BEILSTEIN JOURNAL OF ORGANIC CHEMISTRY

Catalytic multi-step domino and one-pot reactions

Edited by Svetlana B. Tsogoeva

Imprint

Beilstein Journal of Organic Chemistry
www.bjoc.org
ISSN 1860-5397
Email: journals-support@beilstein-institut.de

The *Beilstein Journal of Organic Chemistry* is published by the Beilstein-Institut zur Förderung der Chemischen Wissenschaften.

Beilstein-Institut zur Förderung der Chemischen Wissenschaften
Trakehner Straße 7–9
60487 Frankfurt am Main
Germany
www.beilstein-institut.de

BEILSTEIN JOURNAL OF ORGANIC CHEMISTRY

Catalytic multi-step domino and one-pot reactions

Svetlana B. Tsogoeva

Editorial

Open Access

Address:
Department of Chemistry and Pharmacy, Organic Chemistry Chair I and Interdisciplinary Center for Molecular Materials (ICMM), Friedrich-Alexander-Universität Erlangen-Nürnberg, Nikolaus Fiebiger-Straße 10, 91058 Erlangen, Germany

Email:
Svetlana B. Tsogoeva - svetlana.tsogoeva@fau.de

Keywords:
domino reactions; multi-step reactions; multicomponent reactions; one-pot synthesis; organocatalysis; tandem reactions; transition-metal-catalysis

Beilstein J. Org. Chem. **2024,** *20,* 254–256.
https://doi.org/10.3762/bjoc.20.25

Received: 12 January 2024
Accepted: 30 January 2024
Published: 08 February 2024

This article is part of the thematic issue "Catalytic multi-step domino and one-pot reactions".

Guest Editor: S. B. Tsogoeva

The synthesis of pharmaceutical ingredients, natural products, agrochemicals, ligand systems, and building blocks for materials science has reached a high level of sophistication over the past decades. Most known processes, however, are still frequently hampered by lengthy protecting-group strategies and very costly purification procedures derived from the "stop-and-go" synthetic methods (Figure 1a). Those protocols are still far from the ideal synthesis, implying high atom efficiency, step and pot economies, decreased number of purification steps, or protecting-group-free synthesis.

Multi-step domino [1,2] and one-pot [3] reactions represent a new powerful toolbox in organic synthesis to install molecular complexity economically and sustainably, starting from simple compounds. In particular, catalytic domino reactions and one-pot processes with excellent selectivity and functional-group tolerance are of significant interest to industrial and academic research. In the so-called domino reactions, all of the required reagents, the catalyst, and a solvent are mixed in one flask, in which all reaction steps take place autonomously without the addition of further reactants [1]. The domino process contrasts the conventional "stop-and-go" synthetic approach in the way that multiple reactions proceed in a direct sequence. In such a reaction sequence, one step triggers the next, which in the end yields a complex product. In contrast to a conventional “stop-and-go” method, only a single workup and purification is needed (Figure 1b), and therefore these reaction cascades can be considered superior to stepwise synthetic approaches in the context of green chemistry because they are time-saving, waste-reducing, and atom efficient [1-6]. These efficient and straightforward synthetic methods make the isolation and purification of intermediate products after each reaction step superfluous, thereby drastically reducing the number of workup and purification steps, which is superior to conventional organic synthesis.

The Thematic Issue “Catalytic multi-step domino and one-pot reactions” in the *Beilstein Journal of Organic Chemistry*, which I had the pleasure to edit, covers the recent strategies of domino reactions and one-pot syntheses and presents the advances in the field. A Review article by Pounder, Tam, and co-authors summarizes new transition-metal-catalyzed domino reactions of strained bicyclic alkenes, including both homo- and heterobicyclic alkenes highly useful for the construction of biologically significant compounds with multiple stereocenters [7]. In the Review paper by Kisszékelyi and Šebesta, the diverse variety of chiral metal enolates obtained by asymmetric conjugate addi-

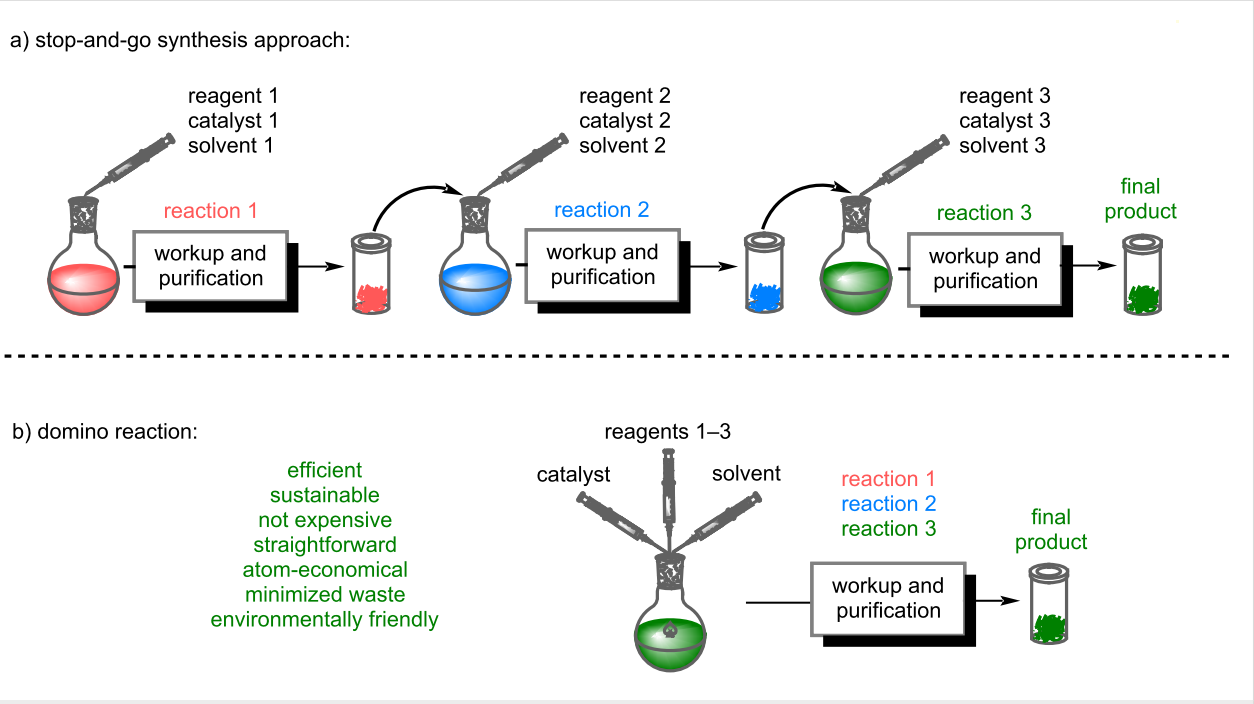

Figure 1: Comparison of a classical “stop-and-go” synthesis with a domino reaction.

tions of organometallic reagents and the possibilities to engage metal enolates in tandem reactions with new electrophiles are presented [8]. A Perspective from X. Zhang, Ma, and W. Zhang reflects the state of the art in the α-amino acid-based [3 + 2] cycloaddition reactions of N–H-type azomethine ylides in multicomponent, one-pot, and stepwise reactions for the synthesis of diverse bioactive heterocyclic compounds and natural products [9].

Computational studies of transannular cycloadditions of cycloalkenone hydrazones catalyzed by BINOL-derived phosphoric acid are reported in the Full Research Paper by Vicario, Merino, and co-workers [10]. Their methodologies can now be used to predict the reactivity of different substrates in other cycloaddition reactions through concerted or stepwise mechanisms. An enantioselective palladium-catalyzed three-component reaction of glyoxylic acid, sulfonamides, and aryltrifluoroborates toward synthetically useful α-arylglycine compounds is described by the Manolikakes group [11]. Moreover, Šebesta and co-workers report a facile stereoselective tandem reaction based on the asymmetric conjugate addition of dialkylzinc reagents to unsaturated acylimidazoles, followed by trapping of the intermediate zinc enolate with carbocations [12]. A practical one-pot synthesis of fluorescent pyrazolo[3,4-*b*]pyridin-6-ones by reacting 5-aminopyrazoles with azlactones under solvent-free conditions, through subsequent elimination of a benzamide molecule in a superbasic medium, is described by the Fisyuk group [13]. A further facile one-pot process toward a new series of copper(II) benzo[*f*]chromeno[2,3-*h*]quinoxalinoporphyrin analogues is described in the Full Research Paper by Nath and co-workers. The newly synthesized porphyrin derivatives displayed significant red-shifted absorption and emission compared to simple *meso*-tetraarylporphyrins [14]. The Carlone group reports an Enders-type triple cascade reaction toward cyclohexenals, using acetaldehyde dimethyl acetal as a masked form of acetaldehyde, which is hydrolyzed in situ, allowing for a higher product yield and fewer byproducts [15]. The group of Müller describes an elegant consecutive four-component reaction involving an alkynylation–cyclization–iodination–alkylation sequence toward trisubstituted 3-iodoindoles, which are valuable substrates for the synthesis of, e.g., blue emitters in good yield [16]. The power of double click reactions toward functionalized bis(1,2,3-triazole) derivatives has been demonstrated in the Full Research Paper by Reissig and Yu. The authors successfully combined nucleophilic substitution of benzylic bromides with sodium azide and a subsequent copper(I)-catalyzed double click reaction in one pot [17].

In summary, these contributions by renowned experts demonstrate the broad diversity of impressive catalytic domino, tandem, and one-pot processes towards many valuable compounds.

Finally, I would like to take this opportunity to warmly thank all the authors of this thematic issue for their beautiful contributions. I also sincerely thank all the referees and the Editorial and

Production Teams of the *Beilstein Journal of Organic Chemistry* for their highly professional assistance and support.

Svetlana B. Tsogoeva

Erlangen, January 2024

ORCID® iDs

Svetlana B. Tsogoeva - https://orcid.org/0000-0003-4845-0951

Data Availability Statement

Data sharing is not applicable as no new data was generated or analyzed in this study.

References

1. Tietze, L. F. *Domino Reactions–Concepts for Efficient Organic Synthesis;* Wiley-VCH: Weinheim, Germany, 2014. doi:10.1002/9783527671304
2. Grondal, C.; Jeanty, M.; Enders, D. *Nat. Chem.* **2010,** *2,* 167–178. doi:10.1038/nchem.539
3. Ishikawa, H.; Suzuki, T.; Hayashi, Y. *Angew. Chem., Int. Ed.* **2009,** *48,* 1304–1307. doi:10.1002/anie.200804883
4. Nicolaou, K. C.; Edmonds, D. J.; Bulger, P. G. *Angew. Chem., Int. Ed.* **2006,** *45,* 7134–7186. doi:10.1002/anie.200601872
5. Held, F. E.; Guryev, A. A.; Fröhlich, T.; Hampel, F.; Kahnt, A.; Hutterer, C.; Steingruber, M.; Bahsi, H.; von Bojničić-Kninski, C.; Mattes, D. S.; Foertsch, T. C.; Nesterov-Mueller, A.; Marschall, M.; Tsogoeva, S. B. *Nat. Commun.* **2017,** *8,* 15071. doi:10.1038/ncomms15071
6. Grau, B. W.; Dill, M.; Hampel, F.; Kahnt, A.; Jux, N.; Tsogoeva, S. B. *Angew. Chem., Int. Ed.* **2021,** *60,* 22307–22314. doi:10.1002/anie.202104437
7. Pounder, A.; Neufeld, E.; Myler, P.; Tam, W. *Beilstein J. Org. Chem.* **2023,** *19,* 487–540. doi:10.3762/bjoc.19.38
8. Kisszékelyi, P.; Šebesta, R. *Beilstein J. Org. Chem.* **2023,** *19,* 593–634. doi:10.3762/bjoc.19.44
9. Zhang, X.; Ma, X.; Zhang, W. *Beilstein J. Org. Chem.* **2023,** *19,* 1677–1693. doi:10.3762/bjoc.19.123
10. Pedrón, M.; Sendra, J.; Ginés, I.; Tejero, T.; Vicario, J. L.; Merino, P. *Beilstein J. Org. Chem.* **2023,** *19,* 477–486. doi:10.3762/bjoc.19.37
11. Jakob, B.; Schneider, N.; Gengenbach, L.; Manolikakes, G. *Beilstein J. Org. Chem.* **2023,** *19,* 719–726. doi:10.3762/bjoc.19.52
12. Mudráková, B.; Marcia de Figueiredo, R.; Campagne, J.-M.; Šebesta, R. *Beilstein J. Org. Chem.* **2023,** *19,* 881–888. doi:10.3762/bjoc.19.65
13. Shuvalov, V. Y.; Vlasova, E. Y.; Zheleznova, T. Y.; Fisyuk, A. S. *Beilstein J. Org. Chem.* **2023,** *19,* 1155–1160. doi:10.3762/bjoc.19.83
14. Tekuri, C. S.; Singh, P.; Nath, M. *Beilstein J. Org. Chem.* **2023,** *19,* 1216–1224. doi:10.3762/bjoc.19.89
15. Brusa, A.; Iapadre, D.; Casacchia, M. E.; Carioscia, A.; Giorgianni, G.; Magagnano, G.; Pesciaioli, F.; Carlone, A. *Beilstein J. Org. Chem.* **2023,** *19,* 1243–1250. doi:10.3762/bjoc.19.92
16. Ledermann, N.; Moubsit, A.-E.; Müller, T. J. J. *Beilstein J. Org. Chem.* **2023,** *19,* 1379–1385. doi:10.3762/bjoc.19.99
17. Reissig, H.-U.; Yu, F. *Beilstein J. Org. Chem.* **2023,** *19,* 1399–1407. doi:10.3762/bjoc.19.101

License and Terms

BEILSTEIN JOURNAL OF ORGANIC CHEMISTRY

Computational studies of Brønsted acid-catalyzed transannular cycloadditions of cycloalkenone hydrazones

Manuel Pedrón[1], Jana Sendra[2], Irene Ginés[1], Tomás Tejero[3], Jose L. Vicario[*2] and Pedro Merino[*1]

Full Research Paper

Open Access

Address:
[1]Instituto de Biocomputación y Física de Sistemas Complejos (BIFI), Universidad de Zaragoza, 50009 Zaragoza, Spain, [2]Departamento de Química Orgánica e Inorgánica, Universidad del País Vasco (UPV/EHU) P.O. Box 644, 48080 Bilbao, Spain and [3]Instituto de Síntesis Química y Catálisis Homogénea (SQCH), Universidad de Zaragoza-CSIC, 50009 Zaragoza, Spain

Email:
Jose L. Vicario[*] - joseluis.vicario@ehu.eus; Pedro Merino[*] - pmerino@unizar.es

* Corresponding author

Keywords:
DFT; distortion model; hydrazones; transannular cycloadditions

Beilstein J. Org. Chem. **2023,** *19,* 477–486.
https://doi.org/10.3762/bjoc.19.37

Received: 28 February 2023
Accepted: 12 April 2023
Published: 20 April 2023

This article is part of the thematic issue "Catalytic multi-step domino and one-pot reactions".

Guest Editor: S. Tsogoeva

Abstract

The contribution to the energy barrier of a series of tethers in transannular cycloadditions of cycloalkenes with hydrazones has been computationally studied by using DFT. The Houk's distortion model has been employed to evaluate the influence of the tether in the cycloaddition reaction. That model has been extended to determine the contribution of each tether and, more importantly, the effect exerted between them. In addition to the distortion induced by the tethers, the entropy effects caused by them has also been studied. The analysis of the evolution of the electron localization function along the reaction revealed the highly concerted character of the reaction.

Introduction

Transannular cycloaddition reactions (TCRs) are useful for the synthesis of complex natural products and other biologically active compounds with high efficiency and stereoselectivity [1-4]. There are several different ways in which TCRs can occur, depending on the nature of the starting materials and the conditions used [5]. Some common types of TCRs include Diels–Alder reactions [6-20], photocycloadditions [21-28], and other types of multistep cycloadditions [29].

Steric hindrance can have a significant effect on the outcome of these reactions. The tether(s) connecting the reactive functional groups affects the spatial orientation of the reacting species and introduces strain into the starting cyclic molecule. As a consequence, the reaction barrier is highly dependent on distortion and entropic effects as Houk and co-workers demonstrated for transannular Diels–Alder cycloaddition reactions of symmetrically tethered large systems (10–18-membered rings) [29].

In this context, we have recently reported the transannular enantioselective (3 + 2) cycloaddition of cycloalkenone hydrazones under Brønsted acid catalysis in route to enantiomerically pure bicyclic 1,3-diamines (Scheme 1) [29]. The reaction led to excellent results when decalines and octahydro-1*H*-indene bicyclic scaffolds were formed (series **a** and **b**) but failed in other cases (series **c**, **d**, and **k**). Series **e**, **f**, **g**, **h**, and **i** have not been tested experimentally.

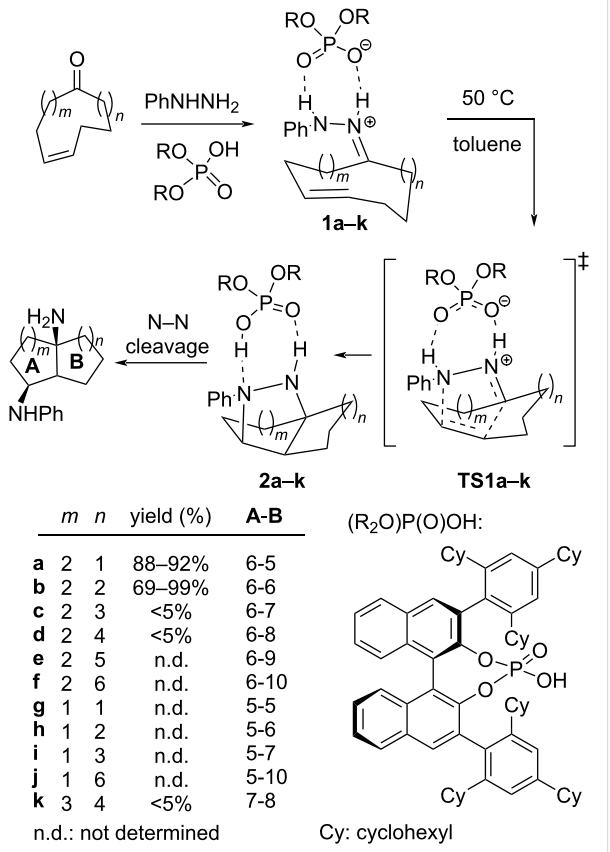

	m	*n*	yield (%)	A-B
a	2	1	88–92%	6-5
b	2	2	69–99%	6-6
c	2	3	<5%	6-7
d	2	4	<5%	6-8
e	2	5	n.d.	6-9
f	2	6	n.d.	6-10
g	1	1	n.d.	5-5
h	1	2	n.d.	5-6
i	1	3	n.d.	5-7
j	1	6	n.d.	5-10
k	3	4	<5%	7-8

n.d.: not determined

Scheme 1: Experimental data (series **a**–**d**, **k**) and non-studied examples (series **e**–**j**) for transannular cycloadditions of cycloalkenone hydrazones.

In this work, we present our results on the computational study of the transannular reaction illustrated in Scheme 1 for several nonsymmetric tether combinations between the hydrazone and double bond moieties leading to a sort of condensed cyclohexanes (series **a**–**f**) and other bicyclic systems (series **g**–**k**) with the aim of explaining the observed lack of reactivity and predicting new reactive substrates. For that purpose, we applied the Houk's distortion model [30] to nonsymmetrically tethered systems and extended the model to estimate the mutual influence of the two different tethers. We have also carried out an analysis of the electron localization function (ELF) [31,32] and the charge transfer along the reaction coordinate to determine the different stages and the polarity of the reaction.

Results and Discussion

The enantioselective intermolecular cycloaddition between hydrazones and alkenes under chiral BINOL-derived Brønsted acid catalysis has been studied by Houk and Rueping in 2014 [33]. These authors established the origin of the enantioselectivity and the differences between the catalyzed and uncatalyzed reactions, suggesting that the catalyzed reaction is, actually, a so-called (3^+ + 2) reaction in which distortion effects are crucial for achieving the required ion-pair geometry in the transition state. Following this precedent, we proceeded to calculate the energy barriers and the corresponding activation parameters for all the reactions illustrated in Scheme 1 (series **a**–**k**), which are listed in Table 1. We used the phosphoric acid derived from 2,2'-biphenol as a model for the catalyst.

Table 1: Calculated activation parameters for transannular cyclizations illustrated in Scheme 1.[a]

reactant	product	system	$\Delta E(0)^{\neq}$	$\Delta H^{\neq}$	$-T\cdot\Delta S^{\neq}$	$\Delta G^{\neq}$
1a	**2a**	6-5	21.3	20.6	2.1	23.2
1b	**2b**	6-6	20.5	19.7	2.1	22.4
1c	**2c**	6-7	27.2	26.4	1.9	28.8
1d	**2d**	6-8	32.2	31.5	1.8	33.7
1e	**2e**	6-9	30.3	28.9	6.1	36.6
1f	**2f**	6-10	35.5	34.5	2.7	37.8
1g	**2g**	5-5	23.0	22.3	1.4	24.0
1h	**2h**	5-6	21.3	20.4	2.8	23.9
1i	**2i**	5-7	30.8	30.1	1.6	32.1
1j	**2j**	5-10	35.6	34.4	2.7	37.8
1k	**2k**	7-8	33.7	32.5	4.1	37.6

[a]Level: m062x/6-311+G(d,p)/SMD=toluene//m062x/6-31G(d).

The optimized geometries of the corresponding transition structures are given in Figure 1 (only those corresponding to fused cyclohexanes are shown, for the rest see Supporting Information File 1).

Only the reactions corresponding to the reaction of **1a** and **1b** show barriers close to 20 kcal/mol thus being plausible to work at ambient temperature or under some heating, which is consistent with the fact that the formation of these adducts were experimentally observed to happen with good yields. Similarly, data of Table 1 predict that the reaction of **1g** and **1h** leading to 5-5 and 5-6 systems (not tested experimentally, yet), respectively could also be observed experimentally. On the other hand, the higher activation barrier of compounds **1c**, **1d**, and **1k** makes the cyclization way more energy demanding, which is fully consistent with the experimental results, where no reaction could be observed. In all these cases, the starting hydrazones were recovered unchanged.

For the other systems (**1e**, **1f**, and **1j**), we predict no reaction at all, since, as before, the energy barriers become unreachable at common reaction conditions.

The reaction has been defined by Houk and Rueping as a (3^+ + 2) monopolar cycloaddition [33] pointing out the protonated state of the imino nitrogen of the hydrazone in contrast to the well-known 1,3-dipolar cycloaddition of azomethine imines in which the terminal nitrogen has a negative charge. While both reacting C–N–N systems fulfil the requirements to give a cycloaddition with an alkene; which are (i) electron density default on the carbon atom and (ii) an electron density excess on the nitrogen atom; the overall positive charge of the hydrazone moiety forces a role inversion of the reagents and whereas in the classical cycloadditions with azomethine imines, they act as a nucleophile (involving their HOMO, interacting with the LUMO of the alkene), in our case, the protonated hydrazone acts as an electrophile (involving their LUMO, interacting now with the HOMO of the alkene) (Figure 2). Thus, we can consider the reaction of hydrazones with alkenes an inverse-demand cycloaddition with respect to that of azomethine imines (Figure 2).

In fact, we monitored the global electron density transfer (GEDT) [34] between the reagents along the reaction coordinate (Figure 3) and we found, in both cases, values lower than 0.4, typical for nonpolar processes.

To assess the concertedness of the reaction we carried out an analysis of the electron localization function (ELF) [31,32]. The ELF analysis applied to an IRC represents the evolution of the

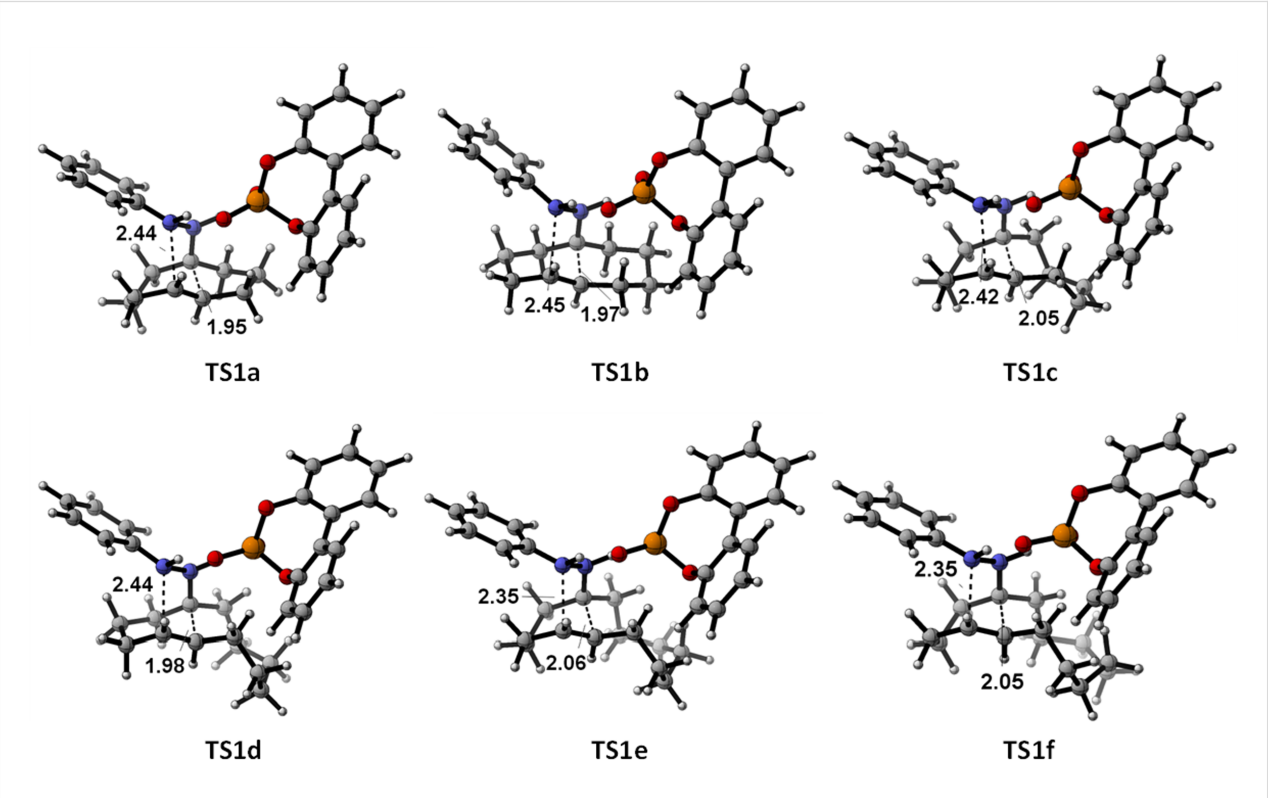

Figure 1: Optimized (m062x/6-31G(d)) geometries for the transition structures of series **a**–**f**.

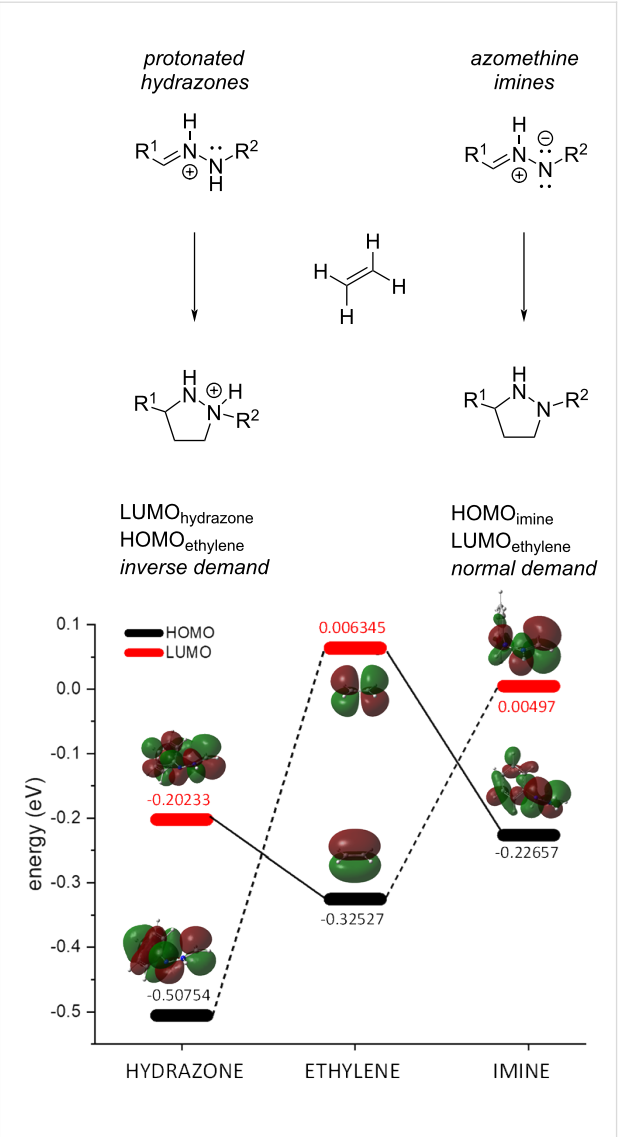

Figure 2: Top: Cycloaddition of protonated hydrazones as inverse-demand reaction of cycloaddition of azomethine imines. Bottom: molecular orbitals involved in the reaction and energy diagram of the reactivity of ethylene with azomethine imine and protonated hydrazone. Energy (eV) of molecular orbitals has been calculated at the m062x/6-311+G(d,p)/SMD=toluene level of theory.

electron density (electron population) during the whole reaction. In consequence, it is possible to analyze the concertedness of the reaction by establishing the moment in which a given bond is broken or formed as well as to analyze changes in the electronic population in bonds and atoms with lone pairs. The ELF analysis of the reaction corresponding to series **b**, leading to a 6-6 system is illustrated in Figure 4.

The first event corresponds to lowering the V(C1,N11) electron population with concomitant decreasing of V(C5,C6) corresponding to the C=N and C=C bonds, respectively. At the same time both V(N11) and V(C1,C6) appear and increase their population till ca. 2 e^- indicating the formation of the C1–C6 bond and the pyramidalization of N11. Although the next bond, corresponding to basin V(C5,N12) seems to be formed with some delay, we can consider the cycloaddition as a highly concerted process, because the bond formation occurs during the other reacting basin's evolution. During the process, N12 loses its lone pair which is involved in the C5–N12 bond formation, and after the cyclization reaction, in a second stage, the lone pair is recovered after the proton (H13) is abstracted by the phosphoric acid. As expected, no significant variations are observed for the bonds N11–N12 and N11–H14, confirming that protonation of N11 is maintained during all the process. In summary, we can define the whole situation as a concerted process taking place in two stages, i.e.: (i) the first one comprises a series of concomitant events in which all bonds involved in the cycloaddition are formed and broken and (ii) a second one consisting of the deprotonation of the nitrogen yielding a neutral compound and liberating the catalyst.

The comparative quantitative analysis of the noncovalent interactions (NCI) [35,36] of fused cyclohexanes clearly showed that NCIs increase with the size of the tether (Figure 5) and the same effect is expected to account for the reagents. In general, a barrier could increase either by a destabilization of the transition structure or the stabilization of the reagents. In our case, the more stable is the reagent the higher is the barrier (for similar transition-state energies) justifying the observed reactivity. Only the two systems (**a** and **b**) with lower values of the integration parameter have barriers compatible with observed reactions upon heating, the rest presenting too high barriers to allow the reaction.

To investigate further the origin of the observed lack of reactivity for medium- and long-size tethers we applied the Houk's distortion model [30] to our substrates using the modified model [9] that allows the analysis of intramolecular reactions. According to that modified model, the two reactive moieties, hydrazone and double bond, are separated from the tethers and capped with hydrogens resulting in hydrazone **3** and ethylene (**4**). In that way, the reactive components preserve the original geometries adopted during the transannular reactions (Figure 6a and 6b). Following the Houk model [30] the distortion energy ($\Delta E^{\neq}_{d}$) corresponds to the difference between the single point corresponding to interacting **3** and **4**, and the sum of single-point calculations for **TS2-a** and **TS2b**.

The apparent activation energy ($\Delta E^{\neq}_{app}$) refers to the energy difference between **TS2** and the interacting reagents **3** and **4** (single point calculations). The difference between $\Delta E^{\neq}_{app}$ and $\Delta E^{\neq}$ is the distortion energy of the tether ($\Delta E^{\neq}_{tether}$) (Equation 1).

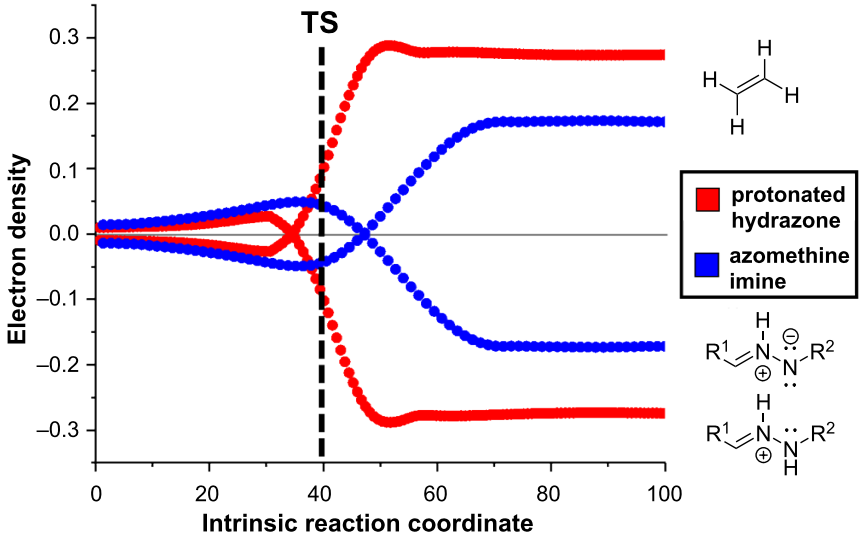

Figure 3: Global electron density transfer (GEDT). Dashed black line indicates both TS.

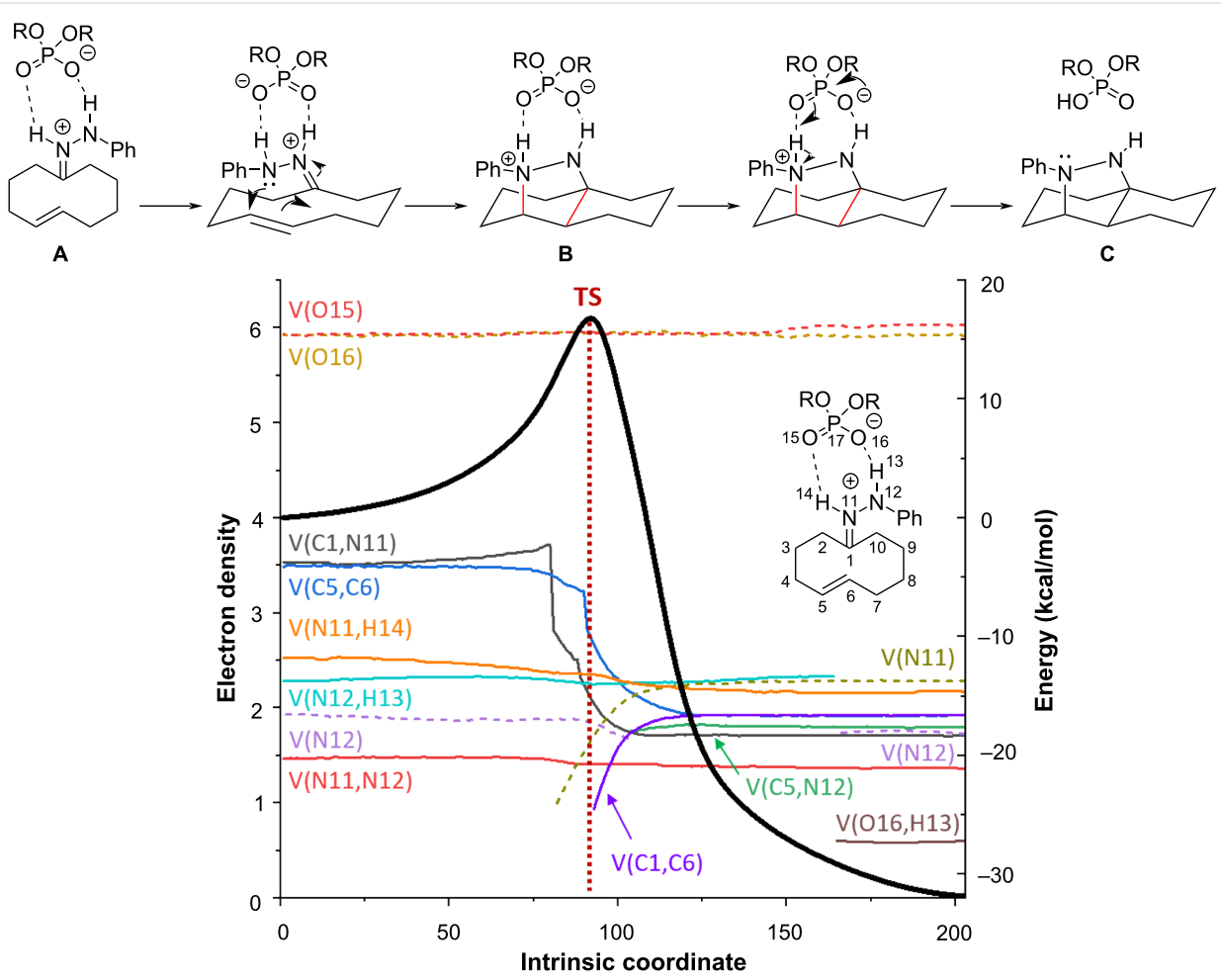

Figure 4: ELF analysis for the reaction of series **b** leading to a system 6-6. Black trace corresponds to IRC. Colored dotted traces refer to lone pairs (monosynaptic basins) and colored plain traces to bonds (disynaptic basins). The vertical red line indicates the transition state (see Supporting Information File 1 for the full data).

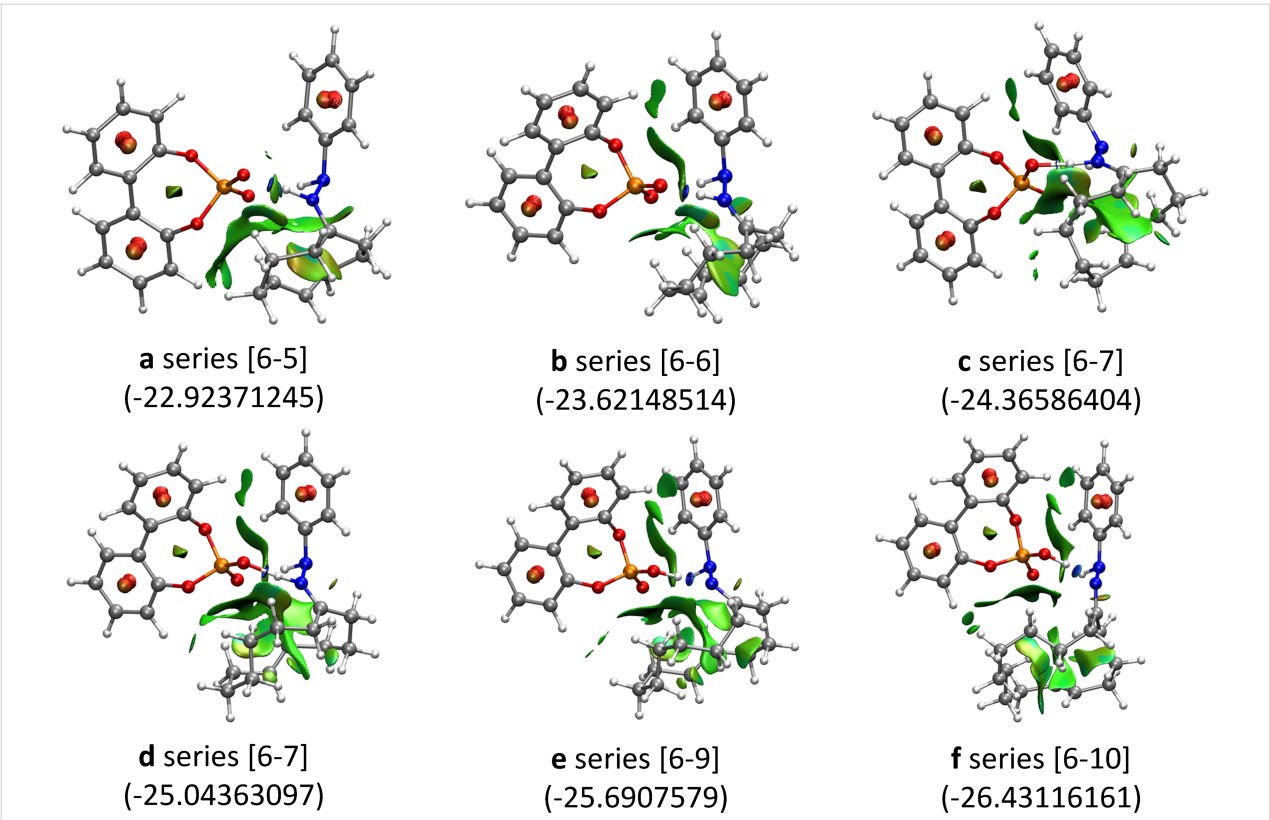

Figure 5: Quantitative NCI analysis [36] for the reaction of series **a**–**f** leading to fused cyclohexanes. The resulting system is given in square brackets. In parentheses the integration over the volumes of $-\lambda^2\cdot\rho^2$ representing the total integration data corresponding to the weak noncovalent van der Waals interactions (represented in green). Higher forces like H-bonds are indicated as blue discs. In red unfavorable interactions are represented.

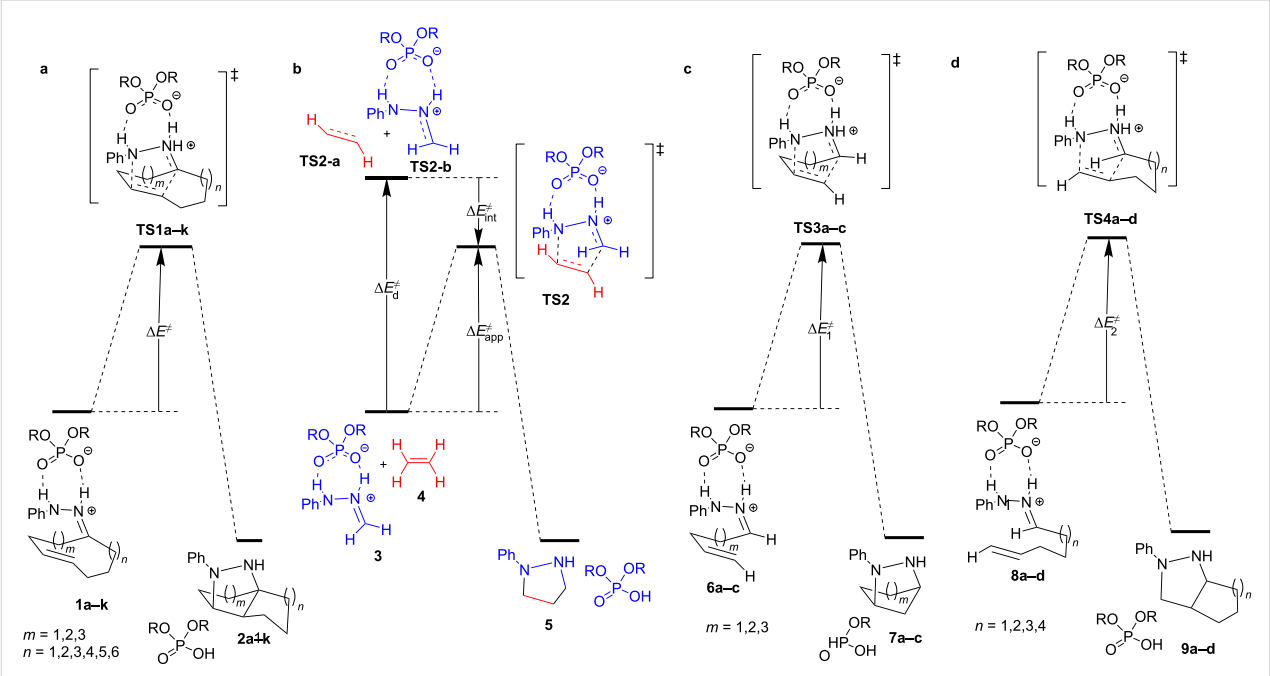

Figure 6: (a) Transannular cycloadditons of compounds **1a**–**k**. (b) Houk's distortion model applied to the reactions. **TS2-a** and **TS2-b** have been calculated separately. (c) and (d) Model reactions with tether **A** and **B**, respectively, to be subjected to the Houk's distortion model, too. Compounds **7a**–**c** and **9a**–**d** have not been calculated because they are not relevant for the distortion analysis.

$$\Delta E^{\neq}_{\text{app}} = \Delta E^{\neq}_{\text{d}} + \Delta E^{\neq}_{\text{int}}$$
$$\Delta E^{\neq}_{\text{tether}} = \Delta E^{\neq} - \Delta E^{\neq}_{\text{app}} \quad (1)$$
$$\Delta E^{\neq}_{\text{tether}} = \Delta E^{\neq}_{\text{t1}} + \Delta E^{\neq}_{\text{t2}} + \Delta E^{\neq}_{\text{ti}}$$

Since our system has two different tethers, we introduced an additional modification by calculating single points of the system with just one tether (Figure 6c and 6d) in order to estimate the individual contribution of each tether to the energy distortion. The corresponding model reactions for tether **A** (**6a–c** to give **7a–c** through **TS3a–c**) and tether **B** (**8a–d** to give **9a–d** through **TS4a–d**) were constructed by eliminating the other tether and keeping the original geometry. From these calculations and applying the Houk's model we can obtain the corresponding distortion energy for each different tether ($\Delta E^{\neq}_{\text{t1}}$ and $\Delta E^{\neq}_{\text{t2}}$; t1 and t2 correspond to tether **A** and **B**, respectively). Besides, we have added an additional term ($\Delta E^{\neq}_{\text{ti}}$) corresponding to the penalty (or synergy) exerted by the combination of the two tethers, which might force additional distortion (or relaxation). That term can be directly calculated from the values obtained by applying the Houk's distortion model to the full system ($\Delta E^{\neq}_{\text{tether}}$) and each of the isolated tether ($\Delta E^{\neq}_{\text{t1}}$ and $\Delta E^{\neq}_{\text{t2}}$). The obtained value for the analysis of the full systems should be the sum of each tether calculated from the individual models plus the term representing the interaction exerted by the combination of both tethers, i.e.: $\Delta E^{\neq}_{\text{tether}} = \Delta E^{\neq}_{\text{t1}} + \Delta E^{\neq}_{\text{t2}} + \Delta E^{\neq}_{\text{ti}}$ (Equation 1). In addition, and for the purpose of comparison, we also calculated the bimolecular reactions for simple models capped with hydrogen and methyl groups without restrictions (Scheme 2).

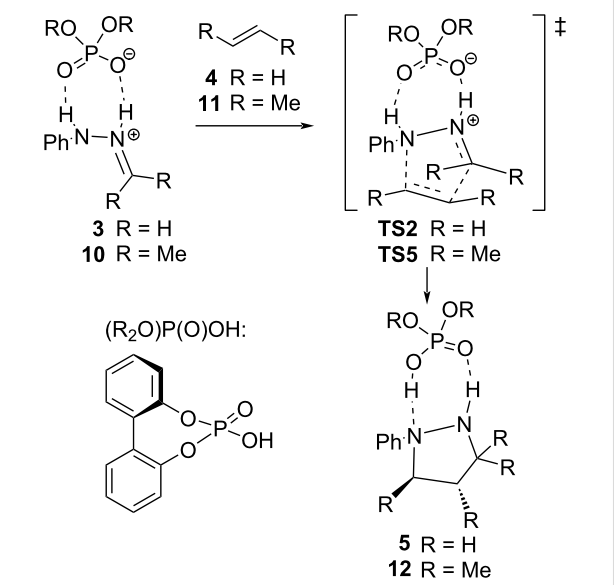

Scheme 2: Reaction with simple models.

Table 2: Calculated activation parameters for transannular cyclizations illustrated in Scheme 2.[a]

reactant	product	$\Delta E(0)^{\neq}$	$\Delta H^{\neq}$	$-T\cdot\Delta S^{\neq}$	$\Delta G^{\neq}$
3	**4**	22.2	20.7	4.2	25.9
10	**12**	6.8	5.3	4.6	11.1

[a]Level: m062x/6-311+G(d,p)/SMD=toluene//m062x/6-31G(d).

The calculated activation parameters for bimolecular cycloadditions for R = H and R = Me are given in Table 2.

Table 3 and Table 4 collect the analyses for fused cyclohexanes and cyclopentanes, respectively.

All the reactions leading to fused cyclohexanes (Table 3) increased tether strain in the transition structures, showing a nega-

Table 3: Distortion–interaction analysis for fused cyclohexanes.

	1a	**1b**	**1c**	**1d**	**1e**	**1f**
system	6-5	6-6	6-7	6-8	6-9	6-10
$\Delta E^{\neq}_{\text{d,dipole}}$	28.6	27.0	25.7	27.2	26.5	33.9
$\Delta E^{\neq}_{\text{d,alkene}}$	4.0	7.1	6.4	6.2	7.9	7.7
$\Delta E^{\neq}_{\text{d,total}}$	32.6	34.1	32.0	33.4	34.4	41.6
$\Delta E^{\neq}_{\text{int}}$	–22.7	–23.4	–20.7	–22.8	–23.3	–23.2
$\Delta E^{\neq}_{\text{app}}$	9.9	10.8	11.3	10.7	11.2	18.4
$\Delta E^{\neq}$	20.9	19.8	26.2	31.2	27.4	31.3
$\Delta E^{\neq}_{\text{d,tether}}$	11.0	9.0	14.9	20.5	16.2	12.9
$\Delta E^{\neq}_{\text{t1}}$	3.5	7.2	7.2	6.3	8.7	3.0
$\Delta E^{\neq}_{\text{t2}}$	11.2	6.9	12.4	18.4	14.6	10.7
$\Delta E^{\neq}_{\text{til}}$	–3.8	–5.0	–4.7	–4.2	–7.1	–0.8

[a]Level: m062x/6-311+G(d,p)/SMD=toluene//m062x/6-31G(d).

Table 4: Distortion-interaction analysis for fused cyclopentanes and system 7-8.

	1g	1h	1i	1j	1k
system	5-5	5-6	5-7	5-10	7-8
$\Delta E^{\neq}_{d,dipole}$	19.4	18.6	27.0	30.5	38.5
$\Delta E^{\neq}_{d,alkene}$	8.2	9.8	11.0	12.3	7.5
$\Delta E^{\neq}_{d,total}$	27.6	28.3	38.1	42.7	46.0
$\Delta E^{\neq}_{int}$	–11.1	–11.9	–13.1	–16.6	–23.2
$\Delta E^{\neq}_{app}$	16.4	16.4	25.0	26.1	22.8
$\Delta E^{\neq}$	23.2	20.8	27.9	31.8	31.8
$\Delta E^{\neq}_{d,tether}$	6.8	4.4	2.9	5.7	9.1
$\Delta E^{\neq}_{t1}$	1.8	6.7	1.5	2.8	8.1
$\Delta E^{\neq}_{t2}$	2.6	1.4	0.9	2.3	16.6
$\Delta E^{\neq}_{ti}$	2.4	–3.7	0.5	0.5	–5.8

[a]Level: m062x/6-311+G(d,p)/SMD=toluene//m062x/6-31G(d).

tive contribution of the tether to the reactivity. The reaction of **1b** has the lowest tether strain, because a decalin is formed. Relatively low values are also observed for the reaction of **1a** and **1f**. However, in the case of **1f** a high distortion of the reactants (particularly of the dipole) is observed contributing to a high barrier. Consequently, only the reactions of **1a** and **1b** are expected to be experimentally observed, as it is confirmed by our previous results. The rest of the compounds are also predicted to be difficult to undergo the transannular reaction as a consequence of the high distortion of the tether. In the case of compounds **1e** distortion of the reagents also contributes to the lack of reactivity.

Interestingly, the Houk's distortion analysis applied to individual tethers shows that tether **B** ($\Delta E^{\neq}_{t2}$) contributes to a greater extent to the barrier of the reaction. Only in the case of the experimentally observed 6-6 both tethers present a similar contribution. Indeed, this case is the only one in which tether **B** ($\Delta E^{\neq}_{t2}$) has a value lower than 10 kcal/mol being the main responsible of the lack of reactivity. Notably, in all cases, $\Delta E^{\neq}_{ti}$ has a negative value indicating that both tethers have a synergic effect, although in any case it is not enough for favoring the reaction. In the case of fused cyclopentanes we observed similar results predicting the only reaction of the observed 5-6 system.

The differences observed between the terms of the distortion analysis corresponding to the transition structures (Figure 6, **TS1a**–**k**) revealed very similar energies, in the range of 2 kcal/mol for both fused cyclohexanes and cyclopentanes, with the exception of the highly constrained system 5-5. Considering the simplest bimolecular model **3**, the fused cyclohexanes contribute with ca. 6–8 kcal/mol while the fused cyclopentanes contribute with ca. 15 kcal/mol (Table 5).

Table 5: Comparison of relative energies (kcal/mol) between transition structure terms of distortion analysis.

system	relative energy[a]
6-5	8.0
6-6	7.2
6-7	6.1
6-8	7.7
6-9	6.8
6-10	7.2
5-5	20.2
5-6	15.4
5-7	14.7
5-10	14.8

[a]Relative to transition structure **TS2**.

Conclusion

In conclusion, the computational topological study (ELF and NCI analysis) of a series of transannular cycloadditions of hydrazones catalyzed by BINOL phosphoric acids, indicated that the process is an apolar concerted process in which all the events (bonds breaking/formation) take place in a concomitant way. In spite of the polarity of the reacting groups the global charge transfer is not so high to be considered a polar process. The reaction, as previously reported by the classical intermolecular reaction takes place smoothly by the action of the organocatalyst that renders a protonated hydrazone as the reacting functional group. However, in several cases the reaction does not work. Application of the Houk's distortion model to those reactions suggested that the observed lack of reactivity for reactions involving the formation of medium-size fused rings is mainly due to the negative effect of the tethers consisting of allowing a more stable (i.e., less distorted) disposition of the

involved functional groups, leading to more stable reagents (rather than more unstable transition structures) which results in an increase of the reaction barrier. In fact NCI analyses points in the same direction. The combined effect of the two tethers is less negative than a simple additive effect as results from the comparison between global and individual distortion analyses of the tethers. Application of these methodologies can be used to predict the reactivity of different substrates in other transannular cycloadditions.

Supporting Information

Supporting Information File 1

Computational methods, energies, and Cartesian coordinates.
[https://www.beilstein-journals.org/bjoc/content/supplementary/1860-5397-19-37-S1.pdf]

Acknowledgements

The authors thankfully acknowledge the resources from the supercomputers "Memento" and “Cierzo”, technical expertise and assistance provided by BIFI-ZCAM (Universidad de Zaragoza, Spain).

Funding

This research was supported by the Spanish AEI (PID2019-104090RB-100, FEDER-CTQ2016-76155-R, FEDER-PID2020-118422GB-I00 and FPI fellowship to J. S.), Basque Government (Grupos IT908-16), and Government of Aragón (Grupos Consolidados, E34_20R and a pre-doctoral contract to M. P.).

ORCID® iDs

Manuel Pedrón - https://orcid.org/0000-0003-4249-6748
Irene Ginés - https://orcid.org/0009-0000-7095-932X
Tomás Tejero - https://orcid.org/0000-0003-3433-6701
Pedro Merino - https://orcid.org/0000-0002-2202-3460

References

1. Deslongchamps, P. *Pure Appl. Chem.* **1992,** *64,* 1831–1847. doi:10.1351/pac199264121831
2. Deslongchamps, P. *Aldrichimica Acta* **1991,** *24,* 43.
3. Marsault, E.; Toró, A.; Nowak, P.; Deslongchamps, P. *Tetrahedron* **2001,** *57,* 4243–4260. doi:10.1016/s0040-4020(01)00121-1
4. Reyes, E.; Uria, U.; Carrillo, L.; Vicario, J. L. *Tetrahedron* **2014,** *70,* 9461–9484. doi:10.1016/j.tet.2014.07.074
5. Reyes, E.; Prieto, L.; Carrillo, L.; Uria, U.; Vicario, J. L. *Synthesis* **2022,** *54,* 4167–4183. doi:10.1055/a-1843-1954
6. Campbell, E. L.; Skepper, C. K.; Sankar, K.; Duncan, K. K.; Boger, D. L. *Org. Lett.* **2013,** *15,* 5306–5309. doi:10.1021/ol402549n
7. Balskus, E. P.; Jacobsen, E. N. *Science* **2007,** *317,* 1736–1740. doi:10.1126/science.1146939
8. Iafe, R. G.; Kuo, J. L.; Hochstatter, D. G.; Saga, T.; Turner, J. W.; Merlic, C. A. *Org. Lett.* **2013,** *15,* 582–585. doi:10.1021/ol303394t
9. He, C. Q.; Chen, T. Q.; Patel, A.; Karabiyikoglu, S.; Merlic, C. A.; Houk, K. N. *J. Org. Chem.* **2015,** *80,* 11039–11047. doi:10.1021/acs.joc.5b02288
10. Prathyusha, V.; Priyakumar, U. D. *RSC Adv.* **2013,** *3,* 15892–15899. doi:10.1039/c3ra42045k
11. Nicolaou, K. C.; Shah, A. A.; Korman, H.; Khan, T.; Shi, L.; Worawalai, W.; Theodorakis, E. A. *Angew. Chem., Int. Ed.* **2015,** *54,* 9203–9208. doi:10.1002/anie.201504337
12. Maiga-Wandiam, B.; Corbu, A.; Massiot, G.; Sautel, F.; Yu, P.; Lin, B. W.-Y.; Houk, K. N.; Cossy, J. *J. Org. Chem.* **2018,** *83,* 5975–5985. doi:10.1021/acs.joc.8b00566
13. Breunig, M.; Yuan, P.; Gaich, T. *Angew. Chem., Int. Ed.* **2020,** *59,* 5521–5525. doi:10.1002/anie.201912613
14. Li, Y.; Palframan, M. J.; Pattenden, G.; Winne, J. M. *Tetrahedron* **2014,** *70,* 7229–7240. doi:10.1016/j.tet.2014.06.090
15. Vasamsetty, L.; Khan, F. A.; Mehta, G. *Tetrahedron Lett.* **2014,** *55,* 7068–7071. doi:10.1016/j.tetlet.2014.10.141
16. Kim, H. J.; Ruszczycky, M. W.; Choi, S.-h.; Liu, Y.-n.; Liu, H.-w. *Nature* **2011,** *473,* 109–112. doi:10.1038/nature09981
17. Mergott, D. J.; Frank, S. A.; Roush, W. R. *Proc. Natl. Acad. Sci. U. S. A.* **2004,** *101,* 11955–11959. doi:10.1073/pnas.0401247101
18. Patel, A.; Chen, Z.; Yang, Z.; Gutiérrez, O.; Liu, H.-w.; Houk, K. N.; Singleton, D. A. *J. Am. Chem. Soc.* **2016,** *138,* 3631–3634. doi:10.1021/jacs.6b00017
19. Yu, P.; Patel, A.; Houk, K. N. *J. Am. Chem. Soc.* **2015,** *137,* 13518–13523. doi:10.1021/jacs.5b06656
20. Zhang, C.; Wang, X.; Chen, Y.; He, Z.; Yu, P.; Liang, Y. *J. Org. Chem.* **2020,** *85,* 9440–9445. doi:10.1021/acs.joc.0c01187
21. Ader, T. A.; Champey, C. A.; Kuznetsova, L. V.; Li, T.; Lim, Y.-H.; Rucando, D.; Sieburth, S. M. *Org. Lett.* **2001,** *3,* 2165–2167. doi:10.1021/ol016076x
22. Fukazawa, A.; Oshima, H.; Shiota, Y.; Takahashi, S.; Yoshizawa, K.; Yamaguchi, S. *J. Am. Chem. Soc.* **2013,** *135,* 1731–1734. doi:10.1021/ja3126849
23. Fukazawa, A.; Oshima, H.; Shimizu, S.; Kobayashi, N.; Yamaguchi, S. *J. Am. Chem. Soc.* **2014,** *136,* 8738–8745. doi:10.1021/ja503499n
24. Liu, J.; Zhou, Y.; Yu, Z.-X. *Org. Lett.* **2022,** *24,* 1444–1447. doi:10.1021/acs.orglett.1c04383
25. Liu, X.; Liu, J.; Wu, J.; Li, C.-C. *J. Org. Chem.* **2021,** *86,* 11125–11139. doi:10.1021/acs.joc.1c00185
26. Chan, D.; Chen, Y.; Low, K.-H.; Chiu, P. *Chem. – Eur. J.* **2018,** *24,* 2375–2378. doi:10.1002/chem.201800019
27. Zhurakovskyi, O.; Ellis, S. R.; Thompson, A. L.; Robertson, J. *Org. Lett.* **2017,** *19,* 2174–2177. doi:10.1021/acs.orglett.7b00834
28. Takao, K.-i.; Kai, H.; Yamada, A.; Fukushima, Y.; Komatsu, D.; Ogura, A.; Yoshida, K. *Angew. Chem., Int. Ed.* **2019,** *58,* 9851–9855. doi:10.1002/anie.201904404
29. Sendra, J.; Reyes, E.; Prieto, L.; Fernández, E.; Vicario, J. L. *Org. Lett.* **2021,** *23,* 8738–8743. doi:10.1021/acs.orglett.1c03190
30. Bickelhaupt, F. M.; Houk, K. N. *Angew. Chem., Int. Ed.* **2017,** *56,* 10070–10086. doi:10.1002/anie.201701486
31. Savin, A.; Nesper, R.; Wengert, S.; Fässler, T. F. *Angew. Chem., Int. Ed. Engl.* **1997,** *36,* 1808–1832. doi:10.1002/anie.199718081

32. Grin, Y.; Savin, A.; Silvi, B. The ELF Perspective of chemical bonding. In *The Chemical Bond: Fundamental Aspects of Chemical Bonding;* Frenking, G.; Shaik, S., Eds.; Wiley-VCH: Weinheim, Germany, 2014; pp 345–382. doi:10.1002/9783527664696.ch10
33. Hong, X.; Küçük, H. B.; Maji, M. S.; Yang, Y.-F.; Rueping, M.; Houk, K. N. *J. Am. Chem. Soc.* **2014,** *136,* 13769–13780. doi:10.1021/ja506660c
34. Domingo, L. R. *RSC Adv.* **2014,** *4,* 32415–32428. doi:10.1039/c4ra04280h
35. Johnson, E. R.; Keinan, S.; Mori-Sánchez, P.; Contreras-García, J.; Cohen, A. J.; Yang, W. *J. Am. Chem. Soc.* **2010,** *132,* 6498–6506. doi:10.1021/ja100936w
36. Boto, R. A.; Peccati, F.; Laplaza, R.; Quan, C.; Carbone, A.; Piquemal, J.-P.; Maday, Y.; Contreras-Garcıa, J. *J. Chem. Theory Comput.* **2020,** *16,* 4150–4158. doi:10.1021/acs.jctc.0c00063

License and Terms

BEILSTEIN JOURNAL OF ORGANIC CHEMISTRY

Transition-metal-catalyzed domino reactions of strained bicyclic alkenes

Austin Pounder*, Eric Neufeld, Peter Myler and William Tam*

Review

Open Access

Address:
Guelph-Waterloo Centre for Graduate Work in Chemistry and Biochemistry, Department of Chemistry, University of Guelph, Guelph, Ontario, N1G 2W1, Canada

Email:
Austin Pounder* - apounder@uoguelph.ca; William Tam* - wtam@uoguelph.ca

* Corresponding author

Keywords:
bicyclic alkenes; cascade; catalysis; domino; transition-metal-catalyzed

Beilstein J. Org. Chem. **2023,** *19,* 487–540.
https://doi.org/10.3762/bjoc.19.38

Received: 06 February 2023
Accepted: 13 April 2023
Published: 24 April 2023

This article is part of the thematic issue "Catalytic multi-step domino and one-pot reactions".

Guest Editor: S. Tsogoeva

Abstract

This review presents a comprehensive overview of transition-metal-catalyzed domino reactions of strained bicyclic alkenes, including both homo- and heterobicyclic alkenes. These compounds are important synthons in organic synthesis, providing an important platform for the construction of biologically/medicinally significant compounds which bear multiple stereocenters. The review has been divided according to the metal used in the reaction. An overview of the substrate scope, reaction conditions, and their potential applications in organic synthesis is discussed. A comprehensive outlook on the reactivity paradigms of homo- and heterobicyclic alkenes is discussed and should shed light on future directions for further development in this field.

Introduction

A well-orchestrated sequence of events – cascade, also known as domino, tandem, and sequential reactions, constitutes a fascinating branch of organic chemistry dedicated to the synthesis of highly functionalized products through sequential transformations in a single reaction. Classically, a domino reaction has been defined by Tietze as a reaction involving two or more bond-forming transformations that take place under the same reaction conditions, without adding additional reagents and catalysts, and in which the subsequent reactions result as a consequence of the functionality formed in previous steps [1].

Bicyclic alkenes, a family of strained ring systems, have seen widespread applications in organic synthesis in the last 20 years [2-6]. Broadly speaking, bicyclic alkenes can be classified into two groups: homobicyclic and heterobicyclic alkenes. Homobicyclic alkenes are hydrocarbons, like norbornadiene, while heterobicyclic alkenes contain at least one heteroatom in the bicyclic framework. Typically, reactions involving these strained bicyclic alkenes are thermodynamically driven forward with the release of ring-strain energy (Figure 1) [7,8]. Intuitively, increasing the number of olefin moieties in the bicyclic system from zero, one, and two, increases the ring-strain

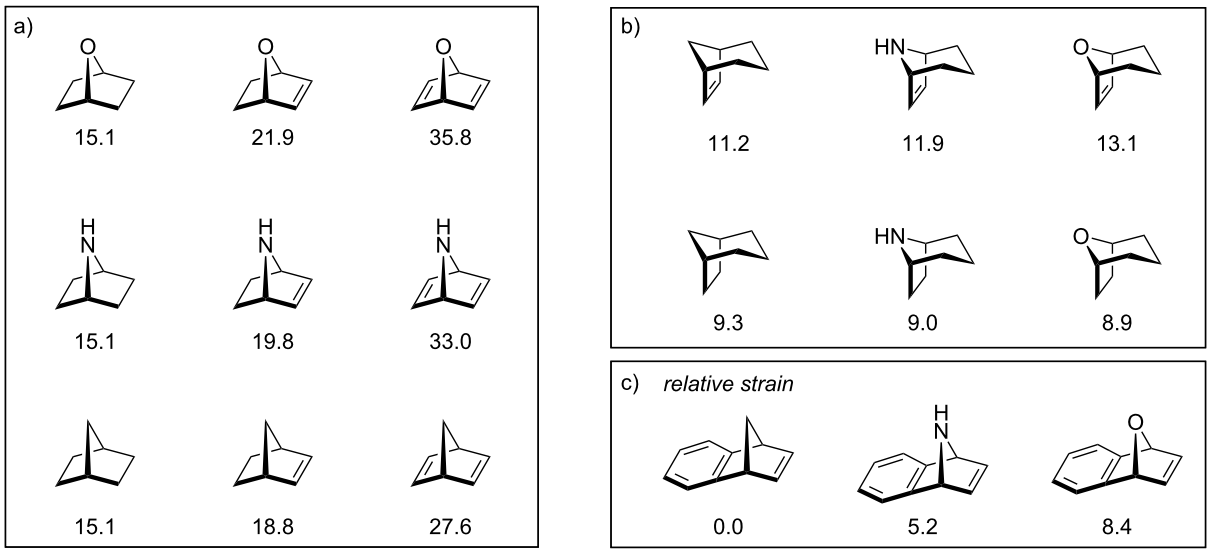

Figure 1: Ring-strain energies of homobicyclic and heterobicyclic alkenes in kcal mol^{-1}. a) [2.2.1]-Bicyclic systems. b) [2.3.1]-Bicyclic systems. c) Benzo-fused [2.2.1]-bicyclic systems; ring-strain energy relative to benzonorbornadiene.

energy. Moreover, the introduction of a bridging heteroatom increases the ring-strain energy of the system, conceptualized by the decrease in bond distances. Typically, there are two modes for ring-strain release. First, functionalization of the double bond mildly alleviates the ring strain by relieving nonoptimal bond angles enforced by the rigid bicyclic framework. Secondly, through ring opening of the bicyclic framework; the C–X bond of a heterobicyclic alkene is much weaker than the corresponding C–C bond of a homobicyclic alkene, which allows the C–X bond to be readily cleaved over the course of a reaction.

The stereochemically well-defined and rigid nature of these bicyclic alkenes creates two diastereotopic faces, namely the *endo* and *exo* face (Figure 2). The *exo* face is sterically less congested than the *endo* face; therefore, the *exo* face will typically interact with metal catalysts through side-on coordination of the olefin, and in the case of heterobicyclic alkenes, the heteroatom. This preferential *exo* coordination is not always the case, as norbornadiene derivatives are known to preferentially form chelated *endo* complexes which can change the stereochemical outcome of the reaction. Nevertheless, the predisposition of metal catalysts towards coordination on the *exo* face biases the reaction outcome towards *exo*-selective functionalization.

Upon *exo* coordination of a metal catalyst with the π system and subsequent migratory insertion, the resulting alkyl metal intermediate is quite limited in how it can propagate. In the case of a carbobicyclic system (Figure 2b), the rigidity of the bicyclic framework restricts β-H elimination. The inability to rotate to achieve an optimal synperiplanar geometry restricts efficient

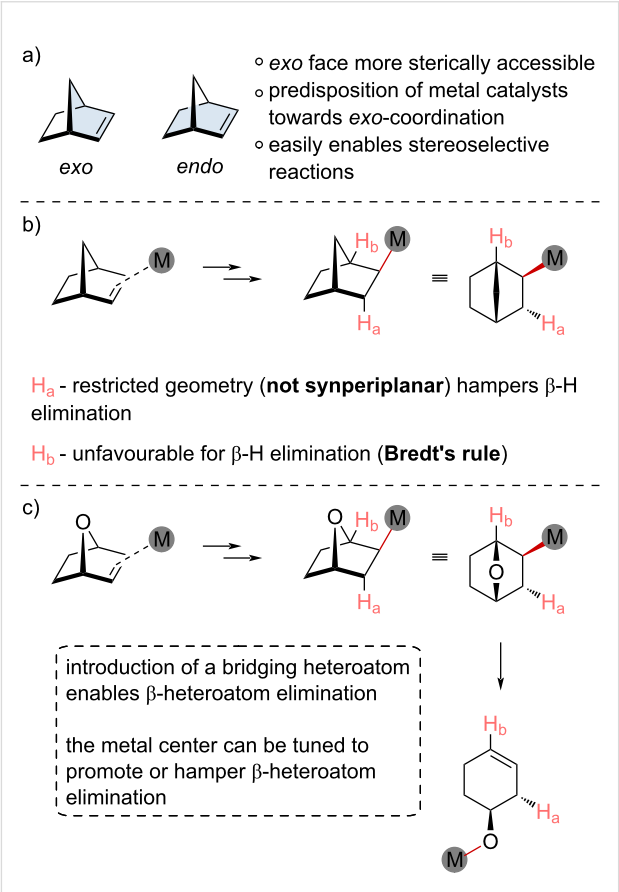

Figure 2: a) *Exo* and *endo* face descriptions of bicyclic alkenes. b) Reactivity comparisons for different β-atom elimination steps for an *exo*-metallated intermediate carbobicyclic system. c) Reactivity comparisons for different β-atom elimination steps for an *exo*-metallated intermediate oxabicyclic system.

elimination (Figure 2b, H_a). Bridgehead protons are in a more favorable geometry for β-H elimination (Figure 2b, H_b); however, their elimination would generate a highly unstable alkene at the bridgehead, violating Bredt's rule [9]. For these reasons, carbobicyclic alkenes have been exploited as propagation mediators, as seen in Catellani-type reactions [10-12]. In this review, we will focus on the functionalization of the bicyclic framework itself rather than its use as a transient mediator for domino reactions [13-17]; however, we point the reader to several excellent reviews. The "trapped" alkyl metal intermediate can undergo subsequent migratory insertion steps with other π systems or can be intercepted by an electrophile.

The introduction of a bridging heteroatom into the bicyclic scaffold can dramatically alter the reactivity (Figure 2c). Besides the apparent increase in the ring strain (vide supra), their potential propagation steps are more complex. After an *exo* coordination of a metal catalyst with the π system and migratory insertion, the resulting heterobicyclic alkyl metal intermediate is not as kinetically stable as its carbocyclic counterpart. While β-H elimination is still limited, these heterobicyclic alkenes will often undergo β-heteroatom elimination to generate ring-opened intermediates (Figure 2c). Fortunately, the metal center can be tuned to promote or hamper the β-H elimination, providing two routes for reaction propagation: ring opening and interception of the ring-opened intermediate or functionalization of the alkyl metal intermediate.

Throughout the past decade, research efforts have demonstrated a broad range of strained bicyclic alkenes can be exploited in domino reactions to selectively generate highly functionalized ring systems. Over the years, several different metal catalysts have been used, each allowing for a breadth of unique coupling partners to either propagate the reaction or to terminate the process.

This review presents a comprehensive examination of domino reactions involving strained bicyclic alkenes. Rather than being exhaustive in the range of potential difunctionalization processes covered, the review will be limited to domino reactions which include at least two distinct reactions. The review is divided on the basis of the transition-metal catalyst used in the reaction and will not cover metal-free methods. The literature is covered up to and including January 2023. For reasons of clarity, newly formed bonds are sketched in red, with newly formed cyclic structures being highlighted.

Review

Earth-abundant metals

Among the transition metal used in organic synthesis, the late transition metals like rhodium, palladium, and iridium have taken center stage when it comes to methodology development. Although these late-stage transition metals have contributed immensely to synthetic organic and organometallic chemistry, increasing societal awareness in terms of sustainable developments and resource management has prompted chemists to explore the use of environmentally benign, inexpensive, and earth-abundant metals [18-27]. In this section, we summarize recent progress in Ni, Fe, Cu, and Co-catalyzed domino reactions of strained bicyclic alkenes.

Nickel-catalyzed reactions

Without close inspection, nickel might seem like the peculiar younger sibling of palladium within the field of transition-metal catalysis. Nickel lies directly above palladium in the periodic table, as such, it readily performs many of the same elementary reactions. Because of their reactive commonalties, nickel is often seen as the budget-friendly replacement; however, this misconception will clearly be refuted in this section, showcasing several diverse nickel-catalyzed domino reactions.

In 2001, Rayabarapu and co-workers investigated the Ni-catalyzed ring-opening/cyclization cascade of heterobicyclic alkenes **1** with alkyl propiolates **2** for the synthesis of coumarin derivatives **3** (Scheme 1) [28]. The reaction initiates with the in situ reduction of Ni(II) to Ni(0) followed by the side-on coordination of the alkene and alkyne substrates to the metal center with subsequent oxidative cyclometallation to form a nickel metallacycle, similar to several reported Ni-catalyzed [2 + 2] cycloadditions [29,30]. Rather than undergoing reductive elimination to afford to [2 + 2] adduct, β-oxygen elimination followed by *E/Z* isomerization and intramolecular lactonization generates the annulated coumarin scaffold. In 2003, the Cheng lab extended on this Ni-catalyzed ring-opening strategy [31]. It was noted the addition of 1.5 equivalents of water interrupted the cyclization step and led entirely to reductively coupled alkenylated ring-opened products. Interestingly, when this methodology was applied to the ester-bearing oxabicyclic **1a**, the anticipated reductive coupling product was not detected; instead, bicyclic γ-lactone **4** was solely observed (Scheme 1). This unprecedented lactone is presumed to be generated through the expected reductive coupling to generate the ring-opened intermediate **5** which undergoes subsequent intramolecular lactonization with the distal ester group. In the same year, Cheng and co-workers observed the identical reactivity when exploring the Pd- and Ni-catalyzed asymmetric reductive ring opening of heterobicyclic alkenes, ultimately generating the bicyclic product **7** (Scheme 1) [32].

In 2003, the Cheng laboratory continued studying Ni-catalyzed routes towards coumarin cores through the Ni-catalyzed ring-opening/cyclization cascade of heterobicyclic alkenes **1** with

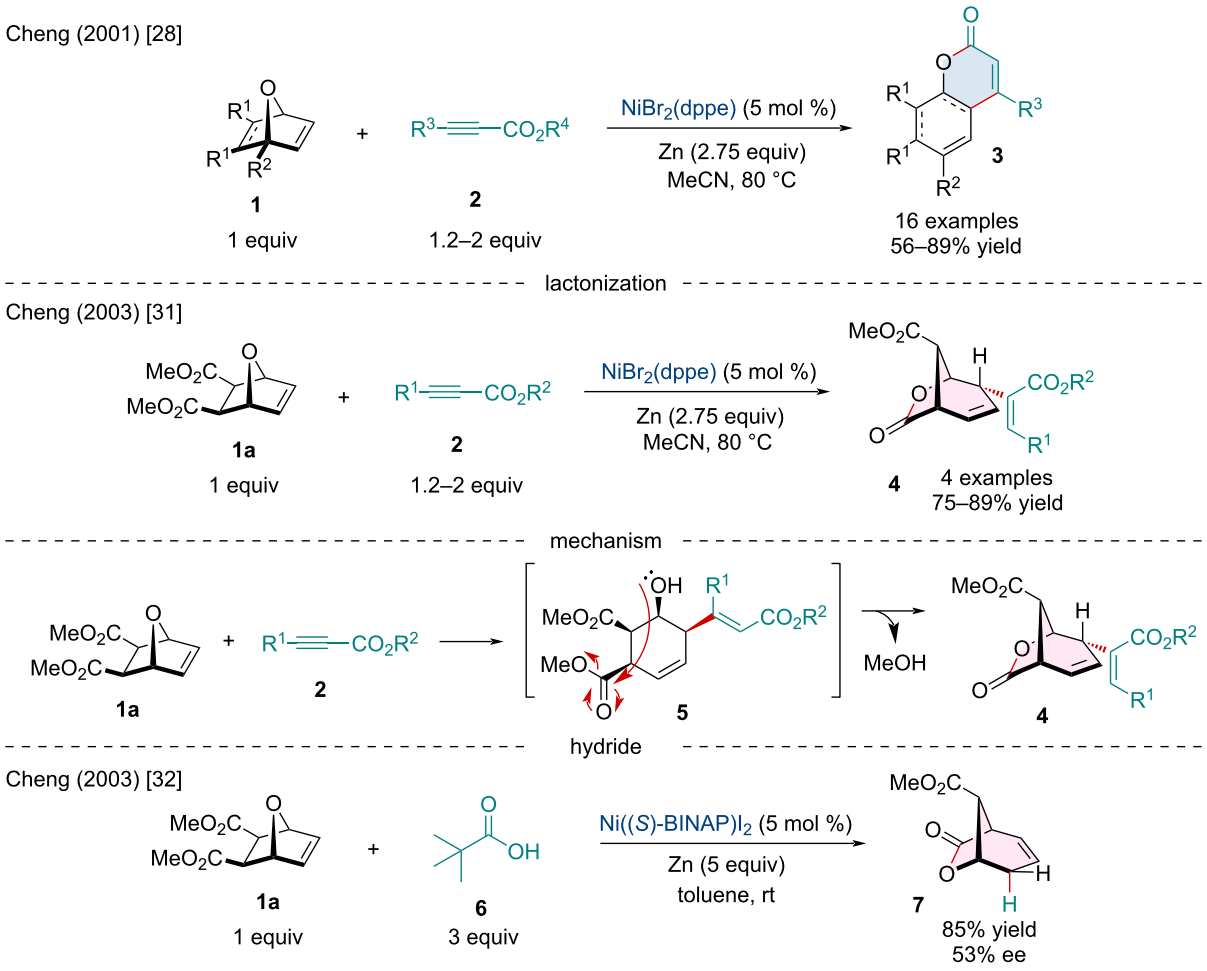

Scheme 1: Ni-catalyzed ring-opening/cyclization cascade of heterobicyclic alkenes **1** with alkyl propiolates **2** to generate coumarin **3** and bicyclic γ-lactone **4** derivatives.

β-iodo-(*Z*)-propenoates and *o*-iodobenzoates **9** (Scheme 2) [33]. The authors noted the ring-opening/cyclization cascade proceeded smoothly for a variety of heterobicyclic alkenes including both oxa- and azabenzonorbornadienes as well as oxanorbornenes; however, the latter two substrates did not undergo dehydrogenation, generating *cis*-selective annulated coumarins (**10b** and **10d**). In 2006, the same group applied this methodology for the total synthesis of arnottin I (**10h**), a coumarin-type natural product isolated from the bark of the *Xanthoxylum arnottianum Maxim* which possesses some antibiotic properties [34]. Mechanistically, the authors proposed the reaction begins with the in situ reduction of Ni(II) to Ni(0) by zinc to generate Ni(0) which undergoes oxidative addition with the organo iodide to yield Ni(II) intermediate **11**. Coordination of **11** to the bicyclic alkene followed by migratory insertion affords intermediate **12** which undergoes β-oxygen elimination to form **13**. Rearrangement of **13** via β-hydride elimination and enolization generates a 1-naphthol species which undergoes intramolecular cyclization with the ester to form the final product **10**. The selectivity for the non-dehydrogenated coumarins **10d** is not understood, but **10b** likely does not undergo dehydrogenation because there is no formation of aromaticity to drive the reaction forward. When the bicyclic alkene is substituted unsymmetrically at the bridgehead position, the reaction is entirely regioselective for the formation of a 1,2,4-trisubstituted pattern. The observed regioselectivity arises from the preferential migratory insertion of the aryl group distal to the bridgehead substituent.

In 2010, Ogata and Fukuzawa explored the Ni-catalyzed two- and three-component difunctionalization of norbornene derivatives **15** with alkynes (Scheme 3) [35]. It was noted the reaction is amenable to both electron-donating groups (EDGs) and electron-withdrawing groups (EWGs); however, yields were diminished with increasing electron deficiency. Moreover, the use of the bulkier *tert*-butyldimethylsilyl-protecting group

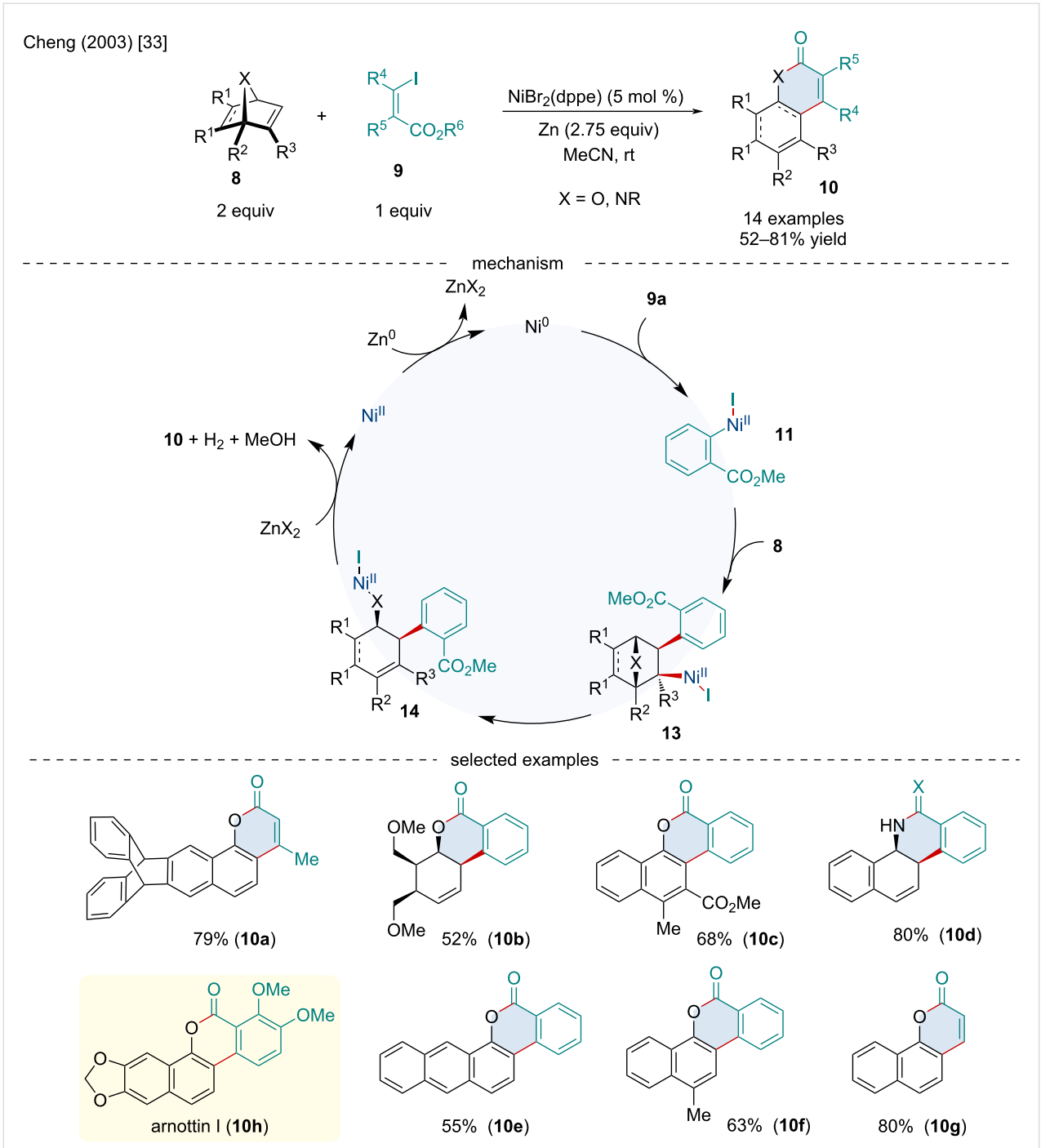

Scheme 2: Ni-catalyzed ring-opening/cyclization cascade of heterobicyclic alkenes **8** with β-iodo-(Z)-propenoates and *o*-iodobenzoates **9**.

resulted in the corresponding 1,5-enyne only being produced in a 33% yield. Several different norbornene derivatives were explored and gave the anticipated *exo,exo*-difunctionalized product in good yield. In contrast, when using an ethylene-bridged bicycloalkene to generate the product **19c**, the latter was obtained in a greatly reduced yield, perhaps due to less ring strain providing a thermodynamic driving force.

In 2013, Mannathan et al. discussed a Ni-catalyzed intermolecular three-component difunctionalization of oxabicyclic alkenes **1** with organoboronic acids **20** and alkynes **17** (Scheme 4) [36]. While broadly successful, when electron-deficient arylboronic acids were used, slightly diminished yields were observed. Moreover, when 3-hexyne was used, the reaction failed to afford any product. The reaction likely begins similarly to

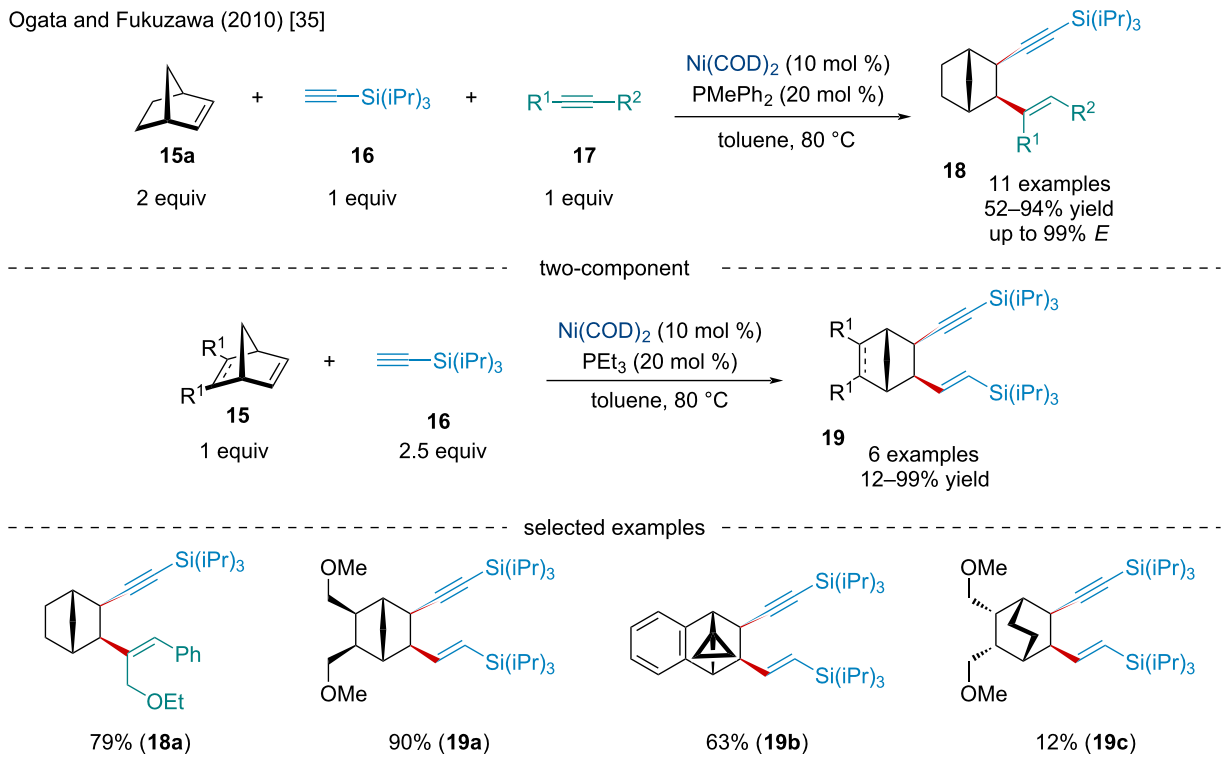

Scheme 3: Ni-catalyzed two- and three-component difunctionalizations of norbornene derivatives **15** with alkynes **16** and **17**.

Cheng's 2003 report (Scheme 1) [31] where the coordination of the alkyne **17** and alkene **1** to the Ni(0) center, followed by oxidative cyclometallation, yields the following nickelocycle **24**. Unlike Cheng's 2003 report, which proposes subsequent β-oxygen elimination (Scheme 1) [31], alkoholysis by MeOH affords an alkyl(methoxy)nickel intermediate **25**. Transmetalation of **25** with the organoboronic acid gives intermediate **26**, which upon reductive elimination affords the difunctionalized product **21** and regenerates the Ni(0) catalyst.

In 2019, the Stanley laboratory explored the Ni-catalyzed intermolecular three-component carboacylation of norbornene derivatives **15** using imides **27** and tetraarylborates **28** (Scheme 5) [37]. The method utilizes C–N bond activation to trigger the reaction. The authors demonstrated a broad reaction scope. Electron-deficient amides were shown to perform worse than their electron-rich counterparts with the *p*-trifluoromethyl substituent forming the ketone product in <10% yield. While substitution of the norbornene was tolerated, both EWGs and EDGs hindered the reaction. Upon several mechanistic studies, the authors proposed the catalytic cycle begins with the oxidative addition of the active Ni(0) catalyst to imide **27** to afford the acyl–Ni(II)–amido intermediate **30**. Side-on coordination followed by migratory insertion of the bicyclic alkene selectively generates the *exo*-alkyl–Ni(II)–amido complex **31**. Transmetalation with triarylborane affords **32** which undergoes reductive elimination to form the carboacylated product **29** as well as regenerates the Ni(0) catalyst. In 2022, the Tobisu group explored a two-component carboacylation of norbornene derivatives. Exploiting a Ni/NHC system, the authors were able to develop an entirely atom-economic carboacylation process utilizing *N*-indoyl arylamides [38].

In 2019, Gutierrez and Molander reported the coupling 4-alkyl-1,4-dihydropyridines **31** with heterobicyclic alkenes **30** under photoredox/Ni dual catalysis (Scheme 6) [39]. In contrast to other photoredox-mediated transformations, the authors utilized the inexpensive organic photosensitizer 4-CzIPN (Scheme 6 and Scheme 7) instead of the more commonly, and expensive, metal-based photocatalysts. While broadly successful, tertiary radicals failed to deliver any desired product. Of note, the reaction was amenable to a broad scope of derivatized heterobicyclic alkenes with mono- and disubstituted bridgeheads having little effect on the reaction (**32b**) with reactions involving unsymmetrically substituted bicyclic alkenes demonstrating complete regioselectivity for either 1,2,3- or 1,2,4-trisubstitued products (**32a**, **32f**). DFT calculations were used to explain the *syn*-1,2-substitution experimentally observed rather than the possible *syn*-1,4-substituted product. It was found the reductive elimination transition state leading to the 1,4-disubstituted prod-

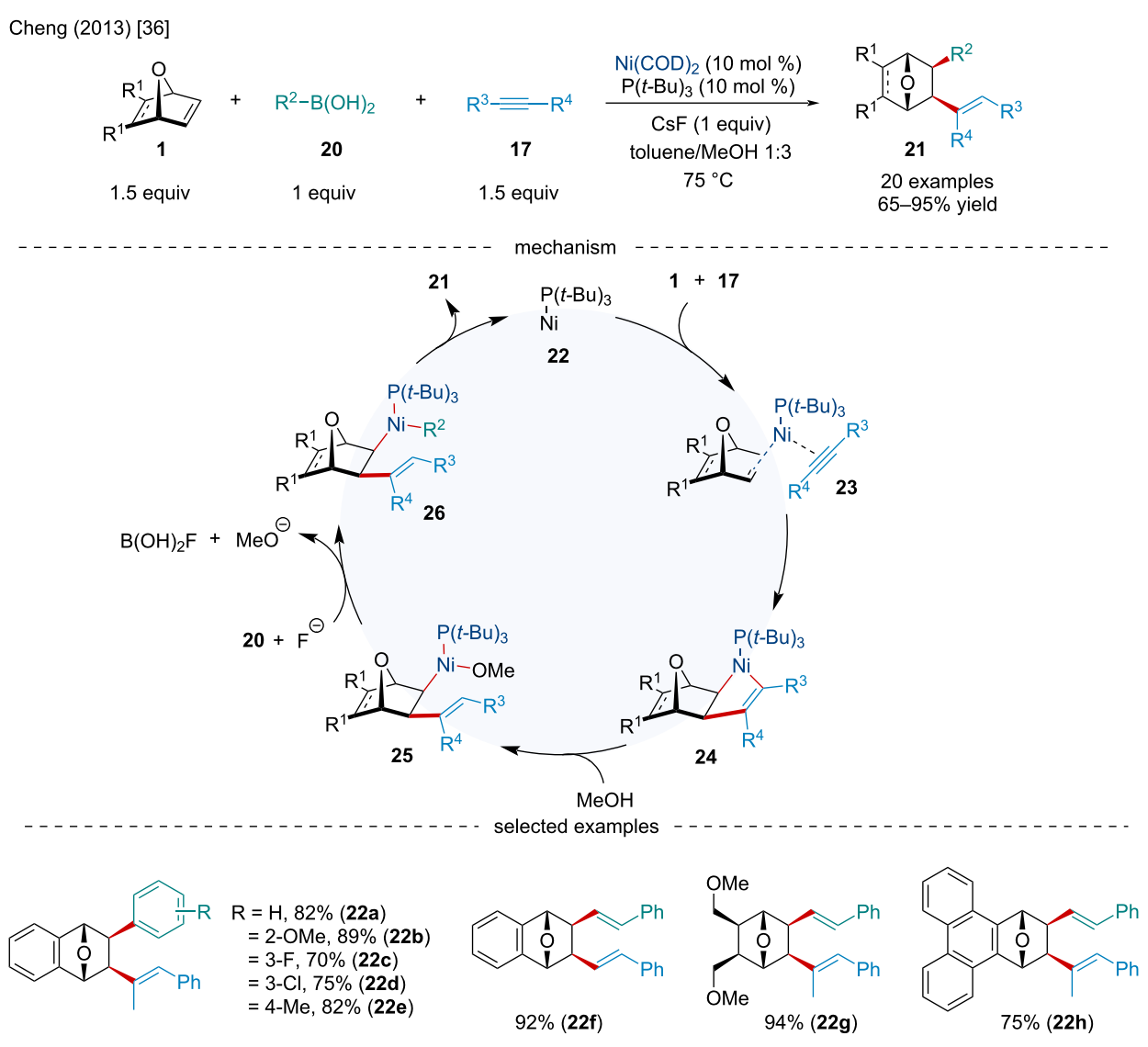

Scheme 4: Ni-catalyzed intermolecular three-component difunctionalization of oxabicyclic alkenes **1** with alkynes **17** and organoboronic acids **20**.

uct $\mathbf{TS_{33\text{-}P1}}$ would require an increase in distortion energy compared to $\mathbf{TS_{35\text{-}P2}}$ which contributes to an overall greater kinetic barrier.

The following year, Lautens and Renaud expanded the scope of the photoredox/Ni dual-catalyzed coupling of alkyl nucleophiles **36** with heterobicyclic alkenes **30** to include α-amino radicals (Scheme 7) [40]. The authors noted the electron-rich oxabenzonorbornadiene derivatives provided the corresponding ring-opened adducts in good yields (63–68% yield) while those bearing EWG led to poor product formation. Unlike Gutierrez and Molander's work (Scheme 6) [39], it was found mono- and disubstituted bridgeheads affected the efficacy of the reaction with the demethylated bridgehead oxabenzonorbornadiene only delivering the product in a 20% yield. Although yields were slightly diminished, unsymmetrical bridgehead-monosubstituted oxabenzonorbornadiene led solely to the 1,2,4-trisubstituted regioisomer (Scheme 7), similar to that observed by Gutierrez and Molander [39]. Selected substituents on the aniline motif were found to hamper reactivity with a few examples failing to provide the desired product when 4-CzIPN was used as the photocatalyst; however, the products were isolated when $[Ir(dF(CF_3)ppy)_2(bpy)]PF_6$ was used. Based on experimental observations and control reactions, the authors proposed the reaction begins with the photoexcitation of the photosensitizer **43** to form **44** which can oxidize aniline **36a** to give radical cation **46** (Scheme 7). Deprotonation by DBU produces the radical **40**. The radical anion photosensitizer **45** can reduce Ni(I) to Ni(0), closing the first catalytic cycle. The Ni(0) complex can undergo oxidative addition into the C–O bond of the

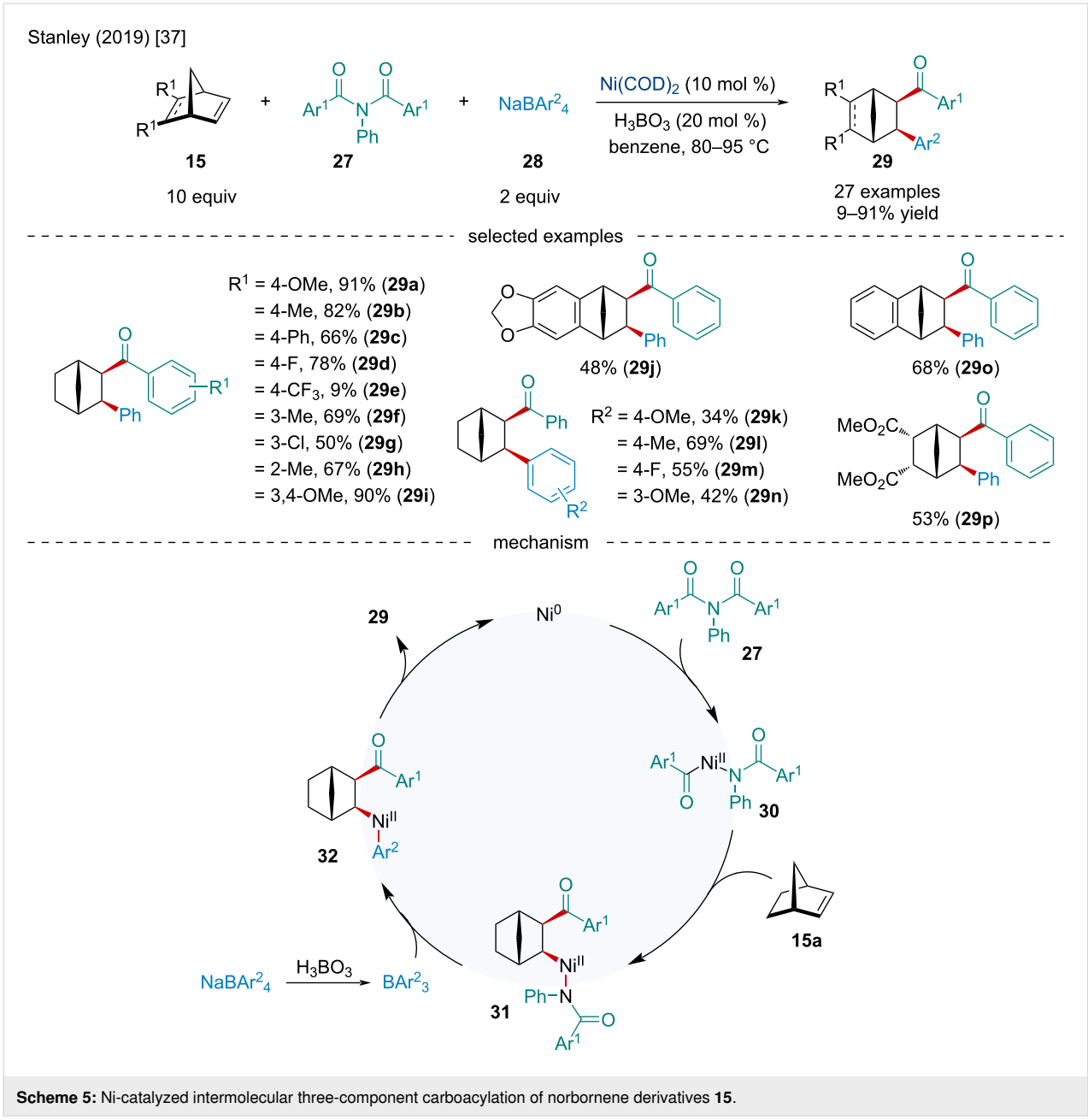

Scheme 5: Ni-catalyzed intermolecular three-component carboacylation of norbornene derivatives **15**.

oxabicyclic alkene **30a** to afford the σ-allyl intermediate **38** which can isomerize to the more stable π-allyl intermediate **39**. Addition of the α-amino radical to the Ni(II) center generates the Ni(III) complex **41**. Reductive elimination, followed by protodemetalation, leads to the final ring-opened adduct **37**.

Copper-catalyzed reactions

In 2009, Pineschi and co-workers explored the Cu-catalyzed rearrangement/allylic alkylation of 2,3-diazabicyclo[2.2.1]heptenes **47** with Grignard reagents **48** (Scheme 8) [41]. The reaction is thought to proceed via the Lewis acid-catalyzed [3,4]-sigmatropic rearrangement of the diazabicycle **47** to form the allylic carbazate intermediate **51**. Nucleophilic attack of an organomagnesium, or organocuprate, in an *anti* S_N2' fashion on **52** furnish the final ring-opened product **49**. The authors note the use of a carbamate protecting group was crucial for the success of the reaction, hypothesizing it inhibited the classical [3,3]-sigmatropic Lewis acid-catalyzed rearrangement often observed. Both alkyl and aryl Grignard reagents were amenable to the reaction; however, heteroaryl Grignard reagents resulted in poor conversion.

The Cu-catalyzed borylative difunctionalization of π-systems is a power tool for the facile synthesis of complex boronate-con-

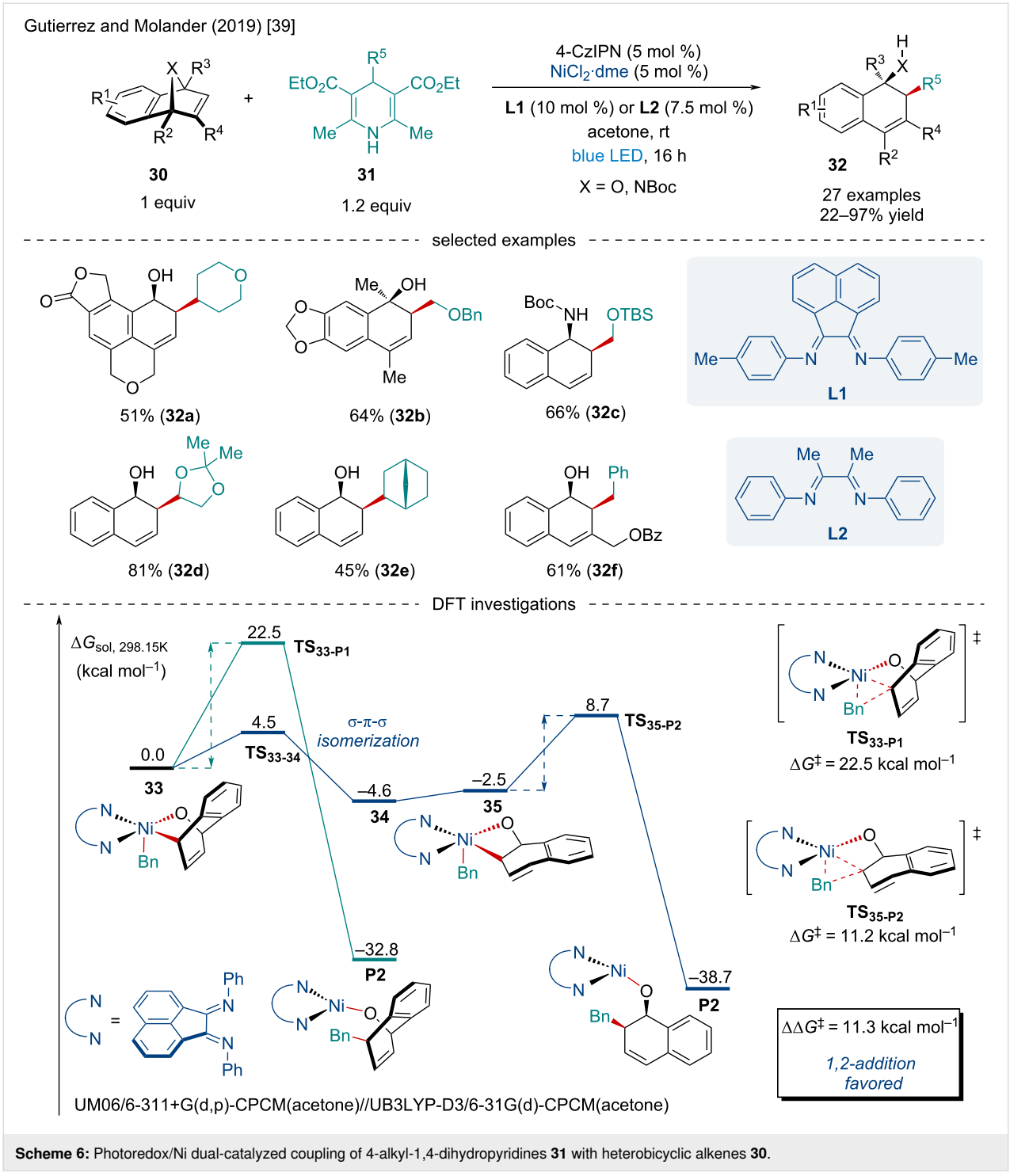

Scheme 6: Photoredox/Ni dual-catalyzed coupling of 4-alkyl-1,4-dihydropyridines **31** with heterobicyclic alkenes **30**.

taining compounds [42]. Generally, these reactions proceed through the generation of a Cu–boryl species via σ-bond metathesis, followed by migratory insertion with a π-system. The subsequent alkyl–Cu intermediate is intercepted by an electrophile to generate the difunctionalized system. This methodology has been applied several times to strained bicyclic alkenes with a variety of electrophiles.

In 2015, Hirano and Miura developed a Cu-catalyzed aminoboration of bicyclic alkenes **1** with bis(pinacolato)diboron (B_2pin_2) (**53**) and *O*-benzoylhydroxylamine derivatives **54** (Scheme 9) [43]. While the scope of bicyclic alkenes was quite extensive with aza-, carbo-, and oxabicyclic alkenes being amenable to the reaction, electron-deficient substrates resulted in lowered yields. Of note, the reaction is highly regioselective

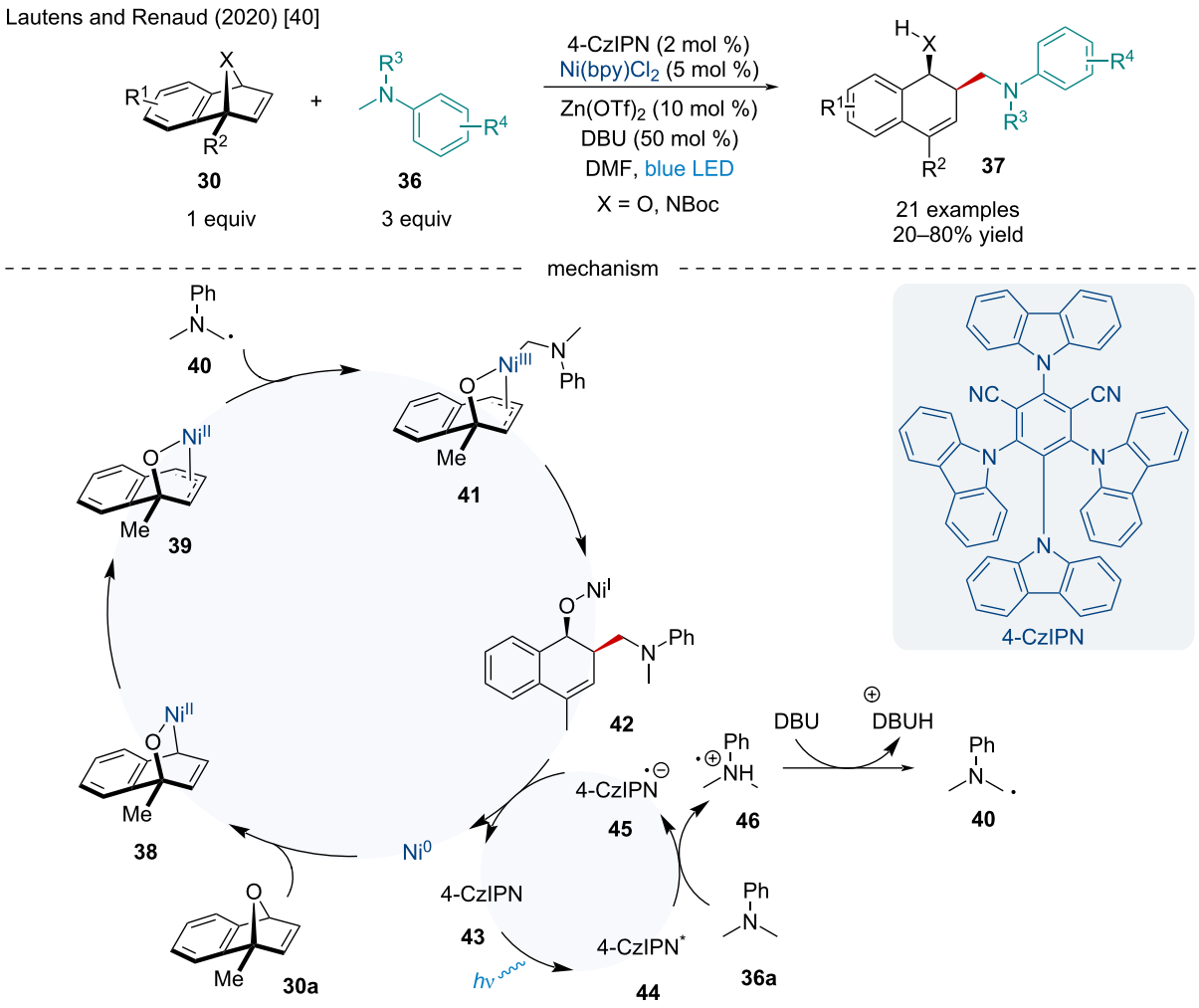

Scheme 7: Photoredox/Ni dual-catalyzed coupling of α-amino radicals with heterobicyclic alkenes **30**.

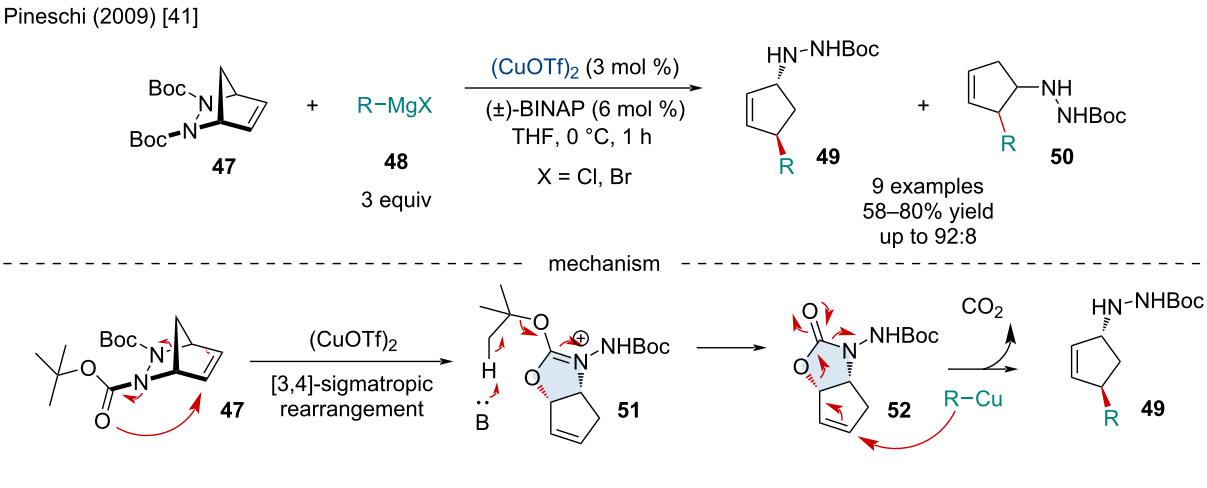

Scheme 8: Cu-catalyzed rearrangement/allylic alkylation of 2,3-diazabicyclo[2.2.1]heptenes **47** with Grignard reagents **48**.

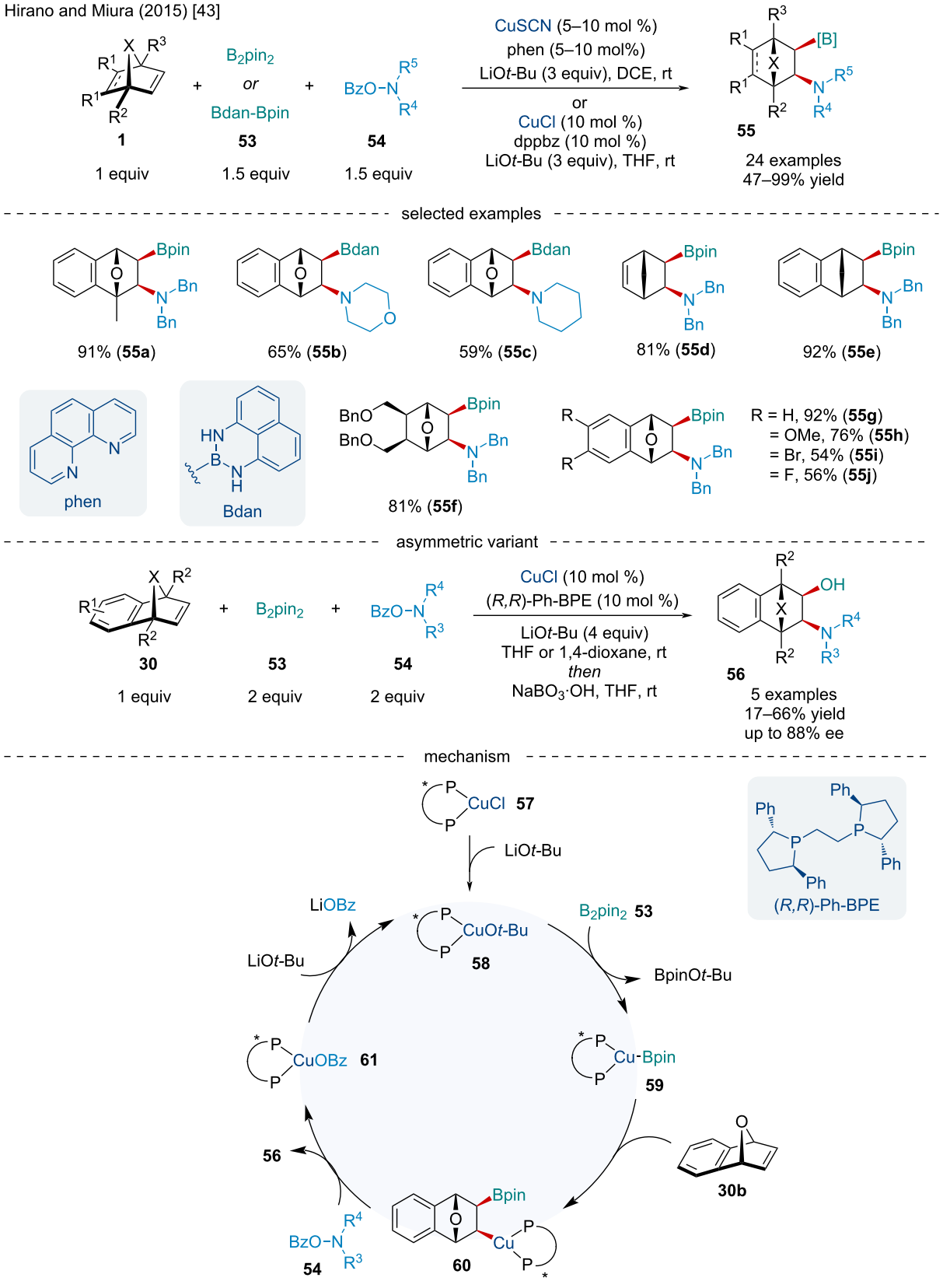

Scheme 9: Cu-catalyzed aminoboration of bicyclic alkenes **1** with bis(pinacolato)diboron (B_2pin_2) (**53**) and *O*-benzoylhydroxylamine derivatives **54**.

with the unsymmetrically methyl-substituted bicyclic alkene producing a single regioisomer **55a**. The authors noted the aminoborylated products bearing a BPin moiety were not always stable upon isolation, so they were either converted into the more stable Bdan (dan = 1,8-diaminonaphthalenyl) or Bpin-Bdan was used directly which showed comparable yields. The authors also reported preliminary results for an asymmetric variant of the reaction using (*R,R*)-Ph-BPE as a chiral ligand. Although the use of the chiral phosphine ligand resulted in slightly diminished yields, the authors were able to achieve ees up to 88%. The authors proposed the reaction begins with the generation of the *tert*-butoxide Cu salt which undergoes σ-bond metathesis with B_2Pin_2 generating the Cu–boryl species **59** (Scheme 9). Side-on coordination on the *exo* face of the bicyclic alkene followed by migratory insertion generates the alkyl–Cu species **60** which after electrophilic amination with the *O*-benzoylhydroxylamine **54** liberates the final aminoborylated product **55** and a benzoyl–Cu complex **61**. To close the catalytic cycle a transmetalation of **61** with LiO*t*-Bu regenerates the active catalyst.

In 2017, Xiao and Fu studied the Cu-catalyzed borylalkynylation of oxabenzonorbornadiene (**30b**) with B_2pin_2 (**53**) and bromoalkynes **62** (Scheme 10) [44]. The scope of the reaction was limited to only two examples of bromoalkynes reacting with oxabenzonorbornadiene (**30b**). Notably, the yield of the reaction dramatically diminished when the terminal triisopropylsilyl (TIPS) group in **63a** was swapped for a Ph (**63b**). Mechanistically, the reaction operates in a similar manner reported by Hirano and Miura (Scheme 9) [43]; however, the alkyl–Cu species **60** is intercepted by the bromoalkyne rather than an *O*-benzoylhydroxylamine.

In the same year, the Brown laboratory investigated the Cu-catalyzed borylacylation of bicyclic alkenes **1** (Scheme 11) [45]. Like the previous borylative difunctionalization reactions, it

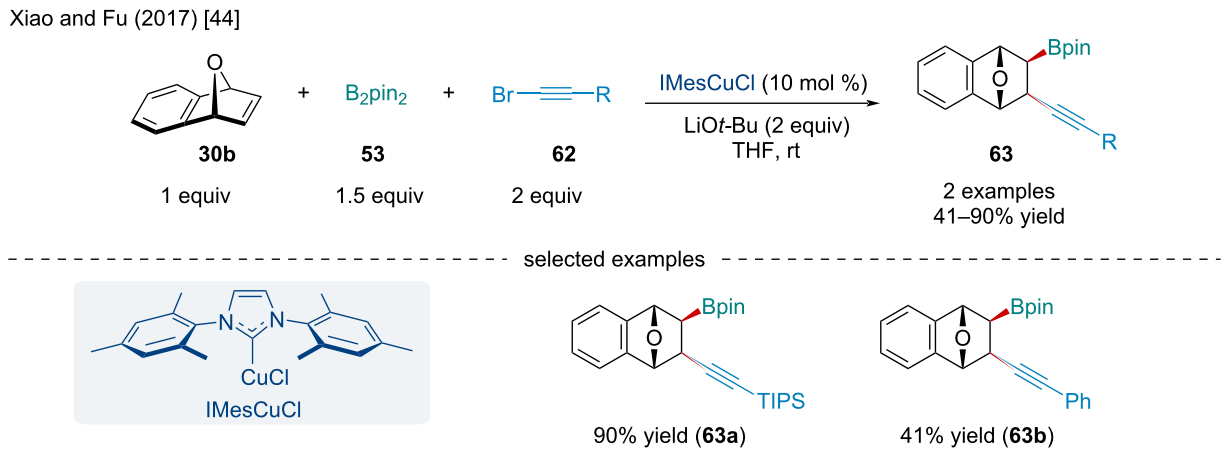

Scheme 10: Cu-catalyzed borylalkynylation of oxabenzonorbornadiene (**30b**) with B_2pin_2 (**53**) and bromoalkynes **62**.

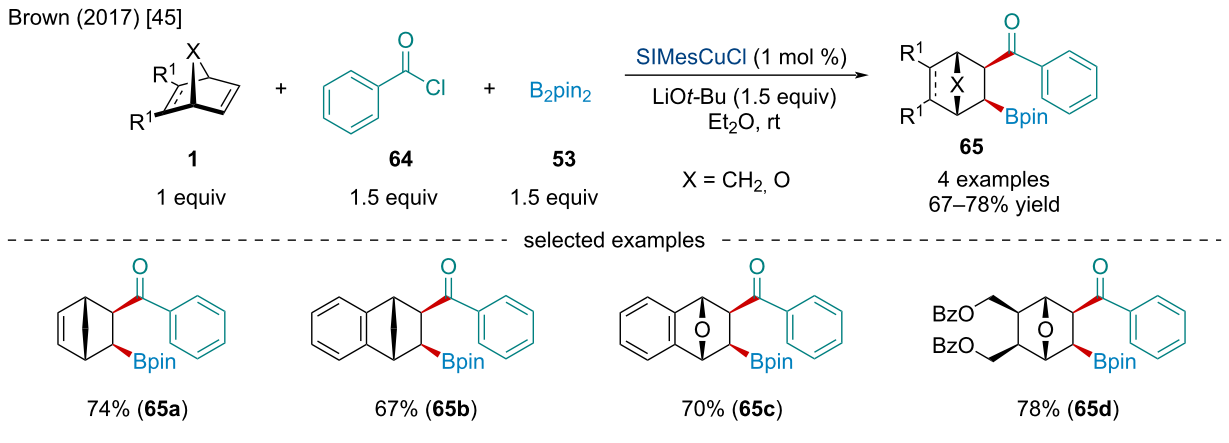

Scheme 11: Cu-catalyzed borylacylation of bicyclic alkenes **1**.

was found the reaction generated a single *exo,exo* diastereomer. A brief investigation into an enantioselective variant of the borylacylation was investigated; however, the methodology was not applied to bicyclic alkenes.

In 2019, the Yang lab examined the Cu-catalyzed diastereoselective 1,2-difunctionalization of oxabenzonorbornadienes **30** for the synthesis of β-thiocyanato thioethers **68** (Scheme 12) [46]. In contrast to the previous difunctionalization reactions, the authors noted the reaction was stereoselective for the *trans*-addition product. Mechanistically, the authors proposed the reaction begins with the Cu-mediated substitution reaction of iodobenzene (**66a**) with KSCN to afford phenyl thiocyanate (**70**). The Cu complex can then undergo oxidative addition into the S–C bond of the thiocyanate **70** to afford intermediate **71** which can side-on coordinate to the *exo* face of **30b**. Subsequently, the thiocyanate attacks the olefin from the *endo* face via **72** to give complex **73**. Reductive elimination furnishes the final difunctionalized product and regenerates the active Cu(I) catalyst. The reaction was broadly successful with the steric and electronic nature of the aryl iodide having little effect on the reaction.

Iron-catalyzed reactions

Being the most earth-abundant d-block element, as well as orders of magnitude less expensive than other transition-metal catalysts, iron is bringing a renaissance to the idea of sustainable, green catalysis. In 2011, Ito et al. reported a diastereose-

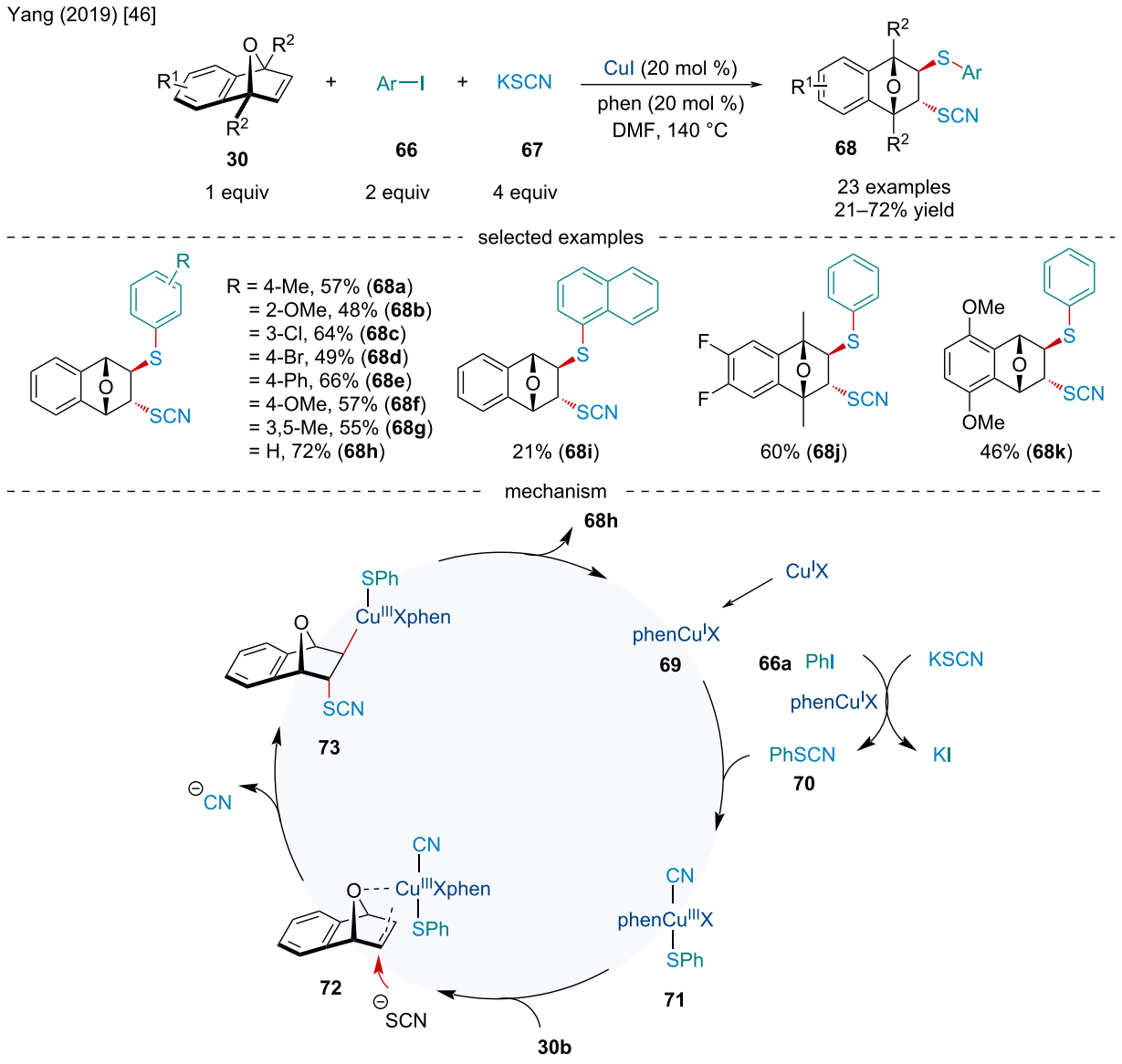

Scheme 12: Cu-catalyzed diastereoselective 1,2-difunctionalization of oxabenzonorbornadienes **30** for the synthesis of β-thiocyanato thioethers **68**.

lective Fe-catalyzed carbozincation of heterobicyclic alkenes **1** with diphenylzinc (**74a**) (Scheme 13) [47]. Using an ortho-phenylene diphosphine ligand **L3**, the authors were able to suppress β-heteroatom elimination enabling sequential electrophilic trapping of the alkylzinc complex. Although this reaction would more closely fall under the definition of a telescoped reaction than a strict domino reaction, this methodology allowed for the synthesis of difunctionalized strained alkenes. While broadly successful, strongly electron-withdrawing groups lowered the yield of the reaction. In 2021, Isozaki and Nakamura reinvestigated the reaction and established an asymmetric variant of the Fe-catalyzed carbozincation of azabicyclic alkenes **77** (Scheme 13) [48]. Using (*S,S*)-chiraphos, the authors were able to achieve enantioselectivities of up to 99%. Unfortunately, only two examples of electrophilic capturing were explored, using CD_3CO_2D to give deuterated products and I_2.

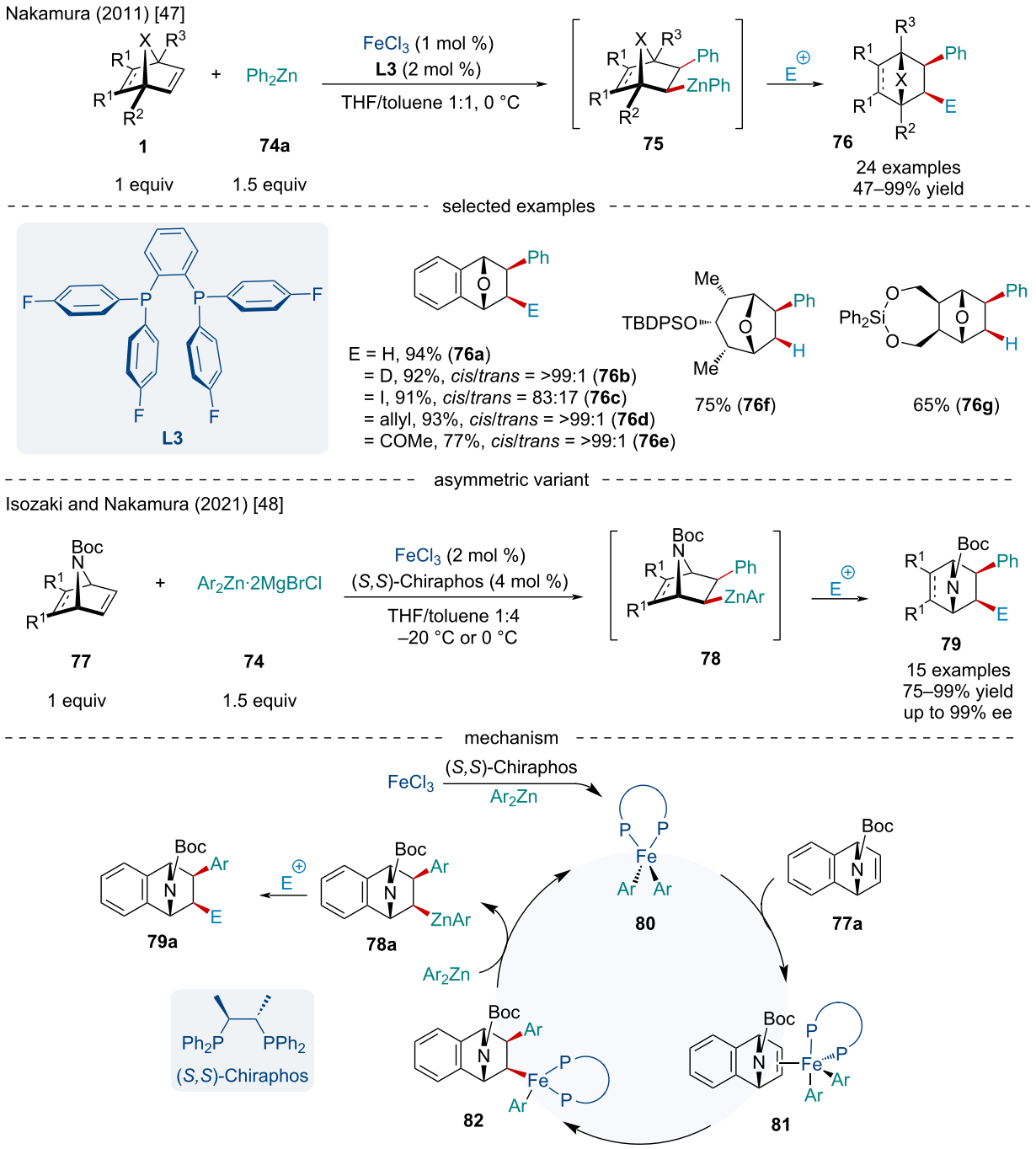

Scheme 13: Fe-catalyzed carbozincation of heterobicyclic alkenes **1** with arylzinc reagents **74**.

Most reports simply underwent protodemetalation upon quenching to afford the monosubstituted bicyclic alkene. The catalytic cycle starts with a diaryl Fe(II)–(*S,S*)-chiraphos complex **80** being generated through the reduction of $FeCl_3$ with excess diarylzinc in the presence of the phosphine ligand. Side-on coordination to the *exo* face of the azabicycle **77a** generates **81** where subsequent migratory insertion affords the alkyl–Fe(II) complex **82**. Transmetalation with an organozinc produces **78a** which can be trapped by an electrophile to generate the final product **79a**.

Cobalt-catalyzed reactions

In 2014, the Yoshikai lab investigated the Co-catalyzed addition of arylzinc reagents **83** of norbornene derivatives **15** (Scheme 14) [49]. In contrast to the 1,2-difunctionalization of bicyclic alkenes via arylzinc reagents reported by Nakamura under Fe catalysis (Scheme 13) [48], this reaction is considered to undergo a 1,4-Co migration ultimately generating 1,4-difunctionalization species. Mechanistically, the reaction likely proceeds similarly to Nakamura's Fe-catalyzed methodology (Scheme 13) [48].

In 2017, the Cheng laboratory investigated the Co-catalyzed ring-opening/dehydration of oxabicyclic alkenes via the C–H activation of arenes (Scheme 15) [50]. First, the group explored the *ortho*-naphthylation of *N*-pyrimidinylindole derivatives **85**. The reaction was amenable for both electron-rich and deficient indoles. When the reaction was attempted on electron-deficient

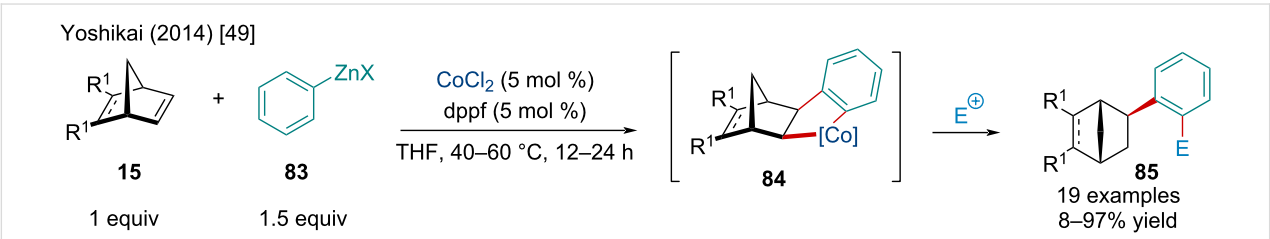

Scheme 14: Co-catalyzed addition of arylzinc reagents of norbornene derivatives **15**.

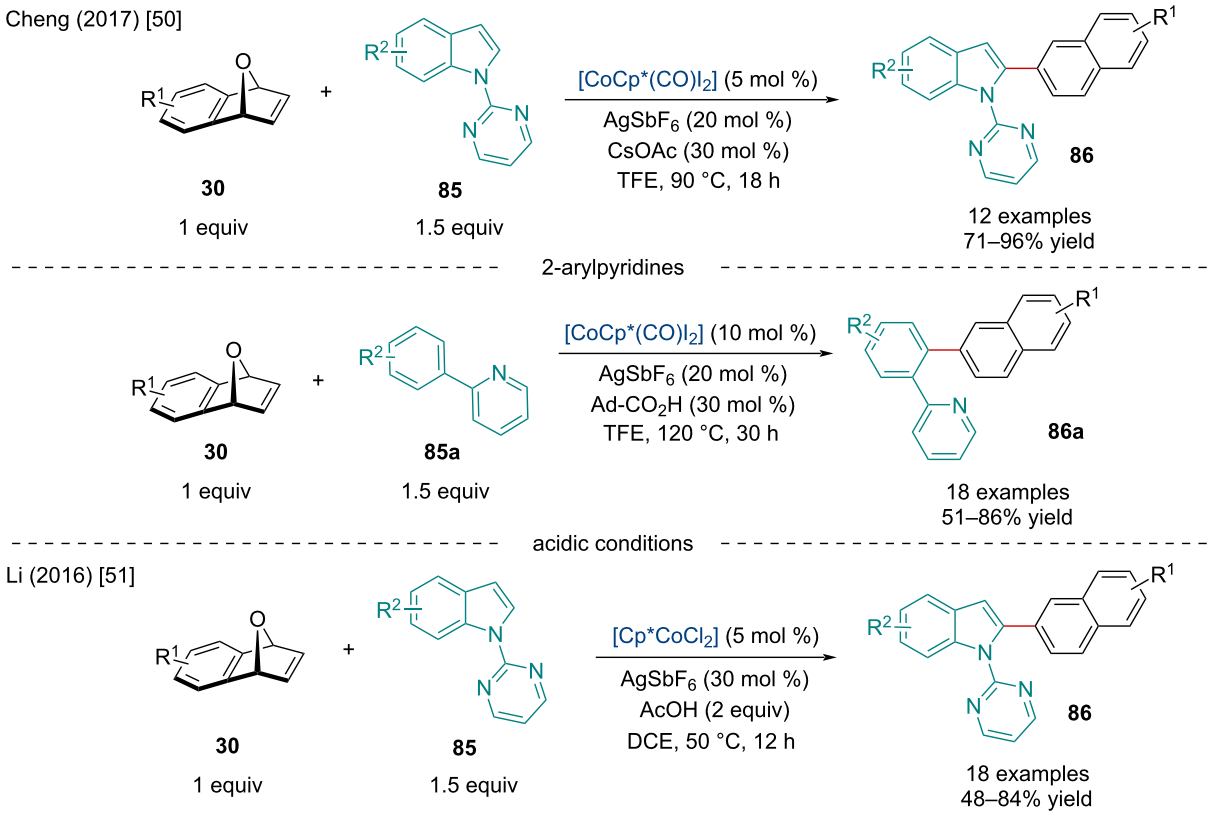

Scheme 15: Co-catalyzed ring-opening/dehydration of oxabicyclic alkenes **30** via C–H activation of arenes.

oxabicyclic alkene derivatives, it was observed the reaction did not undergo dehydration to give the 2-naphthyl product, rather the ring-opened 1,2-hydroxy adduct. When the Lewis acid cocatalyst $AgSbF_6$ was removed from the reaction mixture, it was noted only ring-opened 1,2-hydroxy adducts were formed, so it is likely the Lewis acid is required for dehydration. In contrast, when *N*-pyrimidinylbenzimidazole derivatives were used, the 1,2-C–H addition product was observed exclusively. By slightly altering the reaction conditions, 2-arylpyridines **85a** were able to undergo the ring-opening/dehydration reaction with oxabicyclic alkenes to afford *ortho*-naphthylated products **86a**.

Concurrently, the Li group investigated the same *ortho*-naphthylation of *N*-pyrimidinylindole derivatives **85** (Scheme 15) [51]. In contrast to Cheng's report, it's noted the addition of AcOH rather than CsOAc enabled the same ring-opening/dehydration cascade to occur; however, acidic conditions seem to require less energy to drive the dehydration step.

In 2019, the Zhai Group investigated the Co-catalyzed [3 + 2] annulation/ring-opening/dehydration domino reaction of oxabicyclic alkenes **30** with 2-(1-methylhydrazinyl)pyridine (MHP) directed arenes **87** for the synthesis of benzo[*b*]fluorenones **88** (Scheme 16) [52]. C–H bond functionalization with heterobicyclic alkenes as annulation partners has received considerable attention in recent years. Several different arene and directing groups have been investigated; however, they typically result in the *exo*-selective addition product with the bridge heteroatom intact. Although this limits the applicability of the reaction, the authors noted the use of 5.0 equivalents of Cs_2CO_3 provided the naphthalene core via sequential dehydration. Based on preliminary mechanistic experiments, the authors proposed the reaction begins with the oxidation of Co(II) to Co(III) by O_2. MHP-directed C–H activation of the *ortho*-C–H position generates **90** which can coordinate to the bicyclic alkene forming **91**. Migratory insertion of the olefin affords **92** which undergoes intramolecular nucleophilic addition followed by protodemetalation and elimination of MHP to afford **94**. Base-mediated ring opening

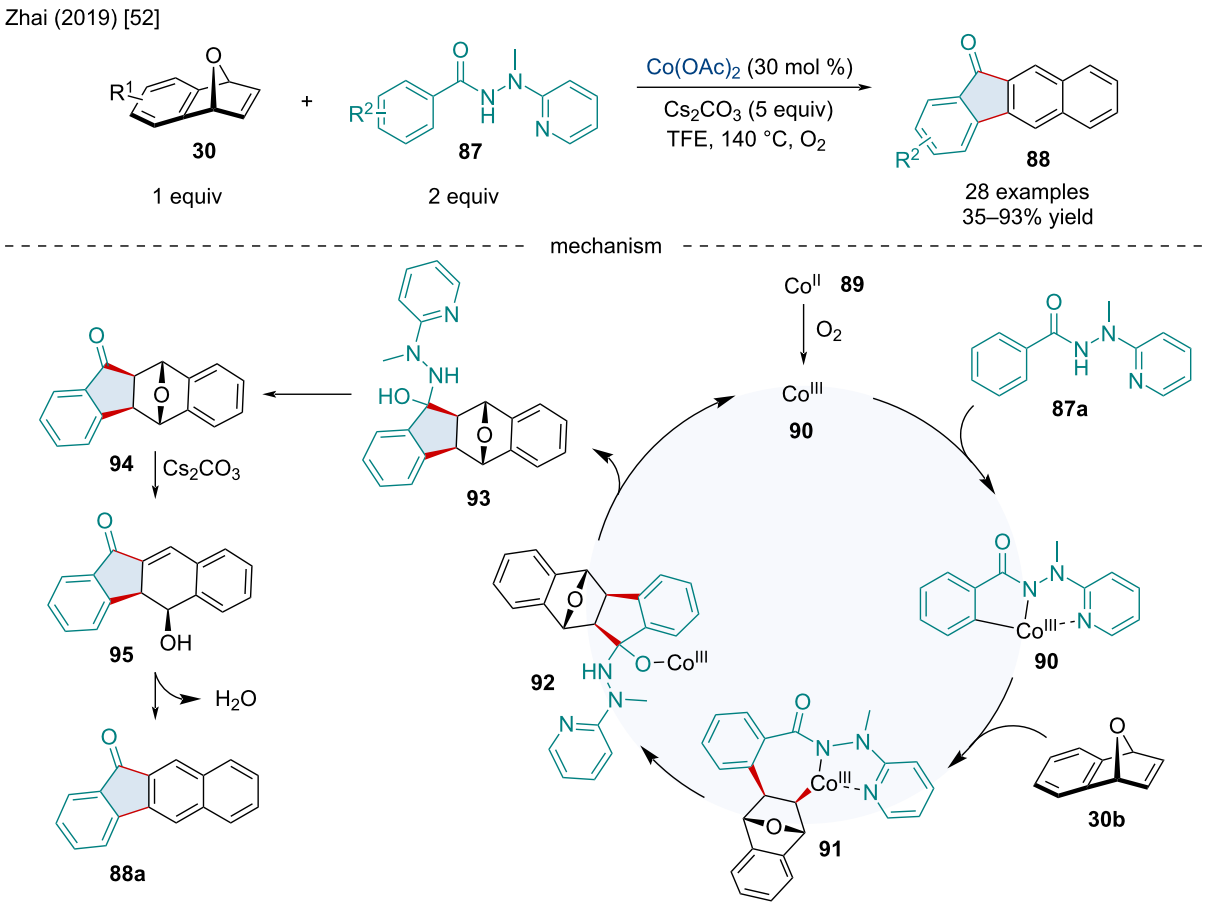

Scheme 16: Co-catalyzed [3 + 2] annulation/ring-opening/dehydration domino reaction of oxabicyclic alkenes **1** with 2-(1-methylhydrazinyl)pyridine (MHP) directed arenes **22**.

of the bridging ether generates **95** which undergoes an elimination reaction to afford the naphthalene product **88a**.

Inspired by Zhao's seminal report on the racemic carboamination of bicyclic alkenes [53], the Cramer laboratory studied the Co-catalyzed enantioselective carboamination of bicyclic alkenes **1** via C–H functionalization in 2021 (Scheme 17) [54]. The authors noted decreasing the steric bulk of the amide moiety of the substrate from isopropyl to ethyl to methyl decreased the enantioselectivity of the reaction. Carbon- and nitrogen-bridging bicyclic alkenes were also identified as competent substrates. In this respect, norbornadiene was found to give the desired carboaminated product in slightly diminished yields while azabicyclic alkenes generated the targeted products in excellent yield, albeit with slightly reduced enantioselectivity. To showcase the synthetic capabilities of this methodology, the authors synthesized the non-natural amino acid derivative **98j** in good diastereoselectivity.

Ruthenium-catalyzed reactions

In 2006, the Tam laboratory investigated the Ru-catalyzed cyclization of oxabenzonorbornene derivatives **30** with propargylic alcohols **99** for the synthesis of isochromenes **100** (Scheme 18) [55]. After coordination of the Ru-center to the *exo* face of **30b**, oxidative cyclization can afford the ruthenacycle **101**. Unlike previous works studying Ru-catalyzed cyclizations involving bicyclic alkenes and alkynes [56-59], the reaction preferentially undergoes β-hydride elimination to generate **102** rather than reductive elimination which would afford the [2 + 2] adduct. Hydroruthenation of the allene produces **103** which can either undergo reductive elimination to afford the cyclopropanated bicyclic alkene or undergo a [2 + 2] cycloreversion to generate the Ru–carbene **104**. The Ru–carbene **104** can rearrange to **100** through a 1,3-migration of the alkoxy group which can finally reductively eliminate the isochromene product. Based on control reactions, the authors proposed the active catalytic species is cationic, as the use of the cationic precatalyst $[Cp^*Ru(CH_3CN)_3]PF_6$ in THF afforded the isochromene as the major product, suggesting a similar cationic species may be generated in MeOH [60].

In 2011, Tenaglia and co-workers investigated the Ru-catalyzed coupling of oxabenzonorbornene derivatives **30** with propargylic alcohols and ethers **106** to access benzonorcaradi-

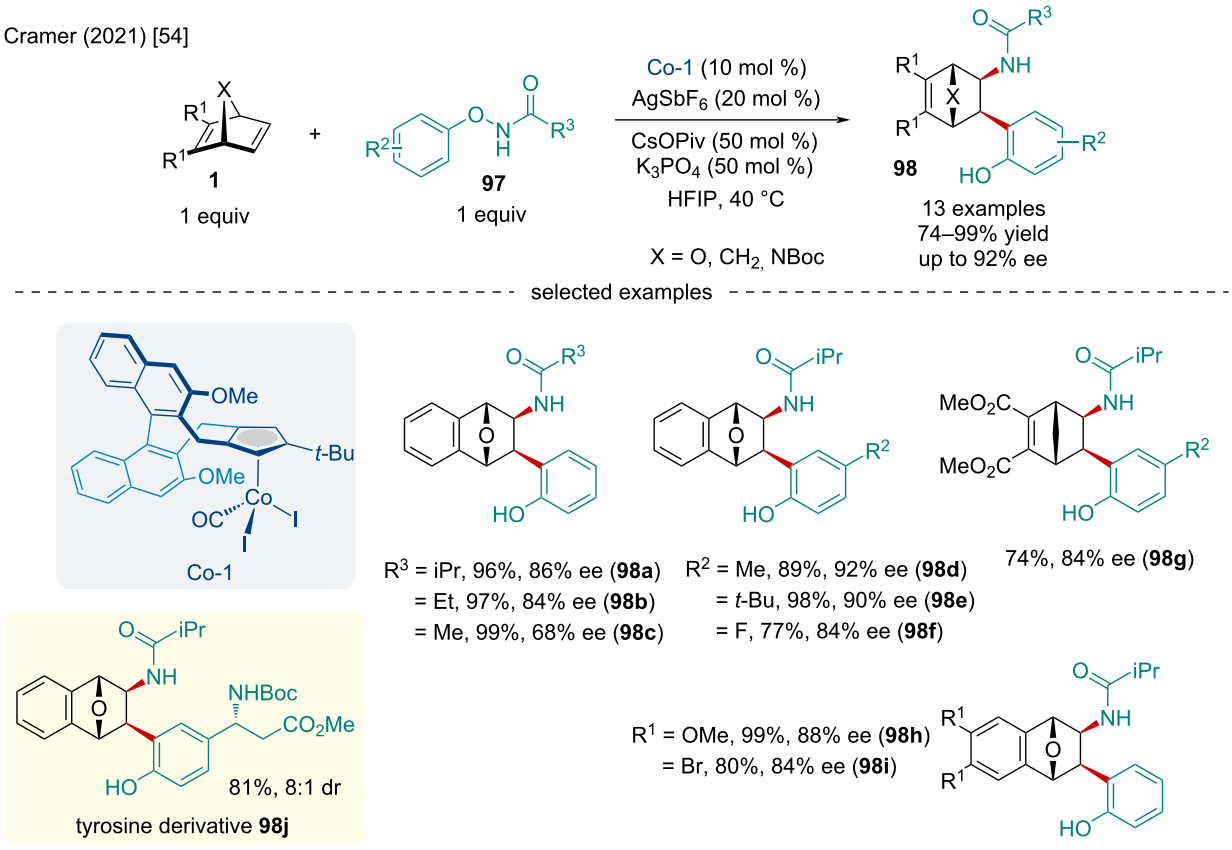

Scheme 17: Co-catalyzed enantioselective carboamination of bicyclic alkenes **1** via C–H functionalization.

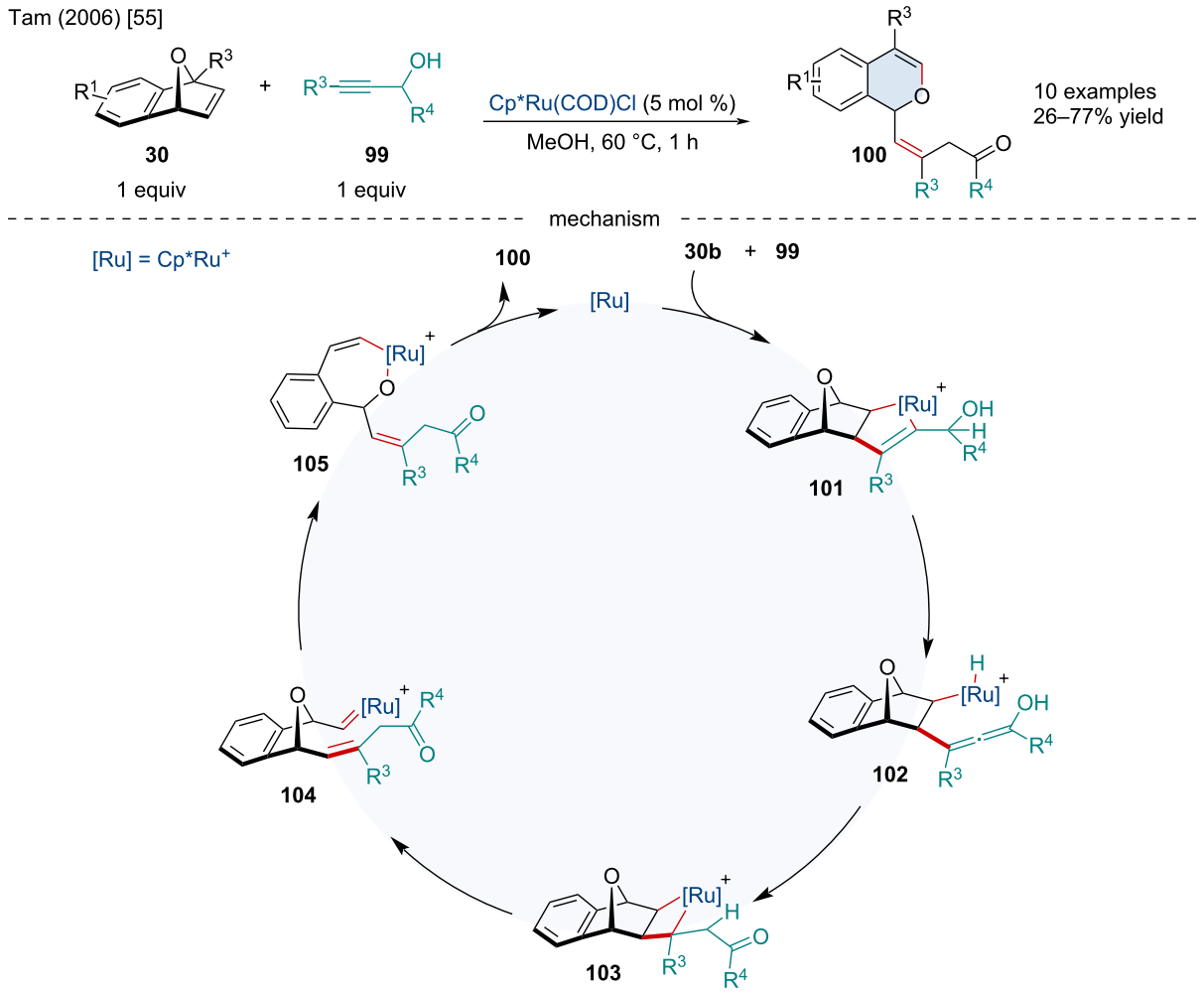

Scheme 18: Ru-catalyzed cyclization of oxabenzonorbornene derivatives with propargylic alcohols for the synthesis of isochromenes.

enes **107** (Scheme 19) [61]. While discriminating between the neutral and cationic active ruthenium species, the authors noted the use of $[Cp^*Ru(CH_3CN)_3]PF_6$ as the precatalyst produced the cyclopropanated bicyclic alkene adducts exclusively. This contrasts with Tam's report (Scheme 18) [55] which found cationic Ru species formed the isochromene **100** preferentially which may be attributed to the solvent playing a more impactful role in the reaction than previously anticipated. Of note, the reaction was amenable to a broad scope of derivatized heterobicyclic alkenes. Electron-deficient bicyclic alkenes were found to react much slower, ultimately affording products in diminished yields. Mono- and disubstituted bridgehead variants were applicable, but with reduced efficacy with the former producing a dihydronaphthofuran **107i** as the major product.

In 2019, the Cramer group continued studying this reaction and developed an enantioselective variant utilizing a chiral Cp* derivative (Scheme 19) [62]. Similar reactivity trends were observed in both accounts. Mechanistically, the transformation was proposed to begin with the coordination of Cp*RuI to the *exo* face of the bicyclic alkene. Oxidative addition into the C–O bond, which is proposed to be the enantiodetermining transition state, followed by coordination to the alkyne generates intermediate **109**. Migratory insertion of the alkyne results in the ruthenacycle **110**. Subsequent reductive elimination generates putative allyl vinyl ether **111** and regenerates the active ruthenium complex**.** The allyl vinyl ether intermediate undergoes a Claisen rearrangement to afford the *endo*-isomer **112**. Thermal isomerization of **113a** by a 6π-electrocyclic ring-opening/closing cascade leads to the to the final *exo*-isomer **107**.

In 2018, the Zhang lab investigated the Ru-catalyzed ring-opening/dehydration of oxabicyclic alkenes **30** via the C–H activation of anilides **114** (Scheme 20) [63]. When the optimized conditions were applied to azabenzonorbornadiene derivatives,

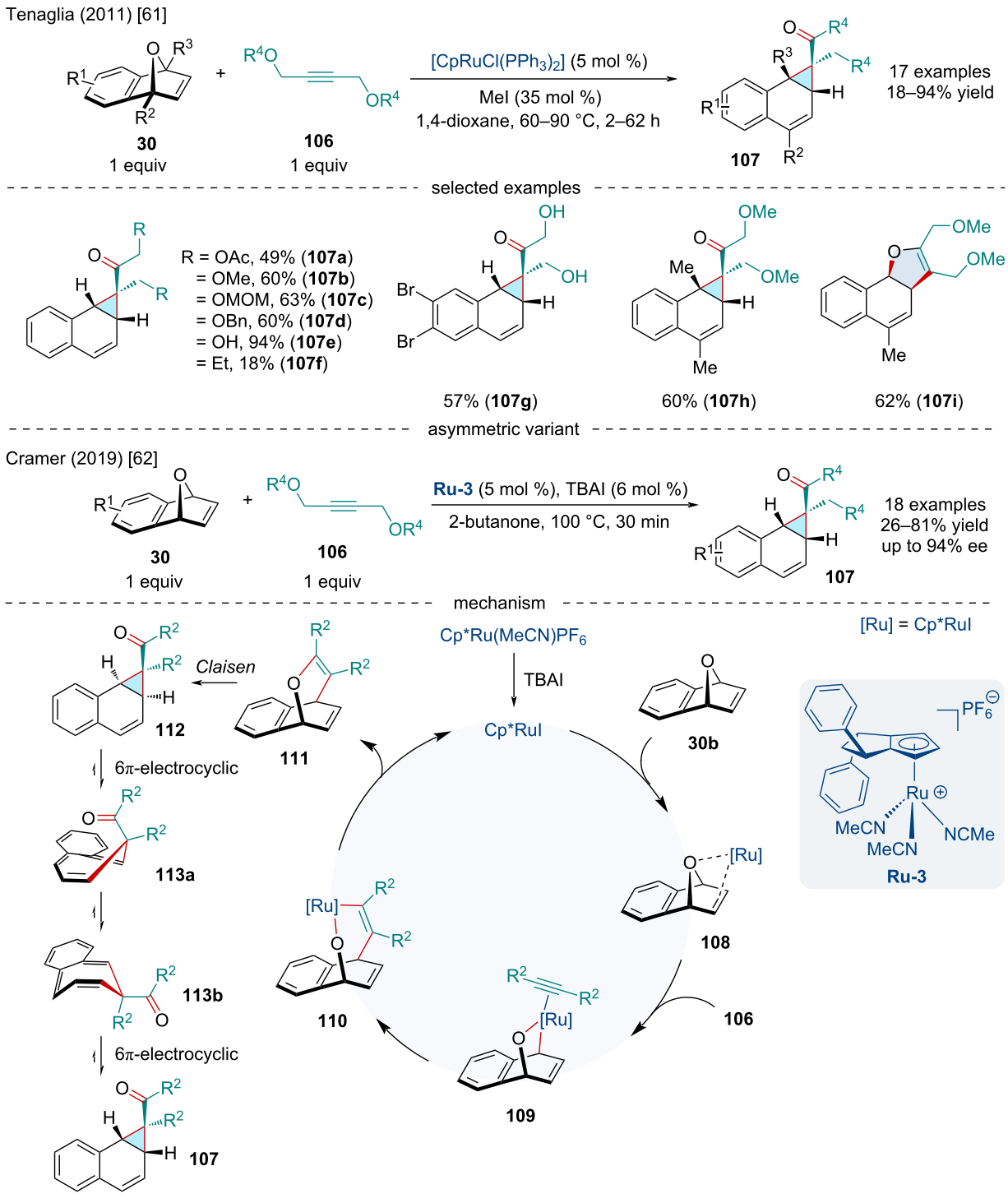

Scheme 19: Ru-catalyzed coupling of oxabenzonorbornene derivatives **30** with propargylic alcohols and ethers **106** to access benzonorcaradienes **107**.

the dehydrative naphthylation sequence did not occur with the reaction being exclusive for *exo*-ring-opened products, similar to that observed in a typical Rh-catalyzed ring-opening reaction (vide infra). The reaction seems to be sensitive to the steric bulk of the amide functionality with *n*-propyl and isopropylamides having diminished yields. While the scope of anilides was quite extensive, electron-deficient substrates resulted in lowered yields.

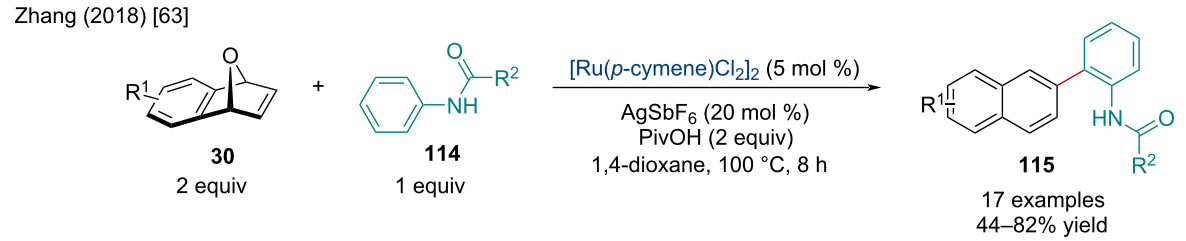

Scheme 20: Ru-catalyzed ring-opening/dehydration of oxabicyclic alkenes via the C–H activation of anilides.

In 2022, the Jeganmohan group investigated the Ru-catalyzed ring-opening/lactamization of azabenzonorbornadiene derivatives **30** with arylamides **116** (Scheme 21) [64]. Weinreb amides outperformed other arylamides, likely serving as a better directing group for the initial aryl-C–H activation. While the scope of functionalized aryl Weinreb amides was quite wide, including different EWGs and EDGs, as well as heterocycles, *ortho*-substitution was not tolerated. The authors applied the methodology for the synthesis of biologically important benzo[*c*]phenanthridine derivatives **117**. Through methylation and subsequent aromatization of the phenanthridinones produced, the authors were able to quickly afford novel fagaronine **117j** and nitidine **117k** derivatives.

Rhodium-catalyzed reactions

In 2002, the Lautens laboratory reported a tandem cyclization of arylboronate esters **118** with a variety of bicyclic alkenes **15** using a water-soluble Rh-catalytic system (Scheme 22) [65]. The authors reported the reaction proceeded smoothly with a limited variety of substituted norbornenes and boronate esters.

In 2004, the same group expanded this Rh-catalyzed cyclization to heterobicyclic alkenes **1** with arylboronate esters **118** for the synthesis of a variety of functionalized indanes **120** (Scheme 22) [66]. This reaction proceeded smoothly with a broad range of [2.2.1] and [3.2.1]-bicyclic alkenes; however, doubly bridgehead-substituted bicyclic alkenes exclusively produced an undesirable demetalated aryl ester byproduct. The authors attributed this to a steric prevention of the attack of the arylrhodium nucleophile to the alkene. Azabicyclic alkenes also proved difficult and failed to react. Mechanistically the authors proposed the arylboronate ester **118** first undergoes a transmetalation with the Rh(I) complex producing **122** which performs an *exo*-carborhodation with the bicyclic substrate to

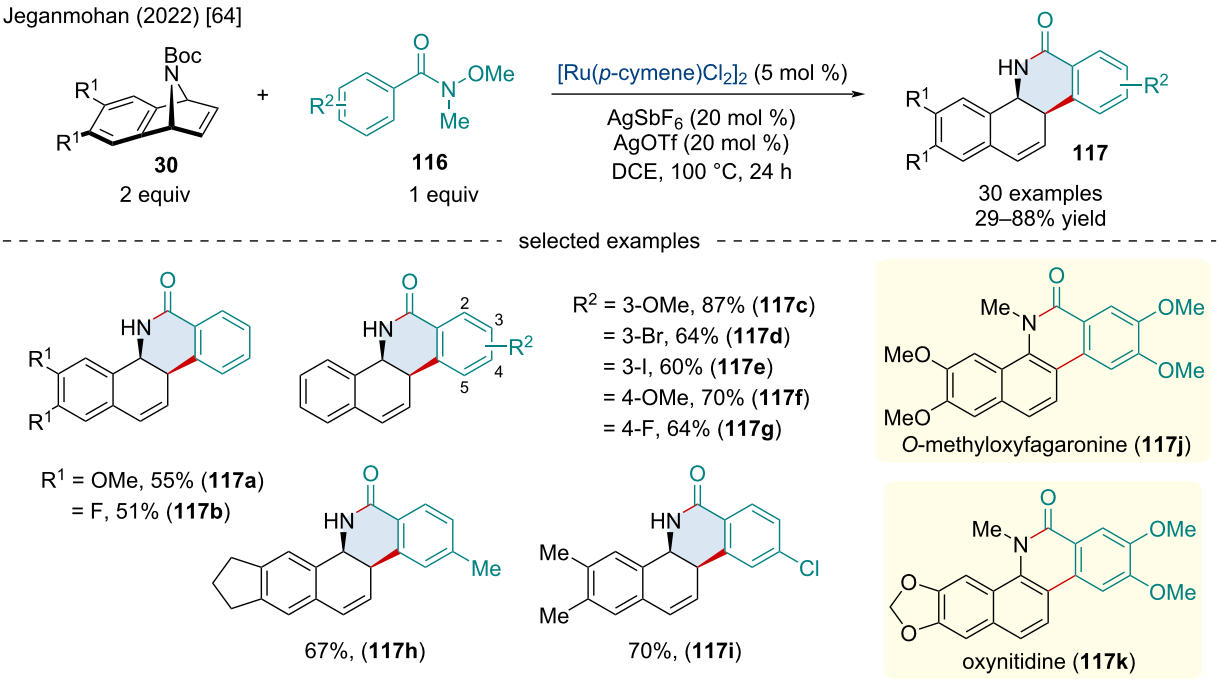

Scheme 21: Ru-catalyzed of azabenzonorbornadiene derivatives with arylamides.

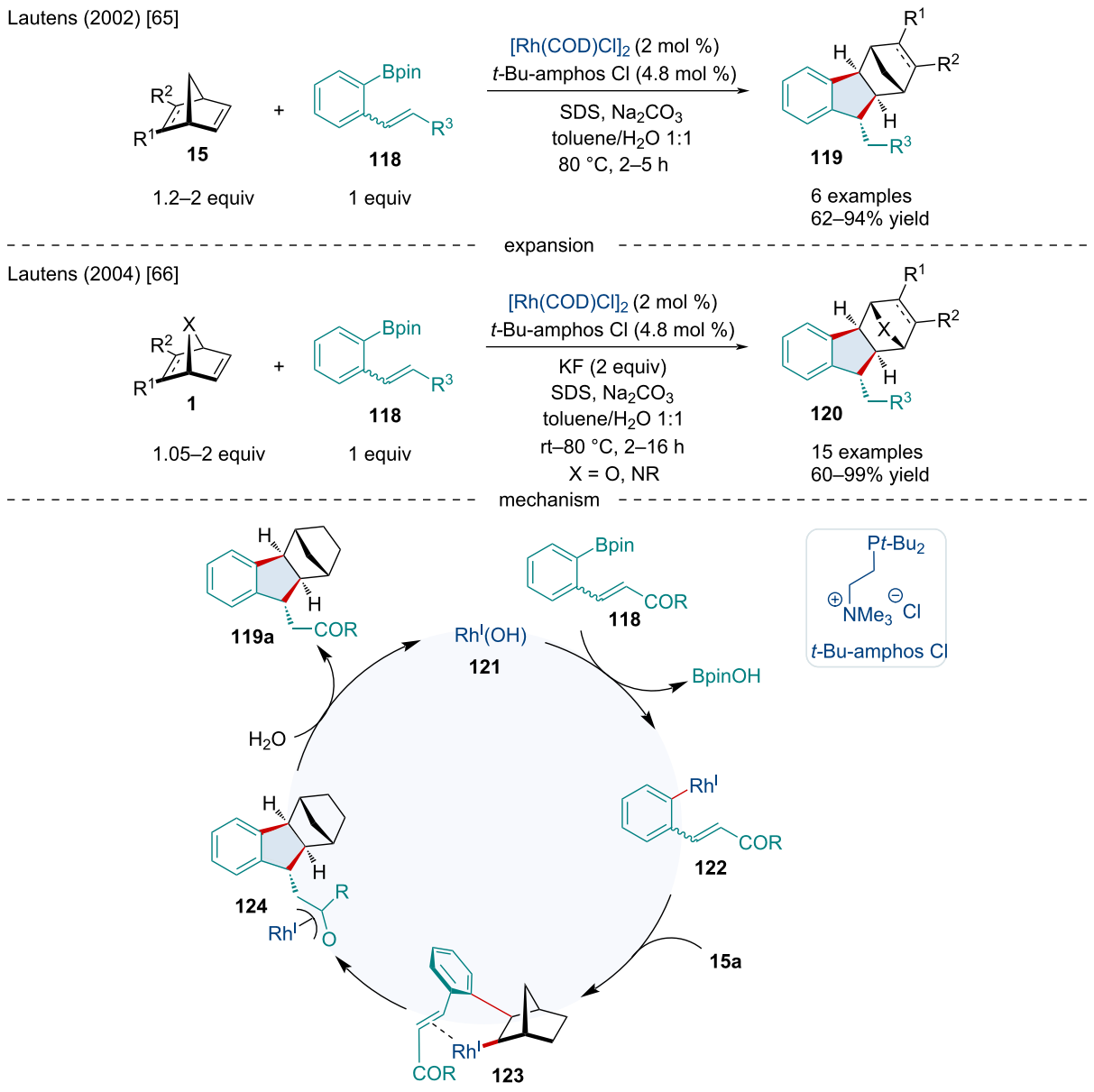

Scheme 22: Rh-catalyzed cyclization of bicyclic alkenes with arylboronate esters **118**.

produce **123**. A 5-*exo-trig* ring closure of **123** produces **124** followed by a rapid protodemetalation with water releasing the final indane product **119a** and regenerating the active Rh(I) species. The authors proposed that the origin of the diastereoselectivity is due to significant steric interactions between the –COR group on the pendant alkene and the bridging group of the bicyclic alkene in **123**.

In 2006, the Lautens lab continued to extend this reaction to include dienylboronate esters **125** and found that an unexpected vinylcyclopropane product **126** was generated (Scheme 23) [67]. Again, nitrogen-containing bicyclic alkenes proved difficult, as diazabicyclic alkenes produced the desired product in low yields while azabenzonorbornadienes failed to react entirely. It was found the introduction of a methyl group α to the boron on the dienylboronate caused the selectivity to be shifted to the 1,4-addition producing a cyclopentene product leading to the conclusion that the substitution pattern on the boronate ester played a significant role in the selectivity between 1,6-addition and 1,4-addition. The mechanism proposed by the authors initially begins in the same manner as Scheme 22 with the transmetalation of the boronate ester with Rh(I) producing **127** which undergoes an *exo*-carborhodation with the bicyclic substrate **15a** producing **128**. The reaction path

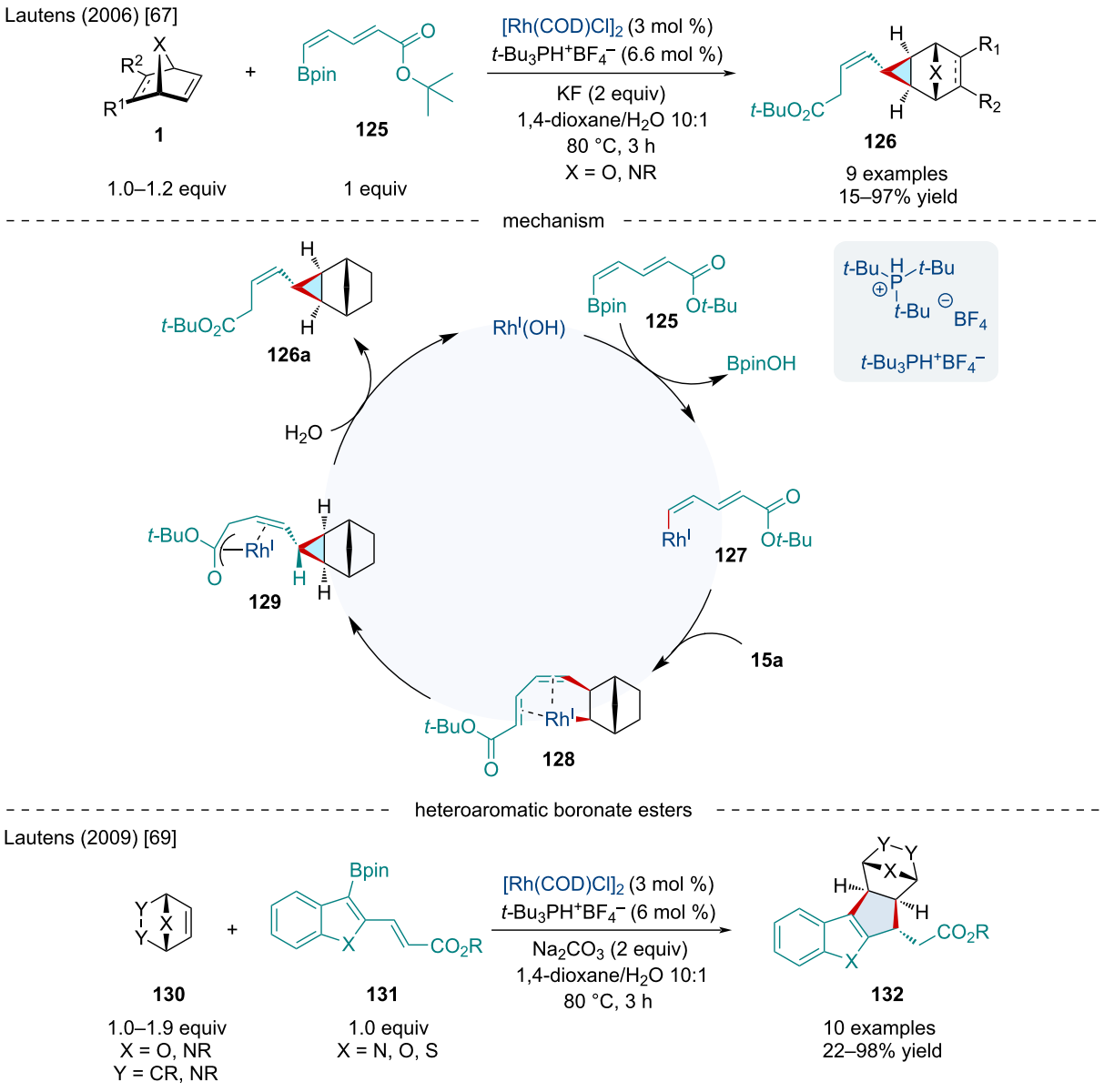

Scheme 23: Rh-catalyzed cyclization of bicyclic alkenes with dienyl- and heteroaromatic boronate esters.

diverges from the previous mechanism undergoing a 1,6-addition resulting in **129**. A rapid protodemetalation with water then occurs releasing the final vinylcyclopropane product **126a** and regenerating the active Rh(I) species. A later 2009 investigation revealed methyl groups α to the ester produced a hydrofunctionalization product [68]. Dienylboronate esters bearing methyl groups β to the ester group produced vinylcyclopropane products **126** while dienylboronate esters bearing methyl groups at the δ or γ position resulted in cyclopentene products.

In 2009, the Lautens lab continued investigating the reactions of bicyclic alkenes **130** with a novel range of heteroaromatic boronate esters **131** (Scheme 23) [69]. This has previously been a challenging transformation due to the propensity of these systems to produce non-cyclized hydroarylation products due to an unproductive rhodium 1,4-migration on heteroaromatic moieties. The use of benzothiophene, benzofurans, and benzopyrrole boronate esters in this investigation prevented this shift as these systems lack the hydrogen to participate in this shift. This reaction proceeded smoothly with a variety of bicyclic alkenes although diazabicyclic alkenes had little to no reactivity. Moreover, benzofuran and benzopyrrole boronate esters resulted in low yields.

In 2011, the Lautens lab reported the Rh-catalyzed domino reaction of doubly bridgehead-substituted oxabicyclic alkenes

134 with secondary amine nucleophiles **135** for the synthesis of bicyclo[2.2.2]lactones **136** (Scheme 24) [70]. This reaction proceeded smoothly with a variety of secondary amine nucleophiles, including those with hydrocarbon, ether, acetal, and ester functionalities; although, aniline nucleophiles only resulted in the one step asymmetric ring-opening (ARO) product under the standard reaction conditions. Fortunately, the authors noted the addition of triethylamine allowed for aniline nucleophiles to undergo the domino reaction, generating the desired bicyclo[2.2.2]lactone **136**. The authors proposed the reaction first takes place through an ARO of the doubly bridgehead-substituted oxabicyclic alkene with the secondary amine nucleophile ultimately producing **137**. The Rh(I) catalyst then facilitates the allylic alcohol isomerization in **137** resulting in the aldehyde **138**. This aldehyde, in close proximity to the tertiary alcohol, leads to the production of the hemiacetal **139** which can finally undergo an oxidation producing the final bicyclo[2.2.2]lactone product **136**.

In 2011, the Radhakrishnan laboratory reported the carboannulation of diazabicyclic alkenes **130a** with 2-cyanophenylboronic acid (**140**) and 2-formylphenylboronic acid (**142**) for the synthesis of indanones **141** (Scheme 25) [71]. This reaction proceeded smoothly with a variety of substituted diazabicyclic alkenes including a variety of ester substituents on the nitrogens and sterically more hindered tricyclic adducts. Mechanistically, the authors proposed the reaction begins with a transmetalation of 2-cyanophenylboronic acid with the Rh(I) species resulting in **143**. Upon association of **143** with the diazabicyclic alkene **132a** a *syn exo*-addition occurs producing **144**. Subsequently, coordination of the Rh(I) to the electrophilic cyano group leads to an intramolecular addition producing **145**. The imine undergoes a hydrolysis releasing the final carboannulated product **141** as well as regeneration of the active Rh(I) catalyst. A similar mechanism can be envisioned for the carbonannulation of diazabicyclic alkenes with 2-formylphenylboronic acid up to the last step which likely operates through a

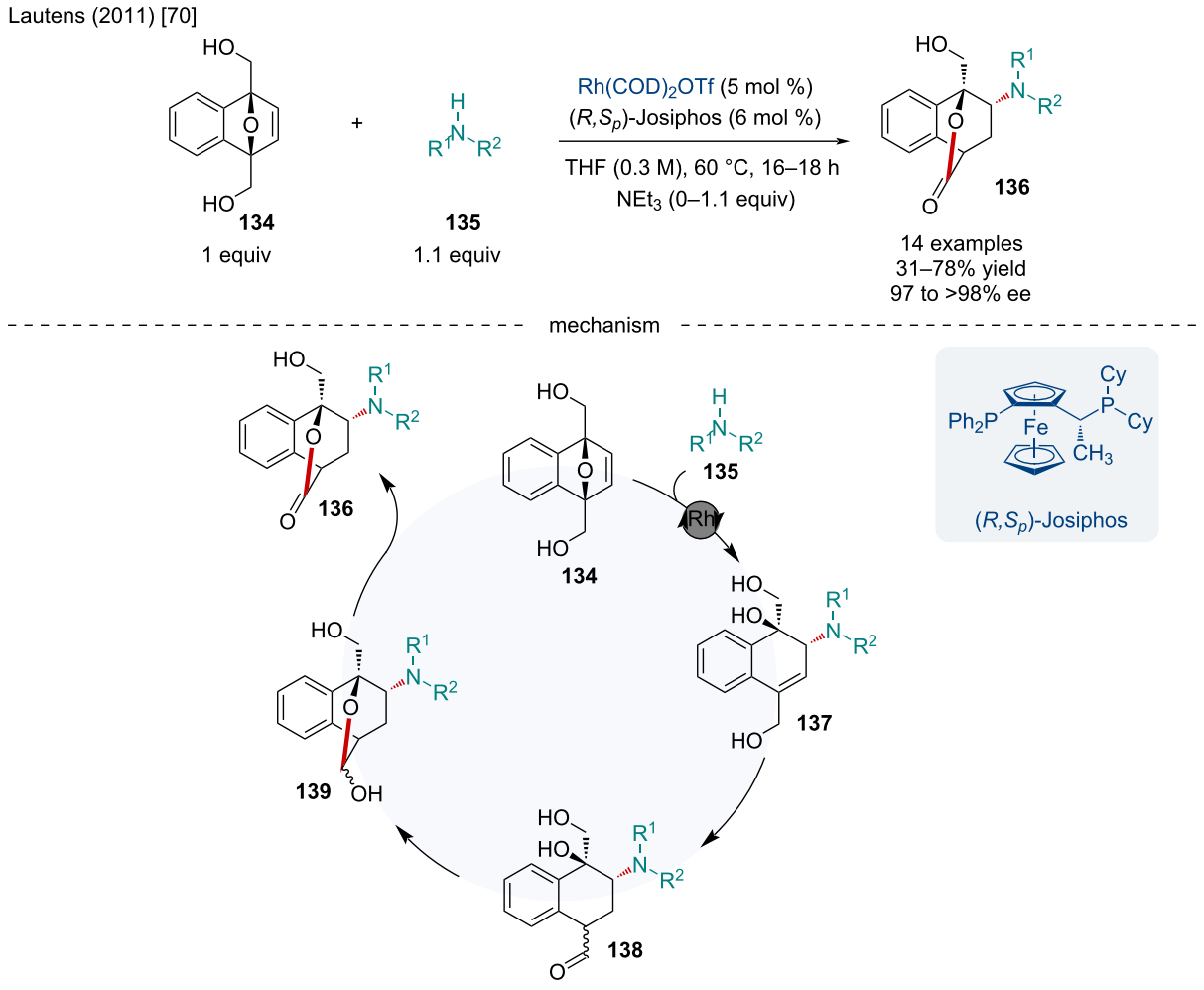

Scheme 24: Rh-catalyzed domino lactonization of doubly bridgehead-substituted oxabicyclic alkenes with secondary amine nucleophiles.

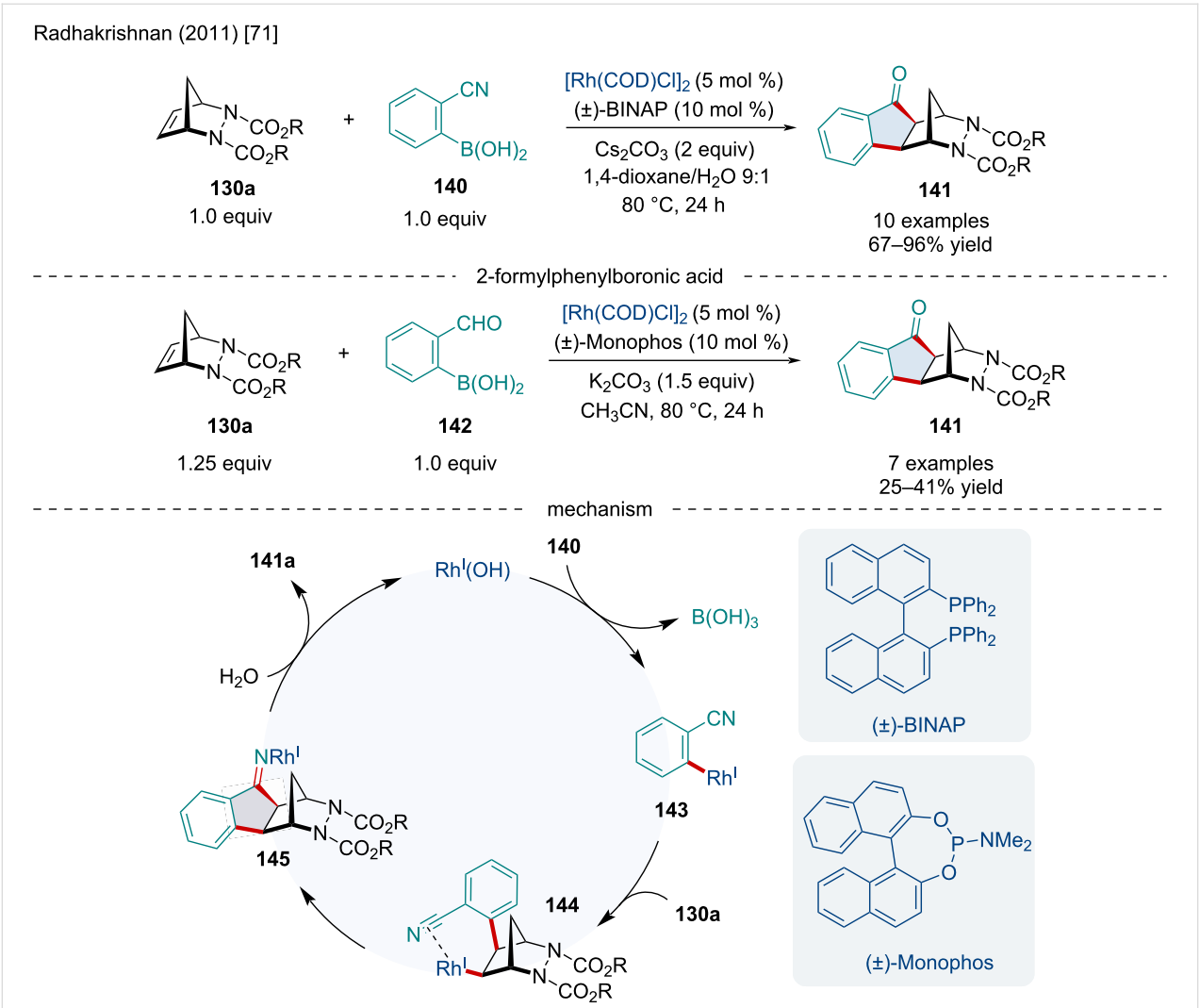

Scheme 25: Rh-catalyzed domino carboannulation of diazabicyclic alkenes with 2-cyanophenylboronic acid and 2-formylphenylboronic acid.

β-hydride elimination of the Rh(I) alkoxide, furnishing the final carbonyl-containing product.

In 2013, Lautens reported the synthesis of oxazolidinone scaffolds **147** through a domino ARO reaction followed by cyclization reaction of oxabicyclic alkenes **30** with sodium cyanate (**146**) (Scheme 26) [72]. This reaction proceeded smoothly with electron-rich oxabenzonorbornadiene derivatives; however, electron-poor oxabenzonorbornadiene derivatives resulted in reduced yield and enantioselectivity. Bridgehead-substituted, non-benzo-fused oxabicycles, as well as azabicyclic alkenes failed to produce the desired product. When the benzo-fused moiety was unsymmetrically substituted, little regioselectivity was observed. Based on X-ray crystallographic data for their final product, and previously reported Rh-catalyzed ARO reactions, the authors hypothesized the reaction begins with the oxidative addition of the Rh(I) catalyst into the bridgehead C–O bond of the oxabenzonorbornadiene producing **148** which is considered the enantiodetermining step. The isocyanate anion then nucleophillically attacks the alkene in an S_N2' fashion producing the *trans*-isocyanate **149**. Subsequently, insertion of the Rh–O bond into the isocyanate results in **150**. Finally, protonolysis produces the oxazolidinone product **147e** as well as regenerates the active Rh(I) catalyst.

In 2013, the Radhakrishnan laboratory reported the Rh-catalyzed oxidative coupling of salicylaldehyde derivatives **151** with diazabicyclic alkenes **130a** producing fused chromanone derivatives **152** (Scheme 27) [73]. It was determined alkyl- and methoxy-substituted salicylaldehydes resulted in a minor reduction of yield while salicylaldehydes with EWGs failed to react. The authors hypothesized the reaction mechanism begins with the association of the Rh(III) catalyst with the hydroxy group of salicylaldehyde (**151a**) resulting in a selective cleavage of the

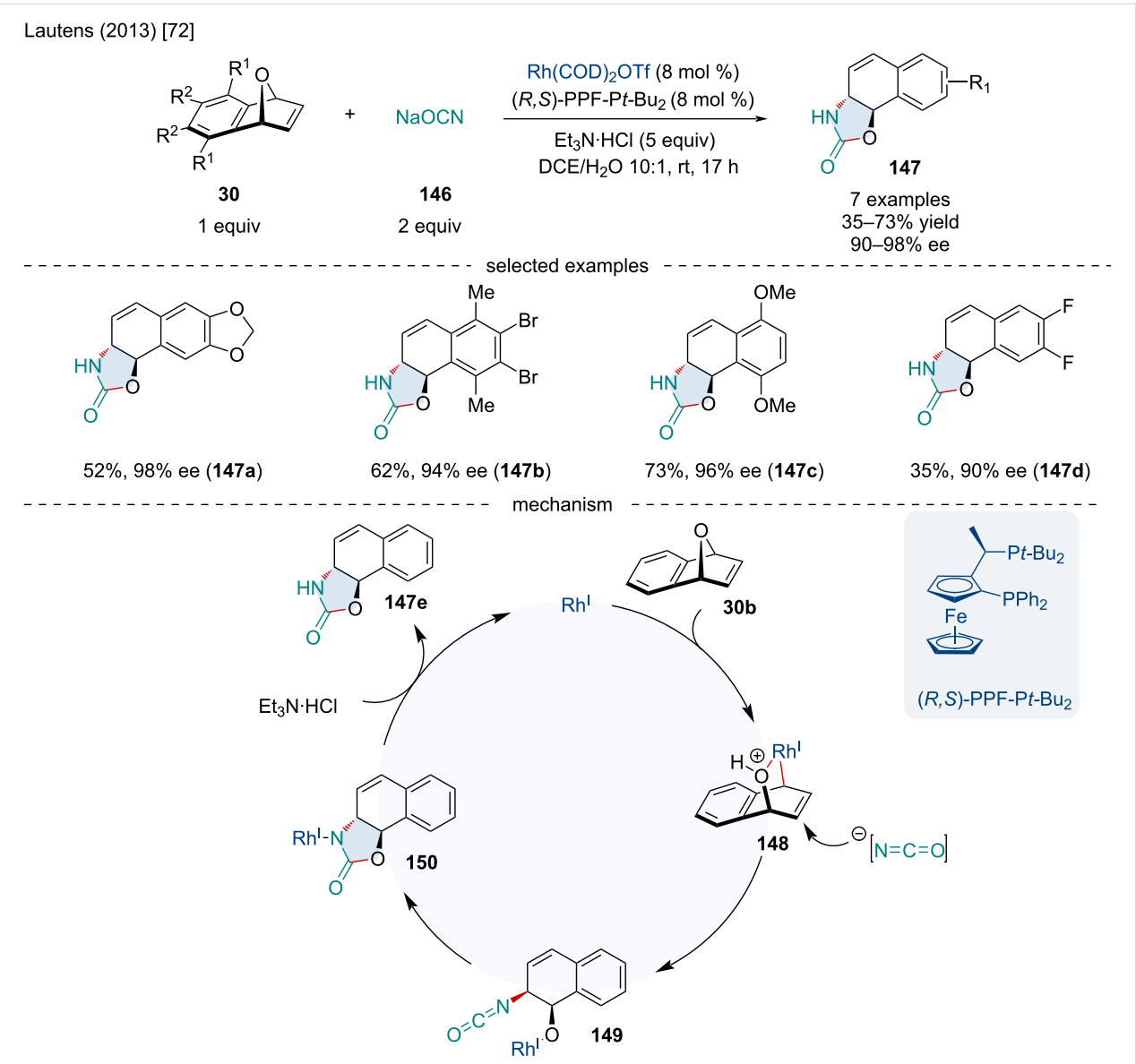

Scheme 26: Rh-catalyzed synthesis of oxazolidinone scaffolds **147** through a domino ARO/cyclization of oxabicyclic alkenes **30** with sodium cyanate (**146**).

aldehyde C–H bond producing the rhodocycle **153** which side-on coordinates with the alkene of the azabicycle producing **154**. A C–N bond cleavage occurs creating π-allylrhodium **155**. Subsequently, the phenol oxygen then adds to the π–allyl species in a *cis* fashion, furnishing **156** which is proposed to be the enantiodetermining step. The carbonyl–rhodium species **156** inserts into the alkene to produce **157**. Following this, β-hydride elimination occurs yielding the final product **152** and a Rh(I) species which is oxidized back to its active Rh(III) state by $Cu(OAc)_2{\cdot}H_2O$.

In 2017, Radhakrishnan reported a Rh-catalyzed annulation of *O*-acetyl ketoximes **159** or *N*-methoxybenzamides **161** with [2.3.1]-bicyclic alkenes **158** for the synthesis of isoquinoline (**160**) or isoquinolone-fused bicycles **162** (Scheme 28) [74]. Compared to their previous C–H functionalization reaction (Scheme 27) [73], no ring opening was observed. This reaction with *O*-acetyl ketoximes was amenable to a variety of *para*-substituents including methoxy and halide groups; however, *O*-acetyl ketoximes with *ortho*- or *meta*-substituents failed to react. A small number of substituted [2.2.1]diazabicyclic alkenes **130a** were successfully employed, albeit with slightly lower yields. In the reaction with *N*-methoxybenzamides **161**, the same substituent trends were seen as that with the reaction with *O*-acetyl ketoximes. Mechanistically, the reaction begins when the Rh(III) catalyst is converted to an active Rh(III)

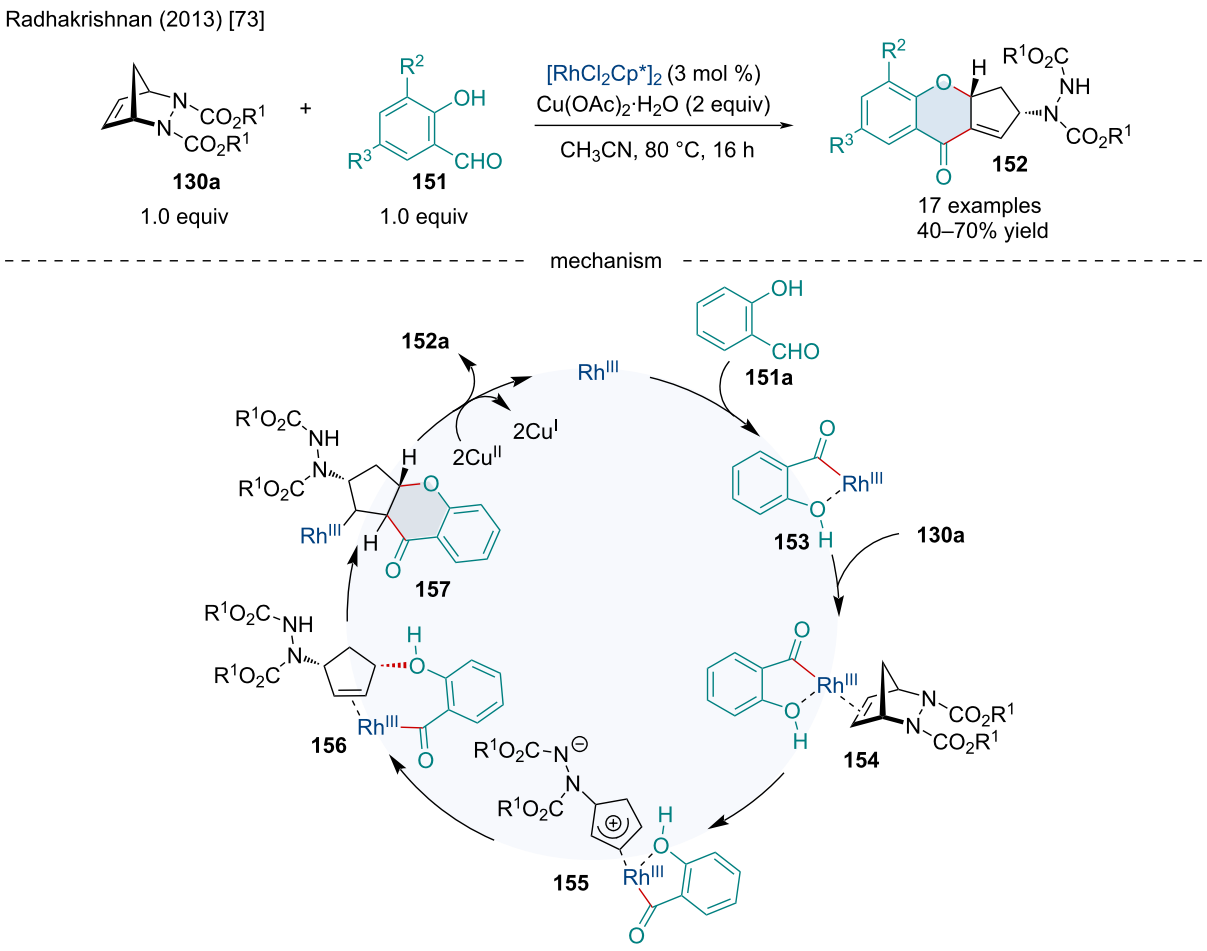

Scheme 27: Rh-catalyzed oxidative coupling of salicylaldehyde derivatives **151** with diazabicyclic alkenes **130a**.

species, by $AgSbF_6$ and $Cu(OAc)_2$, which oxidatively inserts into the *ortho* C–H bond forming **163**. Migratory insertion of the alkene forms **164**. Next, cleavage of the N–O bond followed by an oxidative addition of the Rh(III) to the N–O bond forms intermediate **165** which can finally undergo reductive elimination giving the final product **160a**.

In 2013, Li reported the domino coupling reaction of 2-phenylpyridines **165** with oxa- and azabicyclic alkenes **30** (Scheme 29) [75]. When investigating the reaction with oxabenzonorbornadiene (**30b**), the resulting product was found to exclusively be the dehydrated 2-naphthalene derivative **166**. It was found that the addition of pivalic acid greatly improved the yield, likely due to its facilitation of C–H activation as well as its involvement in the dehydration process. This reaction proceeded smoothly with a variety of both EWGs and EDGs on the 2-phenylpyridine. Interestingly, when swapping the pyridine directing group for thiophene or furan, yields were improved although quinolinyl and pyrimidyl directing groups, despite reacting, resulted in a mixture of mono- and diarylation products. When investigating substituted oxabenzonorbornadienes both mono- and diarylated products were formed with only moderate yield. When azabenzonorbornadienes **30** were investigated in the same redox-neutral conditions no reaction occurred; however, upon the addition of AgOAc a *cis*-fused dihydrocarbazole product was formed (Scheme 29). Mechanistically this reaction was proposed to proceed through first a conversion of the Rh(III) catalyst to the active Rh(III) species by $AgSbF_6$. This active Rh(III) catalyzes the cleavage of the *ortho*-C–H bond of 2-phenylpyridine furnishing **168**. This is followed by the *cis* addition of **168** to the oxabenzonorbornadiene producing **169** whereby subsequent β-oxygen elimination affords **170**, followed by protonolysis producing **171** and regenerating the active Rh(III) species. Finally, a dehydration occurs furnishing the final product **166**. In terms of the azabicyclic substrates, following the β-eliminated heteroatom, a second round of C–H activation/reductive elimination occurs to generate the annulated product **167**.

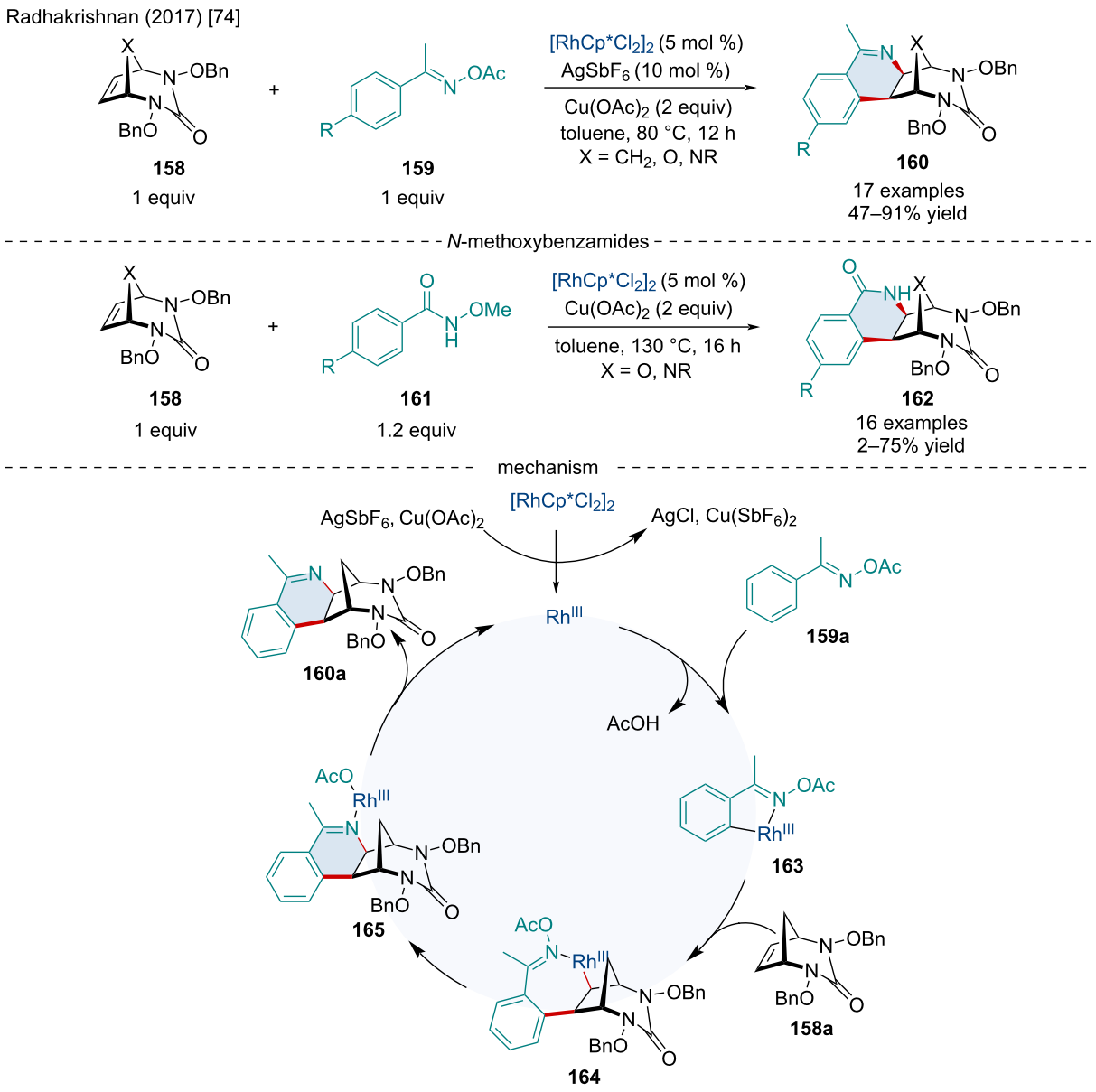

Scheme 28: Rh-catalyzed reaction of *O*-acetyl ketoximes with bicyclic alkenes for the synthesis of isoquinoline-fused bicycles.

In 2014, Chen and Li reported the Rh-catalyzed domino dehydrative naphthylation of oxabenzonorbornadienes **30** with *N*-sulfonyl 2-aminobenzaldehydes **172** (Scheme 30) [76]. This reaction was amenable to a variety of EDG, EWG, as well as a broad scope of sulfonyl groups. Surprisingly, this reaction also proceeded smoothly with nitro substituents on the benzene ring which are typically problematic in C–H activation reactions. Through mechanistic studies, the authors proposed the rate limiting step for this reaction is the C–H cleavage.

In 2015, Miura and co-workers reported the Rh-catalyzed domino dehydrative naphthylation of oxabenzonorbornadienes **30** with arylphosphine derivatives **174** (Scheme 31) [77]. The reaction was amenable to a wide range of substituted arylphosphine derivatives. Moreover, the reaction could be extended to include various phosphinate, phosphonate, and phosphonamide derivatives. The use of triarylphosphine oxides required the reaction to be performed at a 2:1 ratio with oxabenzonorbornadienes **30** to prevent multiarylated products from being formed. Arylphosphine sulfides were also investigated but gave unimpressive yields (8%); however, upon a substitution of the AgOAc for 3 equiv of AcOH moderate yields were obtained (39%). Mechanistically, this reaction likely operates in a similar manner to the previously discussed C–H activation/dehydration domino reactions.

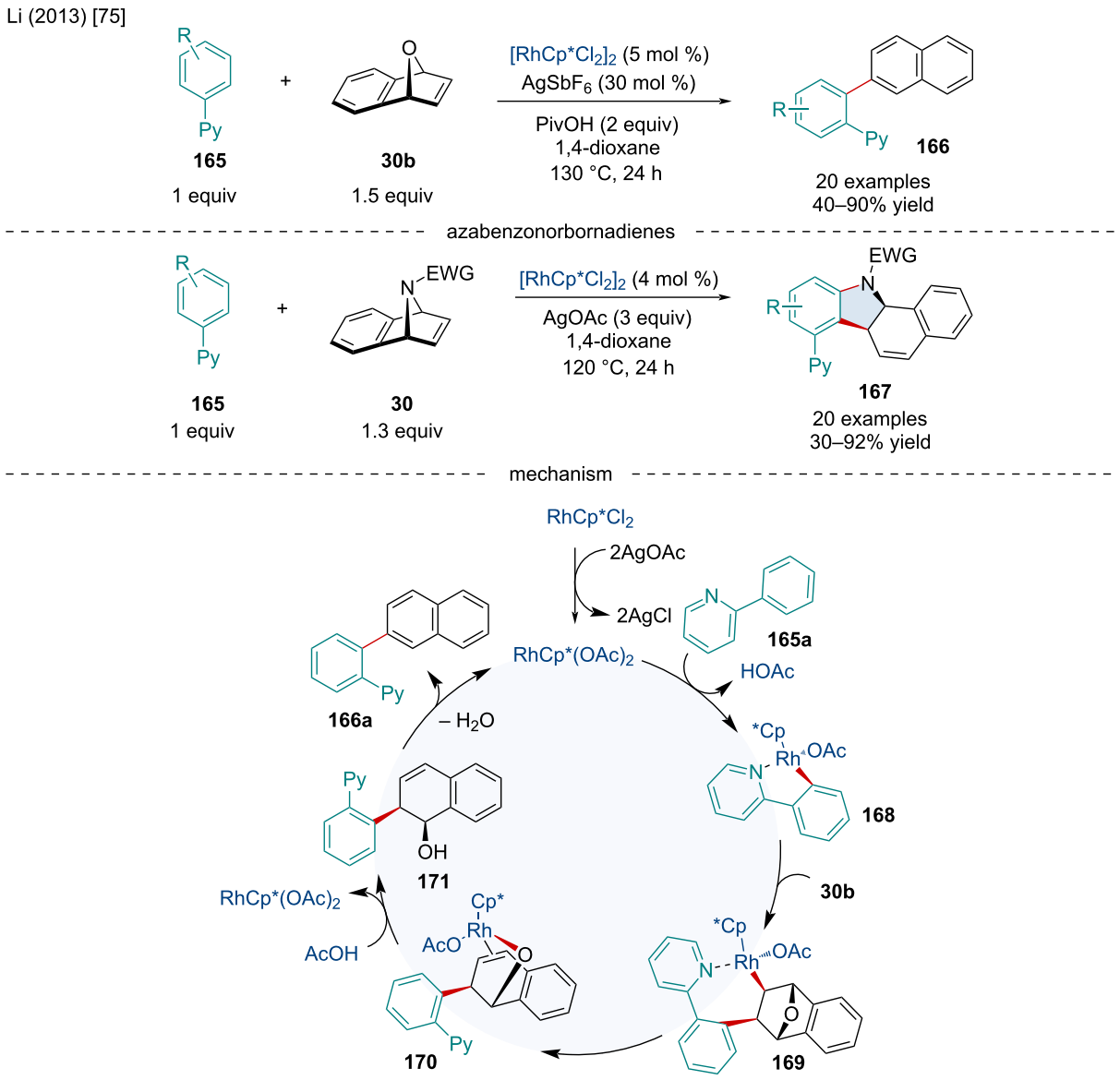

Scheme 29: Rh-catalyzed domino coupling reaction of 2-phenylpyridines **165** with oxa- and azabicyclic alkenes **30**.

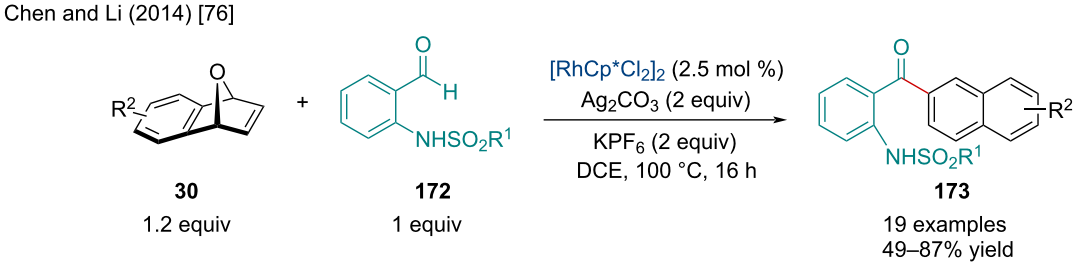

Scheme 30: Rh-catalyzed domino dehydrative naphthylation of oxabenzonorbornadienes **30** with *N*-sulfonyl 2-aminobenzaldehydes **172**.

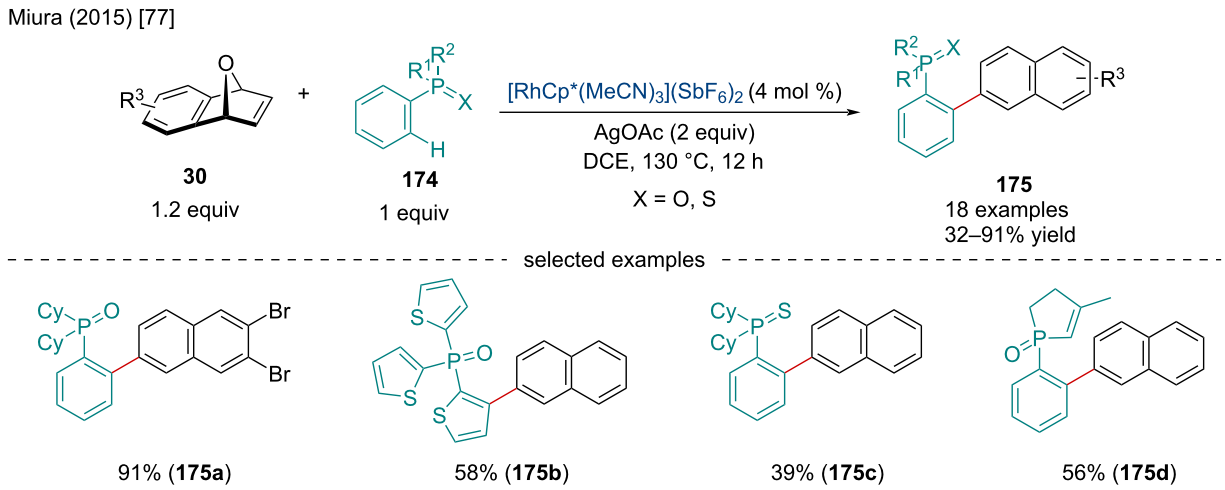

Scheme 31: Rh-catalyzed domino dehydrative naphthylation of oxabenzonorbornadienes **30** with arylphosphine derivatives **174**.

In 2020, a similar method for the construction of 2-aryl-substituted naphthalene cores was discussed by Wang and co-workers who disclosed a Rh-catalyzed C–H bond naphthylation of anilides and benzamides with azabenzonorbornadienes [78]. Interestingly, the dehydration step occurred smoothly with an aza-leaving group rather than the more common oxa-leaving group discussed above.

In 2013, the Radhakrishnan laboratory reported the Rh-catalyzed domino ring-opening coupling reaction of azaspirotricyclic alkenes **176** using arylboronic acids **177** (Scheme 32) [79]. This reaction proceeded well with a variety of ester substituents on the nitrogens of the azaspirotricyclic alkenes. The authors proposed this reaction proceeds first through a transmetalation of the arylboronic acid **177a** with the Rh(I) catalyst producing **179** which undergoes a *cis* addition to the azaspirotricyclic alkene resulting in intermediate **180**. C–H cleavage at the *ortho*-position followed by an intramolecular reductive elimination affords in **182**. Unlike previous reports [80], this arylrhodium complex has a long enough lifetime to propagate further. A subsequent migratory insertion into a second azaspirotricyclic alkene furnishes **183**. Finally, the anion from the catalyst attacks **183** causing a ring opening, forming the final product **178d** and regenerating the Rh(I) catalyst. Keeping with other mechanisms, the Rh(I) may also undergo an *anti*-β-nitrogen elimination to furnish the ring-opened intermediate [80].

In 2016, Liu reported the Rh(III)/Sc(III)-catalyzed domino reaction of oxabenzonorbornadienes **30** with alkynols **184** directed by a transient hemiketal group (Scheme 33) [81]. The use of a transient directing group avoids the tedious process of installation and then removal of directing groups which is a common issue. A variety of substituents were tolerated on both the alkynols **184** and oxabenzonorbornadienes **30**; however, substituted oxabenzonorbornadiene derivatives typically had diminished reactivity. Expansion of the bicyclic scope was limited as other bicycles such as norbornene failed to react. The authors propose the catalytic cycle begins with the Rh(III)-catalyzed hydration of the alkynol to produce **186** followed by a Sc(III)-catalyzed addition to form the transient hemiketal **187**. *Ortho*-C–H activation generates **188** which can undergo migratory insertion with the Sc(III)-coordinated oxabicyclic alkene **189** to form **190**. β-Oxygen elimination, likely assisted by the Sc(III) Lewis acid, produces **191** which subsequently undergoes a protonolysis forming **192** and regenerating the Rh(III) and Sc(III) catalysts. Next, **192** is dehydrated producing **193** which finally undergoes a Prins-type cyclization to afford the final product **185**.

In 2018, the Fan laboratory reported the Rh-catalyzed asymmetric cyclization/addition domino reaction of 1,6-enynes **194** with oxa/azabenzonorbornadienes **30** (Scheme 34) [82]. Both oxa- and azabenzonorbornadienes **30** worked well; however, the authors noted the latter produced better enantioselectivities while sterically bulky substituents led to both reduced yield and enantioselectivities. The authors proposed the reaction mechanistically occurs though the coordination and reaction of the Rh(I) species with the 1,6-enyne **194a** producing **196** which undergoes an oxidative cyclization leading to **197**. Subsequent β-hydride elimination forms **198** which side-on coordinates with azabenzonorbornadiene **30c** forming **199**. Migratory insertion of the olefin followed by reductive elimination of the hydride affords the final product **195a**.

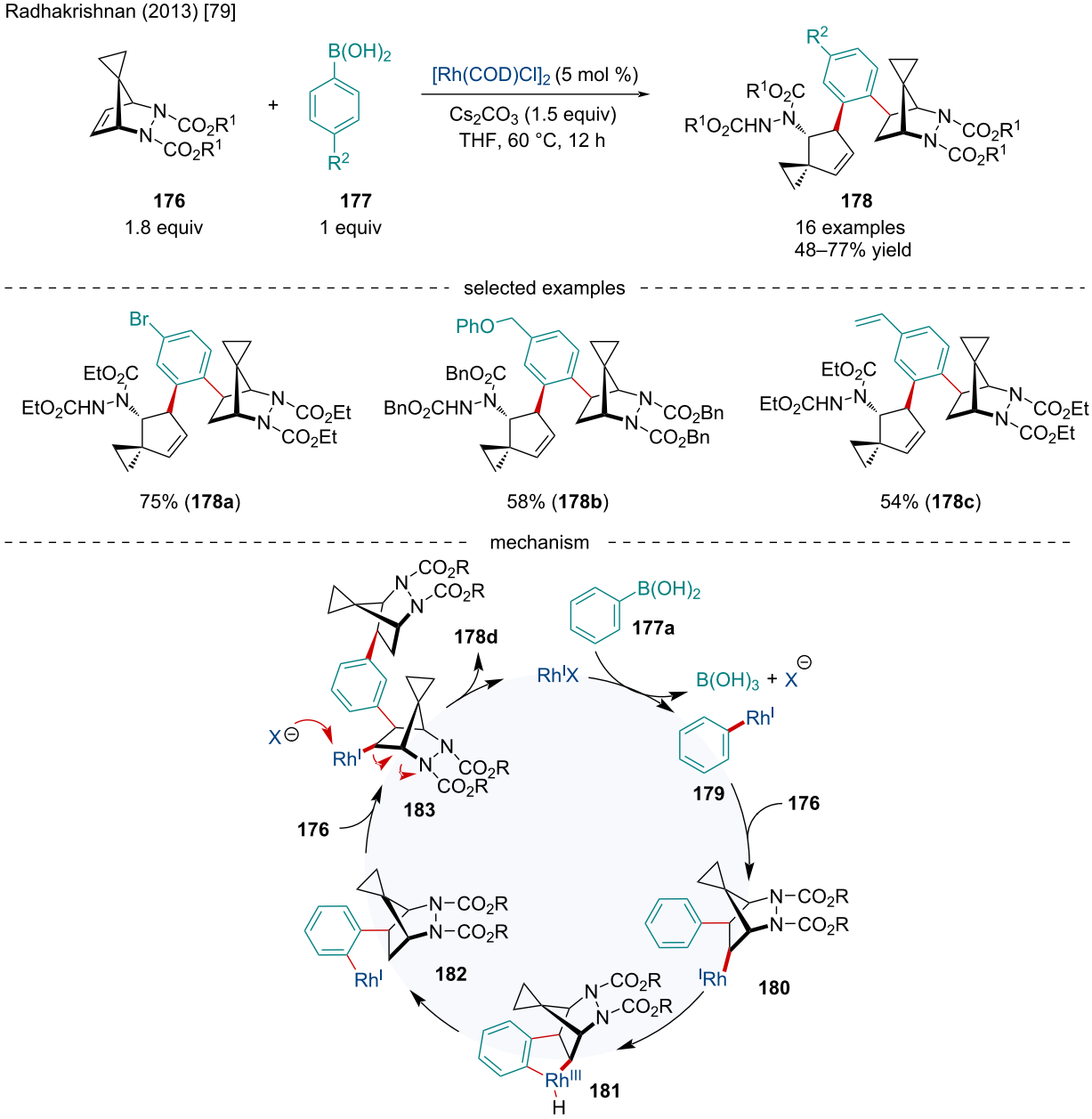

Scheme 32: Rh-catalyzed domino ring-opening coupling reaction of azaspirotricyclic alkenes using arylboronic acids.

In 2019, the Shao group reported the Rh/Zn-catalyzed domino ARO/cyclization of oxabenzonorbornadienes **30** with phosphorus ylides **201** (Scheme 35) [83]. Despite the difficulty of using phosphorus ylides as nucleophiles in metal-catalyzed reactions due to their ability to strongly bind transition metals, this reaction proceeded smoothly with a broad range of ester-, ketone-, and amide-stabilized phosphorus ylides. Oxabenzonorbornadienes bearing both EWG and EDG substituents worked well including bridgehead-substituted substrates which only experienced a slight reduction in yield. Similar to other ARO reactions, the catalytic cycle is proposed to begin with the oxidative insertion of the Rh(I) catalyst into the bridgehead C–O bond producing **204**. The phosphorus ylide attacks **204** in an S_N2' fashion on the *endo* face giving the ring-opened **205** as well as regenerating the Rh(I) catalyst after dissociation. Alternatively, **205** can undergo a ring closure followed by a subsequent C–P-bond cleavage causing a ring opening resulting in **207**. Intramolecular S_N2' and elimination of the phosphine oxide generates the final product **202e** which the authors propose is stereoselective due to significant steric interactions between the carbonyl and aryl groups. The authors proposed that the $Zn(OTf)_2$ Lewis acid cocatalyst may activate the

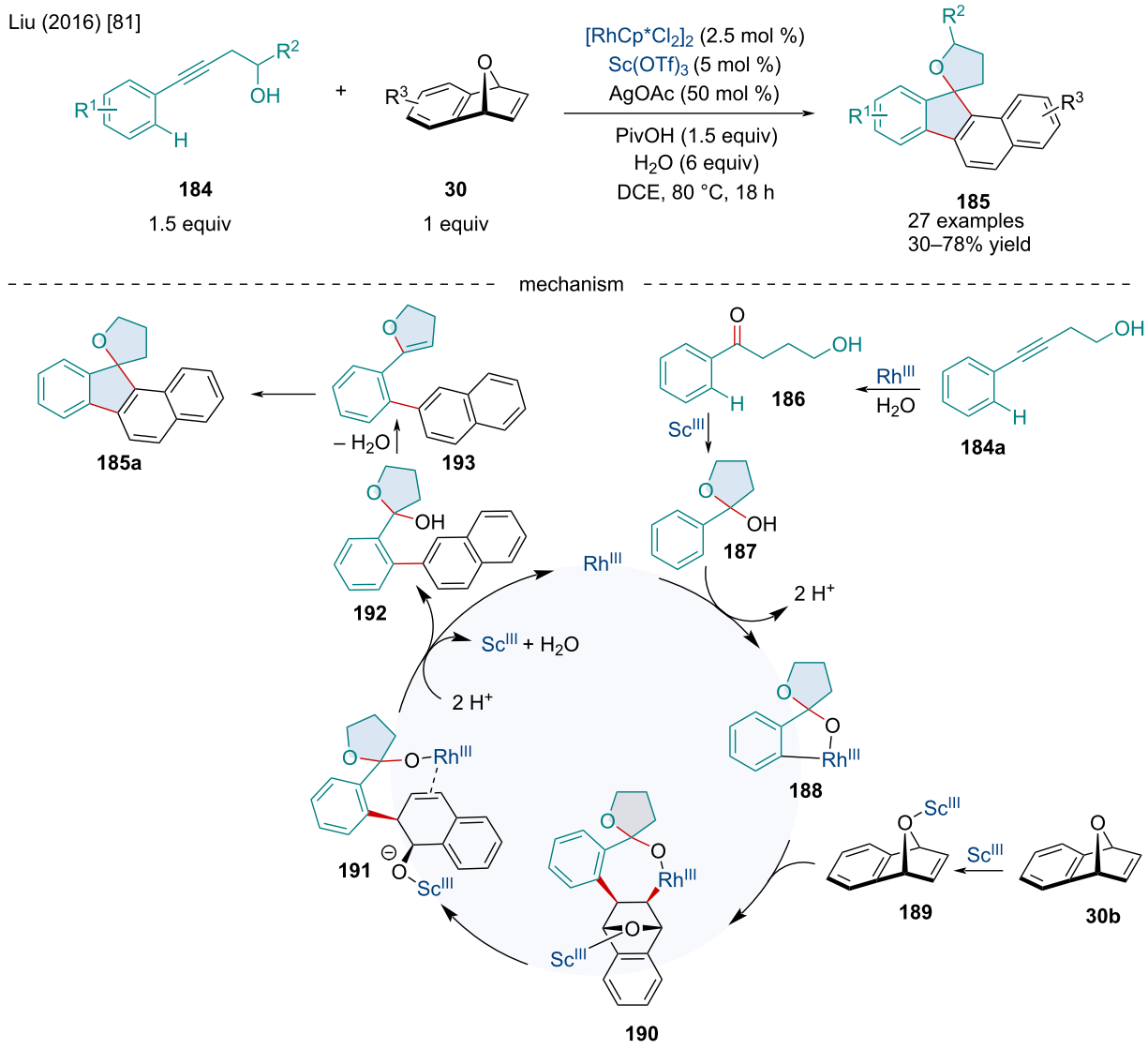

Scheme 33: Tandem Rh(III)/Sc(III)-catalyzed domino reaction of oxabenzonorbornadienes **30** with alkynols **184** directed by a transient hemiketal group.

bridging oxygen of the oxabenzonorbornadiene lowering the kinetic barrier of C–O oxidative addition.

In 2019, Lautens reported the Rh-catalyzed domino ring opening/lactonization of oxabenzonorbornadienes **30** with nosyl-protected amino acid-derived nucleophiles **208** (Scheme 36) [84]. This reaction proceeded smoothly with a range of amino acid derivatives; however, the authors noted that increased steric bulk of the nucleophiles reduced the yields which they attributed to the lactonization being disfavored on steric grounds. In contrast to other ARO reactions, substituents on the oxabicycles were not tolerated well and only two derivatized substrates successfully reacted with greatly diminished yields. Moreover, amino acid derivatives without α-substituents failed to react, leading the authors to conclude that α-substitution is required to make lactonization kinetically feasible.

In 2019, the Punniyamurthy lab reported the Rh-catalyzed domino C–C/C–N bond formation of azabenzonorbornadienes **30** with aryl-2*H*-indazoles **210** (Scheme 37) [85]. This reaction was amenable to both EWGs and EDGs; however, it was noted that an azabenzonorbornadiene bearing a pyridine-2-sulfonyl protecting group only produced a trace amount of product which was attributed by the authors to an unproductive chelation of the Rh(III) by the pyridine nitrogen. Furthermore, aryl-2*H*-indazoles with *para*-substituents failed to react which the authors attributed to both electronic and steric effects.

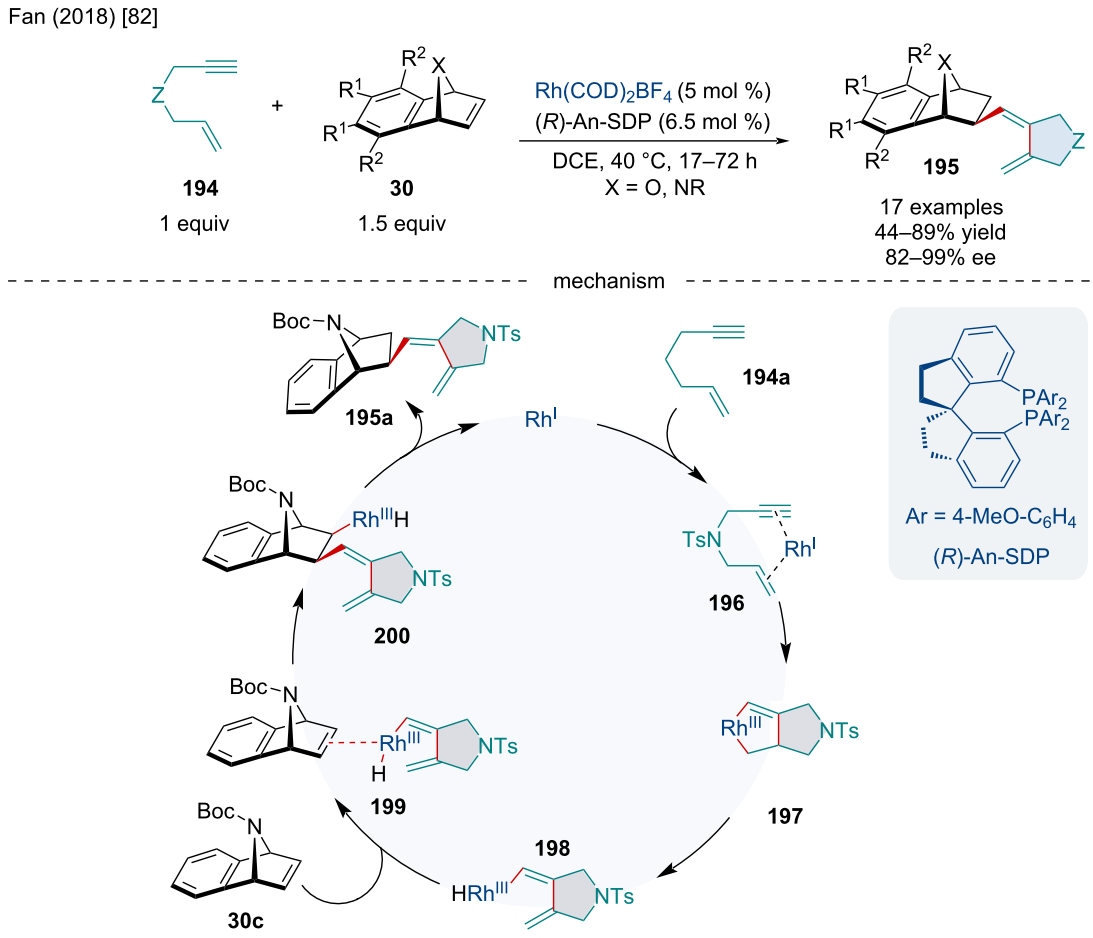

Scheme 34: Rh-catalyzed asymmetric domino cyclization and addition reaction of 1,6-enynes **194** and oxa/azabenzonorbornadienes **30**.

In 2020, Bian and Wang reported the Rh/Pd-catalyzed domino reaction of indole derivatives with 2-(phenylethynyl)anilines **212** and oxabenzonorbornadienes **30** (Scheme 38) [86]. In this reaction, both EWG and EDG substitutions were tolerated; although, the authors noted the latter reduced the yield and enantioselectivity of the final product. These indole derivatives are widely present in many nonsteroidal anti-inflammatory drugs such as indomethacin. The indole derivatives synthesized were subjected to virtual screenings for their anti-inflammatory properties and three of them (**213a**, **213b**, and **213c**) showed better results than indomethacin. Mechanistically, this transformation proceeds initially through a Rh-catalyzed ARO via the aromatic amine nucleophile followed by an Pd-catalyzed cyclization.

In 2021, He and Tian reported the Rh-catalyzed domino 1,2-carborhodation of heterobicyclic alkenes **30** with B_2pin_2 (**53**) (Scheme 39) [87]. EDGs and EWGs were well tolerated on the benzo-fused moiety; however, bridgehead substituents shutdown the reaction. Carbocyclic alkenes, like benzonorbornadiene, failed to produce the desired product leading the authors to conclude the bridging heteroatom of oxa- and azabenzonorbornadiene played a vital role in the carboboration reaction.

In 2021, Ellman reported a Rh(III)-catalyzed three-component 1,2-carboamidation reaction of bicyclic alkenes **30** with aromatic and heteroaromatic C–H substrates **215** and dioxazolones **216** (Scheme 40) [88]. This reaction was successful with a wide range of directing groups and substituents on the heteroaromatic C–H substrate and a broad range of bicyclic alkenes. Bicyclic diene derivatives like norbornadiene failed to react, likely due to non-productive complexation to the catalyst. Using a chiral cyclopentadiene ligand, the authors showcased an asymmetric variant of the reaction producing 5 enantioenriched products with an average enantiomeric excess of 80% ee. The authors proposed the reaction begins with a concerted metalation–deprotonation of the aromatic C–H substrate **215a** with the Rh(III) catalyst yielding **218**. Migratory insertion of the olefin of **15a** to **218** produces **219**. Subsequently, nitrene insertion of the dioxazolone **216a** to **219** furnishes **220**, which after protodemetalation yields the final product **217e**.

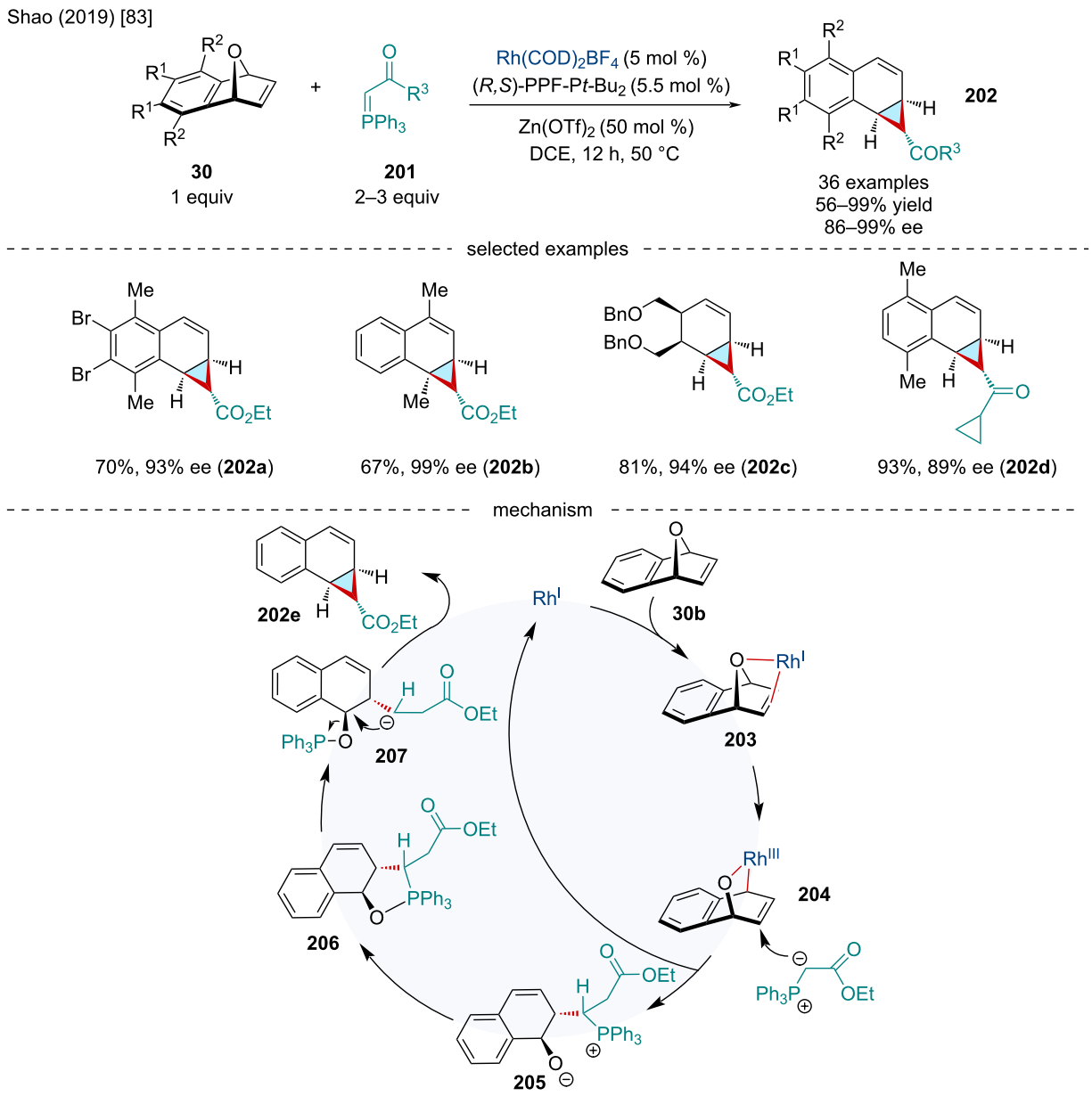

Scheme 35: Rh/Zn-catalyzed domino ARO/cyclization of oxabenzonorbornadienes **30** with phosphorus ylides **201**.

Palladium-catalyzed reactions

In 1998, Kosugi and co-workers explored the Pd-catalyzed diarylation and dialkenylation reactions of norbornene derivatives **8** (Scheme 41) [89]. The authors noted the use of chloroacetone was crucial to the reaction as it acted as an exogenous oxidant. Although not perfect, alkenyl stereochemistry was retained for the majority of examples. In the case of (*Z*)-tributylstannylacrylate, the exclusive product was the *exo-cis*-(*E*,*Z*)-difunctionalized product. Albeit low yielding, heterobicyclic alkenes were tolerated and produced both diarylated and dialkenylated products **222**. On the other hand, benzo-fused heterobicyclic alkenes failed to give the difunctionalized product with the corresponding monofunctionalized ring-opened species being the sole product. Concurrently, the Kang laboratory investigated similar reactivity, disclosing an alternative method for diarylated norbornene derivatives through the three-component coupling of bicyclic alkenes and iodonium salts or diazonium salts with organostannanes, or sodium tetraphenylborate [90]. In 2021, Liu and Chen investigated the use of organoammonium salts and organoboronic compounds as a simple method for the synthesis of diarylated norbornene derivatives [91]. The reaction was also applicable for the addition of benzyl and allyl groups via the organoammonium species.

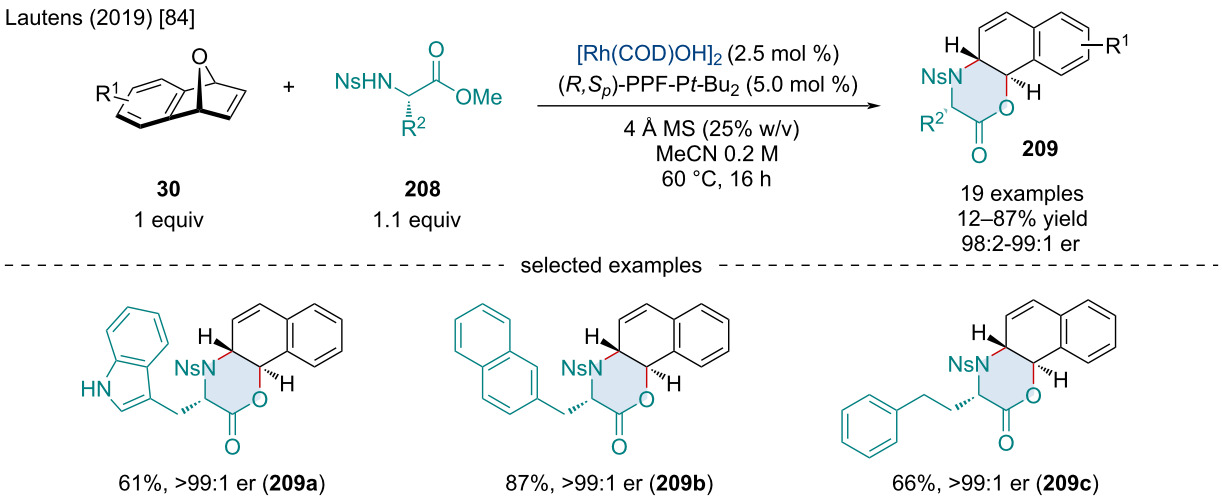

Scheme 36: Rh-catalyzed domino ring opening/lactonization of oxabenzonorbornadienes **30** with 2-nitrobenzenesulfonamides amino acid-derived nucleophiles **208**.

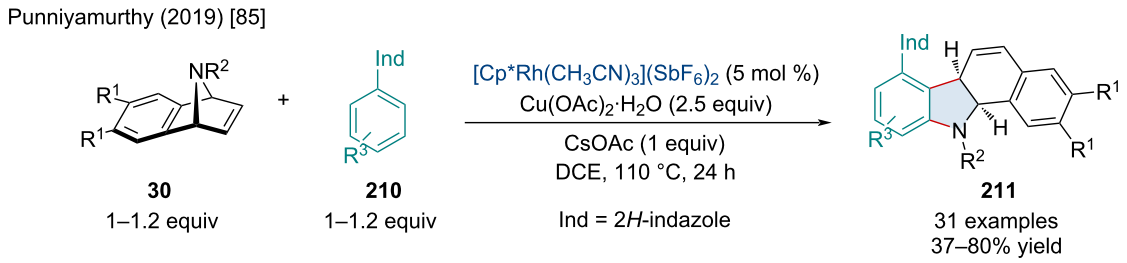

Scheme 37: Rh-catalyzed domino C–C/C–N bond formation of azabenzonorbornadienes **30** with aryl-2*H*-indazoles **210**.

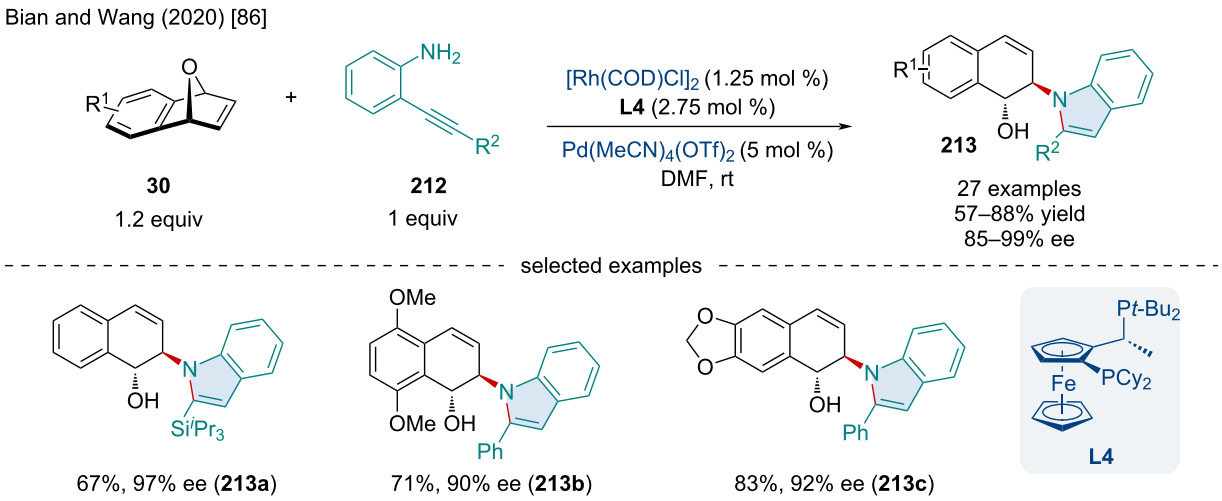

Scheme 38: Rh/Pd-catalyzed domino synthesis of indole derivatives with 2-(phenylethynyl)anilines **212** and oxabenzonorbornadienes **30**.

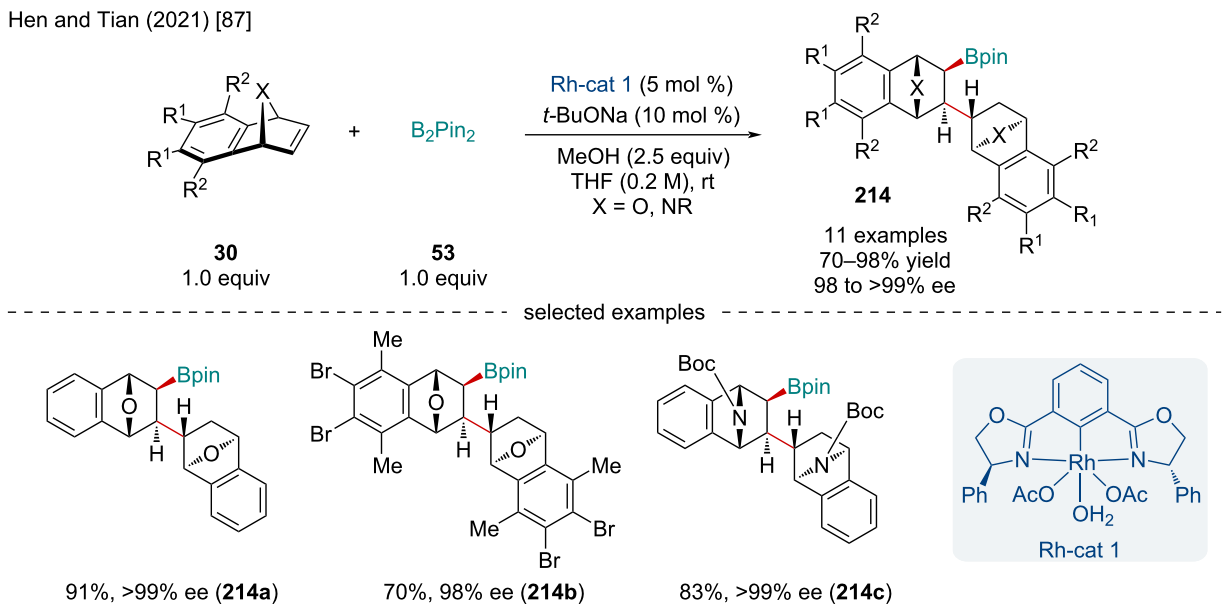

Scheme 39: Rh-catalyzed domino carborhodation of heterobicyclic alkenes **30** with B_2pin_2 (**53**).

In 2008, the Liu laboratory explored the Pd-catalyzed three-component 1,2-arylalkynylation of oxabenzonorbornadiene derivatives **30** (Scheme 42) [92]. Unlike previous reports disclosing the coupling of aryl halides and oxabicyclic alkenes, the authors disclosed the use of 5 M aqueous NaOH to hinder unwanted β-oxygen elimination, promoting difunctionalization of the olefin. The use of the phase-transfer catalyst was paramount, as its removal resulted in little to no conversion. Aryl, alkynyl and alkenyl iodide derivatives, as well as methyl iodide, were shown to operate in the reaction; however, only aryl iodide derivatives routinely gave the desired product in appreciable yield.

In 2022, Wan and Chen explored similar reactivity using aryl triflates (Scheme 42) [93]. The scope of aryl triflates was expansive with derivatives from biologically relevant compounds, like vanillin (**227b**) and eugenol (**227a**), being applicable. Unfortunately, the authors did not expand their scope beyond carbobicyclic frameworks; however, it would be expected the difunctionalization likely does not occur with heterobicyclic alkenes as β-heteroatom elimination could likely be the predominate pathway.

In 2023, Ji and Liu expanded on the Pd-catalyzed three-component arylalkynylation of oxabenzonorbornadiene derivatives (Scheme 43) [94]. Initially reported by Liu and co-workers in 2006 [95], present conditions were altered to avoid aqueous NaOH, opting for Cs_2CO_3. Interestingly, the reaction was applicable to a variety of functional groups, including esters, chlorines, and bromines. In line with similar reports, the scope of bicyclic alkenes was limited with all but a single example being performed on norbornene. DFT calculations were used to explore the reaction mechanism which involves the oxidative addition of the C–I bond, coordination, migratory insertion, transmetalation, and reductive elimination. The authors determined the migratory insertion via $\mathbf{TS_{232–233}}$ is the rate-determining step for the catalytic cycle.

In 2014, Ma and Wang reported the Pd-catalyzed three-component coupling of *N*-tosylhydrazones, aryl halides, and norbornene (Scheme 44) [96]. The reaction tolerated small substituents on the *N*-tosylhydrazone and aryl halide coupling partners, but the reaction was quite sensitive to *ortho*-substitution and steric bulk. Generally, the reaction gave the corresponding product in good yield and excellent diastereoselectivity; however, a few substrates produced diastereomeric ratios of 3:1. As the propensity for an *exo*-selective migratory insertion is well understood, it is surprising some products displayed such poor selectivity. As such, this may indicate some form of stereoisomerization rather than a poorly selective migratory insertion. In the following year, Xu and Liang reported a reaction involving the same three coupling partners [97]. By altering the reaction conditions, the authors observed the first palladium-catalyzed ring opening of norbornene to prepare methylenecyclopentane derivatives via an unusual β-carbon elimination.

In 2016, the Song laboratory reported the Pd-catalyzed arylboration of norbornene derivatives (Scheme 45) [98]. Generally, electron-rich aryl halides afforded the product in a higher yield than those bearing electron-withdrawing groups. Moreover, the

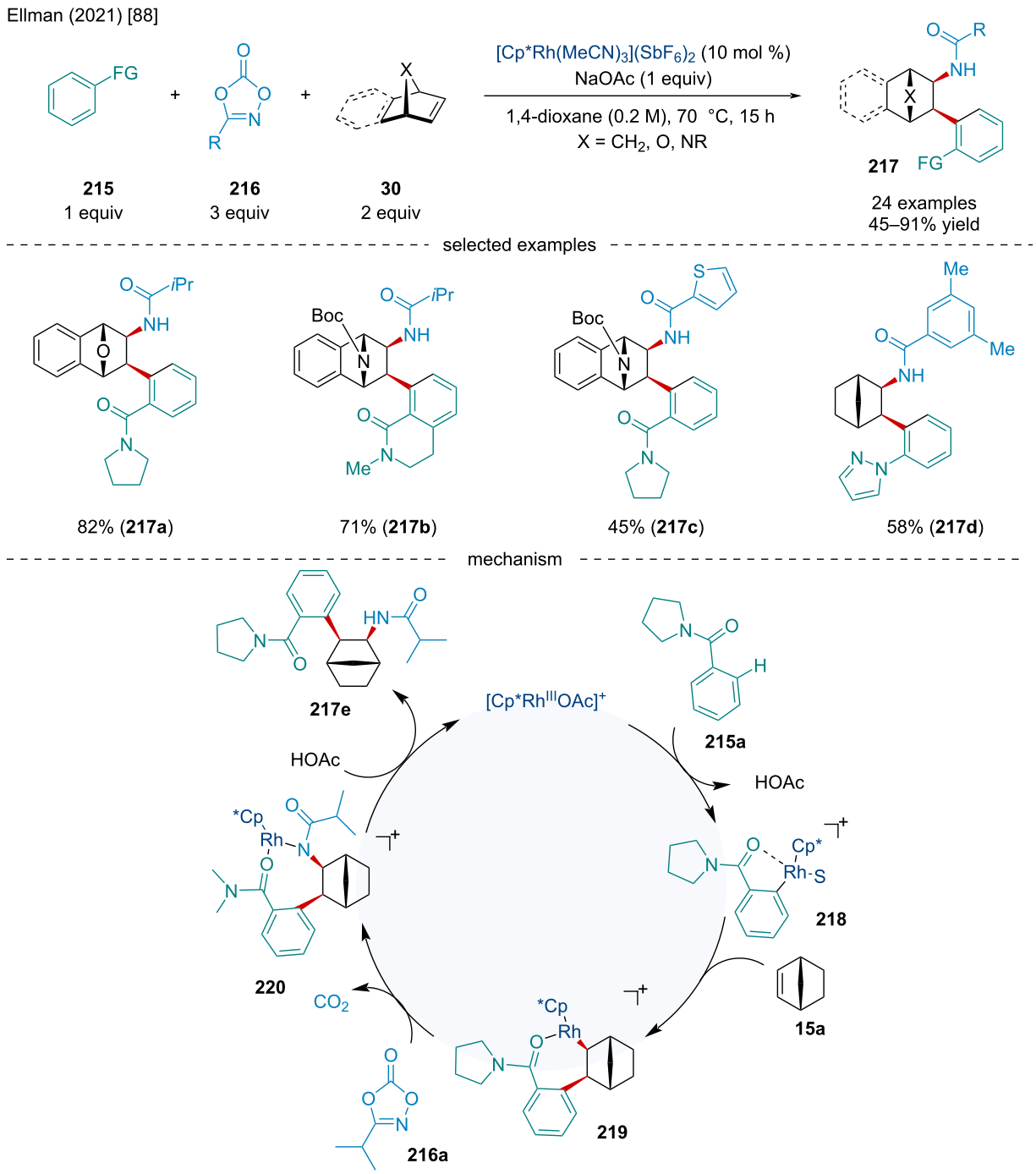

Scheme 40: Rh-catalyzed three-component 1,2-carboamidation reaction of bicyclic alkenes **30** with aromatic and heteroaromatic C–H substrates **215** and dioxazolones **216**.

reaction was amenable to heteroaromatic iodides, but yields were diminished. The authors showed aryl bromides were tolerated albeit with slightly diminished yields relative to their iodide-containing counterparts. The scope of bicyclic alkenes was mainly limited to norbornene with a single example using norbornadiene.

In 2019, Jiang and co-workers expanded on this chemistry and revealed allyl carboxylates can be used as the nucleophilic partner in carboborylation difunctionalization reactions (Scheme 45) [99]. Besides allyl acetates, the authors revealed formates, propionates, and butanoates were able to afford the desired product; however, allyl bromides and chlorides failed.

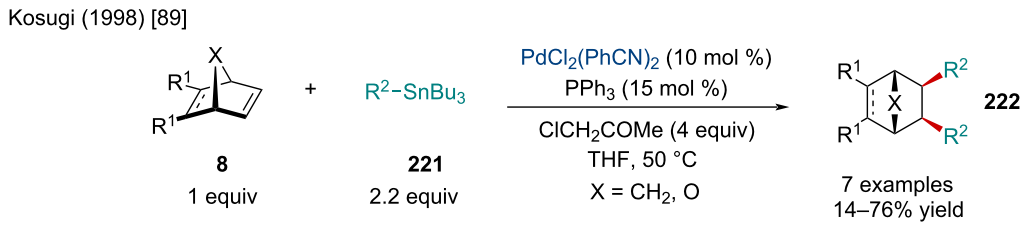

Scheme 41: Pd-catalyzed diarylation and dialkenylation reactions of norbornene derivatives.

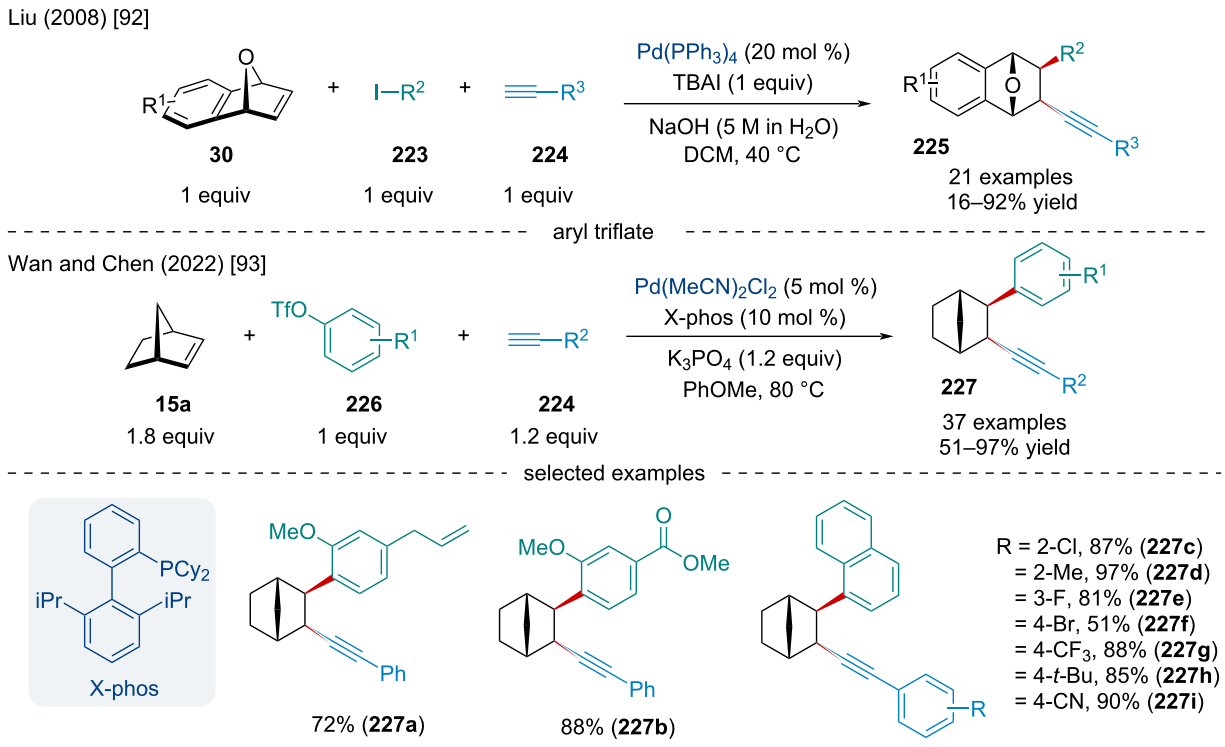

Scheme 42: Three-component Pd-catalyzed arylalkynylation reactions of bicyclic alkenes.

Unfortunately, the reaction was sensitive to the bicyclic alkene used; norbornadiene and 2,3-diester-substituted norbornene were unable to undergo the transformation. Surprisingly, oxabenzonorbornadiene was amenable and afforded the difunctionalized product in 44% yield rather than a ring-opened product.

In 2018, Fu and Chen reported the Pd-catalyzed, three-component annulation of aryl iodides **66**, alkenyl bromides **241**, and bicyclic alkenes **1** (Scheme 46) [100]. Similar reports by the Lautens [101] and Perumal [102] laboratories have demonstrated the use of norbornene derivatives for the synthesis of tetrasubstituted olefins; however, limited work has been done for the synthesis of trisubstituted olefins. The authors noted *ortho*-substituted iodobenzenes delivered products in a greater yield compared to their strictly *meta*- or *para*-substituted counterparts like due to the elimination of complex byproducts. Typically, reactions gave products with very high *Z* stereoselectivity. The authors demonstrated the methodology could be applied towards the synthesis of tetrasubstituted olefins as well, giving the desired product in moderate to good yields. This methodology avoided the use of highly substituted internal alkynes, a substrate which can be more difficult to synthesis than its alkenyl bromide counterpart. The reaction is applicable to other bicyclic alkenes although with slightly diminished yields compared to norbornene. Unsymmetrically substituted bicyclic alkenes bearing relatively sensitive functionalities, such as -CHO and -CN, worked, albeit with no regioselectivity.

In 2019, Perumal and Cho reported a Pd-catalyzed double insertion/annulation reaction for synthesizing tetrasubstituted olefins (Scheme 47) [103]. Mechanistically, the transformation

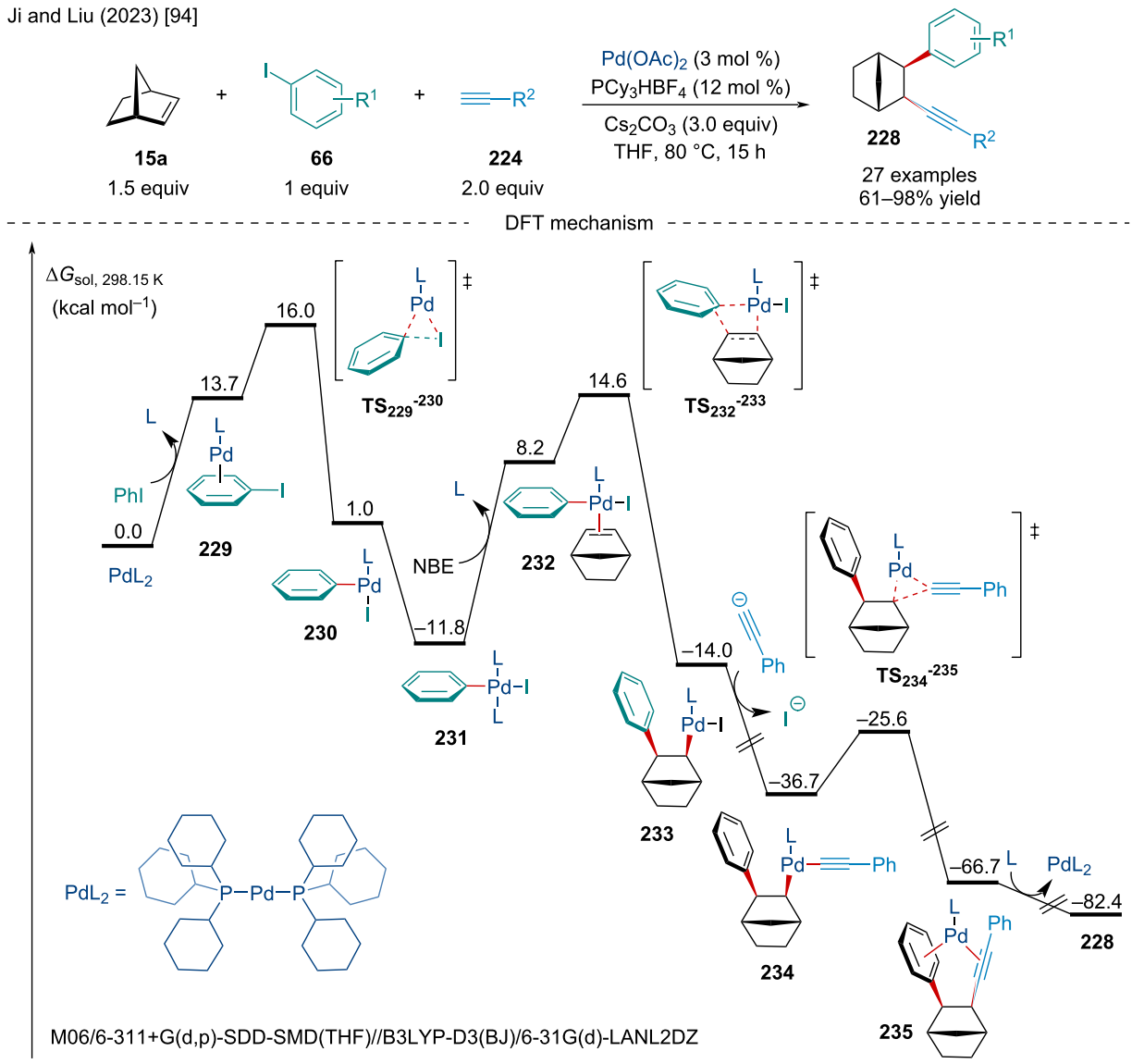

Scheme 43: Three-component Pd-catalyzed arylalkynylation reactions of norbornene and DFT mechanistic study.

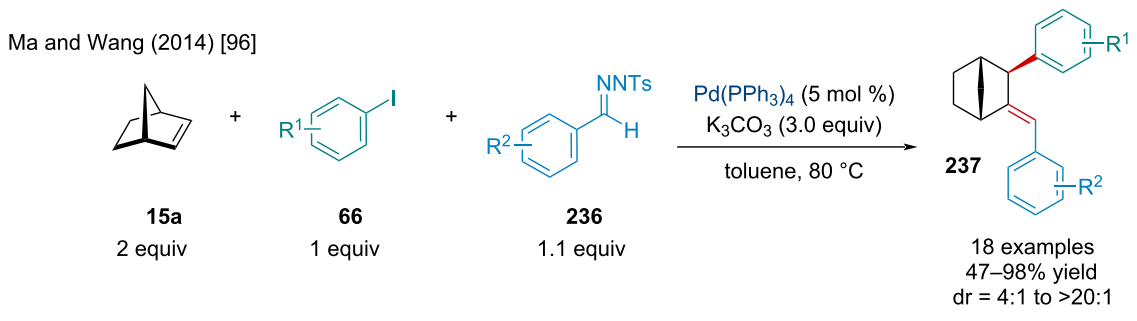

Scheme 44: Pd-catalyzed three-component coupling *N*-tosylhydrazones **236**, aryl halides **66**, and norbornene (**15a**).

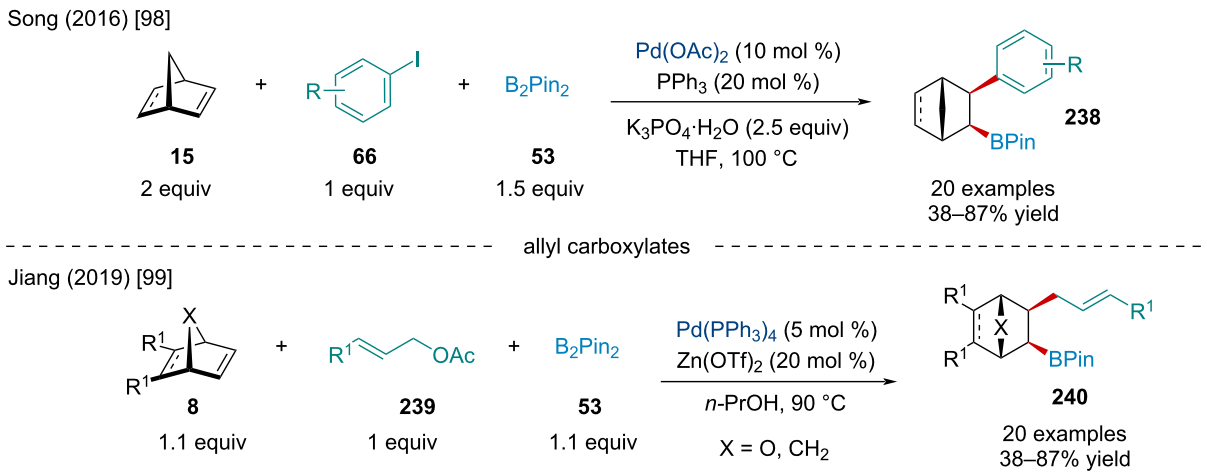

Scheme 45: Pd-catalyzed arylboration and allylboration of bicyclic alkenes.

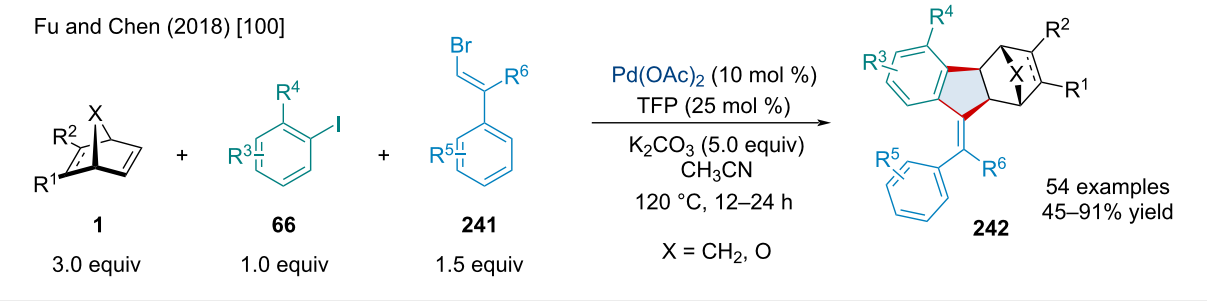

Scheme 46: Pd-catalyzed, three-component annulation of aryl iodides **66**, alkenyl bromides **241**, and bicyclic alkenes **1**.

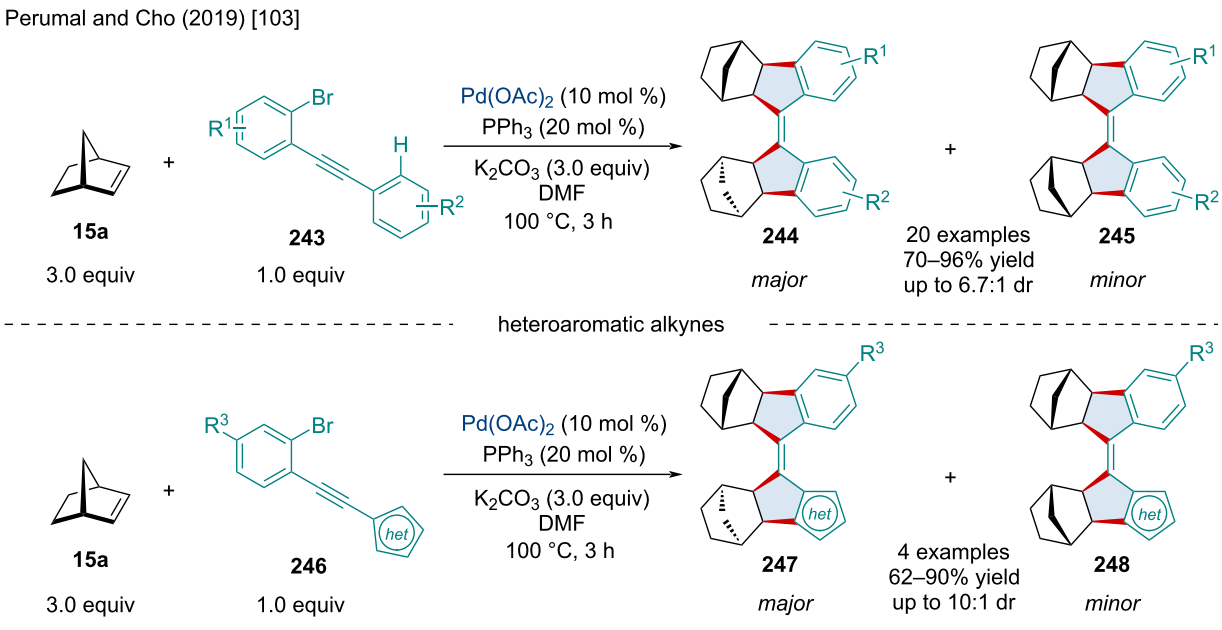

Scheme 47: Pd-catalyzed double insertion/annulation reaction for synthesizing tetrasubstituted olefins.

involves the formation of four new C–C bonds through three consecutive carbopalladations and a C–H activation. Unlike the anticipated *exo* migratory insertion seen almost exclusively in these types of systems, the authors noted the second norbornene moiety undergoes an *endo*-selective reaction, as confirmed through X-ray crystallography. The diastereoselectivity of the reaction was limited due to the production of the unanticipated *exo-endo* adduct **244**/**247** which was formed as the major product while the thermodynamically more stable *exo-exo* product **244**/**248** was only ever achieved in minor yields. The methodology was explored with a broad scope of aryl substituents revealing the robustness of the reaction. Additionally, heteroaromatic alkynes **246** were found to be tolerable but gave slightly diminished yields.

In 2013, van Vranken and co-workers reported the Pd-catalyzed aminocyclopropanation of bicyclic alkenes **1** with 5-iodopent-4-enylamine derivatives **249** (Scheme 48) [104]. The reaction was effective for a range of *N*-substituted derivatives **249**; however, the reaction was sensitive to steric bulk.

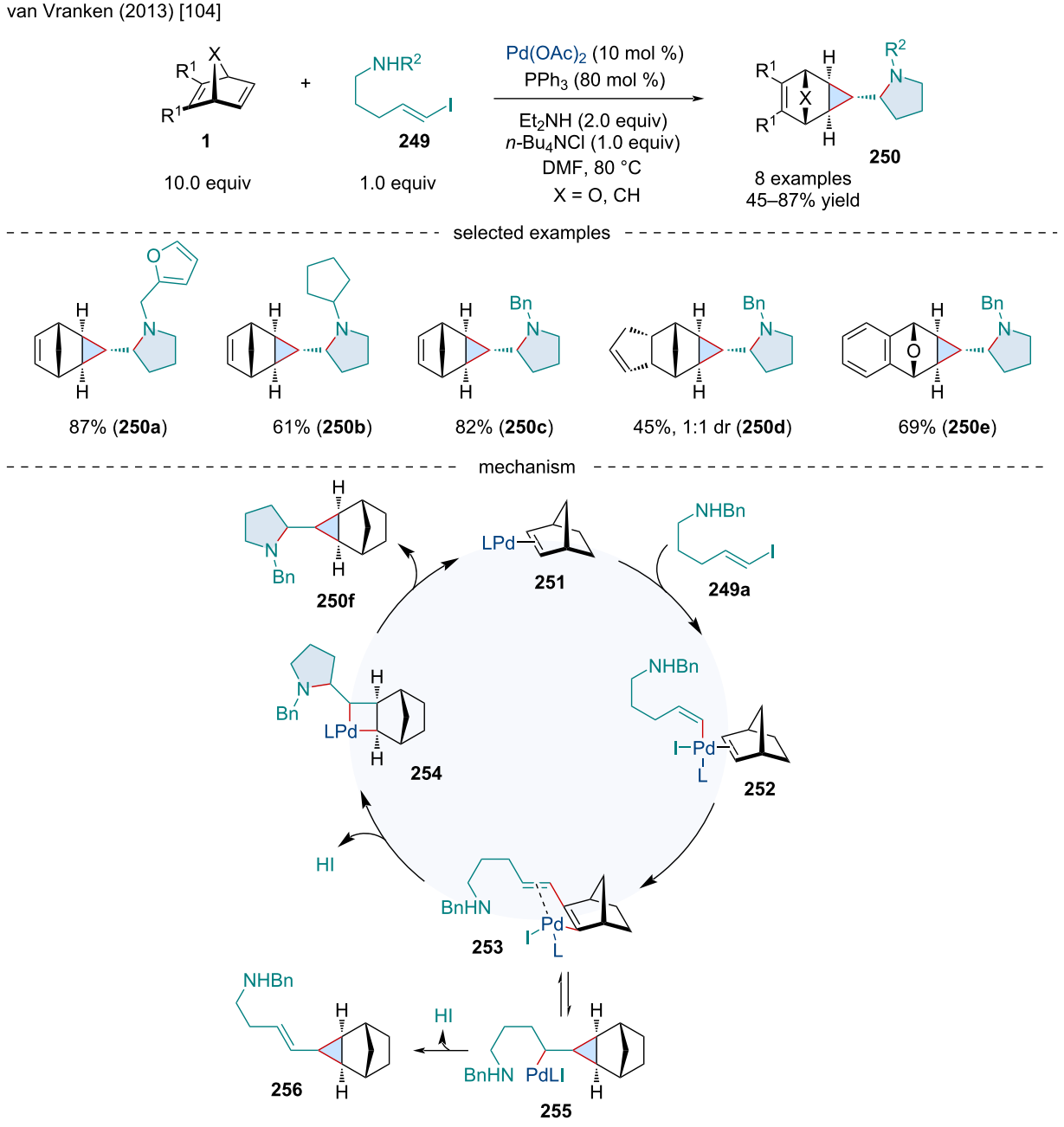

Scheme 48: Pd-catalyzed aminocyclopropanation of bicyclic alkenes **1** with 5-iodopent-4-enylamine derivatives **249**.

With large groups, like *N*-adamantyl, only modest yields of the desired pyrrolidine product were obtained, owing to the formation of the vinylcyclopropane side product. Other bicyclic alkenes were amenable, including an example with an oxabicyclic alkene which underwent the desired reaction rather than the anticipated β-oxygen elimination side reaction. The mechanism for this transformation involves the oxidative addition of the alkenyl iodide to the Pd(0) and side-on coordination to the olefin **252**, followed by the migratory insertion of the bicyclic alkene to afford complex **253**. Aminopalladation of the olefin affords **254** which undergoes a reductive elimination to generate the final product **250**. In the case of the vinylcyclopropane side product, complex **253** preferentially undergoes a carbopalladation to generate a cyclopropane intermediate **255** which undergoes a β-hydride elimination to give **256**.

In 2017, Wu and Jiang reported a Pd-catalyzed, three-component coupling of alkynyl bromides **62**, norbornene derivatives **15**, with electrophilic trapping agents (Scheme 49) [105]. Mechanistically, the transformation begins with the oxidative addition of the alkynyl bromide to the Pd(0) catalyst. From here, four consecutive carbopalladation reactions ultimately end up producing an alkylpalladium intermediate which undergoes a β-carbon elimination to afford a Pd–π-allyl species. First, the authors captured this π-allyl species with *N*-tosylhydrazone derivatives **236**. Notably, alkynyl bromides **62** bearing electron-withdrawing groups typically afforded the desired product in greater yield. The scope of the *N*-tosylhydrazones **236** was expansive with electronic substituents having little effect on the reaction. Heteroaromatic *N*-tosylhydrazones **236** were applicable but gave diminished yields. Moving on, the authors showed the Pd–π-allyl species can be trapped with boronic acids **20**. Like the *N*-tosylhydrazones **236**, the substituents on the boronic acid had little effect on the reaction. Lastly, the authors demonstrated the use of B_2pin_2 **53** to capture the Pd–π-allyl species.

In 2006, the Cheng group investigated the Pd-catalyzed intramolecular cyclization/ring-opening reaction of heterobicyclic alkenes **30** with 2-iodophenoxyallenes **260** (Scheme 50) [106]. Surprisingly, the efficacy of the reaction was more susceptible to derivatization of the benzo-fused moiety with sterically demanding functionalities rather than altering the electronics, as seen with severely diminished yields with phenanthrene-fused oxabicyclic alkenes. The reaction was unaffected by the identity of the bridging heteroatom with both oxa- and aza-bridging atoms performing equally as well; although, the latter was only explored a single time. Altering the tether length of the allene moiety seemed to mildly affect the reaction with 5-membered rings being formed in slightly greater yields compared to their

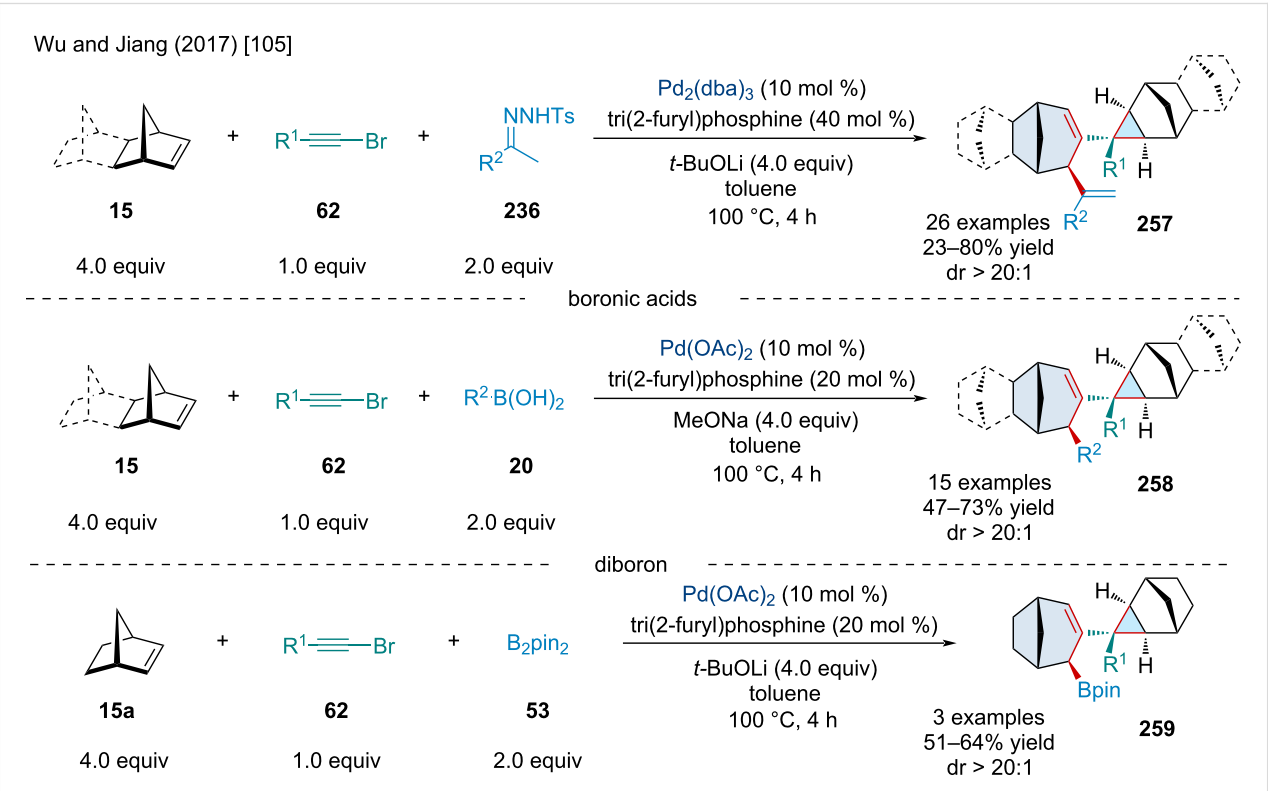

Scheme 49: Pd-catalyzed, three-component coupling of alkynyl bromides **62** and norbornene derivatives **15** with electrophilic trapping agents.

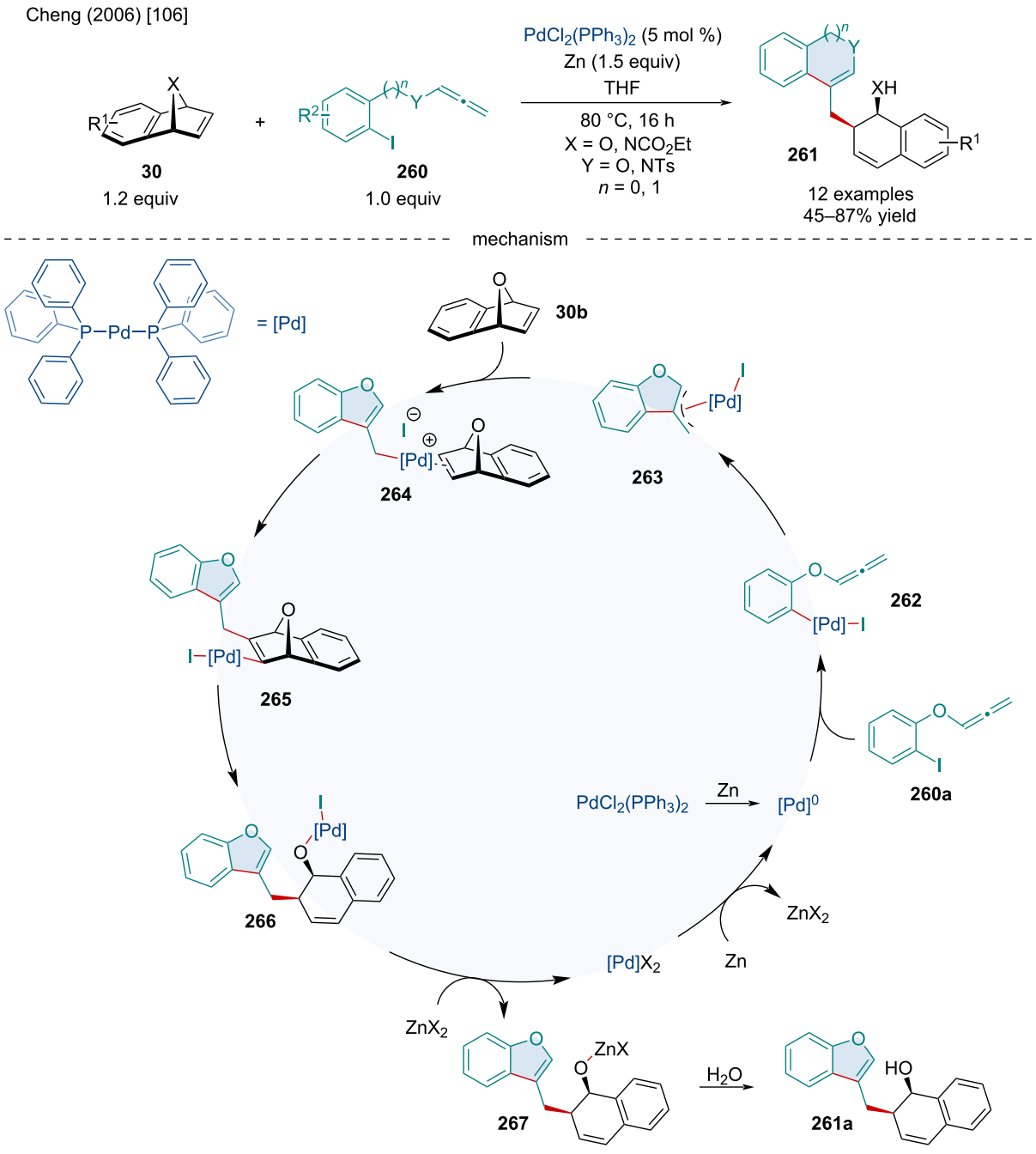

Scheme 50: Pd-catalyzed intramolecular cyclization/ring-opening reaction of heterobicyclic alkenes **30** with 2-iodophenoxyallenes **260**.

6-membered counterparts. Mechanistically, this reaction operates similarly to other cyclization/capture chemistry seminally presented by Griggs [107,108]. First, the Pd(II) catalyst is reduced to the Pd(0) active catalyst with Zn metal. Oxidative addition of the aryl iodide **260a** to Pd(0) gives **262** which can side-on coordinate with the allenyl group. Intramolecular migratory insertion affords the Pd–π-allyl species **263** which can side-on coordinate to the *exo* face of the bicyclic alkene **264**. Rather than dissociation of the iodide ligand to generate a cationic Pd center, it has also been proposed the loss of a phosphine ligand could allow for the generation of a free coordination site. Migratory insertion affords intermediate **265** which undergoes a β-oxygen elimination to **266**. Transmetalation with $ZnCl_2$ affords the zinc alkoxide **267** which is hydrolyzed to give the

final product **261a**. Alternatively, Zn metal could reduce Pd(II) intermediate **266** to Pd(0) directly, bypassing the transmetalation step.

In 2019, the Fan group explored the Pd-catalyzed dimer- and trimerization of oxabenzonorbornadiene derivatives **30** with anhydrides **268** (Scheme 51) [109]. The authors noted electron-deficient oxabenzonorbornadiene derivatives resulted in diminished product yields. When electron-rich bicyclic alkenes were used, the trimer **270** to dimer **269** ratio was increased. When applied to unsymmetrically substituted bicyclic alkenes, the authors propose the dimerized product was formed as a single regioisomer, as evaluated by ^{1}H NMR, with no trimerization observed.

In 2013, the Hu laboratory developed a method to form annulated xanthones **272** using norbornadiene (**15b**), 3-iodochromones **271**, and aryl iodides **66** via a Catellani-type reaction (Scheme 52) [110]. The authors proposed a mechanism beginning with the oxidative addition of Pd(0) to **271a**, followed by migratory insertion across norbornadiene (**15b**) and alkenyl C–H activation of the chromone ring, furnishing the palladacycle **274**. The oxidative addition of **274** to the aryl iodide **66b** yields a Pd(IV) species **275** that can undergo reductive elimination by either an sp^2–sp^3 or sp^2–sp^2 coupling event. The authors probed the regioselectivity of this step using *p*-iodotoluene and, based on the product, concluded that only sp^2–sp^3 coupling occurred. The resulting intermediate **276** undergoes an aryl C–H activation step and a subsequent reductive elimination yielding a norbornadiene-fused xanthone derivative **277**, which forms the final product **272a** via a retro-Diels–Alder reaction. The reaction was generally tolerant of substituted 3-iodochromones; however, substituted aryl iodides were shown to have significant effects. Electron-donating *para*-substituents and bulky *ortho*-substituents resulted in lower yields while bulky *meta*-substituents could be used to influence the regioselectivity of the C–H activation step. The scope was limited to dienes because of the necessity for a retro-Diels–Alder to furnish the desired product but a norbornane-fused xanthone was also produced in 82% yield.

In 2017, Vijayan et al. investigated both the Pd-catalyzed hydroarylation and annulation of urea-derived bicyclic alkenes **158** using aryl iodides **66** (Scheme 53) [111]. In both reactions, the 1,2-migratory insertion of palladium across the olefin resulted in a palladacycle intermediate that was further reacted, either via hydride-donor or an *ortho*-directing group, to form the hydroarylated **280** or annulated products **282**, respectively. For this reason, the formic acid additive was necessary in the hydroarylation but was left out in the annulation to promote capture by the phenolic directing group. The hydroarylation gave moderate to good yields with EWGs and EDGs alike, as well as accommodating *ortho*-substituents. It was also tolerant of spiro-, furan-derived, and *N*-protected pyrrole-derived bicyclic alkenes, all giving similar yields. The heterobicyclic alkenes were shown to be compatible with the annulation as well, though they resulted in slightly reduced yields compared to the carbocyclic examples. Although the authors focused on the use of an alcohol directing group for the annulation to furnish dihydrobenzofurans, they also provided a simple example using methyl bromide and nitrile directing groups giving indane and indanone products in similar yields.

In 2018, the Chen laboratory explored a Pd/norbornene cocatalyzed Catellani annulation reaction of phenyl iodides **66** and NH-sulfoximines **283** in an attempt to produce dibenzothiazines [112]. Though they were successful in this effort, they also reported accessing eight-membered sulfoximine heterocycles when norbornene was not extruded, which was accomplished in two distinct ways (Scheme 54) [112]. The first

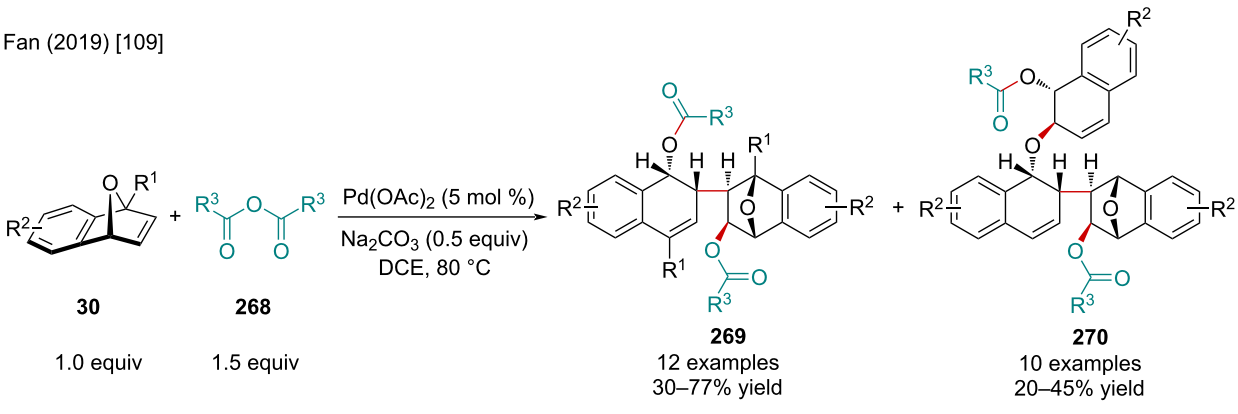

Scheme 51: Pd-catalyzed dimer- and trimerization of oxabenzonorbornadiene derivatives **30** with anhydrides **268**.

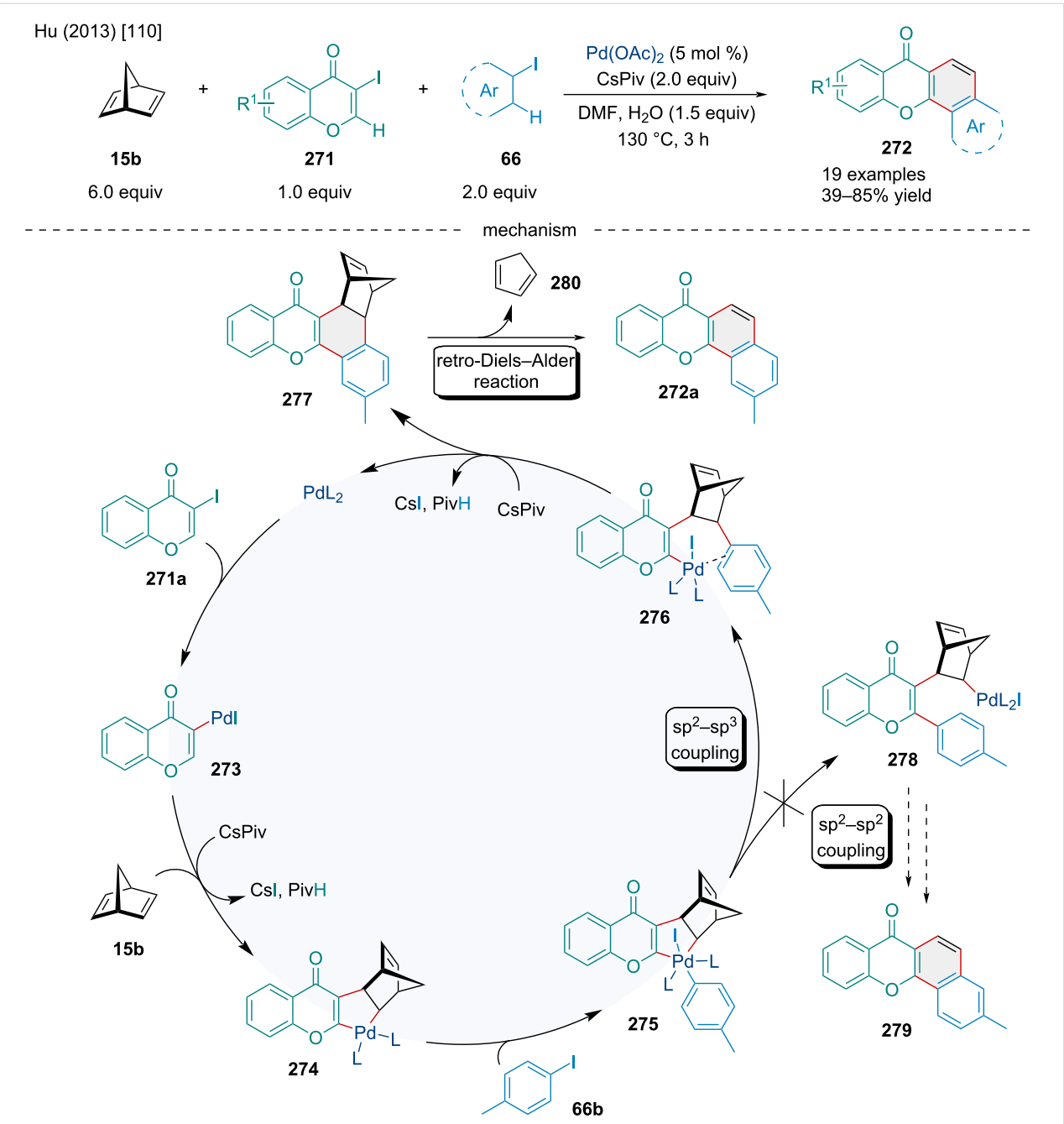

Scheme 52: Pd-catalyzed Catellani-type annulation and retro-Diels–Alder of norbornadiene **15b** yielding fused xanthone derivatives **272**.

requires aryl iodides with *meta*-EWGs, which was shown by DFT calculation to favor sp^2–sp^3 coupling over sp^2–sp^2 coupling. This coupling step prevents the extrusion of norbornane later without restricting the Pd catalyst's access to the sulfoximine directing group, thus allowing the formation of the 8-membered heterocyclic product **284**. The other method requires slightly modified conditions, mainly by increasing the equivalents of NH-sulfoximines **283**, and for the phenyl iodides have two *ortho*-hydrogens. The second hydrogen allows for sequential C–H activation after the standard sp^2–sp^2 coupling, again preventing the extrusion of norbornene, and creating a Pd(II) species that undergoes oxidative addition with the extra sulfoximines provided, eventually forming a heterocycle bearing two sulfoximine moieties **285**. Understandably, the presented examples are limited, as these products were of secondary interest to the authors but yields of up to 94% for product **284** and from 42% to 64% for product **285** were reported.

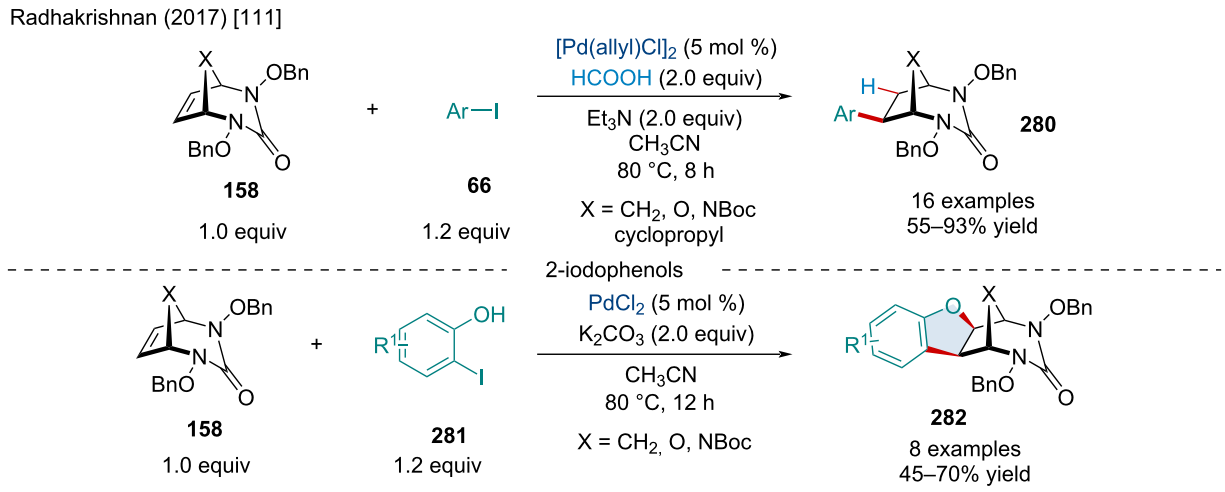

Scheme 53: Pd-catalyzed hydroarylation and heteroannulation of urea-derived bicyclic alkenes **158** and aryl iodides **66**.

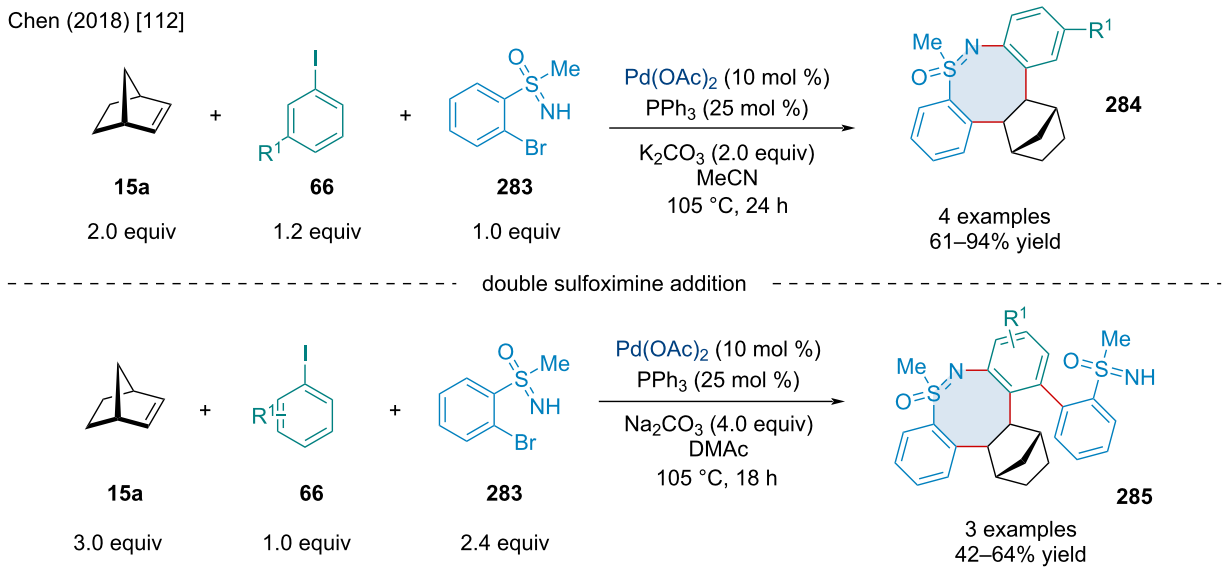

Scheme 54: Access to fused 8-membered sulfoximine heterocycles **284**/**285** via Pd-catalyzed Catellani annulation cascades.

Six years after the work of Hu and co-workers producing annulated xanthones, Yang et al. completed a 2,2-bifunctionalization of bicyclic alkenes **1** to produce xanthone derivatives bearing spirobicyclic moieties **277** (Scheme 55) [113]. This was achieved via a Pd-catalyzed [2 + 3 + 1] annulation of 3-iodochromones **271**, bromoacetones **276**, and bicyclic alkenes **1**. The reaction generally afforded good yield and diastereoselectivity even across the wide swathe of functionalized substrates and few bicyclic alkenes tested and provided a good yield (71%) at the gram scale.

In 2019, Zhong et al. reported a method to produce phenanthrene derivatives **279** using 2-iodotoluenes **66**, *o*-bromobenzoyl chlorides **278**, and norbornadiene (**15b**). This method proceeds through a Pd-catalyzed Catellani reaction; however, norbornadiene extrusion is avoided via the loss of the acyl chloride group as CO, allowing the formation of a 7-membered palladacycle, reductive elimination, and subsequent retro-Diels–Alder reaction to the phenanthrene **279** (Scheme 56) [114]. This was an improvement over past methods that used less reactive *ortho*-haloaryl carboxylic acids which required harsher conditions and longer reaction times to optimally perform. The reaction was shown to be tolerant of diverse functionality, providing excellent yields barring a couple notable examples; 1-iodonaphthalene (64%) and *o*-iodonitrobenzene (75%). The authors were also

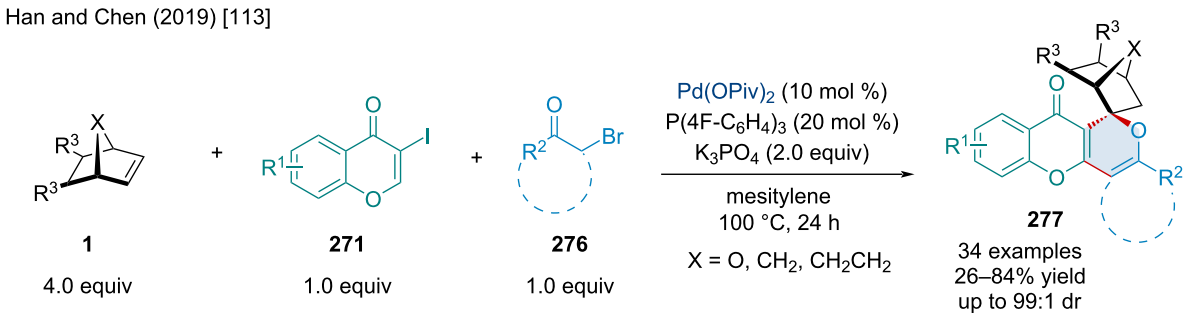

Scheme 55: Pd-catalyzed 2,2-bifunctionalization of bicyclic alkenes **1** generating spirobicyclic xanthone derivatives **277**.

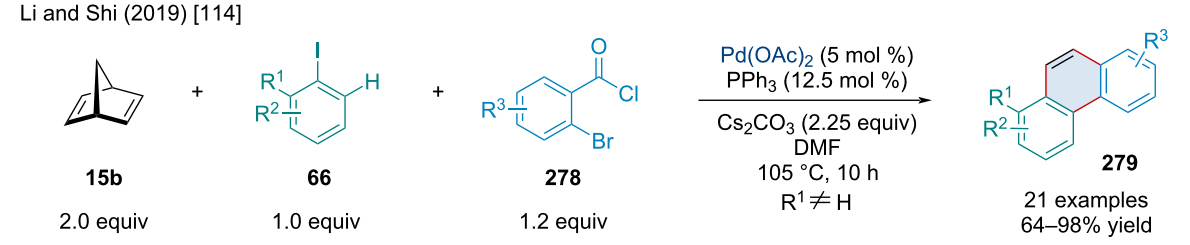

Scheme 56: Pd-catalyzed Catellani-type annulation and retro-Diels–Alder of norbornadiene (**15b**) producing substituted phenanthrenes **279**.

able to demonstrate its efficacy at the gram scale with a yield of 88%.

In 2020, Zhang and colleagues explored a three-component Pd-catalyzed annulation reaction furnishing norbornane-fused indanes **281** (Scheme 57) [115]. This reaction sees an aryl iodide **66** coupled to a bicyclic alkene **30** to produce a 5-membered palladacycle intermediate that is then captured by the third reagent, either methylene bromide (**280**) or an α-diazoester **282**. A reduced yield was seen in the absence of iPrOH, so it was kept as an additive with the authors proposing it functions as a reductant, reducing Pd(II) to the active catalyst Pd(0). A great variety of examples using methylene bromide (**280**) were reported, including using a few different bicyclic alkenes **30**, with up to 96% yield. A similar variety of examples with similar yields were shown using α-diazoesters **282**, however, only norbornene proved suitable in this case with heterobicyclic alkenes unable to afford the desired product.

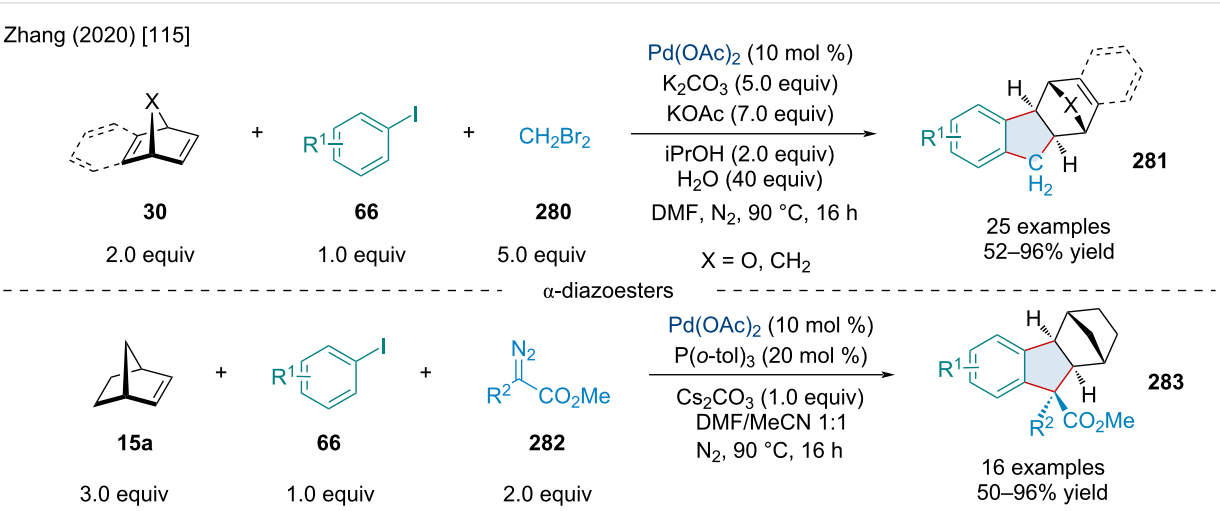

Scheme 57: Pd-catalyzed [2 + 2 + 1] annulation furnishing bicyclic-fused indanes **281** and **283**.

In 2009, the Radhakrishnan laboratory investigated a Pd-catalyzed annulation of diazabicyclic alkenes **130a**, and 2-iodophenols **284** or 2-iodoaniline (**286**) towards fused benzofuran **285** or indole **287** products (Scheme 58) [116]. The reaction begins with the oxidative addition of Pd(0) into the aryl iodide **284a**, followed by migratory insertion across the bicyclic alkene to form **289**. Base-assisted addition of the alcohol and β-nitrogen elimination forms a ring-opened cyclopentene intermediate **290** which then undergoes oxypalladation and β-hydride elimination, furnishing the benzofuran product **284a**. The authors noted that in the absence of the Bu_4NCl additive the reaction did not work. The authors hypothesized the chloride ions are important

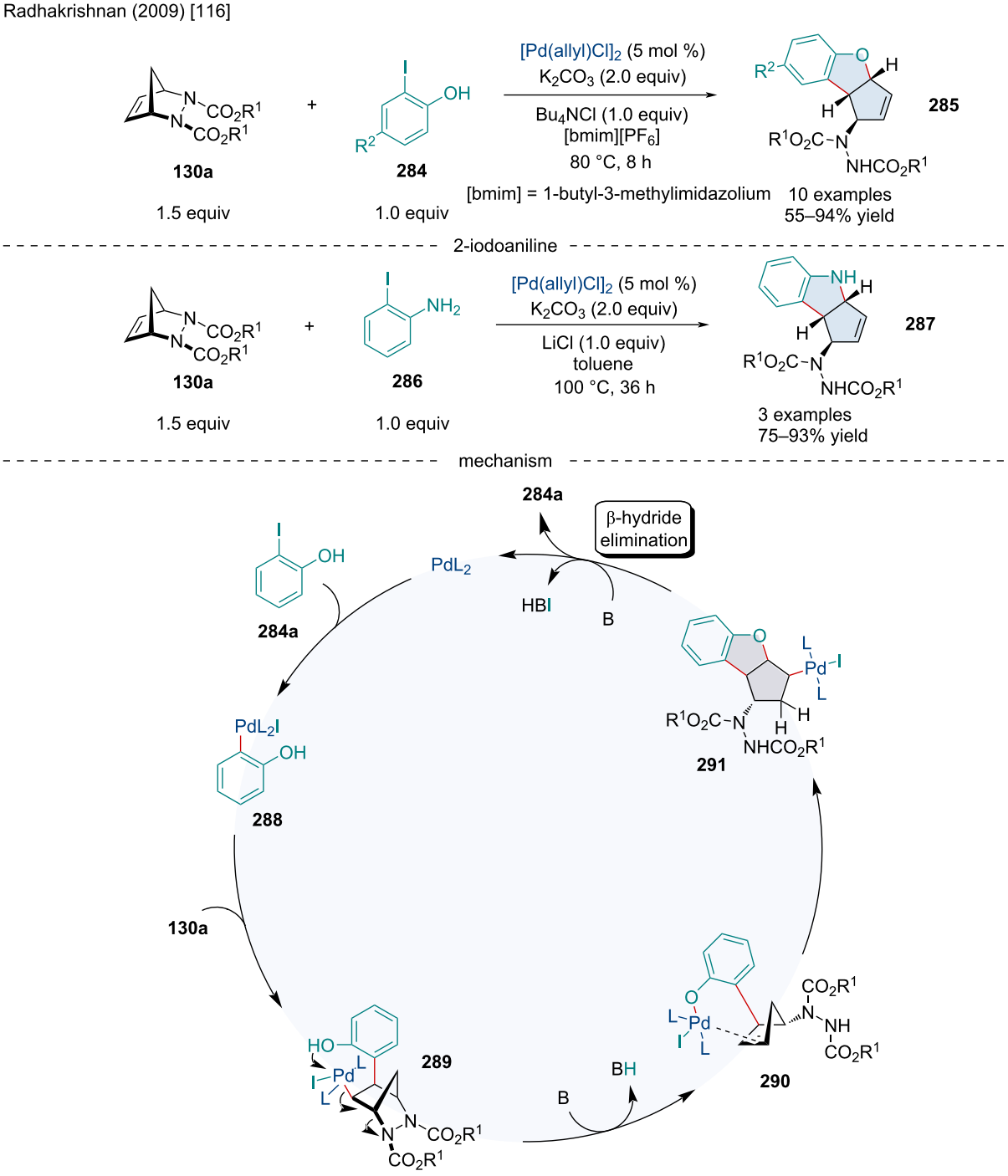

Scheme 58: Pd-catalyzed ring-opening/ring-closing cascade of diazabicyclic alkenes **130a**.

for regenerating and stabilizing the Pd(0) species. While only a handful of examples were reported, it was demonstrated that diazabicyclic alkenes with bulkier ester groups caused reduced yields.

One year later, the Gilbertson laboratory expanded on this annulation reaction, increasing its efficiency and significantly decreasing the reaction time using tweaked conditions and microwave irradiation (Scheme 59) [117]. They also significantly increased the scope of the reaction, providing many examples with up to 98% yield, and utilizing N-substituted anilines to create N-substituted indoles **284**. The authors were also able to apply their methodology to an acetal-protected vanillin derivative, producing the corresponding benzofuran with 90% yield.

Two years after their previous work, the Radhakrishnan group explored a non-ring-opening annulation utilizing 2-iodobenzonitrile (**292**) and 2-formylphenylboronic acids **142** to access diazabicyclic-fused indanones **293** and indanols **294** (Scheme 60) [71]. The authors noted the addition of base increased the yield of 2-iodobenzonitrile (**292**) reactions but reduced it for those with 2-formylphenylboronic acids **142**. Only a few examples producing indanones **293** were presented showing very small changes in yield with different diazabicyclic esters. Different N-substituted triazolinedione-derived bicyclic alkenes were also tested but failed, likely due to their base sensitivity. The annulation reaction yielding indanols **294** was seen to produce the 3,4-disubstituted cyclopentene **295** in ratios of about 1:9 when the diazabicyclic alkenes **130a** were used. However, when using the N-substituted triazolinedione-derived bicyclic alkenes the 3,4-disubstituted cyclopentene **294** could be produced exclusively in yields of up to 90%.

In 2013, Pihko and Radhakrishnan revisited their 2009 annulation reaction using 2-iodophenols **284** and 2-iodoaniline (**286**) in an attempt to access larger polycyclic compounds **296** through the use of spirotricyclic olefins **176** (Scheme 61) [118]. It is proposed that the reaction follows a similar ring-opening/ring-closing mechanism to their 2009 report (Scheme 58), but the cyclopropane moiety allows a second ring opening and the

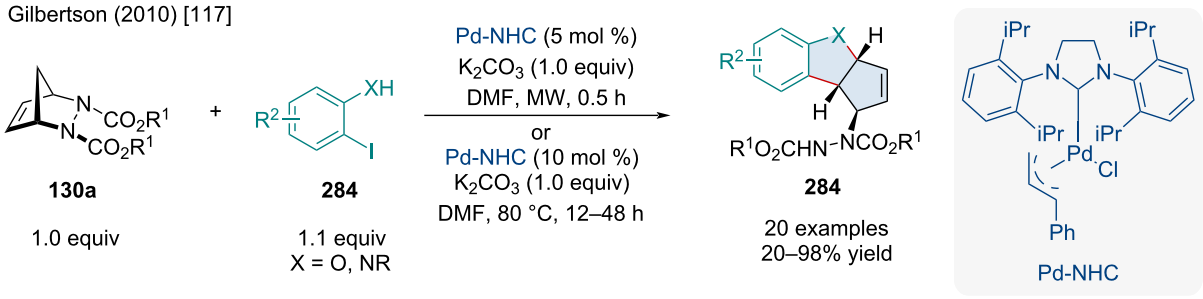

Scheme 59: Pd-NHC-catalyzed cyclopentannulation of diazabicyclic alkenes **130a**.

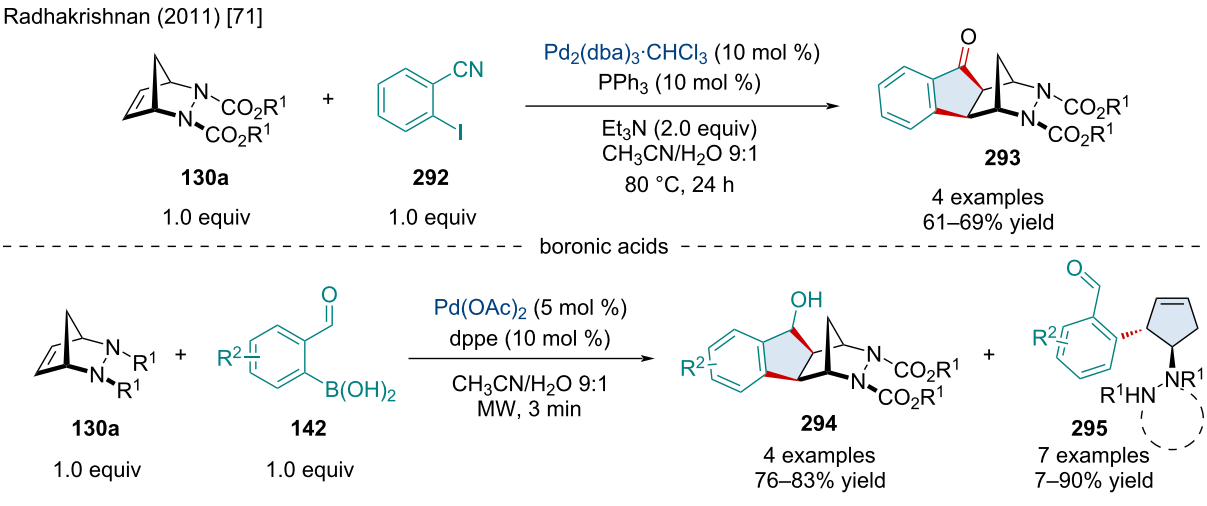

Scheme 60: Pd-catalyzed annulation cascade generating diazabicyclic-fused indanones **292** and indanols **294**.

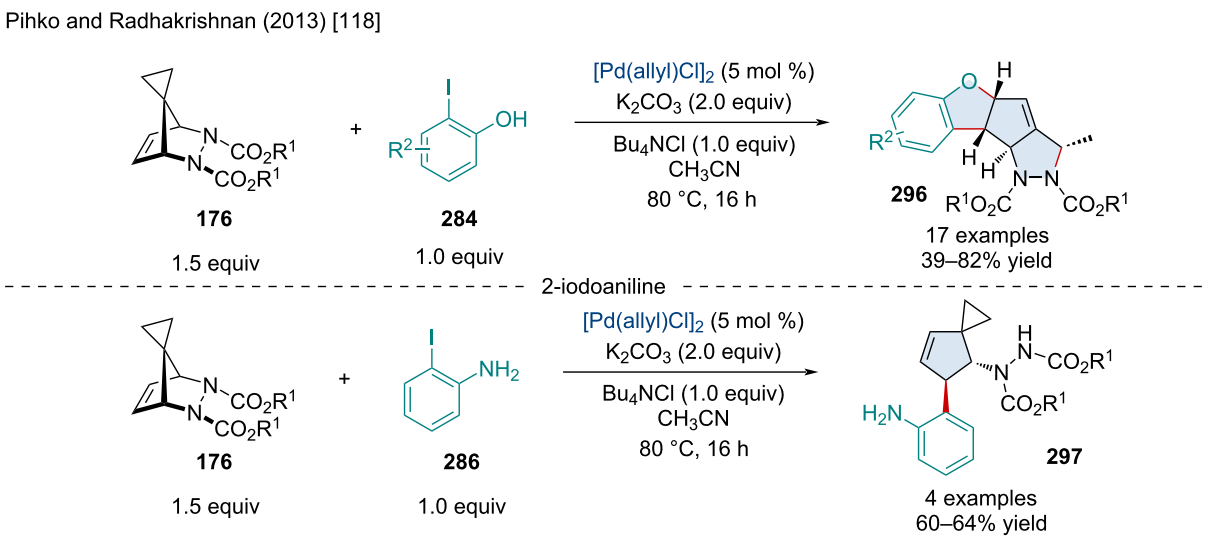

Scheme 61: Pd-catalyzed skeletal rearrangement of spirotricyclic alkenes **176** towards large polycyclic benzofuran derivatives **296**.

subsequent generation of a π-allyl–palladium complex. This complex undergoes an intramolecular nucleophilic attack by hydrazine, forming the fourth fused ring. When the methodology was applied to 2-iodoaniline (**286**), the anticipated polycyclic product was not formed; instead, *trans*-disubstituted spiro[2,4]hept-4-enes **297** were formed. A variety of substituted 2-iodophenols **284** were tested showing significantly reduced yields with *para*-EWGs, emphasizing the importance of an electron-rich alcohol directing group.

In 2017, the Radhakrishnan group investigated another ring-opening/ring-closing reaction of diazabicyclic alkenes **130a**, synthesizing cyclopenta[*b*]pyrroline derivatives **299** using aromatic enamides **298** (Scheme 62) [119]. Since the reaction begins with an alkenyl C–H activation, forming a 6-membered palladacycle intermediate with amide oxygen chelation, $Cu(OAc)_2$ was added as an oxidant to regenerate Pd(II). Afterwards, the transformation progresses similarly to their 2009 report (Scheme 58). The 6-membered palladacycle will undergo migratory insertion into the diazabicyclic alkene **130a** which after a β-nitrogen elimination, adds to the amide via the nitrogen atom. Aminopalladation forms the C–N bond that produces the fused pyrroline moiety in the product **299**. The authors reported several examples using substituted aromatic enamides finding that EWGs were well tolerated while EDGs significantly reduced yields. When applied at the gram scale, the desired product was produced with 60% yield.

In 2018, Radhakrishnan and colleagues again expanded on their past work, attempting to produce 3,4,5-trisubstituted cyclopentenes **300** from diazabicyclic alkenes **130a** and 2-iodobenzoates **9** (Scheme 63) [120]. The authors proposed a charged fused-oxane intermediate is produced after the ring-opening/ring-closing sequence, as anticipated in 2009 (Scheme 58), whose eventual breakdown furnishes a π-allyl–palladium complex which undergoes nucleophilic attack by the acetate or azide anion. Several examples were reported, ranging a 60–85% yield, showing minimal electronic influence by 2-iodobenzoate substituents. However, another reaction path was observed when 2-iodo-3-methylbenzoate (**9a**) was used, producing a cyclopentene-fused indane **302**. The authors suggested that the mechanism of this reaction follows the same

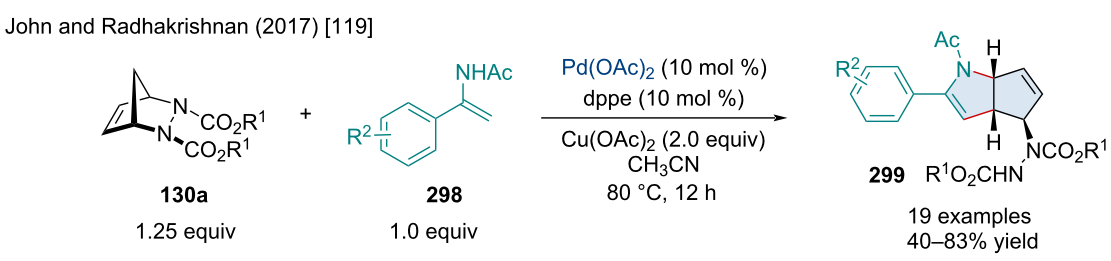

Scheme 62: Pd-catalyzed oxidative annulation of aromatic enamides **298** and diazabicyclic alkenes **130a**.

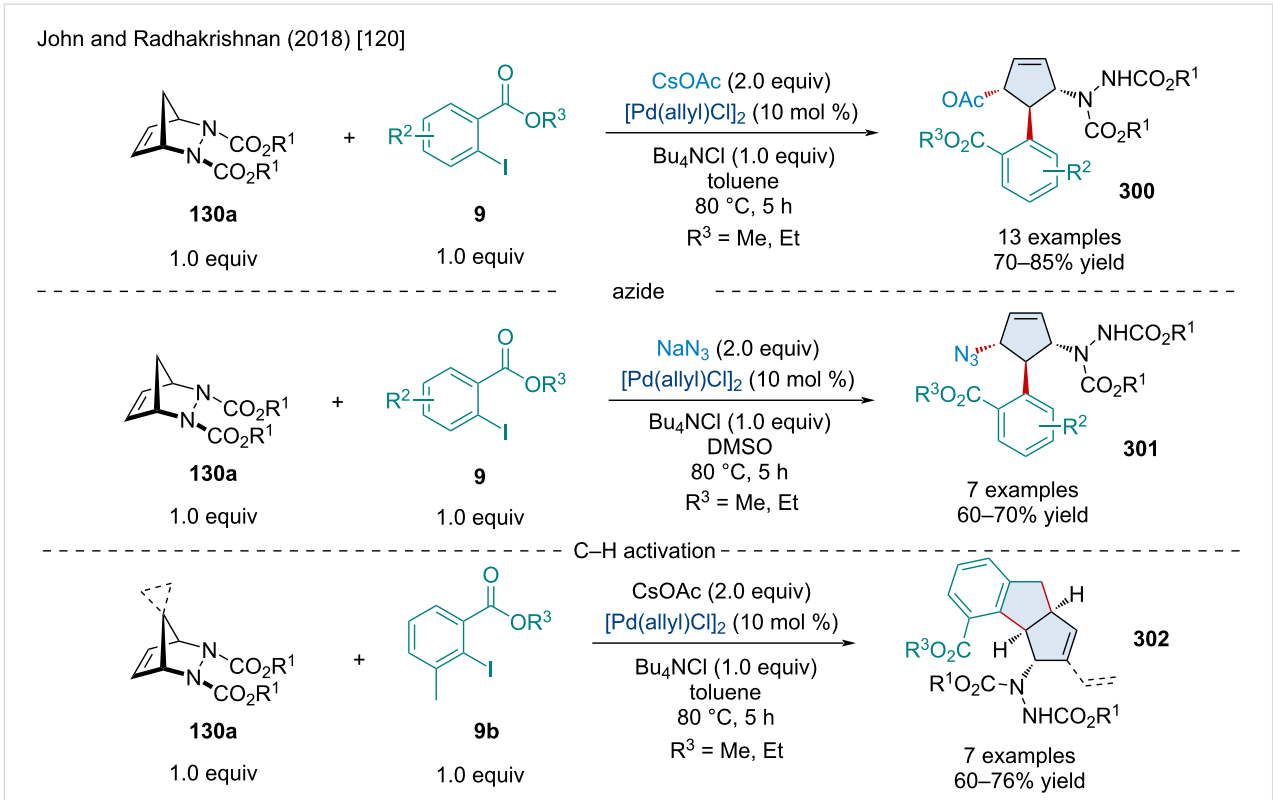

Scheme 63: Accessing 3,4,5-trisubstituted cyclopentenes **300**, **301**, **302** via the Pd-catalyzed domino reaction of diazabicyclic alkenes **130a** and 2-iodobenzoates **9**.

steps until the formation of the π-allyl–palladium complex, which can undergo cyclopalladation via benzylic C–H activation of the 3-methyl group, and subsequently reductive elimination to yield the fused indane product **302**.

In 2012, Ge et al. investigated a palladacycle-catalyzed reaction furnishing highly substituted fused furans **304** using bicyclic alkenes **1** and terminal ynones **302** (Scheme 64) [121]. The authors noted the reaction was sensitive to the identity of both

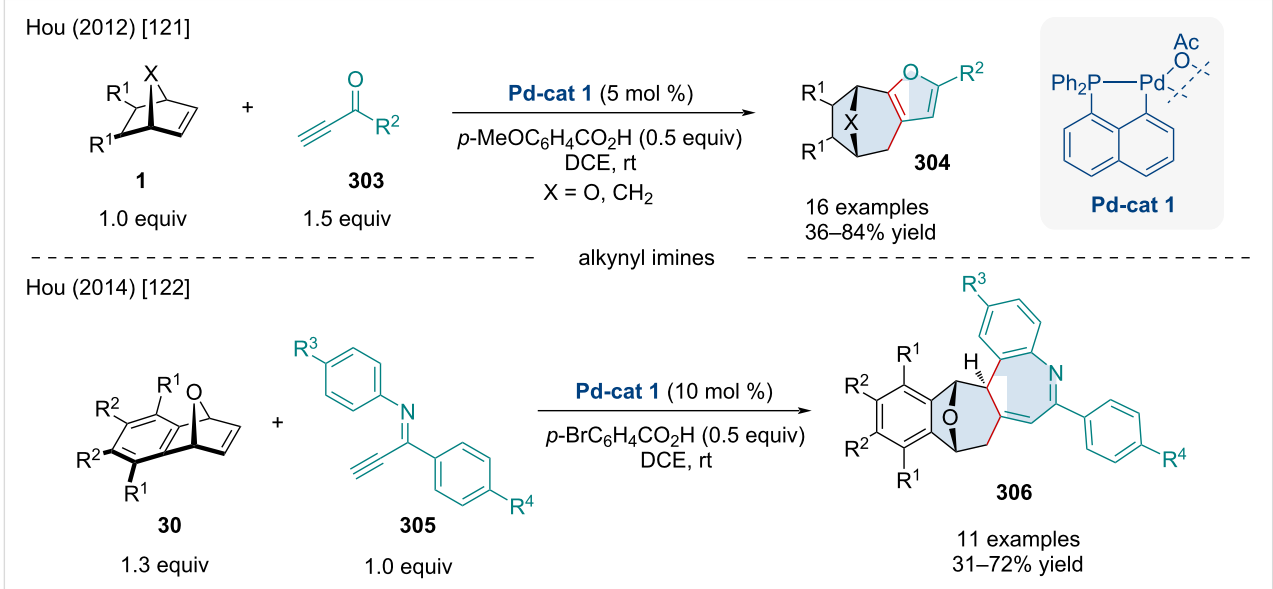

Scheme 64: Palladacycle-catalyzed ring-expansion/cyclization domino reactions of terminal alkynes and bicyclic alkenes.

basic and acidic additives, as bases tended to slow down reactions while stronger acids typically produced only a trace amount of the desired product **304**. Eventually, the authors discovered their goldilocks additive, settling on *p*-methoxybenzoic acid which showed a significant increase in yield. The reaction was generally tolerant of a variety of substituted terminal ynones **303** and bicyclic alkenes **1**, as well as norbornene (**15a**) and norbornadiene (**15b**). Two years later, this methodology was expanded by the same group, using terminal alkynyl imines **305** to access polycyclic 5*H*-benzo[*b*]azepines **306** (Scheme 64) [122]. The authors reported low yields when R^2 or R^3 were weak EWGs and no reaction with strong EWGs at R^3, somewhat restricting the scope of the reaction.

In 2018, the Jiang laboratory explored a Pd-catalyzed carboesterification reaction, using bicyclic alkenes **15** and alkynoates **307**, ynamides **309**, and alkynols **310** to produce α-methylene γ-lactone **308** and tetrahydrofuran derivatives **311** (Scheme 65) [123]. The reaction was shown to be functionally tolerant, boasting a large number of high yielding examples. Largely, the authors noted substitution of the ester or the amide moiety had little influence on the reaction. Only two examples were reported for the reaction of the alkynol **310**, albeit in good yields.

Conclusion

Over the last two decades, there has been remarkable progress in transition-metal-catalyzed domino reactions of homo- and heterobicyclic alkenes. Bicyclic alkenes can be exploited in two ways. Firstly, through the release of ring-strain energy which drives the reaction forward under milder conditions compared to strainless alkene counterparts. Secondly, the stereochemically well-defined, dual-faced nature of these systems can be exploited to synthesize highly stereoselective products.

Multicomponent domino reactions can be challenging due to selectivity issues, but recent advancements have provided straightforward protocols for the construction of complex molecules with multiple carbon–carbon and carbon–heteroatom bonds in a single step. When participating in a well-orchestrated domino sequence, these bicyclic alkenes can quickly generate highly functionalized products with extreme stereo-, regio-, and enantioselectivity.

Currently, a majority of transition-metal-catalyzed domino reactions use simple carbocyclic alkenes, such as norbornene, as the propagative π-system of choice, limiting its relevance. To see further advancements in this field, it is necessary to expand the scope to include more heterobicyclic alkenes and understand

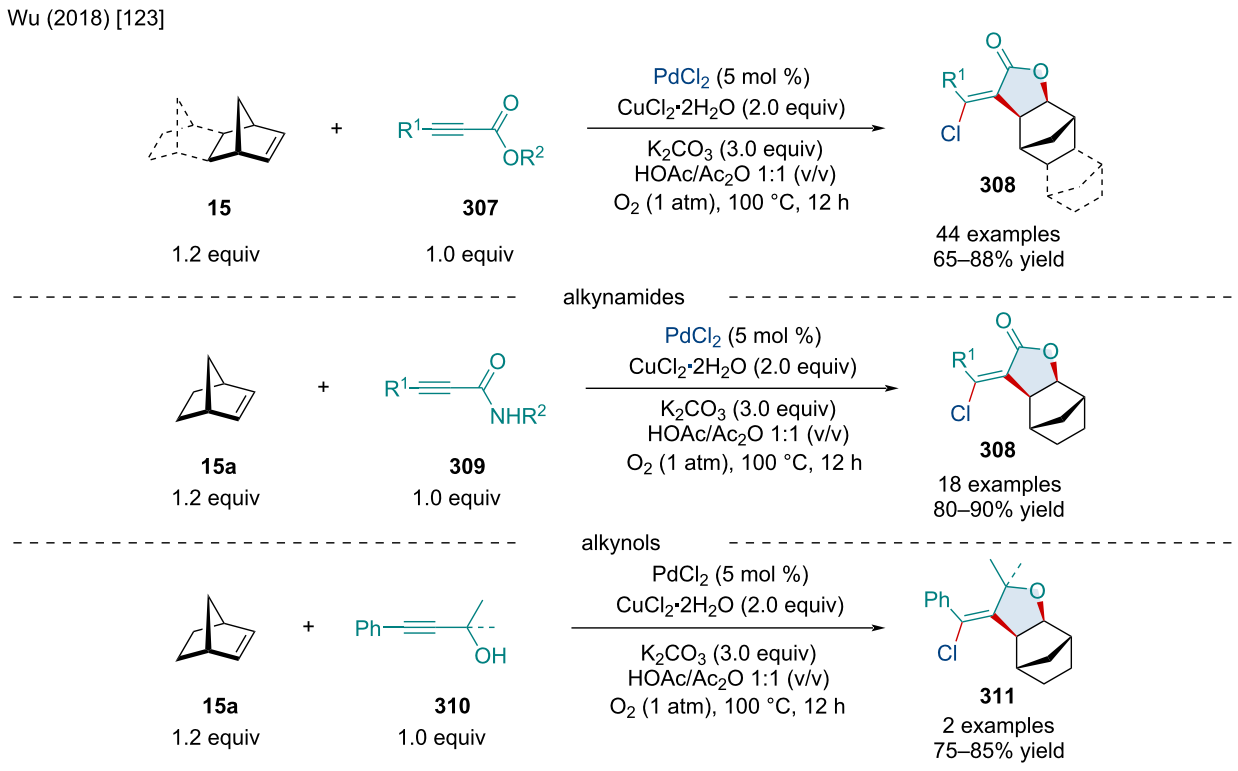

Scheme 65: Pd-catalyzed carboesterification of norbornene (**15a**) with alkynes, furnishing α-methylene γ-lactones **308** and tetrahydrofurans **311**.

their fundamental reactivity. As heterobicyclic alkenes have the tendency to undergo some form a β-heteroatom elimination which can prematurely terminate a cascade, their use requires more thought. However, altering coupling partners, reaction conditions, and the metal center have all been used to promote difunctionalization of heterobicyclic alkenes while hindering β-heteroatom elimination. We hope this comprehensive overview of bicyclic alkene chemistry will drive further advancements in the area of transition-metal-catalyzed domino reactions.

Funding

This work was supported by a Discovery Grant (WT) from the Natural Sciences and Engineering Research Council (NSERC) of Canada. AP also acknowledges NSERC for financial support through the PGS-D Scholarship.

ORCID® iDs

Austin Pounder - https://orcid.org/0000-0002-5843-0922
Peter Myler - https://orcid.org/0000-0002-0089-1056
William Tam - https://orcid.org/0000-0002-1375-881X

References

1. Tietze, L. F. *Chem. Rev.* **1996,** *96,* 115–136. doi:10.1021/cr950027e
2. Pounder, A.; Ho, A.; Macleod, M.; Tam, W. *Curr. Org. Synth.* **2021,** *18,* 446–474. doi:10.2174/1570179417666210105121115
3. Kumar, S. V.; Yen, A.; Lautens, M.; Guiry, P. J. *Chem. Soc. Rev.* **2021,** *50,* 3013–3093. doi:10.1039/d0cs00702a
4. Lautens, M.; Fagnou, K.; Hiebert, S. *Acc. Chem. Res.* **2003,** *36,* 48–58. doi:10.1021/ar010112a
5. Rayabarapu, D. K.; Cheng, C.-H. *Acc. Chem. Res.* **2007,** *40,* 971–983. doi:10.1021/ar600021z
6. Khan, R.; Chen, J.; Fan, B. *Adv. Synth. Catal.* **2020,** *362,* 1564–1601. doi:10.1002/adsc.201901494
7. Khoury, P. R.; Goddard, J. D.; Tam, W. *Tetrahedron* **2004,** *60,* 8103–8112. doi:10.1016/j.tet.2004.06.100
8. Howell, J.; Goddard, J. D.; Tam, W. *Tetrahedron* **2009,** *65,* 4562–4568. doi:10.1016/j.tet.2009.03.090
9. Bredt, J.; Houben, J.; Levy, P. *Ber. Dtsch. Chem. Ges.* **1902,** *35,* 1286–1292. doi:10.1002/cber.19020350215
10. Chiusoli, G. P.; Catellani, M.; Costa, M.; Motti, E.; Della Ca', N.; Maestri, G. *Coord. Chem. Rev.* **2010,** *254,* 456–469. doi:10.1016/j.ccr.2009.07.023
11. Martins, A.; Mariampillai, B.; Lautens, M. Synthesis in the Key of Catellani: Norbornene-Mediated *ortho* C–H Functionalization. In *C-H Activation;* Yu, J. Q.; Shi, Z., Eds.; Topics in Current Chemistry, Vol. 292; Springer: Berlin, Heidelberg, 2009; pp 1–33. doi:10.1007/128_2009_13
12. Catellani, M.; Motti, E.; Della Ca', N.; Ferraccioli, R. *Eur. J. Org. Chem.* **2007,** 4153–4165. doi:10.1002/ejoc.200700312
13. Li, R.; Dong, G. *J. Am. Chem. Soc.* **2020,** *142,* 17859–17875. doi:10.1021/jacs.0c09193
14. Ferraccioli, R. *Synthesis* **2013,** *45,* 581–591. doi:10.1055/s-0032-1318218
15. Cheng, H.-G.; Chen, S.; Chen, R.; Zhou, Q. *Angew. Chem., Int. Ed.* **2019,** *58,* 5832–5844. doi:10.1002/anie.201813491
16. Liu, Z.-S.; Gao, Q.; Cheng, H.-G.; Zhou, Q. *Chem. – Eur. J.* **2018,** *24,* 15461–15476. doi:10.1002/chem.201802818
17. Wegmann, M.; Henkel, M.; Bach, T. *Org. Biomol. Chem.* **2018,** *16,* 5376–5385. doi:10.1039/c8ob01025k
18. Pounder, A.; Tam, W. *Beilstein J. Org. Chem.* **2021,** *17,* 2848–2893. doi:10.3762/bjoc.17.196
19. Chen, J.; Lu, Z. *Org. Chem. Front.* **2018,** *5,* 260–272. doi:10.1039/c7qo00613f
20. Ackermann, L. *Acc. Chem. Res.* **2020,** *53,* 84–104. doi:10.1021/acs.accounts.9b00510
21. Chirik, P.; Morris, R. *Acc. Chem. Res.* **2015,** *48,* 2495. doi:10.1021/acs.accounts.5b00385
22. Reed-Berendt, B. G.; Polidano, K.; Morrill, L. C. *Org. Biomol. Chem.* **2019,** *17,* 1595–1607. doi:10.1039/c8ob01895b
23. Bauer, I.; Knölker, H.-J. *Chem. Rev.* **2015,** *115,* 3170–3387. doi:10.1021/cr500425u
24. Kuzmina, O. M.; Steib, A. K.; Moyeux, A.; Cahiez, G.; Knochel, P. *Synthesis* **2015,** *47,* 1696–1705. doi:10.1055/s-0034-1380195
25. Piontek, A.; Bisz, E.; Szostak, M. *Angew. Chem., Int. Ed.* **2018,** *57,* 11116–11128. doi:10.1002/anie.201800364
26. Czaplik, W. M.; Mayer, M.; Cvengros, J.; von Wangelin, A. J. *ChemSusChem* **2009,** *2,* 396–417. doi:10.1002/cssc.200900055
27. Sherry, B. D.; Fürstner, A. *Acc. Chem. Res.* **2008,** *41,* 1500–1511. doi:10.1021/ar800039x
28. Rayabarapu, D. K.; Sambaiah, T.; Cheng, C.-H. *Angew. Chem., Int. Ed.* **2001,** *40,* 1286–1288. doi:10.1002/1521-3773(20010401)40:7<1286::aid-anie1286>3.0.co;2-i
29. Qin, H.; Chen, J.; Li, K.; He, Z.; Zhou, Y.; Fan, B. *Chem. – Asian J.* **2018,** *13,* 2431–2434. doi:10.1002/asia.201800492
30. Huang, D.-J.; Rayabarapu, D. K.; Li, L.-P.; Sambaiah, T.; Cheng, C.-H. *Chem. – Eur. J.* **2000,** *6,* 3706–3713. doi:10.1002/1521-3765(20001016)6:20<3706::aid-chem3706>3.0.co;2-p
31. Rayabarapu, D. K.; Cheng, C.-H. *Chem. – Eur. J.* **2003,** *9,* 3164–3169. doi:10.1002/chem.200204506
32. Li, L.-P.; Rayabarapu, D. K.; Nandi, M.; Cheng, C.-H. *Org. Lett.* **2003,** *5,* 1621–1624. doi:10.1021/ol034251z
33. Rayabarapu, D. K.; Shukla, P.; Cheng, C.-H. *Org. Lett.* **2003,** *5,* 4903–4906. doi:10.1021/ol036027f
34. Madan, S.; Cheng, C.-H. *J. Org. Chem.* **2006,** *71,* 8312–8315. doi:10.1021/jo061477h
35. Ogata, K.; Sugasawa, J.; Atsuumi, Y.; Fukuzawa, S.-i. *Org. Lett.* **2010,** *12,* 148–151. doi:10.1021/ol9025556
36. Mannathan, S.; Cheng, C.-H. *Chem. Commun.* **2013,** *49,* 1557–1559. doi:10.1039/c2cc38001c
37. Kadam, A. A.; Metz, T. L.; Qian, Y.; Stanley, L. M. *ACS Catal.* **2019,** *9,* 5651–5656. doi:10.1021/acscatal.9b01620
38. Ito, Y.; Nakatani, S.; Shiraki, R.; Kodama, T.; Tobisu, M. *J. Am. Chem. Soc.* **2022,** *144,* 662–666. doi:10.1021/jacs.1c09265
39. Luo, Y.; Gutiérrez-Bonet, Á.; Matsui, J. K.; Rotella, M. E.; Dykstra, R.; Gutierrez, O.; Molander, G. A. *ACS Catal.* **2019,** *9,* 8835–8842. doi:10.1021/acscatal.9b02458
40. Diallo, A. G.; Roy, D.; Gaillard, S.; Lautens, M.; Renaud, J.-L. *Org. Lett.* **2020,** *22,* 2442–2447. doi:10.1021/acs.orglett.0c00593
41. Crotti, S.; Bertolini, F.; Macchia, F.; Pineschi, M. *Adv. Synth. Catal.* **2009,** *351,* 869–873. doi:10.1002/adsc.200900037

42. Whyte, A.; Torelli, A.; Mirabi, B.; Zhang, A.; Lautens, M. *ACS Catal.* **2020,** *10,* 11578–11622. doi:10.1021/acscatal.0c02758
43. Sakae, R.; Hirano, K.; Satoh, T.; Miura, M. *Angew. Chem., Int. Ed.* **2015,** *54,* 613–617. doi:10.1002/anie.201409104
44. Gong, T.-J.; Yu, S.-H.; Li, K.; Su, W.; Lu, X.; Xiao, B.; Fu, Y. *Chem. – Asian J.* **2017,** *12,* 2884–2888. doi:10.1002/asia.201701176
45. Huang, Y.; Smith, K. B.; Brown, M. K. *Angew. Chem., Int. Ed.* **2017,** *56,* 13314–13318. doi:10.1002/anie.201707323
46. Lin, Q.; Yang, W.; Yao, Y.; Chen, S.; Tan, Y.; Chen, D.; Yang, D. *Org. Lett.* **2019,** *21,* 7244–7247. doi:10.1021/acs.orglett.9b02452
47. Ito, S.; Itoh, T.; Nakamura, M. *Angew. Chem., Int. Ed.* **2011,** *50,* 454–457. doi:10.1002/anie.201006180
48. Adak, L.; Jin, M.; Saito, S.; Kawabata, T.; Itoh, T.; Ito, S.; Sharma, A. K.; Gower, N. J.; Cogswell, P.; Geldsetzer, J.; Takaya, H.; Isozaki, K.; Nakamura, M. *Chem. Commun.* **2021,** *57,* 6975–6978. doi:10.1039/d1cc02387j
49. Tan, B.-H.; Yoshikai, N. *Org. Lett.* **2014,** *16,* 3392–3395. doi:10.1021/ol501449j
50. Muralirajan, K.; Prakash, S.; Cheng, C.-H. *Adv. Synth. Catal.* **2017,** *359,* 513–518. doi:10.1002/adsc.201601026
51. Kong, L.; Yu, S.; Tang, G.; Wang, H.; Zhou, X.; Li, X. *Org. Lett.* **2016,** *18,* 3802–3805. doi:10.1021/acs.orglett.6b01806
52. Qiu, S.; Zhai, S.; Wang, H.; Chen, X.; Zhai, H. *Chem. Commun.* **2019,** *55,* 4206–4209. doi:10.1039/c9cc00948e
53. Zhu, Y.; Chen, F.; Zhao, X.; Yan, D.; Yong, W.; Zhao, J. *Org. Lett.* **2019,** *21,* 5884–5888. doi:10.1021/acs.orglett.9b02016
54. Ozols, K.; Onodera, S.; Woźniak, Ł.; Cramer, N. *Angew. Chem., Int. Ed.* **2021,** *60,* 655–659. doi:10.1002/anie.202011140
55. Villeneuve, K.; Tam, W. *Eur. J. Org. Chem.* **2006,** 5449–5453. doi:10.1002/ejoc.200600836
56. Burton, R. R.; Tam, W. *J. Org. Chem.* **2007,** *72,* 7333–7336. doi:10.1021/jo701383d
57. Riddell, N.; Villeneuve, K.; Tam, W. *Org. Lett.* **2005,** *7,* 3681–3684. doi:10.1021/ol0512841
58. Cockburn, N.; Karimi, E.; Tam, W. *J. Org. Chem.* **2009,** *74,* 5762–5765. doi:10.1021/jo9010206
59. Villeneuve, K.; Tam, W. *Organometallics* **2006,** *25,* 843–848. doi:10.1021/om050780q
60. Villeneuve, K.; Tam, W. *Organometallics* **2007,** *26,* 6082–6090. doi:10.1021/om7004518
61. Tenaglia, A.; Marc, S.; Giordano, L.; De Riggi, I. *Angew. Chem., Int. Ed.* **2011,** *50,* 9062–9065. doi:10.1002/anie.201104589
62. Park, S. H.; Wang, S.-G.; Cramer, N. *ACS Catal.* **2019,** *9,* 10226–10231. doi:10.1021/acscatal.9b03858
63. Yan, Q.; Xiong, C.; Chu, S.; Liu, Z.; Zhang, Y. *J. Org. Chem.* **2018,** *83,* 5598–5608. doi:10.1021/acs.joc.8b00604
64. Aravindan, N.; Vinayagam, V.; Jeganmohan, M. *Org. Lett.* **2022,** *24,* 5260–5265. doi:10.1021/acs.orglett.2c01734
65. Lautens, M.; Mancuso, J. *Org. Lett.* **2002,** *4,* 2105–2108. doi:10.1021/ol0260627
66. Lautens, M.; Mancuso, J. *J. Org. Chem.* **2004,** *69,* 3478–3487. doi:10.1021/jo049874k
67. Tseng, N.-W.; Mancuso, J.; Lautens, M. *J. Am. Chem. Soc.* **2006,** *128,* 5338–5339. doi:10.1021/ja060877j
68. Tseng, N.-W.; Lautens, M. *J. Org. Chem.* **2009,** *74,* 2521–2526. doi:10.1021/jo900039g
69. Tseng, N.-W.; Lautens, M. *J. Org. Chem.* **2009,** *74,* 1809–1811. doi:10.1021/jo802622d
70. Boyer, A.; Lautens, M. *Angew. Chem., Int. Ed.* **2011,** *50,* 7346–7349. doi:10.1002/anie.201101773
71. Joseph, N.; John, J.; Rajan, R.; Thulasi, S.; Mohan, A.; Suresh, E.; Radhakrishnan, K. V. *Tetrahedron* **2011,** *67,* 4905–4913. doi:10.1016/j.tet.2011.04.087
72. Tsui, G. C.; Ninnemann, N. M.; Hosotani, A.; Lautens, M. *Org. Lett.* **2013,** *15,* 1064–1067. doi:10.1021/ol4000668
73. Jijy, E.; Prakash, P.; Shimi, M.; Pihko, P. M.; Joseph, N.; Radhakrishnan, K. V. *Chem. Commun.* **2013,** *49,* 7349–7351. doi:10.1039/c3cc43485k
74. Vijayan, A.; Jumaila, C. U.; Radhakrishnan, K. V. *Asian J. Org. Chem.* **2017,** *6,* 1561–1565. doi:10.1002/ajoc.201700377
75. Qi, Z.; Li, X. *Angew. Chem., Int. Ed.* **2013,** *52,* 8995–9000. doi:10.1002/anie.201303507
76. Yang, T.; Zhang, T.; Yang, S.; Chen, S.; Li, X. *Org. Biomol. Chem.* **2014,** *12,* 4290–4294. doi:10.1039/c4ob00704b
77. Unoh, Y.; Satoh, T.; Hirano, K.; Miura, M. *ACS Catal.* **2015,** *5,* 6634–6639. doi:10.1021/acscatal.5b01896
78. Li, H.; Guo, W.; Jiang, J.; Wang, J. *Asian J. Org. Chem.* **2020,** *9,* 233–237. doi:10.1002/ajoc.202000029
79. Prakash, P.; Jijy, E.; Shimi, M.; Aparna, P. S.; Suresh, E.; Radhakrishnan, K. V. *RSC Adv.* **2013,** *3,* 19933–19936. doi:10.1039/c3ra43191f
80. Panteleev, J.; Menard, F.; Lautens, M. *Adv. Synth. Catal.* **2008,** *350,* 2893–2902. doi:10.1002/adsc.200800587
81. Li, D. Y.; Jiang, L. L.; Chen, S.; Huang, Z. L.; Dang, L.; Wu, X. Y.; Liu, P. N. *Org. Lett.* **2016,** *18,* 5134–5137. doi:10.1021/acs.orglett.6b02587
82. Zhou, Y.; Yu, L.; Chen, J.; Xu, J.; He, Z.; Shen, G.; Fan, B. *Org. Lett.* **2018,** *20,* 1291–1294. doi:10.1021/acs.orglett.7b04044
83. Chen, T.; Gan, L.; Wang, R.; Deng, Y.; Peng, F.; Lautens, M.; Shao, Z. *Angew. Chem.* **2019,** *131,* 15966–15970. doi:10.1002/ange.201909596
84. Yen, A.; Pham, A. H.; Larin, E. M.; Lautens, M. *Org. Lett.* **2019,** *21,* 7549–7553. doi:10.1021/acs.orglett.9b02819
85. Vivek Kumar, S.; Banerjee, S.; Punniyamurthy, T. *Org. Chem. Front.* **2019,** *6,* 3885–3890. doi:10.1039/c9qo01120j
86. Li, S.; Wang, Z.; Xiao, H.; Bian, Z.; Wang, J. (Joelle). *Chem. Commun.* **2020,** *56,* 7573–7576. doi:10.1039/d0cc03158e
87. Tan, Y.-X.; Liu, X.-Y.; He, C.-Y.; Tian, P. *Tetrahedron* **2021,** *77,* 131739. doi:10.1016/j.tet.2020.131739
88. Brandes, D. S.; Sirvent, A.; Mercado, B. Q.; Ellman, J. A. *Org. Lett.* **2021,** *23,* 2836–2840. doi:10.1021/acs.orglett.1c00851
89. Fugami, K.; Hagiwara, S.; Oda, H.; Kosugi, M. *Synlett* **1998,** 477–478. doi:10.1055/s-1998-1710
90. Kang, S.-K.; Kim, J.-S.; Choi, S.-C.; Lim, K.-H. *Synthesis* **1998,** 1249–1251. doi:10.1055/s-1998-6086
91. Tang, Y.; Liu, K.; Zhang, J.; Liu, L.; Huang, T.; Li, C.; Tang, Z.; Chen, T. *J. Org. Chem.* **2021,** *86,* 11937–11947. doi:10.1021/acs.joc.1c01339
92. Kuo, C.-J.; Cheng, S.-J.; Chang, S.-T.; Liu, C.-H. *Eur. J. Org. Chem.* **2008,** 485–491. doi:10.1002/ejoc.200700772
93. Xu, T.; Zhou, X.; Han, Y.; Zhang, L.; Liu, L.; Huang, T.; Li, C.; Tang, Z.; Wan, S.; Chen, T. *Tetrahedron Lett.* **2022,** *97,* 153799. doi:10.1016/j.tetlet.2022.153799
94. Shi, Y.; Ji, C.-L.; Liu, C. *J. Org. Chem.* **2023,** *88,* 261–271. doi:10.1021/acs.joc.2c02295
95. Chang, Y.-C.; Kuo, C.-J.; Li, C.-S.; Liu, C.-H. *J. Organomet. Chem.* **2006,** *691,* 4982–4989. doi:10.1016/j.jorganchem.2006.08.058

96. Hu, F.; Xia, Y.; Liu, Z.; Ma, C.; Zhang, Y.; Wang, J. *Org. Biomol. Chem.* **2014,** *12,* 3590–3593. doi:10.1039/c4ob00590b
97. Wu, X.-X.; Shen, Y.; Chen, W.-L.; Chen, S.; Hao, X.-H.; Xia, Y.; Xu, P.-F.; Liang, Y.-M. *Chem. Commun.* **2015,** *51,* 8031–8033. doi:10.1039/c5cc02246k
98. Yang, K.; Song, Q. *J. Org. Chem.* **2016,** *81,* 1000–1005. doi:10.1021/acs.joc.5b02564
99. Li, Z.; Zheng, J.; Li, C.; Wu, W.; Jiang, H. *Chin. J. Chem.* **2019,** *37,* 140–147. doi:10.1002/cjoc.201800536
100. Hao, T.-T.; Liang, H.-R.; Ou-Yang, Y.-H.; Yin, C.-Z.; Zheng, X.-L.; Yuan, M.-L.; Li, R.-X.; Fu, H.-Y.; Chen, H. *J. Org. Chem.* **2018,** *83,* 4441–4454. doi:10.1021/acs.joc.8b00150
101. Gericke, K. M.; Chai, D. I.; Bieler, N.; Lautens, M. *Angew. Chem., Int. Ed.* **2009,** *48,* 1447–1451. doi:10.1002/anie.200805512
102. Naveen, K.; Nikson, S. A.; Perumal, P. T. *Adv. Synth. Catal.* **2017,** *359,* 2407–2413. doi:10.1002/adsc.201700169
103. Naveen, K.; Perumal, P. T.; Cho, D.-H. *Org. Lett.* **2019,** *21,* 4350–4354. doi:10.1021/acs.orglett.9b01543
104. Khanna, A.; Premachandra, I. D. U. A.; Sung, P. D.; Van Vranken, D. L. *Org. Lett.* **2013,** *15,* 3158–3161. doi:10.1021/ol401383m
105. Zhu, C.; Chen, P.; Zhu, R.; Jiang, G.; Lin, Z.; Wu, W.; Jiang, H. *Chem. – Asian J.* **2017,** *12,* 2991–2995. doi:10.1002/asia.201701241
106. Parthasarathy, K.; Jeganmohan, M.; Cheng, C.-H. *Org. Lett.* **2006,** *8,* 621–623. doi:10.1021/ol0527936
107. Burns, B.; Grigg, R.; Santhakumar, V.; Sridharan, V.; Stevenson, P.; Worakun, T. *Tetrahedron* **1992,** *48,* 7297–7320. doi:10.1016/s0040-4020(01)88268-5
108. Grigg, R.; Santhakumar, V.; Sridharan, V. *Tetrahedron Lett.* **1993,** *34,* 3163–3164. doi:10.1016/s0040-4039(00)93407-5
109. Zou, L.; Sun, W.; Khan, R.; Lv, H.; Yang, Y.; Xu, J.; Zhan, Y.; Fan, B. *Eur. J. Org. Chem.* **2019,** 746–752. doi:10.1002/ejoc.201801372
110. Cheng, M.; Yan, J.; Hu, F.; Chen, H.; Hu, Y. *Chem. Sci.* **2013,** *4,* 526–530. doi:10.1039/c2sc21335d
111. Vijayan, A.; Jumaila, C. U.; Baiju, T. V.; Radhakrishnan, K. V. *ChemistrySelect* **2017,** *2,* 5913–5916. doi:10.1002/slct.201701152
112. Zhou, H.; Chen, W.; Chen, Z. *Org. Lett.* **2018,** *20,* 2590–2594. doi:10.1021/acs.orglett.8b00776
113. Yang, S.-Y.; Han, W.-Y.; He, C.; Cui, B.-D.; Wan, N.-W.; Chen, Y.-Z. *Org. Lett.* **2019,** *21,* 8857–8860. doi:10.1021/acs.orglett.9b03565
114. Zhong, Y.; Wu, W.-Y.; Yu, S.-P.; Fan, T.-Y.; Yu, H.-T.; Li, N.-G.; Shi, Z.-H.; Tang, Y.-P.; Duan, J.-A. *Beilstein J. Org. Chem.* **2019,** *15,* 291–298. doi:10.3762/bjoc.15.26
115. Ji, X.; Gu, Y.; Cheng, C.; Wu, Z.; Zhang, Y. *Adv. Synth. Catal.* **2020,** *362,* 1496–1501. doi:10.1002/adsc.201901372
116. John, J.; U., I.; Suresh, E.; Radhakrishnan, K. V. *J. Am. Chem. Soc.* **2009,** *131,* 5042–5043. doi:10.1021/ja900477e
117. Prasad, B. A. B.; Buechele, A. E.; Gilbertson, S. R. *Org. Lett.* **2010,** *12,* 5422–5425. doi:10.1021/ol102270r
118. Prakash, P.; Jijy, E.; Preethanuj, P.; Pihko, P. M.; Sarath Chand, S.; Radhakrishnan, K. V. *Chem. – Eur. J.* **2013,** *19,* 10473–10477. doi:10.1002/chem.201301475
119. Santhini, P. V.; Nimisha, G.; John, J.; Suresh, E.; Varma, R. L.; Radhakrishnan, K. V. *Chem. Commun.* **2017,** *53,* 1848–1851. doi:10.1039/c6cc08753a
120. Santhini, P. V.; Smrithy, A. S.; Irfana Jesin, C. P.; Varughese, S.; John, J.; Radhakrishnan, K. V. *Chem. Commun.* **2018,** *54,* 2982–2985. doi:10.1039/c7cc09521j
121. Ge, G.-C.; Mo, D.-L.; Ding, C.-H.; Dai, L.-X.; Hou, X.-L. *Org. Lett.* **2012,** *14,* 5756–5759. doi:10.1021/ol302586m
122. Ge, G.-C.; Ding, C.-H.; Hou, X.-L. *Org. Chem. Front.* **2014,** *1,* 382–385. doi:10.1039/c4qo00030g
123. Wu, W.; Li, C.; Li, J.; Jiang, H. *Org. Biomol. Chem.* **2018,** *16,* 8495–8504. doi:10.1039/c8ob01799a

License and Terms

BEILSTEIN JOURNAL OF ORGANIC CHEMISTRY

Enolates ambushed – asymmetric tandem conjugate addition and subsequent enolate trapping with conventional and less traditional electrophiles

Péter Kisszékelyi and Radovan Šebesta*

Review

Open Access

Address:
Department of Organic Chemistry, Faculty of Natural Sciences, Comenius University Bratislava, Mlynská dolina, Ilkovičova 6, 842 15 Bratislava, Slovakia

Email:
Radovan Šebesta* - radovan.sebesta@uniba.sk

* Corresponding author

Keywords:
asymmetric catalysis; conjugate addition; electrophile; enolate; tandem reaction

Beilstein J. Org. Chem. **2023,** *19,* 593–634.
https://doi.org/10.3762/bjoc.19.44

Received: 03 February 2023
Accepted: 21 April 2023
Published: 04 May 2023

This article is part of the thematic issue "Catalytic multi-step domino and one-pot reactions".

Guest Editor: S. Tsogoeva

Abstract

Metal enolates are useful intermediates and building blocks indispensable in many organic synthetic transformations. Chiral metal enolates obtained by asymmetric conjugate additions of organometallic reagents are structurally complex intermediates that can be employed in many transformations. In this review, we describe this burgeoning field that is reaching maturity after more than 25 years of development. The effort of our group to broaden possibilities to engage metal enolates in reactions with new electrophiles is described. The material is divided according to the organometallic reagent employed in the conjugate addition step, and thus to the particular metal enolate formed. Short information on applications in total synthesis is also given.

Introduction

The formation of complex chiral molecules is a crucial task of organic synthesis that enables the synthesis of pharmaceuticals, crop-protecting agents, or advanced materials. Their syntheses often involve numerous reaction steps requiring laborious isolation and intermediate product purification steps. An important strategy for improving syntheses' effectiveness is the concept of domino reactions, cascade, or tandem reactions. These transformations combine several reactions into a sequence that uses functionalities generated in previous steps without isolating intermediates [1]. Stabilized carbon-based nucleophiles, or in other words, conjugate bases of weak C–H acids, are termed enolates, and they participate in a large array of organic synthetic transformations. Enolates are usually formed by deprotonation of the corresponding organic compound. However, other synthetic approaches for their generation exist, such as cleavage of enol ethers and esters, halogen–metal exchange, transmetalations, and conjugate additions to α,β-unsaturated carbonyl compounds [2]. In particular, the last-mentioned method is

highly synthetically relevant. This approach has the advantage of being more selective and affording more molecular complexity in one step. In addition, transition-metal catalysis allows the introduction of stereogenic information, thus leading to chiral products. Enolate species are uniquely positioned for reactivity with a broad array of electrophiles and thus allowing quick and efficient construction of highly complex structures from readily available starting materials. Various polar organometallic reagents were successfully employed in asymmetric conjugate additions (ACA) [3-9], mainly organozinc [10], Grignard [11-13], trialkylaluminum [14], or organozirconium reagents [15]. Additions with these reagents lead to corresponding zinc, magnesium, aluminum, and zirconium enolates, which all possess helpful and, to an extent, specific reactivity characteristics. Interesting boron and silicon enolates can be generated by asymmetric conjugate boration [16], or silylation [17]. From several potentially catalytically active transition metals, copper combines beneficial properties for both activation of the Michael acceptor and the formation of intermediate organocuprates from stoichiometric organometallic reagents [18]. Metal enolates formed in this way can react in many transformations (Scheme 1) [19,20]. It has been documented that metal enolates from conjugate additions engaged in aldol, and Mannich-type reactions, Michael addition, nucleophilic substitutions, cyclopropanations, and reactions with carbocations. The field of asymmetric conjugate addition with its extension into enolate trapping reactions began to develop approximately in 1996. In this review article, we analyze more recent realizations of this strategy focusing on lesser-studied trapping reactions and works after 2010. We also present here our attempts to broaden the scope of these enolate trapping reactions by using different types of electrophilic reagents.

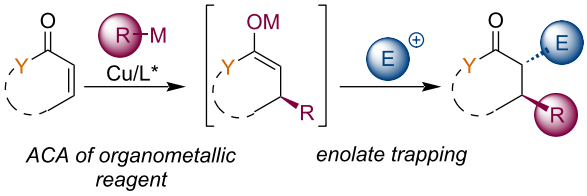

Scheme 1: General scheme depicting tandem reactions based on an asymmetric conjugate addition followed by an enolate trapping.

Review

Conjugate additions with organozinc reagents

Following the seminal work of Feringa in 1997 [21], the tandem asymmetric organozinc conjugate addition followed by subsequent aldol reaction was scarcely applied in the last decade. Welker and Woodward studied the reaction of zinc enolates **2** with chiral acetals **3** (Scheme 2) [22]. The Lewis acid ($TiCl_4$ or TMSOTf) promoted trapping gave the aldol adducts **4** in good to excellent diastereoselectivity (up to a single diastereomer),

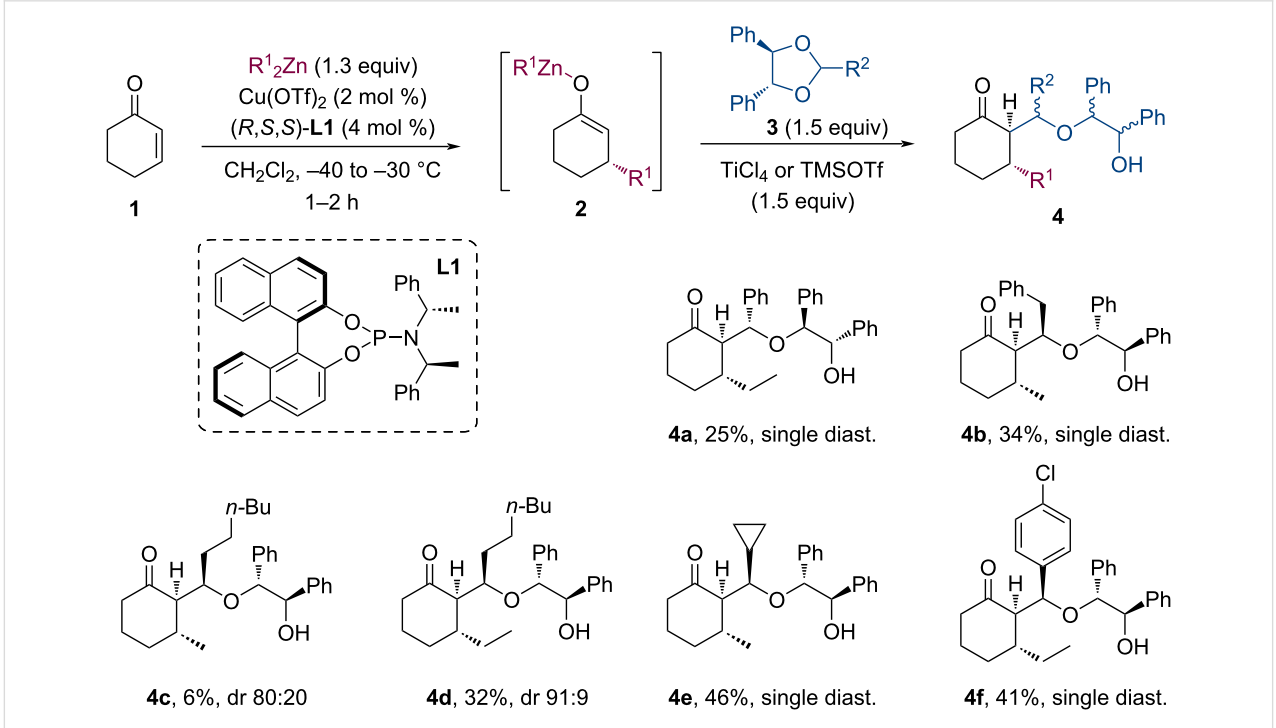

Scheme 2: Cu-catalyzed tandem conjugate addition of R_2Zn/aldol reaction with chiral acetals.

but the yields were relatively low (25–44%). To overcome this limitation, the authors used TMSOTf to prepare and isolate the corresponding silyl enol ethers, which were later successfully applied in the Mukiyama aldol reaction to gain the originally desired aldol adducts with improved yields and still good dr. Finally, the cerium ammonium nitrate (CAN) promoted one-step oxidative removal of the chiral auxiliary group was also successfully demonstrated.

In 2012, Aikawa et al. presented their work on the asymmetric desymmetrization of cyclopentene-1,3-diones **5** (Scheme 3) [23]. Following the $Cu(OTf)_2$-catalyzed conjugate addition of R_2Zn, the enolate **6** was trapped by several aromatic aldehydes **7**. These complex chiral cyclopentane derivatives **8** bearing all-carbon quaternary stereocenters were isolated in excellent yields and high diastereoselectivity. The authors have shown that catalyst loadings as low as 0.5 mol % can still be sufficient to promote the highly stereoselective reaction.

Similarly to aldol reactions, Mannich-type additions are also suitable to trap the metal enolate. González-Gómez et al. studied the tandem conjugate addition of dialkylzincs to cyclic enones (**9**, **12**) and the subsequent reaction of the enolate with *N*-*tert*-butanesulfinylimines **10** (Scheme 4) [24-26]. Their method was applied to a broad range of substrates (5–7-membered rings) with equally high diastereoselectivity and good to excellent yields. In most cases, the authors detected only a single diastereomer in the crude reaction mixture (NMR). Using the enantiomeric form of the ligand or the chiral sulfoximine reagent, four diastereomeric β-aminoketones can be produced in excellent enantiomeric purity. Further transformations of the products were demonstrated in several examples, including reduction, acidic deprotection and subsequent base-mediated cyclization, or Baeyer–Villiger oxidation.

At about the same time, Huang and co-workers have developed similar asymmetric tandem sequences using acyclic enones **14** [27]. Their tandem conjugate addition/Mannich reaction methodology offers access to various non-cyclic β-aminoketones **16** with multiple contiguous stereocenters in high diastereo- and enantioselectivity (Scheme 5a). Additionally, chiral isoindolinones **18** and 2,3,4-trisubstituted azetidines **19** were also synthesized using this methodology (Scheme 5b).

Nitronate anions were also found suitable for Mannich-type trapping reactions [28,29]. Anderson and co-workers accomplished several Cu-catalyzed conjugate additions of R_2Zn to nitroolefins **20**, followed by subsequent reaction with *p*-methoxyphenyl (PMP)-protected imines **21** (Scheme 6A). By varying the reaction conditions, the *syn-anti* and the *syn-syn* diastereomers can be prepared with good yields and excellent stereoselectivity. Using nitroacrylate **23**, the authors have also

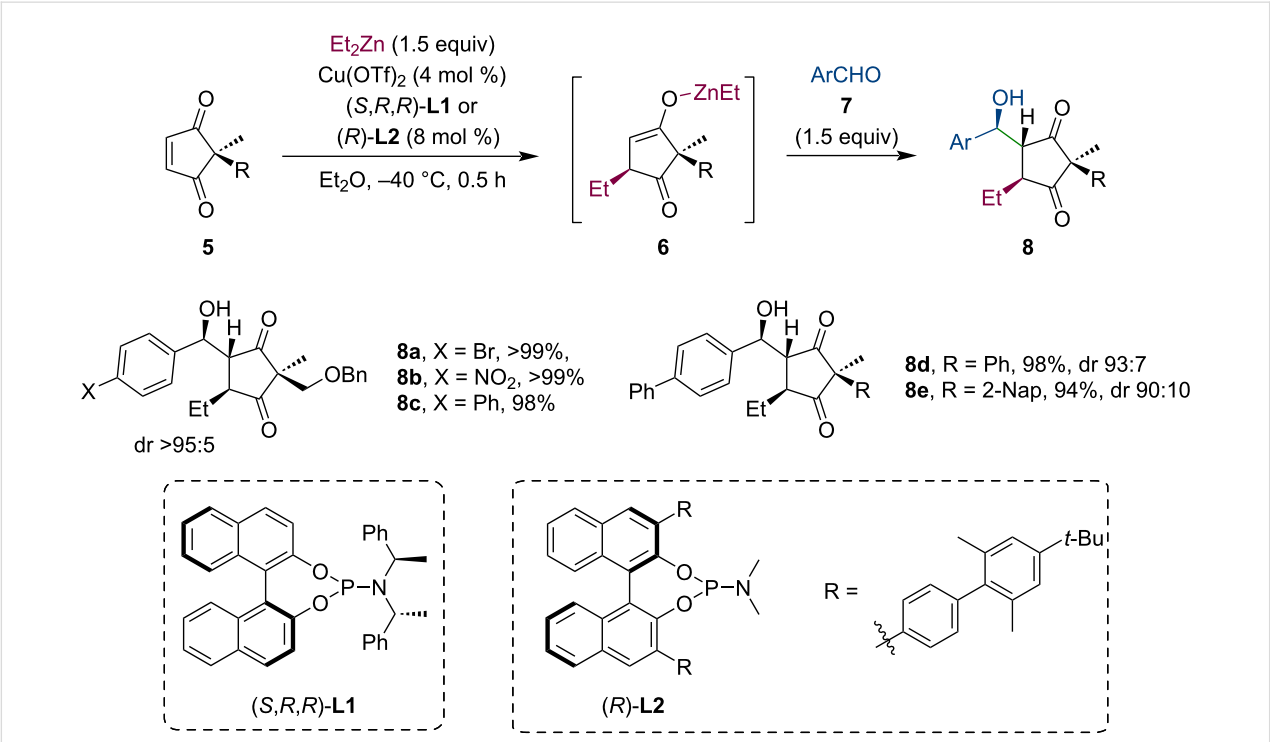

Scheme 3: Cu-catalyzed asymmetric desymmetrization of cyclopentene-1,3-diones using a tandem conjugate addition/aldol reaction sequence.

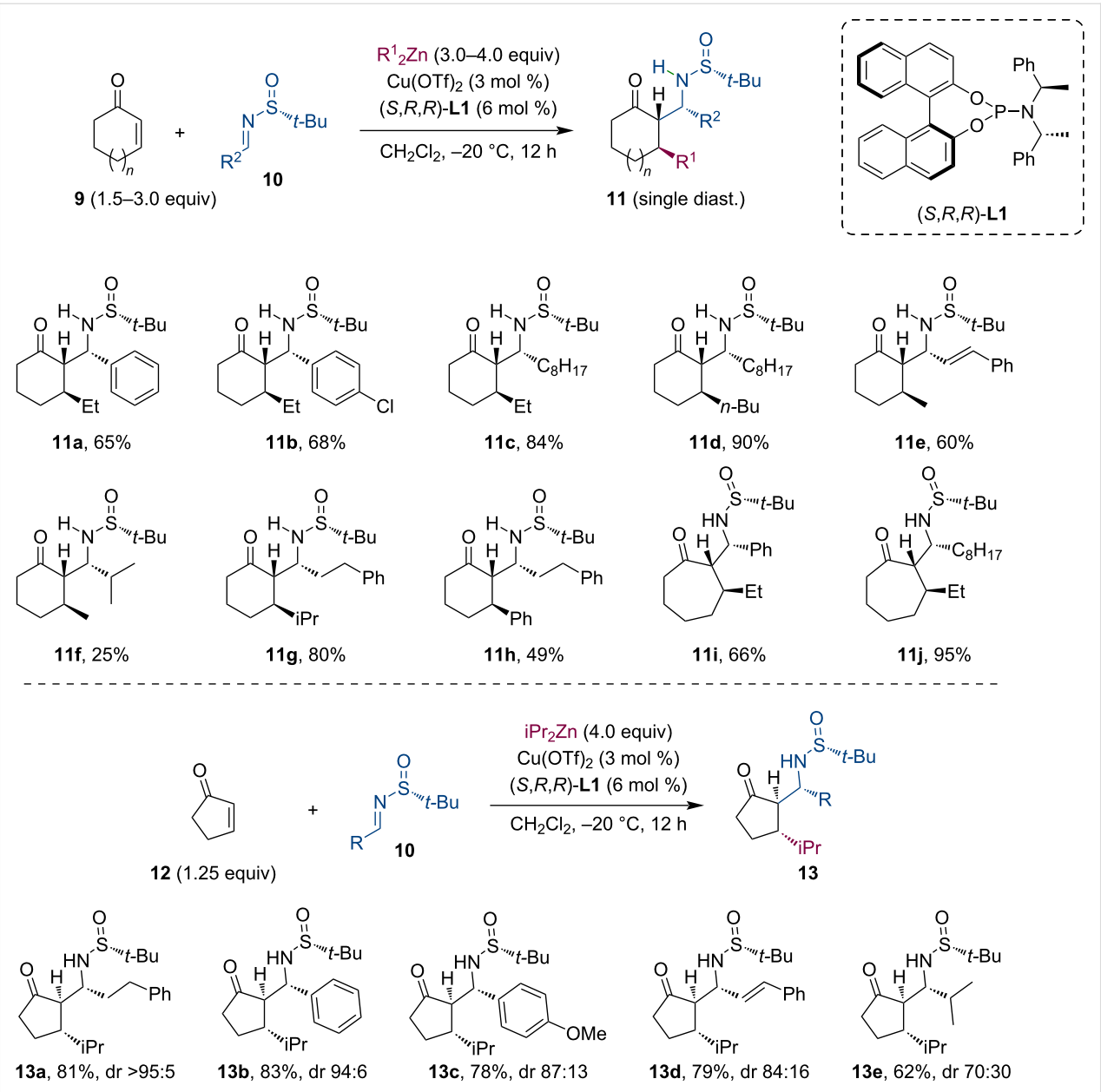

Scheme 4: Stereocontrolled assembly of dialkylzincs, cyclic enones, and sulfinylimines utilizing a Cu-catalyzed tandem conjugate addition/Mannich reaction sequence.

demonstrated a tandem conjugate addition/nitro-Mannich/lactamization three-step reaction sequence resulting in trisubstituted nitropyrrolidinones **24** with exceptional enantioselectivity (Scheme 6B).

In contrast to conjugate additions to nitroolefins, these activated alkenes can also be utilized in the enolate trapping step. In the last decade, several highly stereoselective methodologies have been published that demonstrate the Cu- or Ni-catalyzed conjugate addition of organozincs to α,β-unsaturated ketones **14** followed by the reaction of the metal enolate with a nitroolefin (**20**) (Table 1) [30-33]. These reactions were facilitated by different ligand families (phosphite/phosphine-pyridine amide, phosphine-sulfoxide, phosphoramidite, MINBOL, see Figure 1) and they usually showed excellent diastereoselectivity (dr >20:1). The catalytic systems even with low catalyst loadings tolerated both electron-donating and withdrawing groups on the aromatic substituents. Therefore, numerous structurally distinct substrates were successfully utilized.

Other than nitroolefins, Liao and co-workers have observed a side reaction of the α,β-unsaturated ketone **26** and the enolate

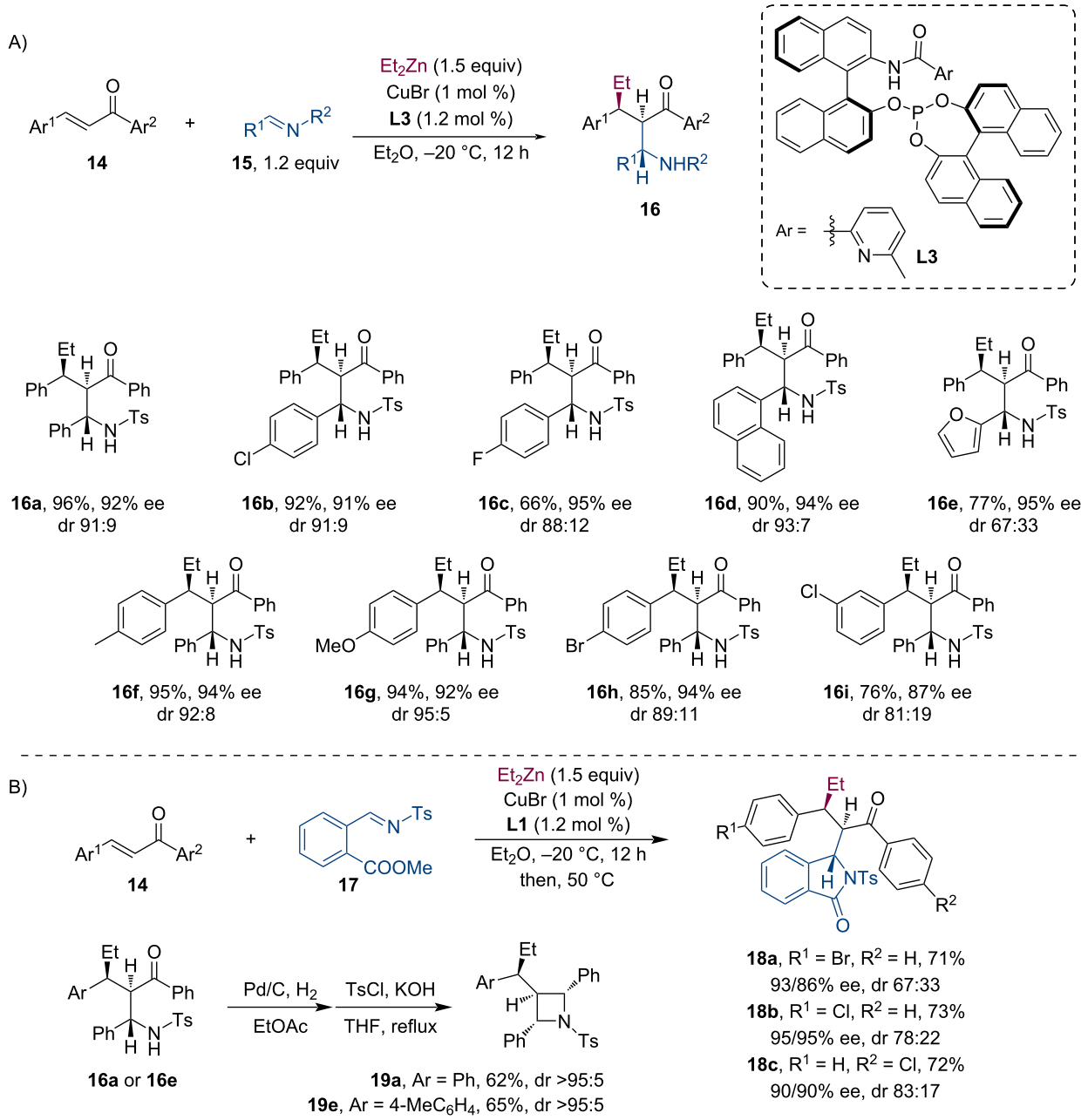

Scheme 5: Cu-catalyzed tandem conjugate addition/Mannich reaction (A). Access to chiral isoindolinones and trisubstituted azetidines with contiguous stereocenters (B).

27 when they studied the conjugate addition of R_2Zn reagents to chalcone and its derivatives (Scheme 7A) [34]. Encouraged by this, they have also attempted an intramolecular tandem conjugate addition/Michael reaction sequence, which has resulted in the expected cyclization product **30** in a diastereopure form (Scheme 7B).

Zinc enolates readily react with allyl iodides **31** or the structurally similar Stork–Jung vinylsilane reagents **33**. Kawamura et al. performed zinc enolate trapping reactions using ligand **L10**, a chiral quinoline-based N,N,P-ligand (Scheme 8A) [35]. The authors have concluded that the strict control of the amount of organozinc reagent added is essential to avoid side-product formation (diallylation) because the strongly basic R_2Zn can form the enolate from the monoallylated product **32**. Therefore, using only 1 equiv of dialkylzinc, the desired allylated products **32** were isolated in good yields and excellent diastereo- and enantioselectivity. Soon after, Jarugumilli et al.

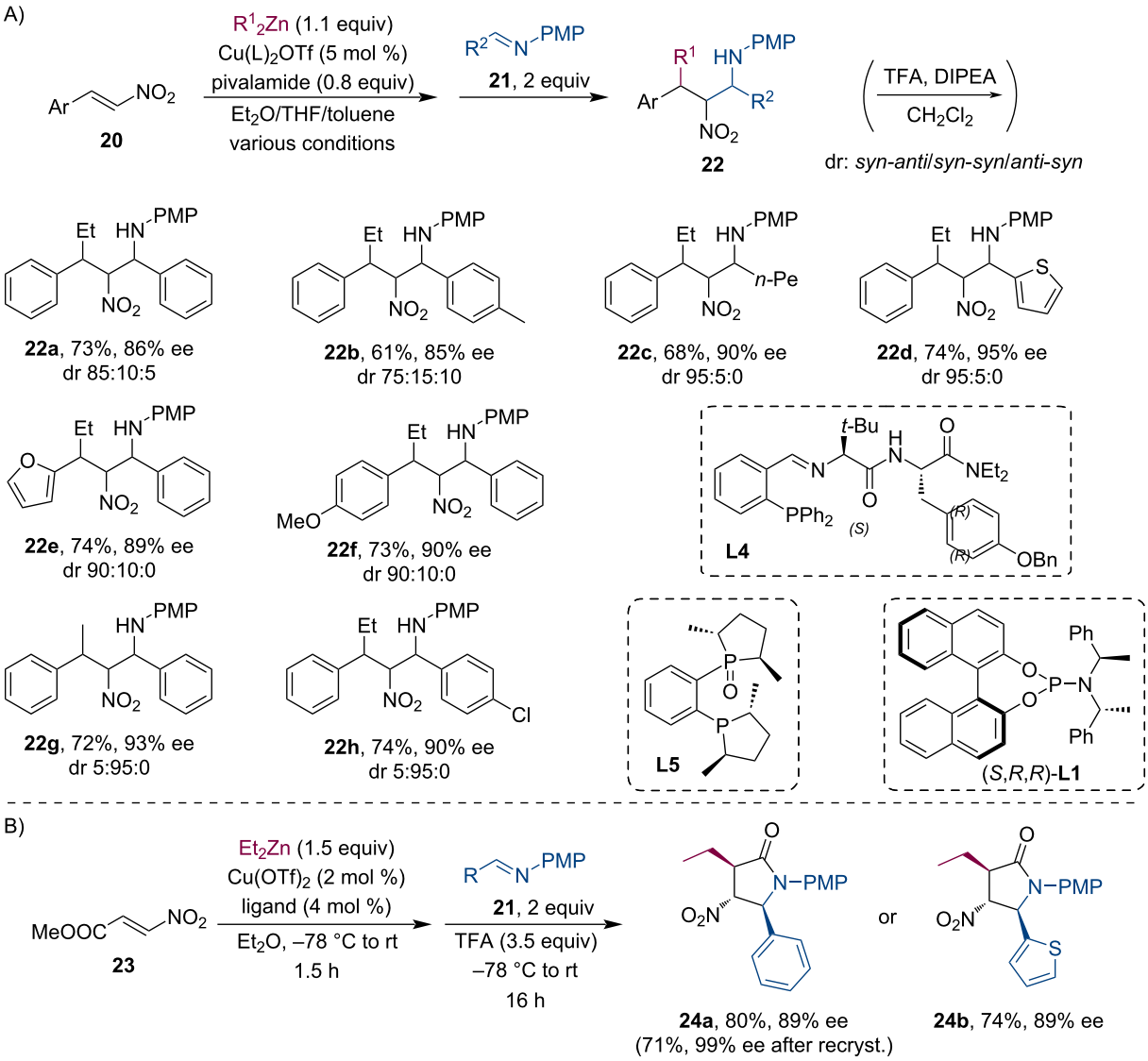

Scheme 6: Cu-catalyzed tandem conjugate addition/nitro-Mannich reaction (A) with *syn–anti* or *syn–syn* selectivity (the products were isolated as trifluoroacetamide). Additional in situ lactamization results in nitropyrrolidinones with excellent stereoselectivity (B).

Table 1: Tandem reactions composed of ACA of R_2Zn and enolate trapping with nitroalkenes.

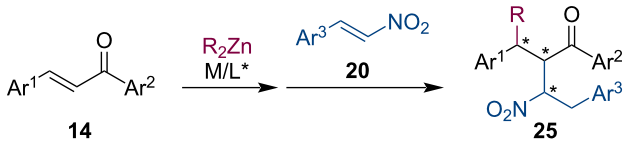

Reference	Catalyst (mol %)	Ligand (mol %)	Conditions	Yield (%)	ee (%)
Huang, 2011 [30]	CuCl (1.0)	**L3** (1.2)	Et_2O, – 20 °C, 24 h	52–90	91–97
Kang, 2011 [31]	$Cu(OTf)_2$ (3.0)	**L6** (6.0)	toluene, –40 °C	25–89	76–96
Uang, 2015 [32]	$Ni(acac)_2$ (0.5)	**L7** (12.5)	CH_3CH_2CN, –50 °C; then, 0 °C, 3 h	66–84	91–97
Hu, 2019 [33]	CuCl (2.0)	**L8** (2.5)	toluene, 0 °C, 12 h	60–88	90–97

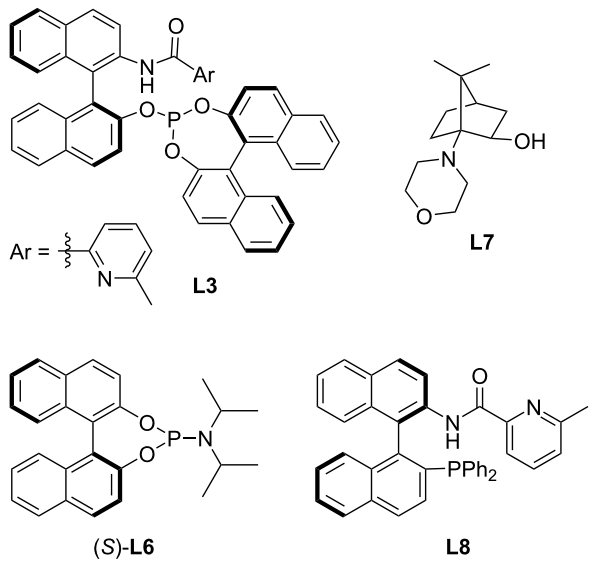

Figure 1: Various chiral ligands utilized for the tandem conjugate addition/Michael reaction sequences.

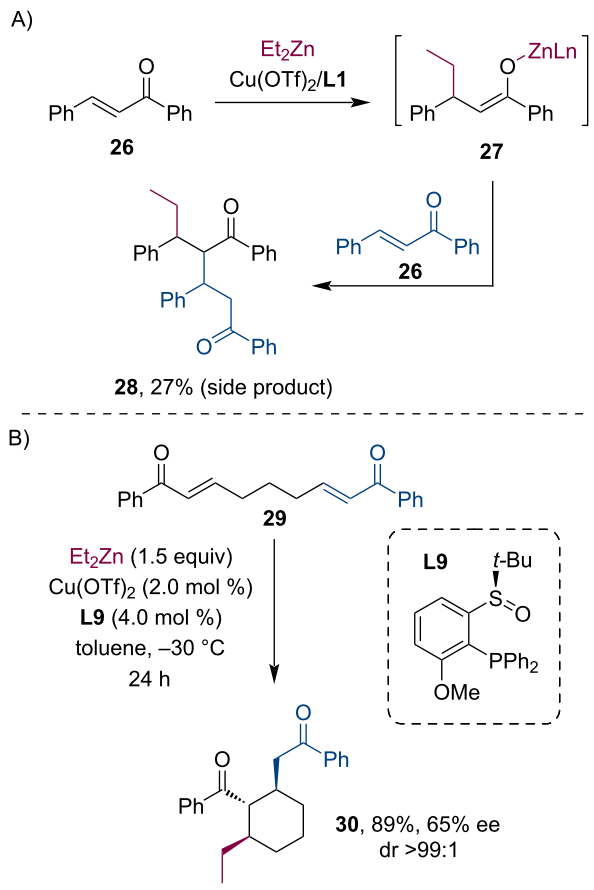

Scheme 7: Cu-catalyzed tandem conjugate addition/Michael reaction: side-product formation with chalcone (A) and application to an intramolecular cyclization reaction (B).

investigated the enolate-trapping tandem sequence using various vinylsilanes **33** (Scheme 8B), allyl halides **35**, and benzyl bromide (**37**) (Scheme 8C) [36]. Although the asymmetric conjugate addition step routinely provided excellent selectivity (93–96% ee), only a moderate to good diastereomeric ratio was achieved.

Entrapping of the Zn enolate directly with acetyl chloride was found inefficient and led to a mixture of C-, O-, and diacylated products as described by Murphy and co-workers [37]. Encouraged by the work of Noyori on the activation of Li enolates using Me_2Zn [38], they have tried to facilitate the enolate trapping by adding MeLi (1.05 equiv), which indeed led to a significant increase in yield and selectivity due to the high reactivity of the lithium dialkyl zincate enolate. Various 1,3-diketones **39** were prepared using this method with good yields and excellent enantioselectivities while only the *trans* diastereomers were detected (Scheme 9A). Furthermore, the authors have also demonstrated a four-component coupling reaction: by simply increasing the amount of the organolithium reagent (2.05 equiv) used for the activation of the Zn enolate, β-hydroxyketones **40** were gained via 1,2-addition of the zincate nucleophile (R_3Zn^-) to the ketone with moderate yields but still good stereoselectivities (Scheme 9B).

In 2018, Wang and co-workers extended the group of applicable electrophiles for the zinc enolate-based tandem reactions. Following the conjugate addition of Et_2Zn to acyclic α,β-unsaturated ketones **41**, they have shown that several electrophilic SCF_3 reagents (e.g., **43**) are suitable for enolate trapping (Scheme 10) [39]. This way, the strong electron-withdrawing SCF_3 group can be efficiently introduced stereoselectively allowing access to structurally diverse compounds with altered pharmacochemical properties. In several cases the α-SCF_3-substituted ketones **44** were isolated in good yields and enantioselectivities but with low diastereoselectivities.

Even though no asymmetric catalyst was involved, Kawano et al. recently demonstrated an attractive one-pot procedure for preparing complex bicyclic and bridged compounds utilizing catalytically generated bicyclic Zn enolates [40].

Welker et al. have introduced the Pd-catalyzed trapping of zinc enolates with various vinyloxiranes [41]. This way, several allylic alcohols **45** were synthesized with moderate yields and excellent enantioselectivities (up to 98%) but low *trans*/*cis* selectivity (Scheme 11). Organoaluminum reagents (Me_3Al, Et_3Al) were also compatible with the reaction, however, they gave lower yields than the corresponding organozincs. The authors have also shown that these products are suitable for forming [6,7]-bicyclic adducts.

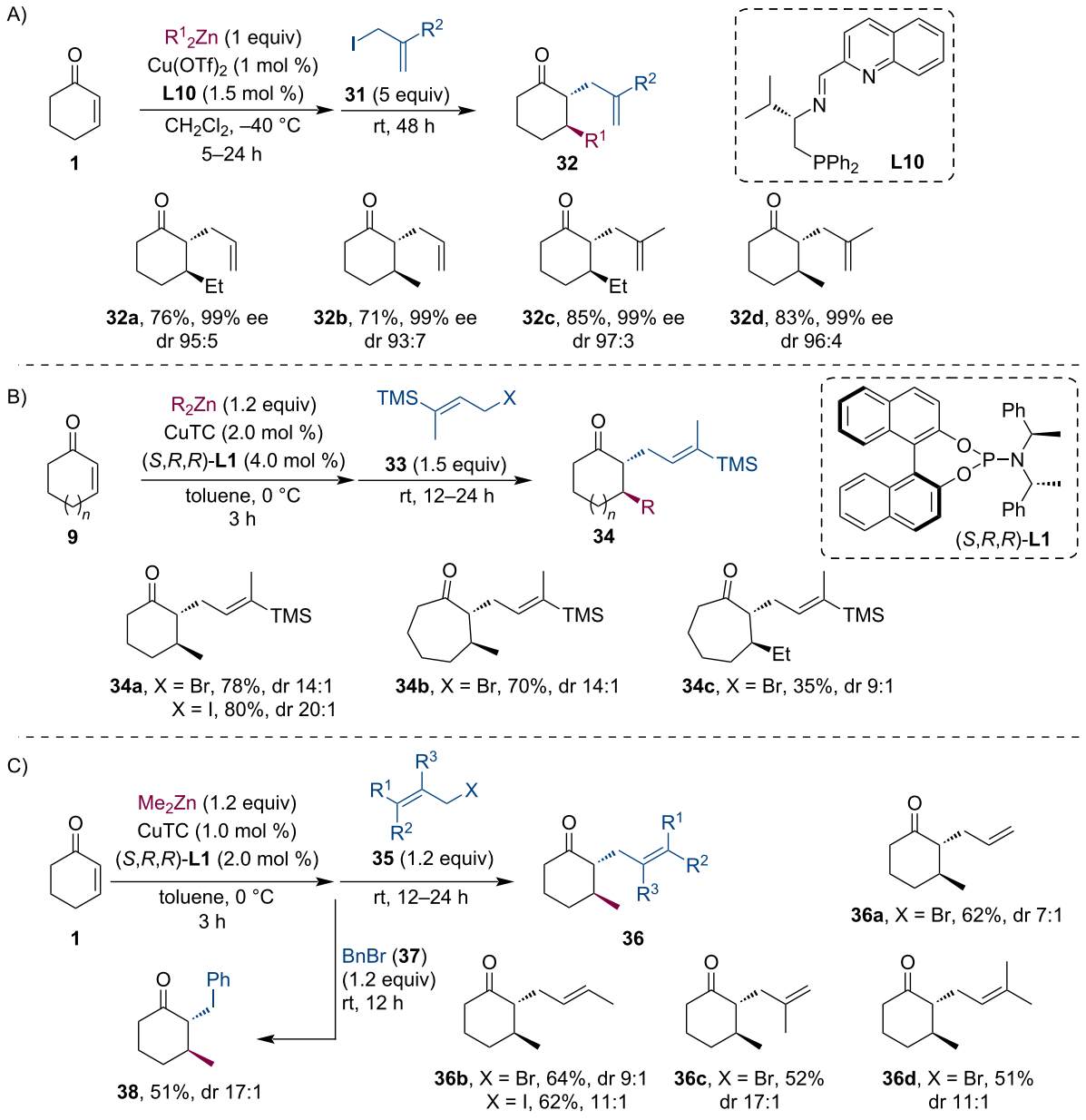

Scheme 8: Zn enolate trapping using allyl iodides (A), Stork–Jung vinylsilane reagents (B), and allyl bromides or benzyl bromide (C).

Conjugate addition with Grignard reagents

Feringa and co-workers realized the tandem conjugate addition of Grignard reagents to 4-chlorocrotonates **46** [42]. The enolate **47**, which was formed in this process, underwent an intramolecular nucleophilic substitution to form cyclopropane derivatives. Thioesters, esters as well as ketones were compatible with this process. The chiral ligand **L12** afforded the highest enantioselectivities of up to 98% ee (Scheme 12).

Conjugate addition of Grignard reagents to coumarin (**49**) generated the corresponding magnesium enolates **50** [43]. In one instance, this enolate was trapped by benzaldehyde (**51**) (Scheme 13a). Related to this work, Feringa´s team realized also the conjugate addition to chromone (**53**) [44]. The enolate was again trapped with benzaldehyde in an aldol reaction (Scheme 13b).

Naphthol derivatives **55** bearing an α,β-unsaturated ester group undergo a copper(I)-catalyzed asymmetric conjugate addition. The magnesium enolates **56** then participated in a copper(II)-mediated intramolecular oxidative coupling to afford benzo-fused spirocyclic cycloalkanones **57** (Scheme 14) [45].

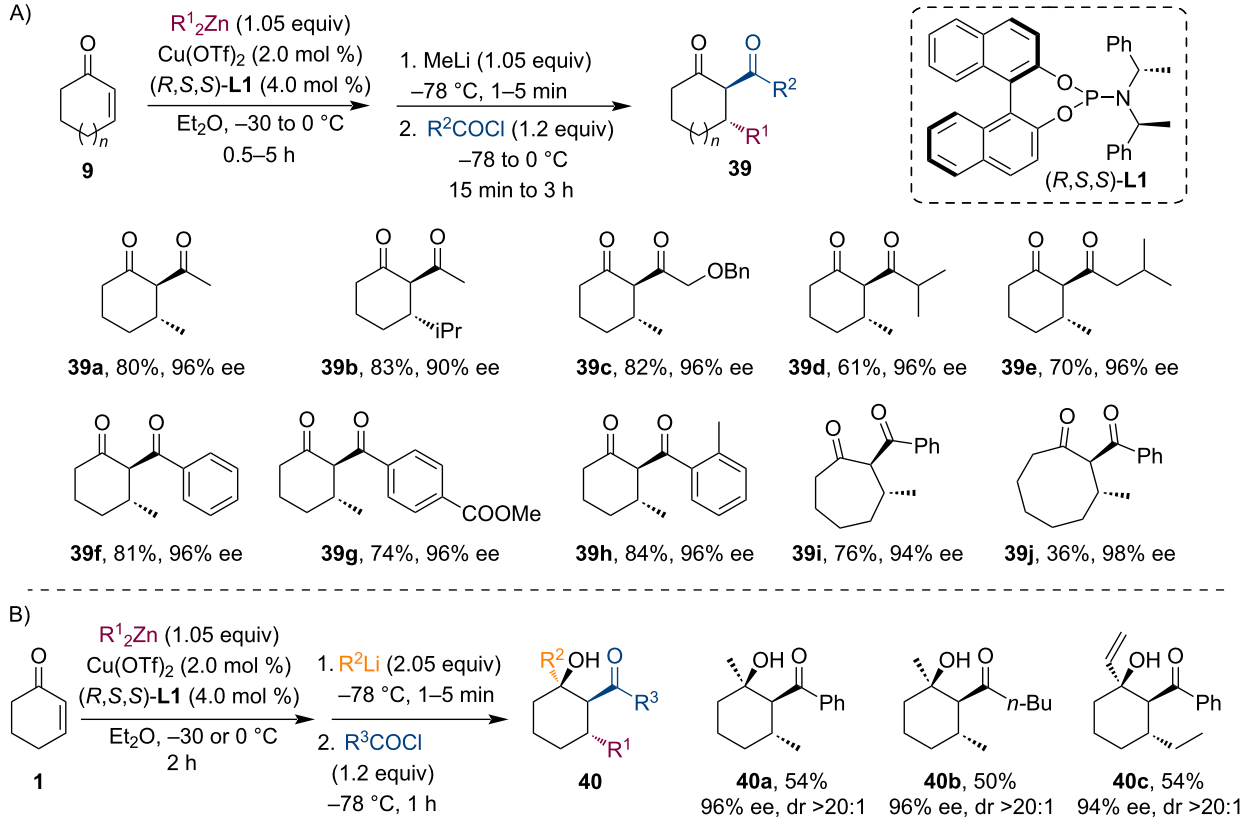

Scheme 9: Cu-catalyzed tandem conjugate addition/acylation through Li R_2Zn enolate (A). A four-component coupling reaction using nucleophilic trialkyl zincate (B).

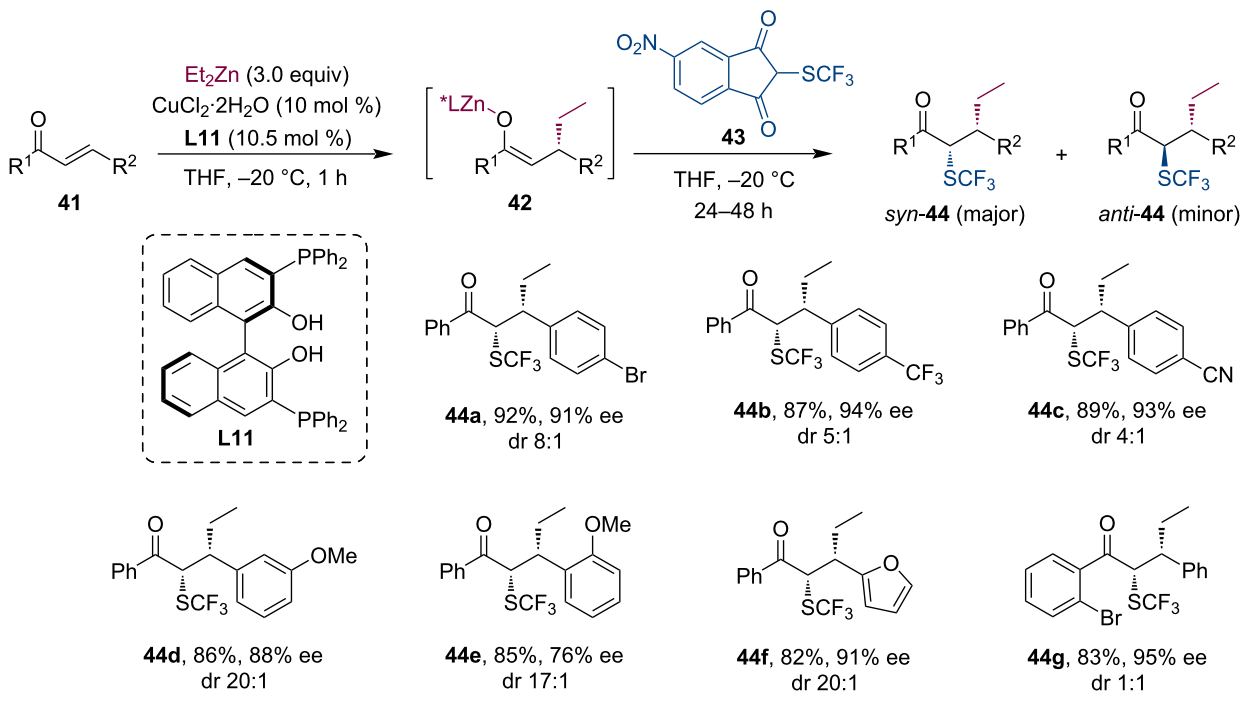

Scheme 10: Selected examples for the Cu-catalyzed tandem conjugate addition/trifluoromethylthiolation sequence.

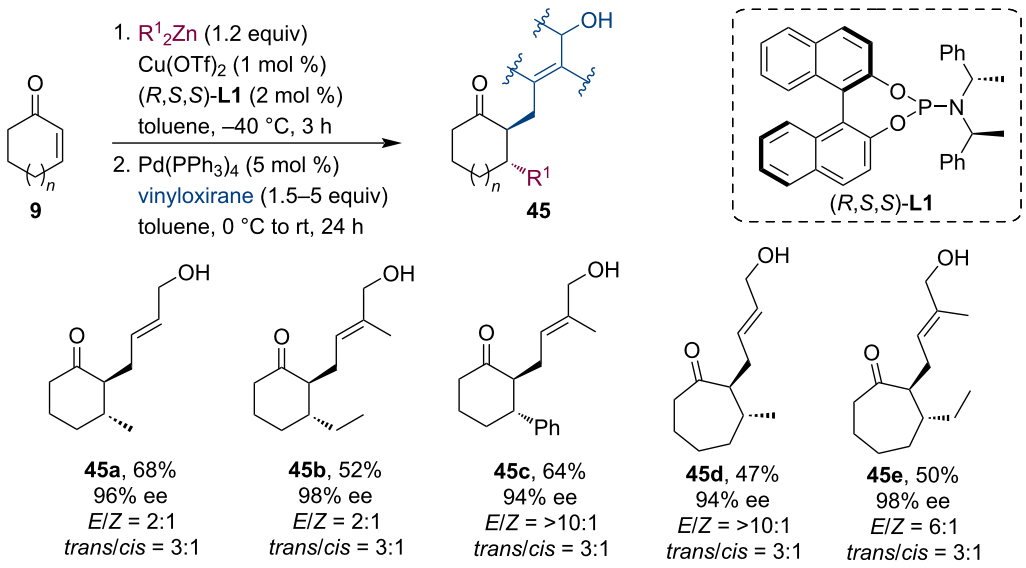

Scheme 11: Zn enolates trapped by vinyloxiranes: synthesis of allylic alcohols.

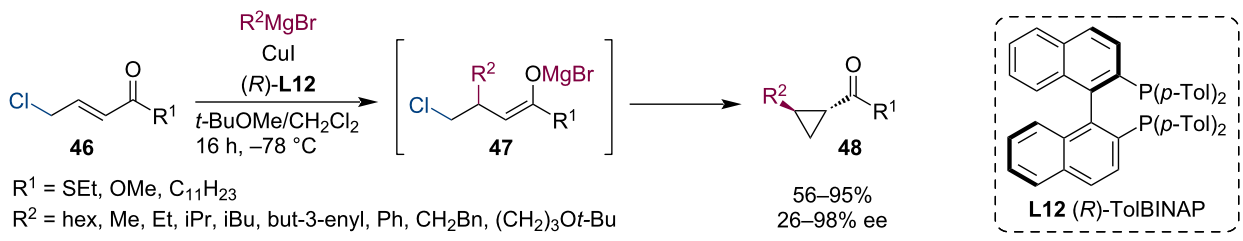

Scheme 12: Stereoselective cyclopropanation of Mg enolates formed by ACA of Grignard reagents to chlorocrotonates.

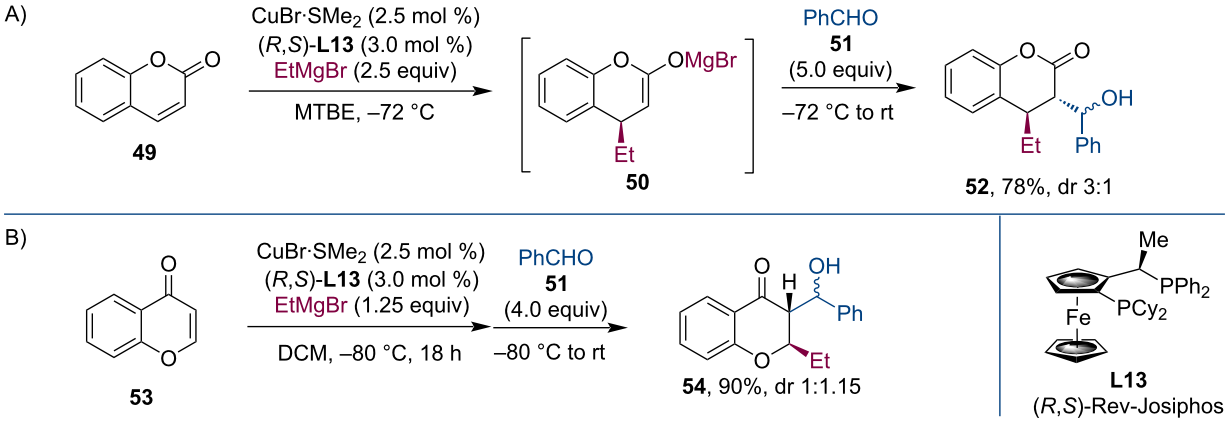

Scheme 13: Domino aldol reactions of Mg enolates formed from coumarin and chromone.

Our team became interested in domino reactions of metal enolates generated by Cu-catalyzed asymmetric conjugate additions of Grignard reagents. At the outset of our studies, there were works in which dialkylzinc additions were utilized to generate zinc enolates, and these enolates were then trapped with chiral sulfonylimines [24]. Specifically, we asked whether these magnesium enolates could be trapped with imines or their synthetic equivalents. Furthermore, we wanted to develop an

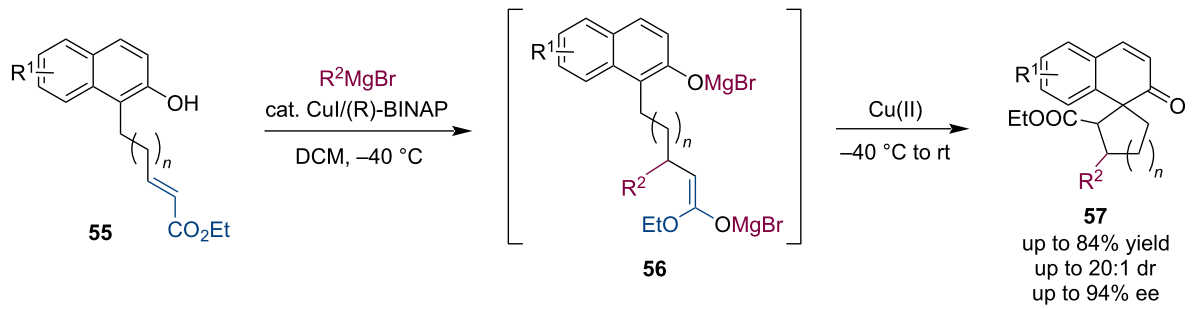

Scheme 14: Oxidative coupling of ACA-produced Mg enolates.

enantioselective and diastereoselective process without adding chirality elements within the reagents.

For our initial studies, we have selected the well-studied cyclic enones as substrates and the Taniaphos ligand (**L14**) that has been shown to impart high levels of enantioselectivity for these ketones [46]. We performed the conjugate addition for 2 h and then added imine **58** having a tosyl protecting group. The workup allowed the isolation of domino products **59** as a mixture of diastereomers with dr 3:2 and enantiomeric purities up to 97:3 er (Scheme 15) [47]. These experiments showed that the concept of interception of magnesium enolates, derived from Cu-ACA, with imines can be realized. As it could have been predicted, chiral enolates reacted with high diastereoselectivity with their *Si*-face (attack *anti* to the R group introduced during the conjugate addition). On the other hand, a typical problem of these reactions was also revealed. The diastereoselectivity with respect to the addition to the imine was only very modest.

To address the problem of low facial selectivity of the imine addition, we continued our study with several imines bearing various *N*-protecting groups [48]. We have argued that this protecting group could influence the enolate addition. Indeed, an effect of the nitrogen protecting group was observed. Interestingly, small sulfonyl-based protecting groups led to the (*R,R,S*)-diastereoisomer of the product **61**. On the other hand, the sterically bulky diphenylphosphorane group afforded the (*R,R,R*)-diastereoisomer **63** as the main product. The large protecting group likely overrides the repulsive interaction between the enolate and a phenyl group in a preferred synclinal Mg-bound arrangement of the reagents (Scheme 16).

Within the framework of these domino reactions, we have mainly employed ferrocenyl phosphane ligands such as Taniaphos or Josiphos. In collaboration with Prof. Schmalz from Cologne University, we have also tested phosphite-

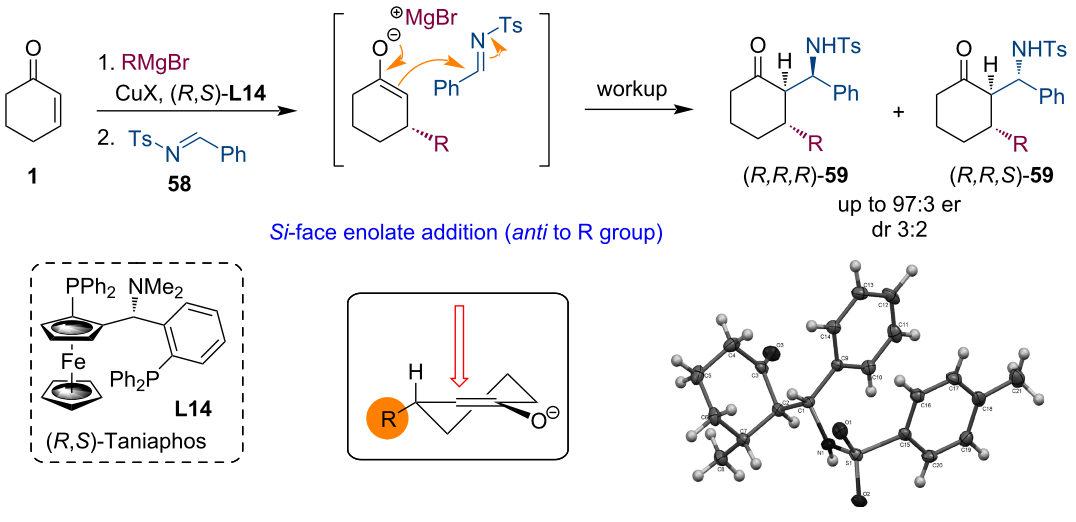

Scheme 15: Tandem ACA of Grignard reagents to enones and Mannich reaction.

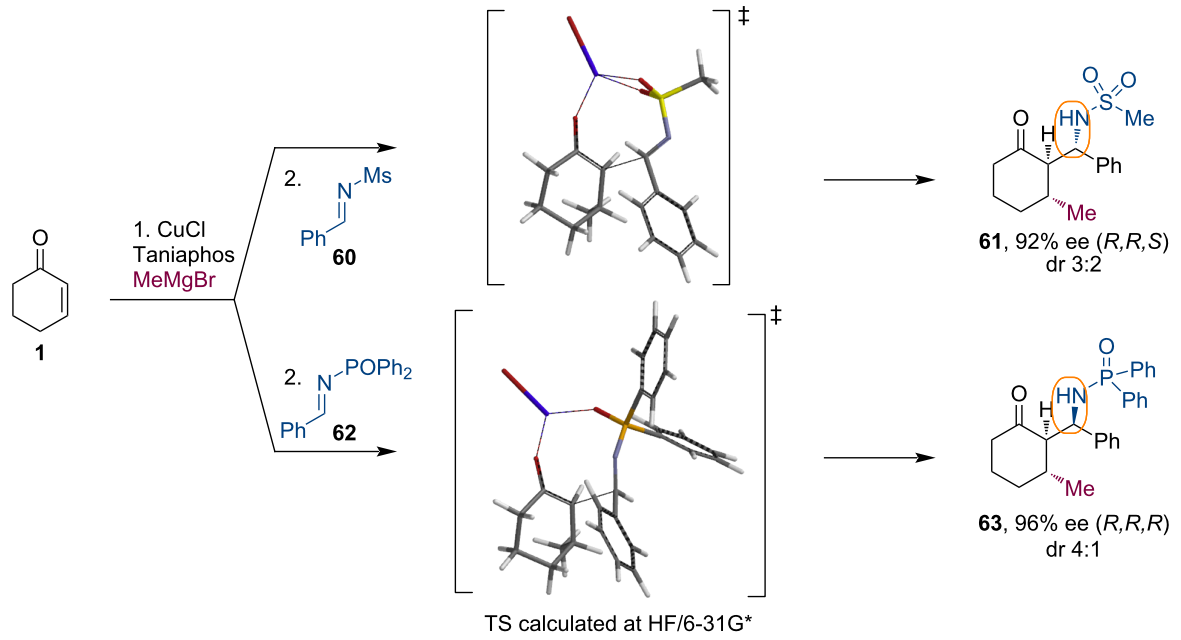

Scheme 16: Diastereodivergent Mannich reaction of Mg enolates with differently *N*-protected imines.

phosphine ligands (e.g., **L15**) from their lab. The advantage of these ligands is that they can also promote the conjugate additions of aryl-based or branched Grignard reagents (Scheme 17) [49].

Further extending this methodology, we have investigated formaldehyde imine equivalents. These kinds of imines are not readily available, but they are highly important synthetic building blocks providing an aminomethyl moiety upon adding nucleophiles. Protected formaldehyde aminals are useful synthetic equivalents to formaldehyde imines. The imine functionality can be unmasked (**68**) in the reaction medium by Lewis acids such as $TiCl_4$. The formed Mg enolates **66** readily react with the transient iminium species **68** to afford the corresponding aminomethylation products **69** (Scheme 18) [50]. As seen from Table 2, the diastereoselectivities were somewhat compromised compared to what one can expect from the reactions of cyclic enolates. This erosion was likely caused by Lewis acid-mediated epimerization.

Guénée et al. described the allylation, benzylation, and propargylation of magnesium enolates. These enolates were generated

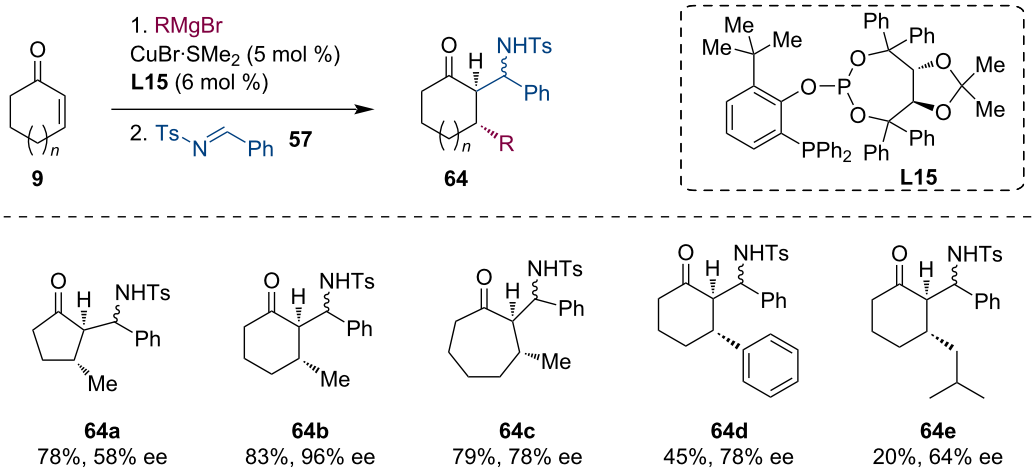

Scheme 17: Tandem Grignard–ACA–Mannich using Taddol-based phosphine-phosphite ligands.

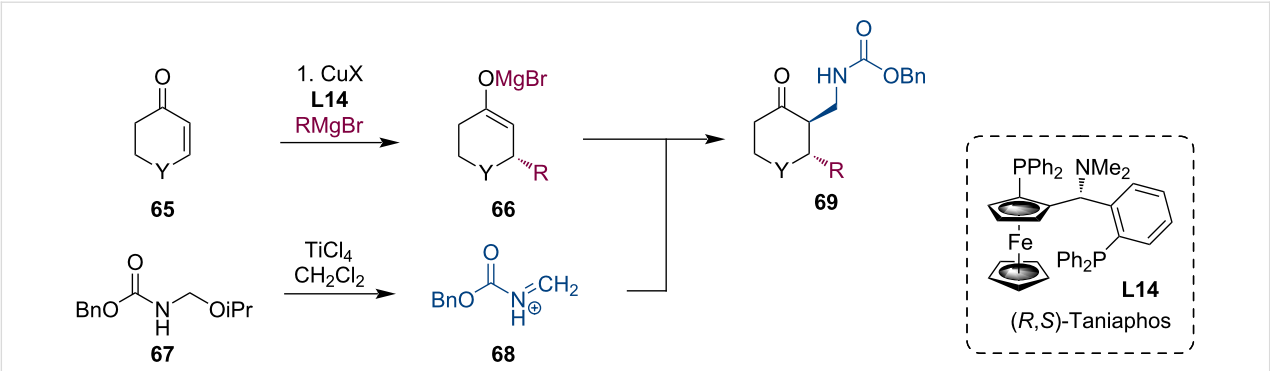

Scheme 18: Tandem reaction of Mg enolates with aminomethylating reagents.

Table 2: Domino aminomethylation of cyclic ketones with Grignard reagents.

RMgX	Yield	dr	ee (*trans*)	ee (*cis*)
MeMgBr	66	2:1	92	95
MeMgI	27	2.7:1	84	88
n-PentMgBr	63	2.4:1	92	60
iPentMgBr	34	2.2:1	92	60
cyclopentylMgBr	16	n.d.	74	74
HexMgBr	41	1.8:1	92	92

by a Cu-NHC-catalyzed conjugate addition of Grignard reagents to β-substituted cyclic enones (**70**) (Scheme 19) [51].

Fox and co-workers developed an intriguing synthesis of enantiomerically enriched cyclobutanes **77** [52]. Their strategy employed a three-component process in which *tert*-butyl (*E*)-2-diazo-5-arylpent-4-enoates **74** were treated with the chiral rhodium catalyst **C1** to provide enantiomerically enriched bicyclobutanes **75**. These highly strained compounds then participated in the Cu-catalyzed homoconjugate addition of Grignard reagents and subsequent enolate trapping to give densely functionalized cyclobutanes **77** with high diastereoselectivity (Scheme 20). The enolates were alkylated, allylated, benzylated, benzoylated, and thienylated.

Minnaard and co-workers developed a copper/Rev-Josiphos-catalyzed asymmetric conjugate addition of Grignard reagents to 2-methylcyclopentenone (**78**), which provided 2,3-disubstituted cyclopentanones in high yields and enantiomeric purities [53]. The one-pot alkylation reaction of the in situ formed magnesium enolate with alkylating reagents required the presence of 1,3-dimethyltetrahydropyrimidine-2(1*H*)-one (DMPU) (Scheme 21). Reactive alkylating reagents such as iodomethane, benzyl bromide, allyl iodide, propargyl bromide, or bromoacetate reacted well and afforded the products **80** in good yields.

In an attempt to expand the available electrophiles for reactions with metal enolates, we were inspired by the work of Cozzi and co-workers. They described reactions of organocatalytically generated enamines with stabilized carbenium ions [54-56].

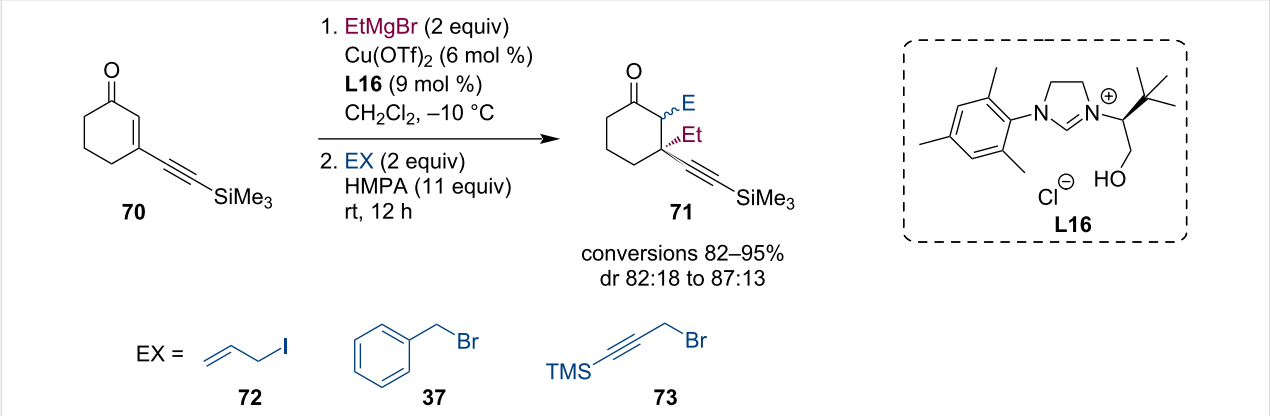

Scheme 19: Tandem reaction composed of Grignard ACA to alkynyl enones.

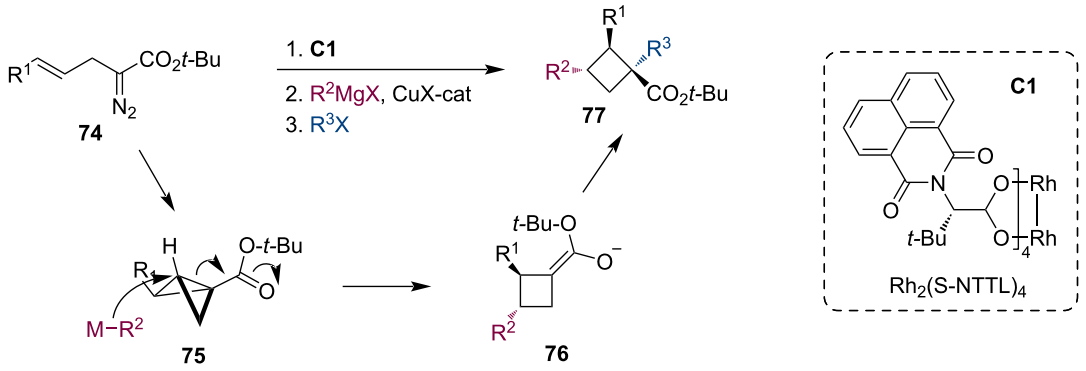

Scheme 20: Rh/Cu-catalyzed tandem reaction of diazo enoates leading to cyclobutanes.

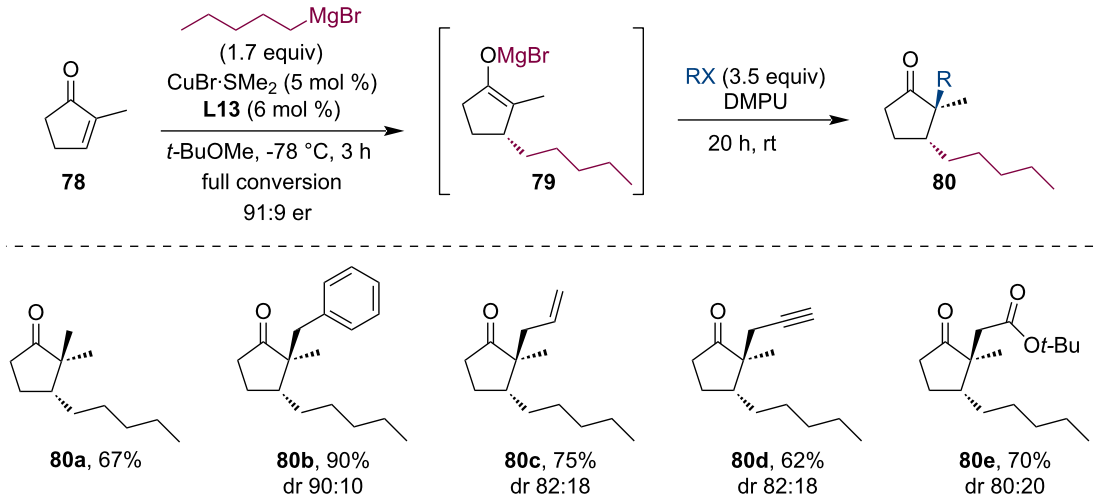

Scheme 21: Tandem Grignard-ACA of cyclopentenones and alkylation of enolates.

These seminal results prompted us to push this question further and we asked whether metal enolates generated by conjugate additions would be compatible and react productively with suitable carbenium ions (Scheme 22). To investigate this question, we started our study with the well-known conjugate additions of Grignard reagents to cyclic and linear enones **1**, **85**, and **87**. At first, the addition of tropylium or benzodithiolium tetrafluoroborates were not highly productive because these onium compounds were not well soluble in typical solvents used for conjugate additions of organometallic reagents, e.g., Et_2O, *t*-BuOMe or CH_2Cl_2. Therefore, we exchanged the BF_4 anion in the onium compounds for the more lipophilic NTf_2. This exchange led to more soluble onium compounds **81** and **83**, and consequently, also significantly improved the reaction with the metal enolates. As a result, the corresponding products were successfully isolated with tropylium and benzodithiolium cations [57]. The reaction worked well with Mg enolates generated from cyclic and linear enones **1** and **85** and enoyloxazolidinones **87**. Apart from the most robust tropylium and benzodithiolium cations, reactions were also possible with the dianisylmethylium cation. Interestingly, tritylium cations reacted only in the *para*-position of a phenyl ring, while flavylium triflate and 2,4,6-triphenylpyrylium tetrafluoroborate were not compatible with our reaction conditions.

Heterodonor ferrocenyl phosphane–carbene ligands efficiently promote the conjugate addition of Grignard reagents to α,β-unsaturated lactones [58]. Building on this knowledge, we have investigated the domino reaction of the formed metal enolates with activated alkenes **91** [59]. Alkenes with two activating groups were needed for efficient enolate-trapping reactions, sulfone or phosphonate activating groups being the most suitable ones (Scheme 23).

Harutyunyan and co-workers developed a Lewis acid-promoted conjugate addition to unreactive Michael acceptors such as

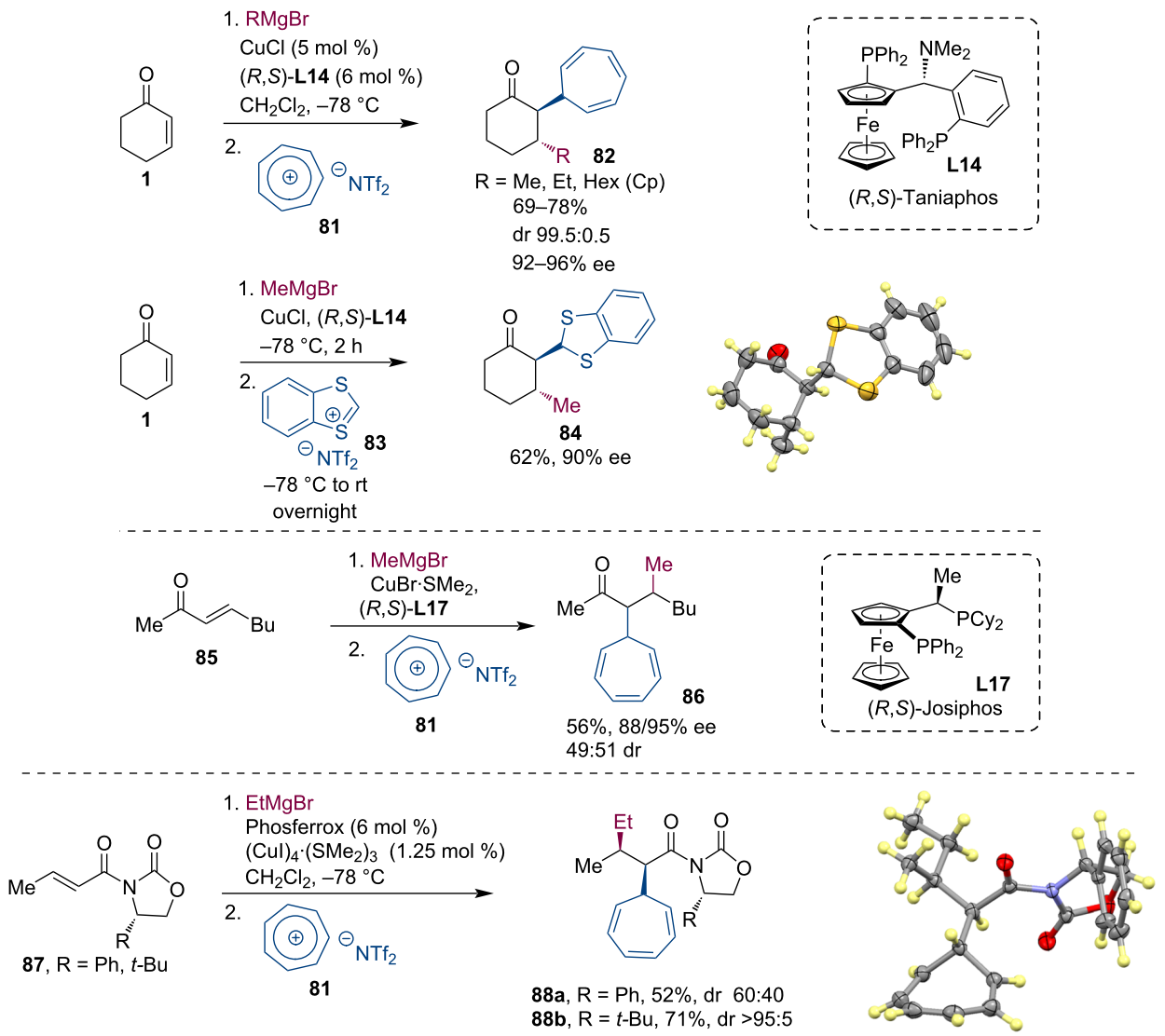

Scheme 22: Tandem ACA of Grignard reagents followed by enolate trapping reaction with onium compounds.

amides or vinyl heterocycles [60]. Trimethylsilyl triflate or boron trifluoride-activated unsaturated amides underwent highly efficient and enantioselective addition of Grignard reagents. When this methodology was applied to a substrate with a pending bromo substituent (**93**), the formed enolate **94** underwent a spontaneous cyclization via an S_N2 displacement (Scheme 24).

The Harutyunyan team showed that this methodology also applies to aza-enolates that are generated by the conjugate addition of Grignard reagents to alkenyl heteroarenes [61]. The aza-enolates were trapped with various Michael acceptors such as unsaturated ketones, esters, and amides (Scheme 25) [62]. The authors noted a strong substrate dependence of this process. The trapping reaction worked best with benzoxazole-derived substrate, while thiazole was also possible. Among electrophilic reagents, unsaturated esters worked best.

In collaboration with the Harutyunyan group, we have further explored the possibilities of chiral enolate trapping which were obtained by asymmetric conjugate addition of organometallic reagents. We intended to employ the Lewis acid-mediated generation of magnesium enolates in the trapping reactions with carbocations. Indeed, unsaturated amides, alkenyl heterocycles, or even unsaturated carboxylic acids successfully participated in this process affording structurally interesting products (Scheme 26) [63].

Apart from unsaturated amides, the trapping worked also with alkenylheterocycles **103**. Interestingly, the corresponding aza-

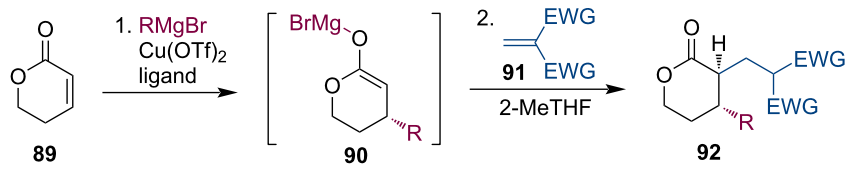

R	EWG	yield	er
Et	SO_2Ph	80	96:4
Et	$PO(OEt)_2$	52	98:2
Et	CO_2Me	33	97:3
Me	SO_2Ph	43	89:11
Me	$PO(OEt)_2$	44	84:16
n-Hex	SO_2Ph	39	94:6

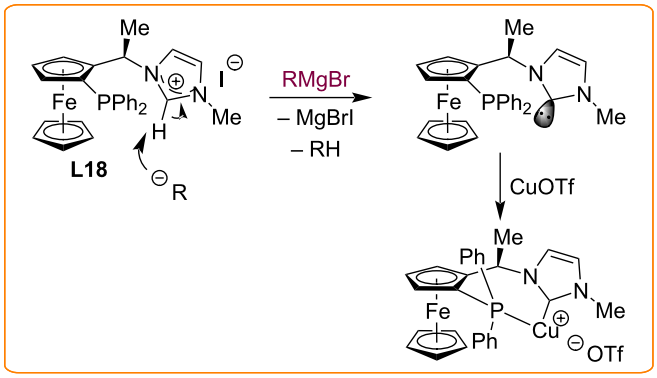

Scheme 23: Mg enolates generated from unsaturated lactones in reaction with activated alkenes.

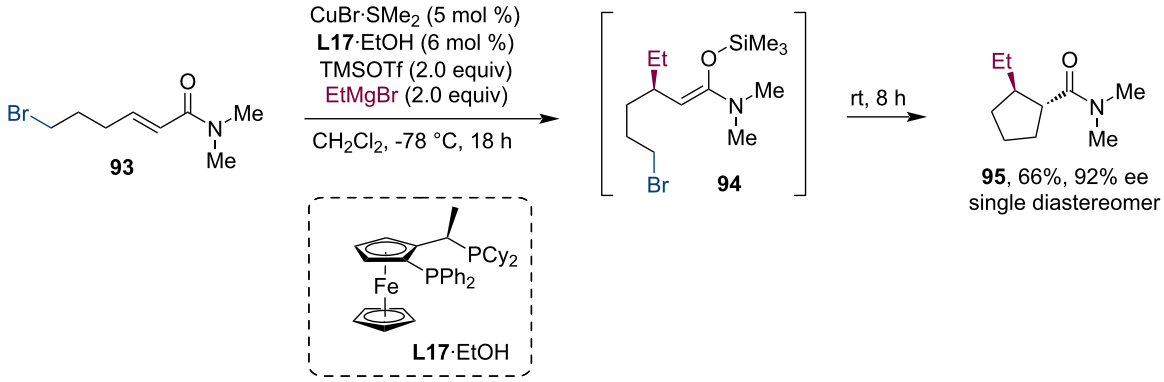

Scheme 24: Lewis acid mediated ACA to amides and S_N2 cyclization of a Br-appended enolate.

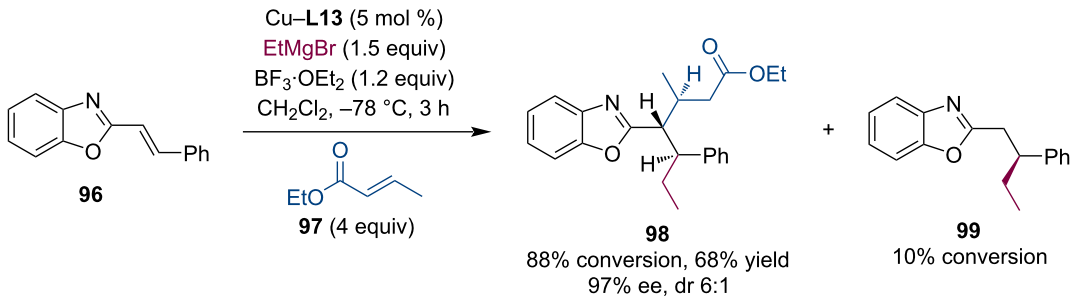

Scheme 25: Trapping reactions of aza-enolates with Michael acceptors.

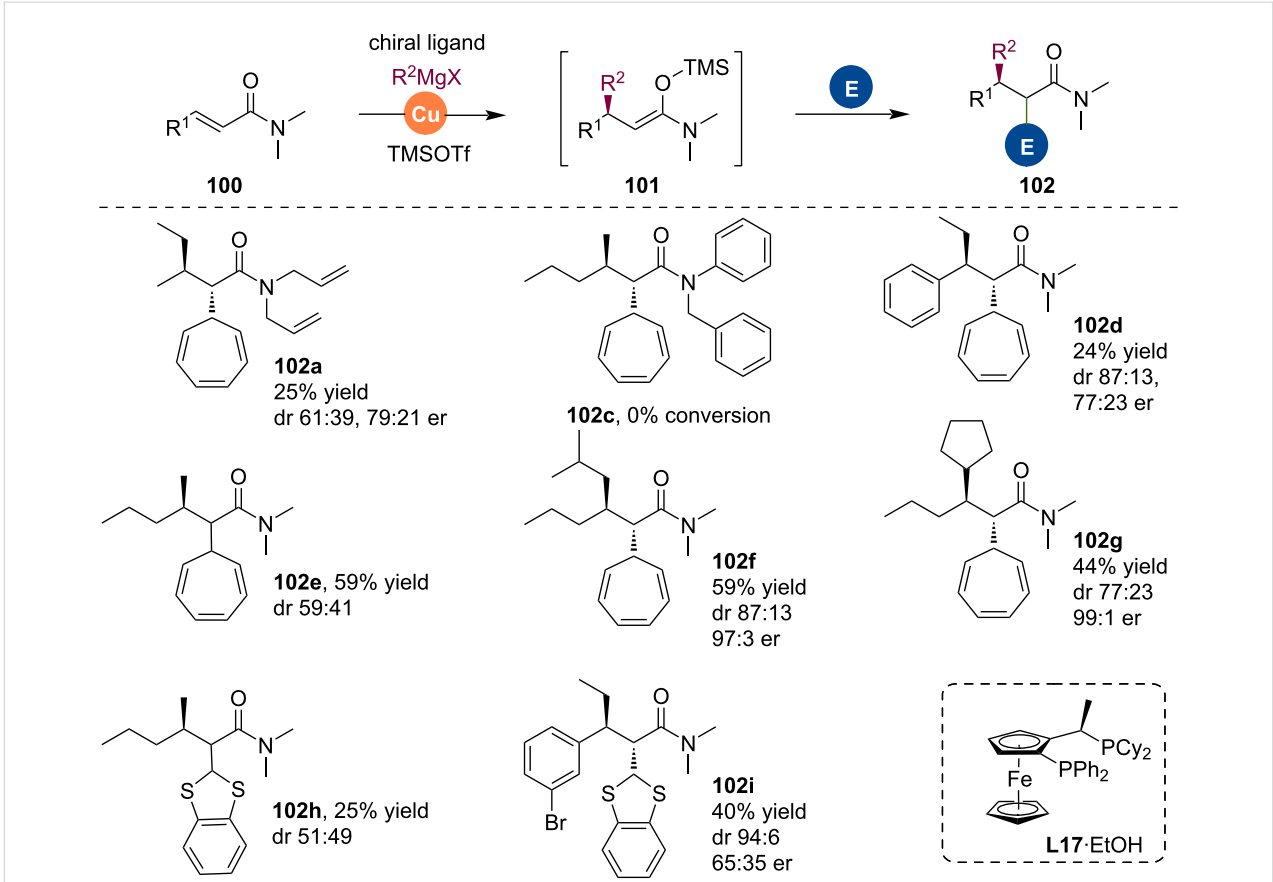

Scheme 26: Si enolates generated by TMSOTf-mediated ACA of Grignard reagents and enolate trapping reaction with onium compounds.

enolates could be generated by two sets of experimental conditions where ACA was promoted either by $BF_3{\cdot}OEt_2$ or TMSOTf (Scheme 27A). Based on the recent Harutyunyan discovery of ACA to unsaturated carboxylic acids [64], we have attempted a similar trapping reaction here as well. Gratifyingly, the corresponding trapping products **106** could be isolated with tropylium and benzodithiolium cations (Scheme 27B).

We have continued our exploration of enolate reactions with carbocations by studying the trapping of heterocyclic enolates **108** generated from coumarin and chromone [65]. The high enantio- and diastereoselectivity of these transformations were ensured by a Josiphos-type ferrocene ligand. The reaction of chiral metal enolates with onium compounds enabled the installation of structurally attractive substituents on the chromenone or piperidinone core (Scheme 28).

Furthermore, cycloheptatrienyl and benzodithiolyl substituents can be further modified, thus, expanding the synthetic possibilities of this methodology. The cycloheptatrienyl substituent allows oxidative ring contraction to form a phenyl ring, which is otherwise not easy to introduce into the C-2 position of carbonyl compounds. Finally, the benzodithiolyl group can be reduced into a methyl group (Scheme 29).

Conjugate additions with trialkylaluminum reagents

Conjugate additions of trialkylaluminum reagents are somewhat less populated as a basis for generating and trapping of reactive metal enolates. The conjugate addition of R_3Al to cyclic enones catalyzed by a combination of copper(II) naphthenate (CuNaph) and SimplePhos ligand **L19** led to the corresponding aluminum enolates. Alexakis and co-workers used these enolates in a Mannich-type reaction with the α-aminoether **118**. This reagent released an iminium ion into the reaction medium that reacted with the Al enolate **117** [66]. Furthermore, the Mannich adduct was then reacted with Grignard reagents that replaced the dimethylamino group (Scheme 30).

Alexakis and co-workers also investigated the trapping of metal enolates by Michael reactions with nitroalkenes **122** and disulfonyl ethylenes **124** (Scheme 31) [67]. The conjugate additions of dialkylzinc, Grignard, and trialkylaluminum reagents to

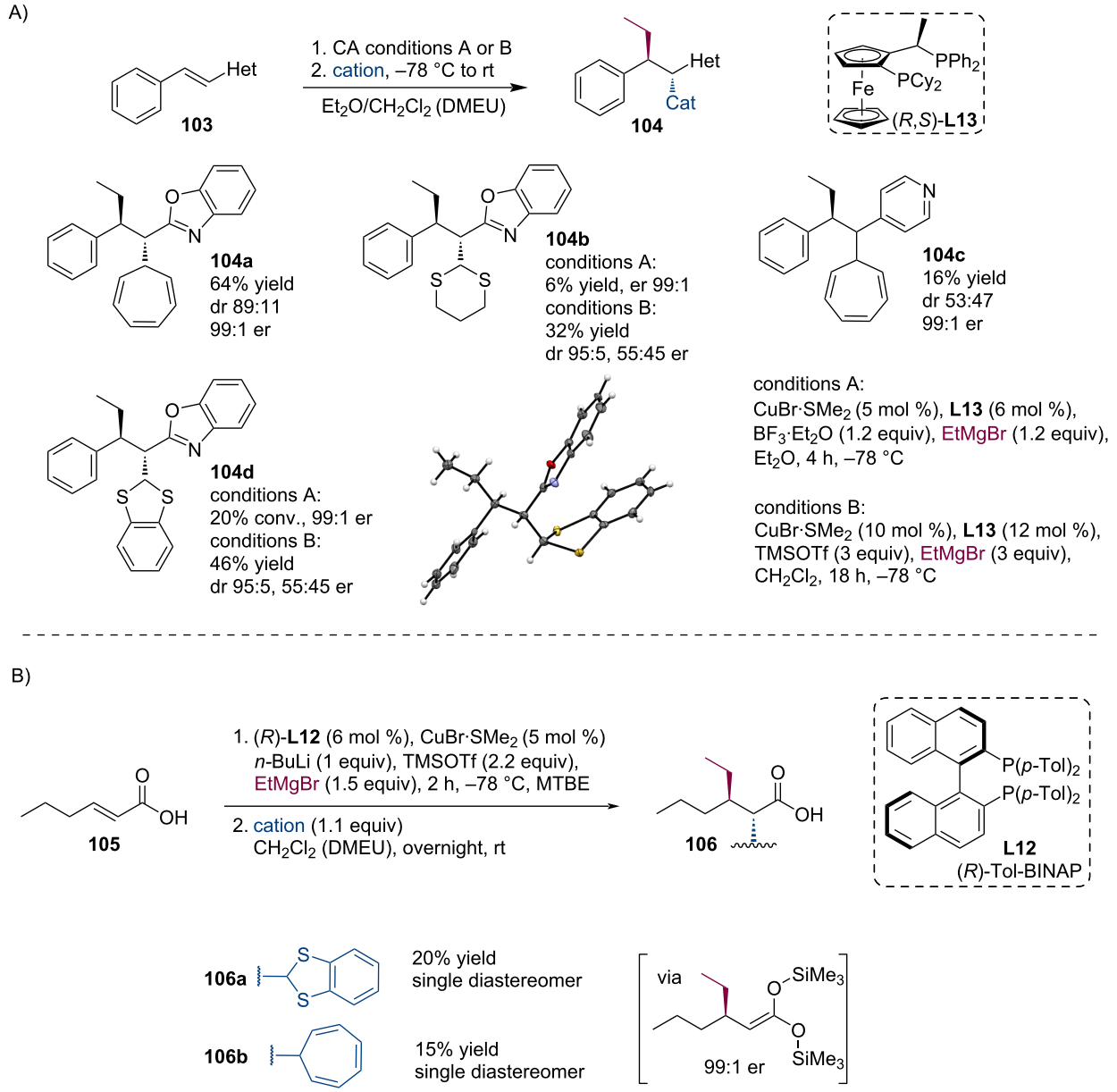

Scheme 27: Trapping reactions of enolates generated from alkenyl heterocycles (A) and carboxylic acids (B) with onium compounds.

cyclic enones **121** were realized using previously established chiral phosphoramidite, carbene or ferrocene ligands. All types of metal enolates generated via these processes were able to react with Michael acceptors and afforded the corresponding products in good yields.

The alkynylation of enolates generated by conjugate addition was described by Teodoro and Silva (Scheme 32) [68]. Even though the conjugate addition of trialkylaluminum or Grignard reagents was realized only in an achiral manner, this work merits discussion here. Aluminum and magnesium enolates were alkynylated with ethynylbenziodoxolone (EBX). This diastereoselective electrophilic alkynylation afforded the corresponding α-alkynylketones **129** in good yields.

Conjugate additions with organozirconium reagents

The hydrozirconation of alkenes and alkynes generates mild organozirconium compounds that can be used in various transformations. Fletcher and co-workers developed the utilization of organozirconium reagents in Cu-catalyzed conjugate additions and allylic substitutions [15]. Given these developments, we posed the question of how would Zr enolates **133**, formed by the corresponding conjugate addition, would react with highly

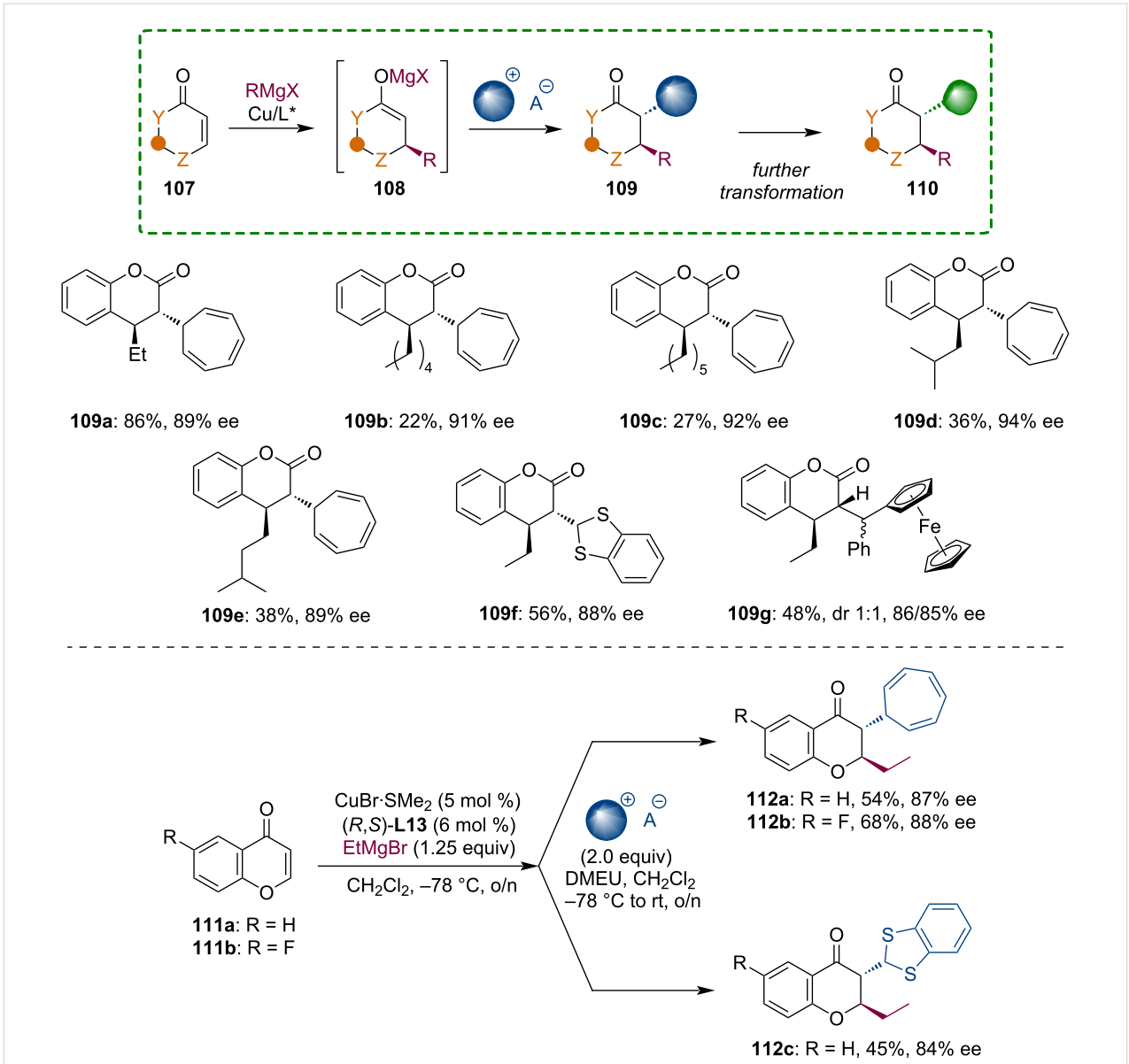

Scheme 28: Reactions of heterocyclic Mg enolates with onium compounds.

reactive electrophiles. With typical electrophiles such as benzaldehyde or nitrostyrene no enolate trapping was observed, however, we isolated trapping products with onium compounds having tropylium, benzodithiolium, and 1,3-dithian-2-ylium cations. The zirconium enolate also reacted with a highly activated alkene (Scheme 33) [69]. A comparison with related Mg and Si enolates revealed a lower reactivity of zirconium enolates, presumably, due to the considerable steric hindrance caused by bulky ligands around the Zr center.

Fletcher investigated the formylation of zirconium enolates with the Vilsmeier–Haack reagent [70]. Interestingly, the reaction afforded chloroformylation rather than simple formylation products. The methodology was later exploited in the expedient synthesis of the Taxol core (Scheme 34) [71].

Tandem conjugate borylations and silylations

Chiral organoboron compounds are well-known synthetic building blocks with diverse possibilities for subsequent derivatization (e.g., oxidation, transformation to potassium trifluoroborate salt, hydrolysis, C–C cross-coupling, base-mediated elimination, radical C–B cleavage) [72]. Therefore, enantioenriched boronates are commonly applied intermediates in organometallic, medicinal, and other fields of chemistry. At the same time, some organoboronic acid derivatives have been found to exhibit potent biological activities, which has

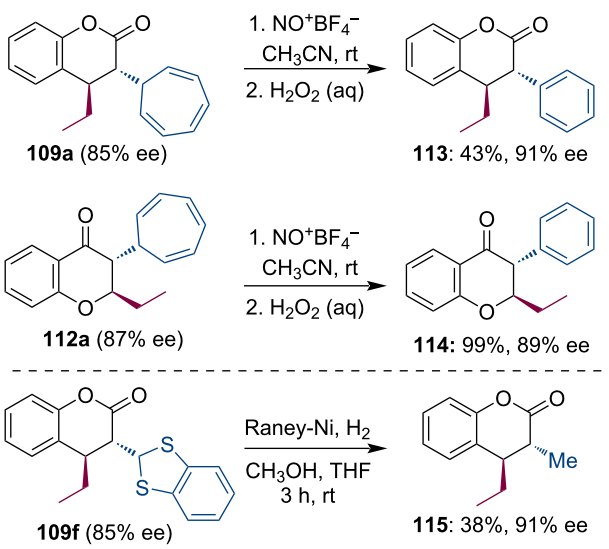

Scheme 29: Synthetic transformations of cycloheptatrienyl and benzodithiolyl substituents.

led to the development of several FDA-approved drug molecules [73,74]. Following the seminal works of Hosomi [75] and Miyaura [76], the synthesis of β-boron-substituted carbonyl compounds by conjugate addition of boron species to activated alkenes has matured into a well-developed strategy (Scheme 35).

Despite its ability to build complex structures, the conjugate borylation with subsequent enolate trapping has rarely been applied in the last decade. These few examples are mostly limited to aldol reactions. In 2009, Shibasaki and co-workers explored the copper-catalyzed asymmetric conjugate borylation of β-substituted cyclic enones using chiral bisphosphine ligand **L21** [77]. Other than the oxidation and hydrolysis of the produced enantiomerically enriched tertiary boronates, in one example, they have demonstrated the utilization of the enolate intermediate in a cascade sequence, including borylation, aldol reaction, and finally oxidation (Scheme 36). The product **146** containing three consecutive stereocenters was ob-

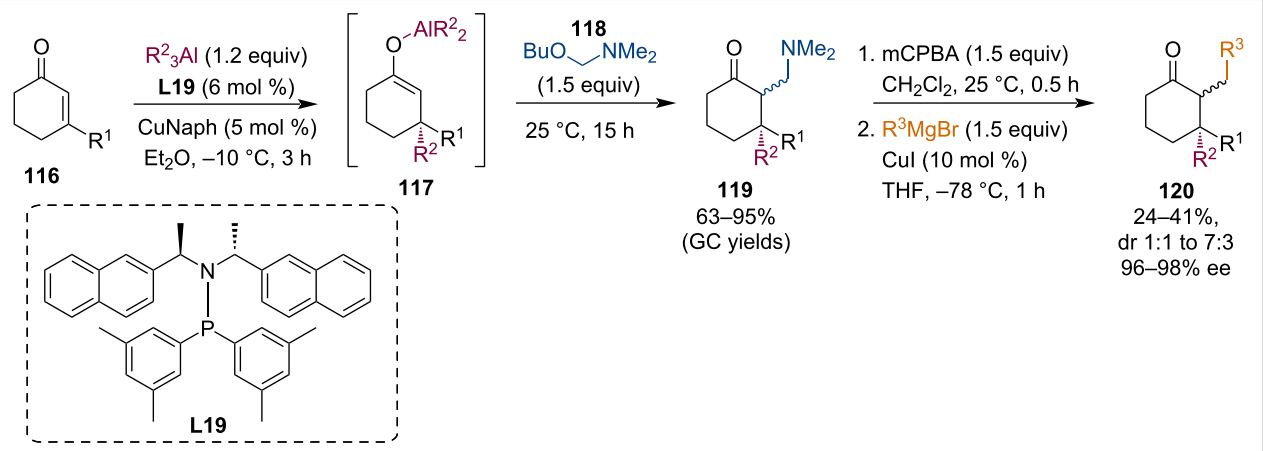

Scheme 30: Aminomethylation of Al enolates generated by ACA of trialkylaluminum reagents.

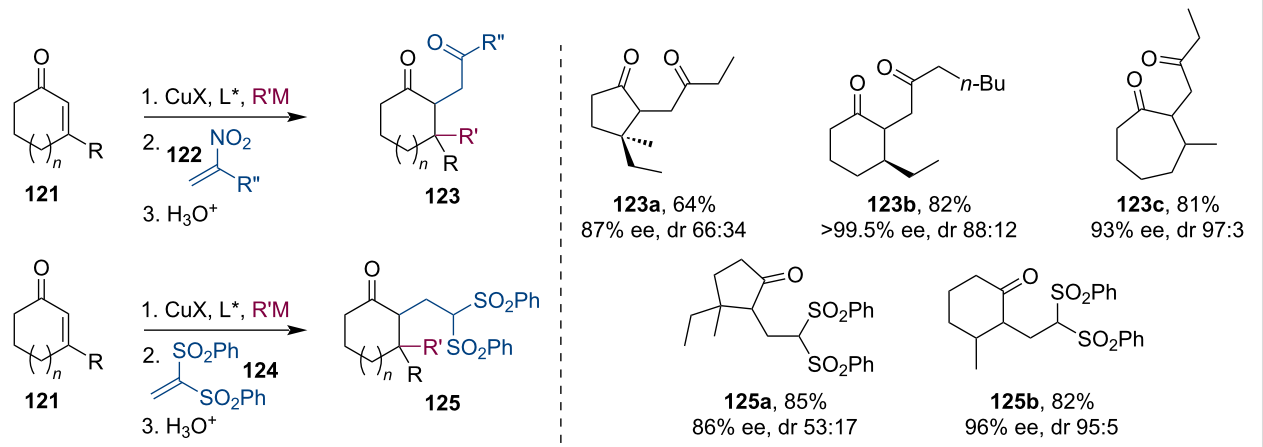

Scheme 31: Trapping reactions of enolates with activated alkenes.

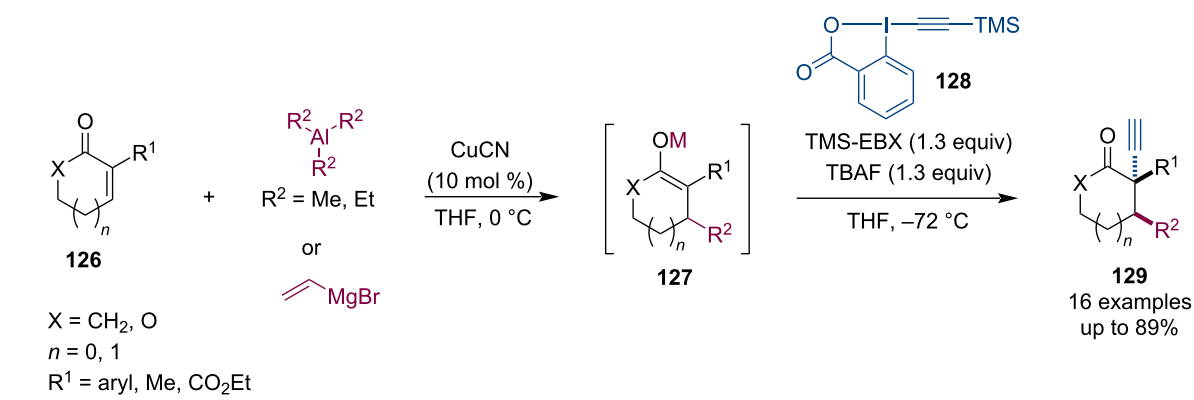

Scheme 32: Alkynylation of racemic aluminum or magnesium enolates.

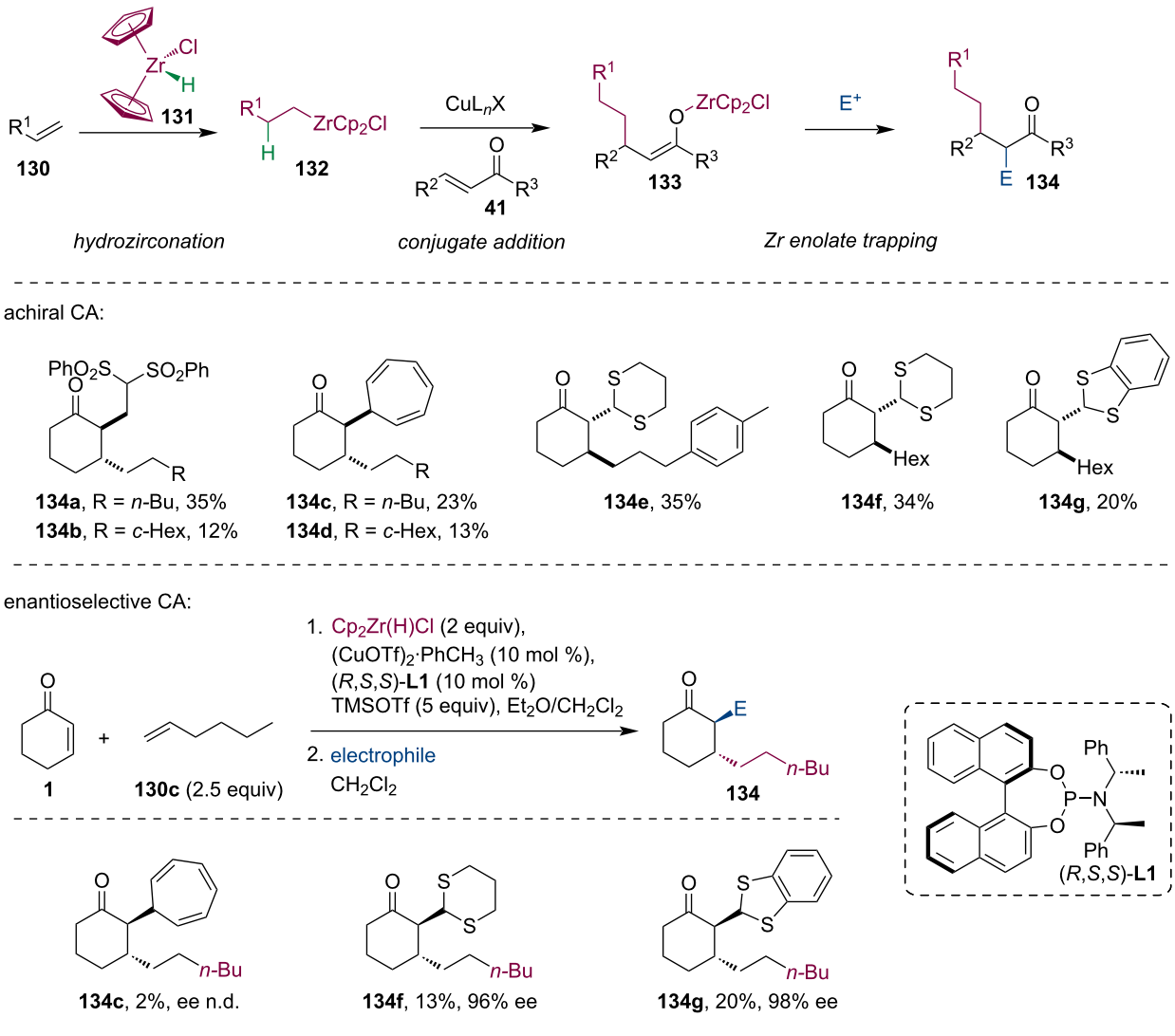

Scheme 33: Trapping reactions of Zr enolates generated by Cu-ACA of organozirconium reagents.

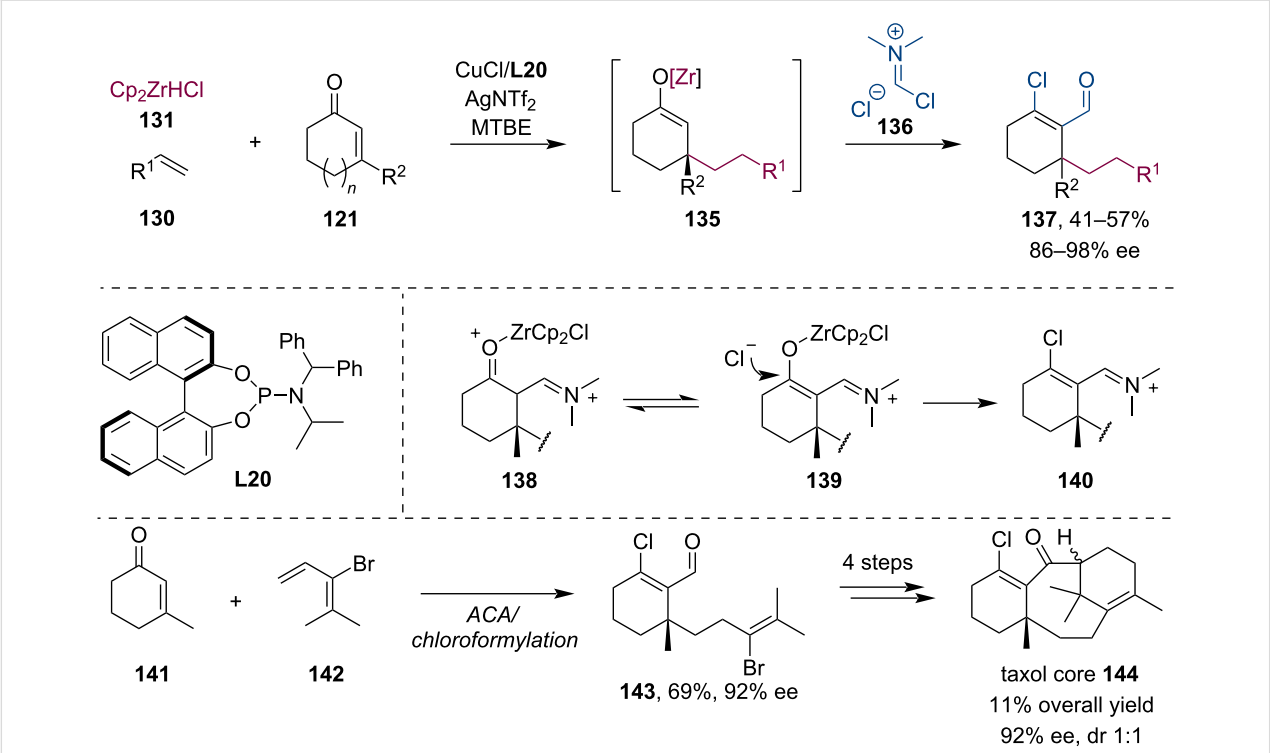

Scheme 34: Chloromethylation of Zr enolates using the Vilsmeier–Haack reagent.

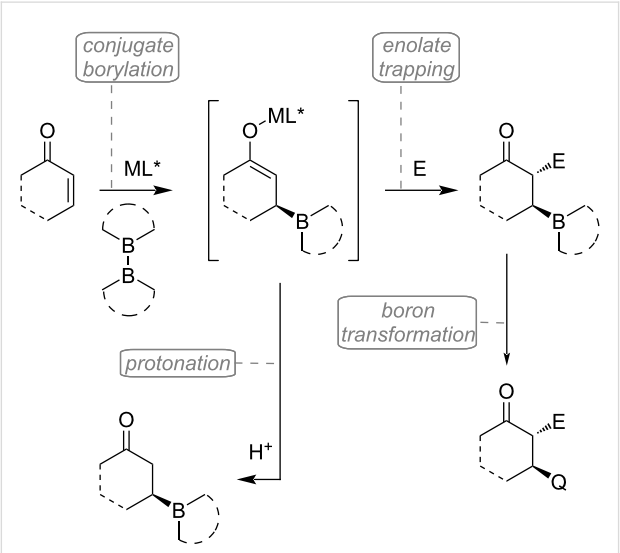

Scheme 35: Tandem conjugate borylation with subsequent protonation or enolate trapping by an electrophile.

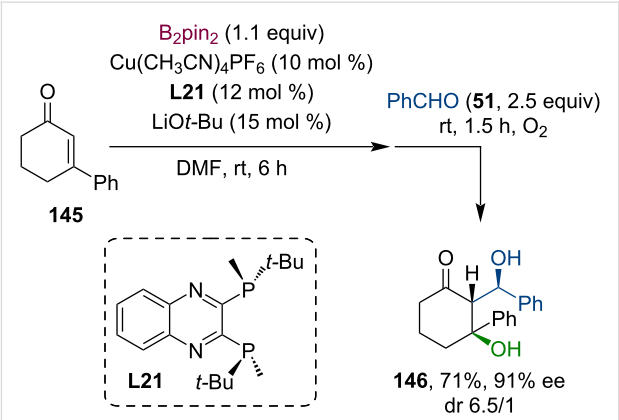

Scheme 36: Tandem conjugate borylation/aldol reaction of cyclohexenones.

tained in a dr of 6.5 to 1 and with good yield and enantioselectivity.

Lam and co-workers described a highly enantioselective tandem borylation/intramolecular aldol cyclization procedure (Scheme 37) [78]. The desymmetrization process of cyclic diones **147** gave the densely functionalized bicyclic products **148** with four contiguous stereocenters usually in a highly diastereoselective fashion. Presumably, the difference in diastereocontrol originates from the preferred *E*/*Z* enolate geometry during the transition state. Interestingly, using *t*-BuOH instead of iPrOH resulted in exceptionally better results for some substrates with different ring sizes.

In 2015, the group of Feringa investigated the copper-catalyzed conjugate borylation of α,β-unsaturated phosphine oxides **149**

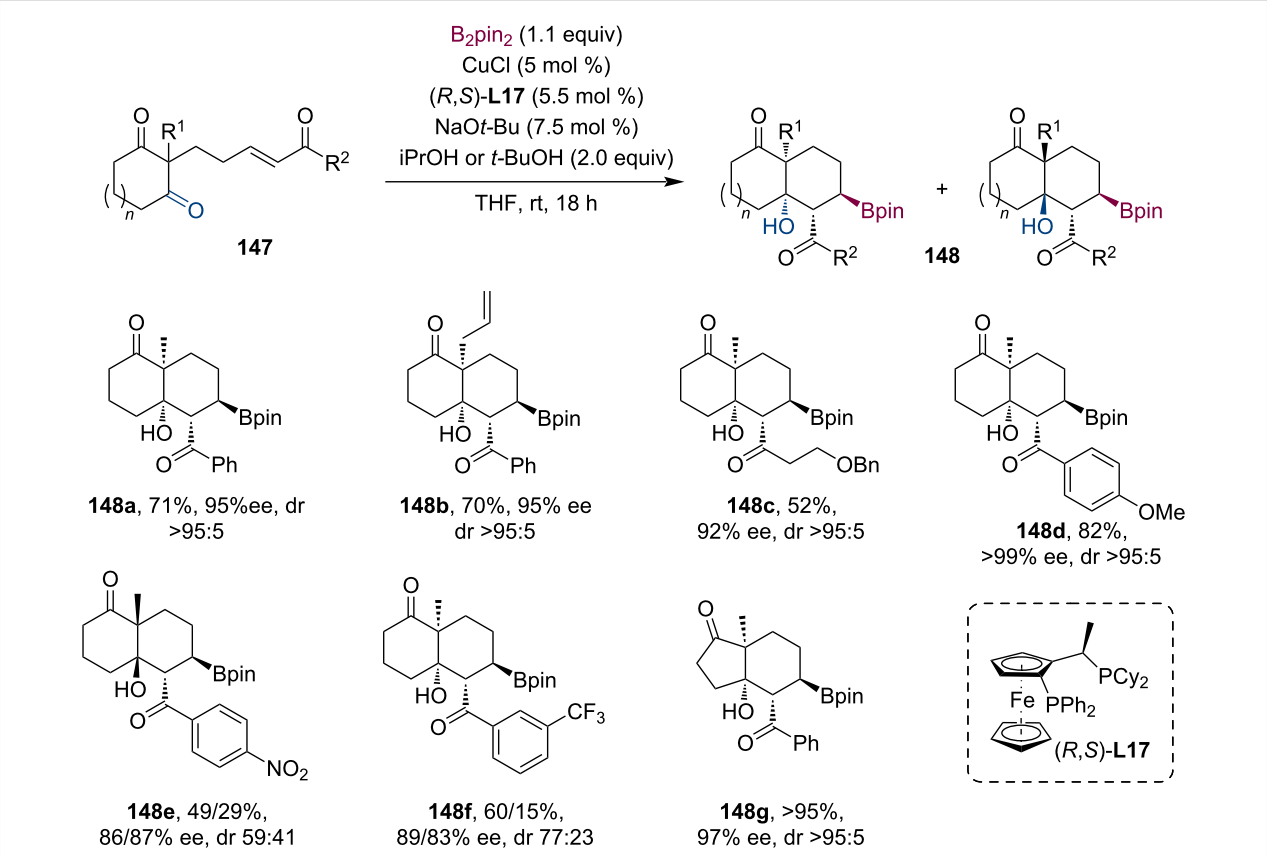

Scheme 37: Selected examples for the tandem asymmetric borylation/intramolecular aldol reaction; synthesis of functionalized bicyclic compounds.

[79]. Their work also included an example of the consecutive trapping of the enolate by MeI (Scheme 38). Using the (R,S_p)-Josiphos ligand (**L17**), the product of the tandem reaction (**150**) was gained in 63% yield (dr 5.2:1).

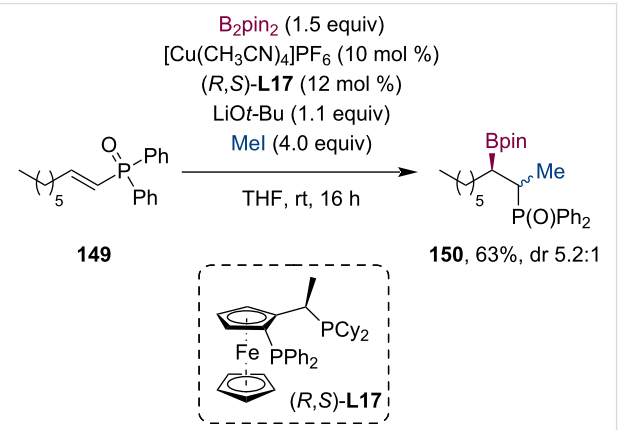

Scheme 38: Cu-catalyzed tandem methylborylation of α,β-unsaturated phosphine oxide in the presence of (R,S_p)-Josiphos ligand (**L17**).

At the beginning of the new decade, Fernández et al. presented a Cu-catalyzed tandem borylation/transannular aldol cyclization using decane and undecane macrocyclic substrates **151** (Scheme 39) [80]. This methodology enabled the synthesis of complex bicyclic scaffolds in a completely diastereoselective and straightforward manner. Based on their NMR experiments (H_α coupling constants ≈ 6.4–8.6 Hz), the high level of diastereocontrol can be associated with the preferred Z-configuration of the cyclic copper enolate intermediate. In the presence of the chiral ligand (R,S)-**L17**, the tandem reaction was accomplished in a highly enantioselective way (ee up to 92%).

In the same year, Lautens and co-workers introduced a novel methodology for preparing enantioenriched N-heterocycles utilizing a Cu-catalyzed tandem conjugate borylation/Mannich cyclization sequence (Scheme 40A) [81]. The procedure was found to be generally relevant as several structurally different Michael acceptors were successfully applied. Their work also included a 3 mmol scale-up (62%, 87% ee, dr >20:1) and various derivatizations of the Mannich products. Furthermore, they have also attempted a multi-electrophile cascade reaction, which harnesses the nucleophilic nature of the secondary amine **157** generated in the cyclization step (Scheme 40B). Consequently, the complex tetracyclic compound **158** was produced in 47% yield and with good stereoselectivity (84% ee, dr 7.5:1).

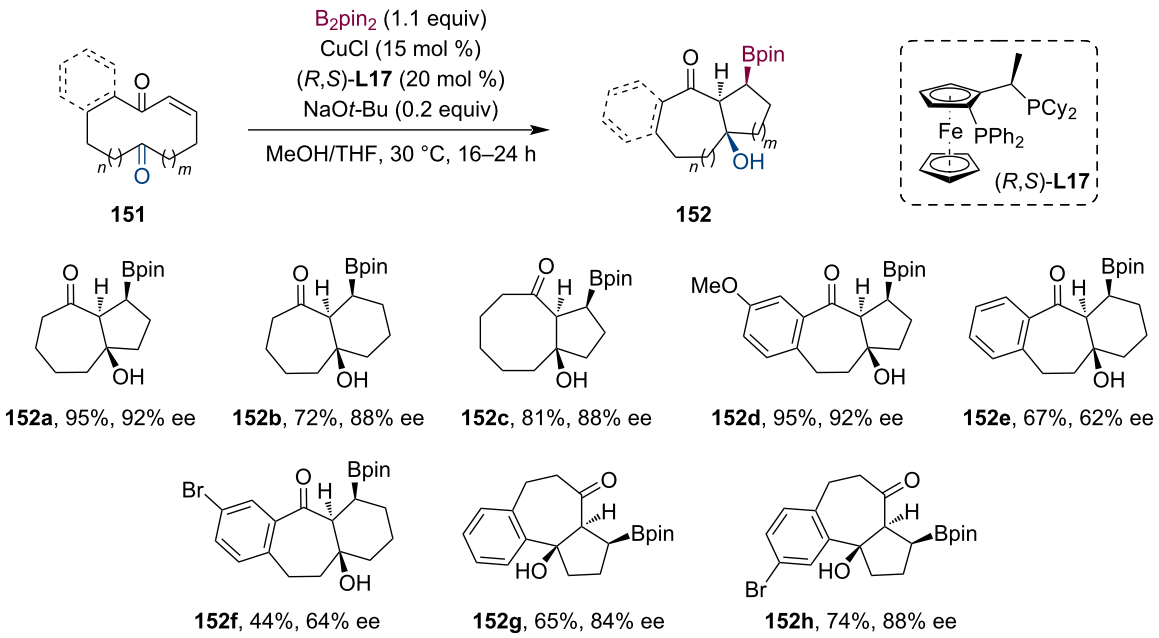

Scheme 39: Cu-catalyzed tandem transannular conjugated borylation/aldol cyclization of macrocycles containing an α,β-unsaturated ketone and an additional ketone moiety.

At about the same time, comparable results were reported by the group of Zhang [82]. Their Cu-catalyzed cascade borylation/aldol cyclization methodology provides rapid access to various indane derivatives **160** (Scheme 41A) with good yields and excellent chemo-, and stereoselectivities. Next, they successfully extended this process to 6-, and 7-membered benzocyclic compounds and the corresponding boronates **162** were isolated with equally good yields and excellent stereoselectivities (98–99% ee) (Scheme 41B). Surprisingly, when the aldehyde was exchanged with imine **163**, the Mannich product **164** was gained only in 23% yield, however, with excellent enantioselectivity of 94%.

In the following year, Aponick et al. systematically modified atropisomeric C1-symmetric stack ligands to identify suitable catalytic systems for a highly enantioselective synthesis of organoboranes (Scheme 42) [83]. Their best attempt to realize a tandem borylation/aldol cyclization reaction resulted in 72% yield, 90% ee, and a diastereomeric ratio of 93:7 using ligand **L25**.

Recently, Chegondi and co-workers have demonstrated an enantioselective Cu-catalyzed tandem borylation/Michael addition reaction of aryl enones **167** and **170** to cyclohexadienones in an intramolecular fashion (Scheme 43A) [84]. The 1,4-conjugate borylation is followed by a desymmetrization step during which the chiral enolate attacks (*Si*-face) the prochiral cyclohexadienone ring via a chair-like transition state. The reaction requires an excess amount of base, resulting in the formation of a more favorable lithium enolate. Subsequent oxidation of the boronates gave the corresponding alcohols without a significant change in yield or selectivity. Interestingly, in the absence of the base, the reaction led to fused dioxane derivatives (Scheme 43B). This can be explained by a borylation/oxidation/oxa-Michael tandem sequence instead of the *C*-Michael addition. The role of the base was thoroughly examined using DFT calculations. Other than the broad substrate scope, the synthetic utility of this method was demonstrated by a scale-up reaction (3.73 mmol scale, 87% yield, 88% ee), and by several different transformations of the tandem products.

Similarly, Ghorai et al. studied a Cu-catalyzed cascade borylation/Michael addition sequence leading to enantioenriched spiroindane boronates **174** (Scheme 44A) [85]. The reaction showed good functional group tolerance. Further derivatization, as well as scale-up (1 mmol) of the reaction were successfully performed (72% yield, 89% ee, dr >20:1). Based on their control experiments and literature mechanistic studies (Chegondi et al.) [84], the role of the base (LiO*t*-Bu) was considered. Following the Cu-catalyzed conjugate addition of B_2pin_2, the Michael cyclization is facilitated by the transmetalation of stoichiometric Li base with the Cu enolate (Scheme 44B). In the end, protonation of the Li enolate affords the spiroindane boronate.

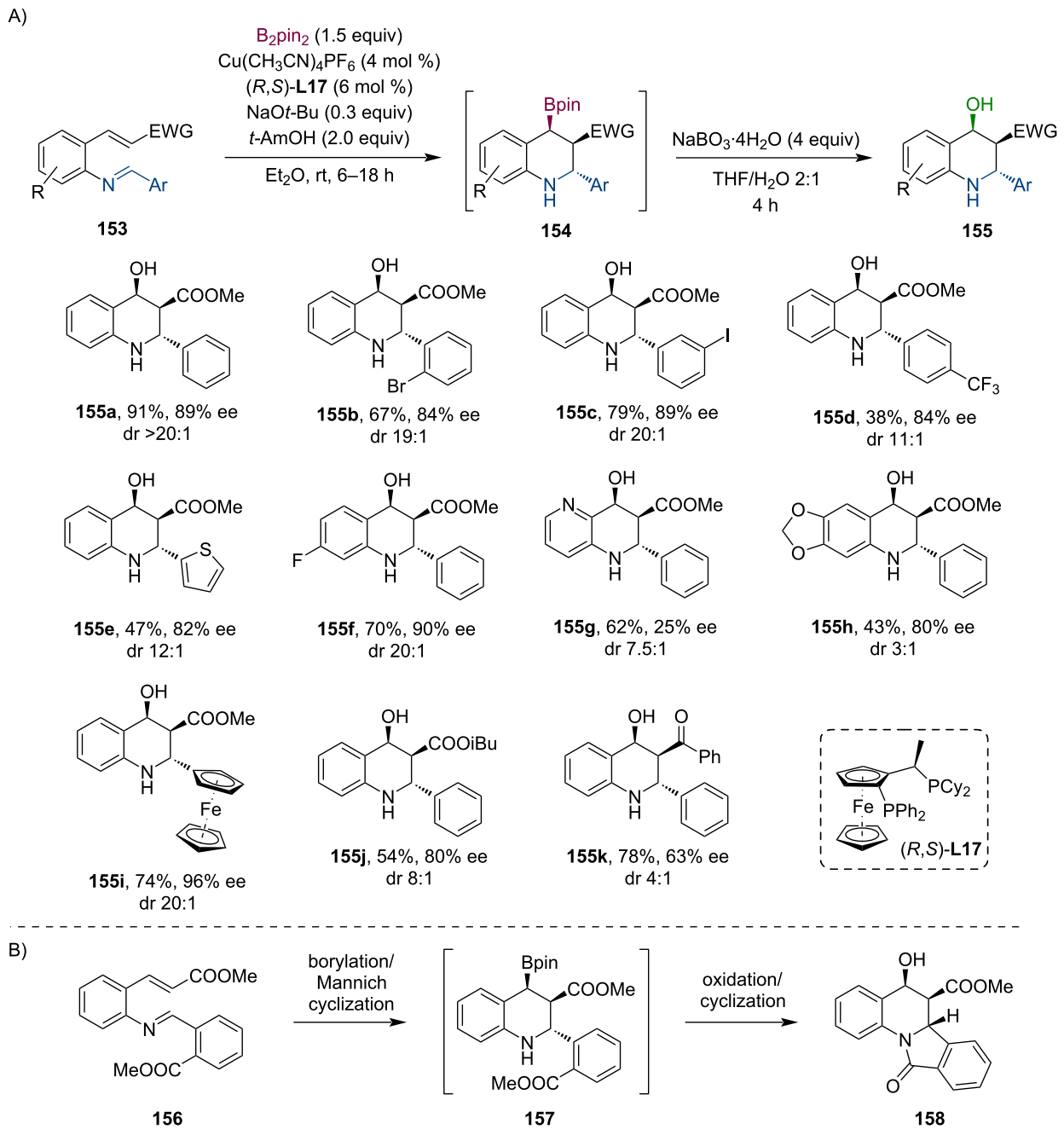

Scheme 40: Stereoselective tandem conjugate borylation/Mannich cyclization: selected examples (A) and a multi-electrophile cascade reaction furnishing a complex tetracyclic scaffold (B).

Due to their paramount role in the fields of bioactive natural products and medicinal chemistry, there is a growing interest in enantioenriched cyclobutanes. Recently, the group of Hall was engaged in developing enantioselective methods for the synthesis of cyclobutylboronates which could serve as important building blocks [86]. Utilizing high-throughput (HTS) chiral ligand screening, they have presented the highly asymmetric conjugate borylation of disubstituted cyclobutenones. Next, they thoroughly studied the stereoselective conjugate borylation of cyclobutene 1-carboxyester **175** (Scheme 45A) [87]. As a result, the *cis*-β-boronyl cyclobutylcarboxyester **176** was prepared on a gram scale with 80% yield and an excellent 99% ee (dr >20:1). Subsequent transformation to the corresponding trifluoroborate salt **177** resulted in a highly beneficial scaffold which was successfully involved in diastereoselective Ni/photoredox dual-catalyzed cross-coupling reactions. Further-

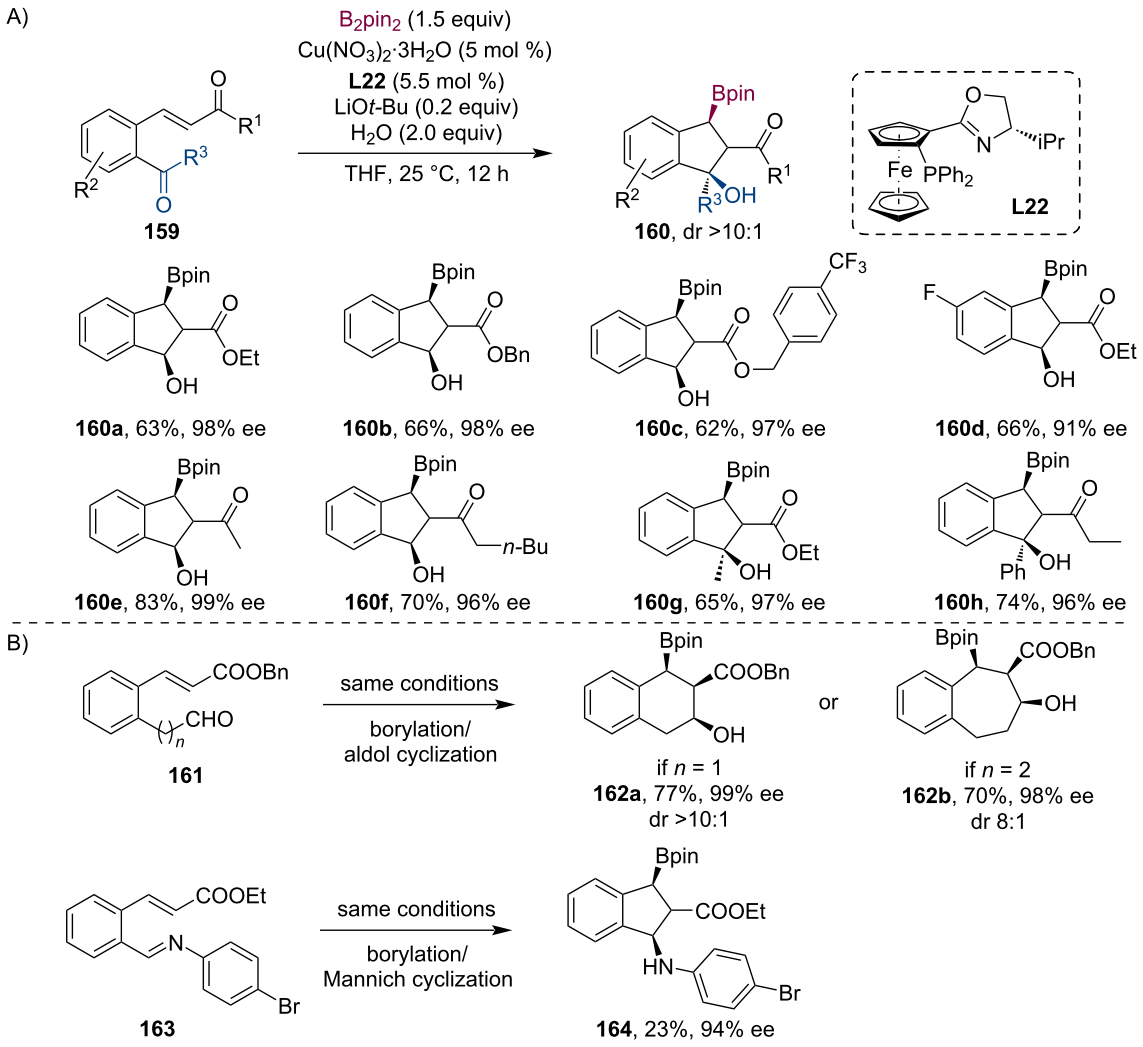

Scheme 41: Some examples of Cu-catalyzed asymmetric tandem borylation/aldol cyclization (A). Application to different ring sizes and combinations with Mannich reaction (B).

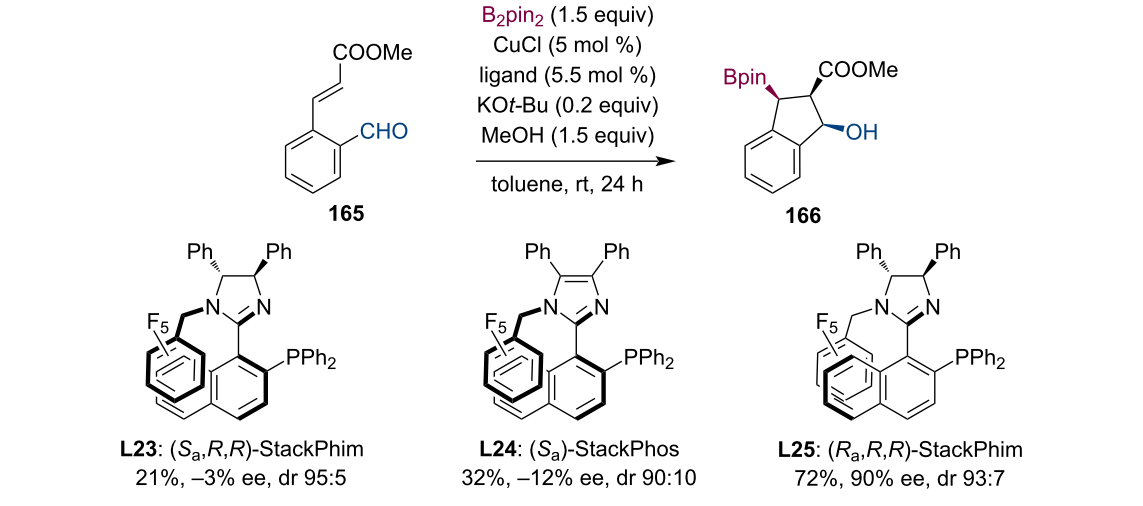

Scheme 42: Atropisomeric P,N-ligands used in tandem conjugate borylation/aldol cyclization sequence.

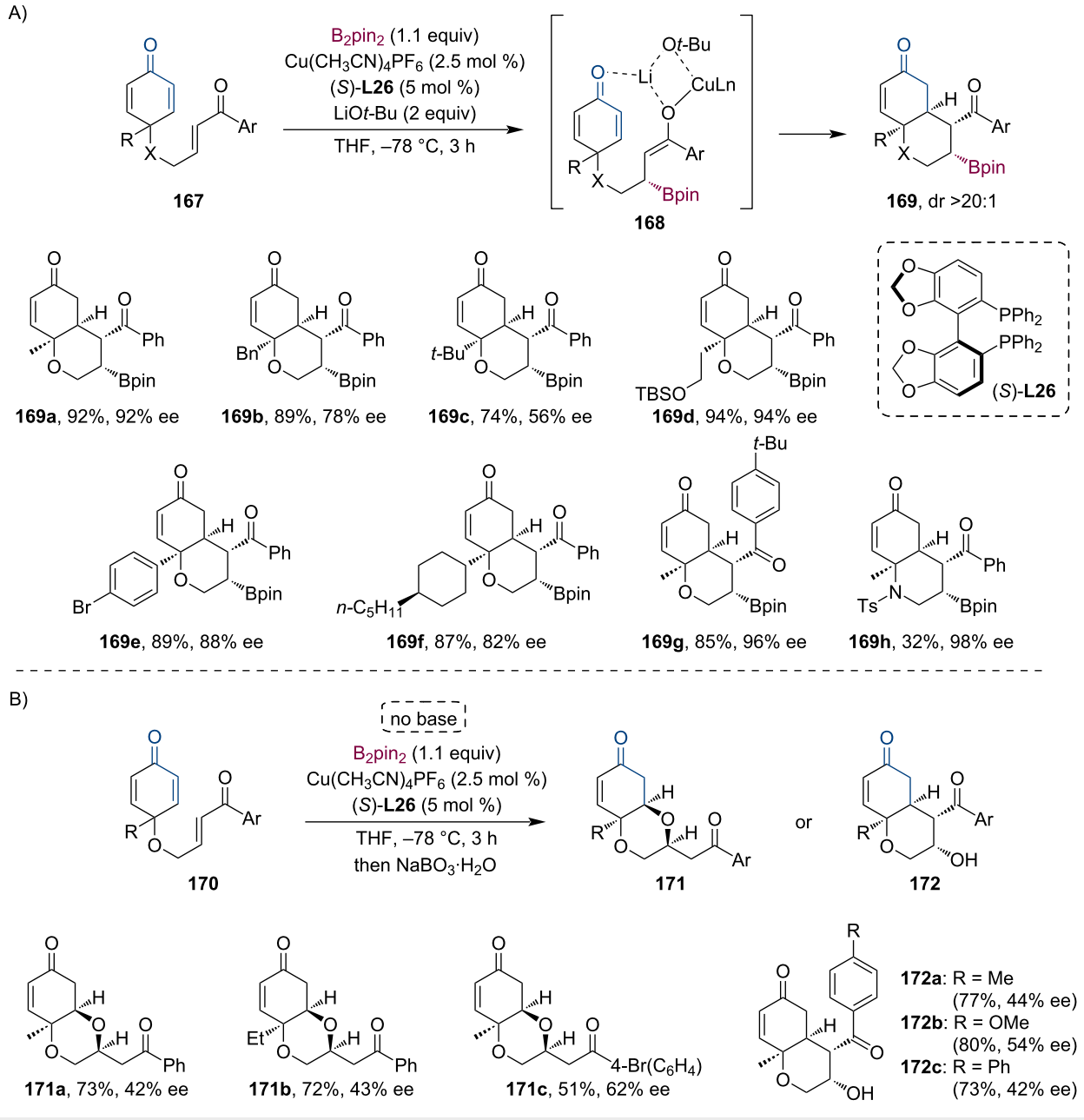

Scheme 43: Selected examples for the enantioselective Cu-catalyzed borylation/intramolecular Michael addition (A). Without the base, the reaction proceeds through a tandem borylation/oxidation/oxa-Michael sequence (B).

more, rather than the stereoselective protonation, they have also demonstrated the successful trapping of the Cu enolate with benzaldehyde (Scheme 45B). This tandem conjugate borylation/aldol reaction gave the aldol product **178** in 79% yield and an exceptional 95% ee (dr 15:1).

Similarly to conjugate borylation, silyl functional groups can be also introduced into activated alkenes. Furthermore, the additional transformation of the silyl motif might be similar or even complementary to boronates (e.g., sensitivity to organometallic reagents). In 2010, the Hoveyda group accomplished the NHC–Cu-catalyzed enantioselective conjugate addition of $PhMe_2Si$-Bpin to α,β-unsaturated enones [88]. Additionally, they have also presented the successful trapping of the Cu enolate intermediate with benzaldehyde (**51**) and methyl bromoacetate (**181**) (Scheme 46).

At about the same time, Riant and co-workers investigated the chiral auxiliary-assisted Cu-catalyzed tandem silylation/aldol reaction between enoyloxazolidinones and different aromatic

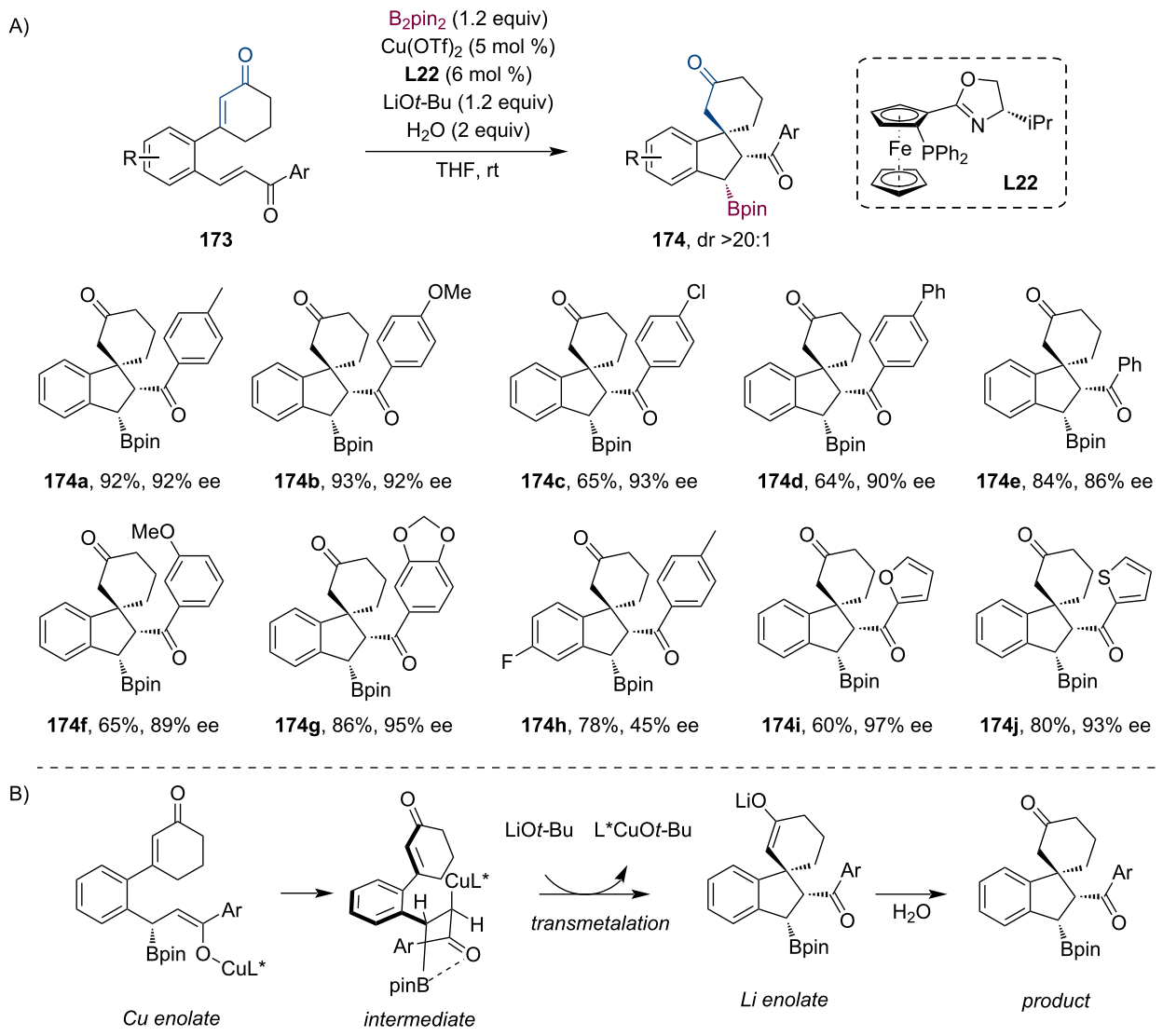

Scheme 44: Selected examples for the preparation of enantioenriched spiroindanes using a Cu-catalyzed tandem conjugate borylation/Michael addition sequence (A). Role of the stoichiometric base (B).

aldehydes [89]. In the case of acryloyloxazolidinone **183**, the reaction gave the expected aldol product **184** in good yields and diastereomeric ratios with a preference toward the *syn*-adduct (Scheme 47A). Interestingly, when they used methacryloyloxazolidinone **185** as a Michael acceptor, the X-ray analysis of the product showed a rearranged structure (Scheme 47B). The authors concluded that the new structure **186** is formed by intramolecular ring opening of the oxazolidine unit initiated by the hydroxy group either following the aldol condensation or during the reaction workup.

In 2021, Zhang and Oestreich presented a Cu-catalyzed tandem conjugate silylation/aldol cyclization sequence where the diastereoselectivity of the reaction is determined by the Si nucleophile used [90]. Using $Me_2PhSiZnX{\cdot}2LiX$ in combination with ligand **L21** leads to the *trans* adduct, while $Me_2PhSiBpin$ together with **L30** provides the *cis* product. Consequently, the authors have successfully synthesized a broad range of bicyclic structures with excellent enantio- and diastereocontrol (Scheme 48). The thermodynamically driven *cis*-to-*trans* isomerization is also available by a retro-aldol–aldol procedure facilitated by a strong base (NaOH or $Me_2PhSiZnX{\cdot}2LiX$). Additionally, further derivatization is possible through the oxidation of the silyl motif to alcohol or the dehydration of the aldol adduct.

Other tandem conjugate addition/enolate-trapping reactions

In 2016, Nishiyama and co-workers have studied a three-component coupling reaction of alkynes, enones, and aldehydes via

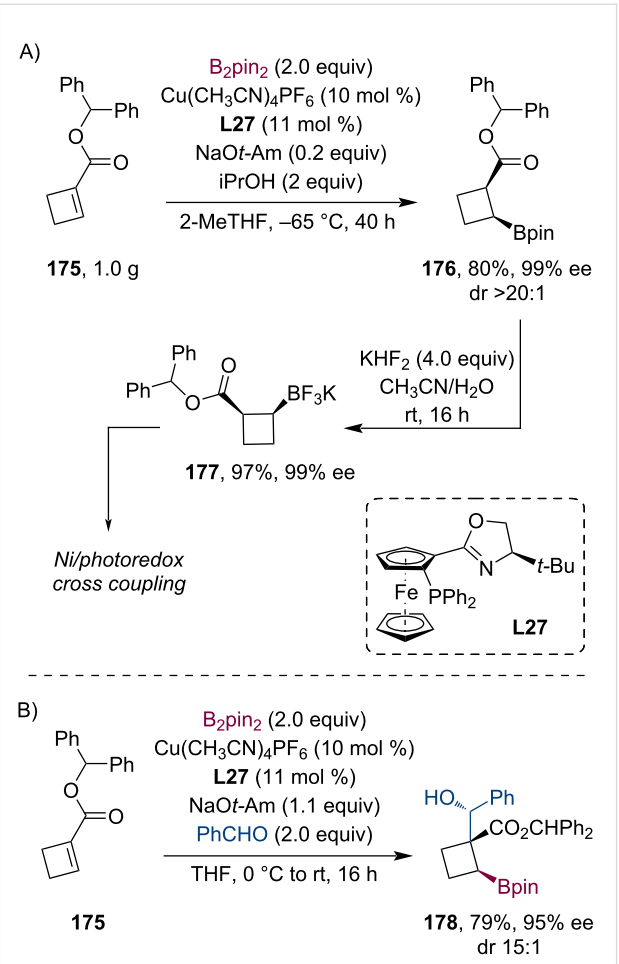

Scheme 45: Enantioselective conjugate borylation of cyclobutene-1-carboxylic acid diphenylmethyl ester **175** with subsequent enolate trapping using benzaldehyde.

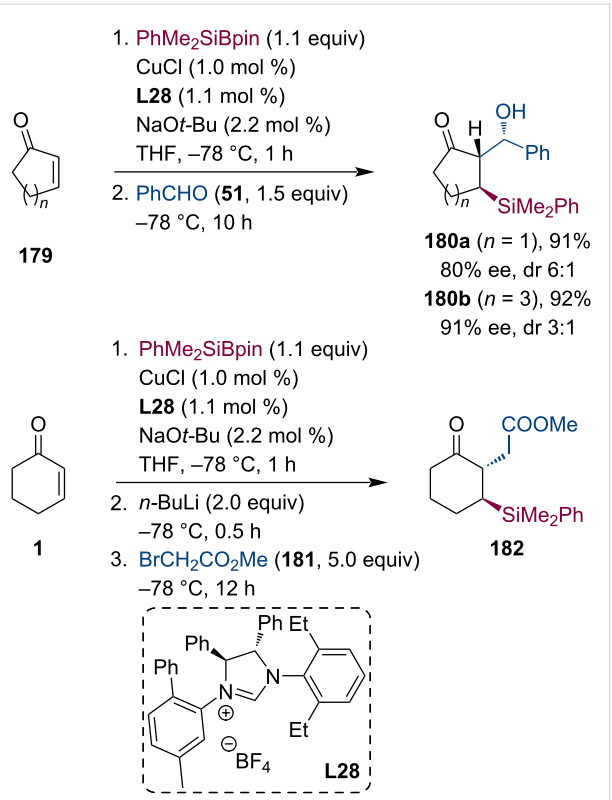

Scheme 46: Cu-catalyzed enantioselective tandem conjugate silylation of α,β-unsaturated ketones with subsequent enolate trapping.

direct conjugate alkynylation and consecutive aldol addition (Scheme 49) [91]. The chiral ruthenium complex **C2** (Phebox-type)-catalyzed procedure delivered β-hydroxyketone derivatives **192** having α-propargyl groups in good yields, however, only with low diastereoselectivities (up to 3:1). While the *syn*-diastereomers had low ee values, the *trans*-products showed better enantioselectivities (up to 78%). Their control experiments suggested that the Ru enolate, formed by the conjugate addition of the alkyne to the enone, plays a significant role in the following aldol reaction.

Later, Tian et al. have also employed a Phebox-based rhodium complex (**C3**) to catalyze the tandem conjugate addition of a terminal alkene followed by reacting the bicyclic dienol silyl ether intermediate with Michael acceptors in a one-pot procedure (Scheme 50) [92]. The bridged cyclic products **196a**,**b**, formed by a double Michael addition sequence, were isolated in moderate to good yields and with high enantiopurities.

Continuing with other Rh-based catalysts, the group of Lautens has also studied the stereoselective conjugate addition of alkynyl species to α,β-unsaturated ketones with subsequent trapping of the metal enolate by aldol cyclization (Scheme 51A) [93]. The reaction starts with the coordination of the Rh catalyst to the propargyl alcohol **198**. In the presence of a base, the rhodium–alkynyl reagent is generated with the concomitant extrusion of benzophenone. Finally, the alkynylation of the enone is followed by the cyclization step which yields the α-propargyl-β-hydroxyketones **201** in good yields and excellent diastereo- and enantiopurities. Soon after, the Lautens group has further extended their methodology to the synthesis of spirooxirane derivatives **203** by implementing a spiro-cyclization step following the aldol reaction (Scheme 51B) [94]. Giving only a single diastereomer with good enantioselectivity using a Rh/bicyclo[2.2.2]octane-2,5-diene (bod) complex, a broad variety of spiro compounds were isolated in good to excellent yields. The authors have also shown that this skeleton provides a great opportunity to prepare complex molecules by further transformations.

Similarly, Huang et al. have recently published their work on the Rh-bod complex-catalyzed highly stereoselective tandem arylation/aldol cyclization [95]. The conjugate addition of aryl-

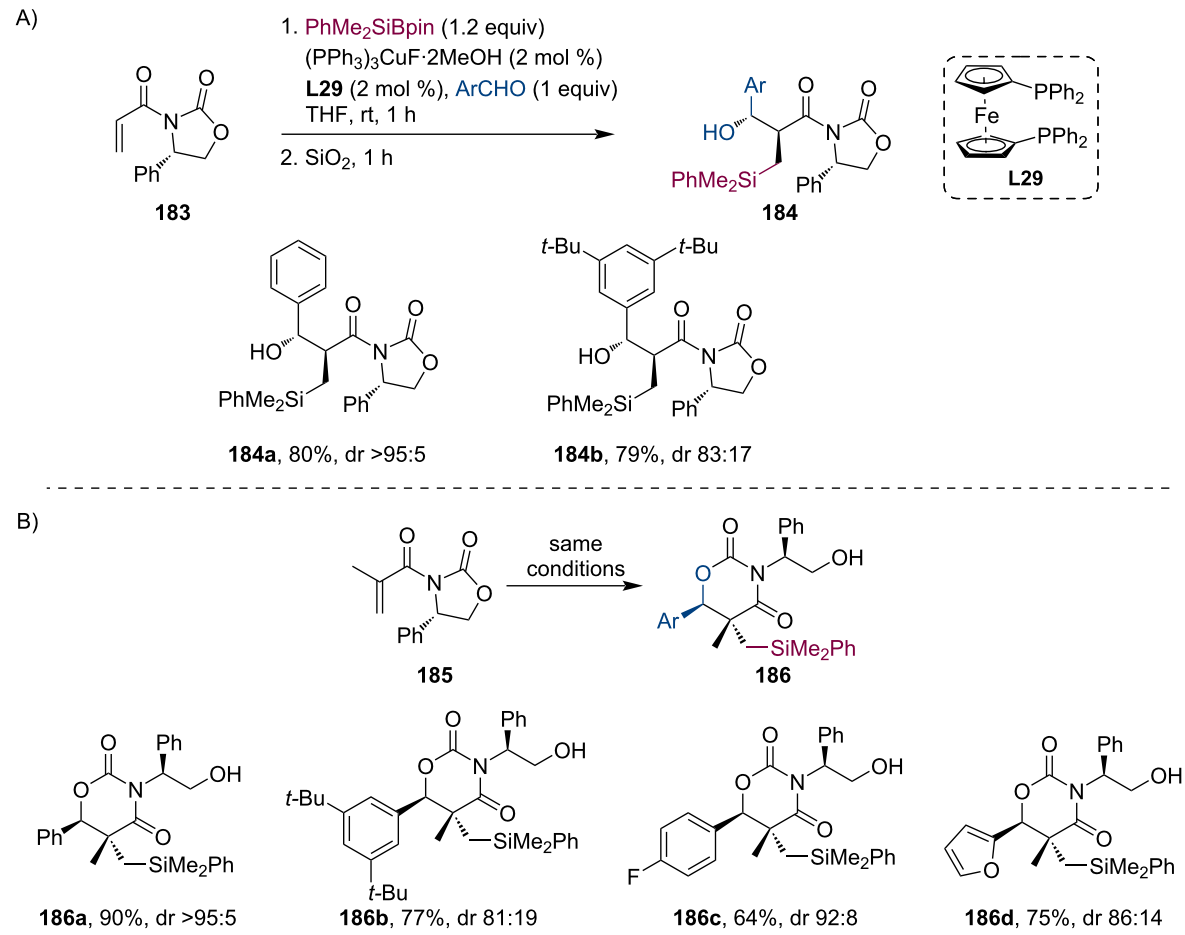

Scheme 47: Cu-catalyzed enantioselective tandem conjugate silylation of α,β-unsaturated ketones with subsequent enolate trapping.

boronic acids to acyclic α,β-unsaturated ketones **147** with sequential intramolecular addition of the enolate to the cyclic dione moiety resulted in various bicyclic compounds with quantitative diastereoselection and excellent yields and enantioselectivities up to 99% (Scheme 52A). Interestingly, when the authors exchanged the Cs_2CO_3 base to Et_3N, the hydroarylated derivative **205** was isolated as the main product (Scheme 52B). Thus far, the direct hydroarylation of such enone-dione substrates was unprecedented, presumably, due to the preferred metal-catalyzed aldol cyclization. Their protocol was further verified by a wide substrate scope. Additionally, the reaction showed high functional group tolerance with excellent stereoselectivities.

In 2016, Ellman and co-workers demonstrated a Rh- or Co-catalyzed highly diastereoselective tandem C–H bond addition/aldol reaction sequence [96,97]. The C–H activation was promoted by pyridine, pyrazole, or imine directing groups, while the aldol addition step was performed either in a two-component (intramolecular aldol) or a three-component (intermolecular aldol) arrangement. The enantioselective implementation of this methodology was realized by Herraiz and Cramer in 2021 (Scheme 53) [98]. The reaction sequence is initiated by the C–H activation of aryl pyrazoles, followed by the asymmetric conjugate addition to the Michael acceptor. Then, the formed cobalt enolate participates in the intermolecular aldol reaction with an aldehyde **207**. The stereochemistry of this tandem procedure is controlled by the chiral Co(III) complex **C4** bearing binaphthyl-derived Cpx ligands. The authors have successfully isolated a broad scope of β-hydroxyketones **208** in good yields and high enantioselectivities. Although only a moderate diastereomeric ratio was achieved, their ligand screening showed that properly tuning the ligand structure can significantly affect the diastereomeric ratio, resulting in even opposite selectivity.

Roush and co-workers have presented a simple stereoselective reductive aldol procedure for the synthesis of tetrasubstituted enolates **210** from substituted morpholine acrylamides **209** (Scheme 54) [99]. Subsequent trapping of the boron enolate with various aldehydes provided the aldol adducts with good

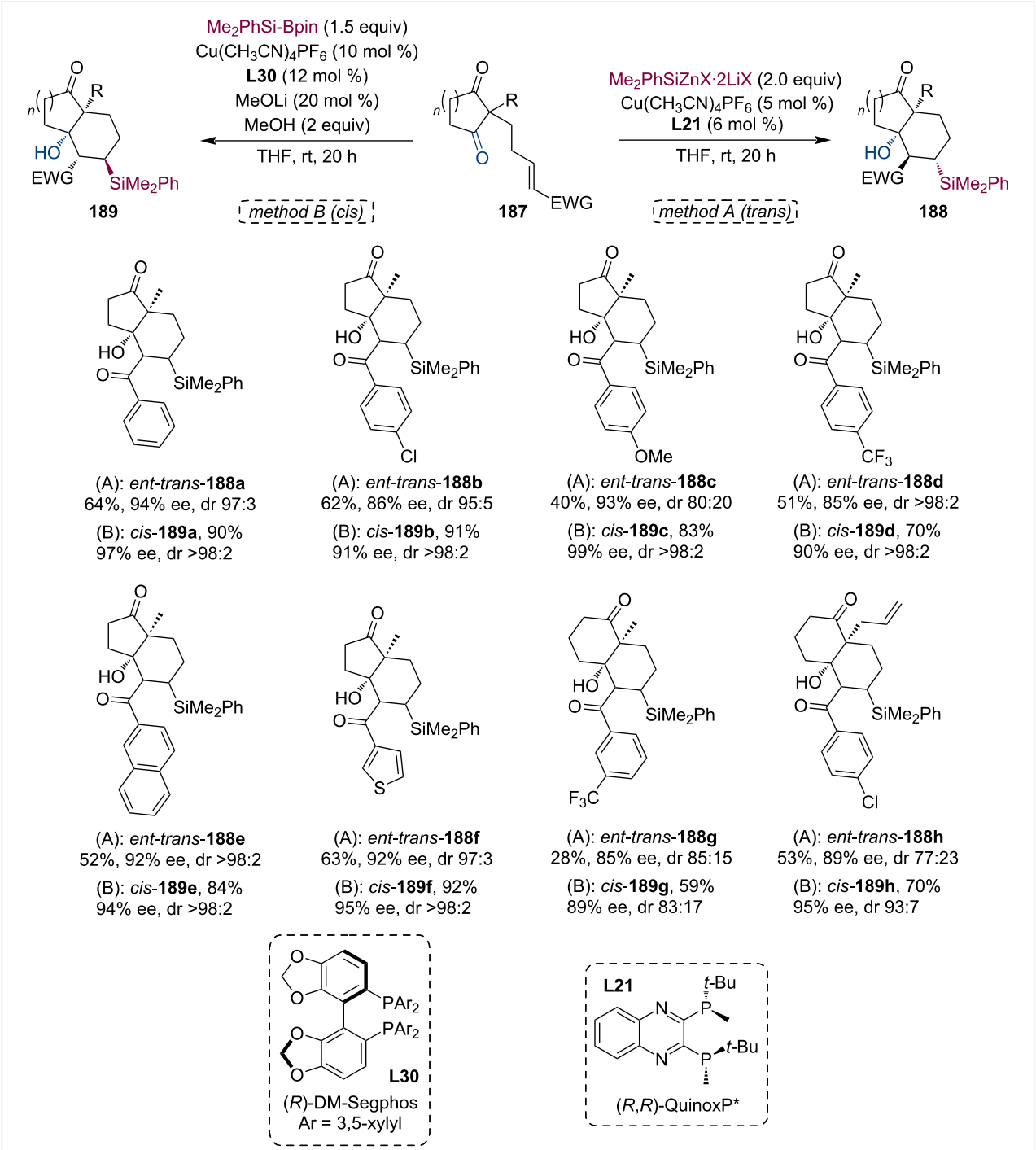

Scheme 48: Cu-catalyzed tandem conjugate silylation/aldol condensation. The diastereoselectivity is controlled by the silicon nucleophile.

yields. Compared to general aldol reactions, the boron enolates showed lower reactivity and required overnight reflux to achieve good conversions. Nevertheless, the stereoselectivity of the reaction was still excellent (up to >95% ee, dr >20:1). Due to the high diastereoselectivity, the authors have concluded that the boron enolates are stable and do not isomerize by reversible formation of C–boryl species. The stereochemical information of the enolate is most likely transferred to the final product via a chair-like transition state.

Application in total synthesis

As shown before, asymmetric tandem conjugate additions followed by enolate trapping are robust methodologies for synthesizing complex structures with multiple stereogenic centers. For

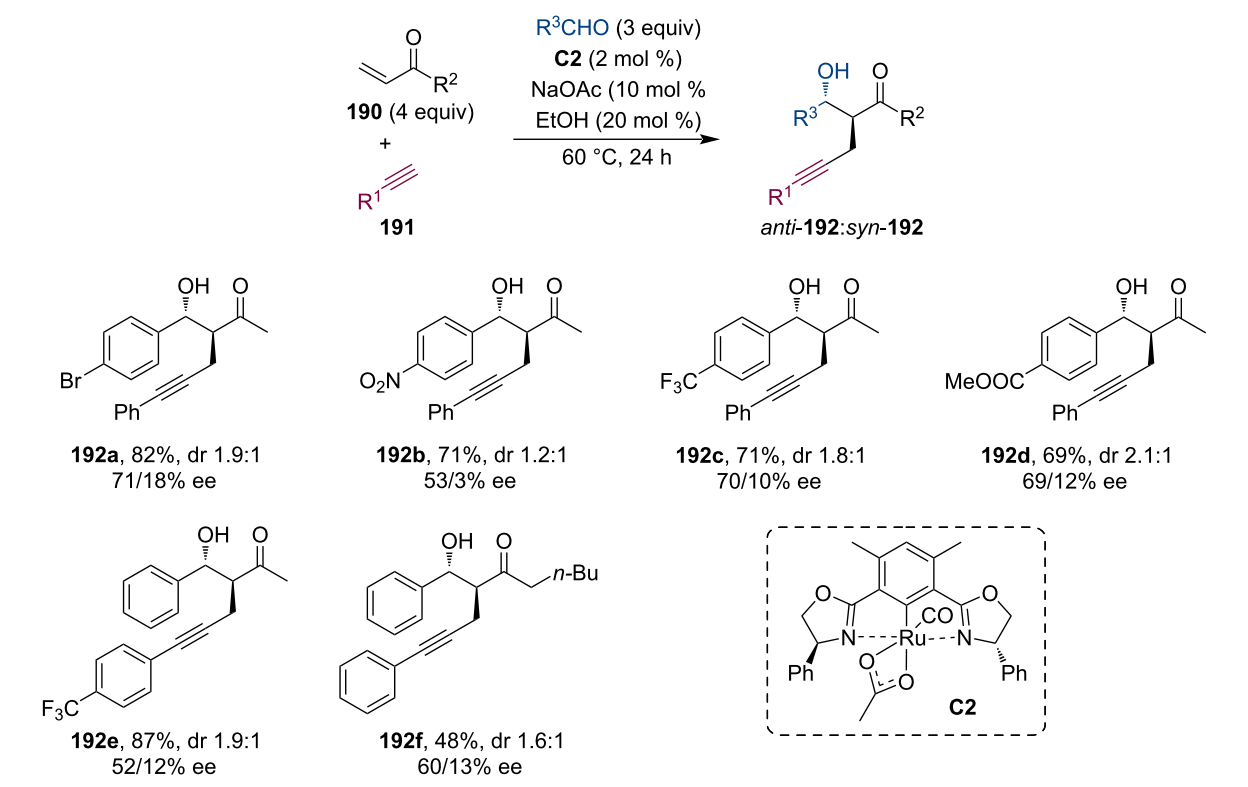

Scheme 49: Chiral Ru-catalyzed three-component coupling reaction.

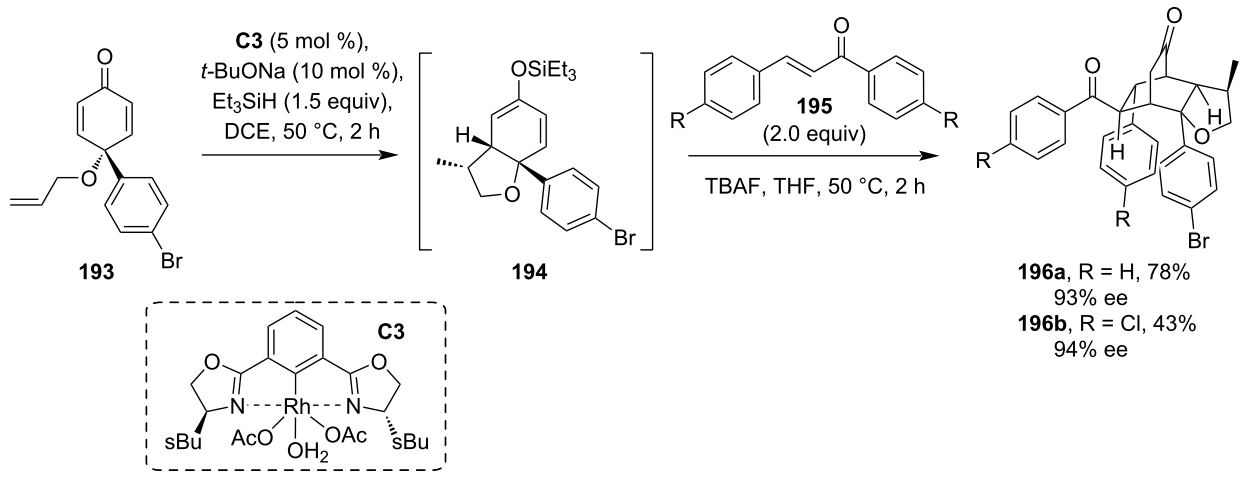

Scheme 50: Rh-Phebox complex-catalyzed reductive cyclization and subsequent reaction with Michael acceptors through the silyl enol ether.

this reason, such stereoselective procedures are commonly used in total synthesis (Figure 2) [100,101]. In this chapter, a few other examples are discussed.

Malaria is one of the most widespread diseases that still poses a severe threat to inhabitants and travelers of tropical regions within Africa, Asia, and Latin America. Uncomplicated cases, caused by *Plasmodium* parasites, are usually successfully treated by artemisinin combination therapy (ACT). Artemisinin can be isolated from the *Artemisia annua* (sweet wormwood) plant. This sesquiterpene lactone bearing a peroxide is a prodrug of the biologically active dihydroartemisinin. In 2012, Zhu and Cook developed a gram-scale asymmetric total synthesis of (+)-artemisinin (Scheme 55) [102]. Using the commer-

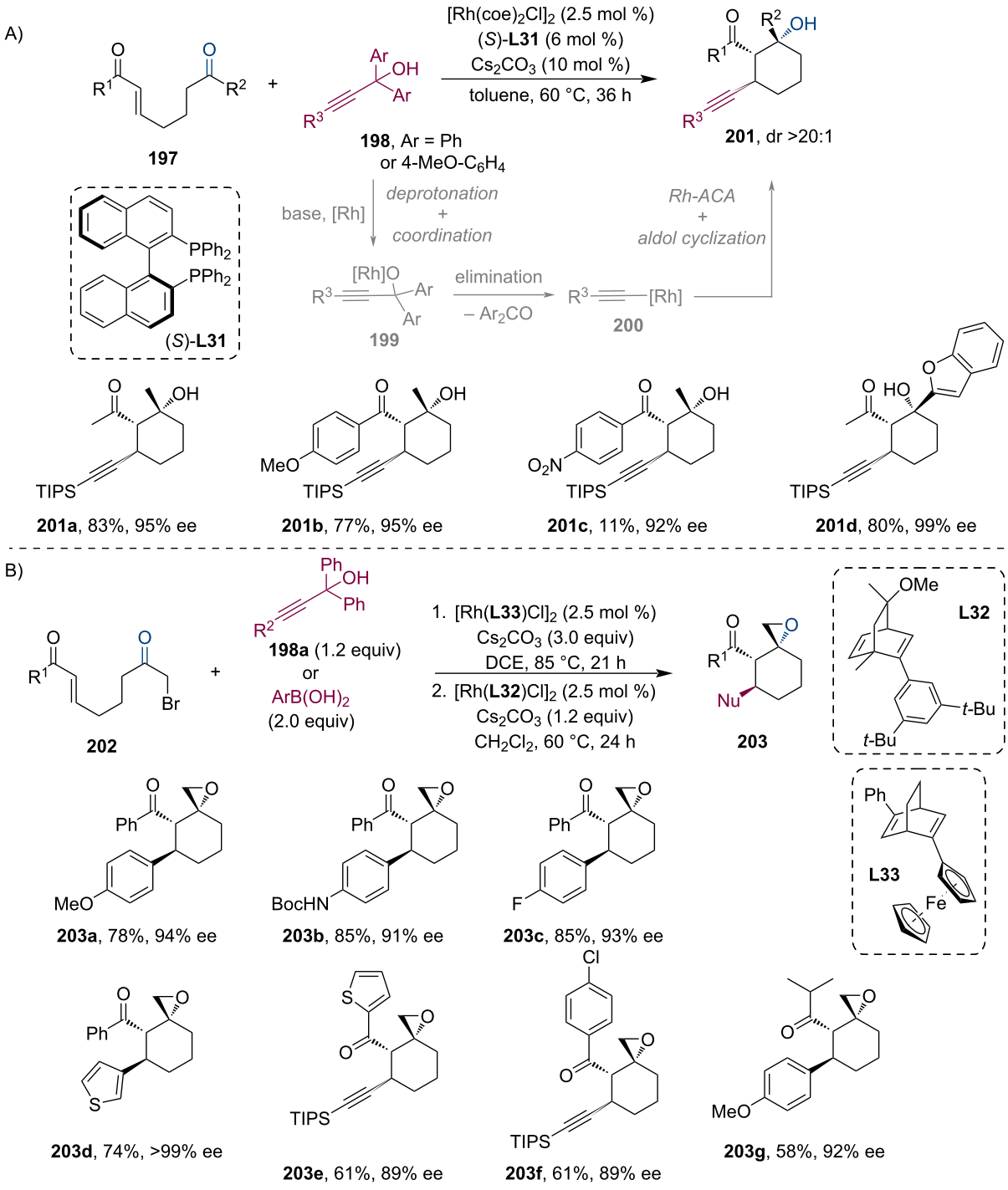

Scheme 51: Rh-catalyzed tandem asymmetric conjugate alkynylation/aldol reaction (A) and subsequent spiro-cyclization (B).

cially available and cheap cyclohexenone **1** as starting material, they have demonstrated an economic synthesis plan in only five steps. In the first step, the Cu-catalyzed conjugate addition of Me_2Zn is followed by alkylation with 1-bromobut-2-ene (**212**). The product of this tandem sequence was isolated on a multigram scale (26 g) in 61% yield and 91% ee with a *trans*/*cis* diastereomeric ratio of 7:1.

Later, Luo and co-workers developed a modular, enantioselective synthetic approach to various amphilectane and serrulatane

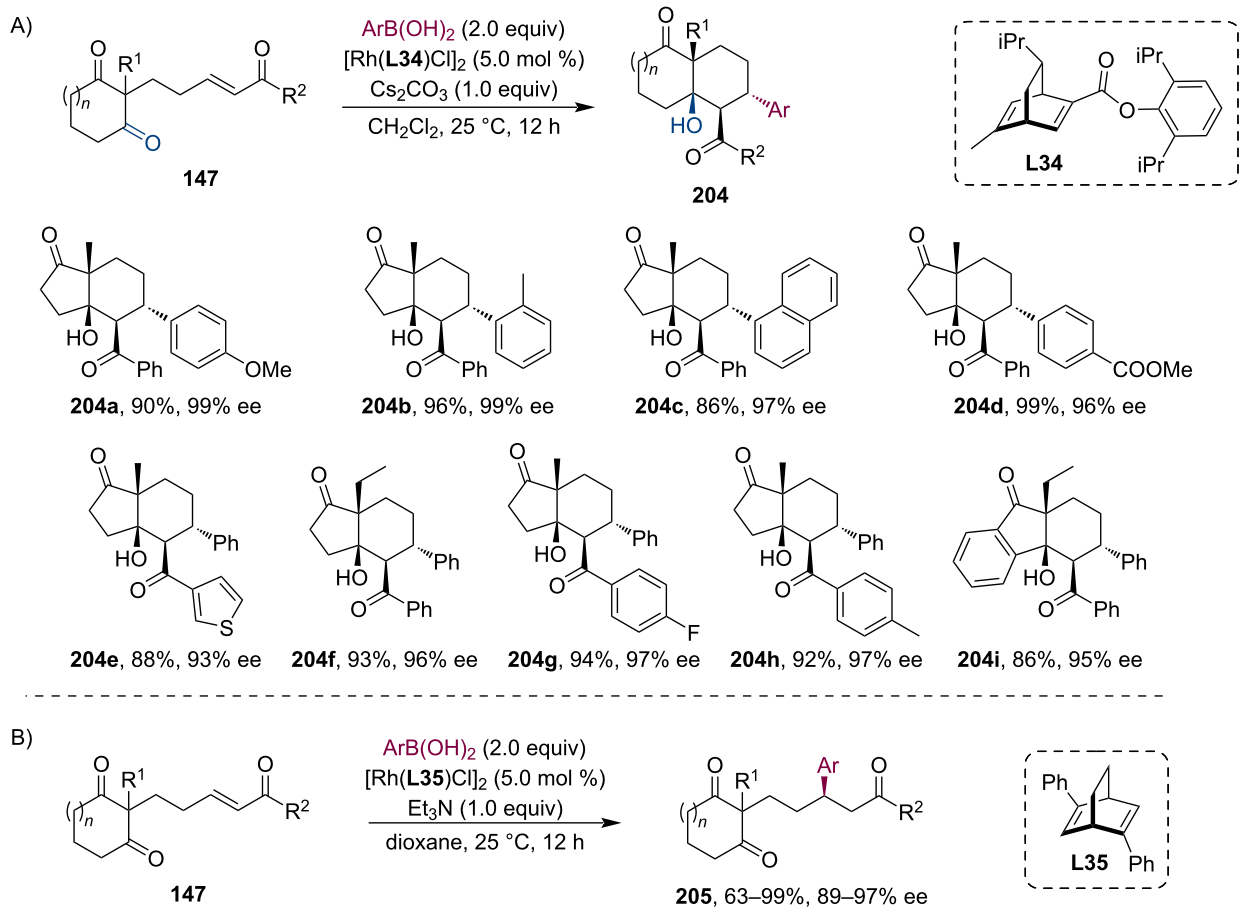

Scheme 52: Rh-bod complex-catalyzed tandem asymmetric conjugate arylation/intramolecular aldol addition (A). Simple asymmetric arylation without the subsequent cyclization in the presence of triethylamine (B).

diterpenoids (Scheme 56B) [103]. These complex natural compounds exhibit strong pharmacological activities like anti-inflammatory, antituberculosis, analgesic properties, etc. The key reaction steps included a highly stereoselective gold-catalyzed or thermally activated Cope rearrangement and a gold-catalyzed 6-*endo*-*dig* cyclization. The chiral starting material was prepared by an asymmetric Cu-catalyzed tandem conjugate addition/acylation sequence using ethyl cyanoacetate (Mander's reagent) as a trapping agent (Scheme 56A). Activation of the zinc enolate by MeLi was necessary, but with optimum reaction conditions the authors were able to isolate product (+)-**214** in good yield (75–85%) and excellent stereoselectivity (>95%) on a multigram scale. Additionally, both stereoisomers are available by simply using the ligand with the opposite stereochemistry.

Pleuromutilin-based antibiotics are an essential line of defense in the war against resistant bacteria strains. The tricyclic diterpene fungal metabolite (+)-pleuromutilin was isolated in 1951 [104]. Since then it has served as a starting point for developing new antibiotics, including semisynthetic derivatives effective against Gram-positive or even both types of bacterial species. The C14 analogs, tiamulin, and valnemulin have been used by veterinarians since the 1980s. The topical antibiotic retapamulin was approved by FDA in 2007 for the treatment of the skin infection impetigo. In 2019–2020, lefamulin was introduced both in the USA and the EU to treat community-acquired bacterial pneumonia. Herzon et al. have demonstrated the modular synthesis of various pleuromutilins and created the foundation for the development of novel antibiotics against complicated infections. The key stereochemical information was usually introduced by a stereoselective tandem Cu-catalyzed conjugate addition and subsequent trapping of the zinc enolate by acylation or aldol reaction with an overall yield of 71–78% and good stereoselectivity (Scheme 57) [105-107]. Recently, Poock and Kalesse demonstrated the first total synthesis of halioxepine, a meridoterpene isolated from the Indonesian sponge *Haliclona* sp. [108]. Their synthesis takes advantage of the same tandem procedure that gives β-ketoester **219**. The asymmetric conjugate 1,4-addition and subsequent acyl-

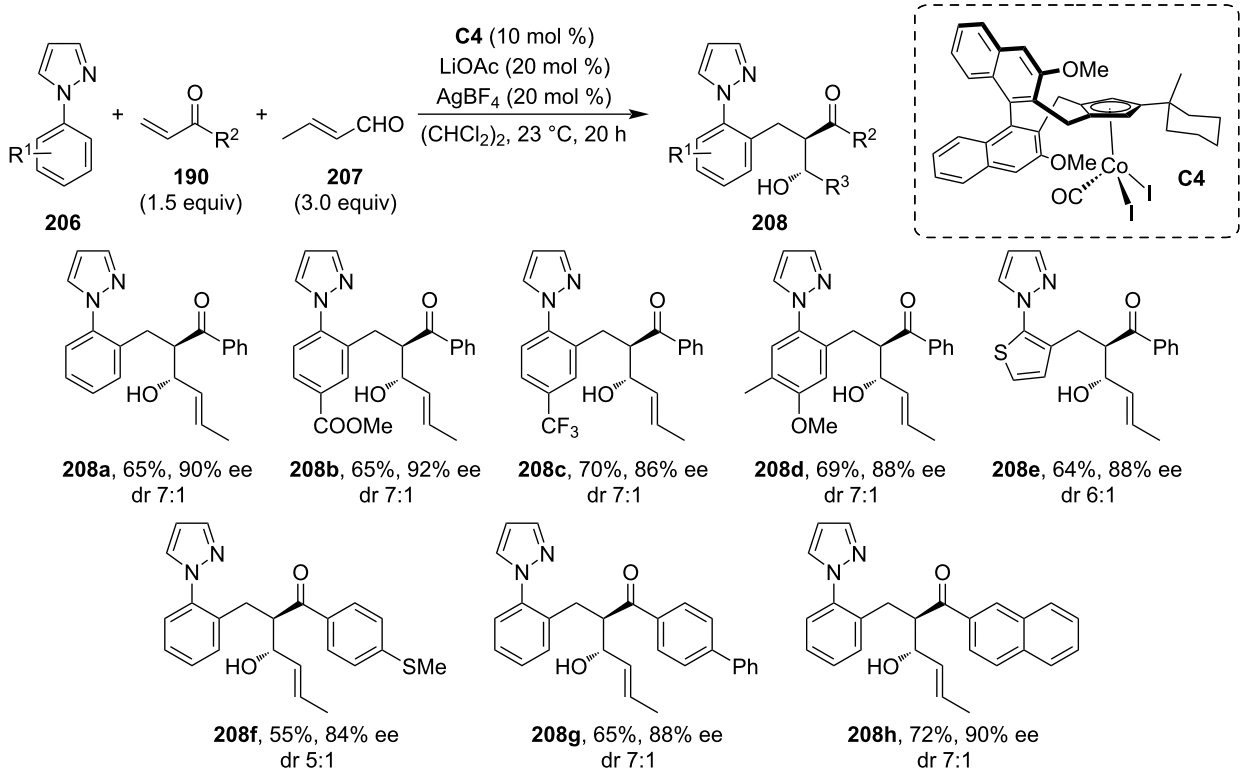

Scheme 53: Co-catalyzed C–H-bond activation/asymmetric conjugate addition/aldol reaction.

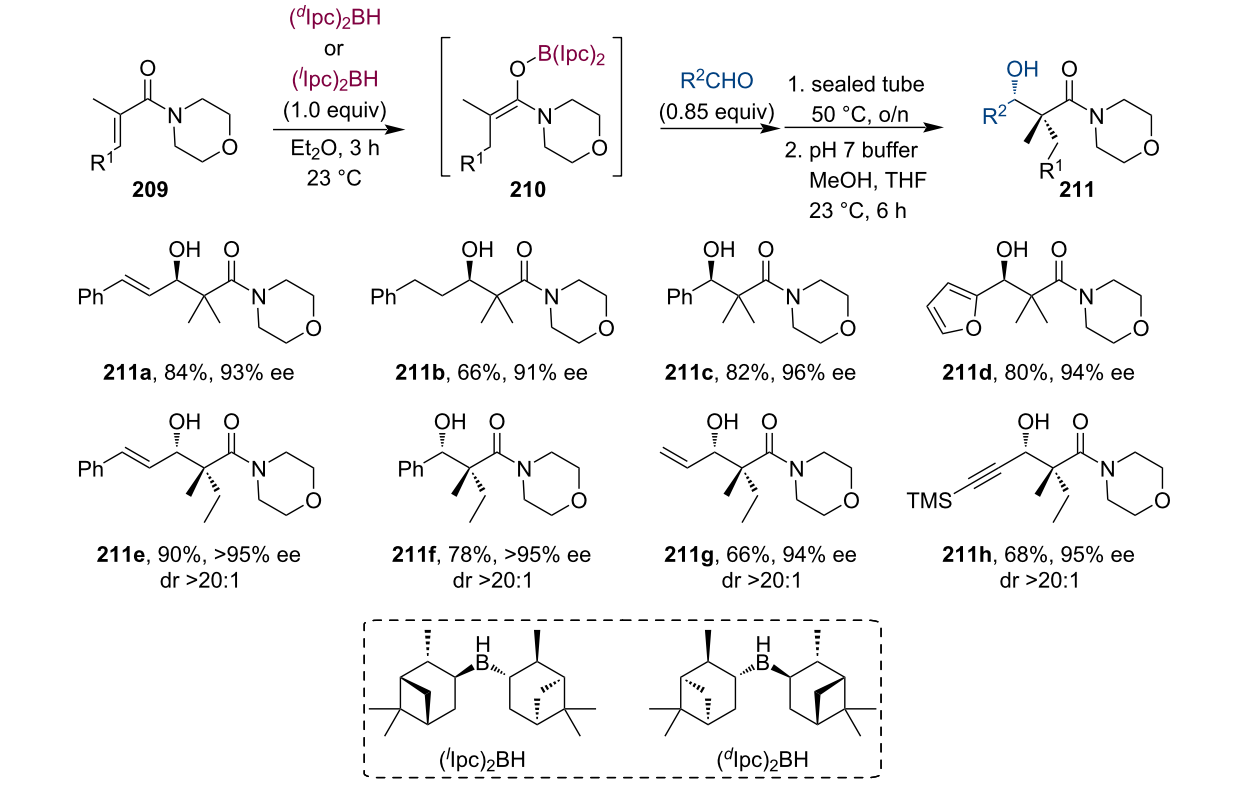

Scheme 54: (Diisopinocampheyl)borane-promoted 1,4-hydroboration of α,β-unsaturated morpholine carboxamides and subsequent aldol reaction.

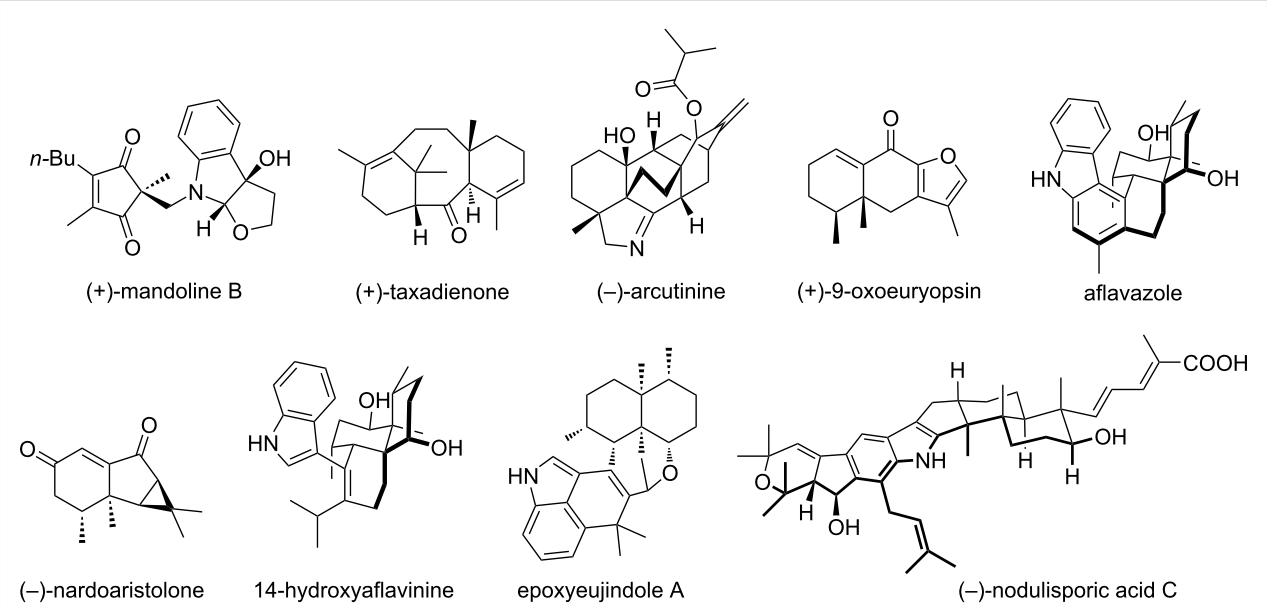

Figure 2: Some examples of total syntheses that have been recently reviewed.

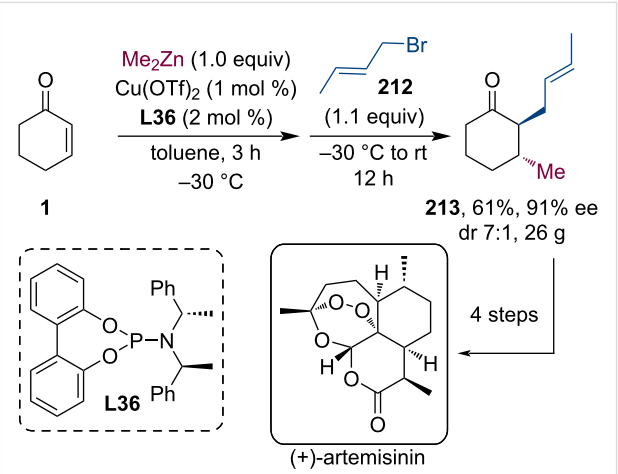

Scheme 55: Stereoselective synthesis of antimalarial prodrug (+)-artemisinin utilizing a tandem conjugate addition/alkylation sequence.

ation provided good stereocontrol and the authors could revise the thus far incorrectly assigned configuration of the target compound.

A similar tandem conjugate addition/acylation reaction sequence was utilized by the group of Jia in their work on the total synthesis of (−)-glaucocalyxin A [109]. Such diterpenoids, containing a 14-oxygenated bicyclo[3.2.1]octane ring system with several continuous stereocenters, are quite challenging targets for total synthesis, however, their biological properties render them highly valuable compounds. The authors utilized a $Mn(OAc)_3$-mediated oxidative cyclization strategy, which begins with the introduction of the fundamental stereochemical information through an asymmetric tandem conjugate addition to cyclohexenone **1**, followed by the trapping of the Mg enolate with ethyl cyanoacetate (**221**). Consequent α-alkylation resulted in the multifunctionalized product **223** in 61% yield (Scheme 58).

Natural products with complex multicyclic structures lacking functional groups (lack of oxygenation) are particularly difficult targets for synthetic chemists. Nevertheless, Huang and co-workers have successfully resolved the total synthesis of waihoensene which was isolated in 1997 from a New Zealand podocarp [110]. This diterpene has a unique substructure with fused 5-membered rings in an angular fashion and contains six contiguous stereogenic centers out of which four are all-carbon quaternary stereocenters. The authors have achieved the stereoselective synthesis of waihoensene for the first time with a 3.8% overall yield (15 steps) (Scheme 59). The construction of the triquinane core included a Cu-catalyzed asymmetric conjugate addition/aminomethylation followed by an oxidation to install the exocyclic double bond. The enone **226** was isolated in 61% yield and 91% ee.

Paclitaxel (taxol) is a highly successful chemotherapy medication that can be isolated from the Pacific jew tree (*Taxus brevifolia*), however, production from the natural source could hardly satisfy the high demand. Therefore, considerable effort was made toward the development of a cost-effective chemical production. In 2020, Fletcher and Wang joined the pursuit of a more efficient approach to produce taxol and related com-

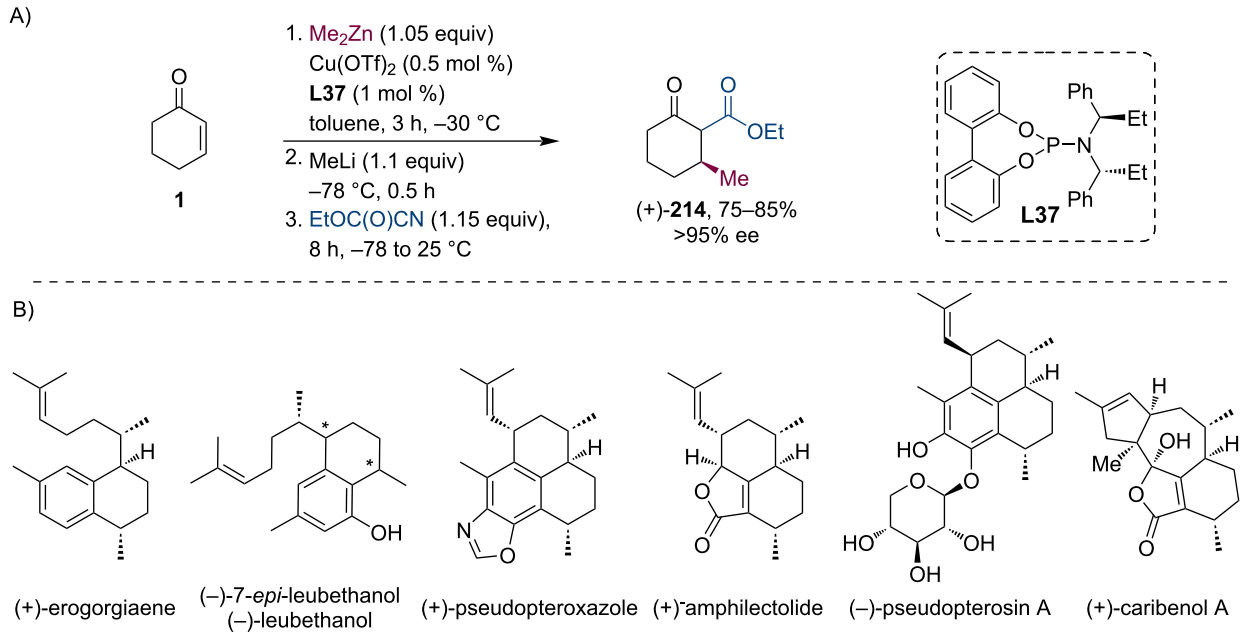

Scheme 56: Amphilectane and serrulatane diterpenoids: preparation of chiral starting material via asymmetric tandem conjugate addition/acylation (A) and structures of prepared molecules (B).

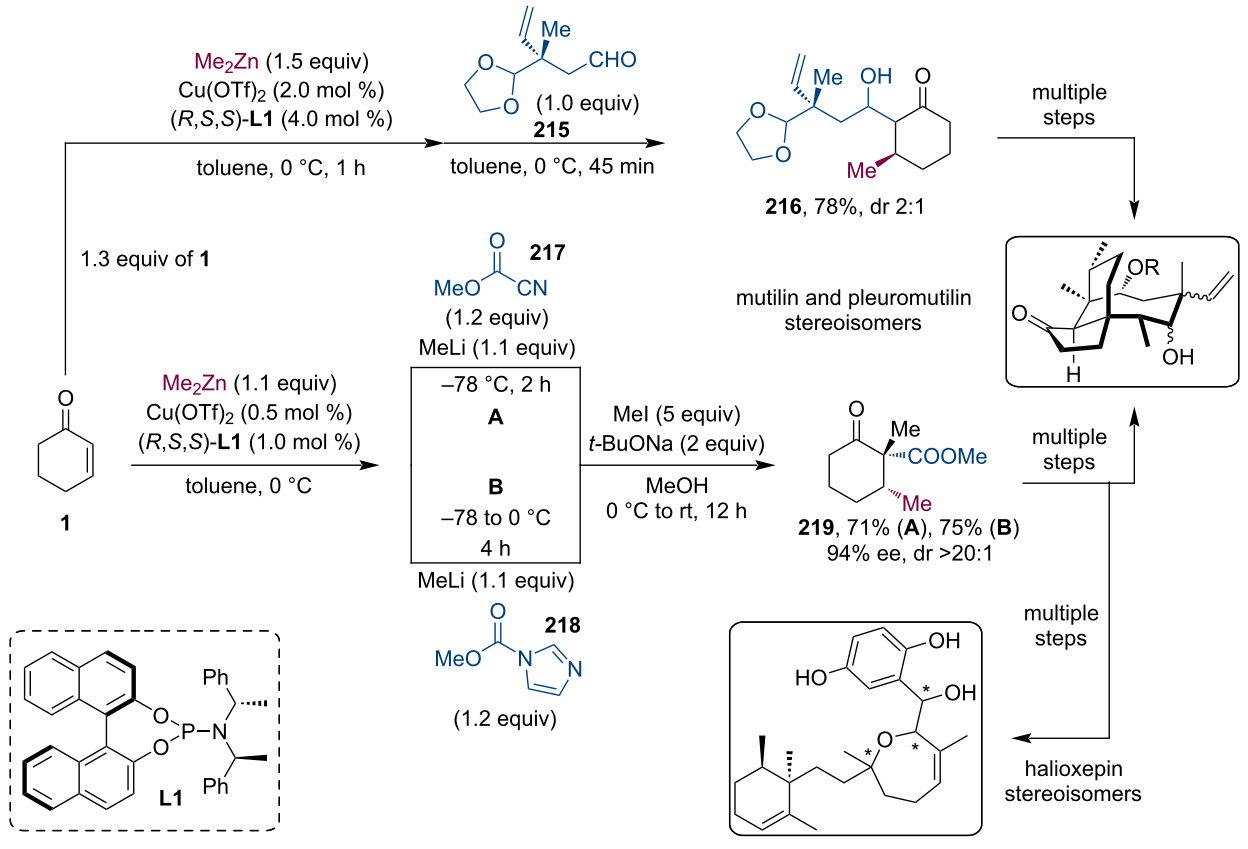

Scheme 57: Various asymmetric syntheses of pleuromutilin and related compounds based on a tandem conjugate addition/acylation sequence. The same procedure provides access to halioxepin as well.

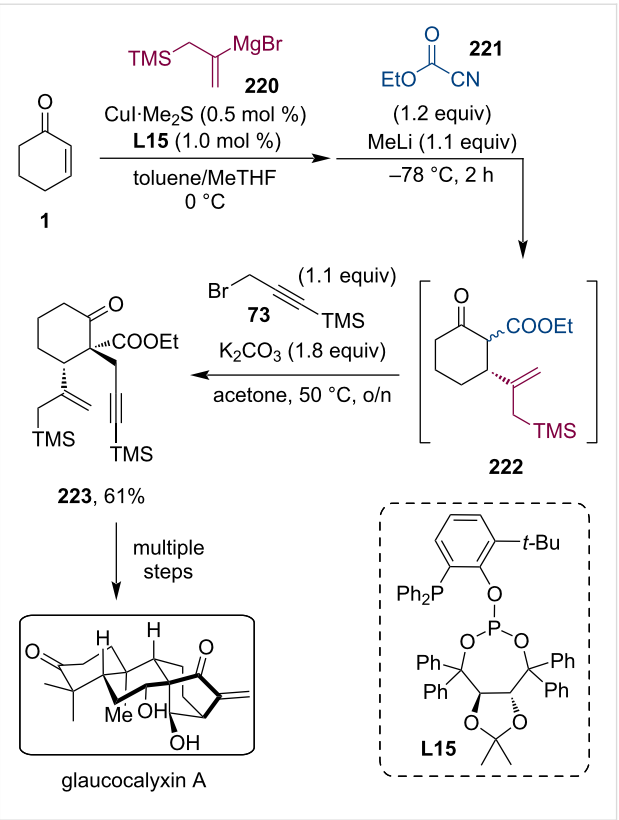

Scheme 58: Total synthesis of glaucocalyxin A utilizing a tandem conjugate addition/acylation reaction sequence.

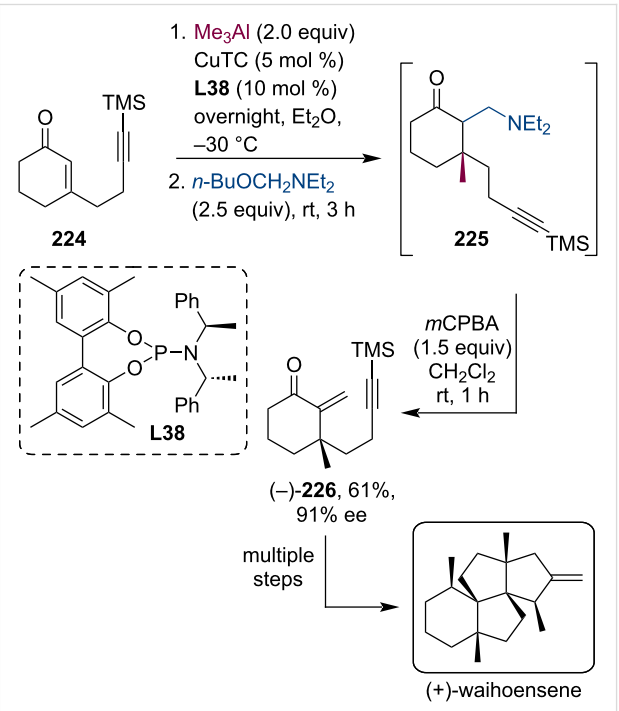

Scheme 59: Installation of the exocyclic double bond using a tandem conjugate addition/aminomethylation sequence followed by oxidation during the total synthesis of waihoensene.

pounds [71]. Their methodology employed a multistep tandem procedure (Scheme 60): first, the alkylzirconium nucleophile was produced by hydrometalation of the functionalized alkene **142**. Next, this organozirconium reagent was used in a Cu-catalyzed asymmetric conjugate addition to 3-methyl-2-cyclohex-2-ene-1-one (**141**) followed by the trapping of the metal enolate with Vilsmeier–Haack reagent. This way, the β-chloroaldehyde **143** was isolated in 69% yield and 92% ee. Further transformation of this compound resulted in the taxol core in only 4 steps with 11% overall yield while retaining the correct stereochemistry introduced in the first step by the phosphoramidite ligand **L39** (92% ee, dr 1:1) (Scheme 60).

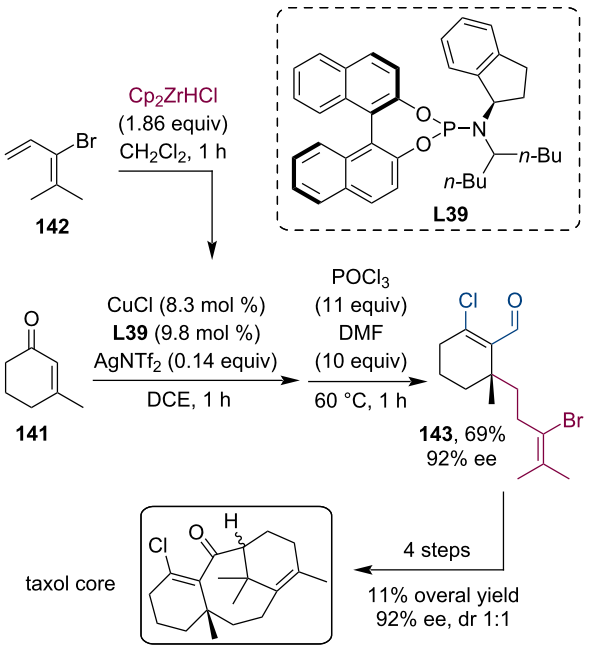

Scheme 60: Synthesis of the taxol core using a tandem conjugate addition/enolate trapping sequence with Vilsmeier–Haack reagent.

Recently, Liu and co-workers reported the stereoselective synthesis of the tricyclic core of dodecahydrodibenzo[*b*,*d*]furan skeleton containing 12-*epi*-JBIR-23 and -24 [111]. Besides their intriguing complex structures, these novel compounds also found interest due to their potential inhibitory activity against malignant pleural mesothelioma (MPM) cell lines. Their synthetic route includes a key tandem sequence producing three neighboring stereocenters. Zirconium enolate **228** was prepared by the Rh-catalyzed conjugate addition of organozirconium reagent **227** to enone **1**. In the presence of the (*R*)-BINAP ligand, the Michael adduct **228** could be isolated in 97% ee. Finally, the Zr enolate was trapped by aldehyde **229** prepared from D-ribose. The aldol adduct **230** was isolated in 80% yield and excellent diastereoselectivity (>20:1). Additional transformation of compound **230** following an A–AB–ABC synthetic

strategy resulted in the desired complex tricyclic skeleton opening the door for the total synthesis of 12-*epi*-JBIR-23/24 (Scheme 61).

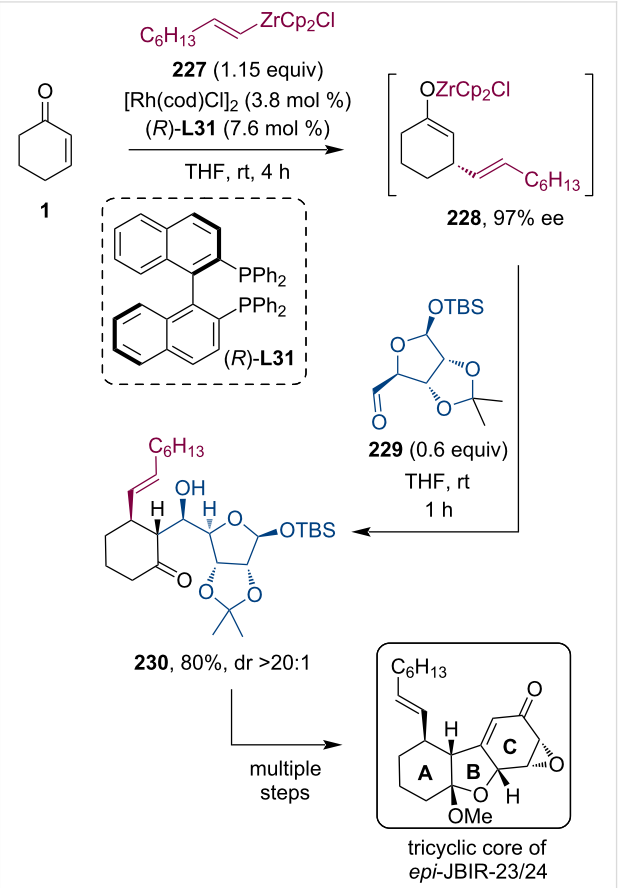

Scheme 61: Synthesis of the tricyclic core of 12-*epi*-JBIR-23/24 utilizing a Rh-catalyzed asymmetric conjugate addition/aldol reaction tandem sequence.

The sulfated β-glycoside peyssonnoside A was isolated only recently from the red algae *Peyssonnelia* sp. This diterpene showed promising biological activity against methicillin-resistant *Staphylococcus aureus* (MRSA) and liver-stage *Plasmodium berghei*. Structurally, peyssonnoside A belongs to a new class of diterpene glycosides with a distinctive tetracyclic carbon skeleton. From the point of view of a synthetic chemist, the most remarkable feature of this structure is the highly substituted cyclopropane ring incorporating two all-carbon quaternary centers, while the whole structure contains 7 stereocenters. Xu et al. recently demonstrated their 13-step total synthesis of (−)-peyssonnoside A, which begins with a Cu-catalyzed enantioselective conjugate addition/enolate alkylation tandem reaction sequence utilizing the N-heterocyclic carbene ligand **L40** [112]. Ketone **232** was isolated in 61% yield and 81% ee. Hereafter, the authors were able to synthesize the complex tetracyclic structure within only 12 additional steps, demonstrating how contemporary catalytic methodologies can facilitate the preparation of synthetically demanding natural products (Scheme 62).

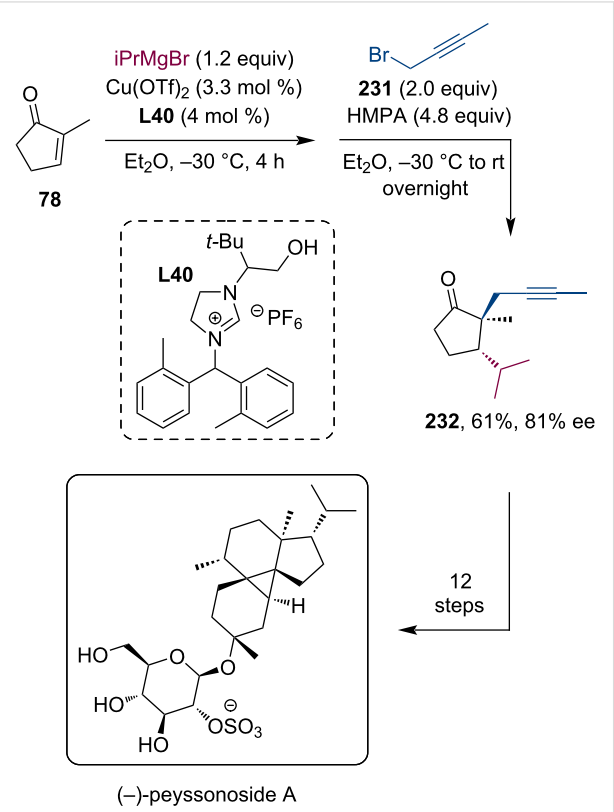

Scheme 62: Total synthesis of (–)-peyssonoside A utilizing a Cu-catalyzed enantioselective tandem conjugate addition/enolate alkylation reaction sequence.

Conclusion

Tandem reactions based on asymmetric conjugate addition and subsequent enolate trapping reactions have undeniably matured into a robust methodology. The multitude of chiral ligands available for the Cu-catalyzed addition of organometallic reagents allows the efficient introduction of chirality and functionalization of various Michael acceptors as substrates. Typical polar organometallics such as dialkylzinc, Grignard, trialkylaluminum, or organozirconium reagents are suitable for fine-tuning the conjugate addition step and the generation of the corresponding metal enolates. Less reactive Michael acceptors can be advantageously activated by Lewis acids (e.g., TMSOTf and $BF_3{\cdot}OEt_2$). These methods likely lead to silicon or boryl enolates that are also highly synthetically relevant nucleophiles. The methodology applies also to asymmetric conjugate silylation or borylation, which directly produces Si or B enolates. The high reactivity of metal enolates generated by these conjugate additions enables them to engage directly with various electrophiles such as carbonyl compounds, imines and their synthetic

equivalents, Michael acceptors, alkyl halides, and carbenium ions. These trapping reactions allow rapid construction of molecules having high synthetic complexity and provide access to great structural variability in the final products. Unsurprisingly, tandem reactions of ACA-formed enolates were utilized in the syntheses of numerous natural products.

Newer advances in this methodology document that the synthetic community is continually pushing the limitations of these transformations, which paves the way to more exciting applications. Among the limitations of this methodology is the high basicity and reactivity of metal enolates formed in the conjugate addition step. This fact stems from the conjugate addition of polar and highly reactive organometallic species, which require careful handling and cryogenic conditions. The utilization of milder organozirconium reagents is an attempt to solve this issue. On the other hand, the high reactivity of metal enolates is advantageous for subsequent trapping reactions with electrophiles. We believe that here lies the possibility for further development. Finding more active catalysts would enable the conjugate addition of less reactive organometallic reagents. At the same time, it is necessary to identify suitable electrophilic reactions that would allow the use of less reactive enolates. The possibility for catalytic activation of these enolate trapping reactions still needs to be explored but it may hide undetected reactivities so far. Another problem is the stereoselectivity of the enolate trapping reactions. Chiral ligands import chirality on the initial Michael acceptor and the chirality of the enolate usually determines the stereoselectivity of the trapping reaction. However, stereoselectivities concerning enolate additions to carbonyl compounds or imines were often poor and new strategies are needed to address this problem.

Intriguing question is whether some less traditional activation techniques such as microwave, photocatalysis, flow chemistry or mechanical activation might not be applicable also to the reactivity of ACA-generated enolates. There are some hints that the use of polar organometallics might be possible and beneficial under these conditions.

In this review, we analyzed recent developments in the trapping reactions of chiral enolates obtained by conjugate additions. We have also highlighted our attempts to explore possibilities for enolate trapping reactions with unusual electrophiles. We hope that we helped researchers working in or interested in this area to navigate this fascinating field of research and stimulate further development of this methodology.

Funding

This work was supported by the Slovak Research and Development Agency under the Contract no. APVV-18-0242.

ORCID® iDs

Péter Kisszékelyi - https://orcid.org/0000-0002-9529-0674
Radovan Šebesta - https://orcid.org/0000-0002-7975-3608

References

1. Tietze, L. F., Ed. *Domino Reactions: Concepts for Efficient Organic Synthesis;* Wiley-VCH: Weinheim, Germany, 2014. doi:10.1002/9783527671304
2. Braun, M. *Modern Enolate Chemistry: From Preparation to Applications in Asymmetric Synthesis;* Wiley-VCH: Weinheim, Germany, 2016. doi:10.1002/9783527671069
3. Alexakis, A.; Benhaim, C. *Eur. J. Org. Chem.* **2002,** 3221–3236. doi:10.1002/1099-0690(200210)2002:19<3221::aid-ejoc3221>3.0.co;2-u
4. Alexakis, A.; Bäckvall, J. E.; Krause, N.; Pàmies, O.; Diéguez, M. *Chem. Rev.* **2008,** *108,* 2796–2823. doi:10.1021/cr0683515
5. Jerphagnon, T.; Pizzuti, M. G.; Minnaard, A. J.; Feringa, B. L. *Chem. Soc. Rev.* **2009,** *38,* 1039–1075. doi:10.1039/b816853a
6. Thaler, T.; Knochel, P. *Angew. Chem., Int. Ed.* **2009,** *48,* 645–648. doi:10.1002/anie.200804446
7. Müller, D.; Alexakis, A. *Chem. Commun.* **2012,** *48,* 12037–12049. doi:10.1039/c2cc34607a
8. Schmid, T. E.; Drissi-Amraoui, S.; Crévisy, C.; Baslé, O.; Mauduit, M. *Beilstein J. Org. Chem.* **2015,** *11,* 2418–2434. doi:10.3762/bjoc.11.263
9. Pichon, D.; Morvan, J.; Crévisy, C.; Mauduit, M. *Beilstein J. Org. Chem.* **2020,** *16,* 212–232. doi:10.3762/bjoc.16.24
10. Baruah, B.; Deb, M. L. *Eur. J. Org. Chem.* **2021,** 5756–5766. doi:10.1002/ejoc.202100828
11. López, F.; Minnaard, A. J.; Feringa, B. L. *Acc. Chem. Res.* **2007,** *40,* 179–188. doi:10.1021/ar0501976
12. Harutyunyan, S. R.; den Hartog, T.; Geurts, K.; Minnaard, A. J.; Feringa, B. L. *Chem. Rev.* **2008,** *108,* 2824–2852. doi:10.1021/cr068424k
13. Wang, S.-Y.; Loh, T.-P. *Chem. Commun.* **2010,** *46,* 8694–8703. doi:10.1039/c0cc03211e
14. von Zezschwitz, P. *Synthesis* **2008,** 1809–1831. doi:10.1055/s-2008-1067097
15. Maksymowicz, R. M.; Bissette, A. J.; Fletcher, S. P. *Chem. – Eur. J.* **2015,** *21,* 5668–5678. doi:10.1002/chem.201405855
16. Mantilli, L.; Mazet, C. *ChemCatChem* **2010,** *2,* 501–504. doi:10.1002/cctc.201000008
17. Hartmann, E.; Vyas, D. J.; Oestreich, M. *Chem. Commun.* **2011,** *47,* 7917–7932. doi:10.1039/c1cc10528k
18. Alexakis, A.; Krause, N.; Woodward, S., Eds. *Copper-Catalyzed Asymmetric Synthesis;* Wiley-VCH: Weinheim, Germany, 2014. doi:10.1002/9783527664573
19. Guo, H.-C.; Ma, J.-A. *Angew. Chem., Int. Ed.* **2006,** *45,* 354–366. doi:10.1002/anie.200500195
20. Galeštoková, Z.; Šebesta, R. *Eur. J. Org. Chem.* **2012,** 6688–6695. doi:10.1002/ejoc.201200875
21. Feringa, B. L.; Pineschi, M.; Arnold, L. A.; Imbos, R.; de Vries, A. H. M. *Angew. Chem., Int. Ed. Engl.* **1997,** *36,* 2620–2623. doi:10.1002/anie.199726201
22. Welker, M.; Woodward, S. *Tetrahedron* **2010,** *66,* 9954–9963. doi:10.1016/j.tet.2010.10.048
23. Aikawa, K.; Okamoto, T.; Mikami, K. *J. Am. Chem. Soc.* **2012,** *134,* 10329–10332. doi:10.1021/ja3032345

24. González-Gómez, J. C.; Foubelo, F.; Yus, M. *J. Org. Chem.* **2009,** *74,* 2547–2553. doi:10.1021/jo802812w
25. González-Gómez, J. C.; Foubelo, F.; Yus, M. *Synthesis* **2009,** 2083–2088. doi:10.1055/s-0029-1216821
26. González-Gómez, J. C.; Foubelo, F.; Yus, M. *Tetrahedron Lett.* **2008,** *49,* 2343–2347. doi:10.1016/j.tetlet.2008.02.076
27. Guo, S.; Xie, Y.; Hu, X.; Xia, C.; Huang, H. *Angew. Chem., Int. Ed.* **2010,** *49,* 2728–2731. doi:10.1002/anie.200907320
28. Anderson, J. C.; Horsfall, L. R.; Kalogirou, A. S.; Mills, M. R.; Stepney, G. J.; Tizzard, G. J. *J. Org. Chem.* **2012,** *77,* 6186–6198. doi:10.1021/jo301000r
29. Anderson, J. C.; Stepney, G. J.; Mills, M. R.; Horsfall, L. R.; Blake, A. J.; Lewis, W. *J. Org. Chem.* **2011,** *76,* 1961–1971. doi:10.1021/jo102408u
30. Guo, S.; Xie, Y.; Hu, X.; Huang, H. *Org. Lett.* **2011,** *13,* 5596–5599. doi:10.1021/ol2023196
31. Ni, C.-Y.; Kan, S.-S.; Liu, Q.-Z.; Kang, T.-R. *Org. Biomol. Chem.* **2011,** *9,* 6211–6214. doi:10.1039/c1ob05903c
32. Hung, Y.-M.; Tseng, C.-H.; Uang, B.-J. *Tetrahedron: Asymmetry* **2015,** *26,* 1369–1374. doi:10.1016/j.tetasy.2015.10.012
33. Wang, Q.; Li, S.; Hou, C.-J.; Chu, T.-T.; Hu, X.-P. *Tetrahedron* **2019,** *75,* 3943–3950. doi:10.1016/j.tet.2019.06.032
34. Yang, T.; Zhang, Y.; Cao, P.; Wang, M.; Li, L.; Li, D.; Liao, J. *Tetrahedron* **2016,** *72,* 2707–2711. doi:10.1016/j.tet.2015.12.062
35. Kawamura, K.; Fukuzawa, H.; Hayashi, M. *Bull. Chem. Soc. Jpn.* **2011,** *84,* 640–647. doi:10.1246/bcsj.20110035
36. Jarugumilli, G. K.; Zhu, C.; Cook, S. P. *Eur. J. Org. Chem.* **2012,** 1712–1715. doi:10.1002/ejoc.201200067
37. Murphy, S. K.; Zeng, M.; Herzon, S. B. *Org. Lett.* **2016,** *18,* 4880–4883. doi:10.1021/acs.orglett.6b02320
38. Morita, Y.; Suzuki, M.; Noyori, R. *J. Org. Chem.* **1989,** *54,* 1785–1787. doi:10.1021/jo00269a006
39. Jin, M. Y.; Li, J.; Huang, R.; Zhou, Y.; Chung, L. W.; Wang, J. (Joelle). *Chem. Commun.* **2018,** *54,* 4581–4584. doi:10.1039/c8cc02097c
40. Tsujihara, T.; Tomeba, M.; Ohkubo-Sato, S.; Iwabuchi, K.; Koie, R.; Tada, N.; Tamura, S.; Takehara, T.; Suzuki, T.; Kawano, T. *Tetrahedron Lett.* **2019,** *60,* 151148. doi:10.1016/j.tetlet.2019.151148
41. Welker, M.; Woodward, S.; Alexakis, A. *Org. Lett.* **2010,** *12,* 576–579. doi:10.1021/ol9027682
42. den Hartog, T.; Rudolph, A.; Maciá, B.; Minnaard, A. J.; Feringa, B. L. *J. Am. Chem. Soc.* **2010,** *132,* 14349–14351. doi:10.1021/ja105704m
43. Teichert, J. F.; Feringa, B. L. *Chem. Commun.* **2011,** *47,* 2679–2681. doi:10.1039/c0cc05160h
44. Vila, C.; Hornillos, V.; Fañanás-Mastral, M.; Feringa, B. L. *Chem. Commun.* **2013,** *49,* 5933–5935. doi:10.1039/c3cc43105c
45. Rudolph, A.; Bos, P. H.; Meetsma, A.; Minnaard, A. J.; Feringa, B. L. *Angew. Chem., Int. Ed.* **2011,** *50,* 5834–5838. doi:10.1002/anie.201102069
46. Feringa, B. L.; Badorrey, R.; Peña, D.; Harutyunyan, S. R.; Minnaard, A. J. *Proc. Natl. Acad. Sci. U. S. A.* **2004,** *101,* 5834–5838. doi:10.1073/pnas.0308008101
47. Šebesta, R.; Bilčík, F.; Fodran, P. *Eur. J. Org. Chem.* **2010,** 5666–5671. doi:10.1002/ejoc.201000773
48. Galeštoková, Z.; Šebesta, R. *Eur. J. Org. Chem.* **2011,** 7092–7096. doi:10.1002/ejoc.201101270
49. Drusan, M.; Lölsberg, W.; Škvorcová, A.; Schmalz, H.-G.; Šebesta, R. *Eur. J. Org. Chem.* **2012,** 6285–6290. doi:10.1002/ejoc.201200729
50. Bilčík, F.; Drusan, M.; Marák, J.; Šebesta, R. *J. Org. Chem.* **2012,** *77,* 760–765. doi:10.1021/jo202146f
51. Tissot, M.; Poggiali, D.; Hénon, H.; Müller, D.; Guénée, L.; Mauduit, M.; Alexakis, A. *Chem. – Eur. J.* **2012,** *18,* 8731–8747. doi:10.1002/chem.201200502
52. Panish, R.; Chintala, S. R.; Boruta, D. T.; Fang, Y.; Taylor, M. T.; Fox, J. M. *J. Am. Chem. Soc.* **2013,** *135,* 9283–9286. doi:10.1021/ja403811t
53. Calvo, B. C.; Madduri, A. V. R.; Harutyunyan, S. R.; Minnaard, A. J. *Adv. Synth. Catal.* **2014,** *356,* 2061–2069. doi:10.1002/adsc.201400085
54. Cozzi, P. G.; Benfatti, F.; Zoli, L. *Angew. Chem., Int. Ed.* **2009,** *48,* 1313–1316. doi:10.1002/anie.200805423
55. Benfatti, F.; Benedetto, E.; Cozzi, P. G. *Chem. – Asian J.* **2010,** *5,* 2047–2052. doi:10.1002/asia.201000160
56. Gualandi, A.; Cozzi, P. G. *Synlett* **2013,** *24,* 281–296. doi:10.1055/s-0032-1317939
57. Drusan, M.; Rakovský, E.; Marek, J.; Šebesta, R. *Adv. Synth. Catal.* **2015,** *357,* 1493–1498. doi:10.1002/adsc.201500074
58. Csizmadiová, J.; Mečiarová, M.; Almássy, A.; Horváth, B.; Šebesta, R. *J. Organomet. Chem.* **2013,** *737,* 47–52. doi:10.1016/j.jorganchem.2013.03.033
59. Sorádová, Z.; Máziková, J.; Mečiarová, M.; Šebesta, R. *Tetrahedron: Asymmetry* **2015,** *26,* 271–275. doi:10.1016/j.tetasy.2015.01.015
60. Rodríguez-Fernández, M.; Yan, X.; Collados, J. F.; White, P. B.; Harutyunyan, S. R. *J. Am. Chem. Soc.* **2017,** *139,* 14224–14231. doi:10.1021/jacs.7b07344
61. Jumde, R. P.; Lanza, F.; Veenstra, M. J.; Harutyunyan, S. R. *Science* **2016,** *352,* 433–437. doi:10.1126/science.aaf1983
62. Lanza, F.; Pérez, J. M.; Jumde, R. P.; Harutyunyan, S. R. *Synthesis* **2019,** *51,* 1253–1262. doi:10.1055/s-0037-1611657
63. Vargová, D.; Pérez, J. M.; Harutyunyan, S. R.; Šebesta, R. *Chem. Commun.* **2019,** *55,* 11766–11769. doi:10.1039/c9cc05041h
64. Yan, X.; Harutyunyan, S. R. *Nat. Commun.* **2019,** *10,* 3402. doi:10.1038/s41467-019-11345-z
65. Mudráková, B.; Kisszékelyi, P.; Vargová, D.; Zakiewicz, D.; Šebesta, R. *Adv. Synth. Catal.* **2022,** *364,* 1337–1344. doi:10.1002/adsc.202101485
66. Bleschke, C.; Tissot, M.; Müller, D.; Alexakis, A. *Org. Lett.* **2013,** *15,* 2152–2155. doi:10.1021/ol400642y
67. Germain, N.; Schlaefli, D.; Chellat, M.; Rosset, S.; Alexakis, A. *Org. Lett.* **2014,** *16,* 2006–2009. doi:10.1021/ol5005752
68. Teodoro, B. V. M.; Silva, L. F., Jr. *J. Org. Chem.* **2018,** *83,* 13604–13611. doi:10.1021/acs.joc.8b02251
69. Némethová, I.; Sorádová, Z.; Šebesta, R. *Synthesis* **2017,** *49,* 2461–2469. doi:10.1055/s-0036-1588968
70. Wang, J. Y. J.; Palacin, T.; Fletcher, S. P. *Org. Lett.* **2019,** *21,* 378–381. doi:10.1021/acs.orglett.8b03520
71. Wang, J. Y. J.; Fletcher, S. P. *Org. Lett.* **2020,** *22,* 4103–4106. doi:10.1021/acs.orglett.0c01165
72. Fyfe, J. W. B.; Watson, A. J. B. *Chem* **2017,** *3,* 31–55. doi:10.1016/j.chempr.2017.05.008
73. Fernandes, G. F. S.; Denny, W. A.; Dos Santos, J. L. *Eur. J. Med. Chem.* **2019,** *179,* 791–804. doi:10.1016/j.ejmech.2019.06.092
74. Plescia, J.; Moitessier, N. *Eur. J. Med. Chem.* **2020,** *195,* 112270. doi:10.1016/j.ejmech.2020.112270
75. Ito, H.; Yamanaka, H.; Tateiwa, J.-i.; Hosomi, A. *Tetrahedron Lett.* **2000,** *41,* 6821–6825. doi:10.1016/s0040-4039(00)01161-8
76. Takahashi, K.; Ishiyama, T.; Miyaura, N. *Chem. Lett.* **2000,** *29,* 982–983. doi:10.1246/cl.2000.982

77. Chen, I.-H.; Yin, L.; Itano, W.; Kanai, M.; Shibasaki, M. *J. Am. Chem. Soc.* **2009,** *131,* 11664–11665. doi:10.1021/ja9045839
78. Burns, A. R.; Solana González, J.; Lam, H. W. *Angew. Chem., Int. Ed.* **2012,** *51,* 10827–10831. doi:10.1002/anie.201205899
79. Hornillos, V.; Vila, C.; Otten, E.; Feringa, B. L. *Angew. Chem., Int. Ed.* **2015,** *54,* 7867–7871. doi:10.1002/anie.201502987
80. Sendra, J.; Manzano, R.; Reyes, E.; Vicario, J. L.; Fernández, E. *Angew. Chem., Int. Ed.* **2020,** *59,* 2100–2104. doi:10.1002/anie.201913438
81. Larin, E. M.; Loup, J.; Polishchuk, I.; Ross, R. J.; Whyte, A.; Lautens, M. *Chem. Sci.* **2020,** *11,* 5716–5723. doi:10.1039/d0sc02421j
82. Liu, B.; Qiu, H.; Chen, X.; Li, W.; Zhang, J. *Org. Chem. Front.* **2020,** *7,* 2492–2498. doi:10.1039/d0qo00654h
83. Dahiya, G.; Pappoppula, M.; Aponick, A. *Angew. Chem., Int. Ed.* **2021,** *60,* 19604–19608. doi:10.1002/anie.202102642
84. Jadhav, S. B.; Dash, S. R.; Maurya, S.; Nanubolu, J. B.; Vanka, K.; Chegondi, R. *Nat. Commun.* **2022,** *13,* 854. doi:10.1038/s41467-022-28288-7
85. Khalse, L. D.; Gorad, S. S.; Ghorai, P. *Org. Lett.* **2022,** *24,* 7566–7571. doi:10.1021/acs.orglett.2c02955
86. Clement, H. A.; Boghi, M.; McDonald, R. M.; Bernier, L.; Coe, J. W.; Farrell, W.; Helal, C. J.; Reese, M. R.; Sach, N. W.; Lee, J. C.; Hall, D. G. *Angew. Chem., Int. Ed.* **2019,** *58,* 18405–18409. doi:10.1002/anie.201909308
87. Nguyen, K.; Clement, H. A.; Bernier, L.; Coe, J. W.; Farrell, W.; Helal, C. J.; Reese, M. R.; Sach, N. W.; Lee, J. C.; Hall, D. G. *ACS Catal.* **2021,** *11,* 404–413. doi:10.1021/acscatal.0c04520
88. Lee, K.-s.; Hoveyda, A. H. *J. Am. Chem. Soc.* **2010,** *132,* 2898–2900. doi:10.1021/ja910989n
89. Welle, A.; Petrignet, J.; Tinant, B.; Wouters, J.; Riant, O. *Chem. – Eur. J.* **2010,** *16,* 10980–10983. doi:10.1002/chem.201000907
90. Zhang, L.; Oestreich, M. *ACS Catal.* **2021,** *11,* 3516–3522. doi:10.1021/acscatal.1c00436
91. Ubukata, S.; Ito, J.-i.; Oguri, R.; Nishiyama, H. *J. Org. Chem.* **2016,** *81,* 3347–3355. doi:10.1021/acs.joc.6b00374
92. Tan, Y.-X.; Peng, P.-Y.; Wang, Y.-J.; Liu, X.-L.; Ye, W.; Gao, D.; Lin, G.-Q.; Tian, P. *Chem. Commun.* **2021,** *57,* 9724–9727. doi:10.1039/d1cc03645a
93. Choo, K.-L.; Lautens, M. *Org. Lett.* **2018,** *20,* 1380–1383. doi:10.1021/acs.orglett.8b00153
94. Choo, K.-L.; Mirabi, B.; Demmans, K. Z.; Lautens, M. *Angew. Chem., Int. Ed.* **2021,** *60,* 21189–21194. doi:10.1002/anie.202105562
95. Li, J.; Sun, J.; Ren, W.; Lei, J.; Shen, R.; Huang, Y. *Org. Lett.* **2022,** *24,* 2420–2424. doi:10.1021/acs.orglett.2c00687
96. Boerth, J. A.; Ellman, J. A. *Chem. Sci.* **2016,** *7,* 1474–1479. doi:10.1039/c5sc04138d
97. Boerth, J. A.; Hummel, J. R.; Ellman, J. A. *Angew. Chem., Int. Ed.* **2016,** *55,* 12650–12654. doi:10.1002/anie.201603831
98. Herraiz, A. G.; Cramer, N. *ACS Catal.* **2021,** *11,* 11938–11944. doi:10.1021/acscatal.1c03153
99. Allais, C.; Tsai, A. S.; Nuhant, P.; Roush, W. R. *Angew. Chem., Int. Ed.* **2013,** *52,* 12888–12891. doi:10.1002/anie.201307302
100. Vargová, D.; Némethová, I.; Šebesta, R. *Org. Biomol. Chem.* **2020,** *18,* 3780–3796. doi:10.1039/d0ob00278j
101. Calvo, B. C.; Buter, J.; Minnaard, A. J. Applications to the Synthesis of Natural Products. *Copper-Catalyzed Asymmetric Synthesis;* Wiley-VCH: Weinheim, Germany, 2014; pp 373–448. doi:10.1002/9783527664573.ch14
102. Zhu, C.; Cook, S. P. *J. Am. Chem. Soc.* **2012,** *134,* 13577–13579. doi:10.1021/ja3061479
103. Yu, X.; Su, F.; Liu, C.; Yuan, H.; Zhao, S.; Zhou, Z.; Quan, T.; Luo, T. *J. Am. Chem. Soc.* **2016,** *138,* 6261–6270. doi:10.1021/jacs.6b02624
104. Kavanagh, F.; Hervey, A.; Robbins, W. J. *Proc. Natl. Acad. Sci. U. S. A.* **1951,** *37,* 570–574. doi:10.1073/pnas.37.9.570
105. Zeng, M.; Murphy, S. K.; Herzon, S. B. *J. Am. Chem. Soc.* **2017,** *139,* 16377–16388. doi:10.1021/jacs.7b09869
106. Murphy, S. K.; Zeng, M.; Herzon, S. B. *Org. Lett.* **2017,** *19,* 4980–4983. doi:10.1021/acs.orglett.7b02476
107. Murphy, S. K.; Zeng, M.; Herzon, S. B. *Science* **2017,** *356,* 956–959. doi:10.1126/science.aan0003
108. Poock, C.; Kalesse, M. *Chem. – Eur. J.* **2021,** *27,* 1615–1619. doi:10.1002/chem.202004847
109. Guo, J.; Li, B.; Ma, W.; Pitchakuntla, M.; Jia, Y. *Angew. Chem., Int. Ed.* **2020,** *59,* 15195–15198. doi:10.1002/anie.202005932
110. Qu, Y.; Wang, Z.; Zhang, Z.; Zhang, W.; Huang, J.; Yang, Z. *J. Am. Chem. Soc.* **2020,** *142,* 6511–6515. doi:10.1021/jacs.0c02143
111. Man, Y.; Zhou, C.; Fu, S.; Liu, B. *Org. Lett.* **2021,** *23,* 3151–3156. doi:10.1021/acs.orglett.1c00853
112. Xu, B.; Liu, C.; Dai, M. *J. Am. Chem. Soc.* **2022,** *144,* 19700–19703. doi:10.1021/jacs.2c09919

License and Terms

BEILSTEIN JOURNAL OF ORGANIC CHEMISTRY

Palladium-catalyzed enantioselective three-component synthesis of α-arylglycine derivatives from glyoxylic acid, sulfonamides and aryltrifluoroborates

Bastian Jakob, Nico Schneider‡, Luca Gengenbach‡ and Georg Manolikakes*

Full Research Paper

Open Access

Address:
Department of Chemistry, RPTU Kaiserslautern-Landau, Erwin-Schrödinger-Str. Geb. 54, D-67663 Kaiserslautern, Germany

Email:
Georg Manolikakes* - manolikakes@chemie.uni-kl.de

* Corresponding author ‡ Equal contributors

Keywords:
amino acids; asymmetric catalysis; multicomponent reaction; palladium catalysis; Petasis reaction; sulfonamides

Beilstein J. Org. Chem. **2023,** *19,* 719–726.
https://doi.org/10.3762/bjoc.19.52

Received: 16 March 2023
Accepted: 17 May 2023
Published: 25 May 2023

This article is part of the thematic issue "Catalytic multi-step domino and one-pot reactions".

Guest Editor: S. Tsogoeva

Abstract

A palladium-catalyzed enantioselective three-component reaction of glyoxylic acid, sulfonamides and aryltrifluoroborates is described. This process provides modular access to the important α-arylglycine motif in moderate to good yields and enantioselectivities. The formed α-arylglycine products constitute useful building blocks for the synthesis of peptides or arylglycine-containing natural products.

Introduction

α-Amino acids play a crucial role in every aspect of our human life [1]. They are important synthetic intermediates in the chemical industry and used for the production of drugs, fertilizers, (biodegradable) polymers or nutritional supplements [2]. More importantly, α-amino acids form the backbone of all proteins and enzymes are therefore essential for almost all biological processes. In the last twenty years non-proteinogenic and chemically synthesized unnatural amino acids received increasing attention due to advances in protein-engineering and the development of protein-based therapeutics [3,4]. Among the different types of non-proteinogenic and unnatural amino acids, α-arylglycines play a particular important role. The arylglycine scaffold can be found in several well-known natural products with interesting biological properties, such as the glycopeptide antibiotics vancomycin and teicoplanin [5] or feglymycin [6], a 13mer peptide which contains nine α-arylglycines in its backbone. α-Arylglycine derivatives are used in the production of important drugs, e.g., the antiplatelet drug clopidogrel [7] or the β-lactam antibiotic amoxicillin [8] (Figure 1).

Therefore, the chemical synthesis of α-aryglycines has received considerable attention. Among the different methods intro-

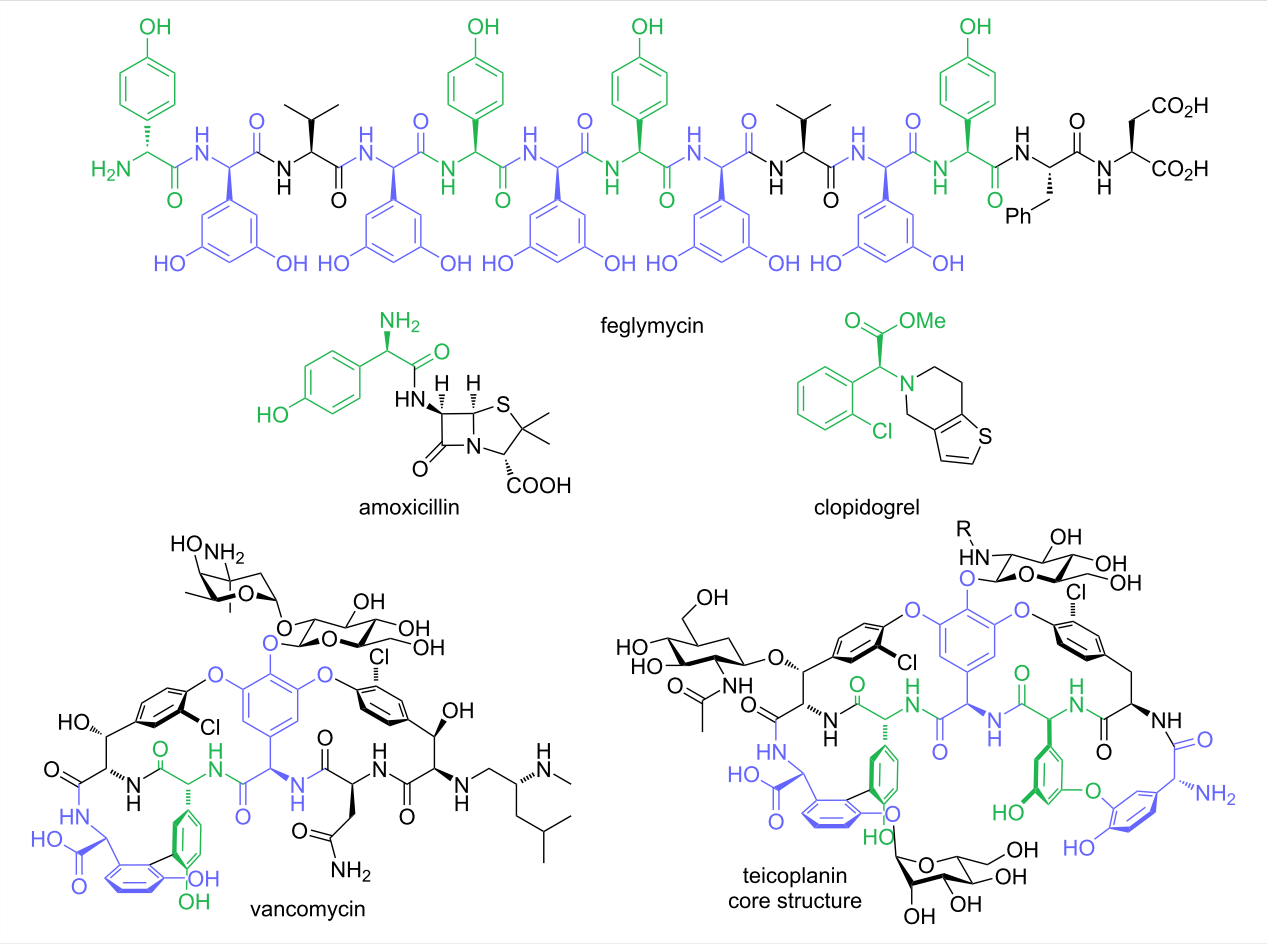

Figure 1: Biologically active molecules containing α-arylglycine motifs (highlighted in green and blue).

duced over time, multicomponent reactions utilizing an in situ generated reactive imine species provide a very flexible approach to the arylglycine scaffold [2,9]. The Petasis borono-Mannich reaction constitutes a prominent example for such an imine-based multicomponent reaction (Scheme 1a). The reaction of glyoxylic acid, an amine component and an arylboronic acid offers a highly modular access to arylglycines from three readily available building blocks [10-12]. The Petasis borono-Mannich reaction usually proceeds in the absence of any external catalyst via zwitterionic intermediates and an intramolecular transfer of the aryl residue form the activated boronate to the electrophilic iminium carbon, leading to the amine product as racemic mixture. Consequently, examples for asymmetric Petasis borono-Mannich reactions are rare [13] and usually rely on the utilization of chiral amine components in stoichiometric amounts [10,11].

As part of our research program utilizing the in situ generation of reactive imine species, we have disclosed iron- and bismuth-catalyzed three-component reactions for the synthesis of α-arylglycines [14-16], in which the arylboronic acid could be replaced with an electron-rich (hetero)arene as nucleophile. In parallel, we have developed palladium-catalyzed three-component reactions between arylboronic or carboxylic acids, amides or sulfonamides and different aldehyde components as attractive and broadly applicable alternative to the classical Petasis borono-Mannich reaction (Scheme 1b) [17-21]. Recently, we were able to extend these transformations to a palladium-catalyzed enantioselective synthesis of α-arylglycine bearing a free carboxylic acid functionality directly from the parent glyoxylic acids (Scheme 1c) [22]. We could show that the desired arylglycine can be synthesized in good to excellent enantioselectivities. However, depending on the nature/substitution pattern of the arylboronic acid, some of the arylglycine products could only be obtained in very low enantioselectivities. This can be attributed to a fast, uncatalyzed racemic background reaction of the boronic acids, in particular for electron-rich or sterically hindered arylboronic acids.

Herein, we report an improved version of this palladium-catalyzed enantioselective three-component reactions using aryltrifluoroborates as replacement of the arylboronic acid building

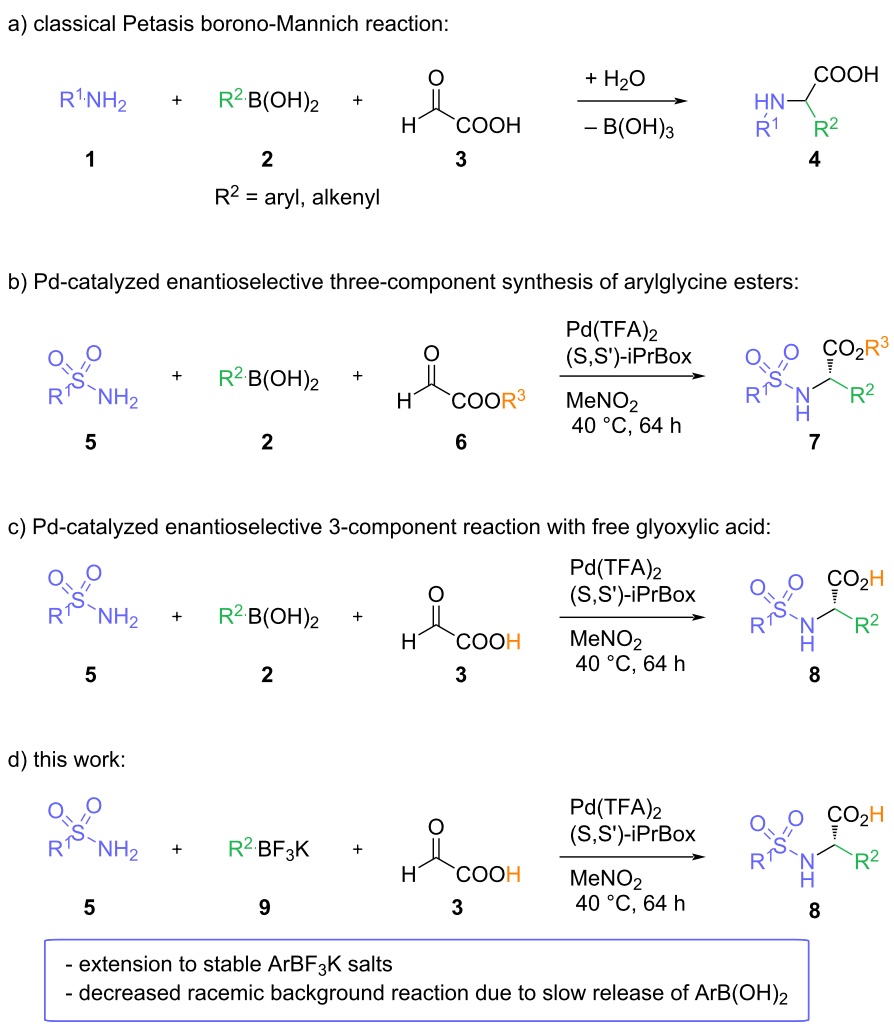

Scheme 1: The Petasis reaction – fundamental reactivities and recent developments.

block (Scheme 1d). The broader scope of this 2nd generation protocol is exploiting a slow release of the boronic acid from the aryltrifluoroborates and enables to enantioselectively synthesize of a broader variety of arylglycines, including a common building block for several biologically active compounds.

Results and Discussion

During our previous studies, we observed that the enantioselectivity of the three-component coupling of glyoxylic acid (employed as its solid, easy-to-handle monohydrate) with 2,2,4,6,7-pentamethyl-2,3-dihydrobenzofuran-5-sulfonylamide, and an arylboronic acid was significantly affected by the nature of the boronic acid. Whereas the reaction with phenylboronic acid afforded the Pbf-protected [23] phenylglycine derivative **10a** in high yield and enantioselectivity, an almost racemic mixture of **10b** was obtained from the corresponding (*p*-methoxyphenyl)boronic acid (**2b**, Scheme 2a). This decrease in enantioselectivity can be attributed to a faster racemic background reaction (pathway A) via ate complex **11a** [10] of the electron-rich, more nucleophilic (*p*-methoxyphenyl)boronic acid (**2b**), which outcompetes the palladium-catalyzed pathway B (Scheme 2b). In turn, suppression or at least a significant deceleration of the uncatalyzed background reaction should lead to an increase in enantioselectivity. Decreasing the arylboronic acid to active catalyst ratio could be one possible opportunity to decrease the rate of the background reaction. Thus, we envisioned that this could be achieved by the slow generation of small amounts of the boronic acid from a suitable precursor. Among different boronic acid derivatives, we identified aryltrifluoroborates as most promising candidates for the slow generation of the corresponding arylboronic acids under our slightly acid reaction conditions [24].

Therefore, we performed two initial control experiments. The reaction of potassium phenyltrifluoroborate with 2,2,4,6,7-

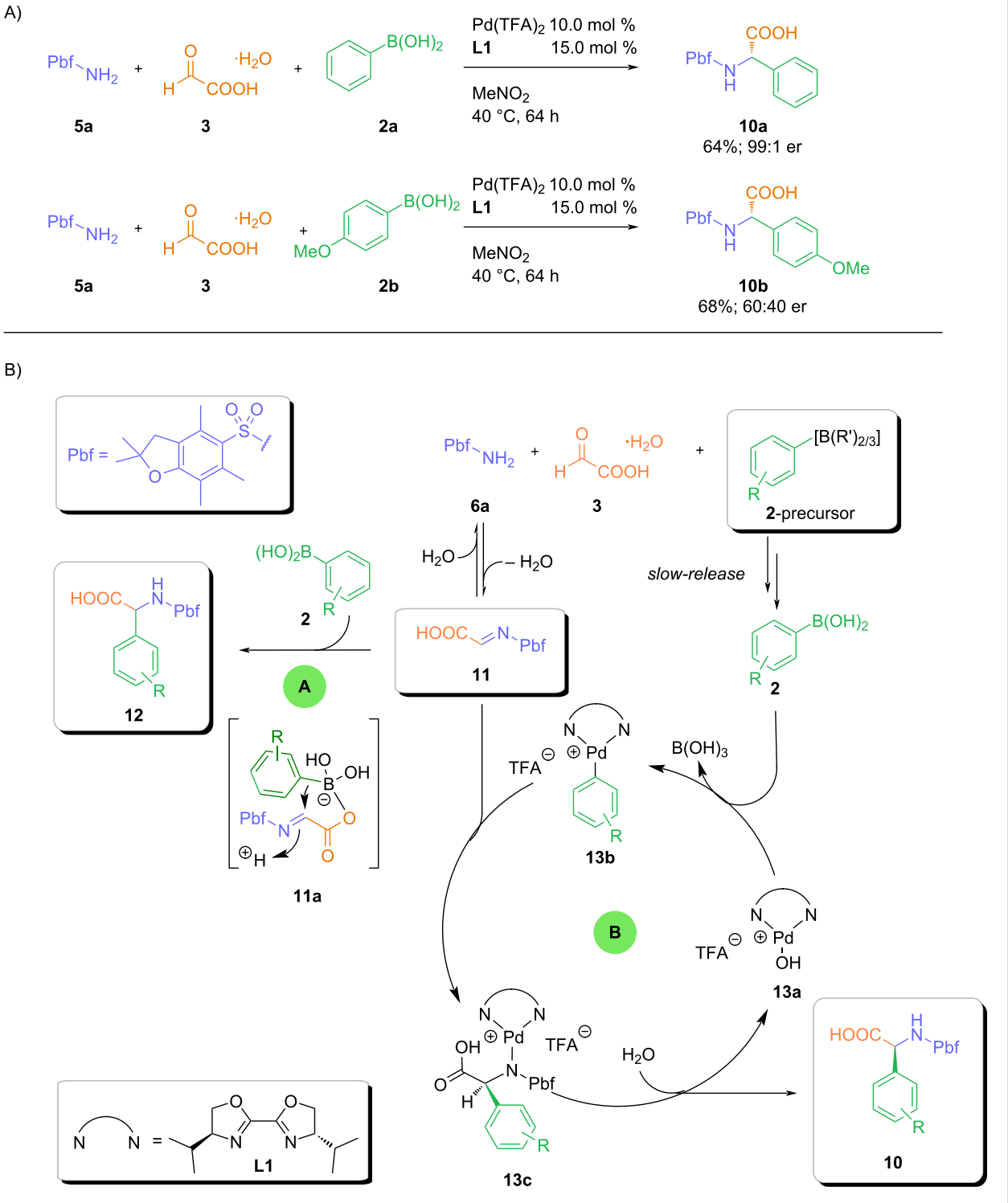

Scheme 2: Observations from previous studies and mechanistic rationale.

pentamethyl-2,3-dihydrobenzofuran-5-sulfonylamide and glyoxylic acid in nitromethane at 40 °C in the presence and absence of our previously established Pd(TFA)$_2$-*S*,*S*-iPrBox catalyst system (Scheme 3). To our delight, the palladium-catalyzed transformation afforded the desired α-arlyglycine in 30% yield and an enantiomeric ratio of 94:6. In the absence of a catalyst, the racemic product was formed in 61% yield. The comparison with the uncatalyzed reaction using free phenylboronic

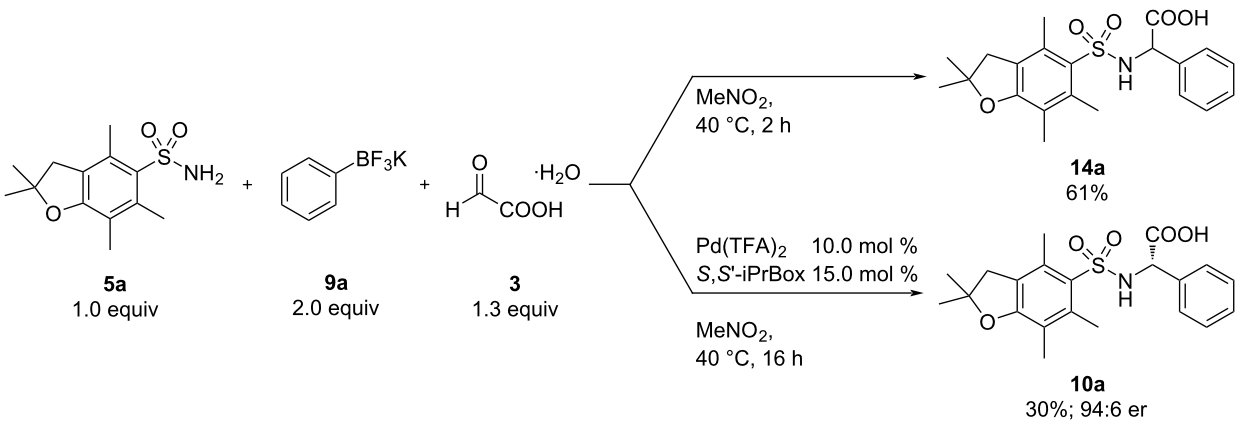

Scheme 3: Initial experiments.

acid showed that the reaction of the phenyltrifluoroborate is considerably slower (61% yield after 16 h vs 89% after 2 h with $PhB(OH)_2$). These preliminary studies confirmed our initial hypothesis that aryltrifluoroborates can be utilized as precursors for a slow release of the free boronic acid in our palladium-catalyzed three-component reaction.

Therefore, we started to optimize the reaction conditions for the use of potassium aryltrifluoroborate salts (Table 1). A quick survey of different solvents showed that the reaction proceeds efficiently only in nitromethane (Table 1, entry 1). Reactions in other common solvents, such as ethyl acetate, acetonitrile, tetrahydrofuran or dichloromethane led to the formation of the arylgylcine in trace amounts (Table 1, entries 2–5). Contrary to our previous report with arylboronic acids, the presence of air is highly detrimental to the reaction outcome (Table 1, entry 6). Therefore, inert conditions were employed throughout all subsequent studies. Increasing the reaction temperature to 60 °C and

Table 1: Reaction optimization.

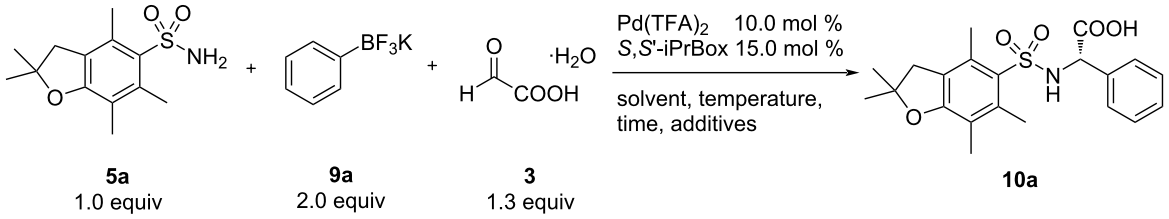

Entry	Conditions	Yield (%)[a]	er
1	10 mol % $Pd(TFA)_2$, 15 mol % ligand **L1**, 40 °C, 16 h, $MeNO_2$	30	94:6
2	EtOAc instead of $MeNO_2$	traces	–
3	MeCN instead of $MeNO_2$	traces	–
4	THF instead of $MeNO_2$	traces	–
5	CH_2Cl_2 instead of $MeNO_2$	traces	–
6	under N_2 atmosphere	40	98:2
7	reaction at 60 °C	54	96:4
8	reaction at 80 °C	55	94:6
9	64 h reaction time	45	98:2
10	with 2.6 equiv glyoxylic acid monohydrate	65	97:3
11	with 2.6 equiv glyoxylic acid monohydrate, 1.0 equiv $CaCO_3$, 2.0 equiv tartaric acid; MS 4 Å	**79**	**96:4**

[a]Isolated yield of analytically pure product.

80 °C furnished the desired product in increased yields of 54 and 55%, respectively, together with a slight erosion of enantioselectivity (Table 1, entries 7 and 8). Prolonging the reaction time to 64 h increased the yield to 45% without affecting the enantioselectivity (Table 1, entry 9). Also, increasing the amount of glyoxylic acid monohydrate to 2.6 equivalents furnished the arylglycine product in an improved yield of 64% and comparable enantioselectivity (Table 1, entry 10). During our experiments, we often observed partial clouding of the used glass vessel, most likely due to slow release of hydrofluoric acid, an effect which has been observed before with trifluoroborate salts [25]. Since the release of hydrofluoric acid could lead to complications with acid-labile substrates (e.g., the Pbf-protected compound **10a**) and safety issues, we decided to investigate the influence of various fluoride scavengers as additives in the three-component process [25,26]. An extensive study (not shown), revealed that most common scavengers either led to a decreased yield, a decreased stereoselectivity or a combination of both. Yet a combination of $CaCO_3$, tartaric acid, and 4 Å molecular sieves, each already employed a HF scavenger by itself, did afford the desired arylglycine in high yields and enantioselectivities (Table 1, entry 11). Although, the use of this scavenger combination did lead to a slightly decreased enantioselectivity (96:4 vs 97:3), we decided to rely on these conditions in order to avoid potential troubles arising from HF release.

With the optimized conditions identified, next we studied the reaction of glyoxylic acid monohydrate and 2,2,4,6,7-pentamethyl-2,3-dihydrobenzofuran-5-sulfonylamide with different aryltrifluoroborate salts. To our delight, these three-component reactions afforded the desired arylglycines in consistently high levels of enantioselectivity, even for electron-rich aryltrifluoroborates (Scheme 4). This can be highlighted by the synthesis of the methoxy-substituted arylglycine **10b**, which

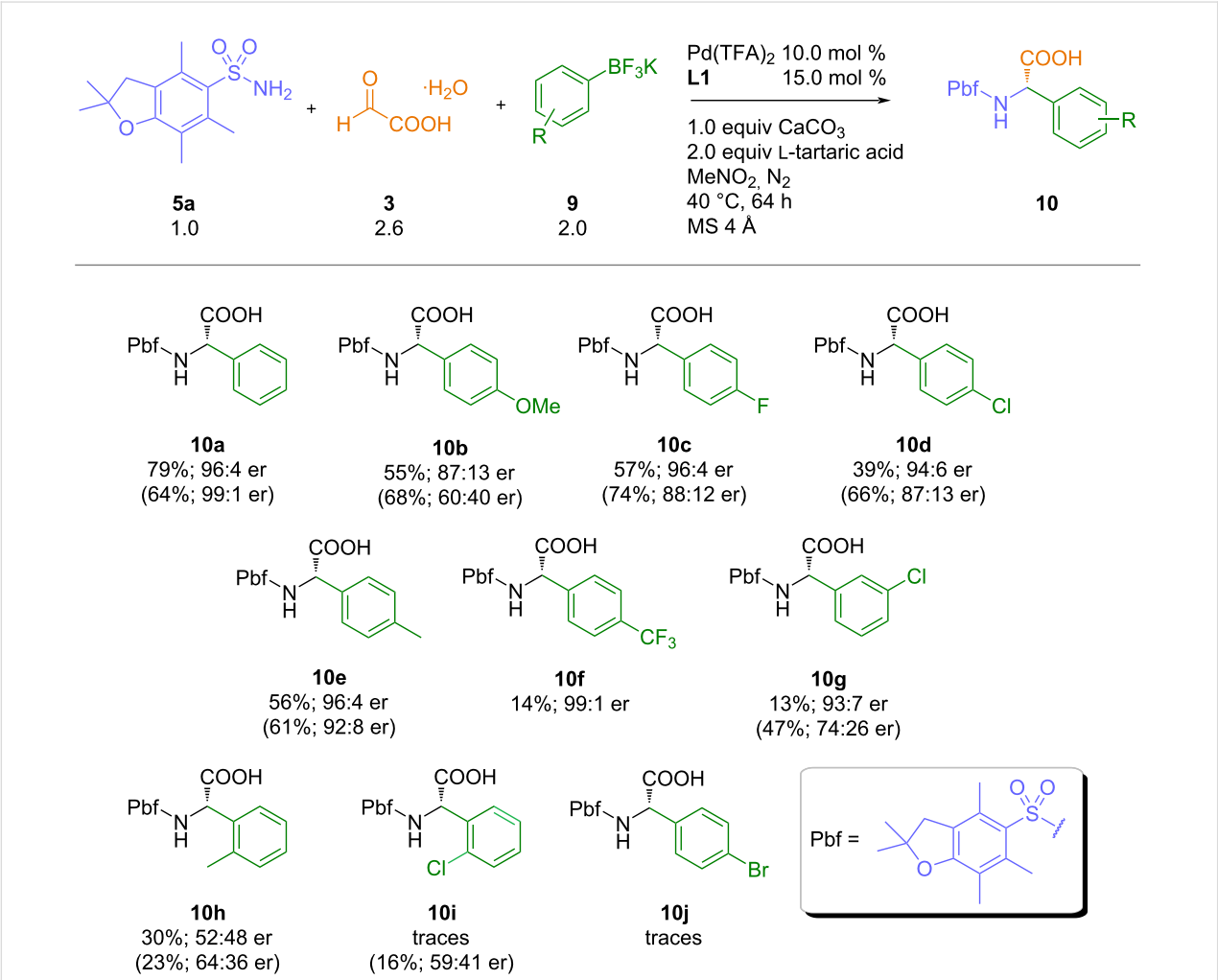

Scheme 4: Reaction scope – aryltrifluoroborates (yields and enantiomeric ratios in parentheses refer to our previous study with the corresponding boronic acids [22]).

was obtained in 55% yield and an enantiomeric ratio of 87:13 (compared to 68% and an enantiomeric ratio of 60:40 with the boronic acid). As in the case of arylboronic acids, reactions with a sterically hindered *ortho*-substituted trifluoroborate furnished the arylglycine product in almost racemic form. Unfortunately, reactions with aryltrifluoroborates did not proceed as efficiently as with the free boronic acid and the arylglycine products **10c–j** were obtained in decreased yields compared to our previous reactions with $ArB(OH)_2$. We assume that a faster protodeborylation, presumably associated with the release of HF, leads to this general decrease of the isolated yields.

As already demonstrated in our previous work, the Pbf-protected arylglycine products can be directly used as building blocks for peptide synthesis [22].

Finally, we utilized our method for the preparation of a protected version of *p*-hydroxyphenylglycine (Scheme 5), a common structural motif in vancomycin, teicoplanin, feglymycin, and amoxicillin. Therefore, the OBn-protected aryltrifluoroborate was subjected to our standard reaction conditions, affording the desired *N*,*O*-protected (*S*)-arylglycine derivative **10k** in 38% yield and an enantiomeric ratio of 88:12. By employing the corresponding *R*,*R*-iPrBox-ligand the second enantiomer, (*R*)-arylglycine **10l** could be prepared with a similar yield and enantioselectivity.

Conclusion

In summary, we have reported a palladium-catalyzed enantioselective three-component reaction of aryltrifluoroborates, sulfonamides, and glyoxylic acid. This method is an improved extension of our pervious protocol with arylboronic acids and provides access to enantioenriched α-arylglycines with an improved substrate diversity. It can be used for the direct synthesis of peptide-like building blocks, which can find direct application in the total synthesis of arylglycine-containing natural products. Currently, we are performing a detailed mechanistic study in order to overcome still existing limitations of the method and to provide a truly general approach to arylglycines with uniformly high yields and enantioselectivities.

Supporting Information

Supporting Information File 1

Experimental section and characterization data.
[https://www.beilstein-journals.org/bjoc/content/supplementary/1860-5397-19-52-S1.pdf]

Funding

Financial support by the research unit NanoKat (RPTU Kaiserslautern-Landau) is gratefully acknowledged.

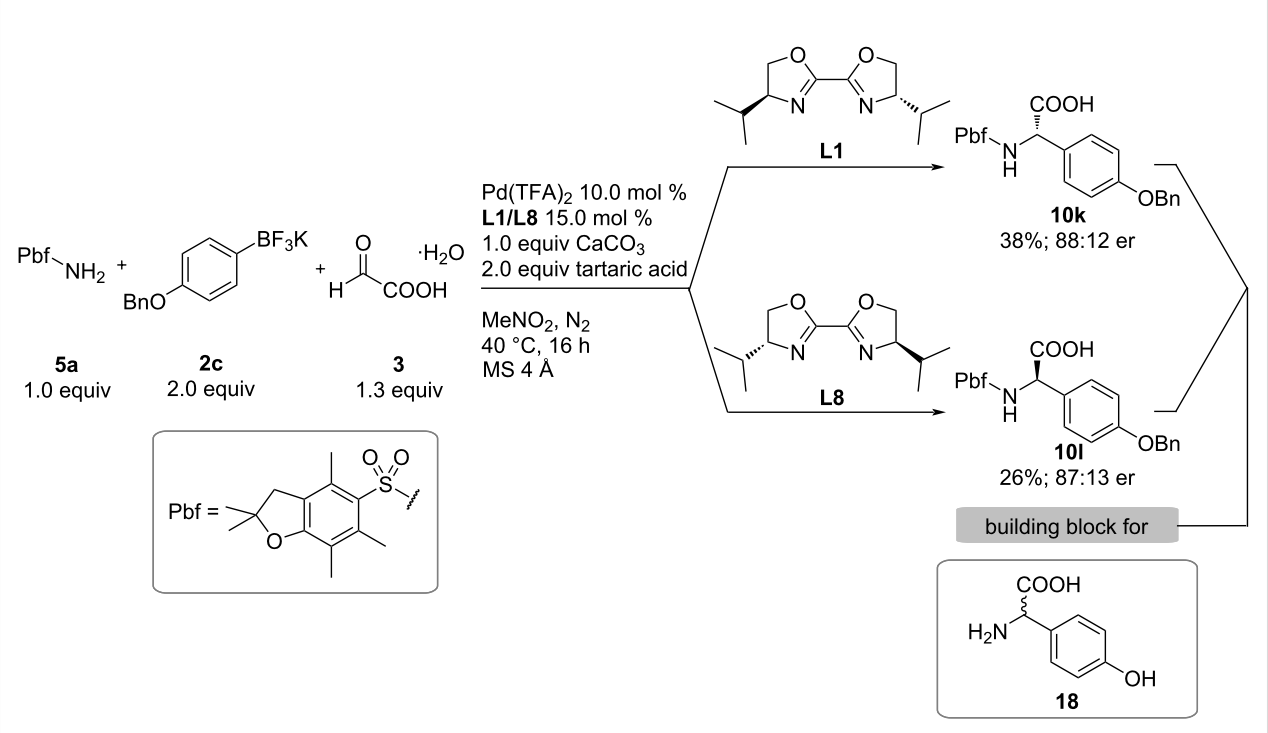

Scheme 5: Synthesis of both enantiomers of arylglycine building block **18**.

ORCID® iDs

Georg Manolikakes - https://orcid.org/0000-0002-4013-5757

Preprint

A non-peer-reviewed version of this article has been previously published as a preprint: doi:10.26434/chemrxiv-2023-cfv7c

References

1. Nelson, D. L.; Cox, M. M. *Lehninger Principles of Biochemistry,* 5th ed.; W.H. Freeman: New York, NY, USA, 2008.
2. Hughes, A. B., Ed. *Amino Acids, Peptides and Proteins in Organic Chemistry;* Wiley-VCH: Weinheim, Germany, 2011. doi:10.1002/9783527631841
3. Tsomaia, N. *Eur. J. Med. Chem.* **2015,** *94,* 459–470. doi:10.1016/j.ejmech.2015.01.014
4. Lutz, S. *Curr. Opin. Biotechnol.* **2010,** *21,* 734–743. doi:10.1016/j.copbio.2010.08.011
5. Van Bambeke, F.; Van Laethem, Y.; Courvalin, P.; Tulkens, P. M. *Drugs* **2004,** *64,* 913–936. doi:10.2165/00003495-200464090-00001
6. Dettner, F.; Hänchen, A.; Schols, D.; Toti, L.; Nußer, A.; Süssmuth, R. D. *Angew. Chem., Int. Ed.* **2009,** *48,* 1856–1861. doi:10.1002/anie.200804130
7. Plosker, G. L.; Lyseng-Williamson, K. A. *Drugs* **2007,** *67,* 613–646. doi:10.2165/00003495-200767040-00013
8. Fisher, J. F.; Mobashery, S. *Bioorg. Chem.* **2014,** *56,* 41–48. doi:10.1016/j.bioorg.2014.05.011
9. Herrera, R. P.; Marqués-López, E. *Multicomponent Reactions: Concepts and Applications for Design and Synthesis;* John Wiley & Sons: Hoboken, NJ, USA, 2015. doi:10.1002/9781118863992
10. Candeias, N. R.; Montalbano, F.; Cal, P. M. S. D.; Gois, P. M. P. *Chem. Rev.* **2010,** *110,* 6169–6193. doi:10.1021/cr100108k
11. Wu, P.; Givskov, M.; Nielsen, T. E. *Chem. Rev.* **2019,** *119,* 11245–11290. doi:10.1021/acs.chemrev.9b00214
12. Paul, J.; Presset, M.; Le Gall, E. *Eur. J. Org. Chem.* **2017,** 2386–2406. doi:10.1002/ejoc.201700038
13. Lou, S.; Schaus, S. E. *J. Am. Chem. Soc.* **2008,** *130,* 6922–6923. doi:10.1021/ja8018934
14. Schneider, A. E.; Beisel, T.; Shemet, A.; Manolikakes, G. *Org. Biomol. Chem.* **2014,** *12,* 2356–2359. doi:10.1039/c4ob00265b
15. Halli, J.; Manolikakes, G. *Eur. J. Org. Chem.* **2013,** 7471–7475. doi:10.1002/ejoc.201301349
16. Halli, J.; Schneider, A. E.; Kramer, P.; Shemet, A.; Manolikakes, G. *Synthesis* **2017,** *49,* 849–879. doi:10.1055/s-0035-1561499
17. Beisel, T.; Manolikakes, G. *Org. Lett.* **2015,** *17,* 3162–3165. doi:10.1021/acs.orglett.5b01502
18. Beisel, T.; Manolikakes, G. *Synthesis* **2016,** *48,* 379–386. doi:10.1055/s-0035-1560910
19. Beisel, T.; Diehl, A. M.; Manolikakes, G. *Org. Lett.* **2016,** *18,* 4116–4119. doi:10.1021/acs.orglett.6b02045
20. Beisel, T.; Manolikakes, G. *Org. Lett.* **2013,** *15,* 6046–6049. doi:10.1021/ol402949t
21. Diehl, A. M.; Manolikakes, G. *ChemCatChem* **2020,** *12,* 3463–3466. doi:10.1002/cctc.202000652
22. Jakob, B.; Diehl, A. M.; Horst, K.; Kelm, H.; Manolikakes, G. *Front. Chem. (Lausanne, Switz.)* **2023,** *11,* 1165618. doi:10.3389/fchem.2023.1165618
23. Carpino, L. A.; Shroff, H.; Triolo, S. A.; Mansour, E.-S. M. E.; Wenschuh, H.; Albericio, F. *Tetrahedron Lett.* **1993,** *34,* 7829–7832. doi:10.1016/s0040-4039(00)61487-9
24. Lennox, A. J. J.; Lloyd-Jones, G. C. *Isr. J. Chem.* **2010,** *50,* 664–674. doi:10.1002/ijch.201000074
25. Lennox, A. J. J. *Organotrifluoroborate Preparation, Coupling and Hydrolysis;* Springer International Publishing: Cham, Switzerland, 2013. doi:10.1007/978-3-319-01134-9
26. Blacker, A. J.; Moran-Malagon, G.; Powell, L.; Reynolds, W.; Stones, R.; Chapman, M. R. *Org. Process Res. Dev.* **2018,** *22,* 1086–1091. doi:10.1021/acs.oprd.8b00090

License and Terms

BEILSTEIN JOURNAL OF ORGANIC CHEMISTRY

Asymmetric tandem conjugate addition and reaction with carbocations on acylimidazole Michael acceptors

Brigita Mudráková[1], Renata Marcia de Figueiredo[2], Jean-Marc Campagne[2] and Radovan Šebesta[*1]

Full Research Paper

Open Access

Address:
[1]Comenius University Bratislava, Faculty of Natural Sciences, Department of Organic Chemistry, Mlynská dolina, Ilkovičova 6, 842 15 Bratislava, Slovakia and [2]ICGM, University of Montpellier, CNRS, ENSCM, Montpellier, France

Email:
Radovan Šebesta[*] - radovan.sebesta@uniba.sk

* Corresponding author

Keywords:
acylimidazole; asymmetric catalysis; carbocation; conjugate addition; enolate

Beilstein J. Org. Chem. **2023,** *19,* 881–888.
https://doi.org/10.3762/bjoc.19.65

Received: 08 March 2023
Accepted: 06 June 2023
Published: 16 June 2023

This article is part of the thematic issue "Catalytic multi-step domino and one-pot reactions".

Guest Editor: S. Tsogoeva

Abstract

We present here a stereoselective tandem reaction based on the asymmetric conjugate addition of dialkylzinc reagents to unsaturated acylimidazoles followed by trapping of the intermediate zinc enolate with carbocations. The use of a chiral NHC ligand provides chiral zinc enolates in high enantiomeric purities. These enolates are reacted with highly electrophilic onium compounds to afford densely substituted acylimidazoles. DFT calculations helped to understand the reactivity of the zinc enolates derived from acylimidazoles and allowed their comparison with metal enolates obtained by other conjugate addition reactions.

Introduction

Asymmetric metal-catalyzed conjugate additions provide access to numerous chiral scaffolds. This type of C–C bond formation efficiently enables the construction of stereogenic centers using polar organometallics [1]. In this way, 1,4-additions of typical organometallics such as dialkylzinc, Grignard reagents, and trialkylaluminum have been developed [2-9]. Recently, also Cu-catalyzed conjugate additions of organozirconium [10,11] or organoboron reagents were realized [12]. Also, in terms of suitable Michael acceptors as substrates, unsaturated ketones, aldehydes, esters, thioesters, amides, alkenyl heterocycles and enoyl heterocycles became viable for conjugate additions. The maturity and robustness of this methodology is documented by its applications in the total syntheses of complex natural products and other molecules of biological relevance [13,14].

Acylimidazoles proved to be versatile building blocks broadly applicable in asymmetric catalysis and organic synthesis. Today, acylimidazoles are used as ester/amide surrogates, because of their particular chemical and physical properties [15]. In addition to ester/amide synthesis, enoyl imidazolides were developed as excellent Michael acceptors. Acylimidazoles are unique electrophiles that demonstrate moderate reactivity, relatively high stability, chemical selectivity, and high solubility in water. Among exceptional properties belongs to

easy post-transformation of acylimidazoles to common carbonyl analogs. These tunable properties allow the use of acylimidazoles in chemical biology research, which includes chemical synthesis of proteins/peptides, structure analysis, and functional control of RNA [16]. Moreover, Campagne and co-workers showed that Cu–NHC-catalyzed conjugate additions of dialkylzinc reagents proceed with high enantioselectivities [17-19]. Furthermore, this methodology allows iterative access to 1,3-disubstituted motifs that are present in various natural products [20].

A salient feature of conjugate additions of organometallic reagents is that they generate reactive metal enolates as primary products. These enolates can be used in a variety of subsequent transformations [21]. Chiral enolates generated by conjugate additions react with carbonyl compounds, imines, other Michael acceptors, or alkyl halides. Our group is developing trapping of metal enolates with stabilized carbocations and could show that magnesium enolates generated from enones [22], unsaturated amides [23], or heterocycles reacted with tropylium, dithiolylium or flavylium cations [24]. These non-traditional electrophiles allow access to structurally highly interesting motifs. In addition, they are amenable to valuable synthetic transformations such as oxidative ring contraction of the cycloheptatrienyl ring or reduction of the benzodithiolyl group.

In this context, we decided to study a tandem reaction comprising the Cu–NHC-catalyzed addition of dialkylzinc reagents to enoyl imidazoles followed by a trapping reaction with various onium compounds (Scheme 1). In this work we show the development of this methodology and its application to a range of acylimidazoles and carbocations.

Results and Discussion

For initial experiments, we have selected the conjugate addition of Me_2Zn to acylimidazole **1a** catalyzed by a chiral NHC ligand derived from imidazolium salt **L1**. This NHC precursor has been described previously by Gérard, Mauduit, Campagne and co-workers [19]. The ligand **L1** is excellent in asymmetric conjugate additions of dialkylzincs to acylimidazoles [25]. The initial reaction conditions were inspired by literature precedence on conjugate additions. As the first electrophile for trapping of the chiral enolate, we have used tropylium bistriflimide (Scheme 2). Following our earlier experience, we employed

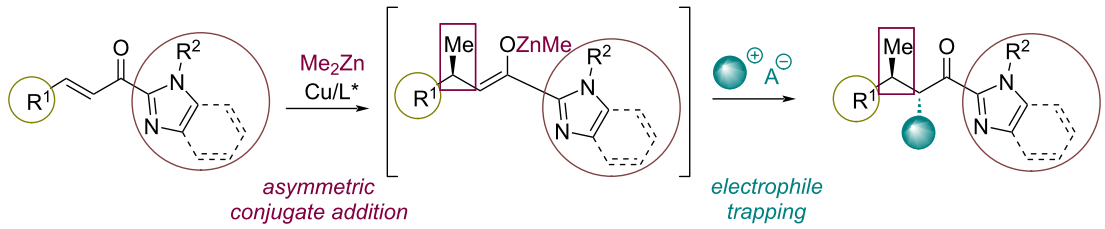

Scheme 1: Concept of this work.

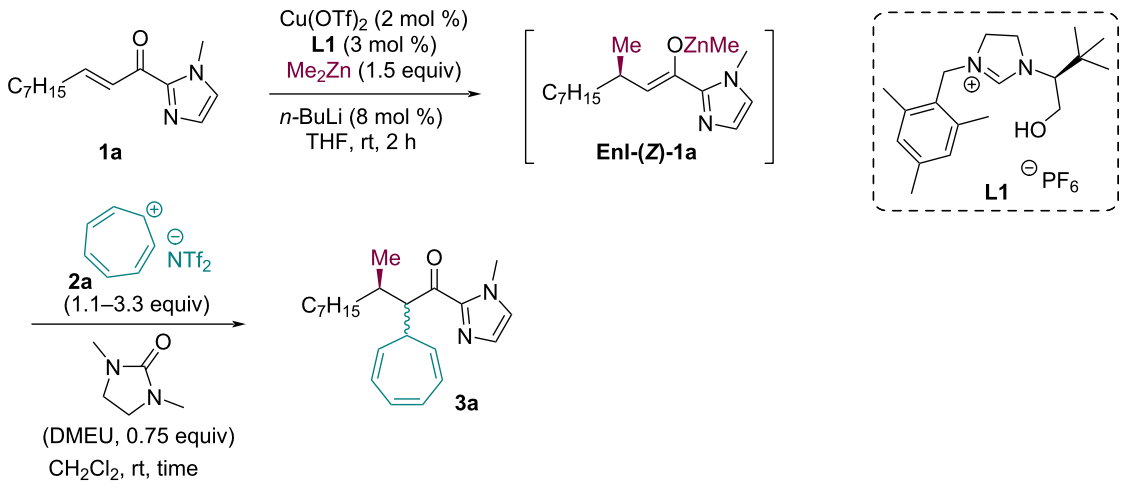

Scheme 2: Initial experiments for the trapping of the intermediate enolate **Enl-1a** with tropylium NTf_2.

the tropylium ion with the more lipophilic bis(trifluoromethane)sulfinimide (NTf_2) anion because of its better solubility in the applied organic solvents than the commercially available tetrafluoroborate (BF_4) form [22-24]. The cyclic urea DMEU (1,3-dimethyl-2-imidazolidinone) [26] additive was used as polar aprotic solvent, which also increases the homogeneity of the reaction mixture.

In the first reaction, 1.1 equiv of tropylium NTf_2 were used. The reaction worked at room temperature and after 16 h the product **3a** was isolated in low 22% yield and a 2:1 diastereomeric ratio (Table 1, entry 1). First we attempted to increase the yield and the diastereoselectivity of the reaction by prolonging the reaction time (Table 1, entry 2). However, a shorter reaction time was preferable as after only one hour the product was isolated in a better yield (33%) with good dr (4:1, Table 1, entry 3). The addition of two equivalents of tropylium NTf_2 led to a decrease of the diastereoselectivity (Table 1, entry 4). In the next tandem reaction, 1.1 equiv of tropylium bistriflimide (**2a**) were added to the reaction mixture every hour until the full conversion of the starting acylimidazole **3a** (Table 1, entry 5) as monitored by TLC analysis. The reaction was completed after 3 hours, meaning that the in situ-formed enolate needed 3.3 equiv of tropylium NTf_2 (**2a**) to complete the reaction. By this route, the tandem product **3a** was isolated in a high yield of 93% but without any diastereoselectivity. The reaction was also carried out using 3.3 equiv of the electrophile added in one portion. The full conversion of the starting acylimidazole **1a** was observed after 30 minutes (TLC monitoring), however, the diastereoselectivity remained low (Table 1, entry 6). Neither an increase nor decrease of the reaction temperature led to improved reaction outcomes (Supporting Information File 1, Table S1, entries 2 and 11). We have continued the evaluation of reaction conditions for improving the diastereoselectivity of the reaction. We have tested transmetallation of the in situ-generated zinc enolate to the ammonium enolate by treatment with *n*-tetrabutylammonium chloride (Table 1, entry 7). For this purpose, the enolate was added to a solution of *n*-Bu_4NCl in THF, and then the reaction mixture was stirred for 30 min before the addition of tropylium NTf_2. Prolonging the transmetallation reaction time led to the formation of only one diastereomer, but in a low yield of 11%. Neither the addition of LiCl helped to increase the diastereoselectivity of the reaction (Table 1, entry 8). See Supporting Information File 1, for complete optimization of the reaction conditions.

Achieving diastereoselective reactions on acyclic systems is often difficult due to small energy differences between reacting conformers. In the case of our trapping reaction of chiral imidazolyl enolates, the lack of diastereoselectivity may be associated with the presence of an *E*/*Z* mixture of enolates. This would also explain why at lower onium salt amount and shorter reaction times the diastereoselectivities are higher but at the expense of the overall yield.

With the optimized reaction conditions in our hands, we next explored the scope of the domino reaction. Structurally diverse onium compounds **2** were tested to probe their reactivity with the Zn-enolate derived from **1a** (Scheme 3). The onium compounds **2a** and **2b** were obtained by anion exchange using $LiNTf_2$ from the commercially available tetrafluoroborate salts. Onium compounds **2c** and **2d** were obtained by acidic dehydration of the corresponding hydroxy derivatives using HBF_4 or CF_3SO_3H (see Supporting Information File 1 for more details). The corresponding tandem products were isolated in medium to good yields as mixtures of diastereomers and high enantiomeric purities were recorded for selected tandem products. The enantioselectivity of this reaction is mainly governed by the conjugate addition step and, in comparison to conjugate addition products described in the literature [19], these tandem products differed only slightly. So, we can assume that all tandem products have high enantiomeric purities.

Table 1: Results of selected optimization experiments.

Entry	Tropylium NTf_2 [equiv]	Additive	Time [h]	Yield [%]	dr (*S,R*)/(*R,R*)-**3a**[a]
1	1.1	–	16	22	2:1
2	1.1	–	72	15	1:1
3	1.1	–	1	33	4:1
4	2.0	–	16	33	2:1
5[b]	3.3	–	3	93	1:1
6	3.3	–	0.5	94	1:1
7	3.3	*n*-$Bu_4N^+Cl^-$	1	11	>99:1
8	3.3	LiCl	16	73	1:1

[a]The diastereoselectivity of the reaction was determined by ^1H NMR spectroscopy of the crude reaction mixture; [b]3 portions (1.1 equiv each) of tropylium NTf_2 were added to the reaction mixture every one hour until the full conversion of **3a**.

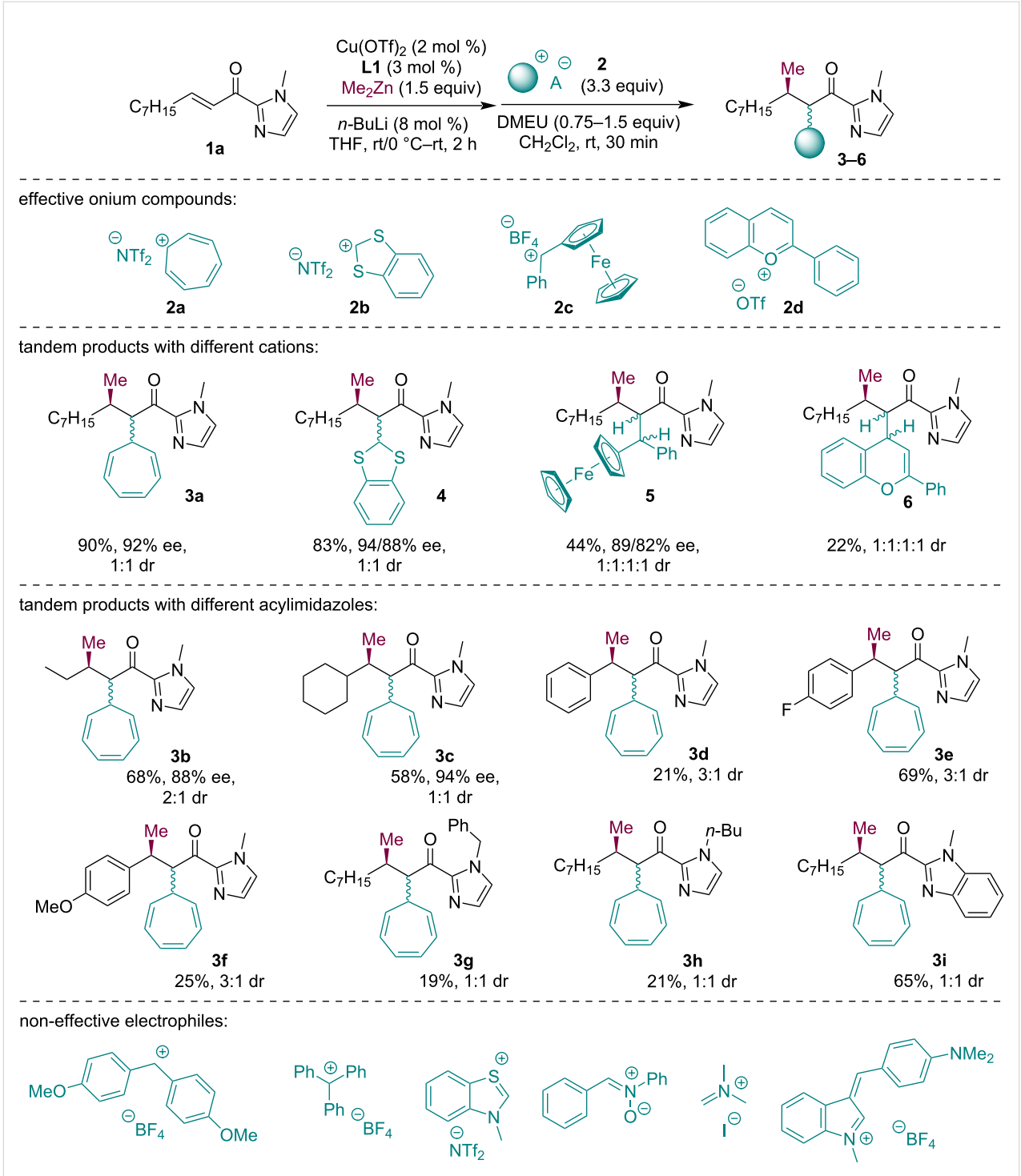

Scheme 3: The reaction scope.

Absolute configurations of tandem products were determined by comparison of experimentally measured electronic circular dichroism (ECD) spectra with those of the DFT-calculated ones (Figure 1 and see Supporting Information File 1 for more details). CD spectra were calculated for the two most populated conformers for both diastereomers of product **4**. The best match between the experimental and averaged calculated spectra was achieved by B97-3c/def2-mTZVP and PBE0-D4/def2-SVP methods. The presence of many conformers in these types of derivatives complicates their analysis and decreased the fit be-

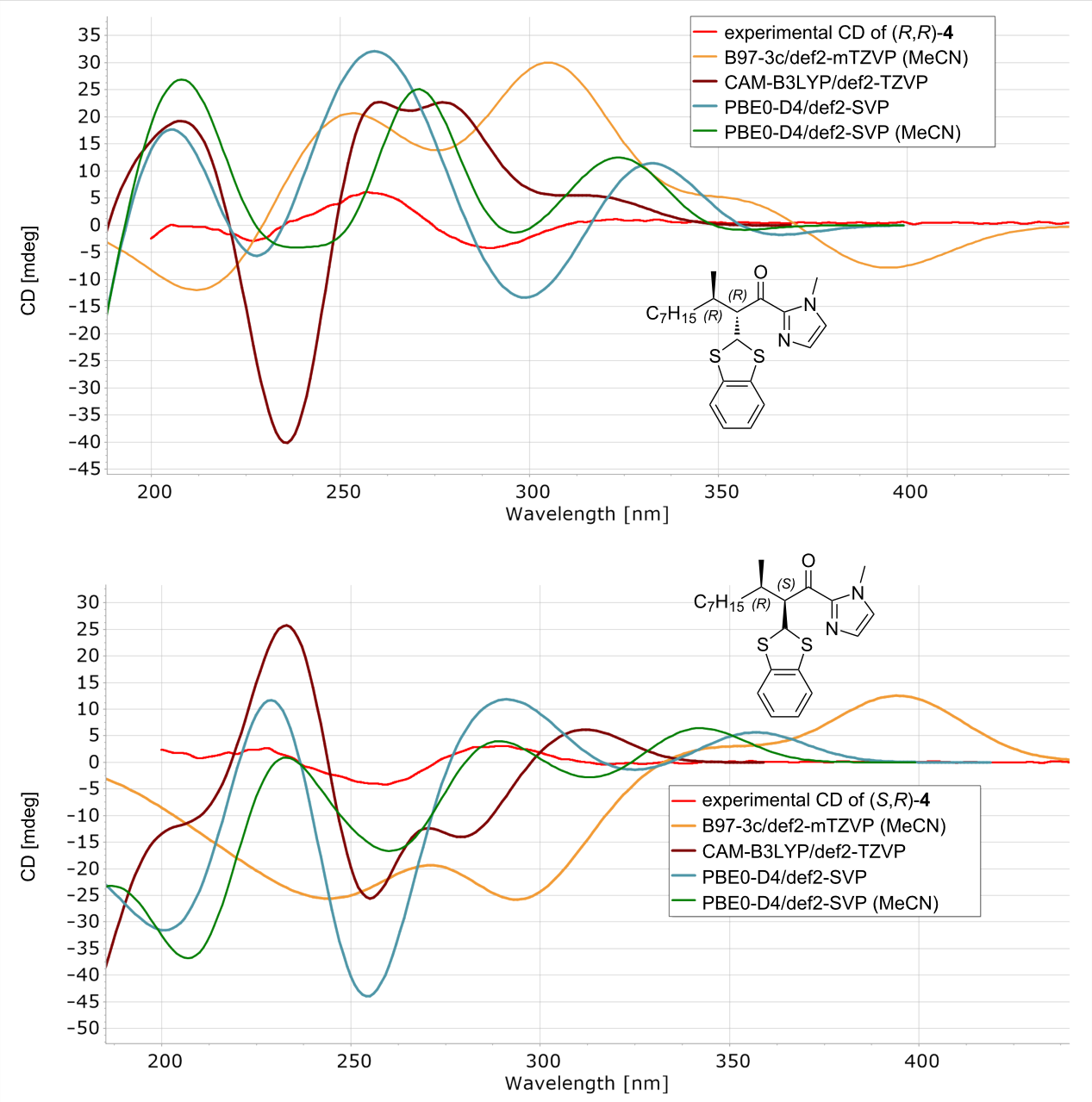

Figure 1: Comparison of DFT-calculated and experimental ECD of (2*R*,3*R*)-**4** and (2*S*,3*R*)-**4**.

tween experimental and calculated CD spectra. Furthermore, the configuration at the position C-3 is determined by the chiral ligand **L1** and was determined previously as (*R*) [19].

To gain insight into the reactivity of enolates formed in this transformation, we evaluated properties of Zn enolates by DFT calculations (Figure 2). The corresponding (*E*) and (*Z*)-enolates were calculated for products **3b** and **3d**, which possess either an alkyl (ethyl) or an aryl (phenyl) substituent on the stereogenic center. To probe the nature of the imidazole moiety, enolates for products **3g** and **3i** were also calculated (with a shorter alkyl chain to simplify the calculations). Single point energy calculations were performed using long-range corrected hybrid density functional ωB97X, which offer very good performance and have been recommended for general use in chemistry [27] with empirical dispersion correction D4 [28] (ωB97X-D4) and the triple-zeta def2-TZVPPD basis set [29]. Geometry optimizations were performed at the PBEh-3c/def2-mSVP level [30]. The energies of HOMOs show only small variations from −7.77 to −7.89 eV and the charges at the C-2 carbon obtained via natural population analysis also ranged only little from −0.254 to −0.291. Differences in HOMO energies and charges at C-2 of

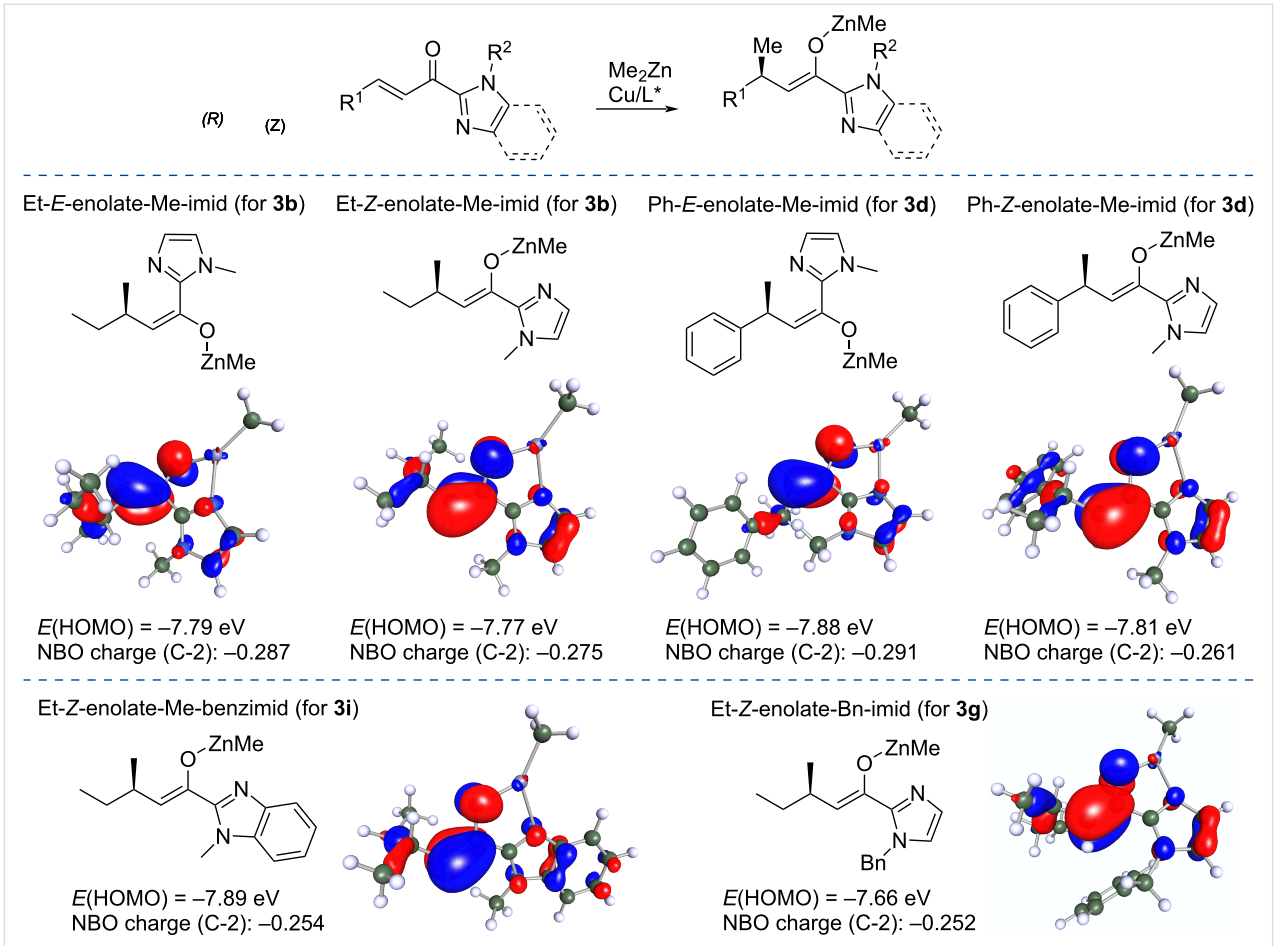

Figure 2: DFT calculated (ωB97X-D4/def2-TZVPPD//PBEh-3c/def2-mSVP) HOMO energies and NBO charges for representative metal enolates.

enolates cannot account for the differences in the yields of the trapping products as these are affected by their specific stabilities and issues during isolation and purification. As an additional question that we tried to answer with these calculations was the comparison of the Zn enolates obtained from acylimidazoles in this work with other metal enolates obtained by related conjugate additions. In comparison, the HOMO energy of a related silyl ketene aminal was similar (−7.87 eV) but its NBO charge was more negative −0.343. The TMS enolate of benzoxazole has a higher HOMO energy of −7.13 eV and an even more negative NBO charge of −0.368 at the C-2 position. We can confer from these data that Zn enolates obtained from acylimidazoles are somewhat less reactive than silyl enol ethers obtained in the Lewis acid-promoted conjugate addition of Grignard reagents [23]. This finding correlates also with the slightly lower yields for the tandem products obtained with Zn enolates from acylimidazoles.

Conclusion

Enantioselective conjugate additions of dialkylzinc reagents afford chiral zinc enolates. These reactive species were trapped with several highly electrophilic onium compounds to introduce synthetically valuable functionalities. In this way, a range of acylimidazoles featuring cycloheptatrienyl, benzodithiolyl, ferrocenyl, and chromenyl substituents were prepared. The DFT calculated HOMO energies and NBO charges of the intermediate zinc enolates allowed placement of these reactive intermediates among other metal enolates obtained in conjugate additions.

Experimental

General procedure for the one-pot conjugate addition of organozinc reagents to acylimidazole followed by trapping with carbocations: In a flame-dried Schlenk flask flushed with Ar, $Cu(OTf)_2$ (1.81 mg, 0.005 mmol, 2 mol %) and chiral NHC ligand **L1** (3.36 mg, 0.0075 mmol, 3 mol %) were dissolved in freshly distilled anhydrous THF (1.0 mL) and the mixture was stirred for 10 min at rt. The reaction mixture was cooled to 0 °C, and then 1.6 M *n*-BuLi (12.5 µL, 0.02 mmol, 8 mol %) was added dropwise and the mixture was stirred for 10 min. Subsequently, 1.2 M dimethylzinc reagent in toluene (0.31 mL, 0.38 mmol, 1.5 equiv) was added dropwise to the solution and

the resulting mixture was also stirred for 10 min. The acylimidazole (0.25 mmol, 1.0 equiv) dissolved in anhydrous THF (0.5 mL) was added dropwise to the mixture. The reaction was stirred for 2 h, while it was slowly warmed up to rt. Then, the electrophile in anhydrous CH_2Cl_2 (1.0 mL) together with DMEU (20.2–40.4 µL, 75–150 mol %, to achieve homogeneity of the reaction mixture) were added to the reaction mixture followed by stirring at rt for 0.5–1 h. The reaction was quenched by the addition of 1 M HCl (6 mL) and EtOAc (6 mL). Then, the organic phase was washed with a sat. aq. solution of $NaHCO_3$ (6 mL), brine (6 mL), dried over $MgSO_4$, and concentrated under vacuum. The residue was purified by flash chromatography on SiO_2 (hexane/EtOAc 15:1).

Supporting Information

Supporting Information File 1

Characterization data for all compounds, computational details, and picture of NMR spectra.
[https://www.beilstein-journals.org/bjoc/content/supplementary/1860-5397-19-65-S1.pdf]

Funding

This work was supported by the Slovak Research and Development Agency under the Contract no. APVV-18-0242 and by the Operation Program of Integrated Infrastructure for the project, UpScale of Comenius University Capacities and Competence in Research, Development and Innovation, ITMS2014+: 313021BUZ3, co-financed by the European Regional Development Fund.

ORCID® iDs

Renata Marcia de Figueiredo - https://orcid.org/0000-0001-5336-6071
Jean-Marc Campagne - https://orcid.org/0000-0002-4943-047X
Radovan Šebesta - https://orcid.org/0000-0002-7975-3608

References

1. Alexakis, A.; Krause, N.; Woodward, S., Eds. *Copper-Catalyzed Asymmetric Synthesis;* Wiley-VCH: Weinheim, Germany, 2014. doi:10.1002/9783527664573
2. Krause, N.; Hoffmann-Röder, A. *Synthesis* **2001,** 171–196. doi:10.1055/s-2001-10803
3. Alexakis, A.; Benhaim, C. *Eur. J. Org. Chem.* **2002,** 3221–3236. doi:10.1002/1099-0690(200210)2002:19<3221::aid-ejoc3221>3.0.co;2-u
4. López, F.; Minnaard, A. J.; Feringa, B. L. *Acc. Chem. Res.* **2007,** *40,* 179–188. doi:10.1021/ar0501976
5. Harutyunyan, S. R.; den Hartog, T.; Geurts, K.; Minnaard, A. J.; Feringa, B. L. *Chem. Rev.* **2008,** *108,* 2824–2852. doi:10.1021/cr068424k
6. Alexakis, A.; Bäckvall, J. E.; Krause, N.; Pàmies, O.; Diéguez, M. *Chem. Rev.* **2008,** *108,* 2796–2823. doi:10.1021/cr0683515
7. Jerphagnon, T.; Pizzuti, M. G.; Minnaard, A. J.; Feringa, B. L. *Chem. Soc. Rev.* **2009,** *38,* 1039–1075. doi:10.1039/b816853a
8. Wang, S.-Y.; Loh, T.-P. *Chem. Commun.* **2010,** *46,* 8694–8703. doi:10.1039/c0cc03211e
9. Müller, D.; Alexakis, A. *Chem. Commun.* **2012,** *48,* 12037–12049. doi:10.1039/c2cc34607a
10. Maksymowicz, R. M.; Bissette, A. J.; Fletcher, S. P. *Chem. – Eur. J.* **2015,** *21,* 5668–5678. doi:10.1002/chem.201405855
11. Némethová, I.; Šebesta, R. *Synthesis* **2021,** *53,* 447–460. doi:10.1055/s-0040-1706055
12. Jang, W. J.; Yun, J. *Angew. Chem., Int. Ed.* **2019,** *58,* 18131–18135. doi:10.1002/anie.201909712
13. Vargová, D.; Némethová, I.; Šebesta, R. *Org. Biomol. Chem.* **2020,** *18,* 3780–3796. doi:10.1039/d0ob00278j
14. Hui, C.; Pu, F.; Xu, J. *Chem. – Eur. J.* **2017,** *23,* 4023–4036. doi:10.1002/chem.201604110
15. Lauberteaux, J.; Pichon, D.; Baslé, O.; Mauduit, M.; de Figueiredo, R. M.; Campagne, J.-M. *ChemCatChem* **2019,** *11,* 5705–5722. doi:10.1002/cctc.201900754
16. Mino, T.; Sakamoto, S.; Hamachi, I. *Biosci., Biotechnol., Biochem.* **2021,** *85,* 53–60. doi:10.1093/bbb/zbaa026
17. Lauberteaux, J.; Crévisy, C.; Baslé, O.; de Figueiredo, R. M.; Mauduit, M.; Campagne, J.-M. *Org. Lett.* **2019,** *21,* 1872–1876. doi:10.1021/acs.orglett.9b00479
18. Halbert, S.; Lauberteaux, J.; Blons, C.; de Figueiredo, R. M.; Crévisy, C.; Baslé, O.; Campagne, J.-M.; Mauduit, M.; Gérard, H. *ChemCatChem* **2019,** *11,* 4108–4115. doi:10.1002/cctc.201900233
19. Drissi-Amraoui, S.; Schmid, T. E.; Lauberteaux, J.; Crévisy, C.; Baslé, O.; de Figueiredo, R. M.; Halbert, S.; Gérard, H.; Mauduit, M.; Campagne, J.-M. *Adv. Synth. Catal.* **2016,** *358,* 2519–2540. doi:10.1002/adsc.201600458
20. Drissi-Amraoui, S.; Morin, M. S. T.; Crévisy, C.; Baslé, O.; de Figueiredo, R. M.; Mauduit, M.; Campagne, J.-M. *Angew. Chem., Int. Ed.* **2015,** *54,* 11830–11834. doi:10.1002/anie.201506189
21. Vargová, D.; Némethová, I.; Plevová, K.; Šebesta, R. *ACS Catal.* **2019,** *9,* 3104–3143. doi:10.1021/acscatal.8b04357
22. Drusan, M.; Rakovský, E.; Marek, J.; Šebesta, R. *Adv. Synth. Catal.* **2015,** *357,* 1493–1498. doi:10.1002/adsc.201500074
23. Vargová, D.; Pérez, J. M.; Harutyunyan, S. R.; Šebesta, R. *Chem. Commun.* **2019,** *55,* 11766–11769. doi:10.1039/c9cc05041h
24. Mudráková, B.; Kisszékelyi, P.; Vargová, D.; Zakiewicz, D.; Šebesta, R. *Adv. Synth. Catal.* **2022,** *364,* 1337–1344. doi:10.1002/adsc.202101485
25. Pichon, D.; Morvan, J.; Crévisy, C.; Mauduit, M. *Beilstein J. Org. Chem.* **2020,** *16,* 212–232. doi:10.3762/bjoc.16.24
26. Leahy, J. W. Dichloroketene. *Encyclopedia of Reagents for Organic Synthesis (EROS);* John Wiley & Sons, 2001. doi:10.1002/047084289x.rd123
27. Chai, J.-D.; Head-Gordon, M. *Phys. Chem. Chem. Phys.* **2008,** *10,* 6615–6620. doi:10.1039/b810189b
28. Caldeweyher, E.; Ehlert, S.; Hansen, A.; Neugebauer, H.; Spicher, S.; Bannwarth, C.; Grimme, S. *J. Chem. Phys.* **2019,** *150,* 154122. doi:10.1063/1.5090222
29. Schäfer, A.; Huber, C.; Ahlrichs, R. *J. Chem. Phys.* **1994,** *100,* 5829–5835. doi:10.1063/1.467146
30. Grimme, S.; Brandenburg, J. G.; Bannwarth, C.; Hansen, A. *J. Chem. Phys.* **2015,** *143,* 054107. doi:10.1063/1.4927476

License and Terms

BEILSTEIN JOURNAL OF ORGANIC CHEMISTRY

New one-pot synthesis of 4-arylpyrazolo[3,4-*b*]pyridin-6-ones based on 5-aminopyrazoles and azlactones

Vladislav Yu. Shuvalov[1], Ekaterina Yu. Vlasova[2], Tatyana Yu. Zheleznova[1] and Alexander S. Fisyuk[*1,2]

Full Research Paper

Open Access

Address:
[1]Laboratory of New Organic Materials, Omsk State Technical University, 11 Mira Ave., 644050 Omsk, Russian Federation and [2]Department of Organic and Analytical Chemistry, F. M. Dostoevsky Omsk State University, Mira Ave., 55a, 644077 Omsk, Russian Federation

Email:
Alexander S. Fisyuk[*] - fisyuk@chemomsu.ru

* Corresponding author

Keywords:
5-aminopyrazole; azlactone; elimination; fluorescence; one-pot synthesis; pyrazolo[3,4-*b*]pyridin-6-one

Beilstein J. Org. Chem. **2023,** *19,* 1155–1160.
https://doi.org/10.3762/bjoc.19.83

Received: 30 May 2023
Accepted: 14 July 2023
Published: 02 August 2023

This article is part of the thematic issue "Catalytic multi-step domino and one-pot reactions".

Guest Editor: S. Tsogoeva

Abstract

An effective one-pot strategy was developed for the synthesis of 4-arylpyrazolo[3,4-*b*]pyridin-6-ones from pyrazolo[3,4-*b*]pyridin-6-ones, obtained by reacting 5-aminopyrazoles with 4-arylidene-2-phenyloxazol-5(4*H*)-ones (azlactones) under solvent-free conditions, through subsequent elimination of a benzamide molecule in a superbasic medium (*t*-BuOK/DMSO). The fluorescent properties of the synthesized compounds were studied. 4-Arylpyrazolo[3,4-*b*]pyridin-6-ones luminesce in the region of 409–440 nm with a quantum yield of 0.09–0.23 when irradiated with UV light.

Introduction

The pyrazolo[3,4-*b*]pyridine scaffold is present in many biologically active compounds [1-12]. Among them, 4-aryl-substituted derivatives should be distinguished, exhibiting antiviral [13] and anti-inflammatory properties [14], being modulators of estrogen-related receptor alpha [15], JAK1 kinase inhibitor [16], GSK3 [17] and GyrB [8] inhibitors (Figure 1).

Despite the high demand, their synthesis methods are few (Scheme 1). To obtain 4-arylpyrazolo[3,4-*b*]pyridin-6-ones, the only known one-step method is most often used, including the acid-catalyzed condensation of aminopyrazoles with ketoesters [1,16,18] (method A). Its significant disadvantage is the low yields of the target products (11–60%). Yields are also low in two-stage synthesis methods. The first of them is based on the three-component condensation of aminopyrazoles, Meldrum's acid, and aromatic aldehydes, followed by the oxidation of the intermediate with DDQ [13,16,19] (method B). The second one includes the reaction of an aromatic aldehyde with thioglycolic acid and aminopyrazole, followed by the extrusion of sulfur from the resulting thiazepine [20] (method C). The three-stage synthesis of 4-arylpyrazolo[3,4-*b*]pyridin-6-ones, involving the preparation of 3-aryl-*N*-(1*H*-pyrazol-5-yl)propiolamides (method D), also leads to the formation of the target products with low yields [21]. Therefore, the development of a new effective method for the preparation of 4-arylpyrazolo[3,4-*b*]pyridin-6-ones is an urgent task.

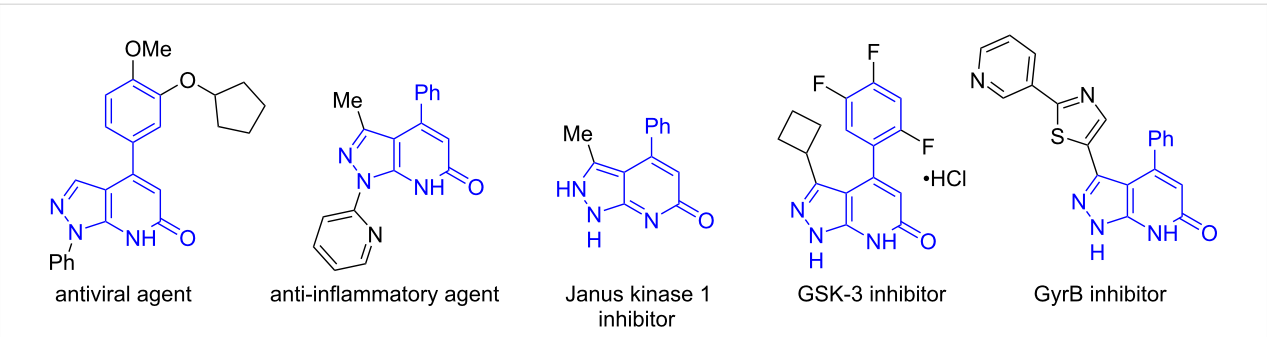

Figure 1: Biologically active 4-arylpyrazolo[3,4-*b*]pyridin-6-ones.

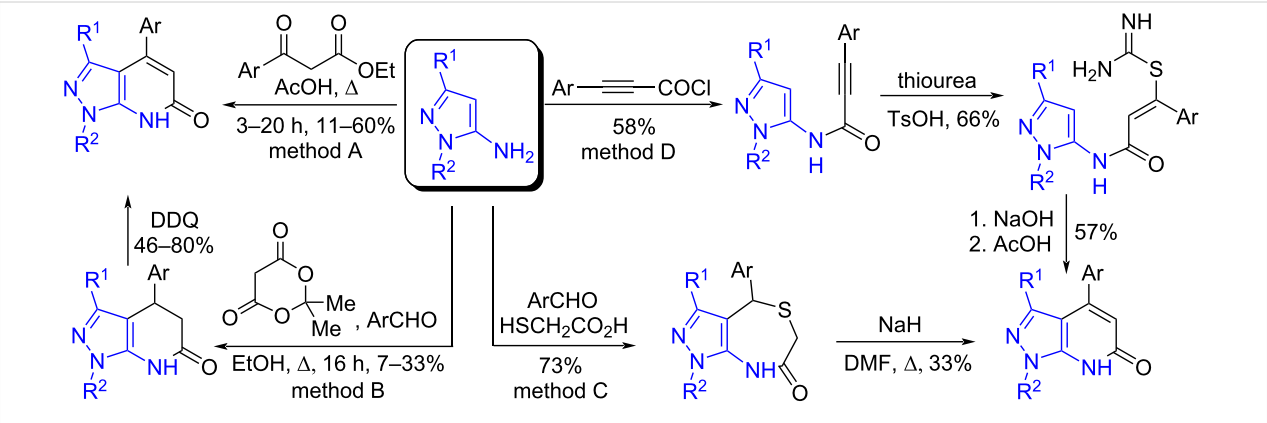

Scheme 1: Methods for the synthesis of 4-arylpyrazolo[3,4-*b*]pyridin-6-ones.

Results and Discussion

One of the rational approaches to the synthesis of fused pyridine derivatives is based on the domino reaction of enamines with azlactones [22-30]. We have previously reported a plausible mechanism of such reactions [22,25]. 1*H*-Pyrazol-5-amines also enter into similar transformations with azlactones in various solvents. The yields of tetrahydro-1*H*-pyrazolo[3,4-*b*]pyridones **3** obtained by this method vary widely [31-33]. Solvent-free reactions are convenient from both economic and environmental points of view. We obtained tetrahydro-1*H*-pyrazolo[3,4-*b*]pyridinone **3a** by heating 5-aminopyrazole **1** with azlactone **2a** in the absence of solvent at 150 °C in 62% yield (Table 1). For compound **3a**, the possibility of benzamide elimination was studied. The benzamide fragment is a poor leaving group; however, in a superbasic medium, we were able to eliminate this group in compound **3a**. In order to select optimal synthesis conditions, we heated compound **3a** in DMSO at temperatures from 90 to 150 °C for 1.5, 3.5 and 6 h in the presence of KOH or *t*-BuOK (Table 1).

The best yield of 4-phenylpyrazolo[3,4-*b*]pyridin-6-one **4a** (81%) was achieved at 150 °C in DMSO containing 1.5 equiv of *t*-BuOK for 1.5 h. Obviously, the preparation of 4-phenylpyrazolo[3,4-*b*]pyridin-6-one **4a** could be carried out as one-pot synthesis, without isolation of the intermediate dihydro derivative **3a**. In this case, the solvent (DMSO) could be added at the stage of obtaining dihydro derivative **3a** or introduced into the reaction together with *t*-BuOK. We have explored both variants. When intermediate **3a** was obtained under solvent-free conditions followed by the addition of *t*-BuOK in DMSO, the yield of pyrazolo[3,4-*b*]pyridin-6-one **4a** was higher (73%, Table 1, entry 5) than when performing the reaction in a solvent (60%, Table 1, entry 6). Therefore, this procedure was used for the synthesis of compounds **4b–i**, **9a**, **10a**. The yields of pyrazolo[3,4-*b*]pyridin-6-ones **4a–i**, **9a**, **10a** obtained by this method are in the range of 55–75% (Scheme 2).

It should be noted that for compounds containing an electron-donating substituent in the C-4 position, such as 4-methoxyphenyl- (**4c**), 3,4-dimethoxyphenyl- (**4d**), 3,4,5-trimethoxyphenyl- (**4e**), 2-furyl- (**4h**) and 2-thienyl- (**4i**), the product yields are reduced to 55–60% (Scheme 2).

All the compounds obtained are colorless crystalline substances. When dissolved, they produce colorless solutions exhibiting

Table 1: Optimization of reaction conditions[a].

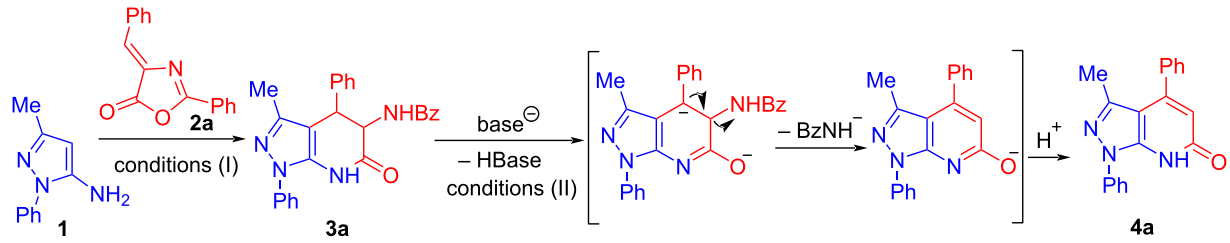

entry	conditions (I)	conditions (II)	yield of **4a** (%)[b]
1	150 °C, 40 min, (62%)[b]	KOH (1 equiv), DMSO, 90 °C, 6 h	traces
2		KOH (1 equiv), DMSO, 150 °C, 6 h	58[c]
3		KOH (1.5 equiv), DMSO, 150 °C, 3.5 h	63
4		*t*-BuOK (1.5 equiv), DMSO, 150 °C, 1.5 h	81
5[d]	150 °C, 40 min then *t*-BuOK (1.5 equiv), DMSO, 150 °C, 1.5 h		73
6[d]	DMSO, 150 °C, 2.5 h then *t*-BuOK (1.5 equiv), 150 °C, 1.5 h		60

[a]Reaction conditions: **1** (2 mmol), **2a** (2 mmol). [b]Isolated yield after column chromatography. [c]Compound **3a** was additionally isolated in 6% yield. [d]One-pot method.

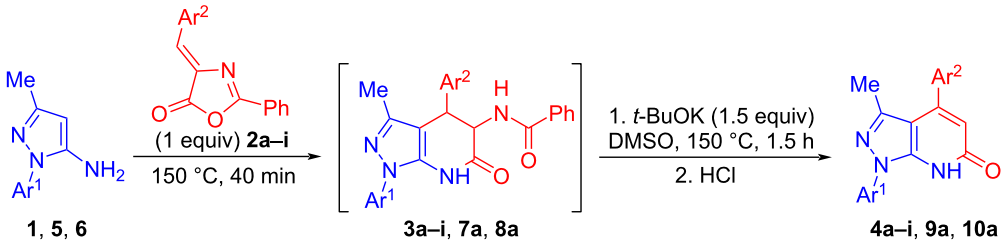

1, **5**, **6** **3a–i**, **7a**, **8a** **4a–i**, **9a**, **10a**

1, **3**, **4**: Ar^1 = Ph; **5**, **7**, **9**: Ar^1 = *p*-Tol; **6**, **8**, **10**: Ar^1 = β-naphthyl; **a**: Ar^2 = Ph, **b**: Ar^2 = C_6H_4-4-Cl; **c**: Ar^2 = C_6H_4-4-OMe; **d**: Ar^2 = C_6H_3-3,4-$(OMe)_2$; **e**: Ar^2 = C_6H_2-3,4,5-$(OMe)_3$; **f**: Ar^2 = C_6H_4-4-F; **g**: Ar^2 = C_6H_4-4-Me; **h**: Ar^2 = 2-furyl; **i**: Ar^2 = 2-thienyl

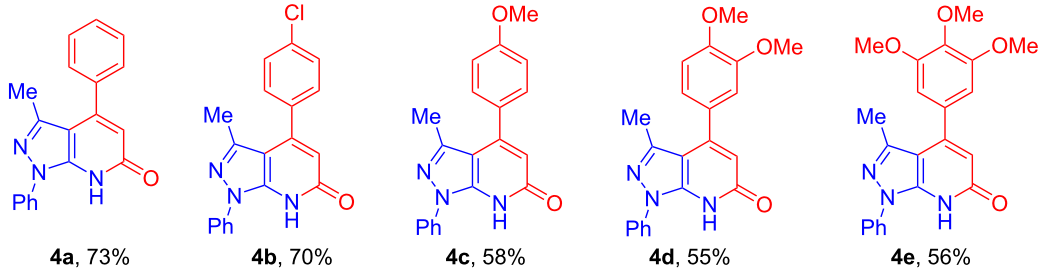

4a, 73% **4b**, 70% **4c**, 58% **4d**, 55% **4e**, 56%

4f, 67% **4g**, 70% **4h**, 58% **4i**, 60% **9a**, 75% **10a**, 56%

Scheme 2: One-pot synthesis of 4-arylpyrazolo[3,4-*b*]pyridin-6-ones **4a–i**, **9a**, and **10a**.

distinct fluorescent properties with blue emission when exposed to UV light. We recorded absorption and fluorescence spectra of ethanolic solutions of compounds **4a–i**, **9a**, and **10a**. The emission and absorption spectra of all the compounds differ slightly from each other. Their spectral parameters are presented in Table 2.

In the UV spectra of ethanolic solutions of compounds **4a–i**, **9a**, and **10a**, a band with a maximum at 260–265 nm is observed, which has a shoulder at 300–305 nm. These signals seem to correspond to π–π* and n–π* transitions. In the luminescence spectra of compounds **4a–i**, **9a**, and **10a**, there is one broadened band with an emission maximum at 409–440 nm (Figure 2).

Table 2: Data of absorption and fluorescence spectra of compounds **4a–i**, **9a**, and **10a**.[a]

Compound	UV–vis		Photoluminescence			
	$^{max}\lambda_{abs}$, nm	ε, 10^3, $M^{-1}\cdot cm^{-1}$ (λ, nm)	λ_{ex}, nm	$^{max}\lambda_{em}$, nm	Stokes shift, nm; eV	Quantum yield Φ_{fl}[b]
4a	260; 302	30.3 ± 0.7 (260)	300; 320	419	117; 1.15	0.22 ± 0.01
4b	260; 302	38.3 ± 0.7 (260)	300; 320	428	126; 1.21	0.23 ± 0.01
4c	262; 302	22.2 ± 0.8 (262)	300; 320	409	107; 1.07	0.16 ± 0.01
4d	260; 301	35.1 ± 0.9 (260)	300; 320	414	113; 1.12	0.15 ± 0.01
4e	262; 301	22.7 ± 0.9 (262)	300; 320	416	115; 1.14	0.18 ± 0.01
4f	260; 302	27.6 ± 0.8 (260)	300; 320	415	113; 1.12	0.20 ± 0.01
4g	261; 300	41.5 ± 0.9 (261)	300; 320	411	111; 1.12	0.20 ± 0.01
4h	265; 305	32.4 ± 1.0 (265)	300; 310	421	116; 1.12	0.23 ± 0.01
4i	263; 301	26.2 ± 0.8 (263)	300; 310	431	130; 1.24	0.09 ± 0.00
9a	259; 303	40.0 ± 0.9 (261)	305	433	130; 1.23	0.19 ± 0.01
10a	261; 288	34.9 ± 0.5 (259)	290	440	152; 1.49	0.11 ± 0.01

[a]In EtOH solution, $c = 1.0\cdot10^{-5}$ mol·L^{-1}. [b]Quantum yield determined relative to quinine sulfate standard in 0.5 M H_2SO_4 ($\Phi_f = 0.546$).

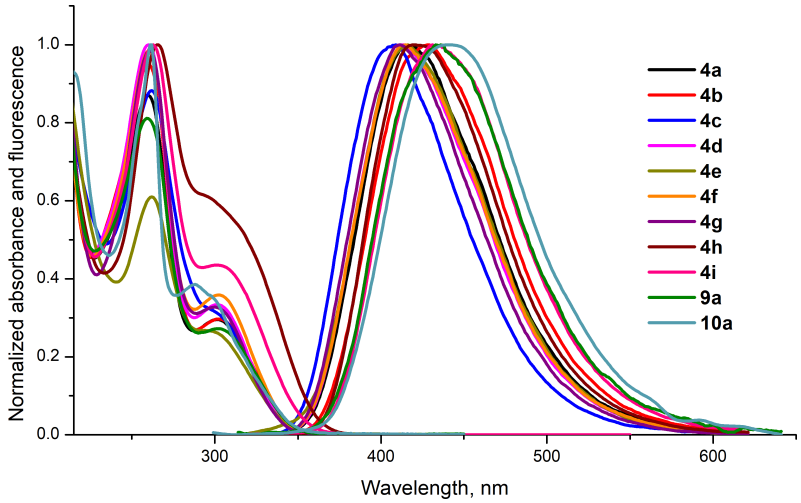

Figure 2: Normalized absorption and fluorescence spectra of solutions of compounds **4a–i**, **9a**, and **10a** in EtOH.

Their diluted alcohol solutions luminesce with a quantum yield of 0.09–0.23. Pyrazolo[3,4-*b*]pyridinones **4a**–**i**, **9a**, and **10a** are characterized by an abnormally high Stokes shift (107–152 nm, 1.07–1.49 eV, Table 2). Such luminophores, which are colorless in daylight but become colored when irradiated with UV light, are used in forensics, in protection against forgery of banknotes, securities, and other important documents [34].

Conclusion

In summary, we developed a simple one-pot synthesis of 4-arylpyrazolo[3,4-*b*]pyridin-6-ones, based on the solvent-free reaction of the available starting compounds 5-aminopyrazoles **1**, **5**, **6** and azlactones **2a**–**i**, followed by heating the resulting intermediate in DMSO in the presence of *t*-BuOK. Photophysical properties of the obtained compounds were studied.

Supporting Information

Supporting Information File 1

Experimental procedures, characterization data, and ^{1}H and ^{13}C NMR spectra for all new compounds.
[https://www.beilstein-journals.org/bjoc/content/supplementary/1860-5397-19-83-S1.pdf]

Funding

This work was supported by the Russian Science Foundation (grant No. 22-13-00356).

ORCID® iDs

Vladislav Yu. Shuvalov - https://orcid.org/0000-0003-2890-1671
Ekaterina Yu. Vlasova - https://orcid.org/0009-0008-0177-8232
Tatyana Yu. Zheleznova - https://orcid.org/0000-0002-0915-1724
Alexander S. Fisyuk - https://orcid.org/0000-0001-6191-9297

Preprint

A non-peer-reviewed version of this article has been previously published as a preprint: https://doi.org/10.3762/bxiv.2023.23.v1

References

1. Cross, J. B.; Zhang, J.; Yang, Q.; Mesleh, M. F.; Romero, J. A. C.; Wang, B.; Bevan, D.; Poutsiaka, K. M.; Epie, F.; Moy, T.; Daniel, A.; Shotwell, J.; Chamberlain, B.; Carter, N.; Andersen, O.; Barker, J.; Ryan, M. D.; Metcalf, C. A., III; Silverman, J.; Nguyen, K.; Lippa, B.; Dolle, R. E. *ACS Med. Chem. Lett.* **2016,** *7,* 374–378. doi:10.1021/acsmedchemlett.5b00368
2. Luo, D.; Guo, Z.; Zhao, X.; Wu, L.; Liu, X.; Zhang, Y.; Zhang, Y.; Deng, Z.; Qu, X.; Cui, S.; Wan, S. *Eur. J. Med. Chem.* **2022,** *227,* 113923. doi:10.1016/j.ejmech.2021.113923
3. Tucker, T. J.; Sisko, J. T.; Tynebor, R. M.; Williams, T. M.; Felock, P. J.; Flynn, J. A.; Lai, M.-T.; Liang, Y.; McGaughey, G.; Liu, M.; Miller, M.; Moyer, G.; Munshi, V.; Perlow-Poehnelt, R.; Prasad, S.; Reid, J. C.; Sanchez, R.; Torrent, M.; Vacca, J. P.; Wan, B.-L.; Yan, Y. *J. Med. Chem.* **2008,** *51,* 6503–6511. doi:10.1021/jm800856c
4. Hamblin, J. N.; Angell, T. D. R.; Ballantine, S. P.; Cook, C. M.; Cooper, A. W. J.; Dawson, J.; Delves, C. J.; Jones, P. S.; Lindvall, M.; Lucas, F. S.; Mitchell, C. J.; Neu, M. Y.; Ranshaw, L. E.; Solanke, Y. E.; Somers, D. O.; Wiseman, J. O. *Bioorg. Med. Chem. Lett.* **2008,** *18,* 4237–4241. doi:10.1016/j.bmcl.2008.05.052
5. Barghash, R. F.; Eldehna, W. M.; Kovalová, M.; Vojáčková, V.; Kryštof, V.; Abdel-Aziz, H. A. *Eur. J. Med. Chem.* **2022,** *227,* 113952. doi:10.1016/j.ejmech.2021.113952
6. Ribeiro, J. L. S.; Soares, J. C. A. V.; Portapilla, G. B.; Providello, M. V.; Lima, C. H. S.; Muri, E. M. F.; de Albuquerque, S.; Dias, L. R. S. *Bioorg. Med. Chem.* **2021,** *29,* 115855. doi:10.1016/j.bmc.2020.115855
7. Sharma, P. K.; Singh, K.; Kumar, S.; Kumar, P.; Dhawan, S. N.; Lal, S.; Ulbrich, H.; Dannhardt, G. *Med. Chem. Res.* **2011,** *20,* 239–244. doi:10.1007/s00044-010-9312-7
8. Mesleh, M. F.; Cross, J. B.; Zhang, J.; Kahmann, J.; Andersen, O. A.; Barker, J.; Cheng, R. K.; Felicetti, B.; Wood, M.; Hadfield, A. T.; Scheich, C.; Moy, T. I.; Yang, Q.; Shotwell, J.; Nguyen, K.; Lippa, B.; Dolle, R.; Ryan, M. D. *Bioorg. Med. Chem. Lett.* **2016,** *26,* 1314–1318. doi:10.1016/j.bmcl.2016.01.009
9. Lu, Y.; Mao, F.; Li, X.; Zheng, X.; Wang, M.; Xu, Q.; Zhu, J.; Li, J. *J. Med. Chem.* **2017,** *60,* 5099–5119. doi:10.1021/acs.jmedchem.7b00468
10. Wager, T. T. Pyrazolo[3,4-*c*]pyridines as gsk-3 inhibitors. PCT Pat. Appl. WO2005000303A1, Jan 6, 2005.
11. Behnke, D.; Cotesta, S.; Hintermann, S.; Fendt, M.; Gee, C. E.; Jacobson, L. H.; Laue, G.; Meyer, A.; Wagner, T.; Badiger, S.; Chaudhari, V.; Chebrolu, M.; Pandit, C.; Hoyer, D.; Betschart, C. *Bioorg. Med. Chem. Lett.* **2015,** *25,* 5555–5560. doi:10.1016/j.bmcl.2015.10.055
12. Choi, P. J.; Lu, G.-L.; Sutherland, H. S.; Giddens, A. C.; Franzblau, S. G.; Cooper, C. B.; Denny, W. A.; Palmer, B. D. *Tetrahedron Lett.* **2022,** *90,* 153611. doi:10.1016/j.tetlet.2021.153611
13. Plemper, R. K.; Lee, E.; Vernachio, J.; Bourque, E. Bicyclic fused pyrazole derivatives for the treatment of rsv. PCT Pat. Appl. WO2017196982A1, Nov 16, 2017.
14. Uchikawa, O.; Mitsui, K.; Asakawa, A.; Morimoto, S.; Yamamoto, M.; Kimura, H.; Moriya, T.; Mizuno, M. Condensed pyrazole derivatives, process for producing the same and use thereof. U.S. Patent US2003187014A1, Oct 2, 2003.
15. Lemmers, J. G. H.; Deretey, E.; Klomp, J. P. G.; Cals, J. M. G. B.; Oubrie, A. Estrogen-related receptor alpha (ERRα) modulators. PCT Pat. Appl. WO2021001453A1, Jan 7, 2021.
16. Hansen, B. B.; Jepsen, T. H.; Larsen, M.; Sindet, R.; Vifian, T.; Burhardt, M. N.; Larsen, J.; Seitzberg, J. G.; Carnerup, M. A.; Jerre, A.; Mølck, C.; Lovato, P.; Rai, S.; Nasipireddy, V. R.; Ritzén, A. *J. Med. Chem.* **2020,** *63,* 7008–7032. doi:10.1021/acs.jmedchem.0c00359
17. Wager, T. GSK-3 inhibitors. U.S. Patent US2005026946A1, Feb 3, 2005.
18. Ratajczyk, J. D.; Swett, L. R. *J. Heterocycl. Chem.* **1975,** *12,* 517–522. doi:10.1002/jhet.5570120315
19. Quiroga, J.; Hormaza, A.; Insuasty, B.; Márquez, M. *J. Heterocycl. Chem.* **1998,** *35,* 409–412. doi:10.1002/jhet.5570350225

20. Swett, L. R.; Ratajczyk, J. D.; Nordeen, C. W.; Aynilian, G. H. *J. Heterocycl. Chem.* **1975,** *12,* 1137–1142. doi:10.1002/jhet.5570120611
21. Minami, S.; Tomita, M.; Kawaguchi, K. *Chem. Pharm. Bull.* **1972,** *20,* 1716–1728. doi:10.1248/cpb.20.1716
22. Shuvalov, V. Y.; Samsonenko, A. L.; Rozhkova, Y. S.; Morozov, V. V.; Shklyaev, Y. V.; Fisyuk, A. S. *ChemistrySelect* **2021,** *6,* 11265–11269. doi:10.1002/slct.202103028
23. Shuvalov, V. Yu.; Chernenko, S. A.; Shatsauskas, A. L.; Samsonenko, A. L.; Dmitriev, M. V.; Fisyuk, A. S. *Chem. Heterocycl. Compd.* **2021,** *57,* 764–771. doi:10.1007/s10593-021-02980-w
24. Shuvalov, V. Y.; Rozhkova, Y. S.; Plekhanova, I. V.; Kostyuchenko, A. S.; Shklyaev, Y. V.; Fisyuk, A. S. *Chem. Heterocycl. Compd.* **2022,** *58,* 7–14. doi:10.1007/s10593-022-03050-5
25. Shuvalov, V. Yu.; Fisyuk, A. S. *Synthesis* **2023,** *55,* 1267–1273. doi:10.1055/a-1993-3714
26. Cunha, S.; dos Santos Filho, R. F.; Saraiva, K. H.; Azevedo-Santos, A. V.; Menezes, D. *Tetrahedron Lett.* **2013,** *54,* 3366–3370. doi:10.1016/j.tetlet.2013.04.055
27. Chen, X.; Zhu, D.; Wang, X.; Yan, S.; Lin, J. *Tetrahedron* **2013,** *69,* 9224–9236. doi:10.1016/j.tet.2013.08.052
28. Vanden Eynde, J. J.; Labuche, N.; Van Haverbeke, Y. *Synth. Commun.* **1997,** *27,* 3683–3690. doi:10.1080/00397919708007288
29. Worayuthakarn, R.; Nealmongkol, P.; Ruchirawat, S.; Thasana, N. *Tetrahedron* **2012,** *68,* 2864–2875. doi:10.1016/j.tet.2012.01.094
30. Liu, X.-Q.; Liu, Y.-Q.; Shao, X.-S.; Xu, Z.-P.; Xu, X.-Y.; Li, Z. *Chin. Chem. Lett.* **2016,** *27,* 7–10. doi:10.1016/j.cclet.2015.10.002
31. Shi, F.; Zhang, J.; Tu, S.; Jia, R.; Zhang, Y.; Jiang, B.; Jiang, H. *J. Heterocycl. Chem.* **2007,** *44,* 1013–1017. doi:10.1002/jhet.5570440506
32. Kim, H. S.; Hammill, J. T.; Scott, D. C.; Chen, Y.; Min, J.; Rector, J.; Singh, B.; Schulman, B. A.; Guy, R. K. *J. Med. Chem.* **2019,** *62,* 8429–8442. doi:10.1021/acs.jmedchem.9b00410
33. Kim, H. S.; Hammill, J. T.; Scott, D. C.; Chen, Y.; Rice, A. L.; Pistel, W.; Singh, B.; Schulman, B. A.; Guy, R. K. *J. Med. Chem.* **2021,** *64,* 5850–5862. doi:10.1021/acs.jmedchem.1c00035
34. Ulyankin, E. B.; Bogza, Y. P.; Kostyuchenko, A. S.; Chernenko, S. A.; Samsonenko, A. L.; Shatsauskas, A. L.; Yurpalov, V. L.; Fisyuk, A. S. *Synlett* **2021,** *32,* 790–794. doi:10.1055/a-1392-2209

License and Terms

BEILSTEIN JOURNAL OF ORGANIC CHEMISTRY

Unravelling a trichloroacetic acid-catalyzed cascade access to benzo[*f*]chromeno[2,3-*h*]quinoxalinoporphyrins

Chandra Sekhar Tekuri, Pargat Singh and Mahendra Nath*§

Full Research Paper

Open Access

Address:
Department of Chemistry, Faculty of Science, University of Delhi, Delhi 110 007, India

Email:
Mahendra Nath* - mnath@chemistry.du.ac.in

* Corresponding author
§ Phone: +91 11 27667794 Extn. 186

Keywords:
bathochromic shift; benzo[*f*]chromeno[2,3-*h*]quinoxalinoporphyrins; catalysis; multicomponent synthesis; one-pot reaction; trichloroacetic acid

Beilstein J. Org. Chem. **2023,** *19,* 1216–1224.
https://doi.org/10.3762/bjoc.19.89

Received: 31 May 2023
Accepted: 02 August 2023
Published: 11 August 2023

This article is part of the thematic issue "Catalytic multi-step domino and one-pot reactions".

Guest Editor: S. Tsogoeva

Abstract

A facile one-pot four-component synthetic methodology is evolved to construct novel copper(II) benzo[*f*]chromeno[2,3-*h*]quinoxalinoporphyrins in good yields via a sequential reaction of copper(II) 2,3-diamino-5,10,15,20-tetraarylporphyrins, 2-hydroxynaphthalene-1,4-dione, aromatic aldehydes, and dimedone in the presence of a catalytic amount of trichloroacetic acid in chloroform at 65 °C. Further, the newly prepared copper(II) porphyrins were transformed to the corresponding free base and zinc(II) benzo[*f*]chromeno[2,3-*h*]quinoxalinoporphyrins under standard demetallation and zinc insertion conditions. The absorption and emission properties of the obtained porphyrins were investigated by using UV–visible and fluorescence spectroscopy. The preliminary photophysical results revealed a significant red-shift in their absorption and emission spectra as compared to the *meso*-tetrakis(4-methylphenyl)porphyrins due to the extended π-conjugation.

Introduction

π-Conjugated porphyrin macrocycles are known for their applications in numerous areas ranging from oxygen transport, photosynthesis, catalysis and medicine [1-3]. In the past several years, diverse organic scaffolds have been incorporated at the porphyrin periphery and different metal ions in the porphyrin core to modulate ground-state and excited-state characteristics of easily accessible *meso*-tetraarylporphyrins. Some of these π-extended tetrapyrrolic macrocycles have emerged as potential candidates in photodynamic therapy and other materials applications [4-7]. Among the previously synthesized synthetically modified porphyrinoids, β,β'-fused *meso*-tetraphenylporphyrins have gained a considerable importance because of their red-shifted absorption and emission due to the extended π-conjugation. In particular, β,β'-fused quinoxalinoporphyrins displayed a wide range of applications in many fields including molecular electronics [8-10]. Additionally, appropriately

functionalized quinoxalinoporphyrin-based photosensitizers are of great interest in the area of dye-sensitized solar cells (DSSC) due to their strong absorption in the visible and near IR regions [11-14]. Similarly, simple quinoxaline-based heterocycles have shown their potential as photosensitizers to induce toxicity in a single cell green algae such as *Chlamydomonas reinhardtii* [15] and also displayed efficacy against *Mycobacterium tuberculosis* and other microbial strains [16,17].

Thorough literature search revealed that the fused heterocycles such as benzo[*a*]pyrano[2,3-*c*]phenazines and benzo[*a*]chromeno[2,3-*c*]phenazines have been prepared as fluorescent materials [18,19]. On the other hand, xanthenes exhibited a number of biological and pharmaceutical profiles such as antimicrobial [20,21], antiviral [22,23], anti-inflammatory [24], anticancer [25], antimalarial agents [26] and are also found to be useful in photodynamic therapy applications [27-29]. In view of above background and also our interest to device convenient protocols for the contruction of periphery-modified porphyrinoids [30-41], we thought to assemble benzo[*f*]chromeno[2,3-*h*]quinoxalinoporphyrins by incorporating porphyrin, quinoxaline and xanthene scaffolds in a single molecular framework using a multicomponent synthetic strategy. The present study discloses an easy and first synthetic approach to build highly π-conjugated copper(II) benzo[*f*]chromeno[2,3-*h*]quinoxalinoporphyrins through a trichloroacetic acid-catalyzed one-pot four-component reaction of 2,3-diamino-5,10,15,20-tetraarylporphyrins, 2-hydroxynaphthalene-1,4-dione, aromatic aldehydes and dimedone in chloroform at 65 °C. The optical properties of the newly prepared porphyrins have been investigated by using UV–vis and emission spectroscopy and the results are presented in this paper.

Results and Discussion

Synthesis

The required precursors, copper(II) 2,3-diamino-5,10,15,20-tetraarylporphyrins **1** were synthesized from the corresponding 2-nitro-*meso*-tetraarylporphyrins in two steps by following the literature procedure [42]. The first step involved an amination of copper(II) 2-nitro-*meso*-tetraarylporphyrins by using 4-amino-4*H*-1,2,4-triazole in the presence of NaOH in refluxing ethanol/toluene 1:10 mixture under inert atmosphere to afford 2-amino-3-nitro-*meso*-tetraarylporphyrins which on reduction through sodium borohydride in the presence of 10% Pd/C in CH_2Cl_2/MeOH provided the desired porphyrins **1** in good yields as key starting materials for the synthesis of newly designed benzo[*f*]chromeno[2,3-*h*]quinoxalinoporphyrins **3**–**8**. For the optimization of the reaction conditions, a model four-component reaction of copper(II) 2,3-diamino-5,10,15,20-tetra(*p*-tolyl)porphyrin with 2-hydroxynaphthalene-1,4-dione (**2**), benzaldehyde and dimedone was carried out in the presence of 20 mol % *p*-toluenesulfonic acid (PTSA) as an acidic catalyst in chloroform at 65 °C for three hours, which provided copper(II) benzo[*f*]chromeno[2,3-*h*]quinoxalinoporphyrin **3** in 40% yield (Table 1, entry 1). To improve the isolated yield of the desired porphyrin **3**, various experiments were performed by reacting copper(II) 2,3-diamino-5,10,15,20-tetra(*p*-tolyl)porphyrin (**1**) with 2-hydroxynaphthalene-1,4-dione, dimedone and benzaldehyde in the presence of different acidic catalysts such as *p*-toluenesulfonic acid (PTSA), $La(OTf)_3$, L-ascorbic acid, *p*-dodecylbenzenesulfonic acid (DBSA), trichloroacetic acid (TCA) and trifluoroacetic acid (TFA) in $CHCl_3$ for 3 hours at 65 °C under one-pot operation (Table 1, entries 1–6). Surprisingly, the reaction did not proceed when $La(OTf)_3$ and L-ascorbic acid were used as acidic catalysts (Table 1, entries 2 and 3). In contrast, the use of Brønsted acidic catalysts such as DBSA and PTSA afforded porphyrin **3** in only 32% and 40% yield, respectively (Table 1, entries 1 and 4). Interestingly, when trichloroacetic acid (TCA) was used as an acidic catalyst under identical conditions, the output of the reaction was improved giving the desired porphyrin **3** in 65% isolated yield (Table 1, entry 5). However, the reaction in the presence of comparatively strong trifluoroacetic acid (TFA) afforded an inseparable mixture of products under the same conditions (Table 1, entry 6). Hence, trichloroacetic acid was found to be an efficient acidic catalyst for the formation of the targeted porphyrin **3** in good yield. Furthermore, various organic solvents such as 1,2-dichloroethane, toluene, 1,4-dioxane and THF were also screened for the synthesis of porphyrin **3** by using 20 mol % of TCA at 65 °C (Table 1, entries 7–10). When the reaction was carried out in 1,2-dichloroethane and toluene at 65 °C, the desired product **3** was obtained in 58% and 10% yields, respectively (Table 1, entries 7 and 8), whereas the reaction did not proceed by using either 1,4-dioxane or THF as a solvent under otherwise identical reaction conditions (Table 1, entries 9 and 10). Thus, chloroform was found to be the best solvent for the synthesis of porphyrin **3**. Further, the effect of catalyst loading on the rate of reaction was examined by varying the concentration of TCA. The yield of the desired product **3** decreased significantly by lowering the amount of TCA from 20 mol % to 10 mol % (Table 1, entry 11). Whereas no increment in the yield of the desired product **3** was observed when the amount of TCA was increased from 20 mol % to 30 mol % (Table 1, entry 12). Therefore, 20 mol % TCA was found to be sufficient to afford the maximum yield of porphyrin **3**.

Finally, the effect of temperature was also investigated by performing the experiments at 80 °C in 1,2-dichloroethane and 50 °C in chloroform under the same reaction conditions which produced the desired porphyrin **3** in lower yields (56% and 34%, respectively; Table 1, entries 13 and 14). In contrast, the

Table 1: Optimization of the reaction conditions for the synthesis of copper(II) benzo[*f*]chromeno[2,3-*h*]quinoxalinoporphyrin **3**.[a]

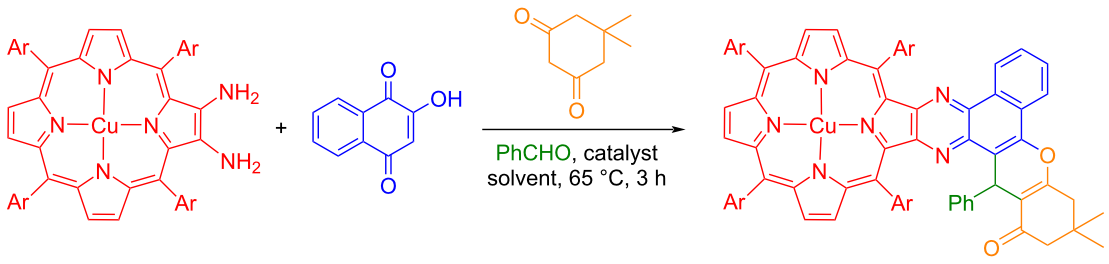

1; Ar = 4-$CH_3C_6H_4$ **2** **3**; Ar = 4-$CH_3C_6H_4$

Entry	Catalyst	Solvent	Time (h)	Yield (%)
1	PTSA (20 mol %)	$CHCl_3$	3	40
2	$La(OTf)_3$ (20 mol %)	$CHCl_3$	3	NR
3	L-ascorbic acid (20 mol %)	$CHCl_3$	3	NR
4	DBSA (20 mol %)	$CHCl_3$	3	32
5	**TCA (20 mol %)**	**$CHCl_3$**	**3**	**65**
6[b]	TFA (20 mol %)	$CHCl_3$	3	0
7	TCA (20 mol %)	$ClCH_2CH_2Cl$	3	58
8	TCA (20 mol %)	toluene	3	10
9	TCA (20 mol %)	1,4-dioxane	3	NR
10	TCA (20 mol %)	THF	3	NR
11	TCA (10 mol %)	$CHCl_3$	3	53
12	TCA (30 mol %)	$CHCl_3$	3	65
13[c]	TCA (20 mol %)	$ClCH_2CH_2Cl$	3	56
14[d]	TCA (20 mol %)	$CHCl_3$	3	34
15[e]	–	$CHCl_3$	3	NR
16[e]	–	toluene	6	NR

[a]NR = no reaction; TCA = trichloroacetic acid; PTSA = *p*-toluenesulfonic acid; DBSA = *p*-dodecylbenzenesulfonic acid; TFA = trifluoroacetic acid; [b]inseparable mixture of products was obtained; [c]reaction was performed at 80 °C; [d]reaction was performed at 50 °C; [e]reaction was carried out at reflux in the absence of TCA.

reaction neither proceeded in chloroform nor in toluene at reflux temperature in the absence of catalyst and always starting material was recovered quantitatively (Table 1, entries 15 and 16). As evident from Table 1, the use of 20 mol % TCA as an acidic catalyst in chloroform at 65 °C was considered to be an optimum condition for the formation of copper(II) benzo[*f*]chromeno[2,3-*h*]quinoxalinoporphyrin **3** in appreciable yield. Further, a new series of copper(II) benzo[*f*]chromeno[2,3-*h*]quinoxalinoporphyrins **3**–**8** were constructed in good isolated yields by using the optimized reaction conditions (Scheme 1).

For a comparative study of absorption and emission properties, the copper complexes of benzo[*f*]chromeno[2,3-*h*]quinoxalinoporphyrins **3**–**7** were converted to the corresponding free-base porphyrinoids **9**–**13** through a standard demetallation process using conc. H_2SO_4 in $CHCl_3$ under cooling conditions (Scheme 1). On complexation with zinc by using $Zn(OAc)_2$ in $CHCl_3$/MeOH, free-base porphyrins **9**, **10** and **13** afforded zinc(II) benzo[*f*]chromeno[2,3-*h*]quinoxalinoporphyrins **14**–**16** in good yields (Scheme 1).

The proposed mechanistic pathway for the formation of copper(II) benzo[*f*]chromeno[2,3-*h*]quinoxalinoporphyrins **3**–**8** under one-pot operation is presented in Figure 1. At the beginning of the reaction, copper(II) 2,3-diamino-5,10,15,20-tetraarylporphyrins **1** react with 2-hydroxynaphthalene-1,4-dione (**2**) in the presence of trichloroacetic acid to form an imine intermediate which on intramolecular cyclization affords a key benzo[*f*]quinoxalinoporphyrin intermediate **17**. Further, a condensation of intermediate **17** with 2-arylidene-5,5-dimethylcyclohexane-1,3-dione **18** (formed in situ through an Aldol condensation of aldehydes with dimedone), to generate copper(II) benzo[*f*]chromeno[2,3-*h*]dihydroquinoxalinoporphyrins which on dehydration produce the desired copper(II) benzo[*f*]chromeno[2,3-*h*]quinoxalinoporphyrins **3**–**8** in 61–68% yields.

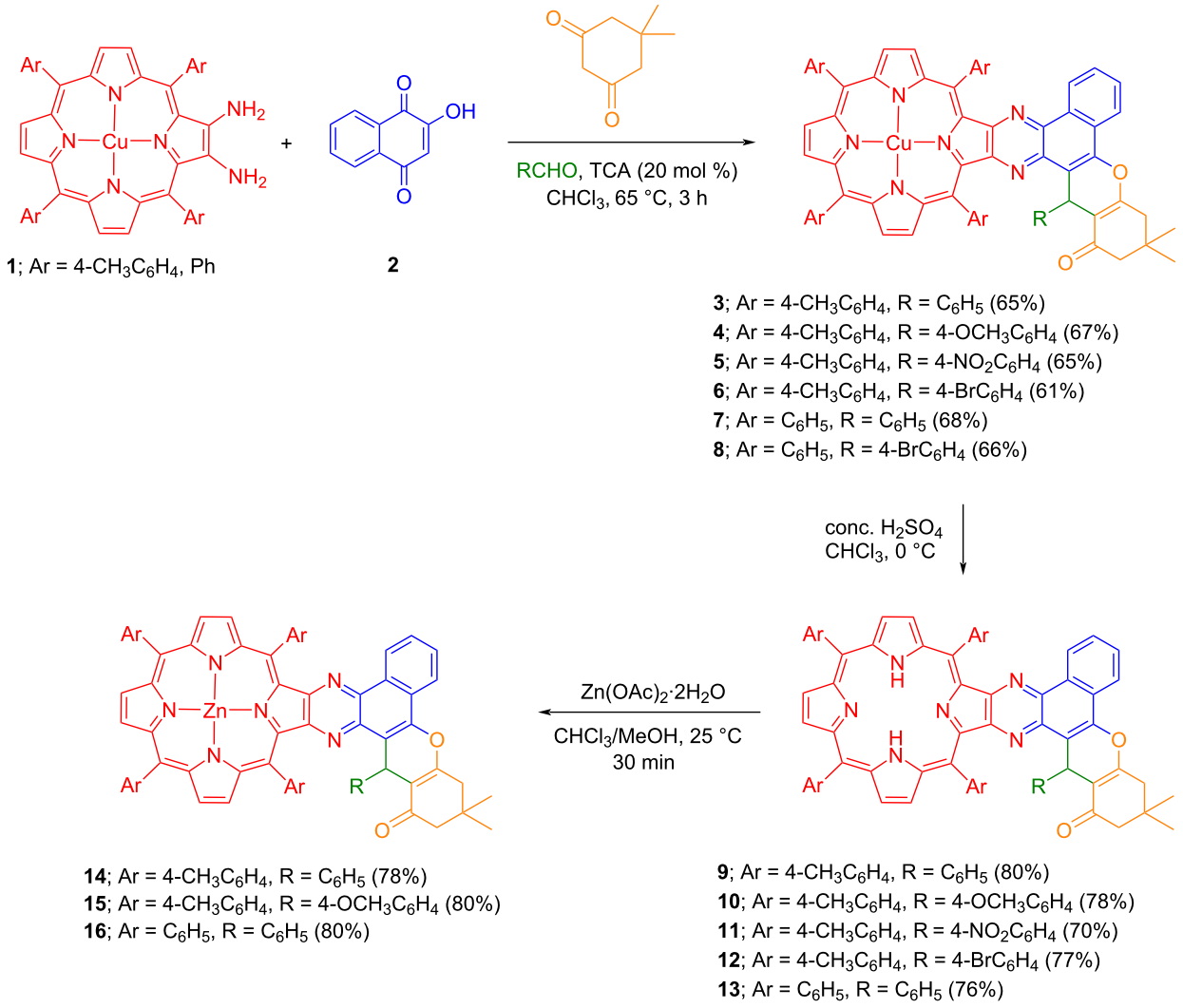

1; Ar = 4-$CH_3C_6H_4$, Ph

2

3; Ar = 4-$CH_3C_6H_4$, R = C_6H_5 (65%)
4; Ar = 4-$CH_3C_6H_4$, R = 4-$OCH_3C_6H_4$ (67%)
5; Ar = 4-$CH_3C_6H_4$, R = 4-$NO_2C_6H_4$ (65%)
6; Ar = 4-$CH_3C_6H_4$, R = 4-BrC_6H_4 (61%)
7; Ar = C_6H_5, R = C_6H_5 (68%)
8; Ar = C_6H_5, R = 4-BrC_6H_4 (66%)

9; Ar = 4-$CH_3C_6H_4$, R = C_6H_5 (80%)
10; Ar = 4-$CH_3C_6H_4$, R = 4-$OCH_3C_6H_4$ (78%)
11; Ar = 4-$CH_3C_6H_4$, R = 4-$NO_2C_6H_4$ (70%)
12; Ar = 4-$CH_3C_6H_4$, R = 4-BrC_6H_4 (77%)
13; Ar = C_6H_5, R = C_6H_5 (76%)

14; Ar = 4-$CH_3C_6H_4$, R = C_6H_5 (78%)
15; Ar = 4-$CH_3C_6H_4$, R = 4-$OCH_3C_6H_4$ (80%)
16; Ar = C_6H_5, R = C_6H_5 (80%)

Scheme 1: Synthesis of benzo[*f*]chromeno[2,3-*h*]quinoxalinoporphyrins **3**–**16**.

To authenticate the proposed reaction pathway, a control experiment was carried out by reacting copper(II) 2,3-diamino-5,10,15,20-tetrakis(4-methylphenyl)porphyrin (**1**) with 2-hydroxynaphthalene-1,4-dione (**2**) in $CHCl_3$ containing 20 mol % TCA at 65 °C as presented in Scheme 2. After workup and chromatographic purification, the isolated product was characterized based on spectral data analysis as copper(II) benzo[*f*]quinoxalinoporphyrin intermediate **17**. Further, porphyrin **17** reacted with benzaldehyde and dimedone in chloroform containing 20 mol% trichloroacetic acid at 65 °C to afford copper(II) benzo[*f*]chromeno[2,3-*h*]quinoxalinoporphyrin **3** in 65% yield (Scheme 2). The successful isolation of intermediate **17** and its conversion to copper(II) benzo[*f*]chromeno[2,3-*h*]quinoxalinoporphyrin **3** as shown in Scheme 2 clearly support the proposed mechanism for the formation of the desired copper(II) porphyrins **3**–**8**.

Finally, the structures of all newly synthesized benzo[*f*]chromeno[2,3-*h*]quinoxalinoporphyrins **3**–**16** and benzo[*f*]quinoxalinoporphyrin **17** were assigned on the basis of IR, ^{1}H and ^{13}C NMR, and HRMS data analysis.

Photophysical characteristics

The UV–vis spectra of the newly synthesized benzo[*f*]chromeno[2,3-*h*]quinoxalinoporphyrins **3**–**16** (Figures 2–4) were recorded in chloroform at 25 °C. Interestingly, the absorption spectra of copper(II) benzo[*f*]chromeno[2,3-*h*]quinoxalinoporphyrins **3**–**8** are significantly broadened and feature split Soret bands between 408–445 nm probably due to the loss in D_{4h} symmetry after the fusion of a large benzo[*f*]chromeno[2,3-*h*]quinoxaline moiety across the porphyrinic β-positions [43], and two Q-bands at ≈562 and 603 nm (Figure 2). Further, the electronic absorpion spectra of free-base benzo[*f*]chromeno[2,3-

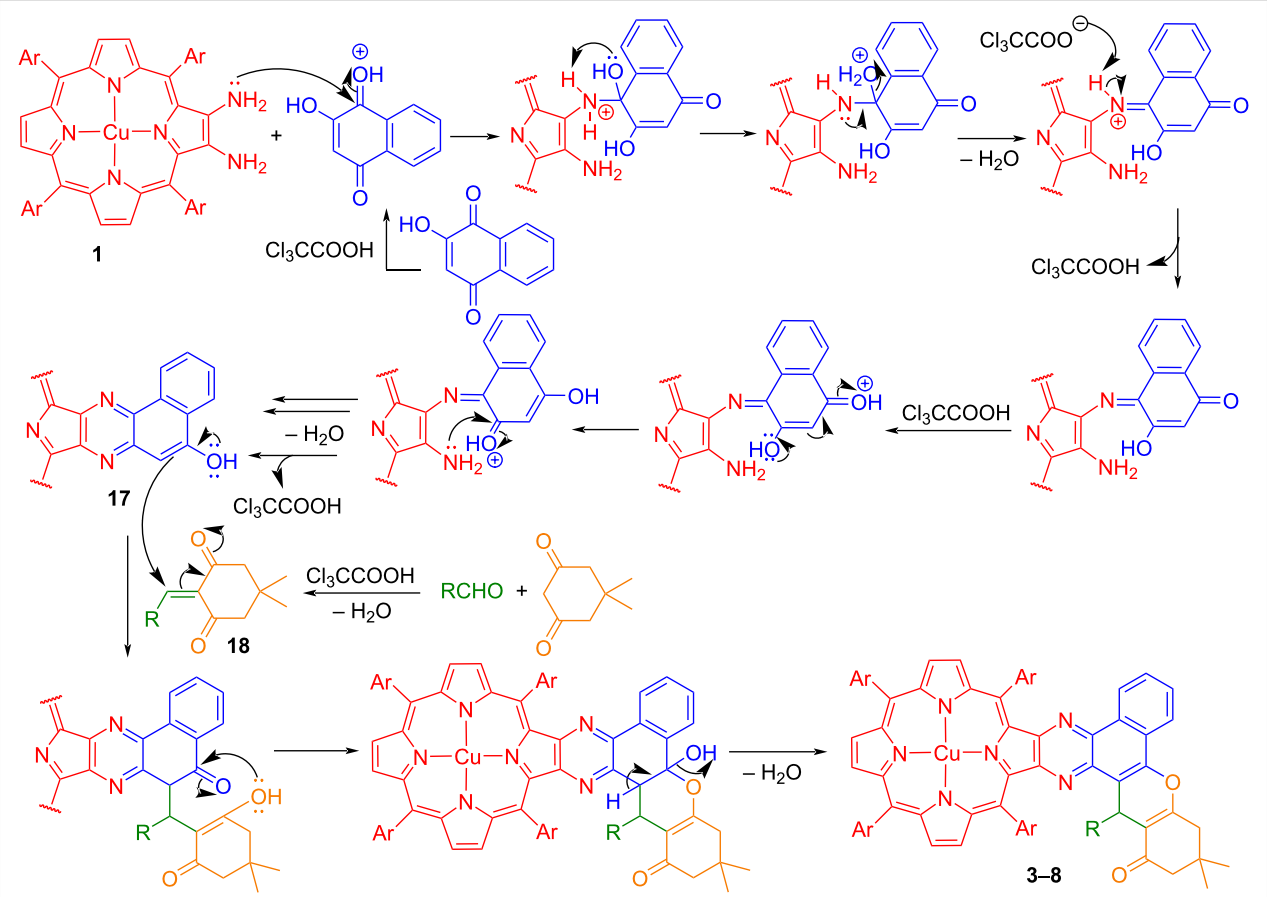

Figure 1: Plausible mechanism for the formation of copper(II) benzo[*f*]chromeno[2,3-*h*]quinoxalinoporphyrins.

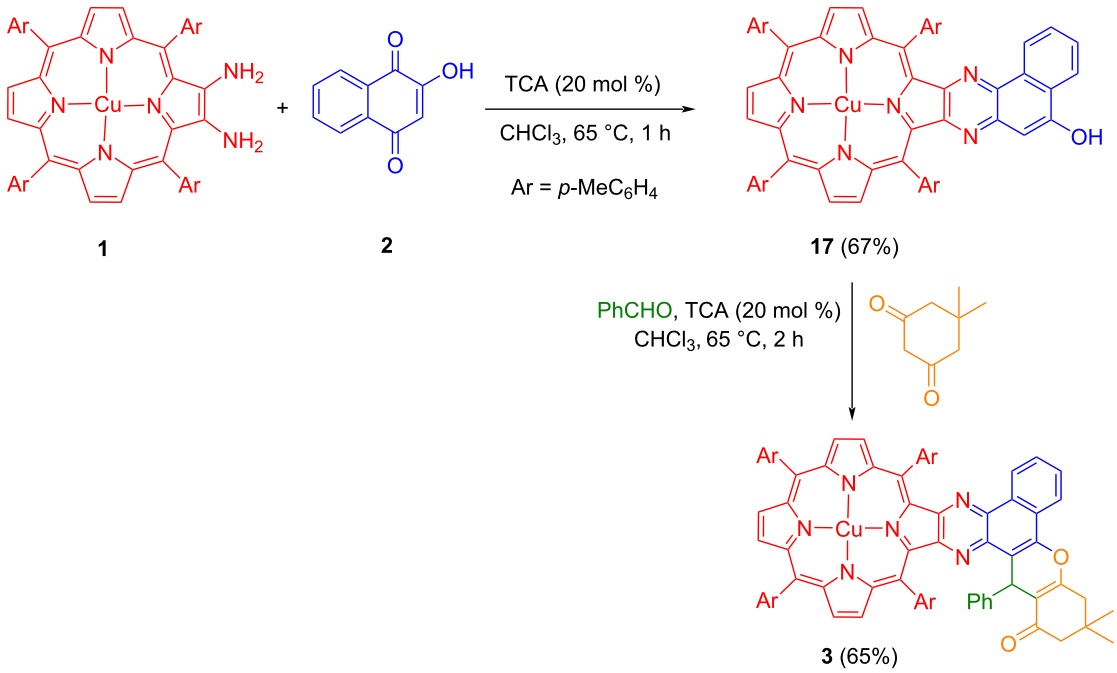

Scheme 2: Sequential synthesis of copper(II) benzo[*f*]chromeno[2,3-*h*]quinoxalinoporphyrin **3**.

h]quinoxalinoporphyrins **9**–**13** exhibited Soret bands between 439–442 nm and four Q-bands between 526 and 642 nm (Figure 3). In contrast, UV–visible spectra of zinc(II) benzo[*f*]chromeno[2,3-*h*]quinoxalinoporphyrins **14**–**16** showed broadened Soret bands with slight splitting between 445–450 nm and two Q-bands at ≈566 and 606 nm (Figure 4).

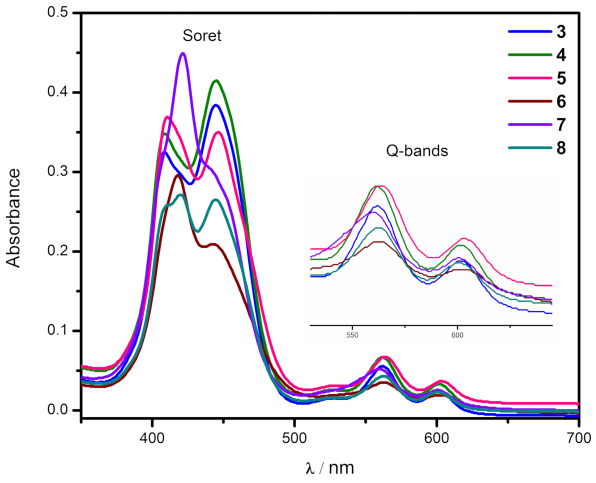

Figure 2: Electronic absorption spectra of copper(II) benzo[*f*]chromeno[2,3-*h*]quinoxalinoporphyrins **3**–**8** in $CHCl_3$ (1.5×10^{-6} M) at 298 K. (Inset shows Q-bands).

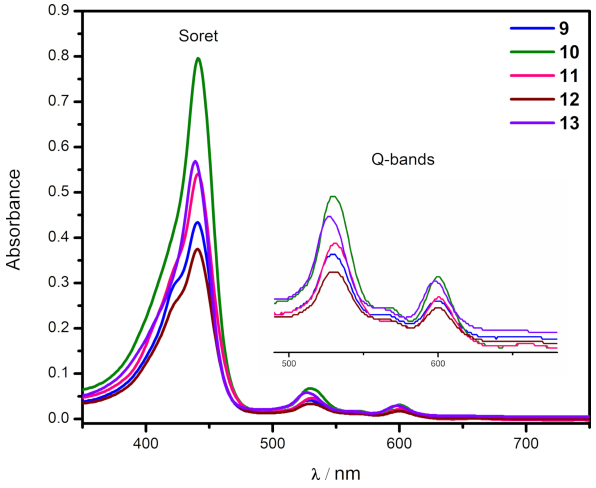

Figure 3: Electronic absorption spectra of free-base benzo[*f*]chromeno[2,3-*h*]quinoxalinoporphyrins **9**–**13** in $CHCl_3$ (1.5×10^{-6} M) at 298 K. (Inset shows Q-bands).

All the newly prepared copper(II), free-base and zinc(II) benzo[*f*]chromeno[2,3-*h*]quinoxalinoporphyrins displayed a significant red-shift in their Soret and Q-bands by ≈20–30 nm as compared to their corresponding *meso*-tertakis(4-methyl-

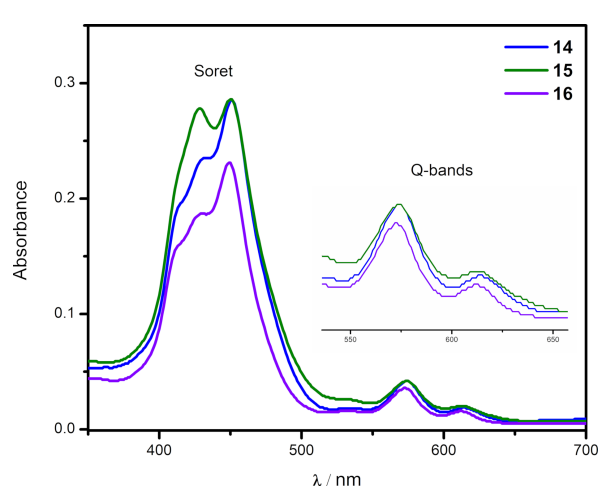

Figure 4: Electronic absorption spectra of zinc(II) benzo[*f*]chromeno[2,3-*h*]quinoxalinoporphyrins **14**–**16** in $CHCl_3$ (1.5×10^{-6} M) at 298 K. (Inset shows Q-bands).

phenyl)porphyrins (Cu-TMPP, Soret band at 416 nm; TMPP, Soret band at 419 nm; Zn-TMPP, Soret band at 425 nm) due to the extended π-conjugation after the fusion of the benzo[*f*]chromeno[2,3-*h*]quinoxaline moiety at the β-pyrrolic positions of the porphyrin macrocycle.

In the fluorescence spectra, free-base benzo[*f*]chromeno[2,3-*h*]quinoxalinoporphyrins **9**–**13** showed emission bands at ≈675 nm and 730 nm (Figure 5a). These newly synthesized free-base porphyrins displayed significant red-shifts in their emission spectra in comparison to *meso*-tetrakis(4-methylphenyl)porphyrin (TMPP; emission bands at ≈652 and 717 nm). Similarly, fluorescence spectra of zinc(II) benzo[*f*]chromeno[2,3-*h*]quinoxalinoporphyrins **14**, **15** and **16** (Figure 5b) showed two emission bands between 623 and 678 nm with a red-shift of 21–25 nm in comparison to zinc(II) *meso*-tetrakis(4-methylphenyl)porphyrin (Zn-TMPP; emission bands at 602 and 653 nm). However, no emission was observed in the case of copper(II) porphyrins due to the paramagnetic nature of copper(II) ions [44].

Conclusion

In summary, we have successfully synthesized a new series of copper(II) benzo[*f*]chromeno[2,3-*h*]quinoxalinoporphyrin analogues in good yields following the one-pot synthetic strategy applying the reaction of copper(II) 2,3-diamino-*meso*-tetraarylporphyrins with 2-hydroxynaphthalene-1,4-dione, aromatic aldehydes and dimedone in the presence of 20 mol % trichloroacetic acid in chloroform at 65 °C. Interestingly, a sequential approach for constructing copper(II) benzo[*f*]chromeno[2,3-*h*]quinoxalinoporphyrin **3** was also followed by capturing a key intermediate, copper(II) benzo[*f*]quinoxalino-

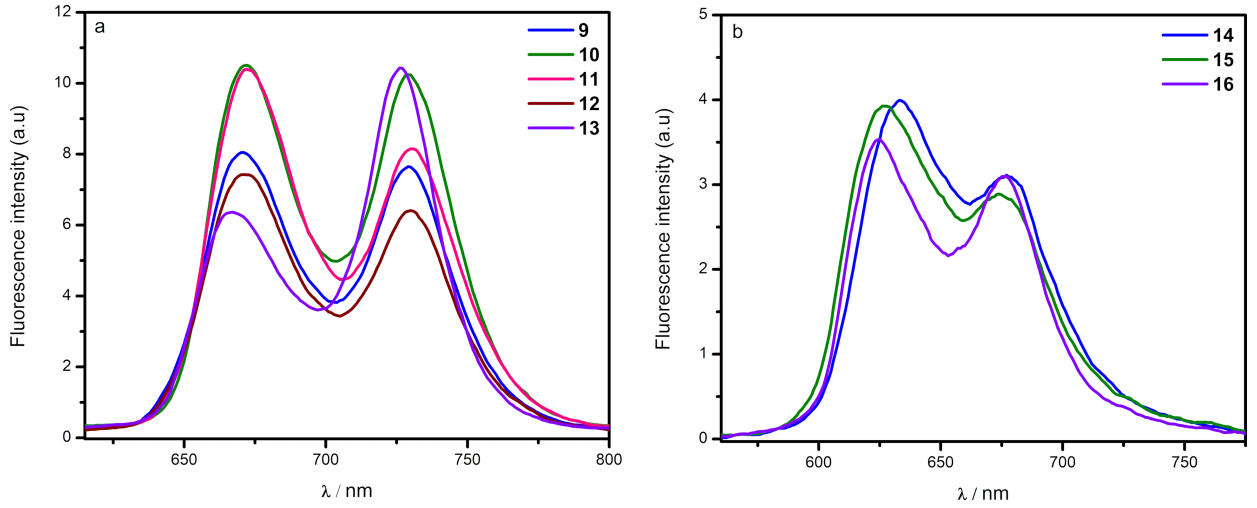

Figure 5: (a) Emission spectra of free-base benzo[*f*]chromeno[2,3-*h*]quinoxalinoporphyrins **9–13** and (b) emission spectra of zinc(II) benzo[*f*]chromeno[2,3-*h*]quinoxalinoporphyrins **14–16** in $CHCl_3$ (1.5×10^{-6} M) at 298 K (λ_{Ex} = 420 nm).

porphyrin **17** for the mechanistic studies. On photophysical evaluation, the newly synthesized porphyrins displayed significant red-shifted absorption and emission as compared to simple *meso*-tetraarylporphyrins due to the extended π-electronic conjugation. Hence, the present study is potentially useful for the development of highly conjugated π-electron rich porphyrinoids with improved light harvesting properties.

Experimental

Materials and instrumentation methods

All reagents and solvents used in this study were purchased from Sigma-Aldrich (Merck) and were used as received unless otherwise stated. The column chromatographic purifications of all products were carried out using either activated neutral aluminium oxide (Brokmann grade I-II, Merck). The melting points of all newly prepared products were determined on a Büchi M-560 melting point apparatus. ^{1}H NMR (400 MHz) and ^{13}C NMR (100 MHz) spectra were recorded in $CDCl_3$ on a Jeol ECX-400P (400 MHz) NMR spectrometer. Chemical shifts are reported in δ scale in parts per million (ppm) relative to $CDCl_3$ (δ = 7.26 ppm for ^{1}H NMR and δ = 77.00 ppm for ^{13}C NMR). The coupling constants are expressed as (*J*) and are reported in hertz (Hz). Infrared (IR) spectra of the synthesized compounds were recorded in film or KBr on Perkin Elmer IR spectrometer and absorption maxima (υ_{max}) are given in cm^{-1}. UV–vis absorption and fluorescence spectra were recorded on an Analytik Jena's Specord 250 UV–vis spectrophotometer and a Varian Cary Eclipse fluorescence spectrophotometer, respectively. The mass spectra were recorded on an Agilent G 6530 AA LC-HRMS QTOF system in positive mode. Spectroscopic grade chloroform was used to measure UV–visible and emission spectra of the samples. Thin-layer chromatography (TLC) was performed on silica gel 60 F_{254} (pre-coated aluminium) sheets from Merck.

General procedure for the synthesis of copper(II) benzo[*f*]chromeno[2,3-*h*]quinoxalinoporphyrins **3–8**

To a solution of copper(II) 2,3-diamino-*meso*-tetraarylporphyrin (**1**; 0.131 mmol) in chloroform (20 mL), 2-hydroxynaphthalene-1,4-dione (**2**; 0.157 mmol) and trichloroacetic acid (0.026 mmol) were added and the reaction mixture was stirred at reflux temperature for 30 minutes. Then, the aromatic aldehyde (0.157 mmol) and dimedone (0.157 mmol) were added and the reaction mixture was refluxed for additional two and a half hours. The progress of the reaction was monitored by TLC. After completion of the reaction, the product was extracted by using chloroform (3 × 50 mL). The organic layers were combined and washed with water (3 × 50 mL), dried over anhydrous sodium sulfate and evaporated under reduced pressure. The crude product was purified on a neutral alumina column by using 20% chloroform in hexane as eluent to afford porphyrins **3–8** in 61–68% yields.

General procedure for the synthesis of free-base benzo[*f*]chromeno[2,3-*h*]quinoxalinoporphyrins **9–13**

To a solution of copper(II) benzo[*f*]chromeno[2,3-*h*]quinoxalinoporphyrin **3–7** (0.090 mmol) in chloroform (20 mL), conc. H_2SO_4 (1.6 mL) was added and the reaction mixture was stirred at 0 °C for 7 min. After completion of the reaction, the reaction mixture was quenched with water and neutralized with saturated sodium bicarbonate solution. The resulting mixture was extracted with chloroform (50 mL). The organic layer was

washed with water (3 × 50 mL), dried over anhydrous sodium sulfate and evaporated under reduced pressure. The crude product was purified on a neutral alumina column by using 40% chloroform in hexane as eluent to afford porphyrins **9**–**13** in 70–80% yields.

General procedure for the synthesis of zinc(II) benzo[*f*]chromeno[2,3-*h*]quinoxalinoporphyrins **14–16**

To a solution of free-base benzo[*f*]chromeno[2,3-*h*]quinoxalinoporphyrins **9**, **10** and **13** (0.038 mmol) in chloroform (10 mL), a solution of $Zn(OAc)_2{\cdot}2H_2O$ (0.136 mmol) in methanol (2 mL) was added and reaction mixture was stirred at 25 °C for thirty minutes. The progress of the reaction was monitored by TLC. After completion of the reaction, the reaction mixture was diluted with chloroform (50 mL). The resulting solution was washed with water (3 × 50 mL), the organic layer was dried over anhydrous sodium sulfate and evaporated under reduced pressure. The crude product was purified on activated neutral alumina column by using 80% chloroform in hexane as eluent to afford porphyrins **14**–**16** in 78–80% yields.

Synthesis of copper(II) benzo[*f*]quinoxalinoporphyrin **17**

To a solution of copper(II) 2,3-diamino-*meso*-tetraarylporphyrin **1** (0.131 mmol) in chloroform (15 mL), 2-hydroxynaphthalene-1,4-dione (**2**; 0.157 mmol) and trichloroacetic acid (0.026 mmol) were added and the reaction mixture was stirred at reflux temperature for 2 hours and the progress of the reaction was monitored by TLC. After completion of the reaction, the crude product was extracted by using chloroform (3 × 50 mL). The organic layer was washed with water (3 × 50 mL), dried over anhydrous sodium sulfate and evaporated under reduced pressure. The crude product obtained was purified on a neutral alumina column by using 20% chloroform in hexane as eluent to afford porphyrin **17** in 67% yield.

Supporting Information

Supporting Information File 1

Characterization data, ^1H and ^{13}C NMR spectra of newly prepared porphyrin products.
[https://www.beilstein-journals.org/bjoc/content/supplementary/1860-5397-19-89-S1.pdf]

Acknowledgements

The authors are grateful to the USIC, University of Delhi, Delhi, India for providing the NMR and high-resolution mass data.

Funding

MN is thankful to IoE, University of Delhi, India for providing a FRP grant. CT and PS are thankful to UGC, New Delhi, India for the award of Senior Research Fellowships.

ORCID® iDs

Pargat Singh - https://orcid.org/0000-0002-0203-0612
Mahendra Nath - https://orcid.org/0000-0002-3088-1422

References

1. Barber, J. *Chem. Soc. Rev.* **2009,** *38,* 185–196. doi:10.1039/b802262n
2. Izbicka, E.; Wheelhouse, R. T.; Raymond, E.; Davidson, K. K.; Lawrence, R. A.; Sun, D.; Windle, B. E.; Hurley, L. H.; Von Hoff, D. D. *Cancer Res.* **1999,** *59,* 639–644.
3. Ethirajan, M.; Chen, Y.; Joshi, P.; Pandey, R. K. *Chem. Soc. Rev.* **2011,** *40,* 340–362. doi:10.1039/b915149b
4. Sternberg, E. D.; Dolphin, D.; Brückner, C. *Tetrahedron* **1998,** *54,* 4151–4202. doi:10.1016/s0040-4020(98)00015-5
5. de Torres, M.; Semin, S.; Razdolski, I.; Xu, J.; Elemans, J. A. A. W.; Rasing, T.; Rowan, A. E.; Nolte, R. J. M. *Chem. Commun.* **2015,** *51,* 2855–2858. doi:10.1039/c4cc09592h
6. Gautam, P.; Dhokale, B.; Shukla, V.; Singh, C. P.; Bindra, K. S.; Misra, R. *J. Photochem. Photobiol., A* **2012,** *239,* 24–27. doi:10.1016/j.jphotochem.2012.04.020
7. Stamati, I.; Kuimova, M. K.; Lion, M.; Yahioglu, G.; Phillips, D.; Deonarain, M. P. *Photochem. Photobiol. Sci.* **2010,** *9,* 1033–1041. doi:10.1039/c0pp00038h
8. Crossley, M. J.; Burn, P. L. *J. Chem. Soc., Chem. Commun.* **1991,** 1569–1571. doi:10.1039/c39910001569
9. Sendt, K.; Johnston, L. A.; Hough, W. A.; Crossley, M. J.; Hush, N. S.; Reimers, J. R. *J. Am. Chem. Soc.* **2002,** *124,* 9299–9309. doi:10.1021/ja020081u
10. Li, L.-L.; Diau, E. W.-G. *Chem. Soc. Rev.* **2013,** *42,* 291–304. doi:10.1039/c2cs35257e
11. Kadish, K. M.; E, W.; Sintic, P. J.; Ou, Z.; Shao, J.; Ohkubo, K.; Fukuzumi, S.; Govenlock, L. J.; McDonald, J. A.; Try, A. C.; Cai, Z.-L.; Reimers, J. R.; Crossley, M. J. *J. Phys. Chem. B* **2007,** *111,* 8762–8774. doi:10.1021/jp0726743
12. Eu, S.; Hayashi, S.; Umeyama, T.; Matano, Y.; Araki, Y.; Imahori, H. *J. Phys. Chem. C* **2008,** *112,* 4396–4405. doi:10.1021/jp710400p
13. Imahori, H.; Hayashi, S.; Hayashi, H.; Oguro, A.; Eu, S.; Umeyama, T.; Matano, Y. *J. Phys. Chem. C* **2009,** *113,* 18406–18413. doi:10.1021/jp907288h
14. Kira, A.; Matsubara, Y.; Iijima, H.; Umeyama, T.; Matano, Y.; Ito, S.; Niemi, M.; Tkachenko, N. V.; Lemmetyinen, H.; Imahori, H. *J. Phys. Chem. C* **2010,** *114,* 11293–11304. doi:10.1021/jp1004049
15. Fischer, B. B.; Krieger-Liszkay, A.; Eggen, R. I. L. *Environ. Sci. Technol.* **2004,** *38,* 6307–6313. doi:10.1021/es049673y
16. Giddens, S. R.; Bean, D. C. *Int. J. Antimicrob. Agents* **2007,** *29,* 93–97. doi:10.1016/j.ijantimicag.2006.08.028
17. De Logu, A.; Palchykovska, L. H.; Kostina, V. H.; Sanna, A.; Meleddu, R.; Chisu, L.; Alexeeva, I. V.; Shved, A. D. *Int. J. Antimicrob. Agents* **2009,** *33,* 223–229. doi:10.1016/j.ijantimicag.2008.09.016
18. Saluja, P.; Chaudhary, A.; Khurana, J. M. *Tetrahedron Lett.* **2014,** *55,* 3431–3435. doi:10.1016/j.tetlet.2014.04.072
19. Khurana, J. M.; Chaudhary, A.; Lumb, A.; Nand, B. *Green Chem.* **2012,** *14,* 2321–2327. doi:10.1039/c2gc35644a

20. Omolo, J. J.; Johnson, M. M.; van Vuuren, S. F.; de Koning, C. B. *Bioorg. Med. Chem. Lett.* **2011,** *21,* 7085–7088. doi:10.1016/j.bmcl.2011.09.088
21. Kaya, M.; Demir, E.; Bekci, H. *J. Enzyme Inhib. Med. Chem.* **2013,** *28,* 885–893. doi:10.3109/14756366.2012.692087
22. Reddi Mohan Naidu, K.; Satheesh Krishna, B.; Anil Kumar, M.; Arulselvan, P.; Ibrahim Khalivulla, S.; Lasekan, O. *Molecules* **2012,** *17,* 7543–7555. doi:10.3390/molecules17067543
23. Maia, M.; Resende, D. I. S. P.; Durães, F.; Pinto, M. M. M.; Sousa, E. *Eur. J. Med. Chem.* **2021,** *210,* 113085. doi:10.1016/j.ejmech.2020.113085
24. Poupelin, J.-P.; Saint-Ruf, G.; Foussard-Blanpin, O.; Narcisse, G.; Uchida-Ernouf, G.; Lacroix, R. *Eur. J. Med. Chem.* **1978,** *13,* 67–71.
25. Mulakayala, N.; Murthy, P. V. N. S.; Rambabu, D.; Aeluri, M.; Adepu, R.; Krishna, G. R.; Reddy, C. M.; Prasad, K. R. S.; Chaitanya, M.; Kumar, C. S.; Basaveswara Rao, M. V.; Pal, M. *Bioorg. Med. Chem. Lett.* **2012,** *22,* 2186–2191. doi:10.1016/j.bmcl.2012.01.126
26. Chibale, K.; Visser, M.; van Schalkwyk, D.; Smith, P. J.; Saravanamuthu, A.; Fairlamb, A. H. *Tetrahedron* **2003,** *59,* 2289–2296. doi:10.1016/s0040-4020(03)00240-0
27. Wu, Y.; Wu, J.; Wong, W.-Y. *Biomater. Sci.* **2021,** *9,* 4843–4853. doi:10.1039/d1bm00128k
28. Ebaston, T. M.; Nakonechny, F.; Talalai, E.; Gellerman, G.; Patsenker, L. *Dyes Pigm.* **2021,** *184,* 108854. doi:10.1016/j.dyepig.2020.108854
29. Pellosi, D. S.; Estevão, B. M.; Semensato, J.; Severino, D.; Baptista, M. S.; Politi, M. J.; Hioka, N.; Caetano, W. *J. Photochem. Photobiol., A* **2012,** *247,* 8–15. doi:10.1016/j.jphotochem.2012.07.009
30. Singh, J.; Singh, P.; Nath, M. *J. Org. Chem.* **2023,** *88,* 7302–7310. doi:10.1021/acs.joc.3c00528
31. Singh, A.; Singh, J.; Nath, M. *Eur. J. Org. Chem.* **2023,** *26,* e202201319. doi:10.1002/ejoc.202201319
32. Singh, P.; Nath, M. *Org. Lett.* **2022,** *24,* 8586–8591. doi:10.1021/acs.orglett.2c02945
33. Tekuri, C. S.; Singh, P.; Nath, M. *Org. Biomol. Chem.* **2020,** *18,* 2516–2523. doi:10.1039/d0ob00171f
34. Singh, P.; Nath, M. *SynOpen* **2020,** *4,* 44–50. doi:10.1055/s-0040-1707429
35. Tiwari, R.; Nath, M. *SynOpen* **2018,** *2,* 133–137. doi:10.1055/s-0036-1591998
36. Tiwari, R.; Nath, M. *Dyes Pigm.* **2018,** *152,* 161–170. doi:10.1016/j.dyepig.2018.01.041
37. Singh, D. K.; Nath, M. *Org. Biomol. Chem.* **2015,** *13,* 1836–1845. doi:10.1039/c4ob02370f
38. Nath, M.; Pink, M.; Zaleski, J. M. *J. Am. Chem. Soc.* **2005,** *127,* 478–479. doi:10.1021/ja045979t
39. Nath, M.; Huffman, J. C.; Zaleski, J. M. *J. Am. Chem. Soc.* **2003,** *125,* 11484–11485. doi:10.1021/ja0302782
40. Boerner, L. J. K.; Nath, M.; Pink, M.; Zaleski, J. M. *Chem. – Eur. J.* **2011,** *17,* 9311–9315. doi:10.1002/chem.201101741
41. Nath, M.; Pink, M.; Zaleski, J. M. *J. Organomet. Chem.* **2011,** *696,* 4152–4157. doi:10.1016/j.jorganchem.2011.07.008
42. Lefebvre, J.-F.; Leclercq, D.; Gisselbrecht, J.-P.; Richeter, S. *Eur. J. Org. Chem.* **2010,** 1912–1920. doi:10.1002/ejoc.200901310
43. Koehorst, R. B. M.; Kleibeuker, J. F.; Schaafsma, T. J.; de Bie, D. A.; Geurtsen, B.; Henrie, R. N.; van der Plas, H. C. *J. Chem. Soc., Perkin Trans. 2* **1981,** 1005–1009. doi:10.1039/p29810001005
44. Szintay, G.; Horváth, A.; Grampp, G. *J. Photochem. Photobiol., A* **1999,** *126,* 83–89. doi:10.1016/s1010-6030(99)00130-6

License and Terms

BEILSTEIN JOURNAL OF ORGANIC CHEMISTRY

Acetaldehyde in the Enders triple cascade reaction via acetaldehyde dimethyl acetal

Alessandro Brusa[‡1], Debora Iapadre[‡1], Maria Edith Casacchia[1,2], Alessio Carioscia[1], Giuliana Giorgianni[1], Giandomenico Magagnano[1], Fabio Pesciaioli[*1] and Armando Carlone[*1,3]

Full Research Paper

Open Access

Address:
[1]Department of Physical and Chemical Sciences, Università degli Studi dell'Aquila, via Vetoio, 67100, L'Aquila, Italy, [2]IUSS Scuola Universitaria Superiore di Pavia, Palazzo del Broletto, Piazza della Vittoria, 15, 27100, Pavia, Italy and [3]INSTM, Consorzio Nazionale per la Scienza e Tecnologia dei Materiali, RU L'Aquila, Italy

Email:
Fabio Pesciaioli[*] - fabio.pesciaioli@univaq.it;
Armando Carlone[*] - armando.carlone@univaq.it

* Corresponding author ‡ Equal contributors

Keywords:
acetaldehyde; acetaldehyde dimethyl acetal; cascade reaction; multicomponent reaction; organocatalysis

Beilstein J. Org. Chem. **2023,** *19,* 1243–1250.
https://doi.org/10.3762/bjoc.19.92

Received: 14 June 2023
Accepted: 09 August 2023
Published: 24 August 2023

This article is part of the thematic issue "Catalytic multi-step domino and one-pot reactions".

Guest Editor: S. Tsogoeva

Abstract

Asymmetric organocatalyzed multicomponent reactions represent an important toolbox in the field of organic synthesis to build complex scaffolds starting from simple starting materials. The Enders three-component cascade reaction was a cornerstone in the field and a plethora of organocatalyzed cascade reactions followed. However, acetaldehyde was not shown as a successful reaction partner, probably because of its high reactivity. Herein, we report the Enders-type cascade reaction using acetaldehyde dimethyl acetal, as a masked form of acetaldehyde. This strategy directly converts acetaldehyde, nitroalkenes and enals into stereochemically dense cyclohexenals in good yield and excellent enantioselectivity.

Introduction

Multicomponent reactions (MCRs) are chemical processes that involve three or more compounds, in which the product contains all the atoms of the reagents, except for condensation coproducts, such as water, hydrogen chloride or other small molecules [1-3]. MCRs have a great advantage over the classical two-component reactions; they allow the construction of complex molecular motifs in only one synthetic operational step starting from simpler building blocks. For this reason, the use of MCRs is appealing in the construction of natural or synthetic products [2-5] or libraries of compounds [2], and is generally

considered an advantage in organic synthesis for atom economy, waste reduction and time saving. Cascade reactions are defined as chemical processes in which two or more bond-forming steps happen under identical reaction conditions, and where a subsequent transformation takes place at the functionality obtained in the former bond-forming event. Cascade reactions are valuable tools for streamlining the synthesis of structurally complex molecules in a single operation and from readily available substrates. Their combination with asymmetric aminocatalysis [4,6-8] has recently led to innovative approaches for the one-step enantioselective preparation of stereochemically dense molecules. Nowadays, organocatalytic cascade processes provide a powerful tool for achieving molecular complexity. Their synthetic potential has been demonstrated by their application in the total synthesis of complex natural compounds [2,4,9-12].

A remarkable example of an amino-catalyzed cascade process was reported by Enders [11], a three-component cascade reaction for the synthesis of polyfunctionalized cyclohexenes bearing multiple stereocenters. The reaction is promoted by a chiral secondary amine, which is capable of catalyzing each step of the process activating the substrates through enamine and iminium ion catalysis towards a Michael/Michael/aldol process. The ingenious crafting of the reaction lies in the selection of the reactivity of the different nucleophiles and electrophiles present in the mixture, both as reagents and as intermediates. First, the chiral aminocatalyst **1** activates the saturated aldehyde **2** via enamine intermediate **A**, which intercepts the nitroalkene **3** in a Michael-type addition forming intermediate **B**. Hydrolysis regenerates catalyst **1** that can then selectively condense with the α,β-unsaturated aldehyde **4** to form chiral iminium ion intermediate **C**. Iminium ion **C** reacts with intermediate **B** in a further Michael-type reaction. The last step involves the enamine intermediate which drives an intramolecular aldol condensation to form the final product **5**. In this elegant cascade process, catalyst **1** promotes three consecutive carbon–carbon bond forming steps generating four stereogenic centers with high diastereoselectivity and complete enantiocontrol (Scheme 1).

This elegantly designed example established a new direction in asymmetric aminocatalysis, leading to an impressive growth of methods based on organocascade processes [8,10,13-16]. The

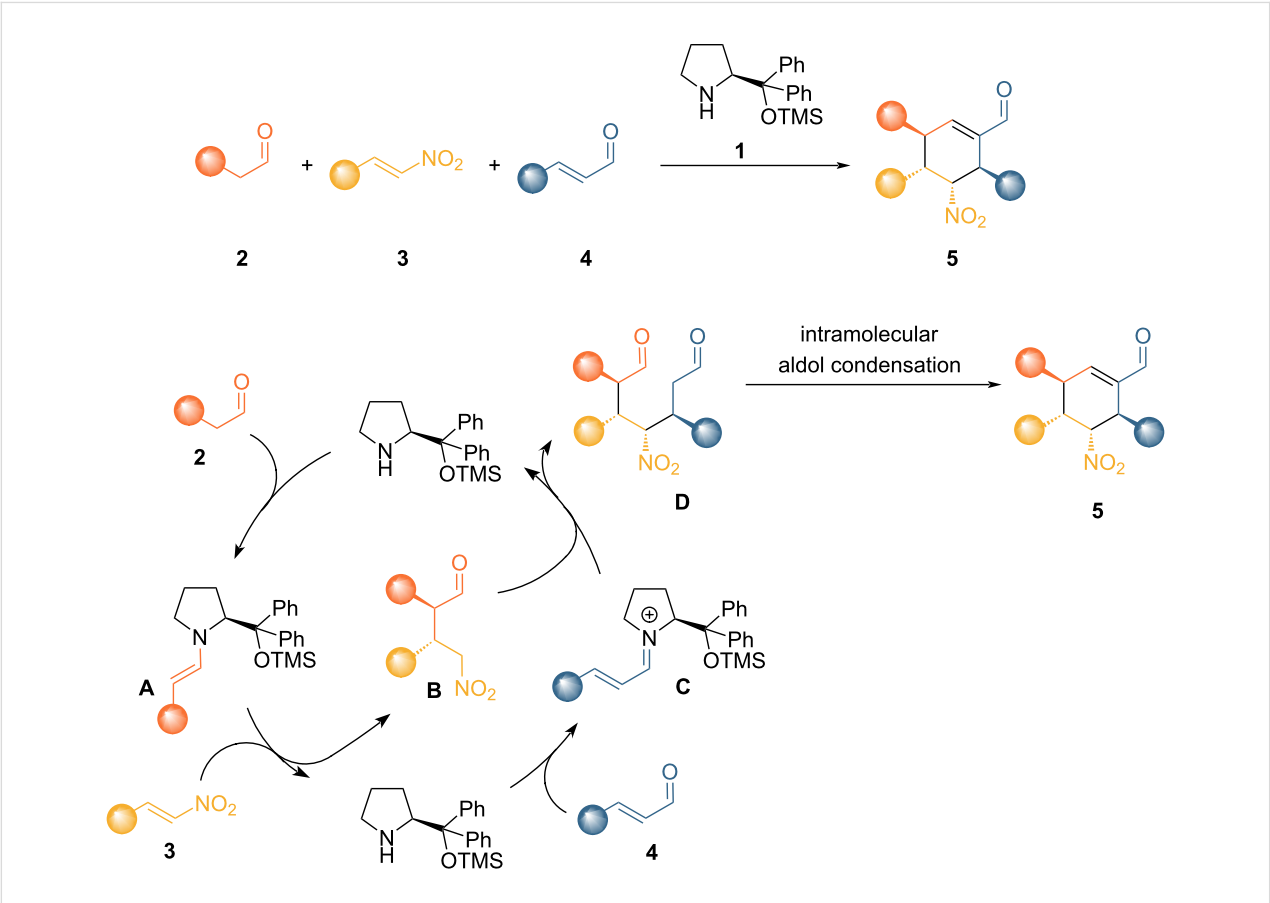

Scheme 1: Original triple organocatalytic cascade reaction developed by Enders.

experimental simplicity of the strategy offers the potential of rapidly increasing structural and stereochemical complexity starting from readily available substrates. The scope of the process was shown to be successful with aliphatic aldehydes **2**, aromatic nitroalkenes **3**, and both aromatic and aliphatic unsaturated aldehydes **4**.

Given our recent interest in the use of a surrogate of acetaldehyde [17-19] to address the challenges of working with free acetaldehyde, we wondered why the scope of this reaction did not include acetaldehyde and questioned whether a three-component triple cascade would indeed work employing this highly reactive substrate. The use of acetaldehyde as a reagent has always been challenging. The low boiling point and high volatility pose a problem with its handling and safety. The small steric hindrance gives rise to a high reactivity both as an electrophile and as a pro-nucleophile, hampering chemoselectivity (further to side reactions such as self-aldol condensations, polymerization and Tishchenko-type processes) and stereoselectivity [20]; the activation of acetaldehyde via aminocatalysis, furthermore, suffers from a lack of proper steric hindrance for the enantio-discrimination process. However, some methodologies enabling the use of acetaldehyde have been reported [20-24].

The safety and handling problems associated with acetaldehyde can be solved by synthetic equivalents that can be generated in situ through different paths. Some examples are represented by vinyl acetate [25], silyl vinyl ethers [26], ethanol, pyruvic acid, (*E*)-3-chloroacrylic acid, 2,4,6-trimethyl-1,3,5-trioxane (paraldehyde) [24,27], and acetaldehyde dimethyl acetal (**6**) [17-19]. On the basis of a long-term project based on masked reagents, our group has previously demonstrated the feasibility of the addition of a masked acetaldehyde **6** to nitroalkene derivatives with low reagent excess and high enantioselectivity; this reaction represents the first step in the Enders triple cascade catalytic cycle.

The use of acetaldehyde in a two-component cascade reaction was previously reported by Enders [27]; however, the scope of this reaction is limited to cyclohexene carbaldehydes bearing a methyl group on the C-6 atom (Figure 1a). On the other hand, these structural motifs can also be synthesized via the condensation of two equivalents of an enal and nitromethane (Figure 1b), although in this case C-4 and C-6 present the same substituent [28]. Interestingly, to the best of our knowledge, the use of acetaldehyde in the original Enders triple cascade reaction has not been explored despite its synthetic value. Indeed, this protocol would enable a wide structural variability in the synthesis of 3-substituted cyclohexene carbaldehydes (Figure 1c).

Results and Discussion

In order to explore the feasibility of the triple cascade reaction with acetaldehyde (**2a**) as a substrate, we tested the original reaction conditions reported by Enders using *trans*-β-nitrostyrene (**3**) and *trans*-cinnamaldehyde (**4**) as the other substrates (Table 1, entry 1). The reaction proved to yield the desired product, indicating that the catalytic system may indeed be applicable. Lowering the amount of organocatalyst **1** to 10 mol % (Table 1, entry 2) resulted in a decrease of both yield and selectivity.

Based on the results obtained (Table 1, entry 2) and the reaction conditions developed in our previous work [17], we tried to introduce **6** as an acetaldehyde equivalent, adding water in the reaction system and Amberlyst-15 as a catalyst to accelerate the hydrolysis process (Scheme 2).

To our delight, **6** as an acetaldehyde surrogate allows a slightly better yield with doubled selectivity, measured as the ratio be-

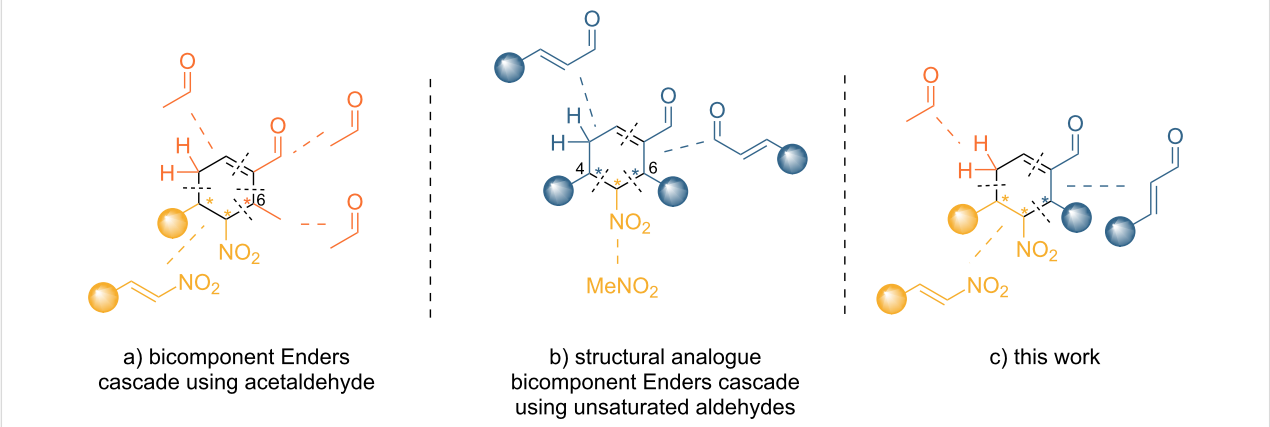

Figure 1: Approaches based on the original Enders cascade reaction to access trisubstituted cyclohexene carbaldehyde derivatives.

Table 1: Enders reaction with acetaldehyde.[a]

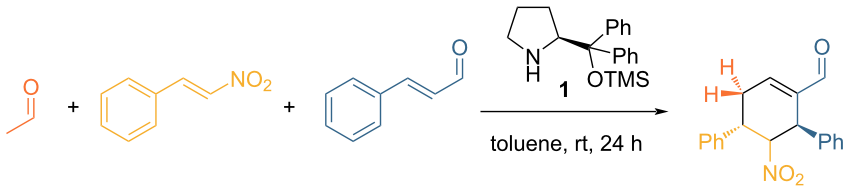

2a 3a 4a 5a':5a" dr ≈ 50:50

Entry	1 (mol %)	ee[b] (%)	Conversion[c] (%)	Yield[c] (%)	Selectivity[d] (%)
1	20	99	91	43	48
2	10	99	95	33	35

[a]Reaction conditions: **3** (0.5 mmol, 1 equiv), **2a** (0.6 mmol, 1.2 equiv), **4** (0.525 mmol, 1.05 equiv) were added to a solution of **1** (0.05 mmol, 0.1 equiv) in toluene (0.625 M wrt limiting reagent) and allowed to stir for 24 hours at room temperature. [b]Determined by chiral HPLC analysis. [c]Calculated by ^{1}H NMR using triphenylmethane as an internal standard. [d]Ratio between yield and conversion.

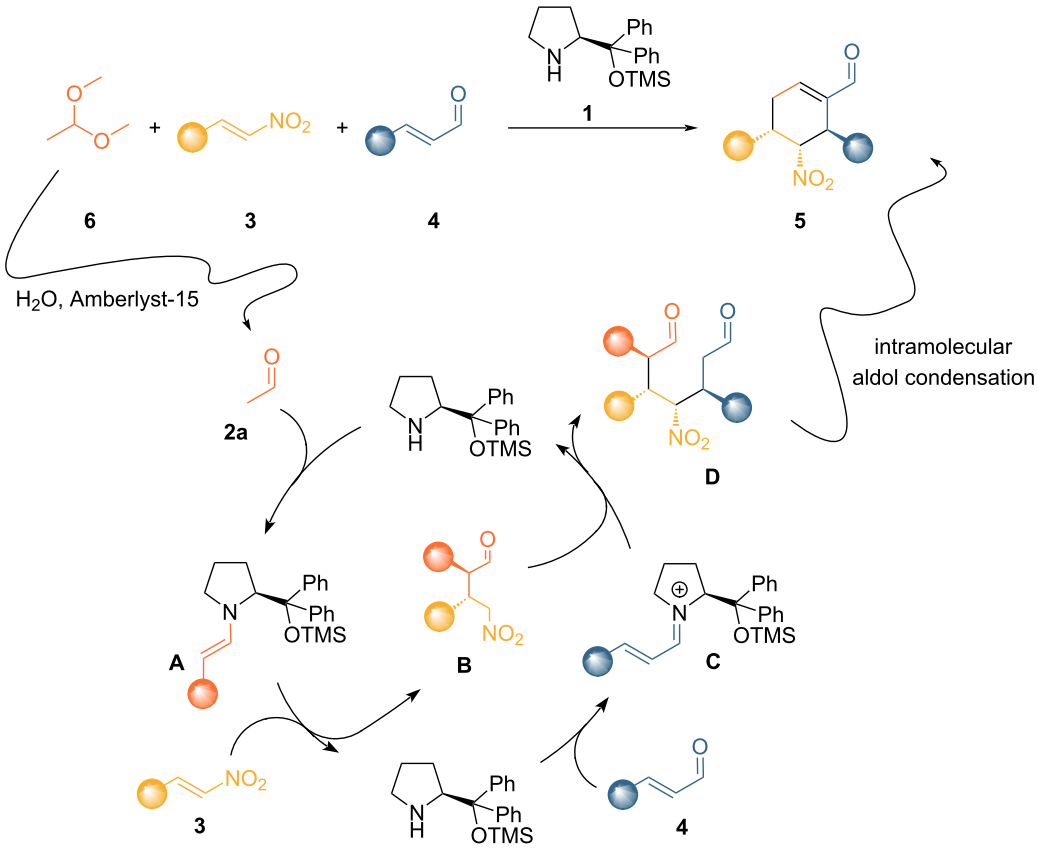

Scheme 2: Acetaldehyde dimethyl acetal (**6**) as an acetaldehyde surrogate to effect a triple organocatalytic cascade reaction.

tween yield and conversion (Table 2, entry 1). This means that the productivity of the reaction using **6** is superior, since far more substrate was converted into the desired product. A solvent screening (see Supporting Information File 1) did not reveal any better alternative to toluene. The use of chloroform (Table 2, entry 2), as in our previous report [17], showed an

Table 2: Selected optimization reaction conditions.[a]

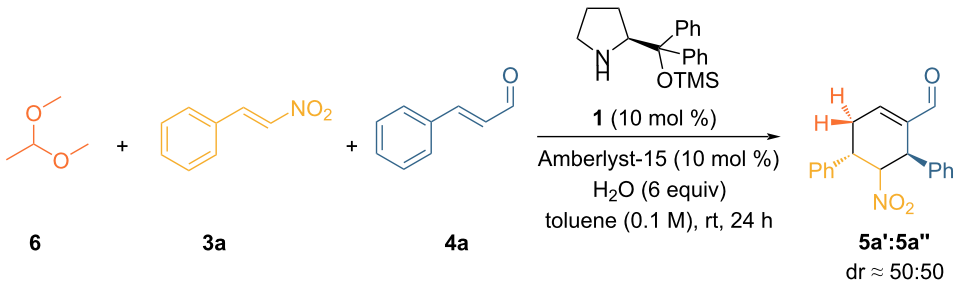

Entry	Deviation from above	ee[b] (%)	Conversion[c] (%)	Yield[c] (%)	Selectivity[d] (%)
1	none	99	61	40	66
2	$CHCl_3$	99	54	43	79
3	0.25 M	99	72	35	48
4	0.5 M	99	93	39	42
5	1 M	99	88	35	40
6	0.25 M, 48 h	99	79	44	56

[a]Reaction conditions: **3** (0.1 mmol, 1 equiv), **6** (0.2 mmol, 2 equiv), **4** (0.1 mmol, 1.05 equiv), H_2O (0.6 mmol, 6 equiv), and Amberlyst-15 (10 mol %) were added to a solution of **1** (10 mol %) in 1 mL of solvent (0.1 M) and allowed to stir for 24 hours at room temperature. [b]Determined by chiral HPLC analysis. [c]Calculated by ^{1}H NMR using triphenylmethane as an internal standard. [d]Ratio between yield and conversion.

improvement on selectivity, however, toluene was chosen as a more benign solvent. After further optimization of the acidic resin, stoichiometry, concentration, temperature, and reaction time (see Supporting Information File 1), we identified the best reaction conditions that yield the desired product in 44% yield, over 48 h (Table 2, entry 6). Unfortunately, side products and unwanted reactions do not allow to have a higher yield. All reactions provide the product in >99% ee, which is expected for a process which involves two consecutives stereoselective reactions. The control of the diastereomeric ratio is, however, difficult to attain as demonstrated by an extensive screening and is always near 50:50 without significant deviations changing the reaction conditions. On the contrary, the use of aldehydes other than acetaldehyde generates higher control [11]. It was previously shown that the first stereogenic center formed in the presented cascade process is formed with high control [17]. Therefore, the second carbon–carbon bond forming step, i.e., the organocatalyzed Michael addition of the nitronate to the α,β-unsaturated iminium ion, should be tackled to improve the diastereocontrol. All efforts to discriminate the two faces of the nitroenolate during the addition proved unproductive during the optimization, therefore, a potential epimerization was envisaged during the course of the reaction, but this hypothesis was discarded after further experimentation; submitting the two isolated diastereomers to the reaction conditions did not show any change. A slight improvement in the dr was found by exposing the mixture of the diastereomers to a strong basic environment (*t*-BuOK/MeOH) to force the formation of secondary nitronates. However, it could not be improved to synthetically interesting values. The observed diastereomeric ratio is, therefore, the direct result of the second Michael addition reaction, as previously reported [29], and no post-process epimerization event could be found.

With the best conditions in our hand, we evaluated the scope of our triple cascade reaction enabled by masked acetaldehyde. As highlighted in Figure 2, the reaction proceeded smoothly regardless of structural and electronic variations of both substrates, giving access to a variety of complex cyclohexenals. Although the scope is limited to aromatic nitroalkenes and enals, the yields are good considering the complexity of the domino process that involves highly reactive partners, and the ees are consistently very high. Finally, albeit there is low diastereocontrol, the diastereomers can be easily separated by simple flash chromatography.

Conclusion

An unprecedented methodology for the synthesis of 4,6-disubstituted 5-nitrocyclohexene carbaldehydes with three contiguous stereogenic centers using acetaldehyde as one of the reaction components of an Enders cascade reaction has been developed. The masked form of acetaldehyde, which is hydrolyzed in situ using Amberlyst-15 as an acid catalyst, instead of directly using acetaldehyde allows for higher yields and fewer byproducts. Using mild reaction conditions, it was possible to obtain a variety of functionalized cyclohexene carbaldehydes in

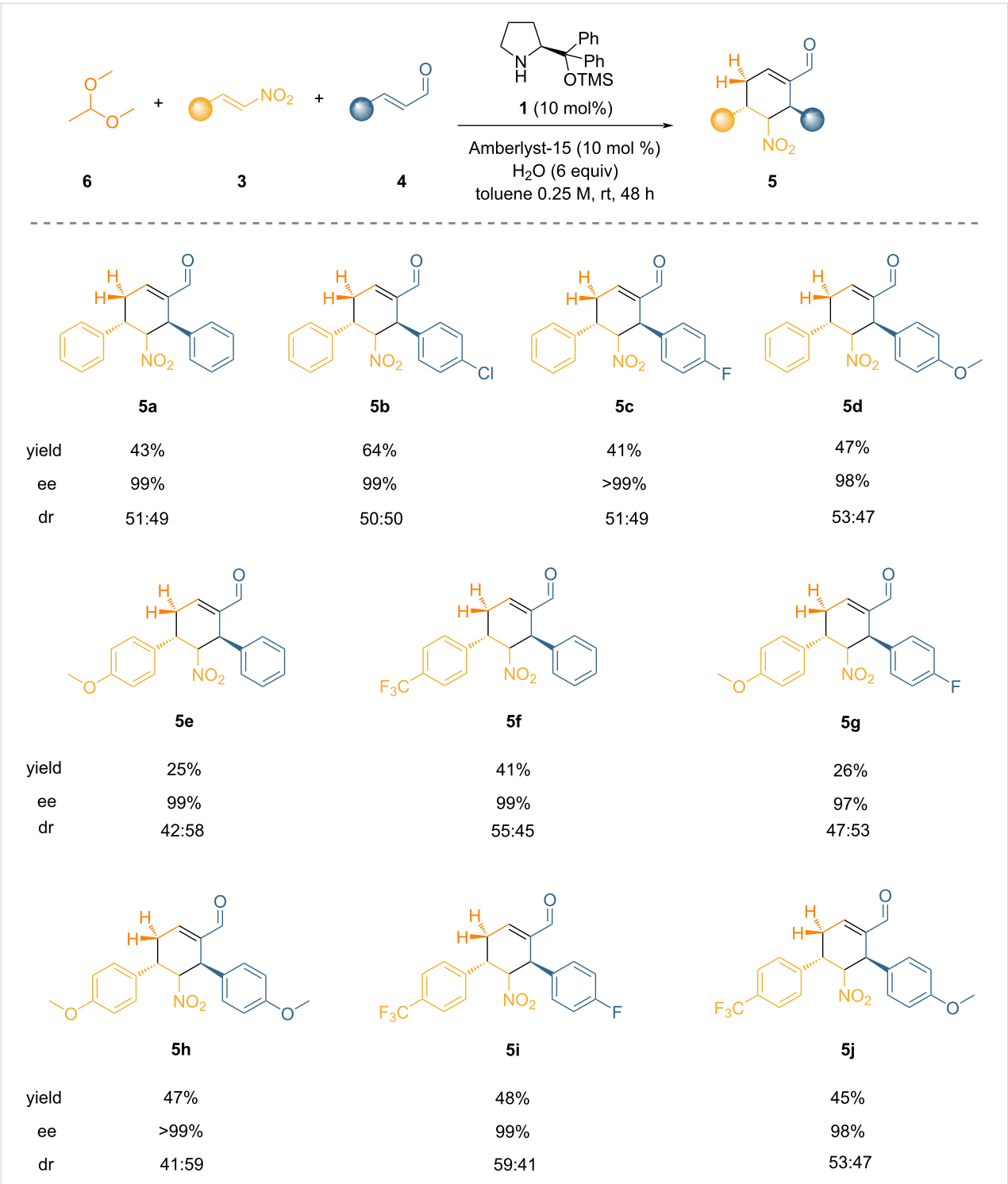

Figure 2: Scope of the cascade reaction using **6** as an acetaldehyde equivalent. Reaction conditions: **3** (0.5 mmol, 1 equiv), **6** (1 mmol, 2 equiv), **4** (0.525 mmol, 1.05 equiv), H_2O (3.0 mmol, 6 equiv), and Amberlyst-15 (10 mol %) were added to a solution of **1** (10 mol %) in 2 mL of solvent (0.25 M) and allowed to stir for 48 hours at room temperature. Yields of isolated compounds are given. Diastereomeric ratio (dr) determined by ^{1}H NMR analysis. Enatiomeric excess (ee) determined by chiral HPLC analysis.

good yields and very high enantiomeric excesses. Unfortunately, the developed methodology is currently limited to aromatic substrates and the formation of one stereocenter is difficult to control, leading to a mixture of two diastereomers. Current efforts in our laboratories are addressing these challenges.

Supporting Information

Supporting Information File 1

Experimental part, NMR and HPLC spectra.
[https://www.beilstein-journals.org/bjoc/content/supplementary/1860-5397-19-92-S1.pdf]

Funding

Fabio Pesciaioli thanks the Ministero dell'Università e della Ricerca (PON-AIM1842894, CUPE18D19000560001) for funding this research. Maria Edith Casacchia thanks the support of the Italian national inter-university Ph.D. course in Sustainable Development and Climate Change. Alessio Carioscia acknowledges Dipharma Francis for supporting his Ph.D. fellowship. Alessandro Brusa and Armando Carlone acknowledge funding by the European Union - NextGenerationEU under the Italian Ministry of University and Research (MUR) National Innovation Ecosystem grant ECS00000041 - VITALITY - CUP E13C22001060006. Giuliana Giorgianni thanks the Ministero dell'Università e della Ricerca (PON-DOT13OV2OC) for an industrial Ph.D. fellowship.

ORCID® iDs

Alessandro Brusa - https://orcid.org/0009-0003-7658-3169
Debora Iapadre - https://orcid.org/0009-0009-9129-9530
Maria Edith Casacchia - https://orcid.org/0000-0002-3435-2923
Alessio Carioscia - https://orcid.org/0000-0002-2091-1173
Giuliana Giorgianni - https://orcid.org/0000-0002-7180-9689
Giandomenico Magagnano - https://orcid.org/0000-0003-4893-4876
Fabio Pesciaioli - https://orcid.org/0000-0002-6792-6292
Armando Carlone - https://orcid.org/0000-0003-2983-6445

References

1. Bienaymé, H.; Hulme, C.; Oddon, G.; Schmitt, P. *Chem. – Eur. J.* **2000,** *6,* 3321–3329. doi:10.1002/1521-3765(20000915)6:18<3321::aid-chem3321>3.0.co;2-a
2. Ruijter, E.; Scheffelaar, R.; Orru, R. V. A. *Angew. Chem., Int. Ed.* **2011,** *50,* 6234–6246. doi:10.1002/anie.201006515
3. Younus, H. A.; Al-Rashida, M.; Hameed, A.; Uroos, M.; Salar, U.; Rana, S.; Khan, K. M. *Expert Opin. Ther. Pat.* **2021,** *31,* 267–289. doi:10.1080/13543776.2021.1858797
4. Wang, Y.; Lu, H.; Xu, P.-F. *Acc. Chem. Res.* **2015,** *48,* 1832–1844. doi:10.1021/acs.accounts.5b00217
5. Ramón, D. J.; Yus, M. *Angew. Chem., Int. Ed.* **2005,** *44,* 1602–1634. doi:10.1002/anie.200460548
6. Volla, C. M. R.; Atodiresei, I.; Rueping, M. *Chem. Rev.* **2014,** *114,* 2390–2431. doi:10.1021/cr400215u
7. Guillena, G.; Ramón, D. J.; Yus, M. *Tetrahedron: Asymmetry* **2007,** *18,* 693–700. doi:10.1016/j.tetasy.2007.03.002
8. Enders, D.; Grondal, C.; Hüttl, M. R. M. *Angew. Chem., Int. Ed.* **2007,** *46,* 1570–1581. doi:10.1002/anie.200603129
9. Grondal, C.; Jeanty, M.; Enders, D. *Nat. Chem.* **2010,** *2,* 167–178. doi:10.1038/nchem.539
10. Zhu, Q.-N.; Zhang, Y.-C.; Xu, M.-M.; Sun, X.-X.; Yang, X.; Shi, F. *J. Org. Chem.* **2016,** *81,* 7898–7907. doi:10.1021/acs.joc.6b01598
11. Enders, D.; Hüttl, M. R. M.; Grondal, C.; Raabe, G. *Nature* **2006,** *441,* 861–863. doi:10.1038/nature04820
12. Ishikawa, H.; Suzuki, T.; Orita, H.; Uchimaru, T.; Hayashi, Y. *Chem. – Eur. J.* **2010,** *16,* 12616–12626. doi:10.1002/chem.201001108
13. Carlone, A.; Cabrera, S.; Marigo, M.; Jørgensen, K. A. *Angew. Chem., Int. Ed.* **2007,** *46,* 1101–1104. doi:10.1002/anie.200604479
14. Tseliou, V.; Faraone, A.; Kqiku, L.; Vilím, J.; Simionato, G.; Melchiorre, P. *Angew. Chem., Int. Ed.* **2022,** *61,* e202212176. doi:10.1002/anie.202212176
15. Kumar, M.; Chauhan, P.; Bailey, S. J.; Jafari, E.; von Essen, C.; Rissanen, K.; Enders, D. *Org. Lett.* **2018,** *20,* 1232–1235. doi:10.1021/acs.orglett.8b00175
16. Barløse, C. L.; Faghtmann, J.; Bitsch, R. S.; Gbubele, J. D.; Jørgensen, K. A. *Org. Lett.* **2023,** *25,* 1209–1213. doi:10.1021/acs.orglett.3c00220
17. Giorgianni, G.; Nori, V.; Baschieri, A.; Palombi, L.; Carlone, A. *Catalysts* **2020,** *10,* 1296. doi:10.3390/catal10111296
18. Nori, V.; Sinibaldi, A.; Giorgianni, G.; Pesciaioli, F.; Di Donato, F.; Cocco, E.; Biancolillo, A.; Landa, A.; Carlone, A. *Chem. – Eur. J.* **2022,** *28,* e202104524. doi:10.1002/chem.202104524
19. Casacchia, M. E.; Giorgianni, G.; Allegritti, E.; Giansanti, L.; Carlone, A.; Pesciaioli, F. *SynOpen* **2023,** *07,* 29–32. doi:10.1055/a-1996-8940
20. Kumar, M.; Kumar, A.; Rizvi, M. A.; Shah, B. A. *RSC Adv.* **2015,** *5,* 55926–55937. doi:10.1039/c5ra05695k
21. García-García, P.; Ladépêche, A.; Halder, R.; List, B. *Angew. Chem., Int. Ed.* **2008,** *47,* 4719–4721. doi:10.1002/anie.200800847
22. Hayashi, Y.; Itoh, T.; Ohkubo, M.; Ishikawa, H. *Angew. Chem., Int. Ed.* **2008,** *47,* 4722–4724. doi:10.1002/anie.200801130
23. Hayashi, Y.; Itoh, T.; Aratake, S.; Ishikawa, H. *Angew. Chem., Int. Ed.* **2008,** *47,* 2082–2084. doi:10.1002/anie.200704870
24. Fan, X.; Rodríguez-Escrich, C.; Sayalero, S.; Pericàs, M. A. *Chem. – Eur. J.* **2013,** *19,* 10814–10817. doi:10.1002/chem.201302087
25. Zhang, W.; Wang, N.; Yang, Z.-J.; Li, Y.-R.; Yu, Y.; Pu, X.-M.; Yu, X.-Q. *Adv. Synth. Catal.* **2017,** *359,* 3397–3406. doi:10.1002/adsc.201700599
26. Boxer, M. B.; Yamamoto, H. *J. Am. Chem. Soc.* **2006,** *128,* 48–49. doi:10.1021/ja054725k
27. Enders, D.; Krüll, R.; Bettray, W. *Synthesis* **2010,** 567–572. doi:10.1055/s-0029-1217146
28. Enders, D.; Jeanty, M.; Bats, J. *Synlett* **2009,** 3175–3178. doi:10.1055/s-0029-1218282
29. Świderek, K.; Nödling, A. R.; Tsai, Y.-H.; Luk, L. Y. P.; Moliner, V. *J. Phys. Chem. A* **2018,** *122,* 451–459. doi:10.1021/acs.jpca.7b11803

BEILSTEIN JOURNAL OF ORGANIC CHEMISTRY

Consecutive four-component synthesis of trisubstituted 3-iodoindoles by an alkynylation–cyclization–iodination–alkylation sequence

Nadia Ledermann, Alae-Eddine Moubsit and Thomas J. J. Müller*

Full Research Paper

Open Access

Address:
Heinrich-Heine Universität Düsseldorf, Institut für Organische Chemie und Makromolekulare Chemie, Universitätsstraße 1, D-40225 Düsseldorf, Germany

Email:
Thomas J. J. Müller* - ThomasJJ.Mueller@uni-duesseldorf.de

* Corresponding author

Keywords:
alkynylation; catalysis; cyclization; indoles; iodination; multicomponent reactions

Beilstein J. Org. Chem. **2023,** *19,* 1379–1385.
https://doi.org/10.3762/bjoc.19.99

Received: 05 July 2023
Accepted: 04 September 2023
Published: 14 September 2023

This article is part of the thematic issue "Catalytic multi-step domino and one-pot reactions" and is dedicated to Prof. Dr. Willi Kantlehner on the occasion of his 80th birthday.

Guest Editor: S. Tsogoeva

Abstract

A library of 19 differently substituted 3-iodoindoles is generated by a consecutive four-component reaction starting from *ortho*-haloanilines, terminal alkynes, *N*-iodosuccinimide, and alkyl halides in yields of 11–69%. Initiated by a copper-free alkynylation, followed by a base-catalyzed cyclizive indole formation, electrophilic iodination, and finally electrophilic trapping of the intermediary indole anion with alkyl halides provides a concise one-pot synthesis of 3-iodoindoles. The latter are valuable substrates for Suzuki arylations, which are exemplified with the syntheses of four derivatives, some of them are blue emitters in solution and in the solid state, in good yield.

Introduction

Indoles and their derived substitution patterns are omnipresent heterocyclic structural motifs in nature [1], many natural products [2,3], drugs [4-8], and dyes [9-11] and their preparation is an evergreen in organic synthesis [12-15]. Although the classical Fischer indole synthesis provides a very reliable and broadly applicable access to indole derivatives [16-18], striving for new indole syntheses is ongoing. In particular, metal-catalyzed processes for accessing indoles have become attractive alternatives over the past decades [19-24]. Besides Larock's indole synthesis employing alkyne anellation [25] and Cacchi's cyclization of *ortho*-alkynylanilines [20,22] catalytic syntheses of indoles from alkynes have become increasingly interesting [26,27]. In addition, as one-pot processes with a huge exploratory potential and diversity-oriented character, syntheses of indoles by multicomponent reactions have aroused considerable interest [28-30].

As part of our program to develop heterocycle syntheses based upon transition-metal catalysis [31], we disclosed an activating group-free alkynylation–cyclization sequence to (aza)indoles

[32,33] that could be readily concatenated with a concluding N-alkylation of the 7-azaindole intermediate in the sense of consecutive three-component coupling–cyclization–alkylation synthesis of 1,2,5-trisubstituted 7-azaindoles [34]. Inspired by the coupling–cyclization–alkylation sequence and the stepwise Sonogashira coupling–cyclization–iodination protocol to give valuable 3-iodoindoles by Amjad and Knight [35], we reasoned that the interception by an electrophilic iodination step prior to terminal alkylation could provide a straightforward entry to trisubstituted 3-iodoindoles, which are valuable building blocks for accessing highly decorated (aza)indoles (Scheme 1). Here, we report the concise consecutive four-component synthesis of trisubstituted 3-iodoindoles.

Results and Discussion

In our previous studies on the alkynylation–cyclization synthesis of 2-substituted (aza)indoles [32-34], we could show that the copper-free Pd-catalyzed alkynylation of 2-aminobromopyridines or 2-bromoanilines and the subsequent base-catalyzed anellation in a one-pot fashion proceeds without nitrogen protection or activation using KO*t*-Bu in DMSO as a base. Under these conditions, the formation of the terminal (aza)indole anion is the driving force (Scheme 1) [34]. As a consequence, the electrophilic trapping of this intermediate with alkyl halides provides as concise access to N-substituted (aza)indoles. As already shown for *N*-alkyl 7-azaindole formation in one case, the crucial 7-azaindole anion could be trapped with electrophilic iodine (from *N*-iodosuccinimide), resulting in a 3-iodo-7-azaindole anion, which could then be alkylated, still in a one-pot fashion [34]. Therefore, we set out to directly employ these standard conditions to the sequence of *ortho*-haloanilines **1**, terminal alkynes **2**, *N*-iodosuccinimide (**3**), and alkyl halides **4** to screen the scope of the one-pot synthesis of trisubstituted 3-iodoindoles **5** in a consecutive four-component fashion (Scheme 2).

The sequence commences with a copper-free alkynylation using DBU as a base at 100 °C. This step is followed by the addition of KO*t*-Bu and reaction at 100 °C for 15 min and subsequent reaction with *N*-iodosuccinimide (**3**) at room temperature. Finally, the reaction with alkyl halides **4** at room temperature gives the title compounds **5** in yields between 11–69% after chromatographic workup. The structures of the products were unambiguously confirmed by ^{1}H and ^{13}C NMR spectroscopy, as well as by mass spectrometry. Assuming that four new bonds are being formed in this one-pot process, the range of yield from 11 to 69% (after isolation) accounts for an average yield of 55–90% per bond-forming step which can be considered to be relative efficient, also because only a single terminal purification step is required. However, noteworthy, the 3-iodoindoles are sensitive to light and prolonged storage at room temperature, even under protective gas atmosphere, leads to slow decomposition. Therefore, storage at low temperature in a dark vial is strongly recommended.

Upon using 2,4-dibromoaniline (**1c**) as the substrate and an excess of phenylacetylene (**2a**), both carbon–bromine bonds are transformed in the alkynylation step affording the alkynyl-substituted 3-iodoindole **6** as product in 42% isolated yield in the sense of a pseudo-five-component reaction (Scheme 3).

Finally, the 3-iodoindole **5a** and arylboronic acids **7** were employed in a standard Suzuki protocol with cesium carbonate

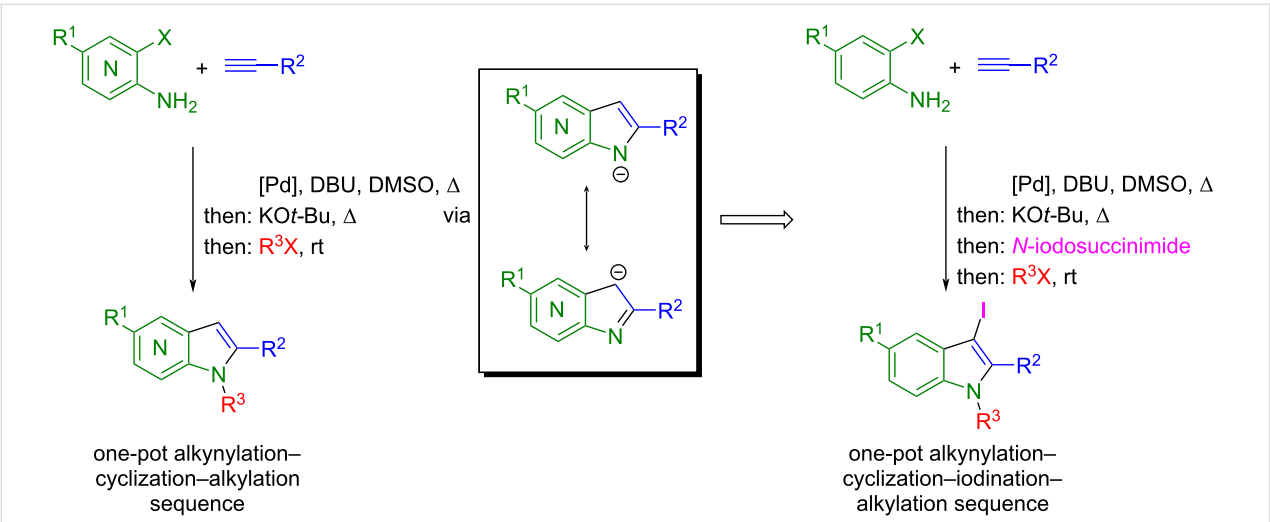

Scheme 1: Consecutive alkynylation–cyclization–alkylation three-component synthesis and conception of a consecutive alkynylation–cyclization–iodination–alkylation four-component synthesis via an (aza)indole anion intermediate.

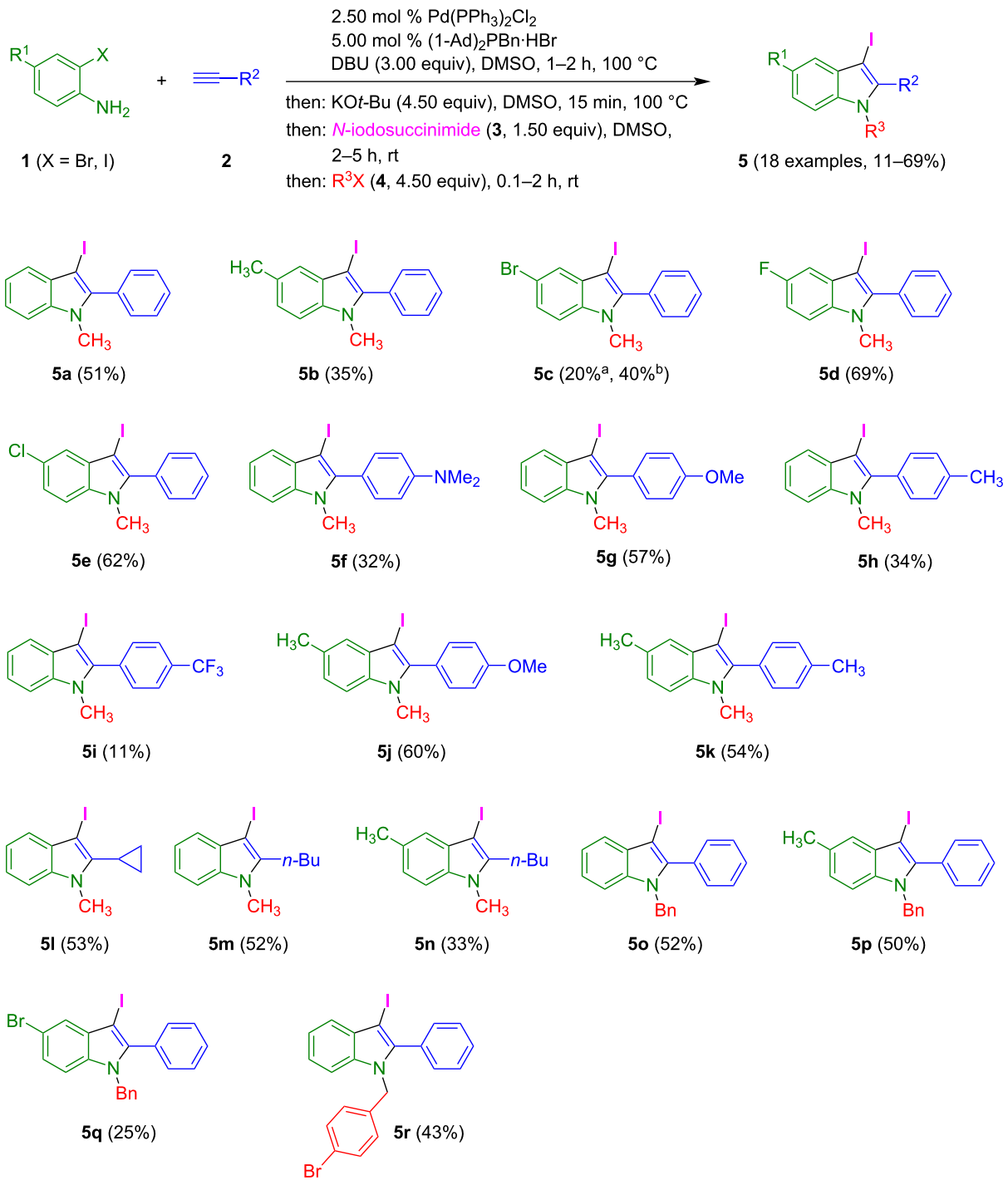

Scheme 2: Consecutive alkynylation–cyclization–iodination–alkylation four-component synthesis of trisubstituted 3-iodoindoles ([a]with 2,4-dibromoaniline (**1c**); [b]with 4-bromo-2-iodoaniline (**1d**)).

as a base to give rise to the formation of 1,2,3-trisubstitued indoles **8** in good yield (Scheme 4). The 1,2,3-trisubstitued indoles **8** were unambiguously confirmed by ^{1}H and ^{13}C NMR spectroscopy, as well as by mass spectrometry and elemental analysis.

Miura et al. could show that 1-alkyl-2,3-diarylindoles constitute a class of blue-emissive indole derivatives that are accessible in two steps from indole carboxylates [36]. Our two-step approach taking advantage of a de novo formation of 3-iodoindoles with variable substitution pattern in a consecutive four-

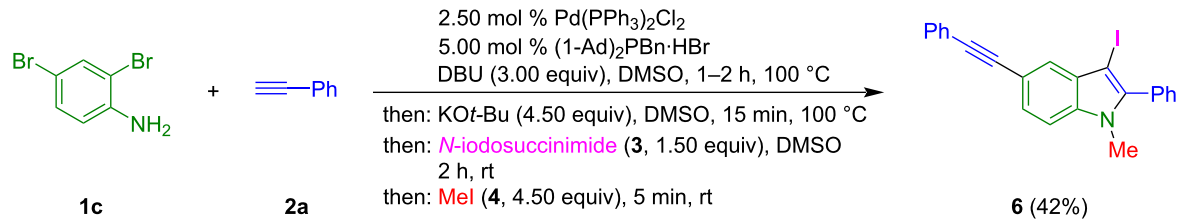

Scheme 3: Consecutive double alkynylation–cyclization–iodination–alkylation pseudo-five-component synthesis of 5-phenylethynyl-1,2-disubstituted 3-iodoindole **6**.

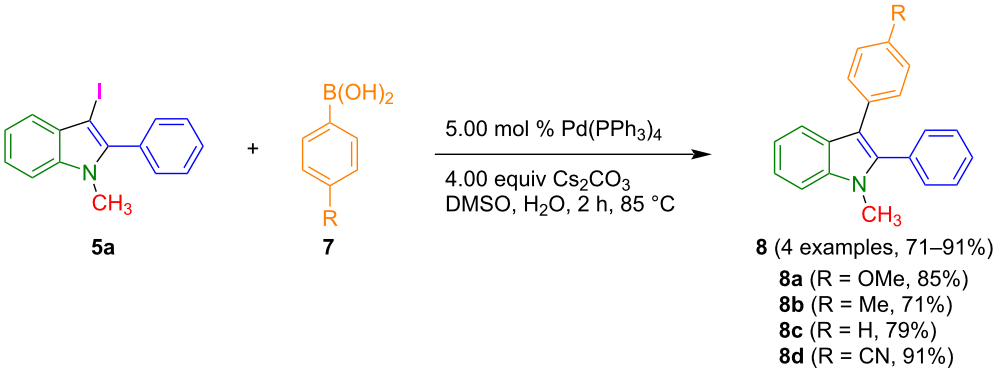

Scheme 4: Suzuki coupling of 3-iodoindole **5a** with arylboronic acids **7** to give 1,2,3-trisubstituted indoles **8**.

component process provides a concise access to the aforementioned class of emitters. For example the absorption maximum of indole derivative **8b** appears at 309 nm with an absorption coefficient ε = 10700 M^{-1} cm^{-1} and the emission maximum is found at 423 nm with a Stokes shift of 8700 cm^{-1} (Figure 1A). Moreover, compound **8b** emits intensively blue in both the solid state and solution (Figure 1B).

Conclusion

In summary the indole anion intermediate resulting from a one-pot alkynylation–cyclization sequence, which has been previously shown to be efficiently trapped by carbon electrophiles to give N-substituted indoles in a consecutive three-component synthesis, can be selectively iodinated in the 3-position with *N*-iodosuccinimide prior to N-alkylation to give substituted

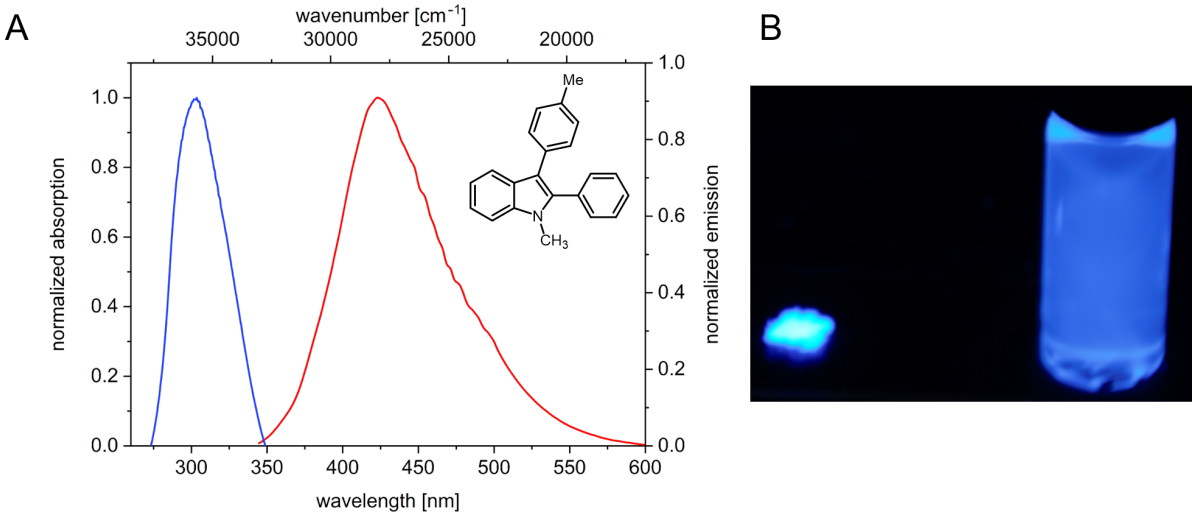

Figure 1: A: Absorption and emission spectra of 1-methyl-2-phenyl-3-(*p*-tolyl)-1*H*-indole (**8b**), recorded in dichloromethane, *T* = 298 K, λ_{exc} = 290 nm. B: Emission of compound **8b** in the solid state (right) and in solution (left) (UV lamp, λ_{exc} = 365 nm.

3-iodoindoles in a concise consecutive four-component fashion in modest to good yields. These target compounds are versatile building blocks for instance for a Suzuki coupling to give 1-alkyl-2,3-diarylindoles that can be of particular interest as indole-based blue emitters in solution and in the solid state. The expansion of this practical concise synthesis of indoles and azaindoles and their exploration as biologically active apoptosis inducers [37] and as functional blue emitters is currently underway.

Experimental

Consecutive four-component synthesis of 1,2-disubstituted 3-iodoindole **5d** (typical procedure)

$PdCl_2(PPh_3)_2$ (17.4 mg, 25.0 µmol) and $(1\text{-Ad})_2$PBn·HBr (23.6 mg, 50 µmol) were placed in an oven-dried Schlenk tube with magnetic stirring bar under nitrogen. Then, 2-iodo-4-fluoroaniline (**1e**, 237 mg, 1.00 mmol), phenylacetylene (**2a**, 122 mg, 1.20 mmol), DBU (457 mg, 3.00 mmol), and DMSO (1.50 mL) were added under nitrogen. The reaction mixture was heated at 100 °C (oil bath) for 2 h. After cooling to room temperature, potassium *tert*-butoxide (505 mg, 4.50 mmol) and DMSO (1.50 mL) were added to the reaction mixture and heated to 100 °C (oil bath) for 15 min. After cooling to room temperature, *N*-iodosuccinimide (**3**, 338 mg, 1.50 mmol) and DMSO (1.00 mL) were added and the mixture stirred at room temperature for a further 2 to 5 h (monitored by TLC). Then, methyl iodide (**4a**, 639 mg, 4.50 mmol) was added and the reaction mixture was stirred at room temperature for 0.1 to 2 h (monitored by TLC). Deionized water (20 mL) was added to the reaction mixture and the aqueous phase was extracted with dichloromethane (3 × 20 mL). The combined organic phases were dried (anhydrous sodium sulfate), filtered, and the solvent was then removed under vacuo. The residue was purified by chromatography on silica gel (*n*-hexane/ethyl acetate 100:1 to 5:1) to give pure compound **5d** (243 mg, 69%) as a beige solid. Mp 118.2 °C; R_f 0.50 (*n*-hexane/ethyl acetate 10:1); ^{1}H NMR (600 MHz, $CDCl_3$) δ 3.68 (s, 3H), 7.02–7.07 (m, 1H), 7.17–7.20 (m, 1H), 7.23–7.26 (m, 1H), 7.46–7.54 (m, 5H); ^{13}C NMR (150 MHz, $CDCl_3$) δ 1.9 (C_{quat}), 32.4 (CH_3), 106.7 (CH), 110.8 (CH), 111.5 (CH), 128.6 (C_{quat}), 129.3, 130.9, 131.5 (C_{quat}), 134.5 (C_{quat}), 143.5 (C_{quat}), 160.0 (C_{quat}); IR (cm^{-1}) ṽ: 604 (w), 619 (w), 662 (w), 689 (s), 733 (m), 756 (s), 789 (m), 860 (w), 907 (w), 934 (w), 957 (w), 997 (w), 1028 (w), 1051 (w), 1074 (w), 1107 (w), 1132 (m), 1165 (w), 1206 (m), 1238 (w), 1261 (w), 1275 (w), 1292 (w), 1315 (w), 1352 (w), 1406 (w), 1445 (w), 1456 (m), 1472 (w), 1541 (w), 1585 (w), 1622 (w), 1865 (w), 2853 (w), 2924 (w), 2961 (w), 3032 (w), 3957 (w), 3103 (w); EIMS (70 eV) *m*/*z* (%): 351 ([M]$^+$, 2), 211 ($C_{14}H_{10}FN^+$, 100), 149 (19), 106 (12), 71 (10), 57 (22); HRMS (*m*/*z*): [M + H]$^+$ calcd for $C_{15}H_{12}FIN$, 351.9993; found, 351.9831.

Consecutive pseudo-five-component synthesis of 3-iodo-1-methyl-2-phenyl-5-(phenylethynyl)-1*H*-indole (**6**)

$PdCl_2(PPh_3)_2$ (17.4 mg, 25.0 µmol) and $(1\text{-Ad})_2$PBn·HBr (23.6 mg, 50 µmol) were placed in an oven-dried Schlenk tube with magnetic stirring bar under nitrogen. Then, 2,4-dibromoaniline (**1c**, 254 mg, 1.00 mmol), phenylacetylene (**2a**, 245 mg, 2.40 mmol), DBU (457 mg, 3.00 mmol), and 1.50 mL DMSO were added and flushed with nitrogen. The reaction mixture was heated at 100 °C until complete conversion of the starting material (via TLC control). Potassium *tert*-butoxide (505 mg, 4.50 mmol) and 1.50 mL DMSO were then added and the reaction mixture was stirred for an additional 15 min. After cooling the reaction mixture to room temperature, NIS (338 mg, 1.50 mmol) and 1.00 mL DMSO were added. After complete conversion (via TLC control), methyl iodide (639 mg, 4.50 mmol) was added and also stirred at room temperature for 5 min. Water was added to the mixture and the aqueous phase was extracted with dichloromethane. The combined organic phases were dried with anhydrous sodium sulfate, filtered, and the solvent was removed under reduced pressure. The residue was purified by chromatography on silica gel (*n*-hexane/ethyl acetate 20:1 to 5:1) to give compound **6** (184 mg, 42%) as a colorless solid. Mp 204.5 °C; R_f 0.35 (*n*-hexane/ethyl acetate 10:1); ^{1}H NMR (300 MHz, $CDCl_3$) δ 3.69 (s, 3H), 7.27–7.30 (m, 1H), 7.31–7.39 (m, 3H), 7.46–7.56 (m, 6H), 7.57–7.60 (m, 2H), 7.72–7.75 (m, 1H); ^{13}C NMR (75 MHz, $CDCl_3$) δ 32.3 (CH_3), 59.2 (C_{quat}), 87.9 (C_{quat}), 90.8 (C_{quat}), 110.1 (CH), 115.5 (C_{quat}), 123.9 (C_{quat}), 125.4 (CH), 126.6 (CH), 128.0 (CH), 128.5 (CH), 128.6 (CH), 129.1 (CH), 130.5 (C_{quat}), 131.0 (CH), 131.4 (C_{quat}), 131.7 (CH), 137.6 (C_{quat}), 142.9 (C_{quat}); IR (cm^{-1}) ṽ: 611 (m), 621 (w), 664 (w), 679 (m), 691 (s), 702 (s), 754 (s), 787 (m), 806 (s), 870 (w), 916 (w), 970 (w), 1022 (w), 1069 (w), 1103 (w), 1148 (w), 1179 (w), 1209 (w), 1229 (w), 1277 (w), 1298 (w), 1337 (w), 1364 (w), 1431 (w), 1441 (w), 1473 (w), 1493 (w), 1595 (w), 1873 (w), 1954 (w), 2029 (w), 2810 (w), 2847 (w), 2893 (w); EIMS (70 eV), *m*/*z* (%): 433 ([M], 100), 304 ([M − I], 38), 227 (11), 153 (29); Anal. calcd for $C_{23}H_{16}IN$: C, 63.76; H, 3.72; N, 3.23; found: C, 63.81; H, 3.74; N, 2.96.

Synthesis of 1,2,3-trisubstituted indole **8b** (typical procedure)

3-Iodoindole **5a** (167 mg, 0.50 mmol), (*p*-tolyl)boronic acid (**7b**, 204 mg, 1.50 mmol), $Pd(PPh_3)_4$ (28.9 mg, 25.0 µmol), and cesium carbonate (652 mg, 2.00 mmol) were placed in an oven-dried Schlenk tube with magnetic stirring bar under nitrogen. Under nitrogen DMSO (5.00 mL) and deionized water

(0.80 mL) were added and the reaction mixture was heated to 85 °C (oil bath) for 2 h. Then, deionized water (20 mL) was added to the reaction mixture and the aqueous phase was extracted with dichloromethane (3 × 20 mL). The combined organic phases were dried (anhydrous sodium sulfate), filtered, and the solvent was removed under vacuo. The residue was purified by chromatography on silica gel (*n*-hexane/ethyl acetate 20:1 to 5:1) to give compound **8b** (105 mg, 71%) as a colorless solid. Mp 150.8 °C (lit.: 157 °C [38]); R_f 0.58 (*n*-hexane/ethyl acetate 10:1); ^{1}H NMR (300 MHz, $CDCl_3$) δ 2.24 (s, 3H), 3.58 (s, 3H), 6.98–7.02 (m, 2H), 7.08–7.14 (m, 3H), 7.40–7.17 (m, 7H), 7.68–7.73 (m, 1H); ^{13}C NMR (75 MHz, $CDCl_3$) δ 21.3 (CH_3), 31.1 (CH_3), 109.7 (CH), 115.1 (C_{quat}), 119.8 (CH), 120.2 (CH), 122.2 (CH), 127.2 (C_{quat}), 128.1 (CH), 128.5 (CH), 129.1 (CH), 129.8 (CH), 131.3 (CH), 132.2 (C_{quat}), 132.2 (C_{quat}), 135.1 (C_{quat}), 137.4 (C_{quat}), 137.6 (C_{quat}); IR (cm^{-1}) ṽ: 698 (s), 721 (m), 741 (s), 783 (w), 810 (m), 918 (w), 939 (m), 1005 (w), 1020 (m), 1037 (w), 1072 (w), 1088 (m), 1117 (w), 1138 (w), 1227 (w), 1261 (w), 1306 (w), 1329 (m), 1368 (m), 1391 (w), 1414 (w), 1431 (w), 1460 (m), 1499 (w), 1512 (w), 1545 (w), 1607 (w), 2855 (w), 2914 (w), 2961 (w), 3013 (w), 3026 (w), 3053 (w); EIMS (70 eV), *m*/*z* (%): 297 ([M], 1), 208 ([$C_{15}H_{12}N$], 100), 180 (12), 165 (12); Anal. calcd for $C_{22}H_{19}N$: C, 88.85; H, 6.44; N, 4.71; found: C, 88.65; H, 6.29; N, 4.52.

Supporting Information

Supporting Information File 1

Experimental details of the synthesis and analytical data of compounds **5**, **6**, and **8**, ^{1}H and ^{13}C NMR spectra of compounds **5**, **6**, and **8**.
[https://www.beilstein-journals.org/bjoc/content/supplementary/1860-5397-19-99-S1.pdf]

Acknowledgements

The authors thank the CeMSA@HHU (Center for Molecular and Structural Analytics @ Heinrich Heine University) for recording mass-spectrometric and NMR spectroscopic data.

The reported results have been summarized in the M.Sc. thesis "Vierkomponenten-Synthese von substituierten 3-Iodindolen" by Dr. Nadia Ledermann, Heinrich Heine University Düsseldorf, 2018.

Funding

The authors cordially thank the Fonds der Chemischen Industrie and the Deutsche Forschungsgemeinschaft (Mu 1088/9-1) for financial support.

ORCID® iDs

Thomas J. J. Müller - https://orcid.org/0000-0001-9809-724X

References

1. Sundberg, R. J. *Indoles;* Academic Press: New York, NY, USA, 1996. doi:10.1016/b978-0-12-676945-6.x5019-4
2. Gul, W.; Hamann, M. T. *Life Sci.* **2005,** *78,* 442–453. doi:10.1016/j.lfs.2005.09.007
3. Sun, H.; Sun, K.; Sun, J. *Molecules* **2023,** *28,* 2204. doi:10.3390/molecules28052204
4. Sravanthi, T. V.; Manju, S. L. *Eur. J. Pharm. Sci.* **2016,** *91,* 1–10. doi:10.1016/j.ejps.2016.05.025
5. Kaushik, N. K.; Kaushik, N.; Attri, P.; Kumar, N.; Kim, C. H.; Verma, A. K.; Choi, E. H. *Molecules* **2013,** *18,* 6620–6662. doi:10.3390/molecules18066620
6. Zhang, M.-Z.; Chen, Q.; Yang, G.-F. *Eur. J. Med. Chem.* **2015,** *89,* 421–441. doi:10.1016/j.ejmech.2014.10.065
7. Dadashpour, S.; Emami, S. *Eur. J. Med. Chem.* **2018,** *150,* 9–29. doi:10.1016/j.ejmech.2018.02.065
8. Thanikachalam, P. V.; Maurya, R. K.; Garg, V.; Monga, V. *Eur. J. Med. Chem.* **2019,** *180,* 562–612. doi:10.1016/j.ejmech.2019.07.019
9. Meredith, P.; Riesz, J. *Photochem. Photobiol.* **2004,** *79,* 211–216. doi:10.1111/j.1751-1097.2004.tb00012.x
10. Li, Q.; Li, Z.; Zeng, F.; Gong, W.; Li, Z.; Zhu, Z.; Zeng, Q.; Yu, S.; Ye, C.; Qin, J. *J. Phys. Chem. B* **2007,** *111,* 508–514. doi:10.1021/jp066489l
11. Nitha, P. R.; Soman, S.; John, J. *Mater. Adv.* **2021,** *2,* 6136–6168. doi:10.1039/d1ma00499a
12. Gribble, G. W. *J. Chem. Soc., Perkin Trans. 1* **2000,** 1045–1075. doi:10.1039/a909834h
13. Humphrey, G. R.; Kuethe, J. T. *Chem. Rev.* **2006,** *106,* 2875–2911. doi:10.1021/cr0505270
14. Taber, D. F.; Tirunahari, P. K. *Tetrahedron* **2011,** *67,* 7195–7210. doi:10.1016/j.tet.2011.06.040
15. Bugaenko, D. I.; Karchava, A. V.; Yurovskaya, M. A. *Russ. Chem. Rev.* **2019,** *88,* 99–159. doi:10.1070/rcr4844
16. Robinson, B. *Chem. Rev.* **1963,** *63,* 373–401. doi:10.1021/cr60224a003
17. Robinson, B. *Chem. Rev.* **1969,** *69,* 227–250. doi:10.1021/cr60258a004
18. Hughes, D. L. *Org. Prep. Proced. Int.* **1993,** *25,* 607–632. doi:10.1080/00304949309356257
19. Hegedus, L. S. *Angew. Chem., Int. Ed. Engl.* **1988,** *27,* 1113–1126. doi:10.1002/anie.198811133
20. Cacchi, S.; Fabrizi, G. *Chem. Rev.* **2005,** *105,* 2873–2920. doi:10.1021/cr040639b
21. Cacchi, S.; Fabrizi, G. *Chem. Rev.* **2011,** *111,* PR215–PR283. doi:10.1021/cr100403z
22. Joucla, L.; Djakovitch, L. *Adv. Synth. Catal.* **2009,** *351,* 673–714. doi:10.1002/adsc.200900059
23. Youn, S. W.; Ko, T. Y. *Asian J. Org. Chem.* **2018,** *7,* 1467–1487. doi:10.1002/ajoc.201800290
24. Mancuso, R.; Dalpozzo, R. *Catalysts* **2018,** *8,* 458. doi:10.3390/catal8100458
25. Herraiz-Cobo, J.; Albericio, F.; Álvarez, M. *Adv. Heterocycl. Chem.* **2015,** *116,* 1–35. doi:10.1016/bs.aihch.2015.04.003
26. Krüger (née Alex), K.; Tillack, A.; Beller, M. *Adv. Synth. Catal.* **2008,** *350,* 2153–2167. doi:10.1002/adsc.200800409

27. Neto, J. S. S.; Zeni, G. *Org. Chem. Front.* **2020,** *7,* 155–210. doi:10.1039/c9qo01315f
28. Shiri, M. *Chem. Rev.* **2012,** *112,* 3508–3549. doi:10.1021/cr2003954
29. Mohammadi Ziarani, G.; Moradi, R.; Ahmadi, T.; Lashgari, N. *RSC Adv.* **2018,** *8,* 12069–12103. doi:10.1039/c7ra13321a
30. Hossein Nia, R.; Taati, Z.; Mamaghani, M. *Polycyclic Aromat. Compd.* **2023,** in press. doi:10.1080/10406638.2023.2173622
31. D'Souza, D. M.; Müller, T. J. J. *Chem. Soc. Rev.* **2007,** *36,* 1095–1108. doi:10.1039/b608235c
32. Lessing, T.; Sterzenbach, F.; Müller, T. J. J. *Synlett* **2015,** *26,* 1217–1221. doi:10.1055/s-0034-1379907
33. Lessing, T.; Müller, T. J. J. *Chem. Heterocycl. Compd. (N. Y., NY, U. S.)* **2018,** *54,* 334–338. doi:10.1007/s10593-018-2269-z
34. Lessing, T.; Müller, T. J. J. *Synlett* **2017,** *28,* 1743–1747. doi:10.1055/s-0036-1590837
35. Amjad, M.; Knight, D. W. *Tetrahedron Lett.* **2004,** *45,* 539–541. doi:10.1016/j.tetlet.2003.10.207
36. Miyasaka, M.; Fukushima, A.; Satoh, T.; Hirano, K.; Miura, M. *Chem. – Eur. J.* **2009,** *15,* 3674–3677. doi:10.1002/chem.200900098
37. Drießen, D.; Stuhldreier, F.; Frank, A.; Stark, H.; Wesselborg, S.; Stork, B.; Müller, T. J. J. *Bioorg. Med. Chem.* **2019,** *27,* 3463–3468. doi:10.1016/j.bmc.2019.06.029
38. Brown, F.; Mann, F. G. *J. Chem. Soc.* **1948,** 847–858. doi:10.1039/jr9480000847

License and Terms

BEILSTEIN JOURNAL OF ORGANIC CHEMISTRY

One-pot nucleophilic substitution–double click reactions of biazides leading to functionalized bis(1,2,3-triazole) derivatives

Hans-Ulrich Reissig*[1] and Fei Yu[1,2]

Full Research Paper

Open Access

Address:
[1]Institut für Chemie und Biochemie, Freie Universität Berlin, Takustrasse 3, D-14195 Berlin, Germany and [2]Asymchem Boston Corporation, 10 Gill Street, Woburn, Massachusetts, 01801, USA

Email:
Hans-Ulrich Reissig* - hreissig@chemie.fu-berlin.de

* Corresponding author

Keywords:
alkynes; azides; copper catalysis; nucleophilic substitution; 1,2-oxazines

Beilstein J. Org. Chem. **2023,** *19,* 1399–1407.
https://doi.org/10.3762/bjoc.19.101

Received: 18 July 2023
Accepted: 04 September 2023
Published: 18 September 2023

This article is part of the thematic issue "Catalytic multi-step domino and one-pot reactions".

Guest Editor: S. Tsogoeva

Abstract

The nucleophilic substitution of benzylic bromides with sodium azide was combined with a subsequent copper-catalyzed (3 + 2) cycloaddition with terminal alkynes. This one-pot process was developed with a simple model alkyne, but then applied to more complex alkynes bearing enantiopure 1,2-oxazinyl substituents. Hence, the precursor compounds 1,2-, 1,3- or 1,4-bis(bromomethyl)benzene furnished geometrically differing bis(1,2,3-triazole) derivatives. The use of tris[(1-benzyl-1*H*-1,2,3-triazol-4-yl)methyl]amine (TBTA) as ligand for the click step turned out to be very advantageous. The compounds with 1,2-oxazinyl end groups can potentially serve as precursors of divalent carbohydrate mimetics, but the reductive cleavage of the 1,2-oxazine rings to aminopyran moieties did not proceed cleanly with these compounds.

Introduction

The concept of click reactions [1,2], in particular, the discovery of the copper-catalyzed alkyne azide (3 + 2) cycloaddition (CuAAC) [3,4], has dramatically changed the approaches to many problems in chemistry, supramolecular chemistry, materials science, biological chemistry and related fields (selected reviews: [5-15]). Mechanistic aspects of the CuAAC have been studied in detail [16,17]. Whereas the traditional 1,3-dipolar cycloaddition (Huisgen reaction) [18-20] of azides and alkynes requires often – but not always – relatively harsh conditions and proceeds with moderate regioselectivity only [21], the copper-catalyzed version can generally be executed at room temperature and it affords exclusively 1,4-disubstituted 1,2,3-triazole derivatives, thus allowing a controlled and highly efficient connection of a variety of molecular building blocks. This “Lego-approach” found countless applications and the bestowal of the Nobel Prize in 2022 to M. Meldal, K. B. Sharpless and C. R. Bertozzi did not come as a surprise.

In most cases the (3 + 2) cycloadditions were performed with isolated (and purified) organic azides, but it was early found that one-pot processes generating the potentially hazardous azides [22] in situ are possible [23]. Later, examples were published showing that these methods are also compatible with the conditions of CuAAC. The earliest case was probably published by Fokin et al. [24,25], one of the inventors of the original copper-catalyzed (3 + 2) cycloaddition. Many examples of nucleophilic substitutions employing sodium azide and organic substrates with potential leaving groups have been reported. The resulting organic azides were trapped in situ by a suitable alkyne to give the 1,2,3-triazoles [26-36]. Fairly recent review articles summarize these results [37,38].

For several years, our group was interested in preparing multivalent carbohydrate mimetics [39-43] on the basis of efficient coupling reactions of aminopyran and aminooxepane derivatives with suitable linker elements. Hence, the aminopyran derivatives **A** could be converted into several multivalent compounds **B** by amine or amide bond formations [44-47]. The transformation of the corresponding azidopyrans and azidooxepanes **C** or **E** into multivalent 1,2,3-triazole derivatives **D** and **F** by Meldal–Sharpless cycloadditions with suitable alkynes proceeded generally in good yields and furnished another set of multivalent carbohydrate mimetics [48-50]. In the current report, we want to disclose our experience with an “inverted” approach to multivalent systems [51]: bicyclic 1,2-oxazine derivatives of type **G** [52,53], which can be regarded as internally protected aminopyrans [54], should be converted into divalent compounds via coupling of the terminal propynyl group with benzylic biazides. Since biazides are potentially explosive [22] it was very desirable to avoid their isolation and to generate these reactive species in situ from the corresponding benzylic halides. In this study we investigated the compatibility of the nucleophilic substitution of 1,2-, 1,3- or 1,4-bis(bromomethyl)benzene **H** with sodium azide and the copper-catalyzed alkyne–azide cycloadditions with compounds of type **G** to provide divalent compounds **I** (Scheme 1). These may serve as precursors of divalent carbohydrate mimetics with aminopyran end groups.

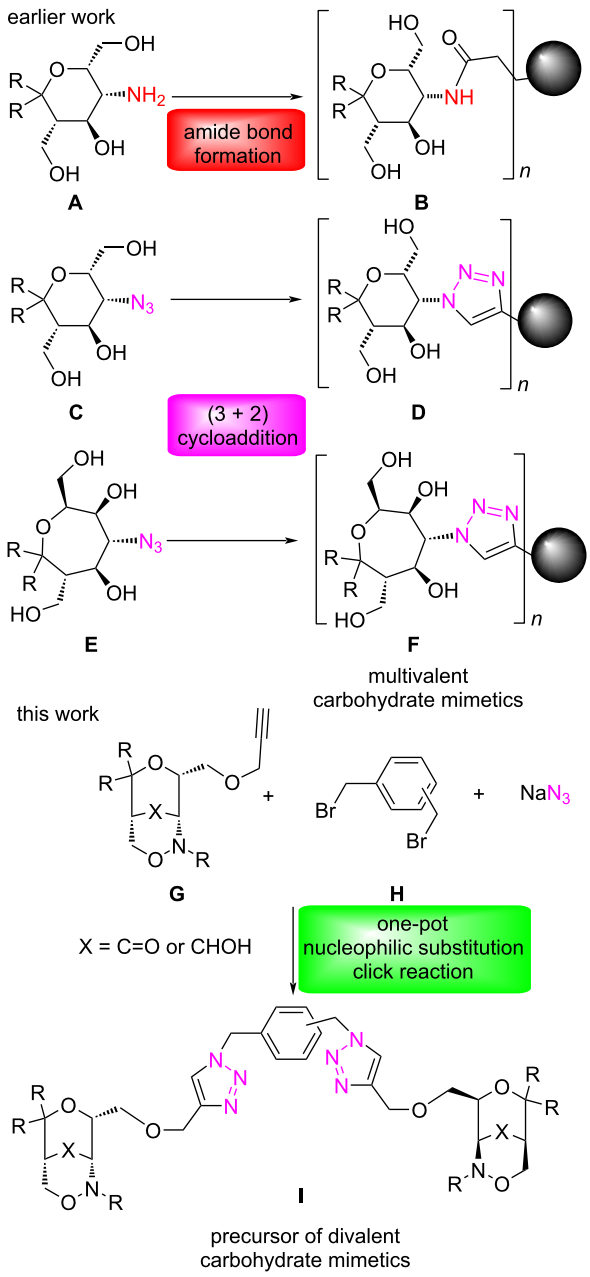

Scheme 1: Earlier approaches to multivalent carbohydrate mimetics **B**, **D** or **F** based on enantiopure aminopyran and aminooxepane derivatives and goal of this study employing alkyne component **G** and biazides in situ-generated from **H**.

Results and Discussion

We started our investigations by preparing the [2-(trimethylsilyl)ethoxy]methyl-substituted 1,2,3-triazole derivative **3** as simple model compound applying different conditions (Scheme 2). The highest yield for **3** was recorded when benzyl azide (**1**) and the simple alkyne **2** were combined in the presence of 0.2 equiv of copper(I) iodide in triethylamine as solvent (Scheme 2, reaction 1). After 16 hours at room temperature and chromatographic purification compound **3** was isolated in 79% yield as colorless liquid. Interestingly, under similar conditions, but employing two equivalents of copper(I) iodide in the presence of Hünig’s base [55] in acetonitrile at 40 °C provided 4,4'-bis(1,2,3-triazole) **4** in low yield (Scheme 2, reaction 2). Performing this reaction at room temperature gave a mixture of **3** and **4**. The formation of oxidative dimers in minor amounts has already been observed by Sharpless and co-workers in their original report on CuAAC reactions [4] and was systematically

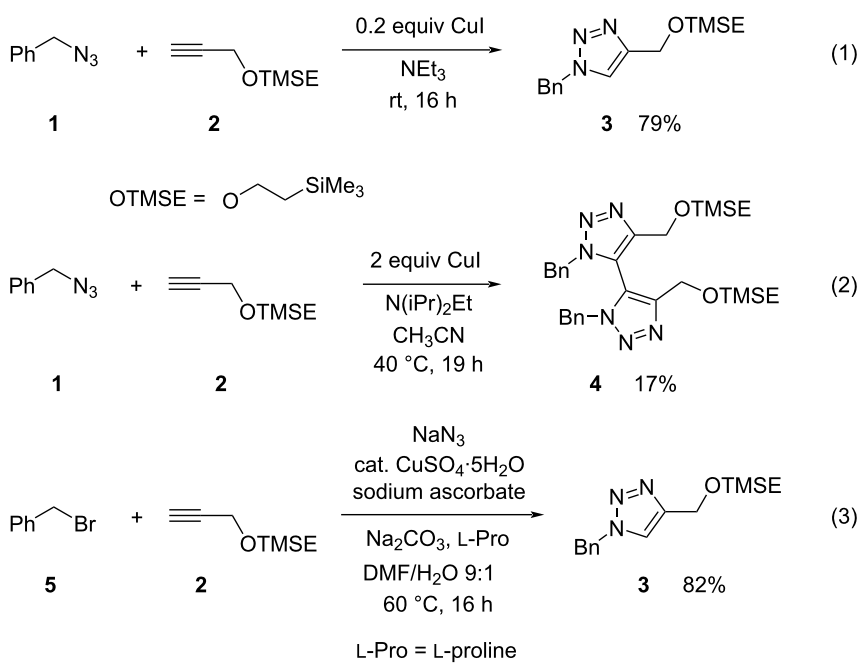

Scheme 2: Synthesis of model compound **3** under conventional conditions and as a one-pot process employing benzyl bromide (**5**), alkyne **2** and sodium azide as precursors for the click reaction.

investigated by Burgess et al. [56] who found that the base plays a crucial role during the formation of this type of bistriazoles. This dimerization was also discussed in a review article [57] dealing with the various types of bis(1,2,3-triazoles). Since we were not interested in compounds such as **4** we did not further investigate details in order to optimize this process. Instead, we looked at the one-pot nucleophilic substitution to generate benzyl azide **3** in situ from benzyl bromide (**5**) and sodium azide and to directly trap the intermediate with alkyne **2**. Under conditions summarized in reaction 3 of Scheme 2 we obtained the desired 1,2,3-triazole derivative **3** in 82% yield. Copper(II) sulfate pentahydrate (0.07 equivalents based on **2**) in the presence of sodium ascorbate as reducing agent and sodium carbonate as base as well as L-proline as ligand in a DMF/water mixture at 60 °C provided this promising result. These conditions applied are similar to those described by Fokin et al. [24], which had also been employed by other groups [37,38].

The conditions found were studied with a second model reaction in order to examine its suitability for the synthesis of potential carbohydrate mimetic precursors (Scheme 3). Sodium azide, benzyl bromide (**5**) and enantiopure bicyclic 1,2-oxazin-4-one derivative **6** [53] which bears a propargylic ether moiety as substituent undergo a one-pot reaction with reasonable efficiency and furnished the expected 1,2,3-triazole derivative **7** in 61% yield under the approved conditions.

Next, we turned our attention to the generation of divalent systems, starting with the reactions of 1,3- (**8**) and 1,2-bis(bromomethyl)benzene (**11**), respectively, in the presence of sodium azide and alkyne **2** (Scheme 4). The conditions employed above converted the *meta*-substituted dihalide into the expected symmetric bis(1,2,3-triazole) derivative **9** in very good yield, but we also isolated azide **10** in small quantities, where the intermediate biazide has undergone only one cycloaddition

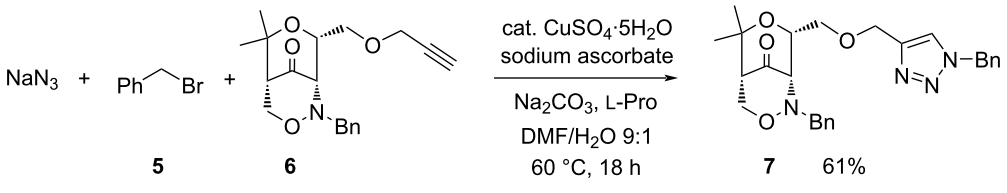

Scheme 3: One-pot reaction employing enantiopure alkynyl-substituted 1,2-oxazin-4-one derivative **6** leading to 1,2,3-triazole **7**.

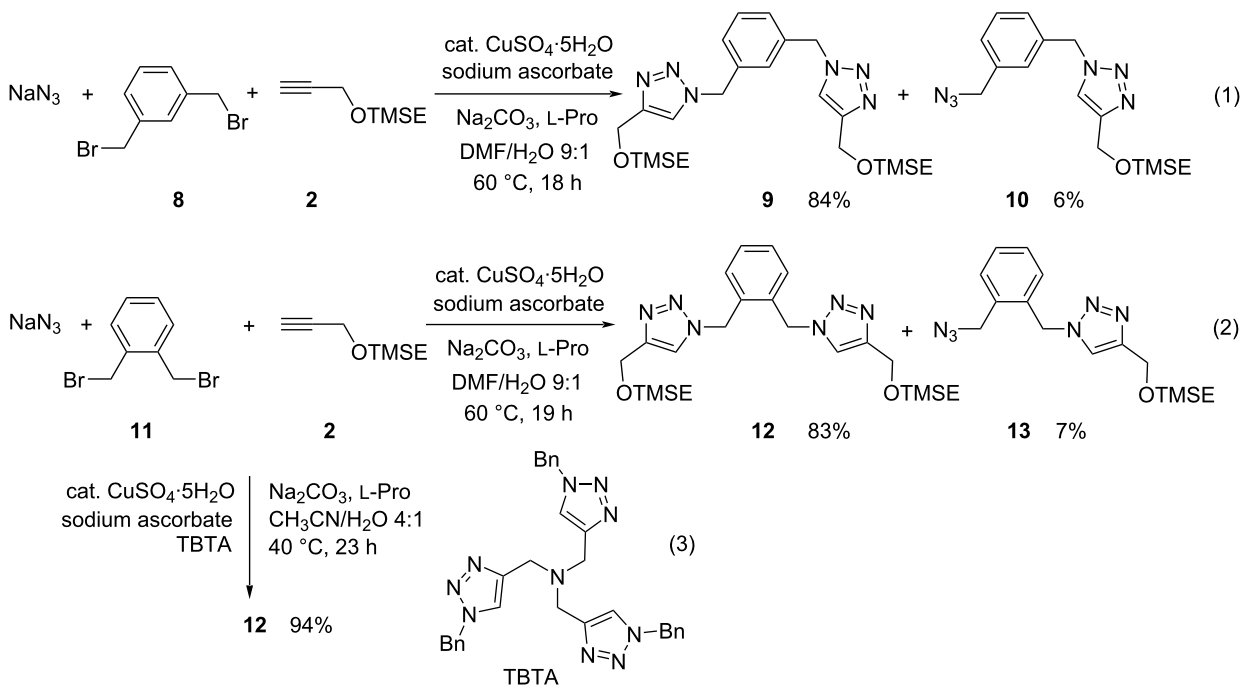

Scheme 4: One-pot reactions of dihalides **8** and **11** with sodium azide and alkyne **2** leading to symmetric divalent bis(1,2,3-triazoles) **9** and **12** as major products.

(Scheme 4, reaction 1). Under the same conditions the *ortho*-dihalide **11** delivered a very similar result, furnishing the expected product **12** in 83% yield. But again, the corresponding azide **13** was obtained in low yield (Scheme 4, reaction 2). In order to improve the process we examined the influence of the ligand tris[(1-benzyl-1*H*-1,2,3-triazol-4-yl)methyl]amine (TBTA) which has been identified by Sharpless et al. [58] as a very beneficial component in CuAAC reactions. After comprehensive optimization, we found that the addition of 0.2 equiv of this ligand not only allowed to lower the reaction temperature from 60 °C to 40 °C, but it also induced full consumption of the intermediate biazide derived from dihalide **11** (Scheme 4, reaction 3); 0.2 equiv of copper(II) sulfate pentahydrate, 0.4 equiv of sodium ascorbate and 0.4 equiv of L-proline in very little of acetonitrile/water as solvent furnished the exclusively isolated bis(1,2,3-triazole) derivative **12** in excellent 94% yield. These conditions of the one-pot nucleophilic substitution double-click reaction became the standard reaction conditions and were applied in most of the following experiments. When the reaction of **2** with **11** in the presence of sodium azide was performed under similar conditions, but without TBTA (not shown), 58% of **12** and 12% of **13** were isolated, clearly emphasizing the rate enhancing effect of this ligand on the (3 + 2) cycloaddition step.

With enantiopure alkynyl-substituted 1,2-oxazin-4-one derivative **6**, a potential aminopyran precursor, as alkyne component similar experience was gathered (Scheme 5). This sterically more demanding component reacted slower under the initially examined conditions and provided the desired bis(1,2,3-triazole) **14** and the mono-cycloadduct **15** in almost equal quantities (Scheme 5, reaction 1). Again, the addition of TBTA as ligand strongly improved the performance of the CuAAC reaction: the symmetric divalent compound **14** with two 1,2-oxazinyl end groups was isolated in very satisfying 87% yield (Scheme 5, reaction 2). When 1,4-bis(bromomethyl)benzene (**16**) was employed as starting material, these conditions afforded the *para*-substituted bis(1,2,3-triazole) **17** in very good yield although the azidomethyl-substituted compound **18** was also isolated in 6% yield in this case (Scheme 5, reaction 3).

Finally, the one-pot click reactions were examined with the alkynyl-substituted 1,2-oxazin-4-ol derivative **19** which is smoothly available from the corresponding ketone **6** by highly stereoselective reduction with sodium borohydride [53]. Starting from 1,3- (**8**) or 1,4-bis(bromomethyl)benzene (**16**), respectively, the approved conditions in the presence of TBTA led to the expected bis(1,2,3-triazoles) **20** or **21** in moderate or very good yield (Scheme 6). We cannot decide whether the lower yields in this series are caused by the unprotected hydroxy group of precursor **19** or the corresponding products. Although we did not isolate the conceivable mono-adducts we cannot rigorously exclude their formation.

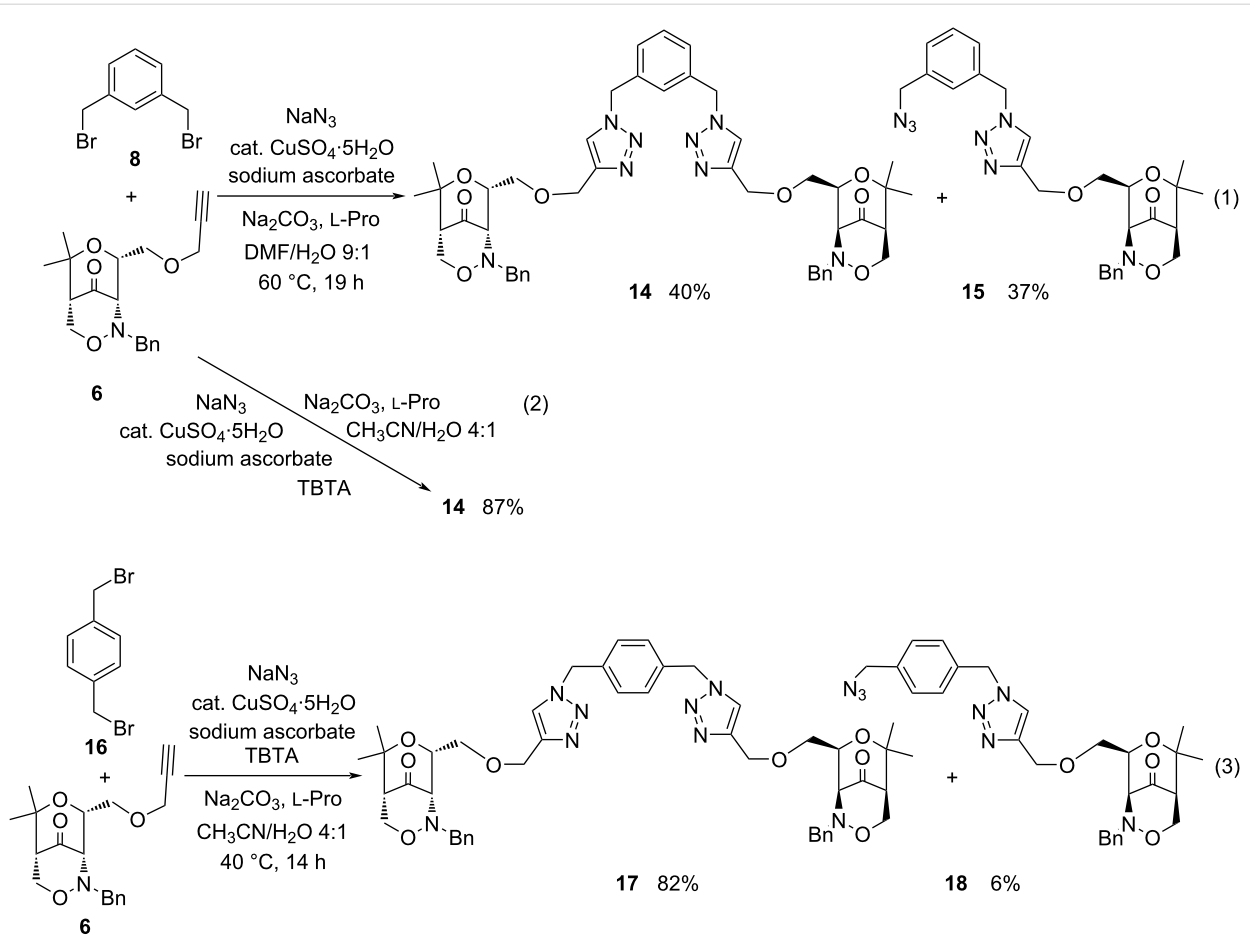

Scheme 5: One-pot reactions employing enantiopure alkynyl-substituted 1,2-oxazin-4-one derivative **6** leading to bis(1,2,3-triazoles) **14** and **17** as major products.

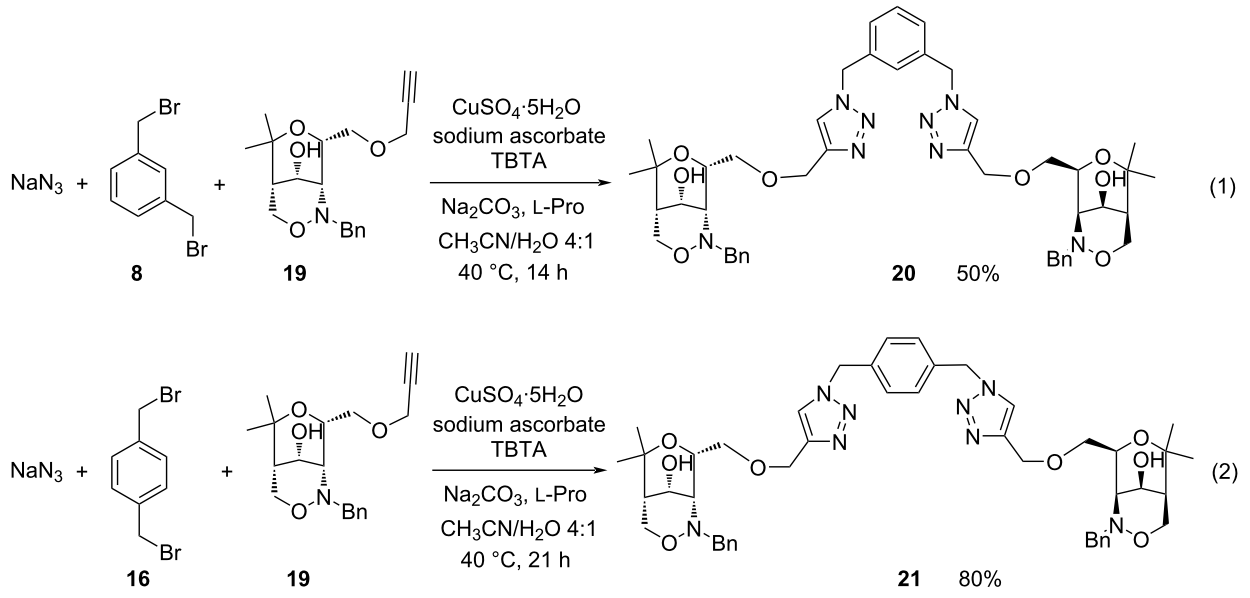

Scheme 6: One-pot reaction employing enantiopure alkynyl-substituted 1,2-oxazin-4-ol derivative **19** leading to bis(1,2,3-triazoles) **20** and **21**.

Compared to bis(1,2,3-triazoles) **14** and **17**, compounds **20** and **21** are one step closer to the desired divalent aminopyran-substituted carbohydrate mimetics, since they already contain a free hydroxy group instead of the carbonyl group. However, their reductive transformation into divalent carbohydrate mimetics turned out to be a difficult task. We started the experiments with the hydrogenolysis of bicyclic 1,2-oxazin-4-ol **19** as simple model compound (Scheme 7). A methanol solution of **19** under an atmosphere of hydrogen was stirred for 17 h in the presence of palladium on carbon and provided the expected (propyloxy)methyl-substituted aminopyran **22** in 81% yield (Scheme 7, reaction 1). The reductive removal of the *N*-benzyl group and the cleavage of the N–O bond occurred apparently without problems. With the second model compound, 1,2,3-triazole **23**, which is almost quantitatively available by sodium borohydride reduction of **7**, we encountered the first problems. Under similar conditions of the hydrogenolysis the expected product **24** could be isolated as major component and characterized (Scheme 7, reaction 2), but the obtained sample contained unknown byproducts. It is possible, that the *N*-benzyl group attached to the 1,2,3-triazole moiety is partially removed under these conditions and/or that even the C–O bond connecting the 1,2,3-triazole part with the aminopyran part is reductively cleaved since this bond also has benzylic character. In earlier investigations with other triazolyl-substituted aminopyran derivatives we encountered similar selectivity problems due to the sensitivity of benzylic bonds to the applied hydrogenolysis conditions [59].

Despite of the discouraging results with model compound **23** we nevertheless examined the reductive cleavage of bis(1,2,3-triazole) **21**. It turned out that the hydrogenolysis of this compound was very capricious and (in part) depended on the batch of palladium on carbon used. In most cases, incomplete consumption of starting material was observed, even after long reaction time. The best result is depicted in Scheme 8 (reaction 1), when after five days of hydrogenolysis and 0.8 equivalents of palladium at least 40% of impure divalent aminopyran derivative **25** was isolated. The major component of the isolated material is certainly fitting to the proposed structure according to the NMR data and their comparison with related compounds, but the sample again contains unknown impurities, which are probably due to additional bond cleavage events. Compound **25** contains four bonds of heteroatoms to carbon atoms which have benzylic character and are possibly attacked under the reaction conditions, in particular, considering the long reaction time and the fairly high amount of catalyst employed.

As an alternative method, which should be more chemoselective, we examined the reduction with samarium diiodide [60].

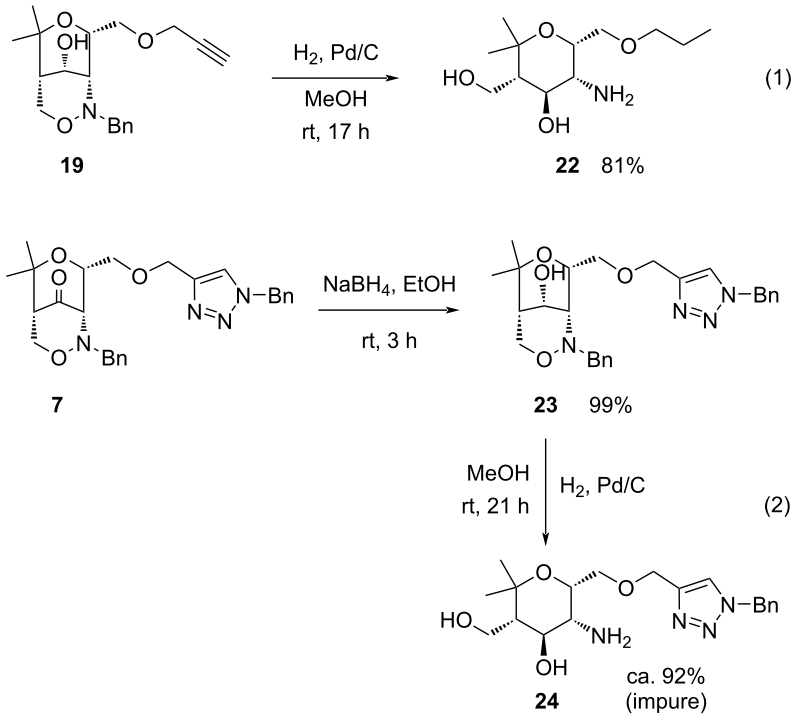

Scheme 7: Reductive ring-openings of 1,2-oxazine derivatives **19** and **23** as simple model compounds by hydrogenolysis in the presence of palladium on carbon leading to aminopyran derivatives **22** and **24**.

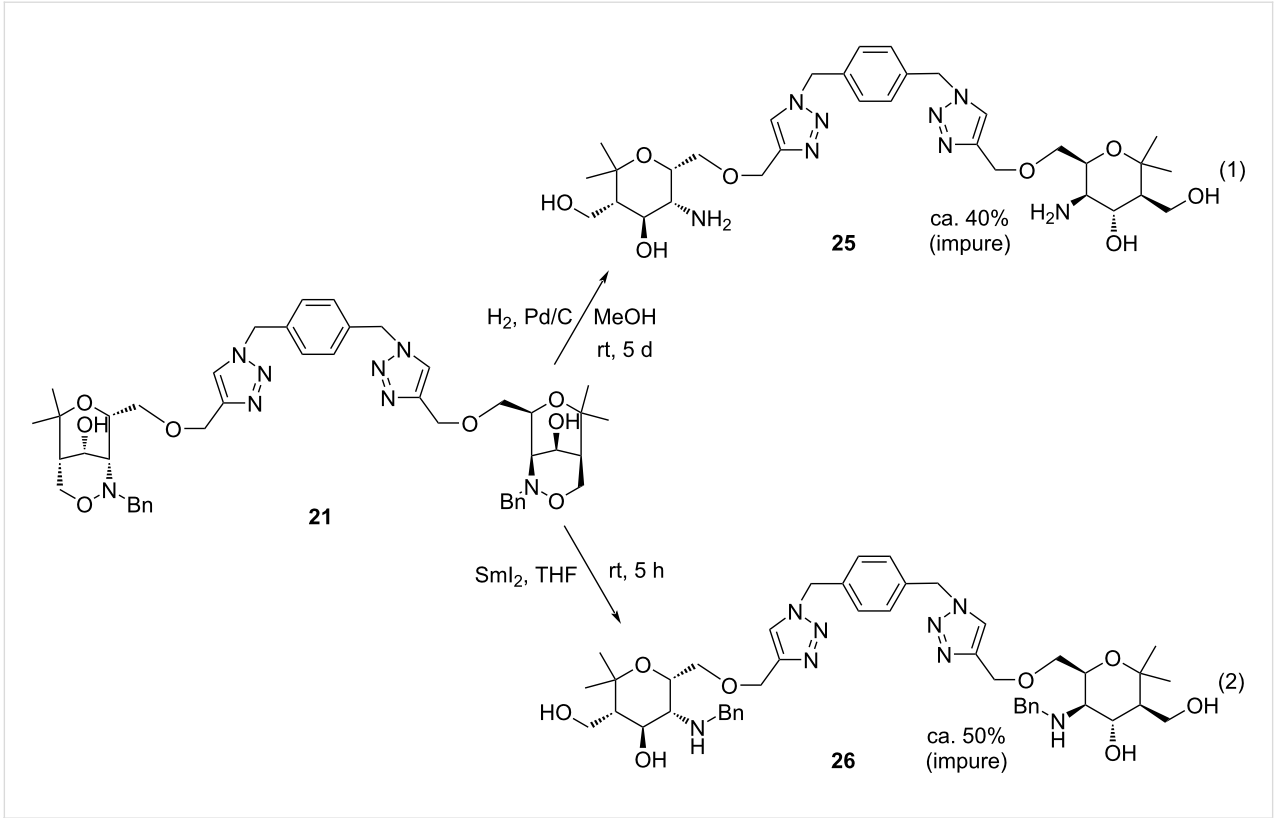

Scheme 8: Attempted reductive ring-openings of compound **21** by hydrogenolysis or by samarium diiodide leading to impure samples of divalent aminopyran derivatives **25** or **26**.

This versatile one-electron transfer reagent is known to cleave N–O bonds with high selectivity [61,62] and was applied several times by our group with good success for reductive ring-openings of 1,2-oxazine derivatives [63,64]. A slight excess of samarium diiodide in tetrahydrofuran completely consumed compound **21** within five hours. Compound **26** was isolated in 50% yield, but again the sample was not clean. The NMR data revealed that the *N*-benzyl groups were still intact, however, we cannot exclude that partial reductions had occurred at other positions of this relatively complex molecule. Thus, better conditions for the clean transformation of compounds such as **21** into carbohydrate mimetics have still to be developed. We abstained from the conversion of compounds **24**, **25** or **26** into their sulfated form due to the presence of the impurities in these samples. However, only the sulfated forms of this type of multivalent carbohydrate mimetics had earlier shown respectable biological activity as ligands of P- and L-selectins [44-50].

Conclusion

We found very good conditions for a one-pot nucleophilic substitution of benzylic bromides with sodium azide and direct subsequent CuAAC reactions with alkynes. The conditions were tested with the simple alkyne model compound **2**, but could be applied to more complex alkynes such as 1,2-oxazin-4-one derivative **6** or 1,2-oxazin-4-ol derivative **19**. With 1,2-, 1,3- or 1,4-bis(bromomethyl)benzene as precursors bis(1,2,3-triazole) derivatives were isolated in good to excellent yields. The use of TBTA as ligand for the click step turned out to be very advantageous. The reductive ring openings of bis(1,2,3-triazole) derivative **21** to divalent carbohydrate mimetics with hydrogen under palladium catalysis or with samarium diiodide did not proceed cleanly and need further optimization.

Supporting Information

Supporting Information File 1

Experimental procedures, spectroscopic and analytical characterization data of new compounds as well as copies of the NMR spectra.
[https://www.beilstein-journals.org/bjoc/content/supplementary/1860-5397-19-101-S1.pdf]

Acknowledgements

We thank Dr. Reinhold Zimmer for his valuable assistance during preparation of the manuscript.

Funding

We gratefully acknowledge support by the Alexander von Humboldt Foundation (research fellowship for Dr. Fei Yu). Funding by the Deutsche Forschungsgemeinschaft (SFB 765) is gratefully acknowledged.

ORCID® iDs

Hans-Ulrich Reissig - https://orcid.org/0000-0002-1912-9635

References

1. Kolb, H. C.; Finn, M. G.; Sharpless, K. B. *Angew. Chem., Int. Ed.* **2001,** *40,* 2004–2021. doi:10.1002/1521-3773(20010601)40:11<2004::aid-anie2004>3.0.co;2-5
2. Rutjes, F. P. J. T. *Click Chemistry;* Science of Synthesis; Thieme: Stuttgart, Germany, 2022. doi:10.1055/b000000077
3. Tornøe, C. W.; Christensen, C.; Meldal, M. *J. Org. Chem.* **2002,** *67,* 3057–3064. doi:10.1021/jo011148j
4. Rostovtsev, V. V.; Green, L. G.; Fokin, V. V.; Sharpless, K. B. *Angew. Chem., Int. Ed.* **2002,** *41,* 2596–2599. doi:10.1002/1521-3773(20020715)41:14<2596::aid-anie2596>3.0.co;2-4
5. Meldal, M.; Tornøe, C. W. *Chem. Rev.* **2008,** *108,* 2952–3015. doi:10.1021/cr0783479
6. Hänni, K. D.; Leigh, D. A. *Chem. Soc. Rev.* **2010,** *39,* 1240–1251. doi:10.1039/b901974j
7. Mamidyala, S. K.; Finn, M. G. *Chem. Soc. Rev.* **2010,** *39,* 1252–1261. doi:10.1039/b901969n
8. Pedersen, D. S.; Abell, A. *Eur. J. Org. Chem.* **2011,** 2399–2411. doi:10.1002/ejoc.201100157
9. Fokin, V. V.; Matyjaszewski, K. CuAAC: The Quintessential Click Reaction. In *Organic Chemistry – Breakthroughs and Highlights;* Ding, K.; Dai, L.-X., Eds.; Wiley-VCH: Weinheim, Germany, 2012; pp 247–277. doi:10.1002/9783527664801.ch7
10. Totobenazara, J.; Burke, A. J. *Tetrahedron Lett.* **2015,** *56,* 2853–2859. doi:10.1016/j.tetlet.2015.03.136
11. Singh, M. S.; Chowdhury, S.; Koley, S. *Tetrahedron* **2016,** *72,* 5257–5283. doi:10.1016/j.tet.2016.07.044
12. Kacprzak, K.; Skiera, I.; Piasecka, M.; Paryzek, Z. *Chem. Rev.* **2016,** *116,* 5689–5743. doi:10.1021/acs.chemrev.5b00302
13. Döhler, D.; Michael, P.; Binder, W. H. *Acc. Chem. Res.* **2017,** *50,* 2610–2620. doi:10.1021/acs.accounts.7b00371
14. Tiwari, V. K.; Mishra, B. B.; Mishra, K. B.; Mishra, N.; Singh, A. S.; Chen, X. *Chem. Rev.* **2016,** *116,* 3086–3240. doi:10.1021/acs.chemrev.5b00408
15. Santos, C. S.; de Oliveira, R. J.; de Oliveira, R. N.; Freitas, J. C. R. *ARKIVOC* **2020,** No. i, 219–271. doi:10.24820/ark.5550190.p011.293
16. Worrell, B. T.; Malik, J. A.; Fokin, V. V. *Science* **2013,** *340,* 457–460. doi:10.1126/science.1229506
17. Berg, R.; Straub, B. F. *Beilstein J. Org. Chem.* **2013,** *9,* 2715–2750. doi:10.3762/bjoc.9.308
18. Huisgen, R. *Angew. Chem., Int. Ed. Engl.* **1963,** *2,* 565–598. doi:10.1002/anie.196305651
19. Huisgen, R. *Angew. Chem., Int. Ed. Engl.* **1963,** *2,* 633–645. doi:10.1002/anie.196306331
20. Breugst, M.; Reissig, H.-U. *Angew. Chem., Int. Ed.* **2020,** *59,* 12293–12307. doi:10.1002/anie.202003115
21. Kirmse, W.; Horner, L. *Justus Liebigs Ann. Chem.* **1958,** *614,* 1–3. doi:10.1002/jlac.19586140102
22. Bräse, S.; Banert, K., Eds. *Organic Azides – Syntheses and Applications;* John Wiley & Sons: Chichester, UK, 2010. doi:10.1002/9780470682517
23. Maksikova, A. V.; Serebryakova, E. S.; Tikhonova, L. G.; Vereshchagin, L. I. *Chem. Heterocycl. Compd.* **1980,** *16,* 1284–1285. doi:10.1007/bf00501836
24. Feldman, A. K.; Colasson, B.; Fokin, V. V. *Org. Lett.* **2004,** *6,* 3897–3899. doi:10.1021/ol048859z
25. Appukkuttan, P.; Dehaen, W.; Fokin, V. V.; Van der Eycken, E. *Org. Lett.* **2004,** *6,* 4223–4225. doi:10.1021/ol048341v
26. Kacprzak, K. *Synlett* **2005,** 943–946. doi:10.1055/s-2005-864809
27. Wang, Z.-X.; Zhao, Z.-G. *J. Heterocycl. Chem.* **2007,** *44,* 89–92. doi:10.1002/jhet.5570440115
28. Odlo, K.; Høydahl, E. A.; Hansen, T. V. *Tetrahedron Lett.* **2007,** *48,* 2097–2099. doi:10.1016/j.tetlet.2007.01.130
29. Bonnamour, J.; Legros, J.; Crousse, B.; Bonnet-Delpon, D. *Tetrahedron Lett.* **2007,** *48,* 8360–8362. doi:10.1016/j.tetlet.2007.09.118
30. Fukuzawa, S.-i.; Shimizu, E.; Kikuchi, S. *Synlett* **2007,** 2436–2438. doi:10.1055/s-2007-986638
31. Kumar, D.; Patel, G.; Reddy, V. B. *Synlett* **2009,** 399–402. doi:10.1055/s-0028-1087556
32. Huang, Y.; Gard, G. L.; Shreeve, J. M. *Tetrahedron Lett.* **2010,** *51,* 6951–6954. doi:10.1016/j.tetlet.2010.10.149
33. Stefani, H. A.; Canduzini, H. A.; Manarin, F. *Tetrahedron Lett.* **2011,** *52,* 6086–6090. doi:10.1016/j.tetlet.2011.09.004
34. Johansson, J. R.; Lincoln, P.; Nordén, B.; Kann, N. *J. Org. Chem.* **2011,** *76,* 2355–2359. doi:10.1021/jo200134a
35. Zhang, J.; Wu, J.; Shen, L.; Jin, G.; Cao, S. *Adv. Synth. Catal.* **2011,** *353,* 580–584. doi:10.1002/adsc.201000791
36. Gonzalez-Olvera, R.; Espinoza-Vázquez, A.; Negrón-Silva, G. E.; Palomar-Pardavé, M. E.; Romero-Romo, M. A.; Santillan, R. *Molecules* **2013,** *18,* 15064–15079. doi:10.3390/molecules181215064
37. Hassan, S.; Müller, T. J. J. *Adv. Synth. Catal.* **2015,** *357,* 617–666. doi:10.1002/adsc.201400904
38. Wang, Z.-Y.; Li, J.; Wang, N.; Liu, H.; Wang, K.-K. *Asian J. Org. Chem.* **2023,** *12,* 202300105. doi:10.1002/ajoc.202300105
39. Sears, P.; Wong, C.-H. *Angew. Chem., Int. Ed.* **1999,** *38,* 2300–2324. doi:10.1002/(sici)1521-3773(19990816)38:16<2300::aid-anie2300>3.0.co;2-6
40. Koester, D. C.; Holkenbrink, A.; Werz, D. B. *Synthesis* **2010,** 3217–3242. doi:10.1055/s-0030-1258228
41. Yang, Y.; Yu, B. *Chem. Rev.* **2017,** *117,* 12281–12356. doi:10.1021/acs.chemrev.7b00234
42. Hazelard, D.; Compain, P. *Org. Biomol. Chem.* **2017,** *15,* 3806–3827. doi:10.1039/c7ob00386b
43. Leusmann, S.; Ménová, P.; Shanin, E.; Titz, A.; Rademacher, C. *Chem. Soc. Rev.* **2023,** *52,* 3663–3740. doi:10.1039/d2cs00954d
44. Dernedde, J.; Enders, S.; Reissig, H.-U.; Roskamp, M.; Schlecht, S.; Yekta, S. *Chem. Commun.* **2009,** 932–934. doi:10.1039/b818263a
45. Roskamp, M.; Enders, S.; Pfrengle, F.; Yekta, S.; Dekaris, V.; Dernedde, J.; Reissig, H.-U.; Schlecht, S. *Org. Biomol. Chem.* **2011,** *9,* 7448–7456. doi:10.1039/c1ob05583f
46. Salta, J.; Dernedde, J.; Reissig, H.-U. *Beilstein J. Org. Chem.* **2015,** *11,* 638–646. doi:10.3762/bjoc.11.72
47. Salta, J.; Reissig, H.-U. *Synthesis* **2015,** *47,* 1893–1898. doi:10.1055/s-0034-1380571

48. Bouché, L.; Reissig, H.-U. *Eur. J. Org. Chem.* **2014,** 3697–3703. doi:10.1002/ejoc.201402191
49. Salta, J.; Reissig, H.-U. *Eur. J. Org. Chem.* **2020,** 4361–4370. doi:10.1002/ejoc.202000618
50. Salta, J.; Arp, F. F.; Kühne, C.; Reissig, H.-U. *Eur. J. Org. Chem.* **2020,** 7333–7342. doi:10.1002/ejoc.202001389
51. Fasting, C.; Schalley, C. A.; Weber, M.; Seitz, O.; Hecht, S.; Koksch, B.; Dernedde, J.; Graf, C.; Knapp, E.-W.; Haag, R. *Angew. Chem., Int. Ed.* **2012,** *51,* 10472–10498. doi:10.1002/anie.201201114
52. Al-Harrasi, A.; Reißig, H.-U. *Angew. Chem., Int. Ed.* **2005,** *44,* 6227–6231. doi:10.1002/anie.200501127
53. Al-Harrasi, A.; Pfrengle, F.; Prisyazhnyuk, V.; Yekta, S.; Koóš, P.; Reissig, H.-U. *Chem. – Eur. J.* **2009,** *15,* 11632–11641. doi:10.1002/chem.200900996
54. Pfrengle, F.; Reissig, H.-U. *Chem. Soc. Rev.* **2010,** *39,* 549–557. doi:10.1039/b914356d
55. Reissig, H.-U. *Angew. Chem., Int. Ed.* **2021,** *60,* 9180–9191. doi:10.1002/anie.202101550
56. Angell, Y.; Burgess, K. *Angew. Chem., Int. Ed.* **2007,** *46,* 3649–3651. doi:10.1002/anie.200700399
57. Zheng, Z.-J.; Wang, D.; Xu, Z.; Xu, L.-W. *Beilstein J. Org. Chem.* **2015,** *11,* 2557–2576. doi:10.3762/bjoc.11.276
58. Chan, T. R.; Hilgraf, R.; Sharpless, K. B.; Fokin, V. V. *Org. Lett.* **2004,** *6,* 2853–2855. doi:10.1021/ol0493094
59. Yekta, S.; Koóš, P.; Reissig, H.-U. unpublished results.
60. Szostak, M.; Spain, M.; Procter, D. J. *Chem. Soc. Rev.* **2013,** *42,* 9155–9183. doi:10.1039/c3cs60223k
61. Chiara, J. L.; Destabel, C.; Gallego, P.; Marco-Contelles, J. *J. Org. Chem.* **1996,** *61,* 359–360. doi:10.1021/jo951571q
62. Keck, G. E.; Wager, T. T.; McHardy, S. F. *Tetrahedron* **1999,** *55,* 11755–11772. doi:10.1016/s0040-4020(99)00486-x
63. Pulz, R.; Al-Harrasi, A.; Reissig, H.-U. *Org. Lett.* **2002,** *4,* 2353–2355. doi:10.1021/ol0260573
64. Bressel, B.; Reissig, H.-U. *Org. Lett.* **2009,** *11,* 527–530. doi:10.1021/ol802514m

License and Terms

BEILSTEIN JOURNAL OF ORGANIC CHEMISTRY

Decarboxylative 1,3-dipolar cycloaddition of amino acids for the synthesis of heterocyclic compounds

Xiaofeng Zhang*[1,2], Xiaoming Ma*[3] and Wei Zhang*[1]

Perspective

Open Access

Address:
[1]Center for Green Chemistry and Department of Chemistry, University of Massachusetts Boston, 100 Morrissey Boulevard, Boston, MA 02125, USA, [2]Department of Medicinal Chemistry, Cerevel Therapeutics, 222 Jacobs St Suite 200, Cambridge, MA 02141, USA and [3]School of Pharmacy, Changzhou University, Changzhou 213164, China

Email:
Xiaofeng Zhang* - xfxiaofengzhang@gmail.com; Xiaoming Ma* - mxm.wuxi@cczu.edu.cn; Wei Zhang* - wei2.zhang@umb.edu

* Corresponding author

Keywords:
[3 + 2] cycloaddition; decarboxylation; 1,3-dipolar; double cycloaddition; one-pot synthesis; multicomponent reaction; semi-stabilized azomethine ylide

Beilstein J. Org. Chem. **2023,** *19,* 1677–1693.
https://doi.org/10.3762/bjoc.19.123

Received: 14 August 2023
Accepted: 25 October 2023
Published: 06 November 2023

This article is part of the thematic issue "Catalytic multi-step domino and one-pot reactions".

Guest Editor: S. Tsogoeva

Abstract

The [3 + 2] cycloadditions of stabilized azomethine ylides (AMYs) derived from amino esters are well-established. However, the reactions of semi-stabilized AMYs generated from decarboxylative condensation of α-amino acids with arylaldehydes are much less explored. The [3 + 2] adducts of α-amino acids could be used for a second [3 + 2] cycloaddition as well as for other post-condensation modifications. This article highlights our recent work on the development of α-amino acid-based [3 + 2] cycloaddition reactions of *N*–H-type AMYs in multicomponent, one-pot, and stepwise reactions for the synthesis of diverse heterocycles related to some bioactive compounds and natural products.

Introduction

The 1,3-dipolar cycloaddition of azomethine ylides (AMYs) [1-6] is a powerful method for the synthesis of bioactive pyrrolidine-containing compounds and natural product analogs [7-15]. AMYs generated from the reaction of aldehydes and α-amino esters (via dehydration) or α-amino acids (via decarboxylation) could be classified based on the substitution groups on the N atom to: 1) N-substituted (*N*–R type), 2) hydrogen containing (*N*–H type), and 3) metal complexes (*N*–M type) (Figure 1) [16,17]. These AMYs could also be classified as stabilized (**A1**–**A4**) which contain an electron-withdrawing group (EWG), semi-stabilized (**B1**–**B4**) which have an aryl (Ar) substituent, and non-stabilized (**C1** and **C2**) which have neither an Ar group nor an EWG on the α-carbon atoms.

The routes to access AMYs of different classes are shown in Scheme 1: **A1**-type AMYs can be generated from the condensa-

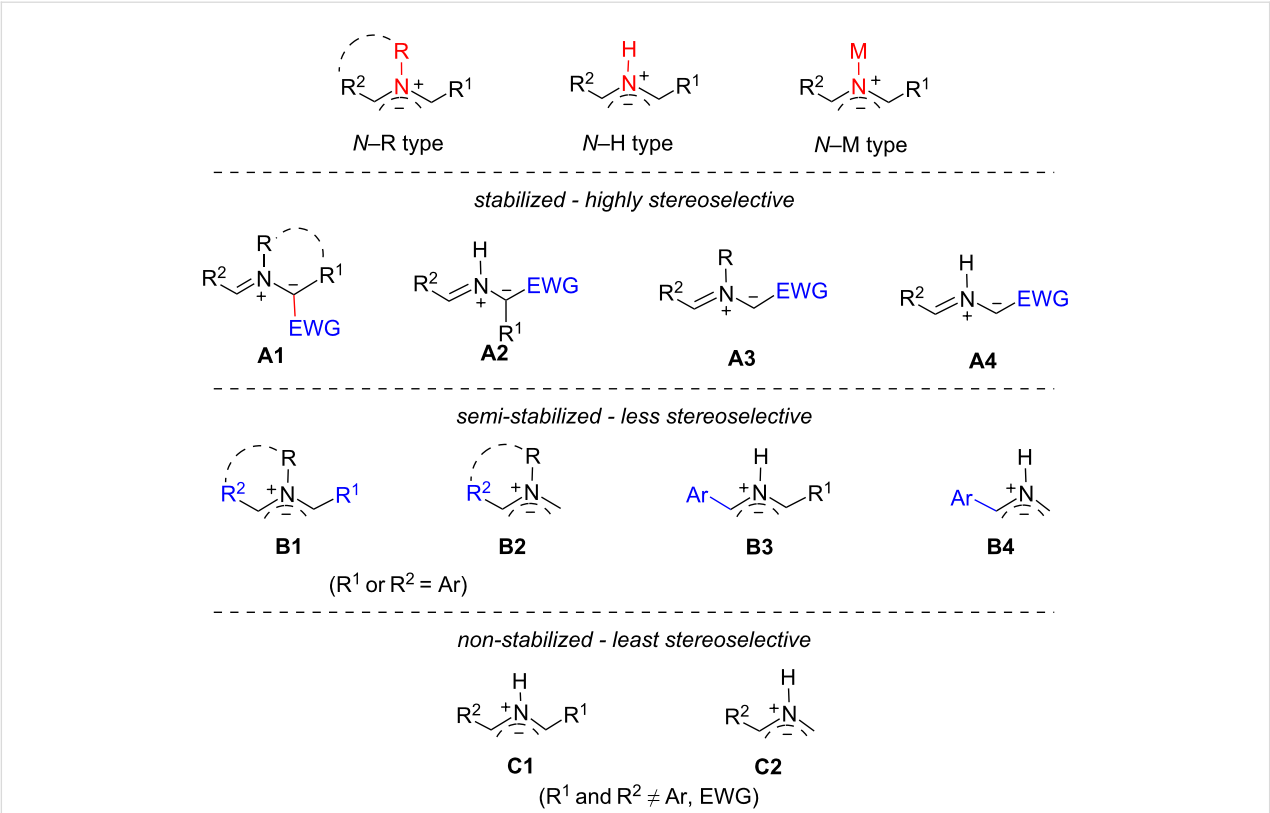

Figure 1: Classification of AMYs.

tion of aldehydes with α- and *N*-dialkylglycine esters, **A2**-type AMYs are derived from α-alkylglycine esters, **A3**-type AMYs are derived from *N*-alkylglycine esters, and **A4**-type AMYs are derived from glycine esters. Stabilized zwitterions **A1**–**A4** have the anionic charge on the α-carbon connecting to the EWG. They are popular AMYs for 1,3-diploar [3 + 2] cycloaddition reactions with alkenes to generate pyrrolidines **1a**–**d** with high regio- and stereoselectivities. They have been reported in a huge number (1,000+) of publications [18-28]. It is worth noting that among the products **1a**–**d**, only compound **1d** has hydrogen atoms on both the nitrogen and α-carbon atoms, which makes it suitable to be used for a second cycloaddition to form double [3 + 2] cycloaddition products **2** [29,30].

The *N*–R-type AMYs **B1** and **B2** bearing an Ar group on the α-carbon atom are semi-stabilized (Scheme 1) [16]. The **B1**-type AMYs can be generated from the decarboxylative condensation of aldehydes with α- and *N*-dialkylglycines or from cyclic amino acids (such as proline) [31-33], while AMYs of type **B2** are accessible through the decarboxylative condensation of *N*-dialkylglycines [34-51]. The *N*–H-type semi-stabilized AMYs **B3** are generated through decarboxylative condensation of arylaldehydes with α-alkylglycines, while **B4**-type AMYs are derived from the reaction of glycine [52-58]. The [3 + 2] cycloadditions of AMYs **B1**–**B4** with alkenes lead to the formation of cycloaddition products **3a**–**d** with attenuated regio- and stereoselectivity, since the Ar group is not strong enough to fully localize the negative charge on the carbon connecting to Ar in the 1,3-dipoles. Both products **3c** and **3d** can be used for a second cycloaddition to form products **4a** and **4b**. The non-stabilized AMYs **C1** and **C2** have neither an EWG nor an Ar group to localize the negative charge. The 1,3-dipolar cycloadditions of **C**-type AMYs lead to the formation of [3 + 2] adducts **5** or **6** with low regio- and stereoselectivity which limits the synthetic utility of non-stabilized AMYs of type **C**.

There are over 300 papers on the amino acid-based decarboxylative [3 + 2] cycloadditions of *N*–R-type AMYs **B1** (such as that derived from proline) and **B2** [31-51]. However, to the best of our knowledge, there are only few examples on the reactions of *N*–H-type semi-stabilized AMYs **B3** or **B4** which were either derived from special carbonyl compounds (such as isatin) [52-55] or the AMYs were reacted with uncommon alkenes as the 1,3-dipolarophiles (such as C_{60}/C_{70} fullerenes) [56-58].

Other than amino esters and amino acids shown in Scheme 1, cyclic amines can also react with arylaldehydes to form **B1**-type semi-stabilized AMYs. In this context, the Seidel group re-

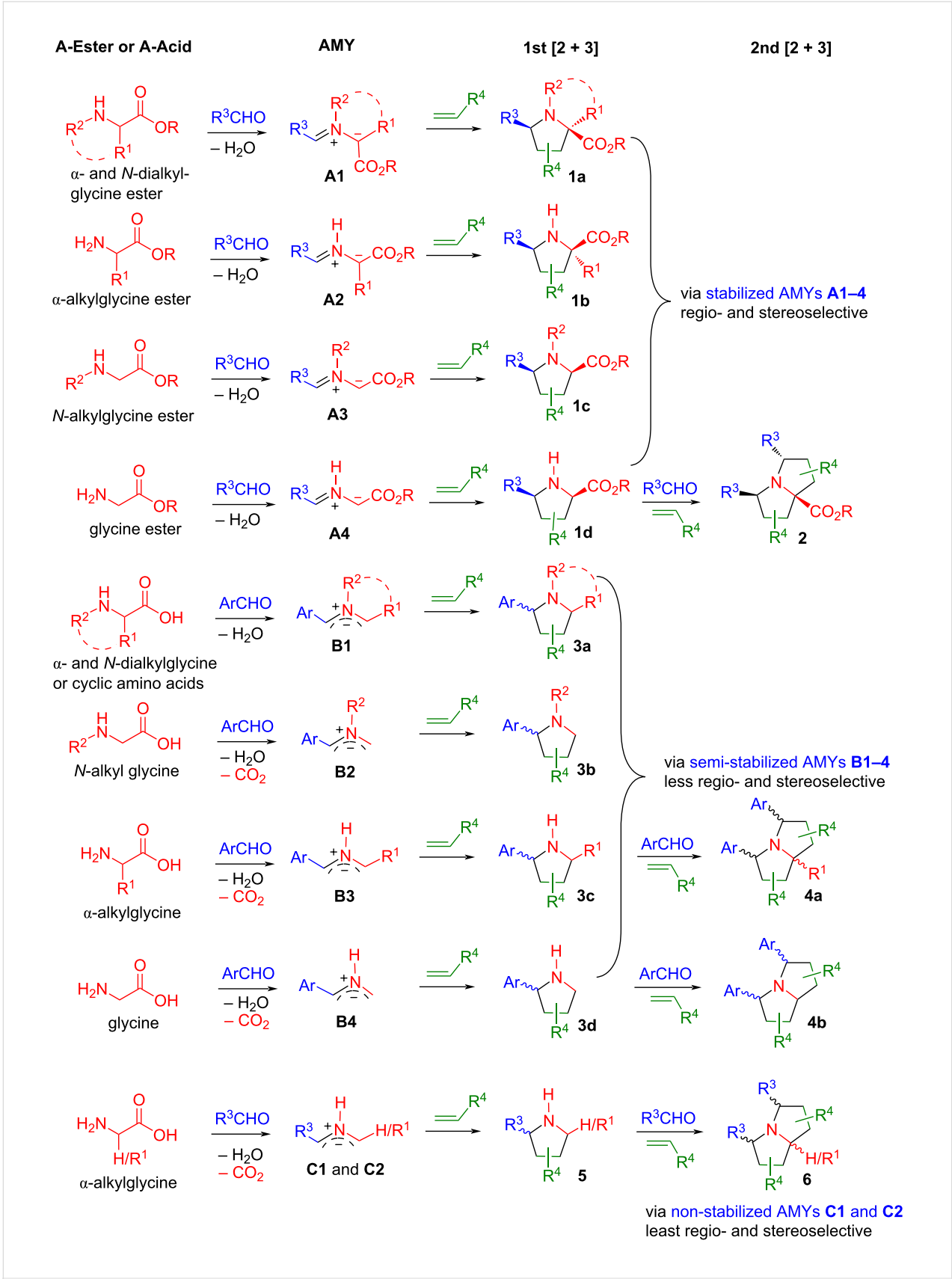

Scheme 1: Aminoester- and amino acid-based AMYs for single and double [3+2] cycloadditions.

ported the reactions of pyrrolidines **5** with arylaldehydes for the formation of AMYs **B1** which then were reacted with nucleophiles to form C–H-functionalized pyrrolidines or subjected to the 1,3-dipolar cycloaddition with olefins to afford bicyclic compounds (Scheme 2A and B) [59,60]. We employed cyclic amines for the synthesis of spirooxindole-pyrrolidines **7a** or **7b** in good stereoselectivity (Scheme 3) [61,62].

From the results shown in Scheme 2 and Scheme 3, we envisioned that pyrrolidines **3c** or **3d** generated from the cycloaddition of AMYs **B3** or **B4** could undergo a second cycloaddition to form double cycloaddition products **4a** or **4b** (Scheme 4). The double cycloaddition process involves two kinds of AMYs, with the first ones (*N*-H-type **B3** or **B4**) derived from amino acids, while the second ones (*N*-R-type **B1**) derived from pyrrolidines **3c** or **3d**. It is worth noting that the double cycloaddition reaction is a pseudo-five-component reaction of amino acids with two equivalents each of aldehydes and alkenes. The first cycloaddition products **3c** or **3d** can also be used as intermediates for other transformations to synthesize novel heterocyclic rings via multicomponent, one-pot, and stepwise synthesis [63,64].

Presented in the following sections is our work on the development of amino acid-based decarboxylative [3 + 2] cycloadditions of *N*–H-type AMYs **B3** and **B4** for double cycloadditions. The stereochemistry of the cycloadditions and the combination of the cycloaddition with other transformations to be one-pot or stepwise reactions are also presented.

Perspective

One-step synthesis of trifluoromethylated pyrrolidines

As mentioned above, the unexpected double cycloaddition and low stereoselectivity are the major challenges for [3 + 2] cyclo-

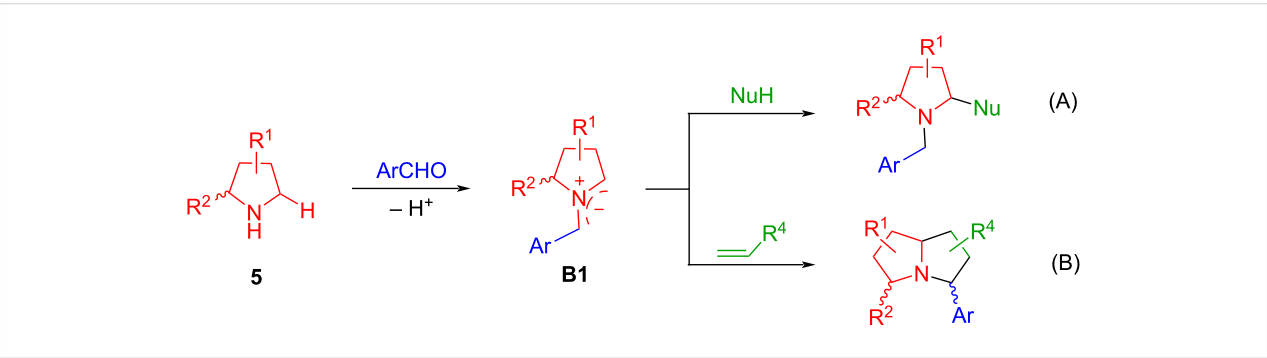

Scheme 2: Formation of semi-stabilized AMYs **B1** from pyrrolidines.

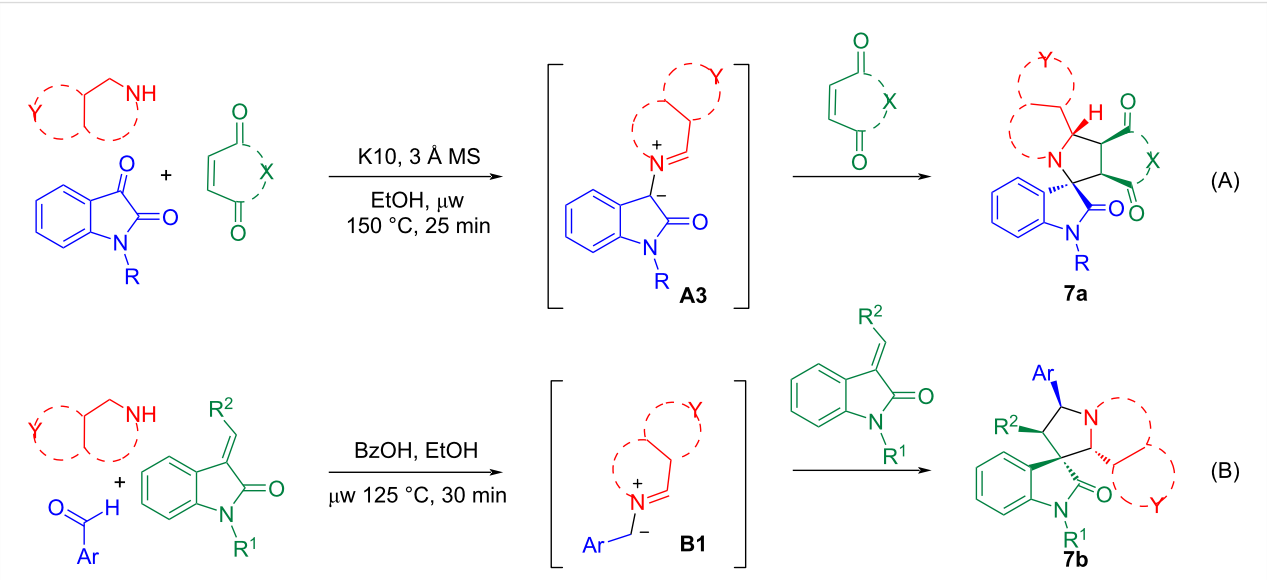

Scheme 3: Cyclic amine-based AMYs **A3** and **B1** for [3 + 2] cycloadditions.

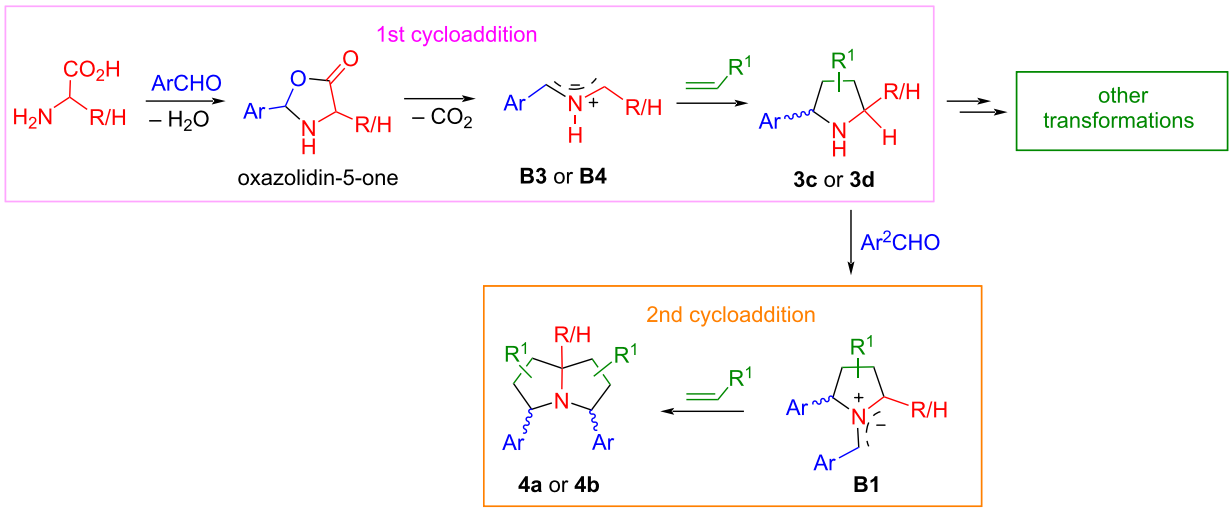

Scheme 4: Proposed double cycloaddition reactions involving semi-stabilized AMYs.

addition reactions of semi- and non-stabilized AMYs derived from the condensation of amino acids with aldehydes. However, the reactions of amino acids with ketones can result in a different kind of AMYs to address the issue. The reaction of trifluoromethyl ketones with glycine or α-substituted amino acids generated stabilized AMY **8** which underwent cycloaddition with maleimides to give 2-CF_3-substituted pyrrolidines **9** in 50–76% yield (Scheme 5) [65]. Both the Ar and CF_3 groups can

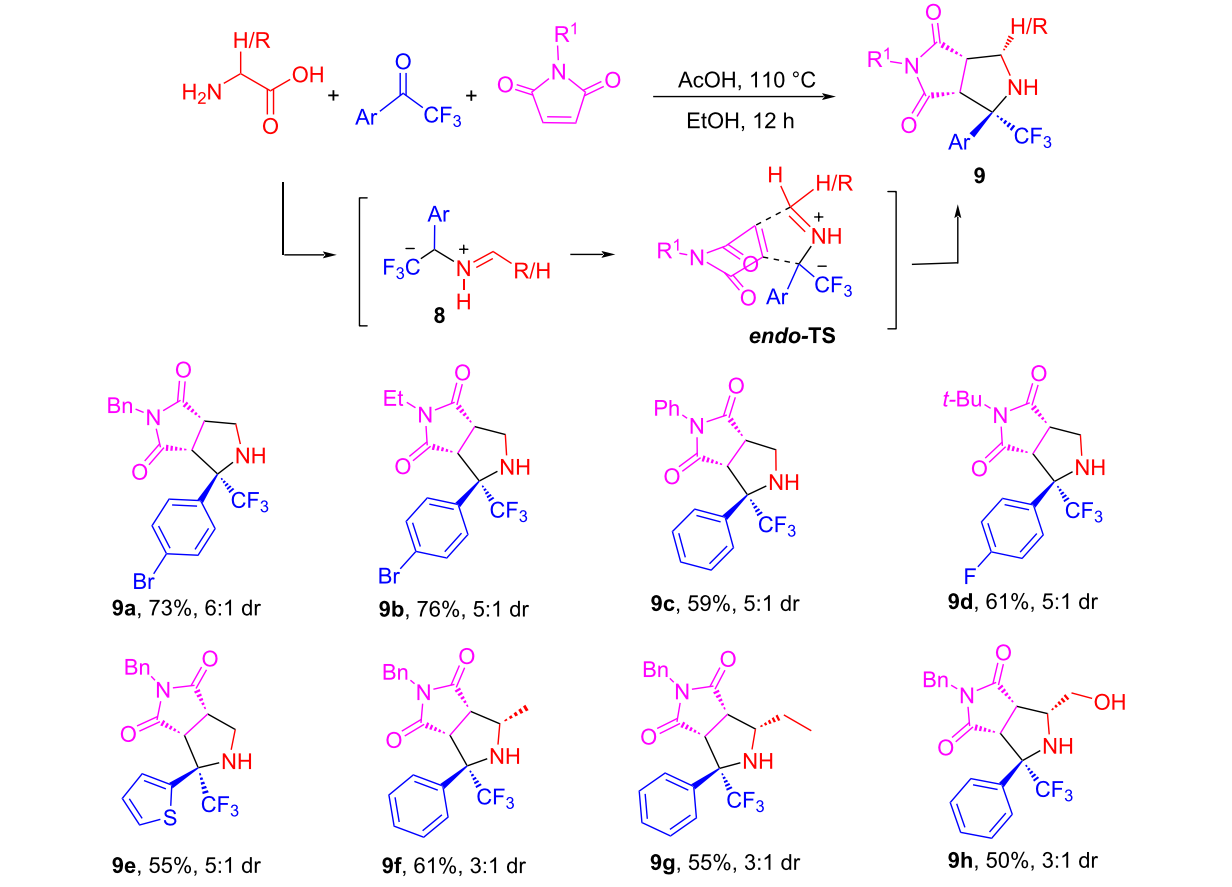

Scheme 5: [3 + 2] Cycloaddition for the synthesis of trifluoromethylated pyrrolidines **9**.

localize the negative charge and also provide steric effects to afford stereoselective cycloaddition products with 3:1 to 6:1 dr. The steric hindrance also prevents products **9** from undergoing a second cycloaddition. The control reactions of methyl ketone or benzaldehydes gave much lower yields and stereoselectivity because of the lacking CF_3 group. This was the first example of synthesizing 2-CF_3-substituted pyrrolidines via decarboxylative [3 + 2] cycloaddition which is more efficient than multistep and metal-assisted syntheses reported in the literature [66,67].

Pseudo-five-component double cycloadditions for polycyclic pyrrolizidines

With the success of the three-component [3 + 2] cycloadditions shown in Scheme 5, we then explored the double cycloaddition reactions proposed in Scheme 4. The reaction has synthetic significance since the resulting pyrrolizidine scaffold can be found in many biologically active compounds and natural products such as 1-epiaustraline, hyacinthacine A1, (−)-isoretronecanol, and (−)-supinidine (Figure 2) [68,69].

After the method development work, a pseudo-five-component double cycloaddition reaction of glycine with two equivalents each of arylaldehydes and *N*-substituted maleimides was carried out in EtOH as a protic solvent at 90 °C for 3 h to afford pyrrolizidines **10** in 73–93% yield with greater than 9:1 dr (Scheme 6). The scope of the reaction could be readily extended for α-substituted amino acids, such as alanine, leucine, serine, and norvaline to give products **11a–f** in 53–88% yields with greater than 8.5 dr (Scheme 7). The reactions with leucine and phenylglycine (R^2 = iPr and Ph) as amino acids gave mainly mono-cycloaddition products and very little double cycloaddition products **11g** and **11h** due to the steric hindrance of the R^2 group.

The stereochemistry of products **10** and **11** was confirmed by X-ray crystal structure and the ^{1}H NMR analysis of both the major and minor diastereomers [69]. The first cycloaddition gives adducts **12** and **12'** as a diastereomeric mixture. At the second cycloaddition, both major and minor adducts from the first cycloaddition generate the same products **10** or **11** (Scheme 8).

We also evaluated the double cycloadditions in two operational steps by using two different sets of aldehydes and maleimides to afford products **13a–d** in 45–60% yields with 2:1 to 3:1 dr (Scheme 9). The low diastereoselectivity is caused by the different $R^2/R^{2'}$ and $R^3/R^{3'}$ groups which no longer have the same stereochemistry as that shown in Scheme 8.

Double cycloadditions for bis[spirooxindole-pyrrolizidine] compounds

After completing the pseudo-five-component double cycloaddition reactions leading to polycyclic pyrrolizidines shown in Scheme 6 and Scheme 7, we then conducted similar reactions in order to synthesize spirooxindole-pyrrolidines. This unique ring skeleton exists in some natural products and biologically active compounds such as (−)-horsfiline, (+)-alstonisine, pteropodine and spirotryprostatin A (Figure 3) [70].

We expected that using olefinic oxindoles **14** as alkenes for the [3 + 2] cycloaddition could afford spirooxindole-pyrrolizidines. The method development revealed that recyclable zeolite HY acid is a good catalyst for the cycloaddition [70]. Thus, the zeolite HY-catalyzed reaction of glycine with two equiv each of arylaldehydes and olefinic oxindoles **14** in EtOH at 90 °C for 6 h gave bis[spirooxindole-pyrrolizidine] compounds **15a–g** in 60–73% yields with up to 6:1 dr (Scheme 10). It is worth noting that this pseudo-five-component reaction gives butterfly-shaped molecules which have a plane of symmetry. The stereochemistry of the products was confirmed by X-ray crystal structure and NMR analysis. The reaction mechanism shown in Scheme 11 suggests that a semi-stabilized AMY **16** generated from the reaction of glycine and arylaldehydes undergoes a [3 + 2] cycloaddition with **14a** via the favorable *endo*-transition state **A** to give spirooxindole-pyrrolizidine **17** which spontaneously reacts with another equiv of arylaldehyde to form ylide **18** in the presence of zeolite HY. The second [3 + 2] cycloaddition of **18** with **14a** affords product **15a** as a major product through an *endo*-cycloaddition and **15a'** as a minor diastereomeric product through an *exo*-cycloaddition.

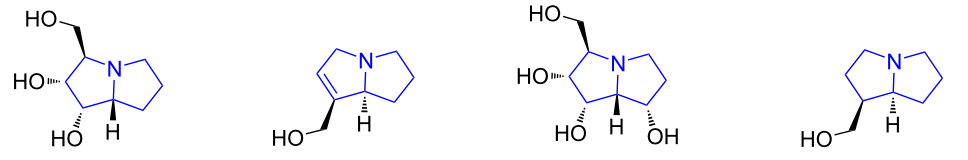

Figure 2: Biologically interesting pyrrolizidines.

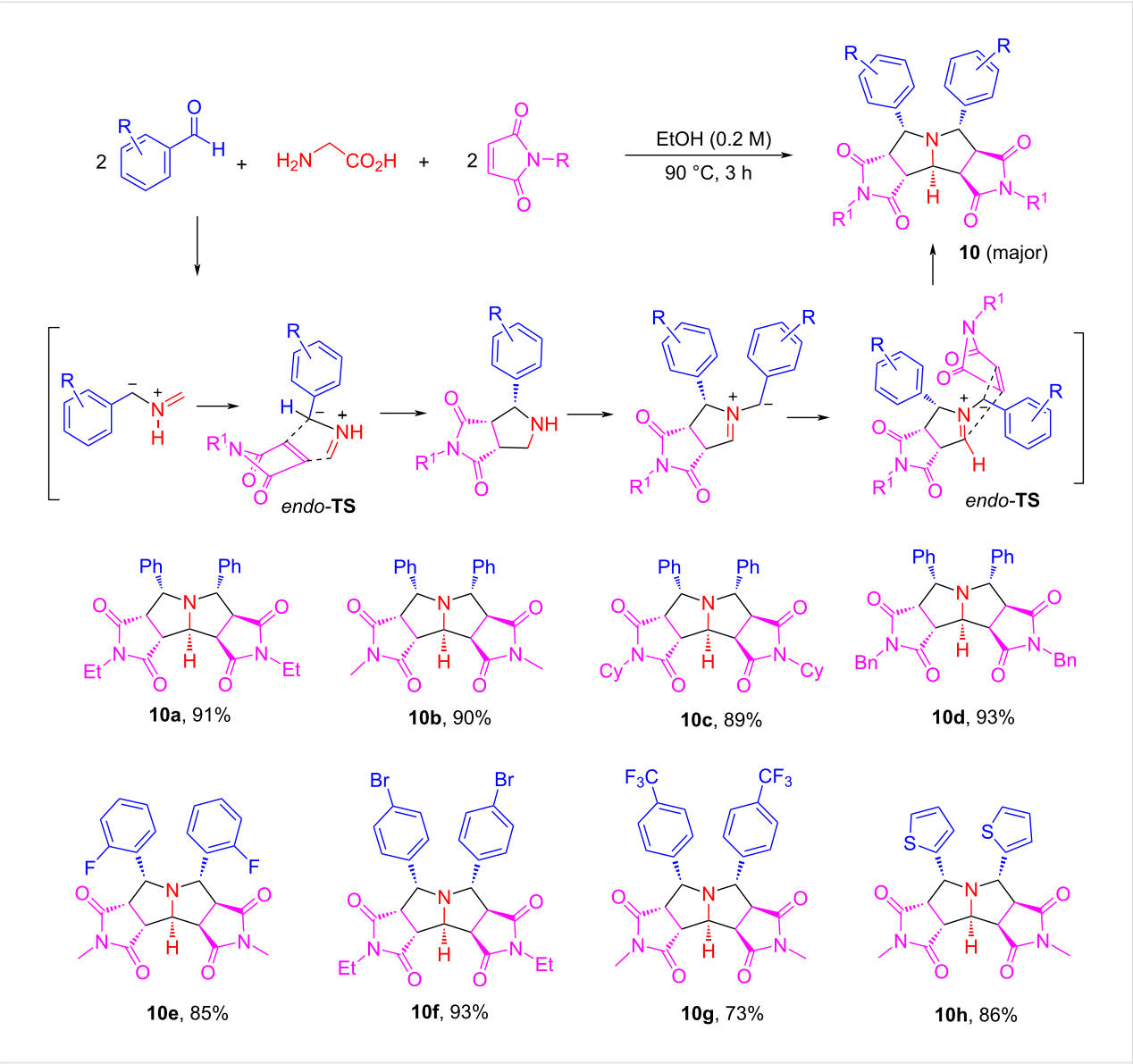

Scheme 6: Double cycloadditions with glycine for the synthesis of products **10** (dr > 9:1).

One-pot synthesis of triazolobenzodiazepines

Other than the multicomponent double cycloaddition reactions shown in the last section, we also utilized the first cycloaddition products for post-condensation reactions to generate new heterocyclic scaffolds. α-Substituted amino acids, such as 2-aminoisobutyric acid, could be used to block the second cycloaddition. Shown in Scheme 12 is a method development for the stepwise synthesis of triazolobenzodiazepines. The reaction of 2-azidobenzaldehyde, 2-aminoisobutyric acid and *N*-ethylmaleimide in MeCN under the catalysis of AcOH at 110 °C for 6 h afforded the monocycloaddition product **19a** in 93% LC yield [71]. The isolated compound **19a** was used for an *N*-propargylation to produce compound **20a** in 94% LC yield. The following Cu-catalyzed click reaction afforded triazolobenzodiazepine **21a** in 88% LC yield (Scheme 12).

Our next goal was to convert the stepwise reaction process into a one-pot synthesis. After optimizing the reaction conditions, a one-pot two-step reaction was developed by the reaction of 2-azidobenzaldehydes, 2-substituted amino acids and maleimides with AcOH as a catalyst in MeCN at 110 °C for 6 h to afford the monocycloaddition compounds. Without isolation, the reaction mixtures were then used for the *N*-propargylation in the presence of K_2CO_3 under microwave heating at 110 °C for 1 h to give triazolobenzodiazepines **21a–f** in 35–65% yields with 2:1 to 7:1 dr (Scheme 13). Other than 2-aminoisobutyric acid, phenylglycine and valine with Ph or iPr groups could also

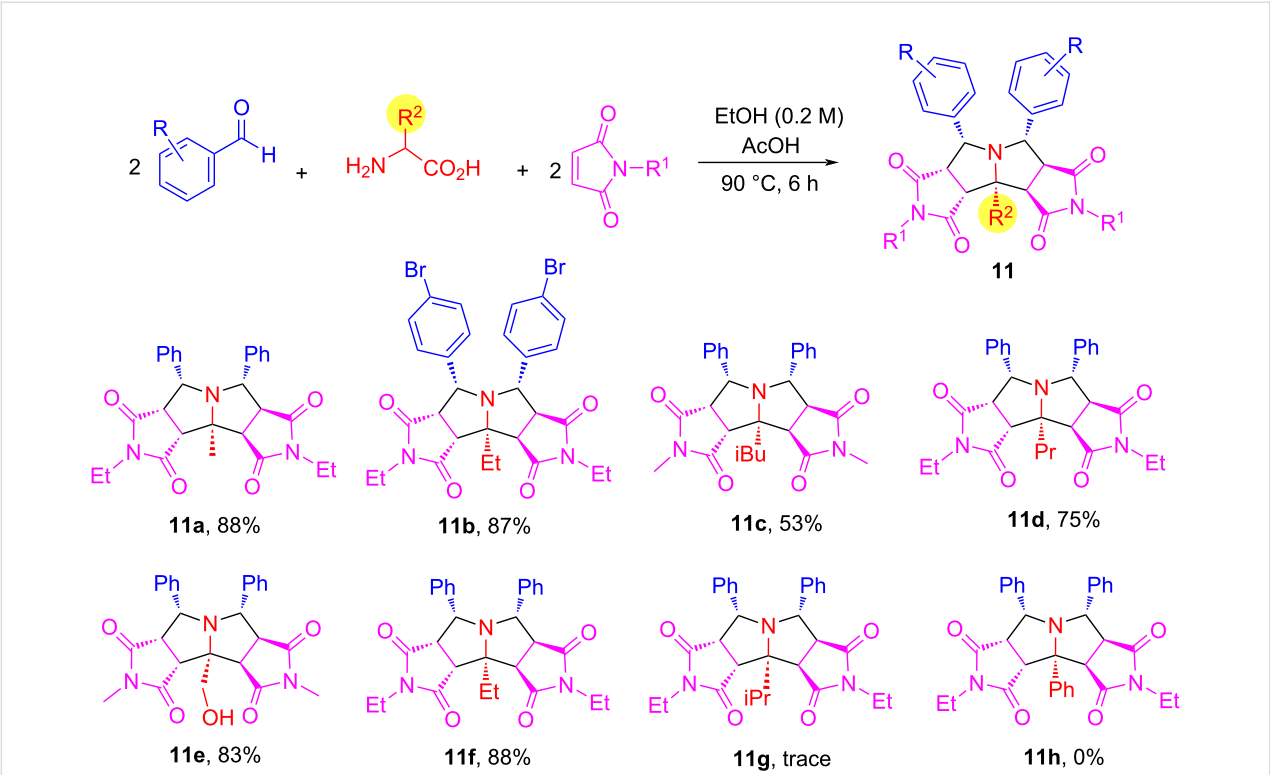

Scheme 7: Double cycloadditions with α-substituted amino acids leading to products **11** (≈8.5:1 dr).

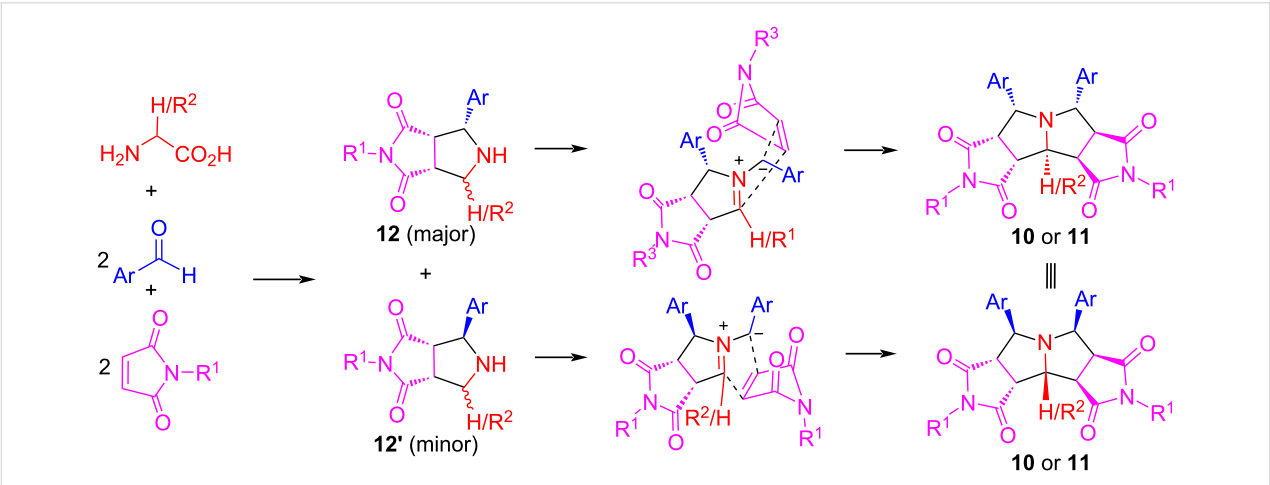

Scheme 8: Stereochemistry for the formation of products **10** or **11**.

be used for the synthesis of the monocycloaddition products for the post-condensation reactions. It is worth noting that in the one-pot synthesis involving an intramolecular click reaction, no Cu catalyst was used. A similar reaction sequence using stabilized AMYs was also reported from our lab [72]. The triazolobenzodiazepines obtained through this highly efficient one-pot synthesis have structure similarity with some drug molecules shown in Figure 4 [71].

One-pot synthesis of pyrroloquinazolines and pyrrolobenzodiazepines

We developed a 2-azidobenzladehyde-based reaction sequence including a one-pot [3 + 2] cycloaddition, *N*-acylation and Staudinger/aza-Wittig reactions for the construction of pyrroloquinazolines and pyrrolobenzodiazepines [73]. The AcOH-catalyzed reaction of 2-azidobenzaldehydes, α-substituted amino acids and maleimides in MeCN at 110 °C for 6 h afforded the

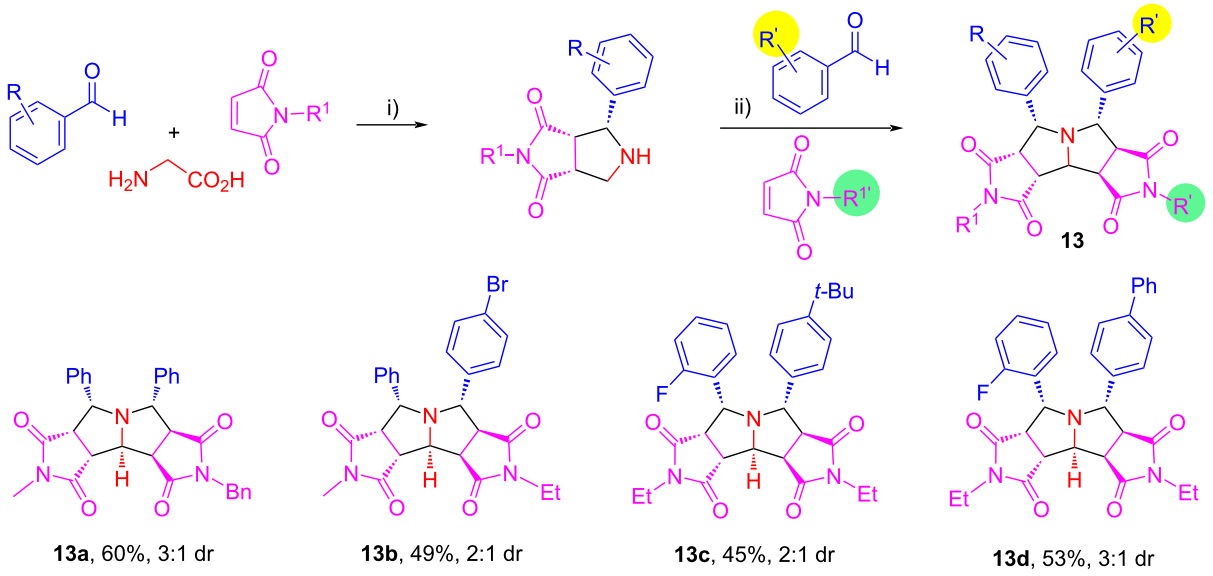

Scheme 9: One-pot and stepwise double cycloadditions. Conditions: i) MeCN (0.02 M), 90 °C, 6 h; ii) then AcOH (0.5 equiv), 125 °C, 12 h.

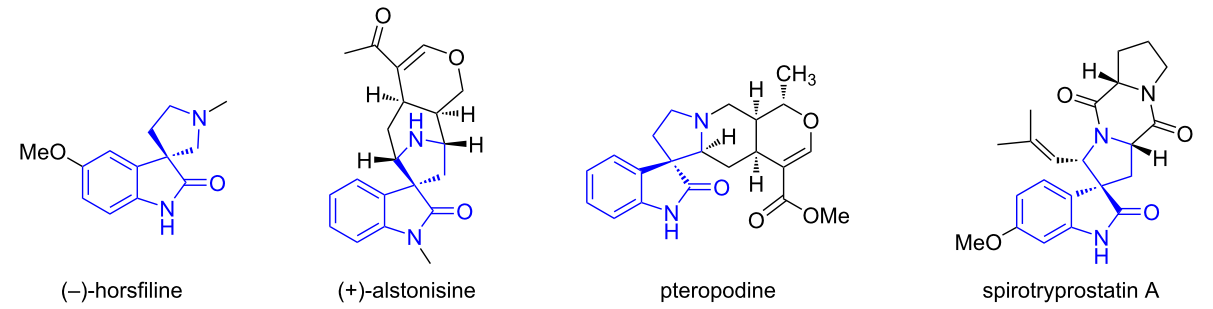

Figure 3: Biologically interesting spirooxindole-pyrrolizidines.

corresponding monocycloaddition compounds followed by acylation to yield intermediates **22**. The subsequent sequential Staudinger/aza-Wittig reaction of intermediates **22** gave products **23a–g** in 48–75% yields with 5:1 to 6:1 dr (Scheme 14). This one-pot reaction could also be applied for the synthesis of pyrrolobenzodiazepines when using 2-bromoketones instead of the acid chlorides affording products **24a–g** in 59–77% yields with 3:1 to 6:1 dr (Scheme 15). The pyrroloquinazolines and pyrrolobenzodiazepines made by this route have structure similarity with bioactive compounds and natural products such as PB1-5 [74], lixivaptan, and (+)-anthramycin (Figure 5) [73].

Stepwise synthesis of pyrrolo[2,1-*a*]isoquinolines

A stepwise synthesis involving [3 + 2] cycloaddition, *N*-allylation and Heck reactions has been developed for the synthesis of pyrrolo[2,1-*a*]isoquinolines. The reaction of 2-bromobenzaldehydes, 2-aminoisobutyric acid, and maleimides in MeCN under the catalysis of AcOH at 110 °C for 6 h afforded the cycloaddition products **26**. The purified intermediates were used for the one-pot *N*-allylation with allyl bromide to afford intermediate **25** followed by a Pd-catalyzed Heck reaction to give products **26** in 65–78% yields (Scheme 16) [75]. The pyrrolo[2,1-*a*]isoquinoline core installed by this route can be found in some natural products and synthetic compounds with antitumor, antibacterial, antiviral, antioxidizing, and other biological activities (Figure 6) [75].

One-pot double annulations for the synthesis of tetrahydropyrrolothiazoles

The unique tetrahydropyrrolothiazole and spiro[indole-tetrahydropyrrolothiazole] scaffolds are found in bioactive compounds such as those shown in Figure 7 [76,77]. Using cysteine as a key reactant, we developed a pseudo-four-component reaction

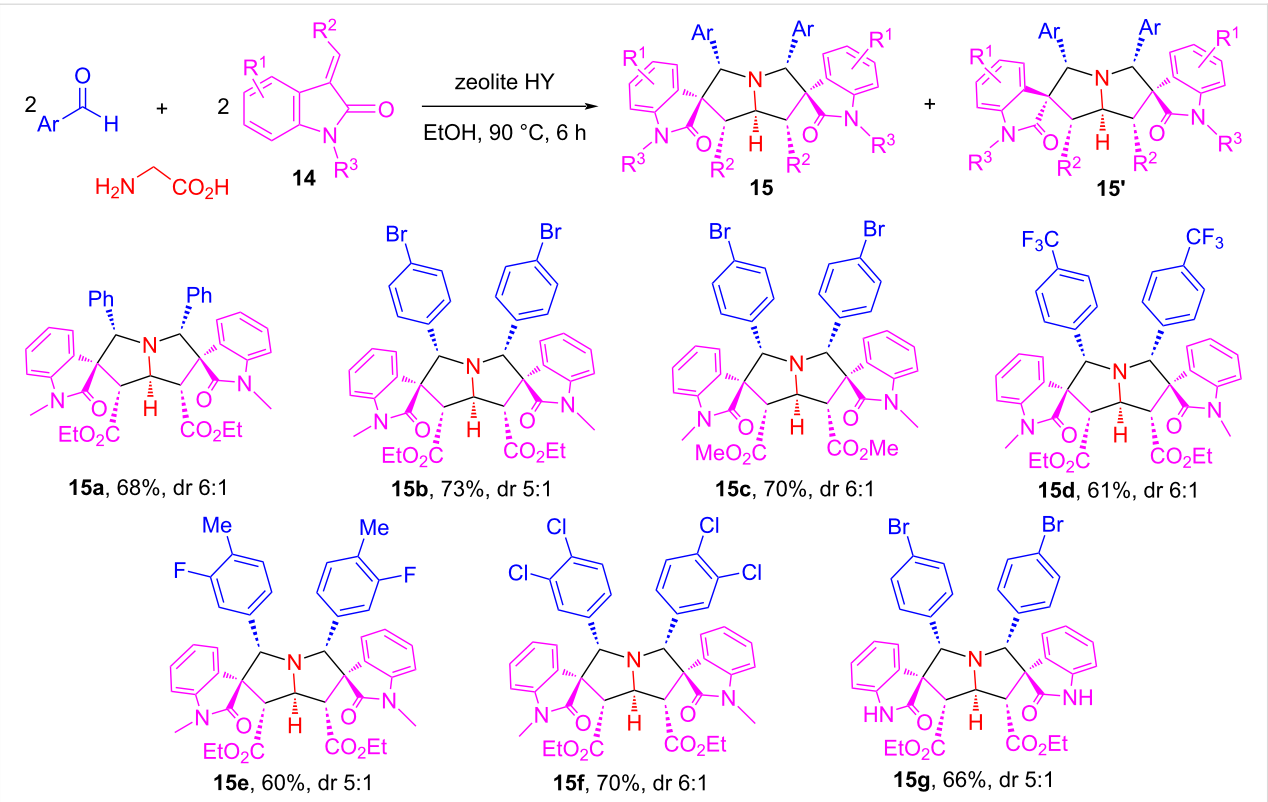

Scheme 10: Double cycloadditions for the synthesis of bis[spirooxindole-pyrrolizidine]s.

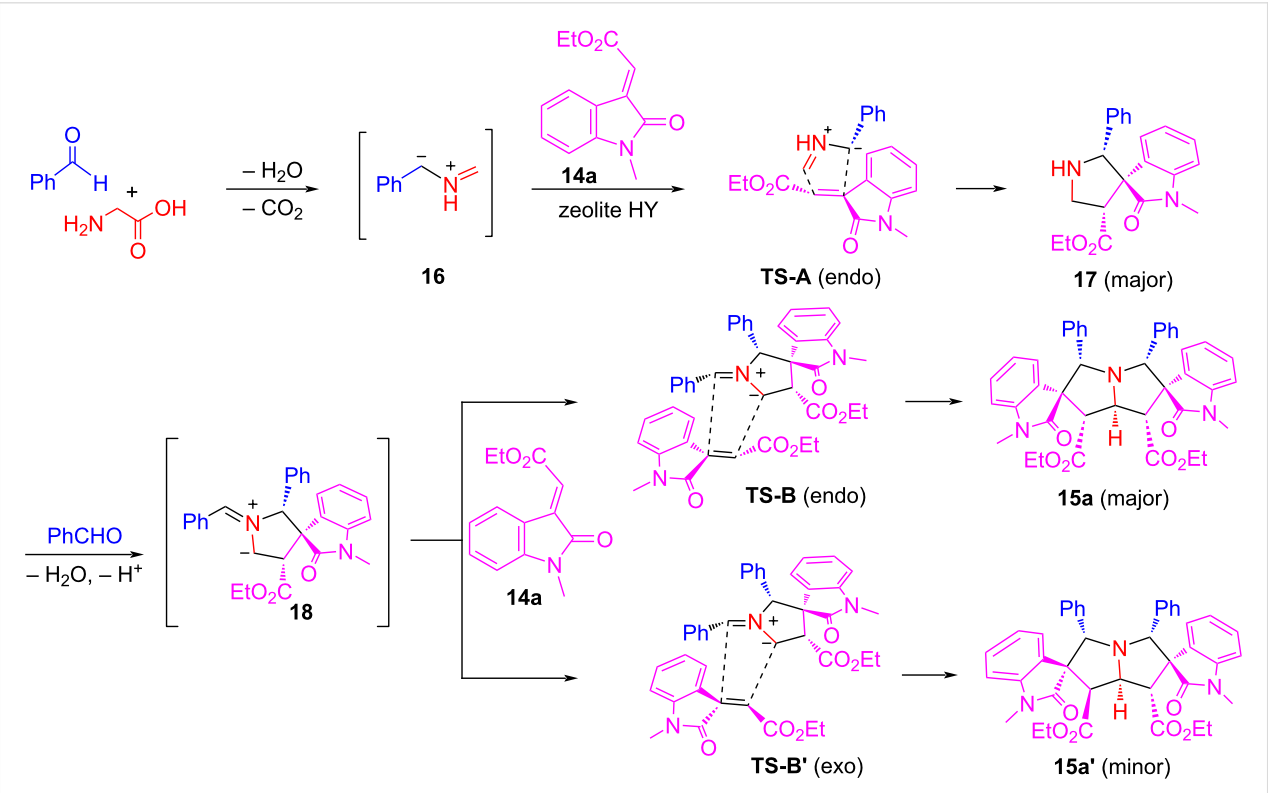

Scheme 11: Mechanism for the diastereoselective synthesis of bis[spirooxindole-pyrrolizidine]s.

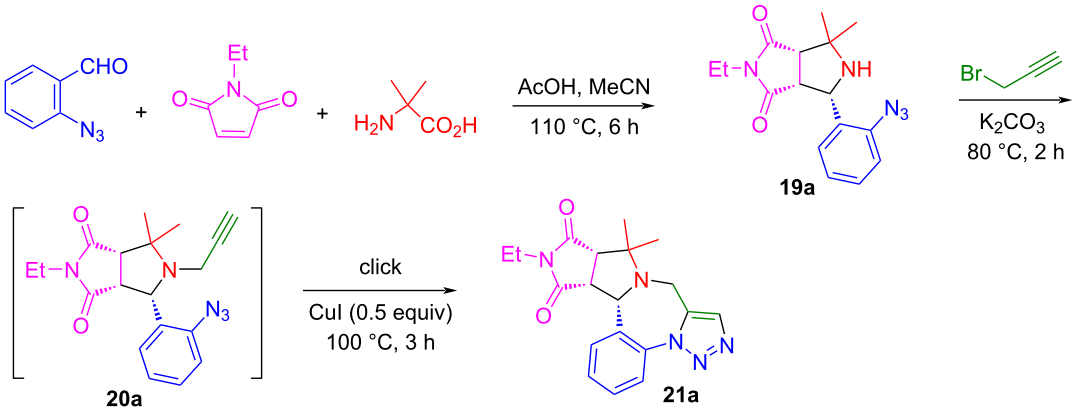

Scheme 12: Stepwise synthesis of triazolobenzodiazepine **21a**.

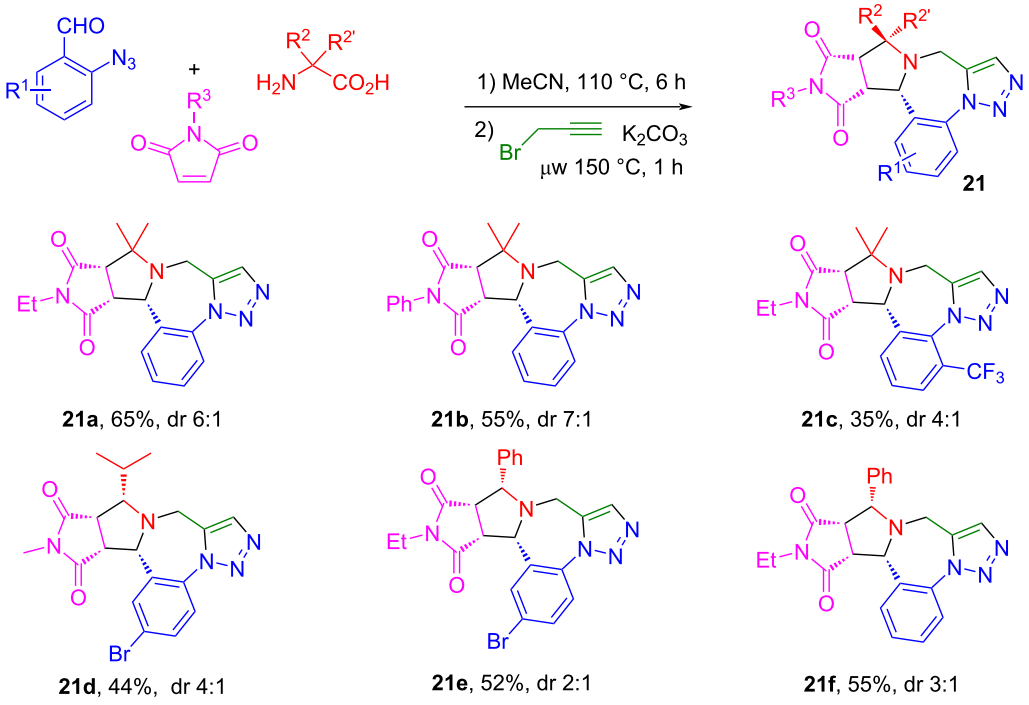

Scheme 13: One-pot synthesis of triazolobenzodiazepines.

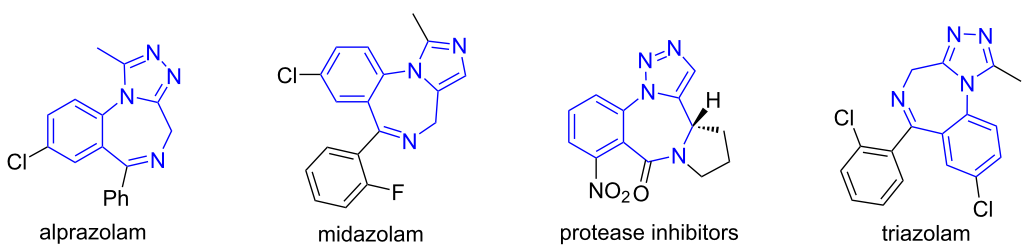

Figure 4: Bioactive triazolobenzodiazepine derivatives.

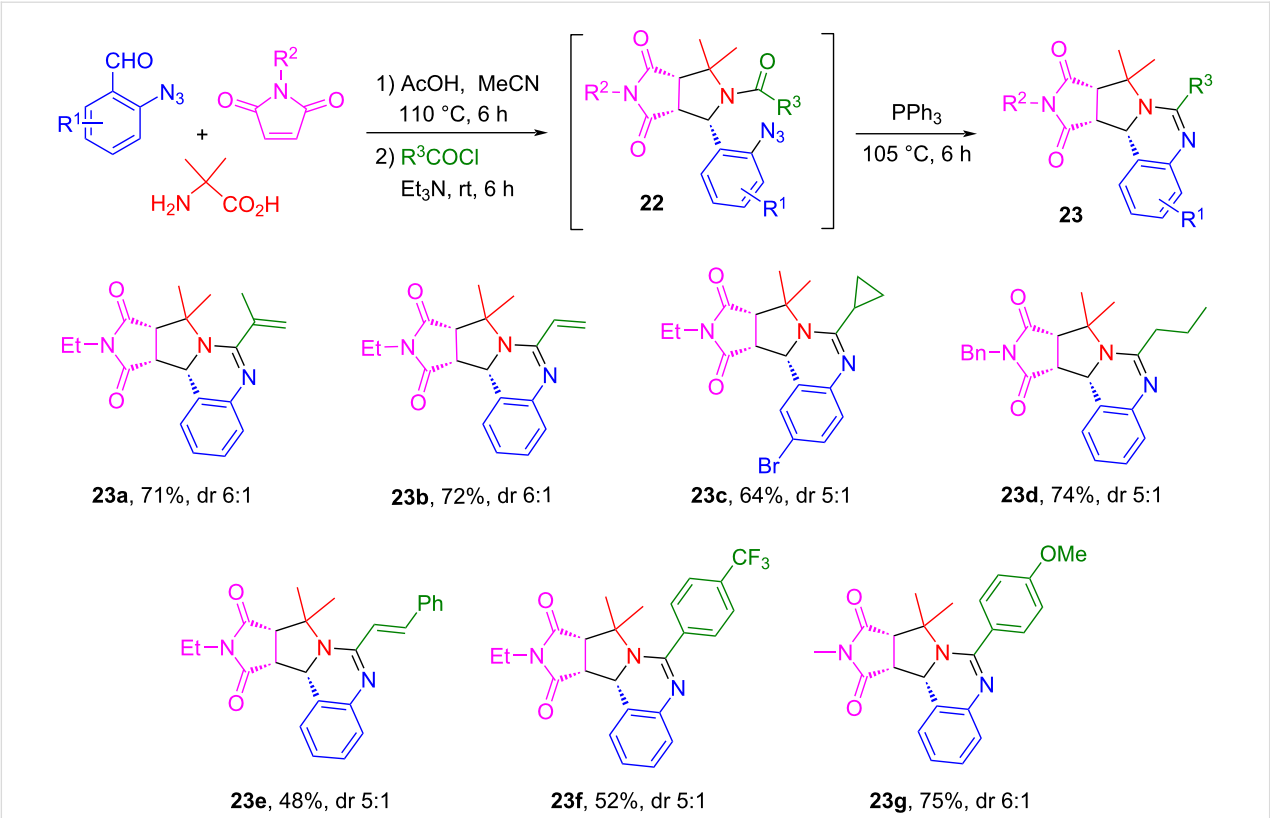

Scheme 14: One-pot synthesis of tetrahydropyrroloquinazolines.

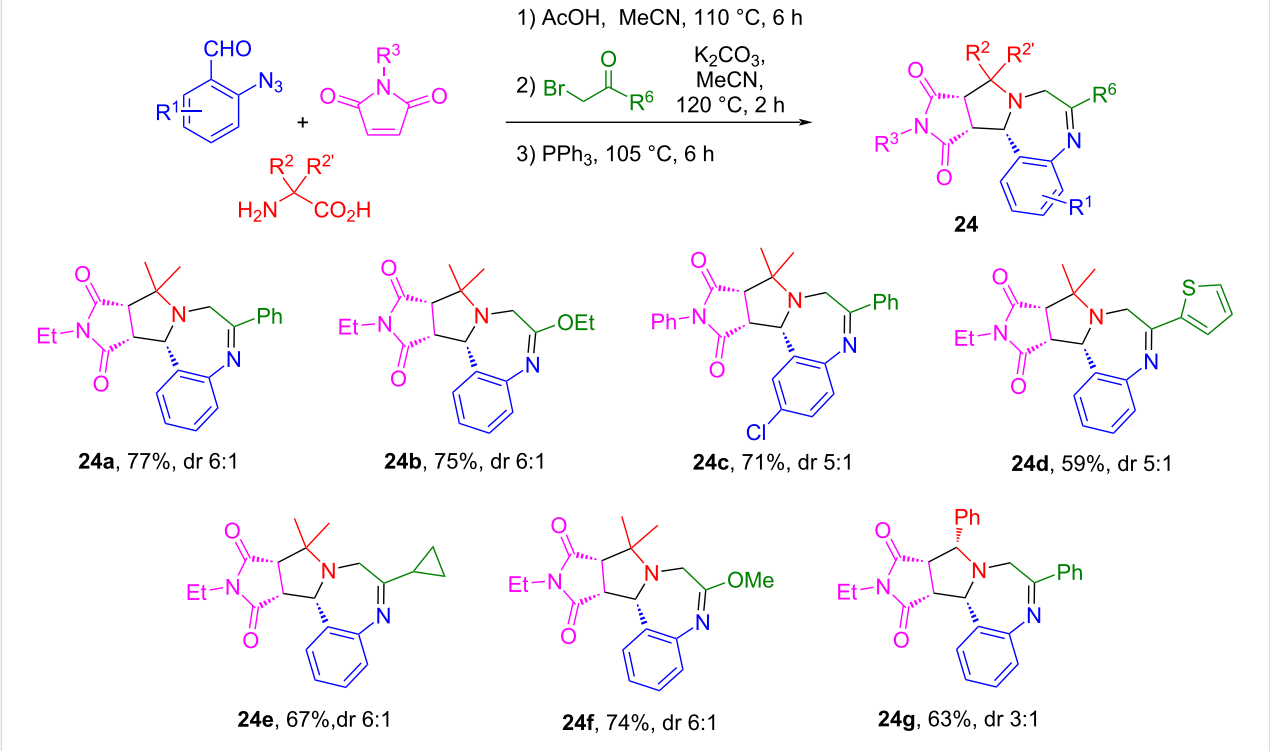

Scheme 15: One-pot synthesis of tetrahydropyrrolobenzodiazepines.

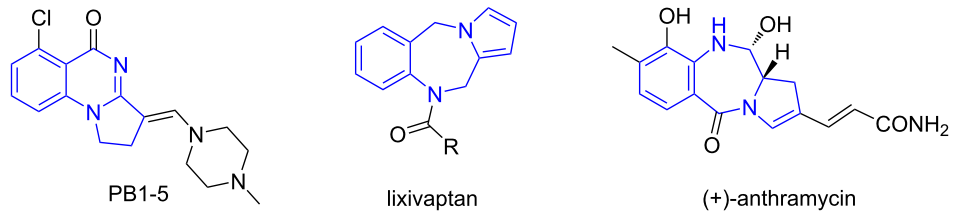

Figure 5: Bioactive pyrroloquinazolines and pyrrolobenzodiazepines.

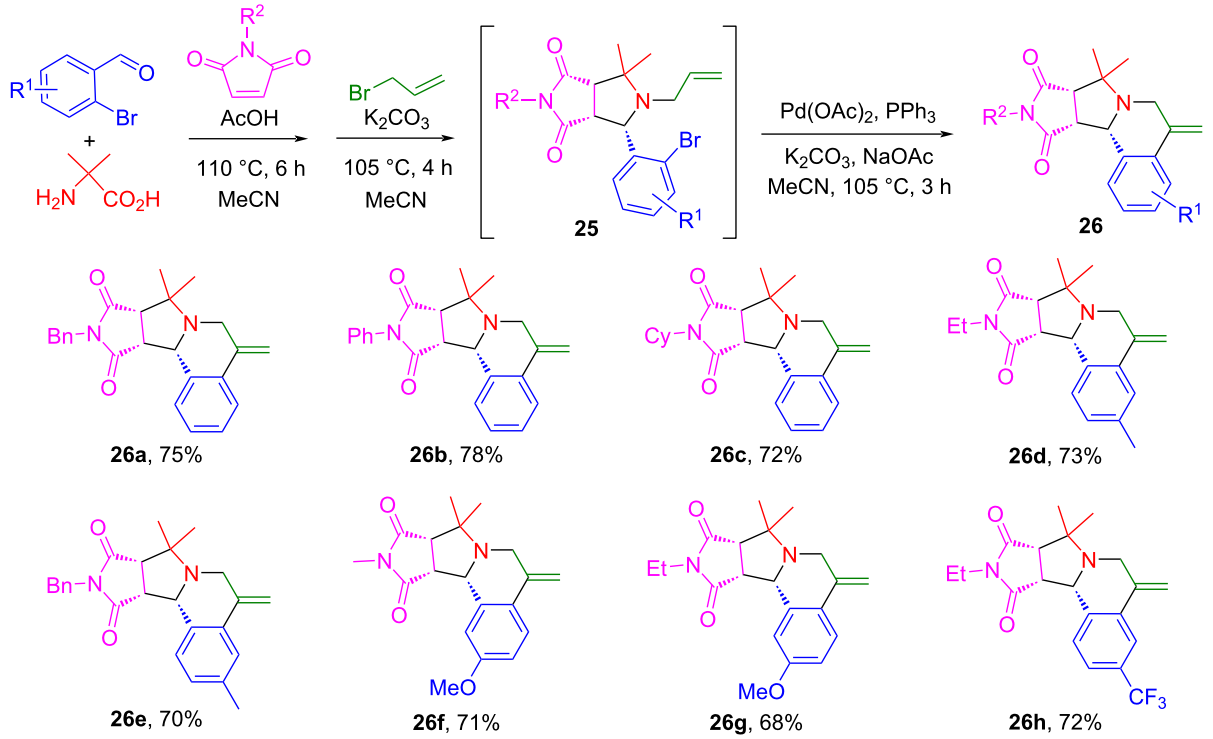

Scheme 16: Stepwise synthesis of pyrrolo[2,1-*a*]isoquinolines.

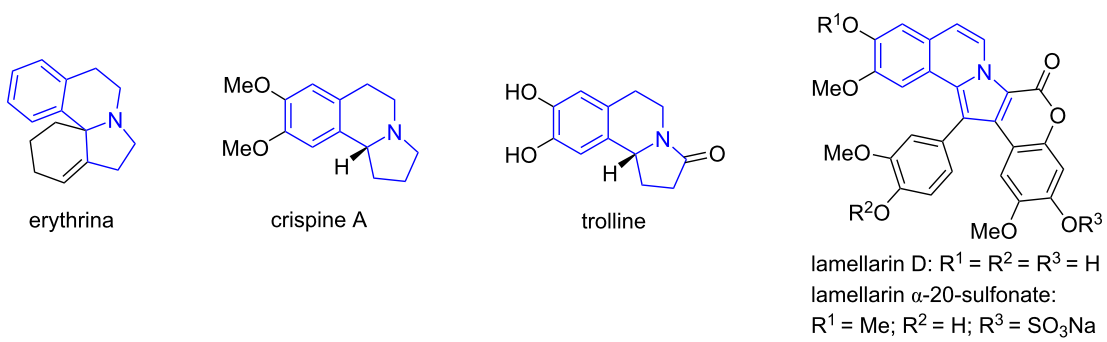

Figure 6: Bioactive pyrrolo[2,1-*a*]isoquinolines and hexahydropyrrolo[2,1-*a*]isoquinolines.

for the synthesis of tetrahydropyrrolothiazole derivatives. The reaction of cysteine with two equiv of arylaldehydes and one equiv of maleimides in EtOH at 90 °C for 12 h afforded tetrahydropyrrolothiazoles **29** in 66–79% yields with up to 7:1 dr (Scheme 17) [76]. Using olefinic oxindoles to replace maleimides, the reactions gave spiro[indoline-tetrahydropyrrolothia-

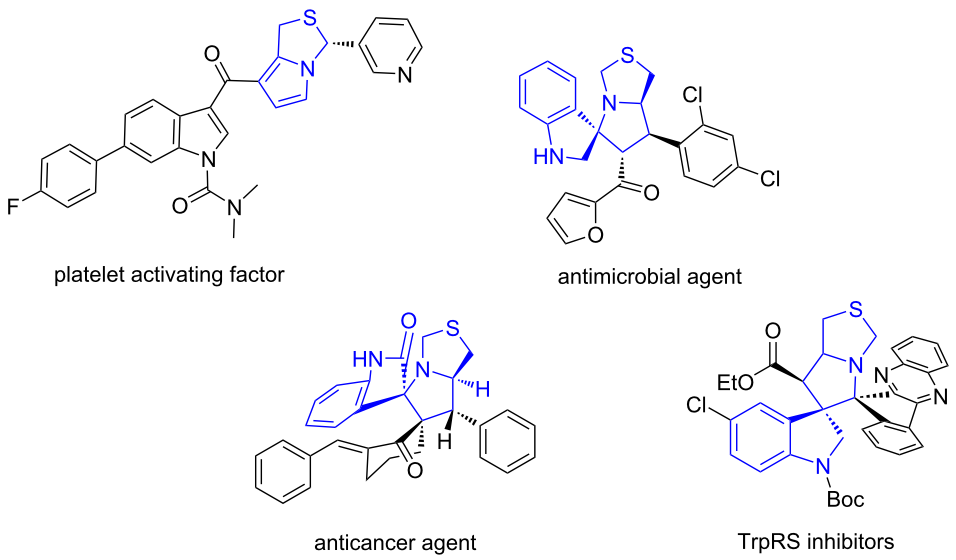

Figure 7: Bioactive tetrahydropyrrolothiazoles.

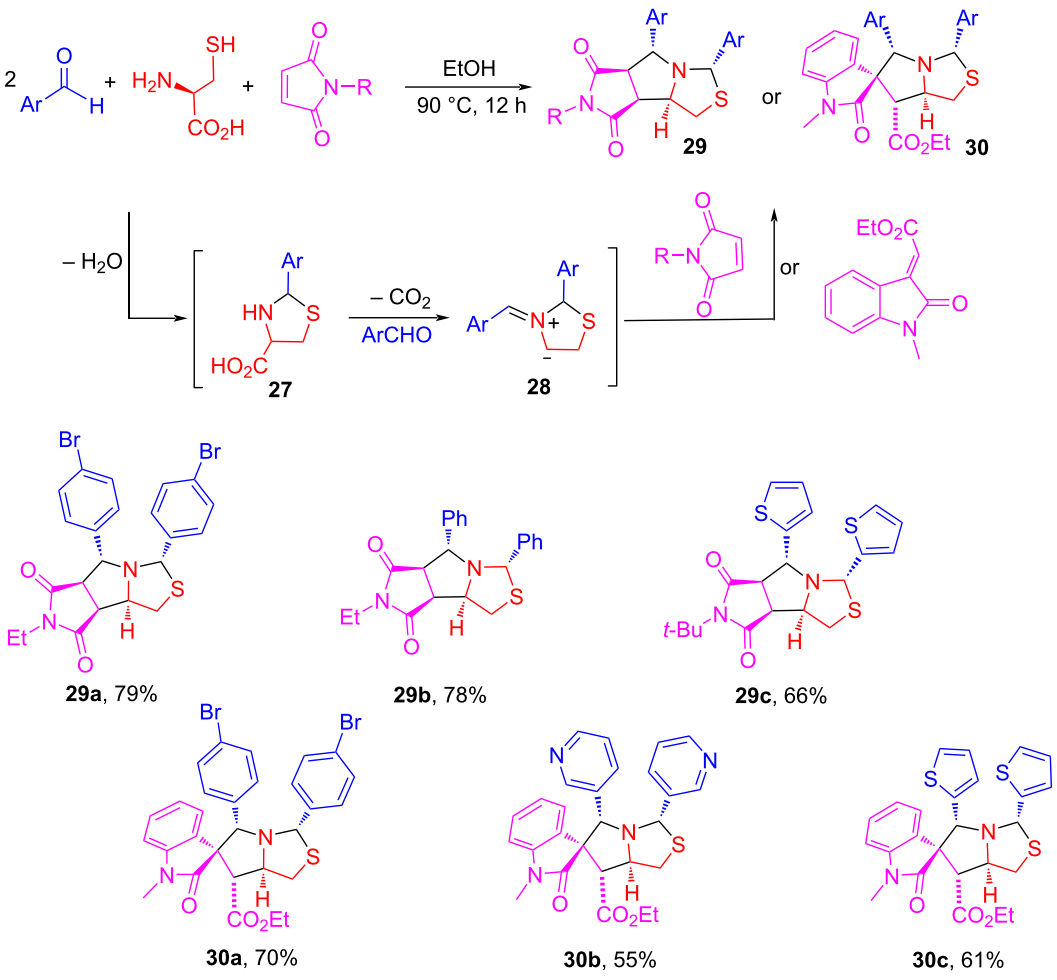

Scheme 17: Pseudo-four-component reaction for the synthesis of tetrahydropyrrolothiazoles **29** and **30** (>4:1 dr).

zole] products **30** in 55–70% with greater than 4:1 dr [76]. The reaction mechanism suggests that the reaction of cysteine with arylaldehydes gives *N*,*S*-acetals **27** which convert to AMYs **28** after decarboxlyation. Cycloaddition of **28** with maleimides or olefinic oxindoles gives products **29** and **30**, respectively. The reactions could be carried out as a two-step synthesis using two different arylaldehydes to give products **31** in 43–72% yields with greater than 4:1 dr (Scheme 18). A similar reaction sequence based on a [3 + 2] cycloaddition of stabilized AMYs has been reported by our lab [78].

Conclusion

The amino acid-based decarboxylative [3 + 2] cycloaddition reactions developed from our lab are summarized in this paper. The semi-stabilized *N*–H-type azomethine ylides derived from amino acids could be used for multicomponent, one-pot, and multistep reactions in the synthesis of heterocyclic compounds. The methods have advantages of using readily available starting materials, performing streamlined reactions, producing diverse product structures, and having high pot, atom, and step economy (PASE) [79-81] for the diversity-oriented synthesis (DOS) [82-88]. The work presented in this paper may also be helpful to understand the reaction mechanism and stereoselectivity of semi-stabilized *N*–H-type AMYs. We hope the new development for 1,3-dipolar cycloaddition chemistry can be used for the synthesis of bioactive heterocyclic compounds in medicinal and drug discovery programs.

Acknowledgements

We would like to thank all our co-workers who worked on the research projects highlighted in this paper, and the Centre for Green Chemistry at the University of Massachusetts Boston.

ORCID® iDs

Xiaofeng Zhang - https://orcid.org/0000-0003-4529-1158
Xiaoming Ma - https://orcid.org/0000-0003-1358-428X
Wei Zhang - https://orcid.org/0000-0002-6097-2763

References

1. Baunach, M.; Hertweck, C. *Angew. Chem., Int. Ed.* **2015,** *54,* 12550–12552. doi:10.1002/anie.201507120
2. Coldham, I.; Hufton, R. *Chem. Rev.* **2005,** *105,* 2765–2810. doi:10.1021/cr040004c
3. Otero-Fraga, J.; Montesinos-Magraner, M.; Mendoza, A. *Synthesis* **2017,** *49,* 802–809. doi:10.1055/s-0036-1588662
4. Wu, S.; Zhu, G.; Wei, S.; Chen, H.; Qu, J.; Wang, B. *Org. Biomol. Chem.* **2018,** *16,* 807–815. doi:10.1039/c7ob03051g
5. Cayuelas, A.; Larrañaga, O.; Selva, V.; Nájera, C.; Akiyama, T.; Sansano, J. M.; de Cózar, A.; Miranda, J. I.; Cossío, F. P. *Chem. – Eur. J.* **2018,** *24,* 8092–8097. doi:10.1002/chem.201801433
6. Zhang, C.; Das, D.; Seidel, D. *Chem. Sci.* **2011,** *2,* 233–236. doi:10.1039/c0sc00432d
7. Snider, B. B.; Ahn, Y.; O'Hare, S. M. *Org. Lett.* **2001,** *3,* 4217–4220. doi:10.1021/ol016884o
8. Vidadala, S. R.; Golz, C.; Strohmann, C.; Daniliuc, C.-G.; Waldmann, H. *Angew. Chem., Int. Ed.* **2015,** *54,* 651–655. doi:10.1002/anie.201409942
9. Gollner, A.; Weinstabl, H.; Fuchs, J. E.; Rudolph, D.; Garavel, G.; Hofbauer, K. S.; Karolyi-Oezguer, J.; Gmaschitz, G.; Hela, W.; Kerres, N.; Grondal, E.; Werni, P.; Ramharter, J.; Broeker, J.; McConnell, D. B. *ChemMedChem* **2019,** *14,* 88–93. doi:10.1002/cmdc.201800617
10. Narayan, R.; Potowski, M.; Jia, Z.-J.; Antonchick, A. P.; Waldmann, H. *Acc. Chem. Res.* **2014,** *47,* 1296–1310. doi:10.1021/ar400286b
11. Pearson, W. H.; Lovering, F. E. *J. Org. Chem.* **1998,** *63,* 3607–3617. doi:10.1021/jo972255+
12. Narayan, R.; Bauer, J. O.; Strohmann, C.; Antonchick, A. P.; Waldmann, H. *Angew. Chem., Int. Ed.* **2013,** *52,* 12892–12896. doi:10.1002/anie.201307392

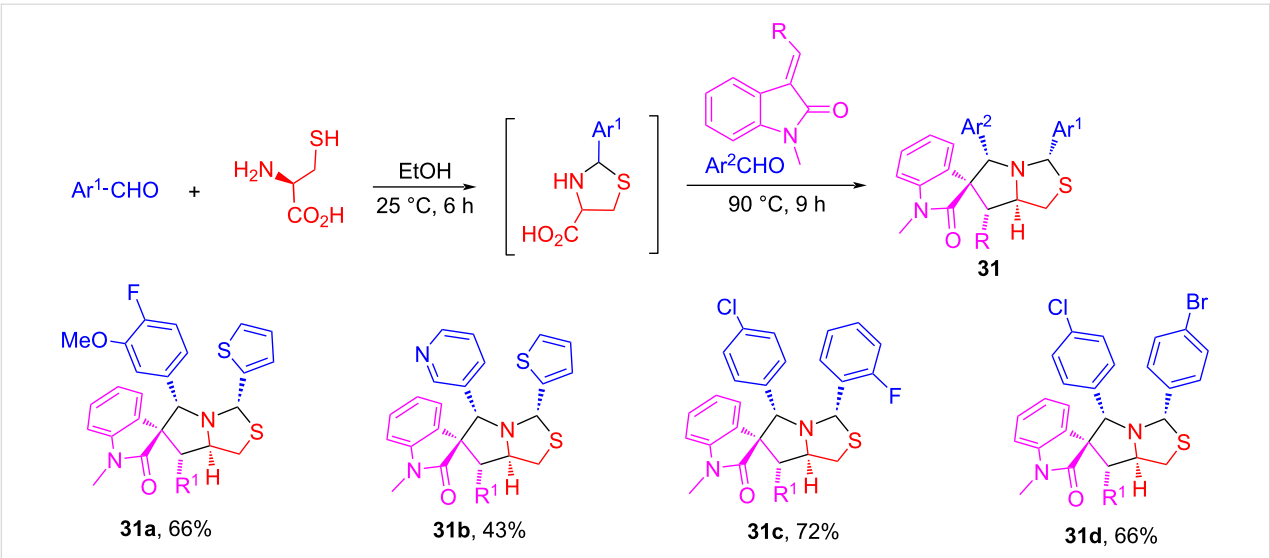

Scheme 18: One-pot two-step synthesis of spirooxindole-pyrrolothiazoles **31** (>4:1 dr).

13. Pearson, W. H.; Postich, M. J. *J. Org. Chem.* **1994,** *59,* 5662–5671. doi:10.1021/jo00098a026
14. Bhat, C.; Tilve, S. G. *RSC Adv.* **2014,** *4,* 5405–5452. doi:10.1039/c3ra44193h
15. Milen, M.; Abranyi-Balogh, P.; Keglevich, G. *Curr. Org. Synth.* **2014,** *11,* 889–901. doi:10.2174/15701794116661408182102 47
16. Tang, S.; Zhang, X.; Sun, J.; Niu, D.; Chruma, J. J. *Chem. Rev.* **2018,** *118,* 10393–10457. doi:10.1021/acs.chemrev.8b00349
17. Banks, H. D. *Org. Biomol. Chem.* **2011,** *9,* 6335–6342. doi:10.1039/c1ob05588g
18. Gothelf, K. V.; Jørgensen, K. A. *Chem. Rev.* **1998,** *98,* 863–910. doi:10.1021/cr970324e
19. Hashimoto, T.; Maruoka, K. *Chem. Rev.* **2015,** *115,* 5366–5412. doi:10.1021/cr5007182
20. Pandey, G.; Banerjee, P.; Gadre, S. R. *Chem. Rev.* **2006,** *106,* 4484–4517. doi:10.1021/cr050011g
21. Chogii, I.; Njardarson, J. T. *Angew. Chem., Int. Ed.* **2015,** *54,* 13706–13710. doi:10.1002/anie.201506559
22. Peng, L.; Wang, H.; Guo, C. *J. Am. Chem. Soc.* **2021,** *143,* 6376–6381. doi:10.1021/jacs.1c02697
23. Adrio, J.; Carretero, J. C. *Chem. Commun.* **2014,** *50,* 12434–12446. doi:10.1039/c4cc04381b
24. Najera, C.; de Garcia Retamosa, M.; Sansano, J. M. *Angew. Chem., Int. Ed.* **2008,** *47,* 6055–6058. doi:10.1002/anie.200801690
25. Potowski, M.; Schürmann, M.; Preut, H.; Antonchick, A. P.; Waldmann, H. *Nat. Chem. Biol.* **2012,** *8,* 428–430. doi:10.1038/nchembio.901
26. Esteban, F.; Cieślik, W.; Arpa, E. M.; Guerrero-Corella, A.; Díaz-Tendero, S.; Perles, J.; Fernández-Salas, J. A.; Fraile, A.; Alemán, J. *ACS Catal.* **2018,** *8,* 1884–1890. doi:10.1021/acscatal.7b03553
27. Zhang, W. *Chem. Lett.* **2013,** *42,* 676–681. doi:10.1246/cl.130504
28. Zhang, X.; Zhang, W. *Curr. Opin. Green Sustainable Chem.* **2018,** *11,* 65–69. doi:10.1016/j.cogsc.2018.04.005
29. Lu, Q.; Song, G.; Jasinski, J. P.; Keeley, A. C.; Zhang, W. *Green Chem.* **2012,** *14,* 3010–3012. doi:10.1039/c2gc36066g
30. Zhang, W.; Lu, Y.; Geib, S. *Org. Lett.* **2005,** *7,* 2269–2272. doi:10.1021/ol0507773
31. Gayen, B.; Banerji, A.; Dhara, K. *Synth. Commun.* **2016,** *46,* 293–308. doi:10.1080/00397911.2015.1135954
32. Madhavan, S.; Okamoto, S. *ChemCatChem* **2018,** *10,* 2014–2018. doi:10.1002/cctc.201702035
33. Malatesti, N.; Boa, A. N.; Clark, S.; Westwood, R. *Tetrahedron Lett.* **2006,** *47,* 5139–5142. doi:10.1016/j.tetlet.2006.05.064
34. De Luca, L.; Chiminazzo, A.; Sperni, L.; Strukul, G.; Scarso, A. *Chem. – Eur. J.* **2017,** *23,* 3474–3478. doi:10.1002/chem.201605878
35. Bolognesi, M. L.; Bartolini, M.; Cavalli, A.; Andrisano, V.; Rosini, M.; Minarini, A.; Melchiorre, C. *J. Med. Chem.* **2004,** *47,* 5945–5952. doi:10.1021/jm049782n
36. Higashino, T.; Yamada, T.; Yamamoto, M.; Furube, A.; Tkachenko, N. V.; Miura, T.; Kobori, Y.; Jono, R.; Yamashita, K.; Imahori, H. *Angew. Chem., Int. Ed.* **2016,** *55,* 629–633. doi:10.1002/anie.201509067
37. Takano, Y.; Herranz, M. Á.; Martín, N.; Radhakrishnan, S. G.; Guldi, D. M.; Tsuchiya, T.; Nagase, S.; Akasaka, T. *J. Am. Chem. Soc.* **2010,** *132,* 8048–8055. doi:10.1021/ja100665q
38. Guldi, D. M.; Swartz, A.; Luo, C.; Gómez, R.; Segura, J. L.; Martín, N. *J. Am. Chem. Soc.* **2002,** *124,* 10875–10886. doi:10.1021/ja012694x
39. Hölzel, H.; Haines, P.; Kaur, R.; Lungerich, D.; Jux, N.; Guldi, D. M. *J. Am. Chem. Soc.* **2022,** *144,* 8977–8986. doi:10.1021/jacs.2c00456
40. Guldi, D. M.; Spänig, F.; Kreher, D.; Perepichka, I. F.; van der Pol, C.; Bryce, M. R.; Ohkubo, K.; Fukuzumi, S. *Chem. – Eur. J.* **2008,** *14,* 250–258. doi:10.1002/chem.200700837
41. Che, J.; Ma, C.; Lu, J.; Chen, B.; Shi, Q.; Jin, X.; Song, R.; Xu, F.; Gan, L.; Li, J.; Hu, Y.; Dong, X. *Eur. J. Med. Chem.* **2022,** *228,* 113954. doi:10.1016/j.ejmech.2021.113954
42. Sato, S.; Takei, T.; Matsushita, Y.; Yasuda, T.; Kojima, T.; Kawano, M.; Ohnuma, M.; Tashiro, K. *Inorg. Chem.* **2015,** *54,* 11581–11583. doi:10.1021/acs.inorgchem.5b01183
43. Wong, W. W. H.; Vak, D.; Singh, T. B.; Ren, S.; Yan, C.; Jones, D. J.; Liaw, I. I.; Lamb, R. N.; Holmes, A. B. *Org. Lett.* **2010,** *12,* 5000–5003. doi:10.1021/ol102166m
44. Clark, R. B.; Pearson, W. H. *Org. Lett.* **1999,** *1,* 349–352. doi:10.1021/ol990677v
45. Kanemasa, S.; Sakamoto, K.; Tsuge, O. *Bull. Chem. Soc. Jpn.* **1989,** *62,* 1960–1968. doi:10.1246/bcsj.62.1960
46. Tsuge, O.; Kanemasa, S.; Hatada, A.; Matsuda, K. *Bull. Chem. Soc. Jpn.* **1986,** *59,* 2537–2545. doi:10.1246/bcsj.59.2537
47. Vedejs, E.; West, F. G. *Chem. Rev.* **1986,** *86,* 941–955. doi:10.1021/cr00075a014
48. Ardill, H.; Grigg, R.; Sridharan, V.; Surendrakumar, S. *Tetrahedron* **1988,** *44,* 4953–4966. doi:10.1016/s0040-4020(01)86199-8
49. Pearson, W. H.; Postich, M. J. *J. Org. Chem.* **1992,** *57,* 6354–6357. doi:10.1021/jo00049a058
50. Pearson, W. H.; Walters, M. A.; Oswell, K. D. *J. Am. Chem. Soc.* **1986,** *108,* 2769–2771. doi:10.1021/ja00270a055
51. Tsuge, O.; Kanemasa, S.; Yamada, T.; Matsuda, K. *J. Org. Chem.* **1987,** *52,* 2523–2530. doi:10.1021/jo00388a033
52. Gollner, A.; Rudolph, D.; Arnhof, H.; Bauer, M.; Blake, S. M.; Boehmelt, G.; Cockroft, X.-L.; Dahmann, G.; Ettmayer, P.; Gerstberger, T.; Karolyi-Oezguer, J.; Kessler, D.; Kofink, C.; Ramharter, J.; Rinnenthal, J.; Savchenko, A.; Schnitzer, R.; Weinstabl, H.; Weyer-Czernilofsky, U.; Wunberg, T.; McConnell, D. B. *J. Med. Chem.* **2016,** *59,* 10147–10162. doi:10.1021/acs.jmedchem.6b00900
53. Rao, M. P.; Gunaga, S. S.; Zuegg, J.; Pamarthi, R.; Ganesh, M. *Org. Biomol. Chem.* **2019,** *17,* 9390–9402. doi:10.1039/c9ob01429b
54. Dong, H.; Song, S.; Li, J.; Xu, C.; Zhang, H.; Ouyang, L. *Bioorg. Med. Chem. Lett.* **2015,** *25,* 3585–3591. doi:10.1016/j.bmcl.2015.06.076
55. Rehn, S.; Bergman, J.; Stensland, B. *Eur. J. Org. Chem.* **2004,** 413–418. doi:10.1002/ejoc.200300621
56. Wang, N.; Jiang, F.; Du, Z.; Bao, X.; Wang, T.; Yang, R. *Supramol. Chem.* **2012,** *24,* 819–825. doi:10.1080/10610278.2012.721551
57. Andersson, C.-H.; Nyholm, L.; Grennberg, H. *Dalton Trans.* **2012,** *41,* 2374–2381. doi:10.1039/c2dt12097f
58. Pérez, L.; Lenoble, J.; Barberá, J.; de la Cruz, P.; Deschenaux, R.; Langa, F. *Chem. Commun.* **2008,** 4590–4592. doi:10.1039/b808730j
59. Seidel, D. *Acc. Chem. Res.* **2015,** *48,* 317–328. doi:10.1021/ar5003768
60. Mantelingu, K.; Lin, Y.; Seidel, D. *Org. Lett.* **2014,** *16,* 5910–5913. doi:10.1021/ol502918g
61. Zhang, X.; Liu, M.; Qiu, W.; Evans, J.; Kaur, M.; Jasinski, J. P.; Zhang, W. *ACS Sustainable Chem. Eng.* **2018,** *6,* 5574–5579. doi:10.1021/acssuschemeng.8b00555
62. Zhang, X.; Liu, M.; Zhan, D.; Kaur, M.; Jasinski, J. P.; Zhang, W. *New J. Chem.* **2022,** *46,* 3866–3870. doi:10.1039/d1nj05538k

63. Ma, X.; Zhang, W. *iScience* **2022,** *25,* 105005. doi:10.1016/j.isci.2022.105005
64. Zhang, W.; Yi, W. B. *Pot, Atom, and Step Economy (PASE) Synthesis;* Springer Nature Switzerland: Cham, Switzerland, 2019. doi:10.1007/978-3-030-22596-4
65. Zhang, X.; Liu, M.; Zhang, W.; Legris, M.; Zhang, W. *J. Fluorine Chem.* **2017,** *204,* 18–22. doi:10.1016/j.jfluchem.2017.10.003
66. Hao, J.; Milcent, T.; Retailleau, P.; Soloshonok, V. A.; Ongeri, S.; Crousse, B. *Eur. J. Org. Chem.* **2018,** 3688–3692. doi:10.1002/ejoc.201800255
67. Corbett, M. T.; Xu, Q.; Johnson, J. S. *Org. Lett.* **2014,** *16,* 2362–2365. doi:10.1021/ol500679w
68. Donohoe, T. J.; Sintim, H. O. *Org. Lett.* **2004,** *6,* 2003–2006. doi:10.1021/ol049397s
69. Zhang, X.; Qiu, W.; Evans, J.; Kaur, M.; Jasinski, J. P.; Zhang, W. *Org. Lett.* **2019,** *21,* 2176–2179. doi:10.1021/acs.orglett.9b00487
70. Zhang, X.; Qiu, W.; Murray, S. A.; Zhan, D.; Evans, J.; Jasinski, J. P.; Wang, X.; Zhang, W. *J. Org. Chem.* **2021,** *86,* 17395–17403. doi:10.1021/acs.joc.1c01797
71. Ma, X.; Zhang, X.; Qiu, W.; Zhang, W.; Wan, B.; Evans, J.; Zhang, W. *Molecules* **2019,** *24,* 601. doi:10.3390/molecules24030601
72. Zhang, X.; Zhi, S.; Wang, W.; Liu, S.; Jasinski, J. P.; Zhang, W. *Green Chem.* **2016,** *18,* 2642–2646. doi:10.1039/c6gc00497k
73. Ma, X.; Zhang, X.; Awad, J. M.; Xie, G.; Qiu, W.; Muriph, R. E.; Zhang, W. *Tetrahedron Lett.* **2020,** *61,* 151392. doi:10.1016/j.tetlet.2019.151392
74. Sutherell, C. L.; Tallant, C.; Monteiro, O. P.; Yapp, C.; Fuchs, J. E.; Fedorov, O.; Siejka, P.; Müller, S.; Knapp, S.; Brenton, J. D.; Brennan, P. E.; Ley, S. V. *J. Med. Chem.* **2016,** *59,* 5095–5101. doi:10.1021/acs.jmedchem.5b01997
75. Ma, X.; Meng, S.; Zhang, X.; Zhang, Q.; Yan, S.; Zhang, Y.; Zhang, W. *Beilstein J. Org. Chem.* **2020,** *16,* 1225–1233. doi:10.3762/bjoc.16.106
76. Ma, X.; Qiu, W.; Liu, L.; Zhang, X.; Awad, J.; Evans, J.; Zhang, W. *Green Synth. Catal.* **2021,** *2,* 74–77. doi:10.1016/j.gresc.2020.11.001
77. Lu, J.; Yao, B.; Zhan, D.; Sun, Z.; Ji, Y.; Zhang, X. *Beilstein J. Org. Chem.* **2022,** *18,* 1607–1616. doi:10.3762/bjoc.18.171
78. Zhang, X.; Ma, X.; Qiu, W.; Awad, J.; Zhang, W. *Green Process. Synth.* **2022,** *11,* 1128–1135. doi:10.1515/gps-2022-0088
79. Hayashi, Y. *Chem. Sci.* **2016,** *7,* 866–880. doi:10.1039/c5sc02913a
80. Sydnes, M. O. *Curr. Green Chem.* **2014,** *1,* 216–226. doi:10.2174/2213346101666140221225404
81. Clarke, P. A.; Santos, S.; Martin, W. H. C. *Green Chem.* **2007,** *9,* 438–440. doi:10.1039/b700923b
82. O' Connor, C. J.; Beckmann, H. S. G.; Spring, D. R. *Chem. Soc. Rev.* **2012,** *41,* 4444–4456. doi:10.1039/c2cs35023h
83. Comer, E.; Duvall, J. R.; duPont Lee, M., IV. *Future Med. Chem.* **2014,** *6,* 1927–1942. doi:10.4155/fmc.14.111
84. Dandapani, S.; Marcaurelle, L. A. *Curr. Opin. Chem. Biol.* **2010,** *14,* 362–370. doi:10.1016/j.cbpa.2010.03.018
85. Galloway, W. R. J. D.; Isidro-Llobet, A.; Spring, D. R. *Nat. Commun.* **2010,** *1,* 80. doi:10.1038/ncomms1081
86. Gerry, C. J.; Schreiber, S. L. *Curr. Opin. Chem. Biol.* **2020,** *56,* 1–9. doi:10.1016/j.cbpa.2019.08.008
87. Mortensen, K. T.; Osberger, T. J.; King, T. A.; Sore, H. F.; Spring, D. R. *Chem. Rev.* **2019,** *119,* 10288–10317. doi:10.1021/acs.chemrev.9b00084
88. Schreiber, S. L. *Science* **2000,** *287,* 1964–1969. doi:10.1126/science.287.5460.1964

License and Terms